PETROGRAPHICAL AND PETRO-CHEMICAL PROPERTIES OF THE ROCK UNITS CROPPING OUT IN ULUKIŞLA TERTIARY BASIN

Ali ÇEVİKBAŞ[1] and Önder ÖZTUNALI[2]

[1] Gen., Direc., Min., Res. Expl.(MTA) Ankara-TÜRKİYE
[2] İstanbul Univ.,Dept. of Geology, İstanbul-TÜRKİYE

ABSTRACT: *Investigated area is limited by Niğde Massif to the north, Bolkardağ to the south and Ecemiş Fault Zone to the east. The basement, Bolkardağ marbles, is tectonically overlain by Alihoca ophiolitic complex.Horoz granodiorite and vein rocks are exposed by cutting the marbles and ophiolitic rocks.*

Ulukışla-Çamardı Basin has studied as three diffrent portion, that stratigraphically and lithologically do not match one another. In the south, the base of the Palaeogene basin starts with Upper Maastrichtian-Lower Paleocene reefal carbonates (Kalkankaya formation), that unconformably rest on the Bolkardağ marbles and ophiolitic complex, and continue with detrital units till to Middle Eocene. The middle portion starts with Cretaceous (Maastrichtian) age detrital Kırkgeçit formation and followed by Middle Eocene age volcano-clastic Tabaklı formation. The base of the north portion starts with Upper Cretaceous carbonates (Ömerli formation) and then formation of the volcano-clastics and various intrusions carry on until Middle Eocene.

In the middle portion of the Ulukışla-Çamardı basin, the first volcanic activity (Karakaya basalt member) formed during Upper Cretaceous together with the basin formation. The second volcanic activity are seen during the Paleocene-Middle Eocene time, however this volcanics carried on their deposition with some other clastics. Volcanism presents volcano-sedimentary character in the middle portion, however, mostly it displays basic character (e.g. Ünlükaya formation and Karlık basalt) and andesitic character (e.g. Ardıçlı formation and Alıçlı andesite), which formed in the shape of lava flow, in the north. Magmatic rock units such as Uçurumtepe monzonite, Yağlıtaş diorite and Elmalı synite stock and dikes are also seen in this part.Well exposed Middle Paleocene-Lower Eocene volcanism also prevailed during Lutetian time. All the units are cut by Kaletepe trachyte. Due to regression occured in the region by the end of Upper Eocene, evaporites, lacustrinal and fluvial deposits formed on the continental environment.

Mineralogically Ulukışla volcanics comprise basalt, sipilitic basalt, andesite, trachyandesite, syenite porphire and trachyte. According to major and trace elements contents, alkaline and calcalkaline rocks formed due to continent- continent collision and so it is proposed that this rocks are the product of a contaminated hybritic magma occured due by thickenning crust.

The background values of the individual metals for Turkish river sediments were represented as mean values which correspond to the natural heavy metal concentration of the waters:

Fe(%)	Co	Cr	Ni	Cu	Pb	Zn	Li	Mn
4	34	215	253	61	24	145	30	957 (mg/kg)
0.87	1.78	2.39	3.73	1.34	1.19	1.53	0.5	1.13-fold values

The above-mentioned heavy metal concentrations were measured in clay fraction and include only those (240) samples with a concentration below the twofold standard deviation values. This represents an area of 240,000 m^2 (one-third of the country's total area).

Geochemical examinatination of fine grain sediment revealed the possible existence of metal deposits with regard to Li, Cu, Pb, and Zn.

Nutrient substance (C_{org} and N) was found to be extremely low with the exception of the Porsuk River, which had high values owing to the waste water coming from to city of Eskişehir. This anthropogenic influence can also be seen in the increased proportion of light bound metals. The lateral distribution of phosphates being quite constant in all rivers, lithogenic origin is indicated. However, a distinct increase in phosphate content was observed downstream after all urban settlements, particularly in Porsuk sediment.

The mean carbonate content is of detritic origin and corresponds to the minerals in the catchment area.

Granulometric analysis showed that sediments are extremely sandy owing to the strong current in all rivers and the prevalence of erosion-proof minerals.

The predominant clay mineral group found was Smectit which is attributed to the extensive areas of volcanic rock and basic magmatites. Illites, caolinites, and chlorites make up almost 50% of the clay minerals in regions of metamorphic and paleozoic rocks.

In summary, the ecologic situation of the rivers can be described as intact, which is largely due to the fact that these waters are unsuitable for navigation. Anthropogenic effects are cleary restricted to the environment of the few large cities.

The high susceptibility of surface water to pollution of all kind demands particular attention in the case of the rivers of Turkey, since they are the main source for drinking water and irrigation even beyond the country's borders. With the growing water scarcity already evident in Israel, the Middle East, Africa, and several Greek islands, a constant observation and protection against contamination has to be given first priority.

367

GEOCHEMICAL AND SEDIMENTOLOGICAL INVESTIGATIONS ON TURKISH RIVER SEDIMENTS-GEOGENIC AND ANTHROPOGENIC EFFECTS-

Dr.H.Emin SEVİM

Kleinschmidtstrasse 46, D-6900 Heidelberg-GERMANY

ABSTRACT: During summer 1988, 250 sediment samples were taken from the flood plain area of Turkey's 7 main rivers (Sakarya, Yeşilırmak, Kızılırmak, Ceyhan, Seyhan, Gediz, and Menderes). The aim of the study was to pinpoint heavy metal deposits and investigate their geochemical and sedimentological background in order to distinguish geogenic from anthropogenic origin. Further, the nutrient substance of the sediment was examined.

The collected samples underwent grainsize fractioning, heavy metal tracing of Cd, Co, Cr, Cu, Fe, Mn, Ni, and Zn, and a sixphase extraction procedure (based on a model by Tessier et al.) to determine the binding forms of the heavy metals in sediment.

Results confirmed the initial assumption that the geogenic base load would be high owing to the extensive deposits of magmatic rock in Turkey. The heavy metal concentration largely reflects the geochemical structure of the hinterland. Analysis of the chemical binding forms revealed a similarity among all the rivers, and that the heavy metals are firmly bound in the sediment. Also, no heavy metal pollution was found in the recent layers of a vertical sediment profile.

The results obtained can therefore be employed as background values in future investigations. Although the mean content in the examined sediment varies, a general tendency was evident. Diverging heavy metal content was found in the case of Ni, Cu, and Mn. Sediments of the Ceyhan and Menderes revealed above average Ni concentration, and the Yeşilırmak showed high Co concentration owing to non-ferrous metal deposits in the East Pontides.

366

NEW GEOCHEMICAL, ISOTOPIC AND RADIOMETRIC DATA RELATED TO PLIO-QUATERNARY VOLCANISM OF ERCIYES MOUNTAIN OF CENTRAL ANATOLIA

Tuncay ERCAN[1], Selçuk TOKEL[2], Jun-İchi MATSUDA[3],
Tadahide Uİ[4], Kenji NOTSU[5], Tatsuya FUJİTANİ[6]

[1] MTA General Directorate , Ankara-TÜRKİYE

[2] Karadeniz Tehc. Univ., Geology Dept.,Trabzon-TÜRKİYE

[3] Department of Earth and Space Science, Faculty of Science, Osaka University, Osaka, JAPAN

[4] Department of Earth Science, Faculty of Science, Kobe University, Nada, Kobe, JAPAN

[5] Laboratory for Earthquake Chemistry, Faculty of Science, Tokyo University, Bunkyo-Ku Tokyo, JAPAN

6 Marine Technical College, Department of Physics,. Ashiyo Hyogo, JAPON

ABSTRACT:"Erciyes Dağı" of Central Anatolia is an important volcanic centre, characterised by eruptions to have started in Pliocene with intermittent historical bursts, and defined as a live volcano due to gas emissions, some of which originating from the mantle. The central cone of Erciyes is 3916 m. high and is surrounded by 70 parasitic cones with diameters ranging between 650-3000 m.

Geochemical, isotopic and radiometric analyses were carried on Plio-Quaternary rocks of generally andesitic and dacitic with minor rhyodacitic and basaltic compositions. Isotopic ratios of $87_{Sr}/86_{Sr}$ varying between 0.70387 and 0. 70548 and evaluation of trace and rare earth element contents, suggest conclusively important contribution from the upper crust. $87_{Sr}/86_{Sr}$ ratio decreases with increase of Sr content, and increases with increase of SiO_2 Erciyes volcanism is a typical example of post-collisional volcanism occurring in the collisional zone between Anatolian and Afro-Arabian plates.

Radiometric dating by K/Ar method yielded ages varying between $2.590.000 \pm 104.000$ y.and 83.000 ± 5.000y. showing that the parasitic cones around Erciyes started in Pliocene and the Erciyes cone started to form approximately 1 million years ago continuing its development until historical times.

365

GEOLOGY OF THE ALAGÖL DAĞI AREA (ÇAMARDI-NİĞDE) IN THE EASTERN TAURIDES

Recep H. EREN [1], Bektaş UZ[1], Işık ÖZPEKER[1]and İhsan SEYMEN[2]

1 İstanbul Techn. Univ. Geology Dept. Ayazağa/İstanbul-TÜRKİYE

2 Selçuk Univ. Geology Dept., Konya-TÜRKİYE

ABSTRACT: Various carbonates with thin quartzite intercalations of the Zindandere formation of the Upper Permian age form the oldest part of the stratigraphical column of the area studied. Situated at the "Black Aladağ Nappe" of the Eastern Taurids. This sequence is followed by another carbonate serie (Çobankaya Fm.) of the Early Jurassic age above an angular unconformity. The youngest units of the stratigraphical column of the area are the alluvium and the slopedebris deposits covering extensive areas.

The Pb-Zn mineralization is observed to be related to the Upper Permian and Jurassic deposits with varying degree. This situation implies that the mineralization is not controlled stratigraphically, in other words, the mineralization is not confined to some sedimentary horizons.

The field observations have showed that the historical mines are situated at the intersection lines of the joints or, more often, are situated in the apex regions of the minor folds situated at the limbs and apex of the Tekneli Anticlinorium. The Pb-Zn occurences seen in the Çobankaya Formation are largely related to the joint planes and the ones seen in the Zindandere Formation are related to the axial zones of the minor anticlines besides the joint planes.

364

ENVIRONMENTAL INTERPRETATION OF THE EARLY MIOCENE DEPOSITS (KAPLANKAYA FORMATION) IN THE ADANA BASIN, S. TÜRKİYE

U.Can ÜNLÜGENÇ[1]* and Ümit ŞAFAK [1]

* Department of Geology, University of Keele, Staffs. ST5 5BG ENGLAND (present address)

1 Çukurova Univ., Geology Department, 01330 Balcalı /Adana-TÜRKİYE (permanent address)

ABSTRACT: Deformed basement units of Palaeozoic and Mesozoic age are overlain by Tertiary deposits with angular unconformity in the study area. The Oligocene Karsantı sub-basin with its alluvial fan, lagoonal, lacustrinal and fluvial sediments were deposited prior to the main Adana Basin deposits. The Karsantı sediments lie disconformably on the allochthonous Upper Cretaceous Kızıldağ melange and Farasa ophiolites to the north of the Adana Basin.

The depositional history of the Adana Basin begins during the Early Miocene as a peripheral foreland basin. The basin fill is both marine and non-marine in character, which show a gradual transition at the northern margin of the basin into one another. Although there is no clear contact observed between the non-fossiliferous terrestrial Gildirli Formation and the Oligocene Karsantı sub-basin fill deposits, it is proposed that, the Karsantı Basin fill is older than the undeformed Gildirli Formation with some substantial intervening deformative event. The Early Miocene Kaplankaya and Karaisalı Formations conformably overlie the Gildirli Formation. They are both seen to sit on the tilted Karsantı basin fill with angular unconformity.

The Early Miocene deposits, formed due to a northerly encroaching marine transgression, with a northerly source for the littoral-brackish and deltaic Kaplankaya Formation deposits. Stratigraphical, sedimentological and palaeontological observations prove that the Kaplankaya Formation formed during the Burdigalian. Its base is characterized by alluvial fan and distributary mouth bar deposits with intermittent fluvial and marine conditions. These pass up into pro-delta clayey facies which consists of shallow marine fossils. The Langhian-Serravallian turbiditic Cingöz Formation cuts the Kaplankaya formation with channelized, erosive contacts.

363

PRELIMINARY FIELD OBSERVATIONS ON THE GEOLOGICAL AND GEOMORPHOLOGICAL FEATURES OF THE NORTH ANATOLIAN FAULT ZONE AROUND DESTEK -ERBAA (AMASYA) REGION, TÜRKİYE

Osman PARLAK and Cavit DEMİRKOL

Dept. of Geology, Çukurova Univ. 01330, Adana-TÜRKİYE

ABSTRACT: *The study area lies on the North Anatolian fault zone in the area between Destek-Erbaa (Amasya). The basement of the investigated area is composed mainly of the low grade metamorphics of the Tokat group. This unit is unconformably overlain by a comprehensive series of Mesozoic sequences containing dominantly carbonate, flysch-type sediments with volcanic intercalation. Middle-Upper Eocene sediments rest on the Mesozoic sequences with an angular unconformity. A wide-spread Pliocene sediments are seen along the fault zone and according to 1943 earthquake, recent deformation patterns in Pliocene deposits are observed in the north of Erbaa region.*

Four sets of faults have been observed in the study area. These are;

1. Approximately 115° trending right -lateral strike slip faults running parallel to the main trace of NAFZ.

2. $130\text{-}140^o$ trending right-lateral strike slip faults

3. $090\text{-}098^o$ trending right-lateral strike slip faults

4. $040\text{-}045^o$ trending left-lateral strike slip faults

Geomorphological features such as elongated hills, sag ponds, pressure ridges, landslides, alluvial fans are the indication of strike slip tectonic regime in the study area.

This study contains the initial observations on general characteristics of the investigated area. Future studies will give much more evidences for neotectonic history of the region.

PALEOMAGNETIC INVESTIGATINOS OF MIOCENE-PLIOCENE AND PLEISTOCENE DEPOSITS OF EAST ANATOLIA.

T.A.ISMAIL-ZADE, A.Kh. IBADOV and T.N. KHUDAYAROV

Institute of Geophysics, Baku-AZERBAIJAN

ABSTRACT: *There were conducted the paleomagnetic investigation of results of fourth sections of deposits of Upper Miocene, Lower Pliocene and Middle Pliocene and Pleistocene of East Anatolia (Araz, Maslakhat, Ishyklar, Araz-chai). The analyses of magnetic clearing results on the basis of Ziyderveld diagram showed that natural residual magnetization of Jn has one ore two components. Viscous components of Jrv varies within the from 3% to 40% of in. Magnetic susceptibility of rock samples of all four sections is varied from 0.4*10 SI, international system of units, to 48*10 SI and natural residual magnetization is varied from 0.2*10 SI to 445*10 SI. In sections of Araz and Maslakhat there were determined one zone of direct magnetization and one zone of reversible magnetization. In Ishyklar section there were determined two zones of direct magnetization and one zone of reversible magnetization. In Araz-chai section there were determined one zone of direct magnetization. Change of zones of direct and reversible magnetization of Araz section coincide with the boundary of Miocene-Pliocene deposits and it is well correlated with transition from Pontic stage to Kinimeric stage of USSR paleomagnetic scale. The average value of the ancient declination D and inclination I according to the sections are equaled: Araz-D=4, I=-60, Maslakhat - D=10, I=-55, Ishyklar - D=203, I=75, Araz-chai - D=230, I=67. Proximity of ancient declination value for two first and two last sections can be related to the features of tectonic development of region. Study of dependence on temperature of residual magnetization saturation of Jrs (T) determined that the carriers of natural residual magnetization are mainly magnetite, hematite, maghemite, hydrogoethite.*

361

Nakhichevan Autonomous Republic and there were not exactly correlated the stratigraphic sections. The same error was made in the Middle Kura depression region. The error made in use of volume of lutecium stage and Middle Eocene related to the stratotypical Paleogene sections located in the West. These stratotypes are located in that part of epicontinental basins where beginning from Danish stage to Oligocene stage inclusive one can observe frequent change of genetic sedimentary origin deposits of the same type (off-shore deposits, lagoon deposits, lacustrine deposits, river deposits, soil fossils of podsol type and others). These deposits have not or have the limited number of characteristic species according to which one can make the wide correlation. Because of sedimentation discontinuity, Paleogene stages of English-French-Belgian basin having insufficient paleontological data overlap each other (Tanet stage, Snarnak stage, Ilerd stage, Ipr stage and others). There were determined according to the fragmentary exposures (Asshai stage, Vemmel stage, Led stage and others). So there were made the great errors in comparison with off-shore Paleogene deposits of East and West up to parallelization of different stage ages (Borton stage, Criabon stage, Bodrak stage and others). Now it is common knowledge that there were not determined the volume of lutecium stage and its correlation with the Middle Eocene in the Crimean scale of Paleogene as well as the West European scale of Paleogene.

Paleogene deposits of Azerbaijan were subdivided into local suits, horizons, layers for a long time. Their ages were determined up to division or subdivision without using of stage separation. It is impossible to determine volume and area of oil-bearing lutecium deposit distributions.

Azerbaijan and Turkey are characterized by heterogenous geological structure which was caused by heterogeneity of their basement, complex geotectonic processes in development of their territories, dislocation features in sedimentary cover, lithofacial variations of areal sections and the presence of magma origin formation in them.

For definition of volume and region of lutecium deposit distributions it is necessary to select from paleontological point of view the best characterized Eocene sections of Azerbaijan and Turkey and make stage separation, zone separation and paleomagnetic separation by them. Paleomagnetic investigation can render invaluable assistance for determination of exact correlation of sections with the common scale of Eocene deprived of faunistic remains. Thus, these investigations enable to correct search and exploration work direction.

THE MAIN REASONS OF SEARCH AND EXPLORATION OF HYDROCARBON ACCUMULATION IN EOCENE DEPOSITS OF AZERBAIJAN AND TURKEY.

M.A.BAGMANOV, T.A.ISMAIL-ZADE and K.M. KERIMOV

Institute of Geophysics, Baku-AZERBAIJAN

ABSTRACT: *Hydrocarbon deposits related to the Eocene section were discovered in a number of areas of Azerbaijan and Georgia. They were localized in lutecium deposit. For definition of further direction of search and exploration work is required to determine the region of these deposit distributions. Difficulty of the problem solution can be explained that firstly, the most of perspective area sections are not exactly controlled from paleontological point of view. There were not determined paleomagnetic zones in them according to which might be conducted the correlation with the common scale. Secondly, Middle Eocene deposits in Azerbaijan and Turkey as well as deposits in the rest regions of the world had been considered only in the volume of lutecium stage up to now.*

In this connection the substantial Above-lutecium part of Middle Eocene in fact not having of large oil and gas show concerned either lutecium stage or Upper Eocene. There was not the great professional error. It was the result of errous practice of stratification section.

For lack of stage separation of Middle Eocene and incapacity of exact definition of lutecium stage in its volume there was not determined the block structure of

359

GEOLOGY AND MINERALOGY OF THE MADSAN ANTIMONY DEPOSIT (ÇAMARDI-NİĞDE)

İlkay KUŞCU and Ayhan ERLER

METU, Dept. Geol. Eng., 06531 Ankara, TÜRKİYE

ABSTRACT: The Madsan antimony deposit is located 1 km north-northeast of Çamardı, and 68 km southeast of Niğde. It lies at the southeastern part of the Niğde Massif, close to its boundary with the Ecemiş Fault.

The Madsan antimony deposit is hosted by white marbles, calc-silicate marbles and sericitized gneisses of the Gümüşler Formation. Wall rocks are silicified, sericitized, chloritized and recrystallized. Silicification, sericitic alteration and chloritization are observed in the gneisses while silicification and recrystallization are dominant in the marbles.

The mineralization is restricted to a zone of structural disturbance. Faults, folds, foliation planes, fractures and rarely joints act as structural controls.

The principal mineralizations are (1) quartz-stibnite veins along the marble-gneiss contacts and at the crests of the folded calc-silicate marbles, (2) quartz-pyrite-stibnite veins along the foliation planes of the gneisses, (3) quartz-pyrite veins along the foliation and fracture planes of the gneisses, and (4) quartz veins along the marble-gneiss contacts. Stibnite is the dominant ore mineral with rare cinnabar. The gangue minerals are pyrite, fine and coarse quartz, calcite and sericite. Stibnites display well developed quasi-plastic deformation textures such as kinking, pressure lamellae, microfractures and annealing, indicating at least five deformation and formation phases.

Lateral secretion and mobilization from source beds appear to explain the mode of formation. According to lateral secretion model, the quartz veins and lenses formed by infilling of fractures and dilational zones by silica and metals and sulphur derived from immediate wall rocks. According to source bed model, stibnite and other minerals are remobilized from syngenetically deposited sulphides within the lower parts of the Gümüşler Formation into structurally controlled places. The role of the Üçkapılı Granodiorite is to provide heat for circulation of the fluids to leach metals from source beds.

GEOCHEMICAL DISCRIMINATION AND PETROGENESIS OF BASALTIC SEQUENCES IN THE ANKARA MELANGE

P.A.FLOYD

Dept. of Geology, Keele University, Staffordshire, U.K

ABSTRACT: *Within the three major thrust-bound tectonic units of the Ankara melange (Ankara zone, Eldivan ophiolitic zone, Kiliclar zone) are numerous megaclasts of submarine basaltic lavas. The lavas are variably altered with secondary assemblages characterized by ubiquitous carbonate, smectite, chlorite, sphene, and Fe oxides; the occurrence of minor pumpellyite suggests low-grades of regional metamorphism.*

Stable incompatible element geochemistry indicates that the majority of the basalts from all three zones exhibit a range of characteristics typical of within-plate ocean islands (OIB) with progressively enriched, chondritenormalized, spidergram distributions peaking at Nb-Ta, light REE-enriched patterns (La/Yb c.10), and low Zr/Nb ratios (3-8). Alkalic basalts from the Kiliclar and Eldivan zones can be broadly distinguished on the basis of variable Zr/Nb ratios. The proportion of lavas comparable to basalts derived from mid-ocean ridges (MORB) are relative small and confined to a few isolated outcrops within all three zones.

Because of the limited and fragmented nature of most outcrops in the melange, a single sequence of basaltic lavas were sampled within the Kiliclar zone to determine the petrogenesis of a small oceanic crustal segment. Near Kiliclar village is an almost continuous sequence of submarine lavas, volcanoclastic debris flows and minor intercalations of oceanic sediments, with a stratigraphic thickness of c.500 m. All the basalts are incompatible element-enriched, alkaline aphyric and phyric OIB, vesicular, quench-textured, and often exhibit pink titanaugite and rare brown magmatic amphibole in a hypocrystalline matrix. Phyric varieties have plagioclase, plagioclase+olivine, and plagioclase+clinopyroxene phenocryst assemblages. On the basis of variable Zr/Y ratios they can be divided into three chemical groups that relate to discrete segments of the lava pile, and reflect a general increase in the degree of partial melting with stratigraphic height.

For many of the Ankara melange basalts the submarine environment is tentatively compared with the volcanically-active arches adjacent to the volcaniclastic debris-filled moats of oceanic islands.

357

MINERALOGY AND ORIGIN OF THE GIBBSITE BEARING KIZILALAN BAUXITE OCCURRENCE (KAŞ-ANTALYA-TÜRKİYE)

M.Kenan YALINIZ and M.Ender ATABEY

Department of Geological Engineering, METU, Ankara-TÜRKİYE

ABSTRACT: *The Kızılalan bauxite occurrence is sited among the Sütleğen bauxite occurrences north of Kaş-Antalya. The occurrence is lens shaped and fills the karstic depression of Upper Cretaceous limestones and unconformably overlain by Burdigalian limestones.*

The bauxite is boehmitic dominantly and gibbsite is present as secondary alumina mineral. However, it's concentration sometimes dominates over boehmite. In contrast, in some samples gibbsite is the only alumina mineral. In addition; kaolinite, hematite, anatase, and goethite are also identified in the samples.

The occurrence also contain gels in considerable amounts. Such as, boehmite, gibbsite, kaolinite gels and alumina silica gels.

The association of above mentioned minerals and gels suggest that, the Kızılalan bauxite occurrence is derived from primary complex gel of Al, Fe, Ti, and Si compounds by gel aging processes.

regarding the formation of the Afiq Canyon.

The first incision is related to the Early Oligocene times, when a submarine canyon was formed on the continental slope of that time.This hypothesis is supported by the occurrence of polymictic conglomerates with a marly pelagic matrix of Oligocene age in the boreholes of Nahal Oz 1 and Gaza 1. Chaotic conglomerates of Oligocene age occur also in the Ashdod Canyon (Buchbinder et al, 1981). These conglomerates are typically mass transported sediments on continental slopes.

The fall of the sea level during the beginning of the Messinian prior to the deposition of the Mavgiim evaporites, exposed the canyon shoulders but not necessarily the canyon floor, thus indicating a fall or sea level not necessarily greater than a few hundred meters only. During the following Messinian rise in sea level, the canyon shoulders were submerged again. Evaporites were deposited within the canyon on the floor and onlapped its shoulders (the Beeri gypsum, Gvirtzman, 1970) thus indicating deposition from a deep hypersaline sea (Cohen and Parchamovsky, 1986). After the deposition of the Mavqiim evaporites at the canyon's shoulders a subsequent drop of the Mediterranean sea level of at least 400 m exposed the canyon's floor, probably for the first time throughout its history. A subsequent development of a fluvial system deposited the conglomerates and sandstones of the Afiq Formation (Buchbinder and Sneh, 1980). A carbonate deposit at the base of Afiq Formation is a reduction product of Mavqiim sulphates.

At the begining of the Pliocene, sea level rose and the canyon and its shoulders were submerged and gradually filled by sediments of the Yafo Formation.

The sudden change in width and shape in the morphology of the Afiq canyon about 4 km east of the present shoreline and its extension as a wide and flat bottomed depression at least some 30 km offshore (Garfunkel et al., 1979); Greenfield, 1985) suggests submarine sliding. Erosion of most of the Early and Middle Miocene sequence in the Gaza 1 borehole (within the broad valley), as compared to the complete section in the Nezarim 1 borehole (on its southern shoulder), is indicated by seismic data, and confirmed by foraminiferal zonation. These data point to a possible Early -Late Miocene time for the sliding event. Late Miocene Ziqim and Mavqiim sediments paved the scar's surface.

THE AFIQ CANYON, SOUTHERN ISRAEL OLIGOCENE TO NEOGENE REPETITIVE SUBMARINE EROSION EVENTS ACROSS THE CONTINENTAL MARGINS OF THE EASTERN MEDITERRANEAN

Y.DRUCKMAN, B.BUCHBINDER, G.M.MARTINOTTI, AND R.SIMAN TOV,

Geological Survey of Israel, Jerusalem-ISRAEL

ABSTRACT: *The buried Afiq Channel is trending NW from Bear Sheva to Gaza, continuing offshore in the same direction. The canyon is entrenched in rocks of the Eocene Avedat Group, Senonian-Paleocene Mt. Scopus and Cretaceous Judea and Talme Yafe groups. Its width ranges between 2-4 km throughout its upper course and changes suddenly to about 15 km, some 4 km inland from the present Mediterranean shoreline.*

It is filled and buried by the Oligocene to Pliocene Saqiye Group. Its depth changes gradually over its upper 20 km from 250 m to 500 m and abruptly from 500 m to 1500 m over its lower 10 km.

The Afiq canyon was interpreted as a late Oligocene erosional feature (Neev, 1960). However, Gvirtzman (1970, 1978) and Gvirtzman and Buchbinder (1978) dated the incision as Middle Miocene. They have inferred two additional erosive phases, one in the early Late Miocene and one at the end of the Miocene. The first two incision phases were regarded as subareal in origin as a result of repeated uplifting of the shelf, and the last one as a result of the sea-level drop during the desiccation of the Mediterranean at the close of the Miocene.

New borehole, paleontological and seismic data led to a revised interpretation

354

moderately large semi-enclosed depocentre in the northeastern Mediterranean Sea.

Detailed interpretation of ~5000 km of seismic reflection profiles from the northeastern Mediterranean Sea showed the followings: (1) During the Pliocene-Quaternary, extension took place in the NE corner of the Mediterranean Sea by listric faulting on a decollement surface at the base of the Messinian evaporites. The former Misis-Kyrenia thrust belt may also have acted as a strike-slip fault, although its surface expression is as a horst block. The decoupling at the base of the evaporites has resulted in listric fault fans and roll-over anticlines almost orthogonal to the bounding faults. (2) The evolution of Pliocene-Pleistocene depocentres was largely controlled by the Misis-Kyrenia horst and the listric fans and associated roll-over anticlines, which shifted position through time, creating a shifting pattern of depocentres. (3) The extensional collapse of the Adana-Clicia-Iskenderun-Latakia basin complex resulted in overall retreat of the coastline in Cilicia and Latakia basins during the mid-to late Quaternary. The continental shelf subsided sufficiently rapidly to trap most sediment on the shelf. (4) Four types of depocentre are distinguished: (A) depocentre landward of the maximum paleoshorelines in which accomodation space between two transgressive surfaces that was created almost exclusively by tectonic subsidence; (B) thick sediment accumulations near paleoshorelines, particularly where a depositional sequence prograded further seaward then the underlying depositional sequence; (C) isolated depocentres in deep water controlled by halokinesis and (D) small deep water turbidite basins fed by fault-controlled channels.

353

TECTONIC EVOLUTION OF BASINS IN NORTHEASTERN MEDITERRANEAN SEA

A.E. AKSU[1], M.ERGUN[2], J.HALL[1], M.DUMAN[2], D.YAŞAR[2], T.CALON[1]

1 Department of Earth Sciences, Centre for Earth Resources Research,

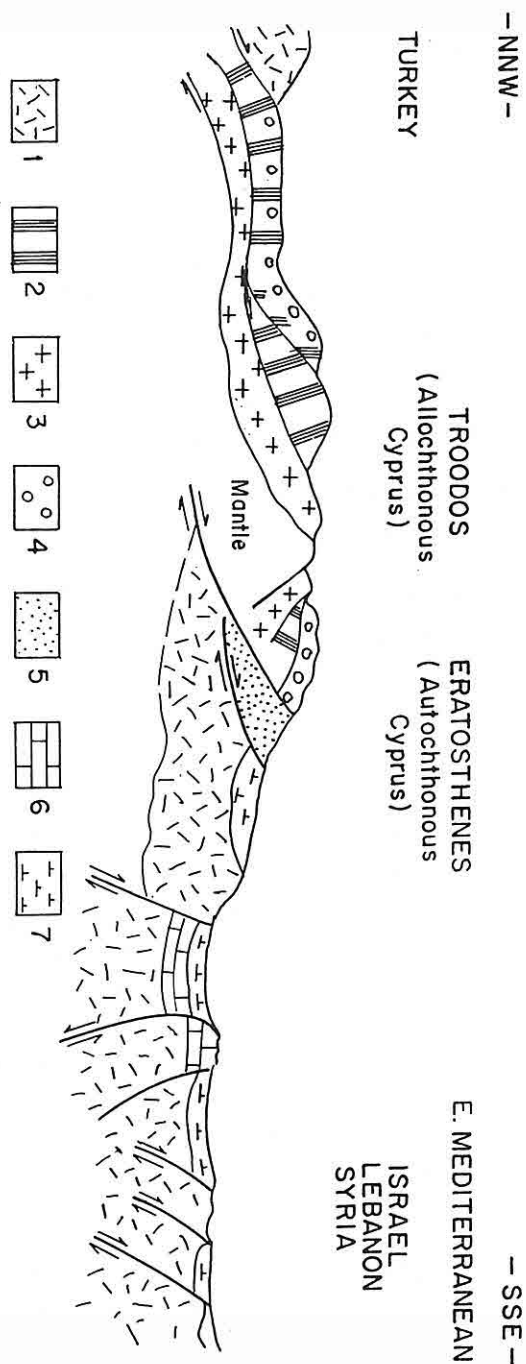*Memorial University of Newfoundland, St. John's, Newfoundland, CANADA*

2 Institute of Marine Sciences and Technology, Dokuz Eylül Univ.,

P.O.Box 478, 35211 İzmir,TÜRKİYE

ABSTRACT:*The present-day tectonic framework of the Eastern Mediterranean is controlled by the last phase of collision between the African and Eurasian plates. The Aegean/Anatolian plate is pushed westwards along strike-slip faults, due to collision between the Arabian/Syrian and Eurasian plates along the Bitlis-Zagros Suture. At its northeastern edge, the African plate is presently moving NNE relative to the Eurasian plate. The boundary between the African and the Anatolian plates is delineated by the Hellenic Arc and Pliny-Strabo Trench in the west and the Cyprus Arc and a diffuse fault systems probably associated with the Amanos Fault in the east. The two arcs are near perpendicular to the relative motion of the African and Anatolian plates, delineating the subduction zones, whereas the Pliny-Strabo Trench and East Anatolian fault zones (including the Amanos and Ecemiş Faults) are sub-parallel to the slip vector, with predominantly transform motion.*

The study area is located at the edge of the Anatolian platform, immediately southwest of the Africa/Arabia/Anatolia triple junction, and includes four genetically related basins: Adana, Cilicia, Iskenderun and Latakia Basins. These four basins collectively form a

352

FIG. 8 :

Late Cretaceous (Senonian) section of Southern Turkey, Cyprus and the Levant, showing active margin processes of subduction (African-Arabian plate), obduction and thrusting (Troodos and other ophiolites) as well as resulting fault inversions and folding of Levantinids. (1) Ancient crust, (2) sheeted dykes, (3) gabbro, (4) pillow lavas, (5) clastics, (6) carbonates, (7) pelagic sediments.
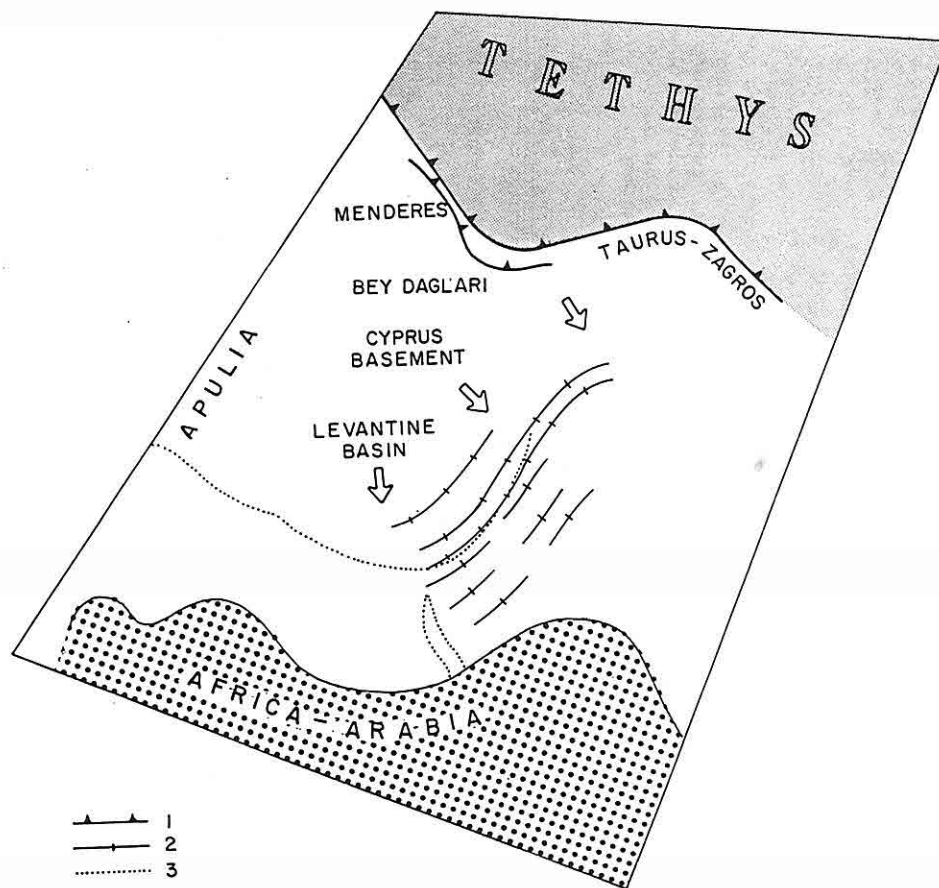
– NNW –

TURKEY

TROODOS
(Allochthonous
Cyprus)

ERATOSTHENES
(Autochthonous
Cyprus)

E. MEDITERRANEAN
ISRAEL
LEBANON
SYRIA

– SSE –

Mantle

1 2 3 4 5 6 7

FIG. 7 :
Late Cretaceous paleogeography, showing front of thrusted Neotethys-terranes, Levantinid folding (Syrian arc) and other elements of Eastern Mediterranean Apulian and African —Arabian plates. (1) thrust-front, (2) folding, (3) present shorelines.

350

PINDOS
ANTALYA
TROODOS
NEOTETHYS

IONIAN   BEY DAGLARI

LEVANT
BASIN

AKKUYU
GEVAR-AM
KIDOD

ARABIA

B

O
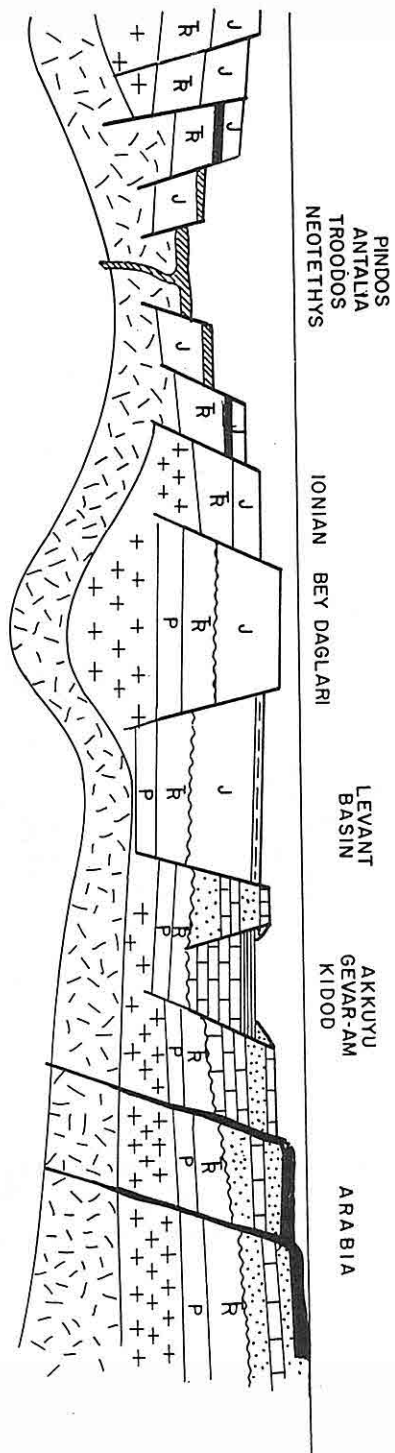
FIG. 6 :

Early Cretaceous palinspastic cross-section
showing: northern edge of Neotethys and its African-Arabian
"Eastern Mediterranean" southern edge. (O) Jurassic and Early
Cretaceous Ophiolites; (B) Basalts; (bars) oceanic and. (crossed)
continental crusts; (P) Paleozoic, (Tr) Triassic and (J) Jurassic
sediments.
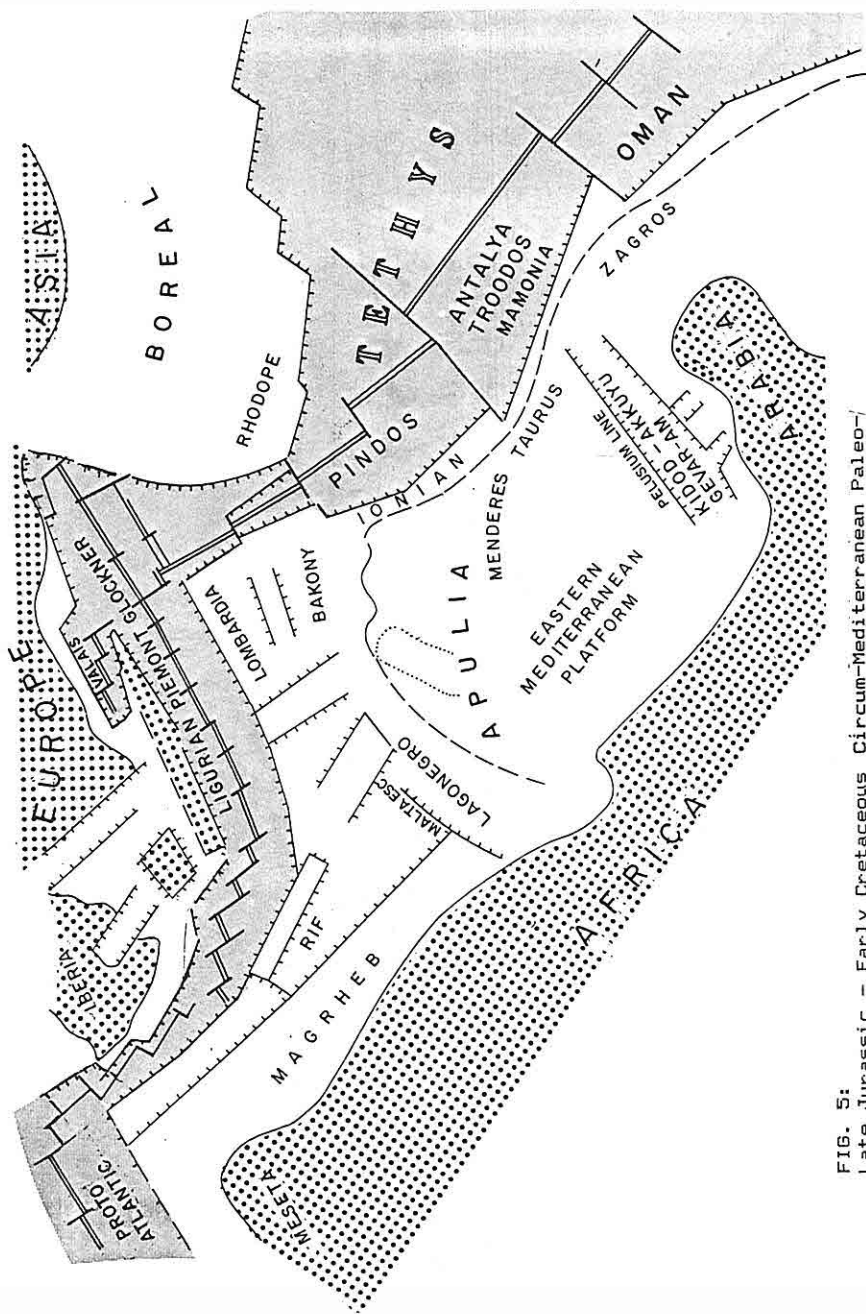
FIG. 5:
Late Jurassic - Early Cretaceous Circum-Mediterranean Paleo-
geography showing Laurasian and Gondwanian plate-elements,
separated by the prograding Tethys (and Neotethyan terranes).
The epicontinental areas are dissected/ by numerous intra-
plate graben - systems as e.g. Gevar-Am.
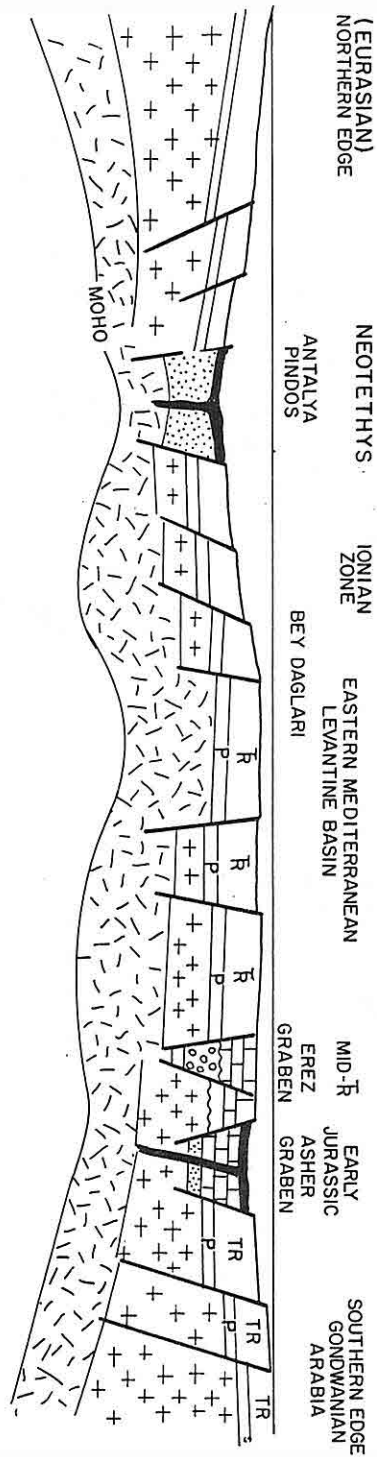(Map contours modified after FOURCADE, E. et al., 1991).

(EURASIAN) NORTHERN EDGE

NEOTETHYS

ANTALYA PINDOS

IONIAN ZONE

BEY DAGLARI

EASTERN MEDITERRANEAN LEVANTINE BASIN

MID-Tr EREZ GRABEN

EARLY JURASSIC ASHER GRABEN

SOUTHERN EDGE GONDWANIAN ARABIA

MOHO

FIG. 4:

Early Jurassic "Eastern Mediterranean" Cross-section showing oceanic (bars) and continental (crossed) crust, (P) Paleozoic and (Tr) Triassic sediments as well as Middle Triassic Erez and Early Jurassic Asher intraplate grabens (the later with basaltic volcanism).

347
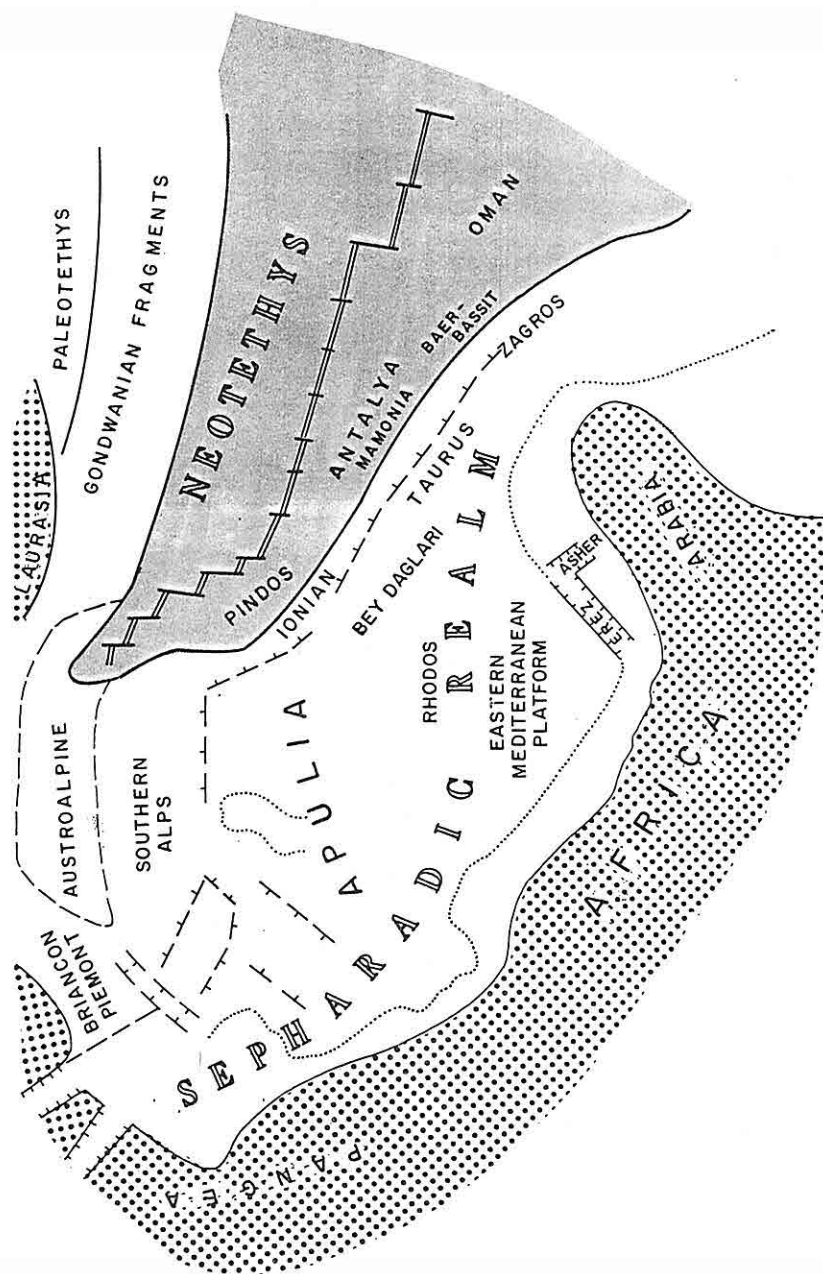
FIG. 3 :
Middle Triassic – Early Jurassic Circum-Mediterranean Paleo-
geography showing Gondwanian and Laurasian plate elements of
Pangea and opening of Neotethys.

346
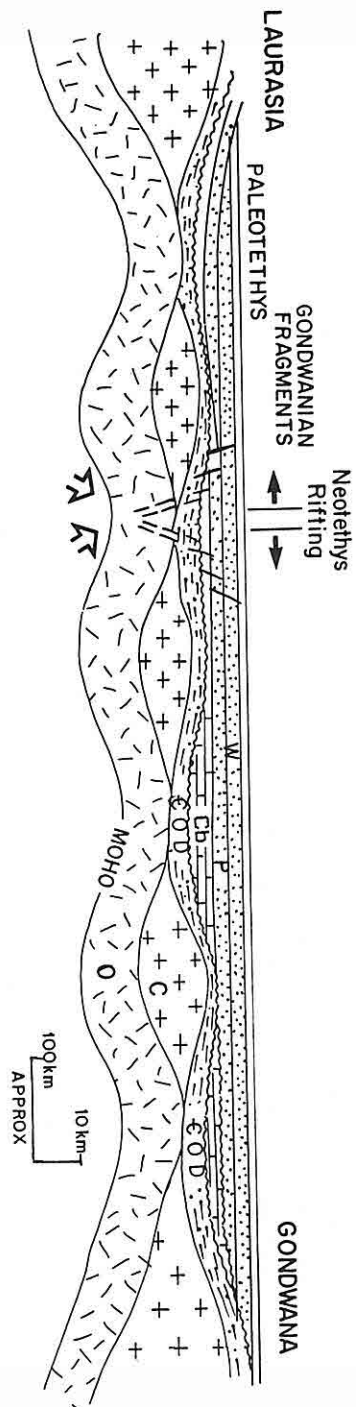
FIG 2 : Early Triassic "Eastern Mediterranean" Cross-section between Laurasia and Gondwana: (C) Continental Crust, (O) Oceanic Crust, (€ O D) Cambrian-Ordovician-Devonian, (Cb) Carboniferous, (P) Permian, (W) Early Triassic Werfen facies, as well as initial "Neotethyan" rifting.

LAURASIA

PALEOTETHYS

GONDWANIAN FRAGMENTS

Neotethys Rifting

GONDWANA

MOHO

100 km APPROX

10 km

344
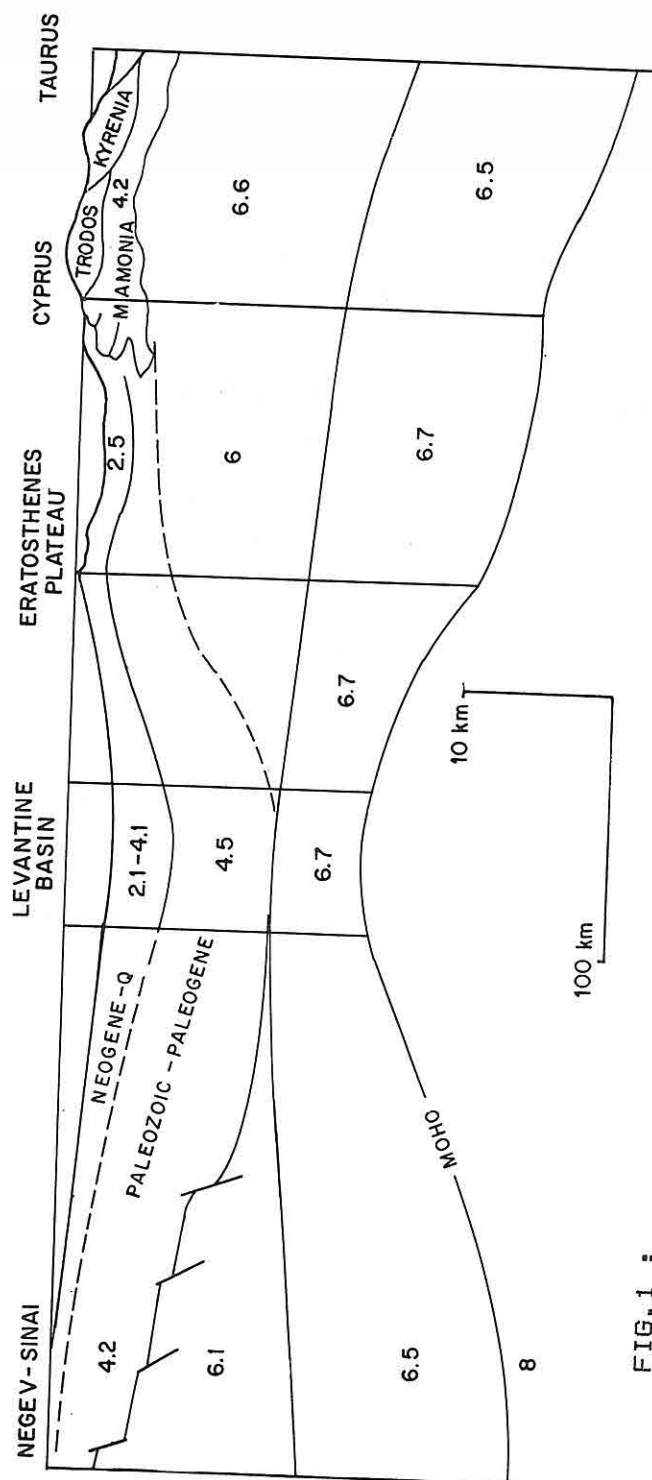
FIG.1 :
Cross-section through the actual Eastern Mediterranean
showing the velocities of the crust (km/sec) from the Levantine
plate to Turkey (after SAGE, L. & LETOUZEY,J., 1990 and BEN-
AVRAHAM, Z. & GINZBURG, A., 1990, modified).

3. Geophysical: Seismic refraction measurements of the present Eastern Mediterranean and Levant crust show a thick sedimentary succession (13-14 km), that most possibly includes Paleozoic-Cenozoic strata. Depths to the Moho and thicknesses of "upper" and "lower" crusts are of continental to semicontinental nature and their distribution "ignores" actual configuration of land and sea.

The present study suggests that, during Mesozoic times, the area of the actual Eastern Mediterranean Sea was part of the African-Apulian-Arabian plate, with a history (Figs. 1-8) of a passive margin: Middle Triassic rifting (Erez), Early Jurassic rifting, blockfaulting and volcanism (Asher, Mishhor-Cayir), Late Jurassic blockfaulting (Kidod-Akkuyu), Early Cretaceous rifting and volcanism (Gevar Am - Akkuyu, Tayasir) and Middle Cretaceous volcanism (Carmel), whereas rifting, spreading, oceanization and subduction of the Neotethys arching, took place north of the Taurid platform-edge. It turned into a more active continental margin during Late Cretaceous-Paleogene Levantinid (Syrian Arc) folding and rotation, that accompanied the Alpidic thrusting and obduction, long before Neogene subduction of the Eastern Mediterranean plate.

We therefore suggest, on the basis of a broad geological view, that the Levant Basin is mostly paved by continental crust with possibly embedded old Infracambrian ocean-crust relics. This agrees well with the seismic refraction measurements and explains its enormous thick sedimentary cover.

THE EASTERN MEDITERRANEAN MESOZOIC HISTORY: TO WHAT EXTENT WAS IT OCEANIC AND HOW PASSIVE ITS MARGIN?

F. HIRSCH[1] , A. FLEXER[2] and A. ROSENFELD[1]

[1]The Geological Survey of Israel, 30 Malkhei Yisrael Street, 95501 Jerusalem, Israel
[2]Dept.of Geophysics and Planetary Sciences, Sackler, Faculty of Exact Sciences, Tel Aviv University, 69978, Tel Aviv, Israel

ABSTRACT: *Nature and tectonic setting of the Levant Basin (Eastern Mediterranean) still puzzle the scientific community. Is it built of oceanic crust (Makris et al., 1983; Ben Avraham, 1989; Ben Avraham & Ginzburg, 1990) or of continental crust (Woodside, 1977; Malovitskiy, 1982) ? If oceanic, why does it reach 8-10 km thickness instead of the consistent 5-6 km of typical oceanic crust? Why were so far no magnetic anomalies detected and no tripartite oceanic crust of gabbro, sheeted dykes and pillow lavas found?*

These questions are analyzed from three points of view:

1. Stratigraphical and Palaeogeographical: The Palaeozoic-Mesozoic stratigraphic column and the palaeogeography of its biota suggest a fair continuous unity of epicontinental African, Apulian and Arabian areas from the Early Triassic opening to the Late Cretaceous closure of Neotethys. (Monod, 1977; Hirsch, 1976, 1988; Enay, 1976; Masse, 1985; Philip, 1985; Cariou et al., 1985; Damotte and Babinot, 1985; Marcoux, 1978).

2. Tectonical: Field observations fit best within a palinspastic model of one single Tethys ocean, north of the African-Apulian-Arabian paleo-edge, from which ophiolite-bearing thrusts originated, resting now on parts of the Gondwanian plate. (Laubscher and Bernouilli, 1977; Ricou et al., 1984; Whitechurch et al., 1984; Michard et al., 1984).

EVOLUTION AND STRUCTURE OF THE ANAXIMANDER SEAMOUNT

M.ERGÜN, E. ÖZEL, M.AVCI and D. YAŞAR

Dokuz Eylül Univ., Inst. of Marine Sci. and Tech. P.O. Box 478, 35211 İzmir-TÜRKİYE

ABSTRACT:*There are several prominent bathymetric features exist in the eastern Mediterranean in addition to Cyprus. One of them is the large seamount, the Anaximander Seamount, which is associated with gravity anomalies, suggests that it might also be a microcontinental fragment. During the Maastrichtian, Cyprus began to break away from Türkiye. As the result of this break up, the Antalya and Adana basins were formed. In the Paleocene the Anaximander and Eratosthenes Seamounts collided with the Cyprean arc. This collision is still going on at present determined from the distribution of earthquake epicentres in the region.*

The objective of this paper is to give some insight information about this very interesting feature as well as its relation with the Antalya Basin and the Cyprus Arch. A detailed neotectonic survey was carried out in June 1991 with the Russian research vessel Gelincik in the context of the UNESCO/TREDMAR project. The four mountains in the complex were imaged with OKEAN long range side scan sonar, and profiled at a line spacing of about 15 km by high resolution seismic techniques and gravity and magnetic observations.

The Anaximander Seamount is characterised by block faulting and very pronounced and active vertical uplift with the Messinian reflector intermittently detectable. Structures and their trends indicate influences both from the northeast-southwest transpressive regime along the Mediterranean Ridge southwest of Crete and from an assumed northeast-southwest compression across the Florence Rise. The concomitant subsidence and tilting of the sediments toward the north and south margins of the E-W trending Finike Basin which is at the north of the Anaximander Seamount, is attributed to extensional block faulting. The western peaks comprise large folded strata tilted to the northwest. The eastern peaks show more northeasterly tilting. Faulting appears to lie between the different peaks. The age, provenance, and evolution of the deformed and tectonically-active sedimentary rocks comprising these structures will be facilitated with the new data.

341

SULUCADERE (BOLKARDAĞ) POLYMETALIC OCCURRENCES

Mehmet YILDIRIM

MTA Bölge Müdürlüğü-Adana-TÜRKİYE

ABSTRACT: *Sulucadere polymetalic outcrops discovered by MTA during large scale prospecting project at Bolkardağ region.*

Sulucadere is a small valley on the west flank of Bolkardağ. Polymetalic mineralization crops out on this flank along the contact zone in between Bolkardağ marble and the ophiolitic melange.

Nearly 2000 m long and 50 m wide contact zone are completely deformed and occuring breccias are silisified and carbonitized by the hydrothermal activities. The hydothermal activities are derived from the Horoz Granite batholith which is very near to the zone. The aphophises of it crops out along the contact zone near Sulucadere valley.

Mineralization of contact zone are due to late cristalization and hydrothermal phases of granite intrusion. Molybdanite and chalcopyrite minerals are concentrated in quartz-porphyry veins, but these minerals are mobilised later by means of hydrothermal activities and redeposited at the fissure lines with minerals such as sphalarite, galena, stibnite, chalcopyrite, pyrite and the others within the contact zone.

THE PALEOCEANOGRAPHIC REGIME OF UPPER CRETACEOUS ORGANIC-RICH CARBONATE AND PHOSPHORITE SEQUENCES IN ISRAEL

Ahuva ALMOGI-LABIN[1], Amos BEIN[1] and Eytan SASS[2]

[1] Geological Survey of Israel, Jerusalem -ISRAEL

[2] Department of Geology, The Hebrew University, Jerusalem-ISRAEL

ABSTRACT: Upper Cretaceous rocks which include chalks, phosphorites, organic-rich carbonates, cherts, pocrelanites and marls, are widely distributed throughout Israel and the neighboring countries. The unique diverse lithology of this sequence reflects the combination of three major events, namely, the worldwide intensive Late Cretaceous transgression, the Syrian Arc folding system and the enhancement in productivity along the southern margins of the Tethys.

In the southern and eastern parts of the country a threefold lithostratigraphic subdivision is commonly accepted: Upper Coniacian to Early Campanian chalks; Middle to Upper Campanian cherts, phosphorites, organic-rich carbonates and Maastrichtian organic-rich carbonates and marls. Toward the northern and western parts of the country, this threefold division disappears and the entire sequence is dominated by organic-rich carbonates. Deposition in the southeastern parts of the country occurred in tectonically-controlled northeast-trending shallow shelf basins. Toward the northwest deposition took place in somewhat deeper water in the outer shelf and slope environments.

Paleontological, sedimentological and geochemical criteria are used to characterize the paleoceanographic conditions which have prevailed in Upper Cretaceous sequences in Israel. The investigated region was influenced by a continuous highly productive upwelling system. The proximity of each area to the upwelling core controlled the rate of primary productivity and consequently the type of sediment which accumulated underneath (cherts and porcelanites vs. organic-rich carbonates). The overall oxygen depleted bottom water, between near anoxic to dysaerobic, controlled the type of the accumulated sediment only to a certain degree: porcelanites, cherts, phosphorites and some of the organic-rich carbonates were deposited in near anoxic bottom water conditions while some other organic-rich carbonates were associated with somewhat better bottom aeration conditions.

339

Les Ophiolities de Pozantı-Karsantı, (Unité 2), sont génétiquement différentes des Ophiolites de l'alignement méridional de la Méditerranée Orientale, (Vourinos, Troodos, Baër-Bassit.), alors que le magmatisme de l'Unité 3 est fort comparable à celui de ces dernières.

REFERENCES

Bebien, J., 1980, *Magmatismes Basiques Dits "Orogéniques" et "Anorogéniques" et Tencurs en TiO$_2$: les Associations "Isotitanées" et "Anisotitanées".* Journ. Volcanology and Geothermal Res. Vol.8. pp 337-342.

Bingöl, A. F., 1978, *Pétrologie du Massif de Pozantı-Karsantı (Taurus Cilicien-Turquie). Etude de la Partie Orientale, Thèse de Spécialeté.* Univ. Strasbourg, 277 p..

Çakır, U., 1978, *Pétrologie du Massif de Pozantı-Karsantı (Taurus Cilicien-Turquie). Etude de la Partie Centrale. Thèse de Doctorat d'Ingénieur.* Univ. Strasbourg, 251 p.

Çataklı, A. Ş., 1983, *Assemblage Ophiolitique et Roches Associées de la Partie Occidentale du Massif de Pozantı-Karsantı (Taurus Cilicien-Turquie). Thèse de Doctorat d'Etat,* Univ. Nancy I, 760 p+annexes.

Çataklı, A. Ş., 1984, *Volcanisme ophiolitique du Massif de Pozantı-Karsantı (Turquie).* Ofioliti Suppl. Vol.9, "Ophiolities Through Time", p.17.

Çataklı, A. Ş., 1992-1993, *Kaersutites et Oxykaersutites: Proposition d'un Diagramme Discriminant.* Eur. J. Mineral. (sous presse).

trachytes en passant par des basaltes alcalins et des laves intermédiaires (hawaites-mugéarites).

Le magmatisme alcalin de cette série corresponderait bien à celui des séries "anorogéniques" et non "orogéniques" définies par Bébien (1980), comme le confirme le chimisme des clinopyroxènes (Çataklı, 1983) et celui des kaersutites (Çataklı, 1993 sous presse).

Ainsi, les formations magmatiques de cette série sont très probablement mises en place dans un système de "rifting" intracontinental précédant une océanisation, amorcée par une expansion océanique après la déchirure continentale.

Sur la pétrogénèse de l'Unité 2 :

-Les Tectonites sont toujours de nature harzburgitique.

-Les Cumulats sont de nature dunitique, pyroxénolitique et gabbroique. Les gabbronorites et les ferrogabbros caractérisent la zone gabbroique. La présence d'unités cycliques et l'absence d'une évolution cryptique confirment que pendant la cristallisation de ces cumulats il y a eu plusieurs injections succesives du magma.

-La série volcanique, découverte pour la première fois dans le Taurus en Méditerranée Orientale (Çataklı, 1983), comprend des coulées de pillows–lavas de nature basaltique vitreuse et sphérolitique avec ou sans olivine. Ces basaltes montrent des caractères tholéiitiques à olivine de type dorsale océanique.

Ces laves basaltiques démembrées du reste de cet assemblage ophiolitique, lui sont apparentées génétiquement (Çataklı, 1983; 1984).

Sur la pétrogénèse de l'Unité 3 :

Les dykes de dolérites-diabases isolés de direction générale parallèle à celle du massif (NE-SW), sont de deux types :

-Type I: dolérites-diabases quartziques issues d'un magma basaltique tholéiitique à quartz, produit par la fusion partielle de matériaux mafiques hydratés à des pressions et profondeurs relativement faibles.

-Type II : dolérites-diabases non quartziques issues d'un magma basaltique tholéiitique à olivine, produit par la fusion partielle de même materiaux mais à des pressions assez élevées et à des profondeurs relativement grandes.

Ces deux magmas, (Th. à Ol et Th. à Qz), appartiennent à un environnement géodynamique identiqu de type "arc insulaire"; par conséquent ne présentent aucun lien de parenté avec le volcanisme ophiolitique de l'Unité 2 (Çataklı, 1983).

Les deux types de dykes, recoupant les formations de l'Unité 2 et les formations métamorphiques, sont totalement absents dans l'Unité 1. Par conséquent leur injection est probablement antérieure au charriage général sur la marge continentale arabo-africaine.

337

LE MASSIF DE POZANTI - KARSANTI
(Taurus Cilicien - Turquie)

Ahmet Şevket ÇATAKLI

Laboratorie de Pétrologie, Université de Nancy I
B.P. 239 - 54506 Vandoeuvre-lès-Nanacy Cédex

ABSTRACT: *Le Massif de Pozantı-Karsantı, étudié par Bingöl ,1978, Çakır ,1978, et Çataklı ,1983, est situé à 100 km au nord de la Plaine d'Adana dans le Taurus Cilicien. Il comprend un assemblage ophiolitique d'âge supposé Crétacé moyen à supérieur et des formations non ophiolitiques, telles que la série volcanique et sédimentaire triasique supérieur et l'ensemble des dykes de dolérites-diabases, isolés d'âge Crétacé supérieur. Ce massif est charrié sur les calcaires de plate-forme de la Chaîne des Taurus, qui servent d'autochtone relatif.*

Nous avons mis en évidence la présence de trois unités dont l'association constitue ce que l'on appelle le massif de Pozantı-Karsantı (Çataklı, 1983). Ce sont dans l'ordre chronologique:

UNITE 1 : "anté ophiolitique", comprenant la série volcanique et sédimentaire d'âge triasique supérieur dont le volcanisme appartient à une souche magmatique alcaline. Elle est attribuée à un environnement de type "rift intracontinental en voie d'océanisation".

UNITE 2 : "ophiolitique", comprenant l'assemblage ophiolitique composé d'un ensemble plutonique (tectonites et cumulats), d'une association filonienne peu développée et d'une série volcanique tholéiitique à olivine de type dorsale océanique.

UNITE 3 : "post ophiolitique", comprenant l'ensemble des dykes de dolérites-diabases isolés. Leur magmatisme de caractère tholéiitique (à Olivine et à Quartz), est attribué à un environnement d'arc insulaire immature.

Sur la pétrogénèse de l'Unité 1 :

Cette série comprend d'une part des formations volcanique (coulées de laves massives ou en coussins) et bréchiques, d'autre part des formations sédimentaires détritiques voire pélagiques. Leur volcanisme appartient à une lignée magmatique de caractère alcalin, différenciée dans la suite sous-saturée et sodique allant des ankaramites jusqu'aux

336

RECENT ADVANCES IN PETROLEUM EXPLORATION IN THE CENTRAL PALMYRID MOUNTAINS, SYRIA.

D.C. BLANCHARD, B.G.WOOD, S.G. SMITH, J.H. COCKINGS, S.N. DAHER, J.C. LAUGHRY, B.M. ARNOLD, B.J. RUSSELL, G.M. WOOD, H. DEMBICKI, L.E. MAXWELL, R.E. POLLOCK, M. MOUTY AND Z.R. BEYDOUN.

Marathon Oil company, Marathon, Houston,Texas-USA

ABSTRACT: *Recent exploration drilling campaigns during the past 4 years in the central Palmyrids between the Syrian cities of Homs and Tudmor (Palmyra) have produced several hydrocarbon discoveries in Triassic and Jurassic carbonate reservoirs and have greatly advanced understanding of the geology in this area. Prior to the current campaign, the relationship between source, seal, migration and structure was poorly constrained. Reprocessing of vintage seismic and gravity data, acquisition of new data and computer manipulation of these data has produced a startling reappraisal of structural relationships Pre- and Post Mid-Triassic evaporitic deposition. Understanding of source distribution and potential migration paths have likewise been re-evaluated. Considerable effort in regional stratigraphic correlations has resulted in an enhanced appreciation for Tethyan depositional regimes.*

There is optimism that the application of these advances in relating source, seal, migration and structure will result in continued exploration success in this region of Syria.

with both sedimentary and structural contacts with the Andırın carbonates, or, less often, with serpentinites. The sedimentary contacts typically show a gradation from "basement" through a breccia sheath into a Paleogene mud-matrix breccia and finally to calcilutites. The panel sediments range from Eocene to late Oligocene in age and include both hemipelagic and mass flow strata. Although the Andırın complex has been interpreted as an "olistostrome" it bears a closer resemblance to massively extended units in regions of crustal extension. Clearly deformation occurred before, during, and after mixing of the Paleogene strata into the complex, all at moderate water depth. In many aspects the Andırın complex resembles extensional "chaos" deposits of the U.S. basin and range province. This similarity is strengthened by structural relationships in the northeastern part of the Misis-Andırın block where the Andırın complex with its Paleogen panels overlies massive Malatya metamorphic rocks. Although the contact between Andırın and Malatya rocks was not seen, the two units appear to be stratigraphic correlatives, suggesting large scale horizontal displacement along the contact.

Another zone of possible extension involving Andırın complex rocks lies north of the Engizek (Bitlis) fault zone. Not only is the Andırın complex in this area structurally mixed with Paleogene sediments, but it is also separated from the underlying Malatya Rocks by a zone of strong shearing. Because this shearing was observed early in our survey, before the possibilty of massive extension was entertained, no data was collected that would have confirmed this zone as an extensional decollement, nor was the direction of motion determined. It is possible that a single direction of stretching existed throughout the region, before the development of the early Miocene basins that defined the Neogene triple junction. If the Andırın complex is a result of regional crustal extension, it would have been in a widespread marine environment, as may now be occurring in the northern Aegean Sea.

MID-TERTIARY REGIONAL EXTENSION IN THE MARAŞ AREA

Daniel E. KARIG

Department of Geological Sciences Cornell University, Ithaca, N.Y. - U.S.A.

ABSTRACT: *The history of the Anatolian-Arabian plate collision, between the late Cretaceous closure of Neotethys and the present phase of transpression, is complex and poorly understood. There clearly has not been continuous convergence near the present Ar-An-Af triple junction, and there is reasonable evidence for regional extension from sometime in the Paleogene into the mid Miocene. Because the evidence for extension is not yet widely recognized, and the resultant tectonic implications remain speculative, this talk is intended primarily to challenge orthodox perspectives and to promote interest in the problem.*

The easiest example of regional extension to document is the series of N to NW trending, early to mid Miocene half-graben in the Misis-Andırın block, well exposed west of Maraş. These basins are developed on a sub-strate of Andırın complex rocks and are probably related to transtension along the Aslantaş fault zone. The fault margin of the best-studied of these basins is associated with steep flexuring of the older strata and very high-angle unconformities within basinal strata. The basin fill is bimodal, consisting of hemipelagic calcilutites and much coarser mass flow deposits. These basins appear to have been local depocenters in a generally marine region and were fed from local highs of Andırın complex rocks.

The Andırın complex itself is also suspected to have been created by Paleogene extension. The complex consists of a intimately shattered sequence of late Paleozoic-Mesozoic carbonates, as well as late Cretaceous ophiolitic components and Paleogene sediments. The Paleogene strata occur in steeply dipping but coherent panels,

333

feature variations on lateral. According to the basement surface bedding character there were separated 4 blocks divided by transverse faults. Central blocks are elevated. The largest accumulation of weak earthquakes epicenters are concentrated within their blocks.

High-precision gravimagnetic survey was conducted by the reference network with single profile passage having two gravimeters. The survey was conducted along four profiles within the range of 120 km, step between the reference points was from 1000 to 2000 m, step between the ordinary points was 100 m. As a result of the above mentioned data there were related Khorasan gravitational maximum of North-West-South-East strike. Lateral parts of maximum is characterized by gradients of 5-6 Mgal/km. It shows the presence of fault zones. This feature is also traced in the character of magnetic and geotermal fields and it is confirmed by the seismological observation results.

The unique geophysical data on the Earth's crust structure of Norman-Khorasan earthquakers obtained for the first time can be the basis of the further investigation. This information is required for revealing Earth's crust structure feature relations with high seismisity and geodynamic activity of region. It is recommended to continue these works, to enlarge their areas, to organize geophysical monitoring of strained state of medium in connection with erthquake predictions.

GEOPHYSICAL INVESTIGATIONS OF EARTH'S CRUST OF NORMAN-KHORASAN EARTHQUAKES FOCUS ZONE

M.M.RADZHABOV[1], R.J.SUDZHADRINOV[1], S.G.MAMEDOV[1] and S.P.AGAMIRZOEV[2]

[1]*Institute of Goeophysics, Baku-AZERBAIJAN*

[2]*Geoseism", Baku-AZERBAIJAN*

ABSTRACT: *The Earth's crust of Norman-Khorasan earthquakes focus zone was studied by complex geophysical methods. Seismological observations were carried out by apparatus "Cherepacha". Seismological observations included local seismicity analysis and Earth's crust section construction by alternating wave method of distant earthquakes. Field works were conducted by profile-areal system in continuous recording regime. During the observations there were recorded more than 300 local earthquakes and 234 distant earthquakers identified according to Obninsk bulletine. According to the local earthquake data there were determined parameters of hypocenters and energetic characteristic values. There was suggested velocity model of Earth's crust of earthquakes focus zone according to the distant earthquake data there were conducted time sections and deep sections. There were separated 10 boundaries related to the sedimentary strata, basement surface and its internal structure as well as Moho boundary.*

Time field features show separateness of medium, presence of faults and boundary

331

RECENT TECTONIC EVENTS IN THE SİVAS BASIN (SİVAS AREA) TÜRKİYE

H.GÜRSOY[1], H.TEMİZ[1] and A.M. POISSON[2]

[1]*Cumhuriyet Univ., Geology Department, 58140 Sivas-TÜRKİYE*

[2]*Univ. Paris Sud, Geol. Structurale Unite CNRS 1369 91405 Orsay FRANCE*

ABSTRACT:*During Cenozoic times the Anatolia area as a whole was submitted to a N-S tectonic shortening in response to the N-S convergence of the Eurasian and Arabo-African plates. This convergence was repturted to have provoked a westward escape of the Anatolian block located in between the Nort and East Anatolian Faults. In spite of many local arguments (and focal mechanisims), in favour of this westward motion the total amount of displacement does not seen very important. A N-S shortening which produced many thrusts and folds, and a related crust thickening, seems to be the main effect of the collisional processes.*

In this general context the Sivas basin is located in the central E-W Anatolian depression and is bordered by the Pontic and Taurus belts . Since Late Cretaceous-Paleocene times it was the site of an active sedimentation accompanied by a more or less important subsidence (depending the period). During the same period the basin was submitted (and has registered) the global regional tectonic events.

Many important tectonic features resulted from this tectonic activity the most spectacular of which being flat or high angle thrust faults such as the Sivas fault (north of the city) which affect Pliocene deposits. The recent deposits of the Kızılırmak river around Sivas are cut by many faults. These deposits are represented by conglomerates, sands and silty clays which have been observed in several terraces at different altitudes from the river level up to aproximately 50 m above the present day alluvial plain. These faults are mainly tension faults striking in variable direction. The corresponding extensional directions vary but two main directions have been observed N030 and N120 and a subordinate N170-180 other direction. This variability can not be explained in a simple model of extension but has to be replaced in the general context of N-S convergence and shortening and could be a local superficial accommodation of more deep seated flat thrust faults.

THE KARAKAYA COMPLEX, NW TURKEY: A PALAEOTETHYAN ACCRETIONARY COMPLEX?

E.A. PICKETT, A.H.F. ROBERTSON and J. E. DIXON

Dept. of Geology and Geophysics, Grant Institute, Univ. of Edinburgh, UK

ABSTRACT: *The Permo-Triassic Karakaya Complex is a low-grade metamorphic assemblage of deformed deep-sea sediments and volcanics. It is part of the suture system of northern Turkey which formed by closure of the Palaeozoic Tethyan ocean, the Palaeotethys. The role of the Karakaya Complex in Palaeotethyan evolution is poorly understood but is critical to the testing of alternative models. Current work focuses on the Biga Peninsula in NW Turkey. Here, the Karakaya Complex is composed of tectonostratigraphic units which may be interpreted in terms of oceanic subduction and accretion. One unit comprises spilitized basalts showing within-plate geochemistry. It also contains volcanoclastics and limestone blocks, features suggestive of a seamount origin. A basalt-chert-sandstone association forms an adjacent unit. Pillow lava of E-MORB/IAT type is overlain by radiolarian chert and a coarsening-upward turbidite succession in a possible trench sequence. The Karakaya units were deformed by imbricate thrusting, folding and intense shearing, characteristic subduction-accretion processes. Upper Triassic sediments lying unconformably on the Karakaya Complex may represent fore-arc basin deposits. They are capped by a Jurassic carbonate platform (Bilecik Limestone), laid down after the cessation of Palaeotethyan accretionary tectonics in this area. In conclusion, the studied Karakaya Complex can be reinterpreted as part of an accretionary complex formed at a long-lived active margin, as seen in W USA and SW Japan.*

329

DEEP STRUCTURE AND TECTONIC DEVELOPMENT FEATURES OF EAST PART OF MEDITERRANEAN SEGMENT OF BALKAN-PAMIR FOLDED BELT

Kerim M.KERIMOV[1], Rauf J.SUDZADINOV[1], M.M. ZEINALOV[1],
ROBERT B. TALLYN[2], DAVID KENT[2], OLEG RODKIN[2] and
HENRY M. LIBERMAN[2]

[1]Institute of geophysics, Baku-AZERBAIJAN

[2]UNOCAL, USA

ABSTRACT: *The considered part of Mediterranean segment of Balkan-Pamir folded belt is located approximately in co-ordinates of 22 and 51 of North latitute and 24 and 69 of East longitude. It is characterized by complex geological-tectonical structure and history development. It is naturally reflected both in all geodynamic situation and in common regularities of distribution and location of mineral deposits in the region. First of all, the talk is about cover thickness of main boundaries of Earth's crust divisions, its physical state and region block structure features on the different hypsometrical and stratigraphic levels. The solution of many practical and theoretical problems of tectonic oil and gas-bearing region and also prediction of all the geodynamic processes occuring in it to a great extent depends on the exact interpretation of these factors. The report considers all these problems on the basis of new geological-geophysical material analyses and aerocosmic investigation data from two main tectonic conception standpoints.*

It is shown that network of regional dislocations with the breaks in continuity in the region including the largest areal distribution has the various genetic base and its origin is related to the platform displacement in horizontal direction of Earth's crust blocks and their vertical movements. The role of vertical movements noticeably increases in the sedimentary cover. It increases in particular in its subsurface part. The character of the various landslide phenomena and varities of seismological processes to a great extent depend on the activity of horizontal and vertical movements of Earth's crust blocks.

The mineralogical composition of all sediments in this basin was determined by x-ray diffraction. There are two dominating facies: carbonaceous and magmatic. Dolomit is the main mineral in the carbonaceous layers and the calcite content is low. Surprising was the occurrence of pure magnesit (> 99% $MgCO_3$), partially in layers up to one meter thick. Heulandt and Philipsit were found in the volcanic tuffs.

There are three thick sequences of bituminous material, separated by persistent, interclast horizons up to several meters thick. The economic-grade oil shale averages 12.8 m thick, it is persistent and is distributed over a relatively wide area. The upper calorific value is 813 kcal/kg (dry) and the oil content 5.5 % (dry or 60 l/t oil).

The reserves of the economic grade oil is 1.058 million t. This result shows that the area of Beypazarı ranks as the largest oil shale deposit in Turkey known to date. From these reserves, however, only 60 million t are minable by open cast mining.

Organic material is present mainly in fine layers with very sharp boundaries. Continuous horizons with prebitumina (parts of sporomorphs) are widespread in the area. The layers contain an intimate mixture of organic and inorganic material showing a rapid growth and sedimentation rate. No fossils were found besides small silicified organisms.

A number of tectonic events during the genesis of the basin rocks formed special basins, big deltas, changes in water level, etc. Tephra and tuffs were deposited during volcanic eruptions of the Teke volcano. An unusual oil shale was formed as a result.

Zeolites were formed from volcanic glass; surplus silicate formed opal. At a very early stage calcite changed to dolomite due to increasing Mg/Ca ratio during evaporation. Magnesium ions originated from ultrabasic rocks of the basement. Reduced water flow, increasing salinity and dehydratation finally led to magnesite.

In contrast to the Green River oil shales, the Beypazarı oil shales contain trona seams $Na_3H(CO_3)_2 \cdot 2 H_2O$ between the bituminous sequences. In general, oil shale represents a transgressive phase and evaporites a regressive phase. Therefore, we can distinguish several cycles.

OIL SHALE, TECTONICS AND VOLCANISM-AN UNUSUAL GENESIS IN WEST ANATOLIA/TURKEY

H.H.SCHMITZ

Federal Institute For Geosciences and Natural Resources

ABSTRACT: *Turkey, except in eastern Anatolia. As an energy resource oil shales could be important in the future for local use. The Miocene occurrence near Beypazarı, 100 km NW of Ankara, has an unusual geological genesis. It is in the central part of a 1500 km² Neogen basin. Strong volcanism-accompanied sedimentation changed the relief considerably. While the bottom of the basin sunk, the marginal rims were elevated. The closed basin filled with fluviatil, lacustrine, and igneous material. Lignite formed in quiet tectonic times. Sodium carbonate minerals precipitated in smaller basins around the main one. Several seams are more than 30 m thick. The sodium source is mainly volcanic tuff in which the sodium-bearing silicates were weathered under the influence of carbonic acid, also of magmatic origin. Only in the U.S.A. larger sodium deposits are known.*

The oil shale was folded by post Miocene tectonics. The northern part of the basin was elevated. It is now about 150 m above the plain, the oil shale crops out the entire length of the basin.

A permanent change in environmental conditions led to a great variety of bituminous, carbonaceous, and magmatic. About 1,200 m of core samples give an overview of sedimentation.

northeast of the Town of Diyarbakır. All of these faults form a geometry similar to the system of strike-slip faults formed as a result of strains created by a rigid indenter during and after a continent-continent collision (cf. Tapponnier et al., 1982; Ratschbacher et al., 1991). Many of these fault zones including the East Anatolian and the Bozova fault zones, show evidence of Late Miocene to Pliocene movement and are probably still active. The Late Miocene to Pliocene initiation age of the indentation tectonics has been also confirmed by the radiometric ages of the basalt samples in the western part of southeast Anatolia where basaltiç rocks produced as fissure eruptions along the faults have yielded radiometric age determinations (K/Ar) of 10 to 5 Ma old.

It has been long proposed that the extensional tectonics in western Anatolia is caused by the Miocene collision in southeastern Anatolia. Our recent field observations along the Koçhisar fault zone of Central Anatolia suggest to us that this fault is probably the easternmost fault zone effected by the westerly escape of the Turkish plate. The main evidence for this is the lithology of the Miocene Kochisar Formation which is well exposed on the northeastern block of the Kochisar fault zone. The formation shows a fining upward sequence and several lateral facies changes. We interpret this formation as deposited due to oblique-slip normal movement along the Kochisar fault zone which is caused by the westward movement of the Turkish plate.

INDENTATION TECTONICS IN SOUTHEASTERN ANATOLIA AND ITS EFFECT IN CENTRAL ANATOLIA.

İbrahim ÇEMEN[1], M.Cemal GÖNCÜOĞLU[2], Hüseyin KOZLU[3], Doğan PERİNÇEK[4] and Kadir DİRİK[2]

1 School of Geology, Oklahoma State Univ. Stillwater, Oklahoma, U.S.A.

2 Dept. of Geological Engineering, Middle East Technical Univ., Ankara, Turkey.

3 Turkish Petroleum corp. An kara, TÜRKİYE

4 9 Sunhill Rd., Mt. Waverly, Vic. AUSTRALIA.

ABSTRACT:*The Miocene to present continent-continent collision between the Arabian and Eurasian Plates produced the present form of the southeastern Anatolian fold and thrust belt. This collision also resulted in the westward escape of the Turkish plate which is bounded by the North Anatolian fault to the north and the East Anatolian fault to the southeast (Şengör and Yılmaz 1981; Şengör and others 1985).*

Recent geological mapping in southeastern Anatolia suggests the presence of several southeasterly trending strike-slip fault zones which are the Mutki, Şemdinli and Hakkari fault zones. These fault zones and the East Anatolian fault zone truncate the southeast Anatolian fold and thrust belt with an acute angle. In the forelands of the fold and thrust belt, there are two prominent strike slip fault sets. The first set is the northeasterly trending faults which include the faults of the eastern margin of the Hatay Graben, the Adıyaman fault, and the Lice fault. The second set is the northwesterly trending faults which include the Bozova fault, the Kalecik fault and the unnamed faults

characterizing an evaporitic lacustrine basin comprise "gypsum-bearing green clay" member, "sepiolite-dolomite" member (Dacian) and "silicified limestone" member, together with "red mudstone-conglomerate" member having the characteristics of a braided fluviatile environment, showing lateral gradation into the former.

The sepiolite-dolomite member, on which our research work has been concentrated is the product of an alkaline lake which was rather extensive and shallow, fed by seasonal discharge and reflecting arid climatic conditions. Within this member a rough mineralogical zonation as illite, smectite, palygorskite, palygorskite sepiolite, sepiolite and magnesite, from the margins to the centre. At the periods when the lake greatly or wholly dried up, insufficient fresh water discharge through channels constituted small bounded lakes of the playa type. These swamps gave rise to the formation of sepiolite lenses with varying thickness, which may be considered as sub-facies.

Bioturbation root marks, gas exit structures, flow marks and mud cracks are common within the sepiolite lenses.

Sepiolite has formed by direct precipitation in this environment with a pH around 8-8.5 from the Mg^{2+} enriched waters. It may occur as filling the vacancies between the detrital sepiolite and dolomite material, that has previously formed or as pure laminar sepiolite. In addition, late diagenetic occurrences within the cavities formed by drying or gas exit structures may also be observed.

Pure sepiolite lenses may contain organic material, generally not exceeding 8 %. Some of the lenses may exhibit a distribution of clay minerals such as palygorskite+ sepiolite-sepiolite from the margins to the centre. Moreover, vertical and lateral gradation into dolomite may occasionally be observed.

LITHOFACIAL FEATURES OF THE UPPER SAKARYA SECTION OF CENTRAL ANATOLIAN NEOGENE BASIN (SİVRİHİSAR-GÜNYÜZÜ-ÇELTİK) AND THE SEPIOLITE OCCURENCES

Hakan GENÇOĞLU, Taner İRKEÇ, Nusret GÜNGÖR, Mahmut
DEMİRHAN and Semih ÇOKYAMAN

Gen. Dir. Min. Res. Expl.(MTA). Ankara-TÜRKİYE

ABSTRACT: *Evolution of the Central Anatolian Basin, which employs an important rank within the Neotectonics of Turkey, exhibit remarkable variations. Upper Sakarya Section of the basin, on the other hand, is particularly very significant, considered the sepiolite occurences. In order to carry out precise evaluations on the formation, stratigraphic setting, sedimentologic and mineralogic features of the economic sepiolite deposits, which occur as lenses in a very wide area, this section of the basin has been given priority in the basinal research work.*

Neogene sequence of the area is represented by İlyaspaşa Formation, which characterizes the final drying stage of the tectonically controlled Miocene lake, whose basal relations cannot be observed due to overburden. This formation with frequent synsedimentary faults crop out with well stratified limestones, bearing fresh water algae horizons, and progress with alternations of claystone-siltstone sandstone tuffite silica and siliceous limestone. The sequence ends with thick gypsum deposits, which overlie the former and show lateral gradation. Conglomeratic lenses showing the characteristics of braided fluviatile intra-channel deposition are widely distributed throughout the formation. Sakarya Formation, which has been assigned to Pliocene according to its fossil content, overlies the former by angular unconformity. This formation

322

METALLOGENIC DEVELOPMENT OF THE RHODOPES, BULGARIA

Bogdana MANEVA

Research Institute for Mineral Deposits, Sofia-BULGARIA

ABSTRACT: *The Rhodopes are one of the most important metallogenic units within the Mediterranean Alpine belt. Their metallogenic development is in close relationship with the geodynamic and tectonic processes and at present is considered corresponding to the newest ideas about Mid-Mesozoic collage of the Rhodope microplate.*

Two main periods of geodynamic and metallogenic evolution of the Rhodopes can be distinguished: accretion and postaccretion.

The accretion period (up to K2) occurred along the sutures of the actually determined four collage integral terranes. During that period syngenetic, synmetamorphic and synmigmatic deposits of siderophile (Cr, Fe, Ni, Mg) and lithophile (Li, Be) elements were formed.

The postaccretion period (K2 - Ng) is a transcollage, affecting the Rhodope unit as a whole. On the basis of the different geodynamic conditions it has been divided into several stages: subduction (K2); blocking with transversal shearing (P1); collision (P2); and quaziplatform (Ng-Q). The metallogeny of the separate stages is characterized as follows: K2 -by skarn and high-hydrothermal deposits of a wide metallogenic spectrum (Fe, Cu, Pb, Ag, Au, Mo, W), related to anatectic intrusions and layer boundaries in the crust; P1- by lithophile specialization (Mo, U, F, P) of the mineralizations, related to deep drained fluids and transcurrent faults; P2 - by base-metallic vein and metasomatic type of deposits of industrial significance and nonmetalliferous ones, associated to volcanic sources and rocks and controled by a fault network; Ng-Q - by supergenic, alluvial occurrences and placers of Fe, Mn, Mg, Au and sedimental bedded bodies of clays and diatomites. A tendency of the increase of the metallogenic activity eastwards throughout the whole period, has been established.

METALLOGENIC CHARACTERISTICS OF AZERBAIJAN AND ADJACENT COUNTRIES

G.V.MUSTAFAEV

Geological Institute of Azerbaijan Academy of Sciences, Baku, AZERBAIJAN.

ABSTRACT: *Geological structure of Azerbaijan, Turkey and Iran have a great deal in common in as much as they are part of the Alpine folding system. Tectonic structures are traced in adjacent countries and are characterized by wide spread of the Mesozoic-Cenozoic magmatism of calc-alkali and subalkaline type. In this case with granitoid intrusives in these regions are associated the skarn deposits of iron, veined polymetalls, copper-porphyritic mineralization etc., with the Miocene volcanism-mercury deposits, probably, antimonite; with ultrabasite complex-chromium, nickel, gold deposits. Similarity of geology and metallogeny of the countries mentioned at the same time sets a number of common tasks for them. Thus, for example, in Azerbaijan granitoid intrusives are subdivided by isotopic methods in age mere in details therefore, further study on granitoid geochronology of adjacent countries is also necessary, as different age granitoids of Azerbaijan have different geochemical specialization.*

Another example is the occurrence of commercial stratiform deposits of copper, plumbum, zinc of the copper-pyrrhotite and pyrite-polymetallic formations in black shale strata of the Greater Caucasus Southern slope within Azerbaijan. Search for stratiform deposits in Turkey and Iran can be of a great practical interest. At the same time there are strontium deposits in Turkey and Iran, strontium-bearing (deposits) basins are found. In Azerbaijan, however, the strontium deposits were not found and practically they were not concerned with their search.

Working out of searching criterion for gold, silver and different rare and ore metals is of a great importance for Azerbaijan, Turkey and Iran. Therefore, co-ordination of specialists efforts of these countries, practical exchange of experience as well as joint researches can be very efficient.

320

THE ECONOMIC EVALUATION OF GREEN MARBLES OF BÜKRÜCE (DENİZLİ)

Remzi KARAGÜZEL, Mahmut MUTLUTÜRK and Yaşar KİBİCİ

Akdeniz Univ., Isparta Eng., Fac. Geology Dept., 32001, Isparta-TÜRKİYE

ABSTRACT: *The marbles outcroped in the Karahallı (Uşak), Bükrüce (Denizli) region are light to dark green-grey in colour according to dark coloured mineral paragenesis. This mineral paragenesis controls the physical-mechanical and petrographical properties of the marbles. Piedmontit and pistacite are dominant minerals at light green marbles whereas hornblende and actinolite are dominant minerals at dark green marbles.*

The green coloured marbles exposed in the investigated area have great demand from overseas and have economical importance. In the Bükrüce (Denizli) region the petrographical physical and mechanical properties are determined and the correlection between there are searched on the outcroped marbles, approximately 7 km square. The prepared maps from these properties show the changes of colour, mineral, physical and mechanical features and the discontiniuty positions. The economicly and technologically operatable sites are determined, by the evaluation of these map which connected to each other but giving different properties. In the determined open git locations, the block dimensions are investigated and the operational models which will give optimum efficiency are prepared, by making discontiniuty analysis.

319

SLOPE STABILITY OF THE NAMRUN AREA

Altay ACAR[1,2], Tolga ÇAN[1], and Aziz ERTUNÇ[1]

1, Dept. of Geology, Çukurova Univ., Adana, TÜRKİYE
2Dept. of Earth Science , Leeds Univ., Leeds LS2 9JT , ENGLAND (Present Address)

ABSTRACT: *Sixteen slopes, in Namrun town located 50 km north of Mersin, were examined to identify problems of slope stability, instability and associated mass movement process of slope failure in the region. A quantitative assessment of the stability of a slope was, therefore, judged for the design of an engineering structure, such as a two storey building.*

Tertiary aged units are exposed in the area under investigation, which are Gildirli formation comprising conglomerate, generally sandstone, carbonate-cemented sandstone, siltstone, and mudstone, Kaplankaya formation comprising gravelly sandstone, sandstone and sandy-clayey carbonate, sandy-silty limestone, and Karaisalı formation comprising reef limestone. The overlying unit included by the research consists mainly of talus.

The method applied here depends upon terrain classification, weather conditions at time of field inspection and failure, annual rainfall records, vegetation cover and type on slopes, influence of groundwater, remedial works, structure on or adjacent to slopes, materials, evidences of instabililty, and geometry of slopes.

In the current study a case history is presented, where a slope failure took place along a shear plane, and the material is described as sandy clay.

ENGINEERING GEOLOGICAL INVESTIGATION AND REDESIGN OF TWO ROAD CUT SLIPS IN NEOGENE MARL IN WESTERN TURKEY

A.ABDULAZIZ[1], AKTAN, E., M.Y. KOCA[2], and N.TÜRK[2]

1 DeLEUW Cather-Kutlutaş, JV, Bornova, İZMİR

2 D.E.U., Geol. Eng. Dept., Bornova, İZMİR

ABSTRACT: *İzmir Ring Road forms a major part of the İzmir-Aydın Motorway presently under construction in western Turkey. The ring road passes through Neogene marl, limestone and colluvium. Two major slides have occurred between Km. 212+100 and Km. 212+500 of the ring road during the excavation of slopes.*

The initial road cut slopes were designed at an inclination of 2H:1V using moderately reduced peak shear strength parameters obtained from laboratory testing of the intact marl samples recovered from boreholes drilled in the area and assuming low water levels in the slope stability analyses.

The post slip investigation has shown that the failures had taken place along preexisting slip planes. It also determined the geometry of the slides, the position of the groundwater levels and slaking properties of the marl.

Back analyses of the slips have given shear strength parameters equivalent to the residual values. Cut slopes were redesigned using these more realistic values. Thus, the slope angles of the road cuts were flattened to 3.75H:1V and remedial measures applied, including subsurface drainage to increase the stability of the cut slopes. These cut slopes have been performing satisfactorily for over a year, after being redesigned.

In this paper, details of the site investigation studies, stability analyses, and redesign scheme suggested for the slips in section 2.4 of the İzmir Ring Road will be presented.

317

LITHOSTRATIGRAPHIC AND PALEOGEOGRAPHIC EVOLUTION OF SYRIA DURING THE JURASSIC

Mikhail MOUTY

Dept. of Geology,Damascus-SYRIA

ABSTRACT: *The lithostratigraphic studies reveal that the carbonaceous Jurassic sediments in Syria and the adjacent areas dominated by dolostone, limestone and limited marly intercalations, have been precipitated in a shallow sea, which, since the Jurassic onset, has transgressed the entire region with the exception of a NE-SW elongated uplift in the east and southeast of Syria (Al Hammad Uplift).*

The correlation of the geologic sections performed evidence, that since the end of the Lower Jurassic, this uplift has further extended.

At the end of the Middle Jurassic the sea regressed northwestwards, where an important subsiding structure oriented NNE-SSW took shape (Homs-Lebanon trough), in which the thickness of the Jurassic sediments is in excess of 1000 m.

By the end of the Upper Jurassic the sea further regressed from the last submerged areas. Consequently, the entire Syrian territorie remained emerged until the Cretaceous transgression initiated in the Barremian-Aptian time.

appear to be syntectonic katazonal granites intruding into and growing on and replacing the micaschist concordantly. In the syntectonic granites augen, nebulitic, blastomylonitic and ribbon textures are common. In this area, it is clearly observed that the augen gneisses can not be core complexes but rather they are younger than the micaschists upon which they were grown as migmatitic granites. Toward the gneisses, metamorphic grade increases in the micaschists and close to the boundary staurolite-kyanite- sillimanite assemblages appear. The increase in the temperature gradient was related to the emplacement of the granites.

The third area examined is between Kocarlı and Bafa Lake. Around Bafa Lake the gneisses appear to be true granites and the boundary is clearly intrusive. Just along the contact a zone of garnet-fels is present with a thickness of 10-100 m. The gneissic granites cut the micaschists and enclose marble lenses that were previously lenses within the schists. In the western shore of the lake the granites intrudes further up in the succession nearly touching just 50 m below the lower part of the Mesozoic marble succession.

In all these three regions, large and small-scale features all indicate that the gneisses are syntectonic granites intruding various stratigraphic levels of the micaschists, which was called as envelope of the massif. So that, the gneisses can not be the Precambrian in age but rather syntectonic granites emplaced in the period of the main Menderes metamorphism, that is known as the Late Cretaceous-Eqrly Eocene in age.

PROBLEM OF CORE-MANTLE BOUNDARY OF MENDERES MASSIF

Burhan ERDOĞAN

Dokuz Eylül Univ., Geology Department , İzmir / TÜRKİYE

ABSTRACT:*In previous studies, stratigraphy of the Menderes Massif has been defined to compose a core complex of the Precambrian and a mantle association of the Paleozoic and Mesozoic ages. The core complexes are represented by augen gneisses and the envelope association by Paleozoic micaschists and Mesozoic platform-type marbles. Between the core and mantle, an angular unconformity has been considered but, although extensive open outcrops present, in nowhere this boundary has been defined unquestionably.*

In this study three regions where the main core complexes crop out, are studied and the mantle-core boundary has been examined. The first region is the Selçuk-Bayındır-Ödemiş area, in which the Menderes metamorphics form a large- scale anticline with one of the thickest stratigraphic section. The centre of the anticline consists of micaschists of more than 3 km thickness overlain by emery - bearing platformal marbles. No gneissic core complexes are present in the stratigraphically and structurally lowermost part of the succession, but along the flank of the anticline seams of gneissic rocks start to appear around Bayındır. Toward Ödemiş gneissic rocks become dominant and they are found to grow over the micaschists. The boundary relations indicate that the gneissic rocks intruded into the micaschists and replaced and cut these rocks.

The Akhisar region is the second area studied, where a marble succession is underlain by very thick micashists. Toward the Demirköprü Dam, the micaschists form a large anticline a d along the eastern flank of which gneisses crop out. The boundary between the gneisses and micaschists show all kinds of gradation and the gneisses

314

ABOUT THE GEOLOGY OF THE NUR MOUNTAIN RANGE (NMR)

İlyas YILMAZER[1] and Cavit DEMİRKOL[2].

[1]*Dar Müh.Müşavirlik A.Ş. Adana-TÜRKİYE*

[2]*Çukurova Univ., Geology Department, 01330 Balcalı /Adana-TÜRKİYE*

ABSTRACT: *A 55 km long stretch of the Tarsus-Adana-Gaziantep Motorway (TAGM) is being constructed across the Nur Mountain Range (NMR) between the towns Düziçi-Bahçe-Kömürler Sakçagöz. Stratigraphy and structural geology of approximately 15 km wide area along the TAGM and route of a proposed railway, has been studied in detail.*

A suit of medium grade schist, phyllite and slate (Dhm) constitutes an essential part of the NMR. The following units occur in order from east to west: Recrystallized dolomitic limestone (Dhl), serpentinite (Kbs) as a well preserved component of the ophiolitic melange (Kb), approximately 350 m thick conglomerate/siltstone alternation (Kk), deformed spilitic basalts (Kp) and limestone blocks, slabs and bedchunks (Kp) belonging to border zone of the ophiolitic melange, and Upper Miocene aged shallow marine facies (Mib) . Recrystallized dolomitic limestone- silicified dolomitic limestone (Dhl), serpentinite (Kbs), and peridotite (Kbp) crop out eastward. Further east, tan alternation of the Upper Eocene aged unit (Es) comprising basically limestone, siltstone, calcareous mudstone, calcilutite, and calcarenite crops out.

The NMR trends in the direction of NEN-SWS along the eastern coast of the Mediterranean Sea. It constitutes the northern middle portion of a 100 km long chain of mountains (Amonos), which is bounded by a sinistral lineament and the Çukurova basin on eastern and western sides respectively. The neotectonic frame of the region has been influenced mainly by Arabian-Eurasian collision to the east. However, the mountain range has formed under NW-SE compressional regime which prevailed during the Upper Cretaceous time. Thrust planes between rock units which are diverse in origin are distinct. Furthermore, highly dissected topography enables investigators to recognize subsurface geology. NEN-striking reverse faults, high angle thrusts, overturned-recumbent folds, drag folds, and schistosities exhibit monoclinal structures dipping basically NW. This situation likely arose from compressional forces which have acted towards the SE. The Paleozoic units and Miocene units along the border zone are severely tectonized and deformed. Therefore, numerous active and potential landslides are mainly distributed along these zones.

313

GEOLOGY OF THE ÇAMARDI (NİĞDE-TURKEY) REGION

İlkay KUŞCU, Ayhan ERLER and M.Cemal GÖNCÜOĞLU

METU, Dept. Geol. Eng., 06531 Ankara-TÜRKİYE

ABSTRACT: *The Çamardı region lies in the southern part of the Central Anatolia 68 km southeast of Niğde province. The rock units of the Çamardı region are, Paleozoic-Mesozoic Niğde Group, Cenomanian Üçkapılı Granodiorite, Late Cretaceous-Paleocene Çamardı Formation and Early-Middle Eocene Evliyatepe Formation. The rock units of the Ulukışla Basin are included within Late Cretaceous-Late Paleocene Eskiburç Group.*

Niğde Group consists of (1) the Gümüşler Formation composed of sillimanite-biotite-muscovite gneisses with lenses of white marbles and calc-silicate marbles, and (2) the Aşıgediği Formation characterized by thick bedded marbles intercalated with amphibolites and followed upward by cherty marbles. The Aşıgediği Formation overlies the Gümüşler Formation with a pre-metamorphism unconformity. The Üçkapılı Granodiorite intrudes the Niğde Group and crops out as patches crossed by pegmatite dykes. Narrow zones of contact metamorphism are observed along its contacts with the Aşıgediği Formation. Çamardı Formation consits of conglomerates and sandstones derived from the Niğde Group. The Evliyatepe Formation unconformably overlies the Çamardı Formation and includes conglomerates and alternations of sandstones, siltstones and silty limestones.

The Eskiburç Group consists of (1) Ovacık Formation characterized by flysch-like sequences and chaotic mixture of volcanic and volcano-sedimentary rocks, and (2) Ulukışla Formation with volcano-sedimentary and volcanic rocks. Alluvial deposits cover the older rock units.

Foliation and schistosity are the distinct structures for the gneisses of the Gümüşler Formation with N55-65E and N75-85E as significant trends. Small and large scale overturned folds are observed within metamorphic and sedimentary rocks. Joints as single and rarely conjugate sets are commonly observed in intensely folded metamorphic rocks and occasionally in the sedimentary rocks. The significant faults in the region are the Üçkapılı Normal Fault trending N30-35W and the Celaller Thrust Fault. The rock units of the Niğde Region are thrusted over the Eskiburç Group along the Celaller Thrust Fault.

the Kırankaya formation is conformably underlain by the flysch deposits of the Ulupınar formation and is conformably overlain by the dolomitic limestones of the Zorbehan formation. The Zorbehan formation deposited within a shallow to lagoon environment is Upper Maastrichtian in age and the top most geological unit of the Upper Cretaceous sequences. In addition to these formations, the volcanics and volcanosedimenter deposits cutting the almost all Upper Cretaceous succession to the Kırankaya formation's deposits are named as the Deveci formation and relatively aged to be Maastrichtian. The volcanosedimets of the formation is separated as the Çanakpınar member.

In the region, Tertiary and Upper Cretaceous sequences have an unconformable relationship. The conglomerates, gypsiferous conglomerates and clayey limestones of the Nadartepe formation occurs at the bottom of the Tertiary sequences. It is conformably overlain by the gypsum deposits of the Hüyük formation. Eocene aged the limestones of the Asartepe formation deposited within a very shallow sea environment is unconformably (?) underlain by the gypsums and is conformably overlain by the clayey limestones of the Yenice formation. The Miocene aged limestones of the Tahtalıtepe formation covers unconformably the Paleogene succession. In addition to these formations, the Plio-Quaternary aged the Ayrancıdağı volcanics cut and overlie the other geological units. The volcanosedimentary deposits within the formation is named as the Otolar member. The youngest deposits in the area are alluviums.

STRATIGRAPHY OF THE HEKİMHAN AND SURROUNDING AREAS (NW MALATYA)

Muhittin GÖRMÜŞ

Akdeniz Univ., Isparta Eng.Fac., Geology Dept., Isparta-TÜRKİYE

ABSTRACT: *The investigation includes the stratigraphy of the Hekimhan and surrounding areas located at 70 km northwest of the Malatya city, Türkiye. In the area, the Güvenç Complex occurs at the basement of the sequences and contains ultrabasic, volcanic and sedimentary rocks. The volcanics and the deep sea sediments are separated as the Karakısıksırtı volcanic member and the Kızılceviztepe member of the formation.*

The Upper Cretaceous sequences unconformably overlies the Güvenç Complex and they are from bottom to top as follows: the Hekimhan conglomerates, the Tohma reefs, the Ulupınar formation, the Deveci formation, the Kırankaya formation and the Zorbehan formation. Among these, the bottom sequence Hekimhan conglomerates deposited within an alluvial environment are conformably overlain by the Tohma reefs. The age of the conglomerates is thought to be Campanian?. The reefs, Upper Campanian to Middle Maastrichtian in age, are also conformably overlain by the Ulupınar formation. These two formations have lateral and vertical changes. The Ulupınar formation deposited within the various depths of sea environment from deep to shallow contains rhythmically developed conglomerates, sandstone, claystones, siltstones and clayey limestones. The age of the formation is Lower to Middle Maastrichtian and it outcrops widely in the area. The mapped conglomerates of the formation is separated as the Kızılsırtı conglomerate member. The clayey limestones of

310

PALYNOSTRATIGRAPHY OF THE COAL BEARING NEOGENE DEPOSITS IN BÜYÜK MENDERES GRABEN, WESTERN ANATOLIA

Funda AKGÜN and Erol AKYOL

Dokuz Eylül Univ., Geology Dept., 35100 Bornova, İzmir-TÜRKİYE

ABSTRACT:*The Büyük Menderes Graben is a part of the Aegean graben system in Western Anatolia. The deposition of the sediments filling Büyük Menderes Graben is controlled by approximately E-trending faults which are formed stepwise.*

In 160 samples of palynomorphs of the coal-bearing Neogene deposits, in eight localities in the Büyük Menderes graben, between Aydın-Söke and Denizli-Sarayköy, include 5 spores, 22 Angiospermae and 8 Gymnospermae taxa. This allows detailed age divisions the infull of the Graben. The precence of the two palynomorphs assemblages have been recognized by the quantitative and qualitative palynomorph contents of the samples. The first palynomorph assemblage, which is Middle Miocene in age, is recognized in Aydın-Söke, İncirliova, Şahinali, Köşk, Köşk-Başçayır, Kuloğulları and the lower coal layer of Nazilli-Hasköy. The variation of the frequencies of spores and nonarboreal pollen forms, in this assemblage indicate that Kuloğulları and Köşk-Başçayır coals are early Middle Miocene in age and the other coals are middle Middle Miocene. The second palynomorph assemblage, which is late middle Miocene-earliest Late Miocene in age, is recognized in the upper coal layer of Nazilli-Hasköy and Denizli-Sarayköy.

On the bases of the above age assignments Büyük Menderes rifting occurre as a result of extentional forces in Western Anatolia started at the begining of the Middle Miocene.

FACIES CHANGES AND NEW STRATIGRAPHICAL -PALEONTOLOGICAL DATA IN THE CRETACEOUS-TERTIARY BOUNDARY AROUND SÖBÜDAĞ (ÇÜNÜR-ISPARTA)

Muhittin GÖRMÜŞ and Erkan KARAMAN

Akdeniz Univ., Eng., Fac., Geology Dept., ISPARTA

ABSTRACT: The study area is located at the northwest of the Isparta Engineering Faculty's campus area. The investigation includes the micritic limestones of the Senirce limestone and the mudstones of the Kızılkırma formation in the Cretaceous-Tertiary boundary.The Senirce limestone is the top most geological unit of the Upper Cretaceous sequences and the Kızılkırma formation is the bottom geological unit of the Tertiary sequences in the region. Both formations indicate deep sea environments in the boundary. Some stratigraphical sections were measured and systematic samples were collected from these two formations with the aims of investigation and interpretation of the C/T boundary.

The top most unit of the Upper Cretaceous sequences is fossiliferous limestones having abundant **Globotruncana** fossils. The limestones known as the Senirce limestone includes micritic and turbiditic levels having very shallow to shallow microfauna. The upper part of the formation contain rhytmitically deposited, grey and red coloured micritic limestones. The Paleocene-Eocene aged, red coloured Kızılkırma formation overlies the Cretaceous deposits and have abundant globigerins. It starts with red coloured limestone level, continuous red coloured mudstone levels and ends with rhytmitically developed calcarenitic sandstone and mudstone levels. Sandstones are mostly composed of litic fragments, ophiolitic pebbles, benthonic foraminifera such as nummulits and calcareous cement, and increase towards the upper part of the formation.

In the boundary, the upper age limit of the Senirce limostone was found to be Upper Maastrichtian according to **Abathomphalus mayaroensis** (Bolli) and the lower age limit of the Kızılkırma formation was determined to be Montian according to Globigerina species.

Besides, the paleoenvironmental interpretations and the relationships between the formations are also presented.

GEOCHEMICAL STUDY OF CHROMITITES AND REPARTITION OF P.G.E. ELEMENTS IN THE MERSIN OPHIOLITE (SOUTHERN TÜRKİYE)

Servet YAMAN

Çukurova Univ. Geology Dept. Adana-TÜRKİYE

ABSTRACT: *Mersin ophiolite outcrops as an erosional window at the bottom of post tectonic Tertiary cover units. Ophiolites are made up of a pile of tectonic slices having harzburgites, gabbroic and pyroxenic cumulates, and pillow-lawas. They are all intersected by isolated diabase dykes. These units have a tectonic contact with a typical ophiolitic melange containing limestone blocks metamorphic slices, radiolarites and pillow-lavas.*

Tectonized harzburgites are chromiferous vein-like ore lense-like deposits that consist of disseminated, massif or schlieren ore bodies at Akarca, Yapraklı and Musalı.

The major chemical composition of chromite ores show that the repartition of major constitutes are similar to those of podiform deposits. Chromite has an average composition as $Cr_2O_3 > 49.32$ % and $Cr/Fe > 2$, total $Fe < 1.20$% constant Fe^{+2}/Mg^{+2} atomic ratio and relatively low TiO_2 % (<0.3).

The concentration of P.G.E. in massif disseminated or schlieren ores range from less than 100 pbb to few hundred ppb. The P.G.E. concentrations seem to be unrelated to any ore facies. The chondrite normalised P.G.E patterns of chromites show depletion in the P.G.E with respect to chondrite average concentrations. Os, Ir and Ru depletions are smaller than of Pt and Pd resulting in chracteristic patterns with negative slopes. These patterns may be used to indicate the ophiolitic character of the chromiferous bodies as it's a case of the chromites within the ultramafic zone of Mersin ophiolite.

ABSTRACTS

PLATE III

1

2

3

4

5

6

7

8

9
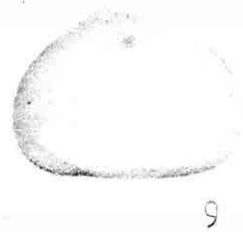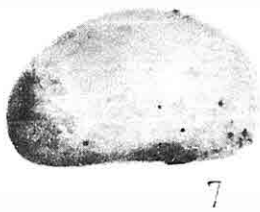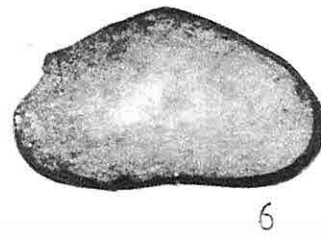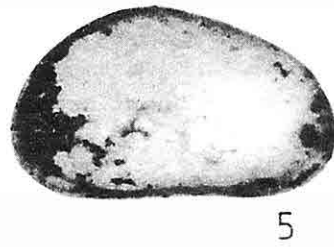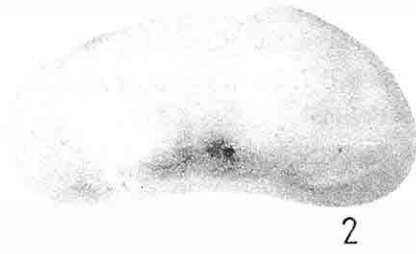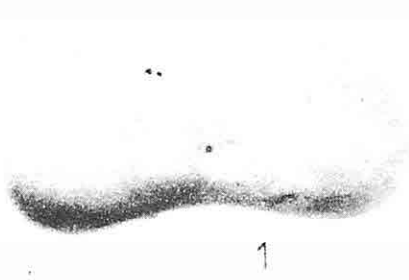
PLATE III

Figure 1-2: **Candona (Candona) altoides** Petkovski

    1 .Right valve, outer wiev, X30, Borehole P-7, Sample number 24

    2. Right valve, inner wiev, X30, Borehole P-7, Sample number 24

Figure   3: **Candona (Candona) luminosa** Bodina

    3. Left wiev of carapace, X30, Borehole P-15, Sample number 1

Figure   4: **Heterocypris salina salina** (Brady)

    4. Right wiev of carapace, ( ), X30, Borehole P-10, Sample number 14

Figure 5-6: **Eucypris dulcifons** Diebel and Pietrzenuik

    5. Right valve, outer wiev, X22, Borehole P-7, Sample number 28

    6. Left valve, outer wiev, X21, Borehole P-7, Sample number 28

Figure 7-9: **Cypridopsis** sp.

    7. Left valve, outer wiev, ( ), X24, Borehole P-3, Sample number 30

    8. Right valve, inner wiev, ( ), X30, Borehole P-13, Sample number 9

    9. Right valve, outer wiev, ( ), X30, Borehole P-13, Sample number 9

PLATE 11

1

2

4

3

5

6

8

7

302
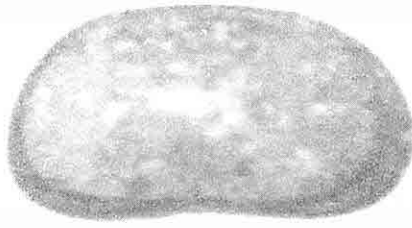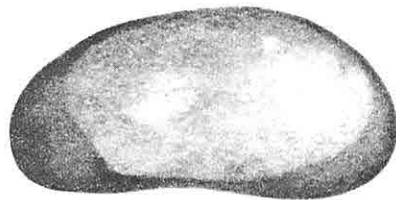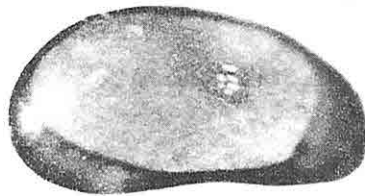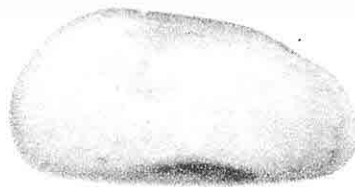
PLATE II

Figure   1: **Candona (Candona) parallela pannonica** Zalanyi
          1. Left valve, inner wiev, X90, Borehole P-3, Sample number 21
Figure 2-3: **Candona (Candona) devexa** Kaufmann
          2. Right valve, inner wiev, X30, Borehole P-3, Sample number 30
          3. Right valve, outer wiev, X30, Borehole P-3, Sample number 30
Figure 4-5: **Candona (Candona) burdurensis** Freels
          4.Right valve, inner wiev, X30, Borehole P-3, Sample number 21
          5.Right valve, outer wiev, X30, Borehole P-3, Sample number 21
Figure 6-7: **Candona (Candona) decimai** Freels
          6.Left valve, inner wiev, X24, Borehole P-3, Sample number 11
          7.Left valve, outer wiev, X25, Borehole P-3, Sample number 11
Figure   8: **Candona (Caspiocypris) alta** Zalanyi
          8.Left valve, outer wiev, X23, Borehole P-20, Sample number 28

PLATE I

1

2

3

4

5

6

7

8

10

9

300
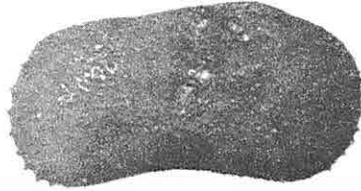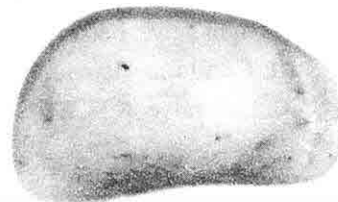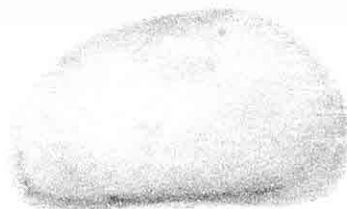
PLATE I

Figure 1-2: **Darwinula cylindrica** Straub

        1.Left valve, outer wiev, X21, Borehole P-3, Sample number 22

        2.Right valve, outer wiev, X20, Borehole P-3, Sample number 22

Figure   3: **Darwinula stevensoni** (Brady and Robertson)

        3.Left valve, outer wiev, X19, Borehole P-3, Sample 22

Figure 4-5: **Ilyocypris gibba** Ramdohr

        4.Right valve, outer wiev, X24, Borehole P-10, Sample number 24

        5.Right valve, outer wiev, X21, Borehole P-10, Sample number 16

Figure   6: **Ilyocypris bradyi** Sars

        6.Left valve, outer wiev, X24, Borehole P-15, Sample number 1

Figure   7:**Cyprideis (Cyprideis) sohni** Bassiouni

        7.Dorsal wiev of carapace, . X17, Borehole P-13, Sample number 10

Figure 8-9: **Candona (Pseudocandona) marchica elbistanensis** Freels

        8.Right valve, inner wiev, X24, Borehole P-3, Sample number 28

        9.Right valve, outer wiev, X24, Borehole P-3, Sample number 28

Figure   10: **Candona (Pseudocandona)** sp.

        10. Left valve, X27, Borehole P-10, Sample 14

5. ACKNOWLEDGEMENT

6. REFERENCES

Blumental, M. M., 1944.Kayseri ile Malatya Arasındaki Toros bölümünün Permo-Karbonifer Arazisi. M.T.A.Dergisi No. 1/31, s.105.

Demirtaşlı, E., 1967. Pınarbaşı-Sarız-Mağara İlçeleri Arasındaki Sahanın Litostratigrafi birimleri ve Petrol imkanları. Rapor No. 4389 (unpublished).

Erkan,E.N., Sümengen, M. ve Terlemez, İ., 1978. Sarız-Şarkışla-Gemerek-Tomarza Arasının Temel Jeolojisi, MTA Rap., No:5646 (Yayınlanmamış), Ankara.

Gökçen, N., 1979. Denizli-Muğla Çevresi Neojen İstifinin Stratigrafisi ve Paleontolojisi. Doçentlik Tezi, H.Ü., Ankara, 178 s.

Morkhoven,F.P.M.van, 1962. Post Paleozoic Ostracoda.Elsevier edit,1:1-244.

Morkhoven, F.P.M.van, 1963. Post Paleozoic Ostracoda, Elsevier edit,2:1-478.

Metin, S., 1984. Doğu Toroslarda Derebaşı (Develi), Armutalan ve Gedikli (Saimbeyli) Köyleri Arasının Jeolojisi, İstanbul Üniv. Müh.Fak. Yerbilimleri Dergisi, C.4, s.1-6, 45-66.

Özgül, N., Metin, S. ve Dean, W.T., 1972. Doğu Toroslarda Tufanbeyli İlçesi (Adana) Dolayının Alt Paleozoyik Stratigrafisi ve Faunası M.T.A.Dergisi Sayı. 72, s.9-17.

Özgül, N., Metin, S., Erdoğan, B., Göğer, E., Bingöl, I. ve Baydar, O., 1973. Tufanbeyli dolayının (Doğu Toroslar, Adana) Kambriyen-Tersiyer kayaları, TJK Bült.,16,82-100.

Şafak, Ü., Nazik, A. ve Şenol, M., 1992. Kayseri Güneydoğusu (Sarız) Pliyosen Ostrakod ve Gastropod Faunası, Ç.Ü.Müh-Mim.Fak. Dergisi, C.7, S.1, 171-197.

Şenol, M., Karaman, C., Ağlagül, S. and Çözeli, F., 1992. Tufanbeyli (Adana) Bölgesinin Jeolojisi ve Pliyo-Kuvaterner Zamanında Oluşmuş Toprak Materyalinin Mineralojisi, Ç.Ü.Ziraat Fak., Toprak Materyalinin Kil Sempozyumu, (in press).

Tağa, H., 1992.Tufanbeyli (adana) yöresi Pliyosen istifinin Mikropaleontolojik İncelemesi, Ç.Üniv.Jeoloji Müh.,Bitirme Ödevi, No:309, 60 s, Adana (unpublished).

Yalçınlar, İ., 1955.Structures Geologiques de la Region de Feke-Saimbeyli, İstanbul Üniversitesi Jeoloji Enst. Rev. (İnst. Ed. No.13 (1970-71) page 55-56.
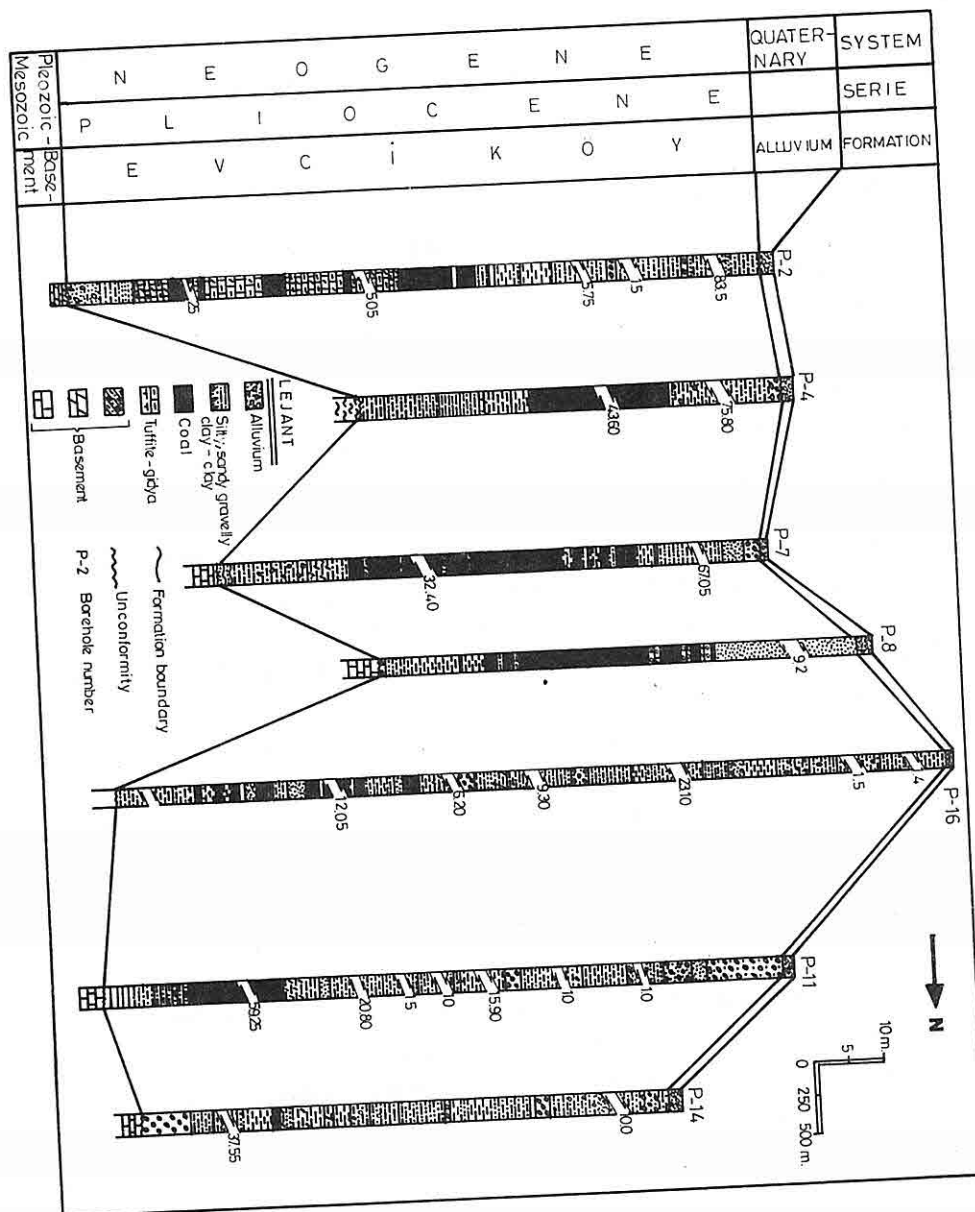
Figure 10. Borehole Correlations of Investigated Area

297

In conclusion, Pliocene formations with coal were deposited as a rapid sedimentation with a salinity of fresh-oligohaline in local small water-filled depressions in water-included terrestrial environments (Table 2),(Gökçen, 1979; Morkhoven 1962, 1963).

The Quaternary age alluviums are the youngest units in the basin, which rest upon other units unconformably.

4. CONCLUSIONS

The results obtained from the present study carried out on the Evciköy formation in the Tufanbeyli area may be summarized as follows:

a) The environment and degree salinity defined by ostracodes and the identification of gastropods, Bryozoa, and charophyte observed together in the current study show that the Evciköy formation was deposited in a terrestrial environment containing small isolated lakes, where essentially fresh water but slightly oligohaline salinity conditions prevailed.

Table 2. The degree salinity of environment identified by Ostracoda in the study.
*Percentage of salinity taken from Remane (1958) as referred in Gökçen (1979)

OSTRACODA	SALINITY*		
	FRESHWATER °/₀ 0.5-3	BRAHIK / SOMATR °/₀ 3-8 (10)	MARINE °/₀ 18-45
Cyprideis	—	—	
Heterocypris	———	—	
Darwinula	———		
Eucypris	———		
Limnocythere	———		
Ilyocypris	———		
Candona(Typhlocypris)	———	—	
Candona (Candona)	———		
Candona (Pseudocandona)	———	———	

b) Coals observed in the formation were irregularly distributed and created by physico-chemical conditions as a result of the continuous burial of the organic materials
c) The formation was deposited during the Pliocene. This age is assigned from the ostracode fauna and also from the distributions of the gastropod fauna.
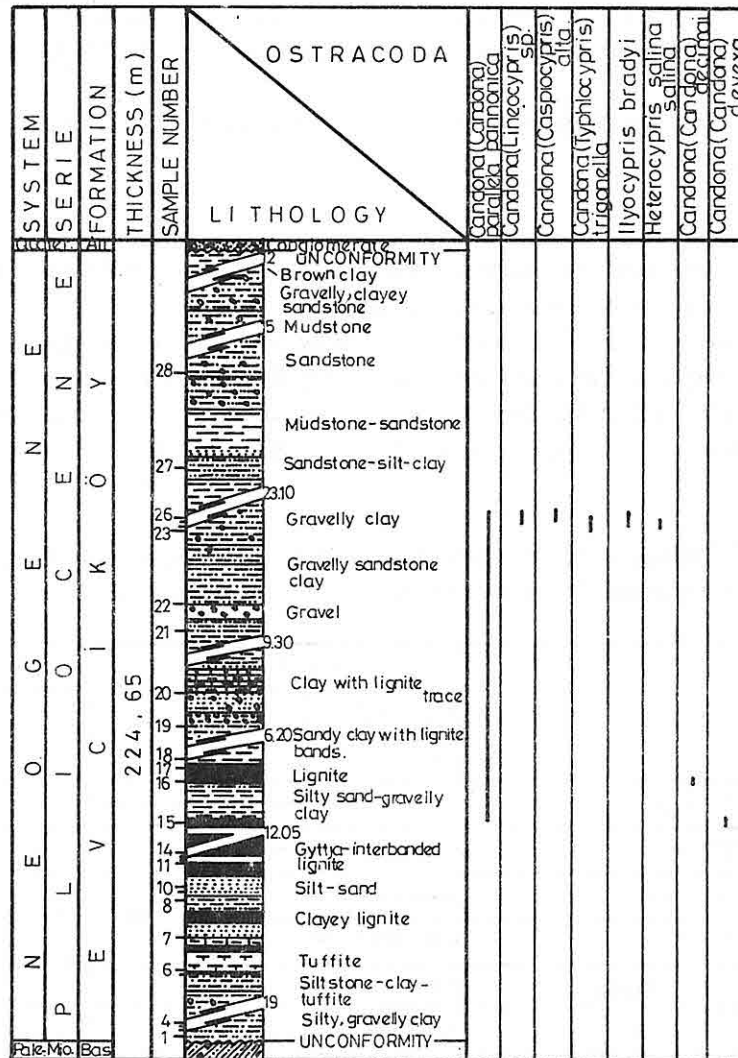
296

Figure 9. Stratigraphic Columnar Section and Ostracoda Distribution of the P-16 Borehole from Tufanbeyli-Pınarlar Location.

have abundant fossils, from south to north, are shown in Fig. 10. As a result of the borehole interpretation carried out to identify the distribution of coals and other units in the basin, which is much deeper towards north, the units, various in age, are unconformably overlain by Pliocene the Evciköy formation.

Candona (Candona) parallela pannonica Zalanyi

Candona (Candona) decimai Freels

Candona (Candona) burdurensis Freels

Ilyocypris gibba Ramdohr

Heterocypris salina salina (Brady)

Xestoleberis sp.

These zones are overlain by clay, silty clay, clayey silt, silt and gravelly units that are unsorted, and 3 m thick. The uppermost part comprises a 115 m thick brown mudstone gravel-sand succession that is overlain by a 2 m thick conglomerate.

Borehole No: P-16

This borehole is located approximately 250 m east of Veletleryaylağı Hill and the coordinates and depth are given in Table 2.

Up to 145 m, gravelly, clayey gyttja-interbanded lignite coals rest upon the units including gastropod shells in which greenish-gray shale is unconformably underlain by gravelly, clayey, silty and locally tuffite levels at the basement and a very thin bedded lignite rank was recovered at the depth of 185.05 m (Figure 9).

The results of paleontologic examination of this zone are as follows:

Candona (Candona) parallela pannonica Zalanyi

Candona (Candona) decimai Freels

Candona (Candona) devexa Kaufmann

The overlying zone is composed of a succesion of conglomerate, claystone and siltstone and includes the following fossils:

Candona (Candona) parallela pannonica Zalanyi

Candona (Typhlocypris) trigonella (Hejjas)

Heterocypris salina salina (Brady)

Ilyocypris bradyi Sars

Candona (Lineocypris) sp.

Candona (Caspiocypris) alta (Zalanyi)

The uppermost part consists of alluvial materials, approximately one meter in thickness.

3. BOREHOLE CORRELATIONS

The correlations between P-2, P-3, P-7, P-8, P-16, P-11 and P-14 boreholes, which

294

This zone is overlain by clay, clay-silt and abundant carbonates, gravelly clay up to 155 m, and the overlying unit is a thin-bedded coal. **Candona (Candona) parallela pannonica** Zalanyi are observed in this zone.

From this level to the upper level at 143 m, plant trace-bearing abundant carbonates, lignite-painled clay, gravelly siltstone-sondstone and gravelly silt. The results of paleontologic examination are as follows;
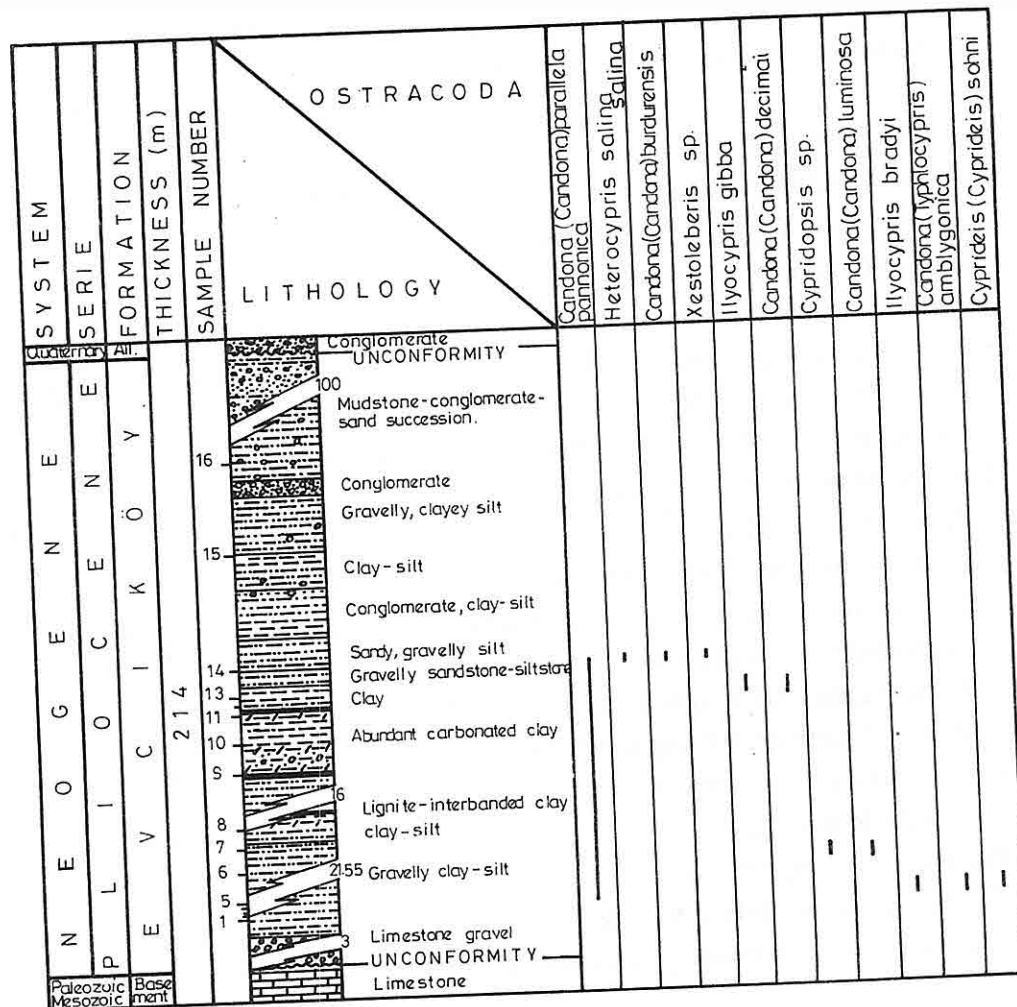

Figure 8. Stratigraphic Columnar Section and Ostracoda Distribution of the P-14 Borehole from Tufanbeyli-Pınarlar Location.
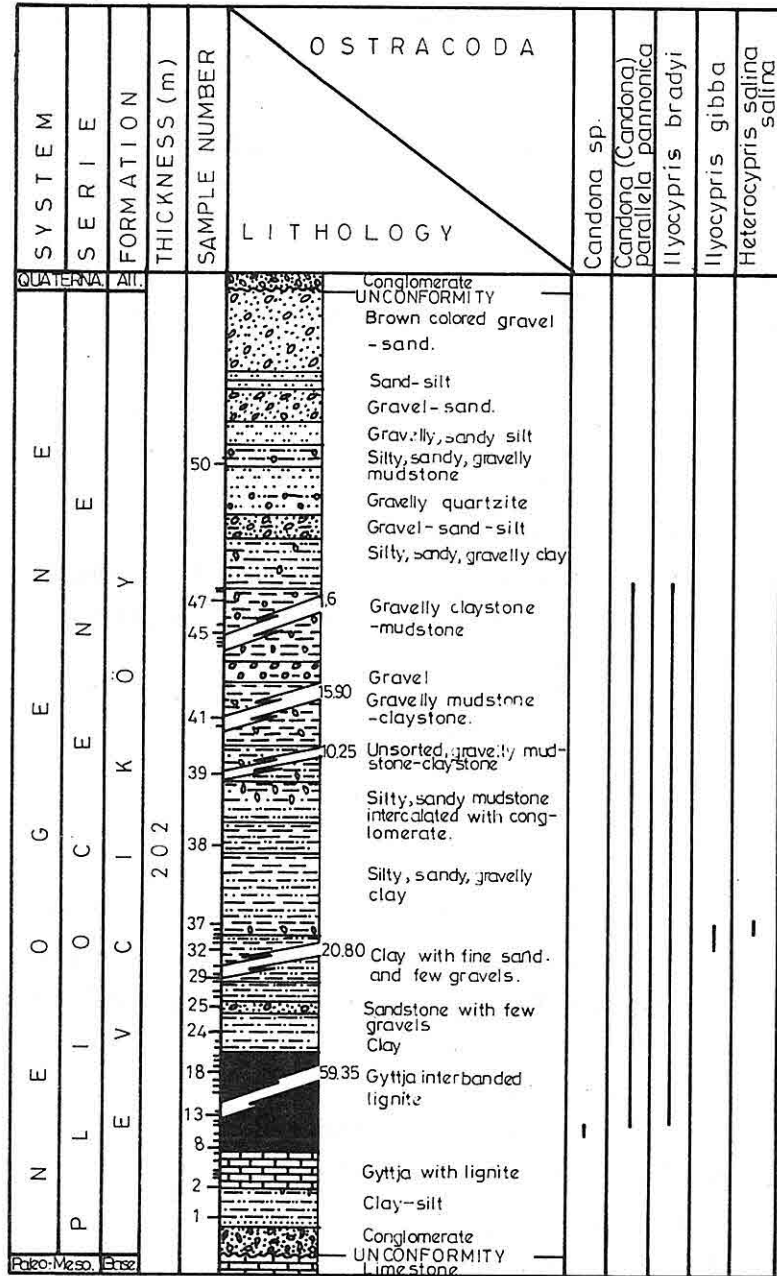
Figure 7. Stratigraphic Columnar Section and Ostracoda Distribution of the P-11 Borehole from Tufanbeyli-Pınarlar Location.

292

conglomerate with limestone materials. This is succeeded by clay-silt and gyttja with lignite up to 185 m (Figure 7).

Gyttja-interbanded, locally clayey lignite rests upon, up to 162 m, and **Candona sp., Candona (Candona) parallela pannonica** Zalanyi were identified from this zone. Up to 154 m, this sequence is succeeded by gray in color, clay and silt, and then slightly gravelly sandstone, approximately 3 m in thickness and

Ilyocypris bradyi Sars

Candona (Candona) parallela pannonica Zalanyi were defined.

Between 151 and 90 meters;

Ilyocypris bradyi Sars

Ilyocypris gibba Ramdohr

Candona (Candona) parallela pannonica Zalanyi

Heterocypris salina salina (Brady)

were defined from gray, plant-traced, fine sandy clay cotaining plant traces, and yellowish brown in color, silty, conglomerate-interbedded mudstone.

Between 90 and 2 meters;

Candona (Candona) parallela pannonica Zalanyi

Ilyocypris bradyi Sars

were defined from claystone, gravelly, sandy, silty claystone, siltstone and conglomerates overlain by alluvial materials with a thickness of 2 m.

Borehole No: P-14

The borehole is located to the North of Doruk Hill and its coordinates and depth are given in Table 1. It begins with coarse limestone gravels, and up to 170 m, continues with gray in color, abundant carbonates, locally fossilferrous, locally lignite-painted clay and clay-silt (Figure 8) .

The identified fossils from this zone are as follows:

Candona (Candona) parallela pannonica Zalanyi

Candona (Candona) aff luminosa Bodina

Ilyocypris bradyi Sars

Candona (Typhlocypris) amblygonica Freels

Cyprideis (Cyprideis) sohni Bassiouni

Candona (Pseudocandona) marchica elbistanensis Hartwig

In addition, Charophytes and gastropods were distinguished.

The thickness of gray in color, clayey, silty sardstone rested upon this zone is approximately 112 m, and then alluvium materials, 2.20 m in thickness is placed (Fig.6).
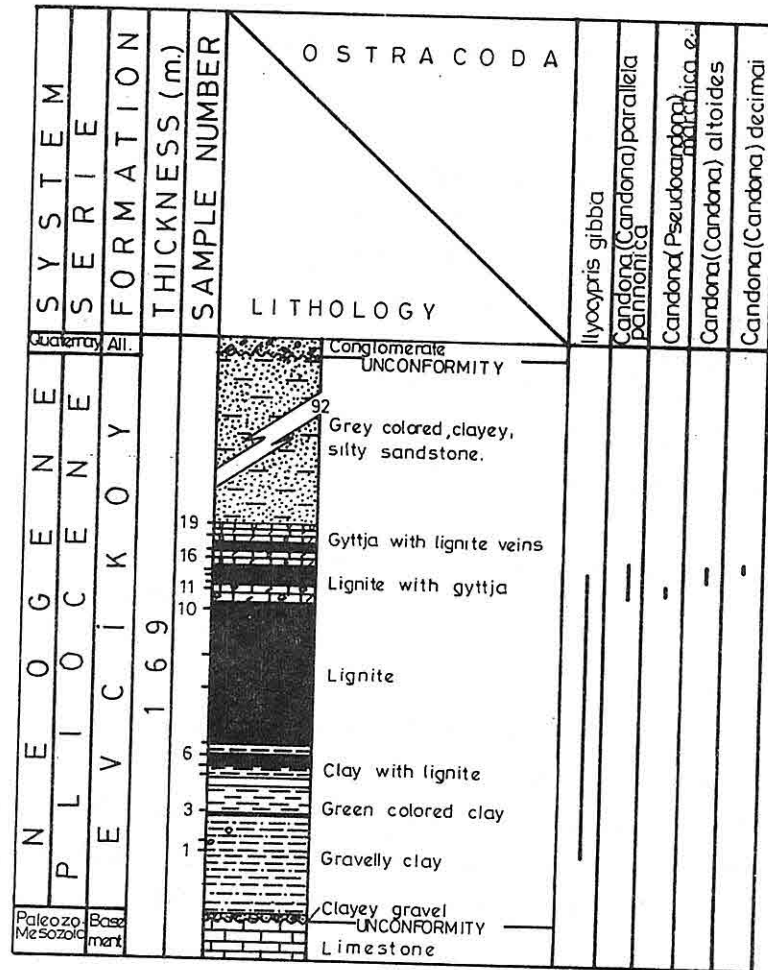

Figure 6. Stratigraphic Columnar Section and Ostracoda Distribution of the P-8 Borehole from Tufanbeyli-Pınarlar Location.

Borehole No: P-11

The borehole located in the NW of Mağara and in the W of Sarız river begins with limestone in the lower part and the unconformably overlying unit is unsorted

(Figure 5). **Ilyocypris gibba** Ramdohr was identified from the paleontological examination of gravelly clay placed over by coally, clay-intercaleted coal and clay-interbanded coals, having a thickness of 90.50 m with the following fossils:

Cyprideis (Cyprideis) cf. torosa (Jones)

Ilyocypris gibba Ramdohr

Candona (Candona) parallela pannonica Zalanyi

Candona (Candona) decimai Freels

Candona (Candona) aff. candida (Müller)

Candona (Candona) burdurensis Freels

Candona (Candona) altoides Petkovski

Candona (Pseudocandona) marchica Hartwig

Darwinula stevensoni (Brady and Robertson)

Darwinula cylindrica Straub

Eucypris dulcifons Diebel and Pietrzenuik

Candona (Typhlocypris) amblygonica Freels

Candona (Caspiocypris) alta (Zalanyi)

Cyprideis sp.

In addition, various gastropods and Bryozoa were also observed.

This zone is overlapped by gray, clayey, silty sandstone, where its thickness is 112 m, and then overlain by the alluvial materials, measured to be 2.20 m thick

Borehole No:8

The depth and coordinates of the borehole located to the west of the Sarız river and to the SE of Veletleryaylalığı Hill are given in Table 1.

At the bottom, limestone belonging to the basement, measured to be 5m is recovered, and unconformably overlain by clayey gravel, green slightly gravelly clay and gray-green clay (Figure 6). **Ilyocypris gibba** Ramdohr was observed only from these units in this borehole.

Between 150 and 114.50 meters, clayey, locally coal with gyttja and coal ranks were observed, and the ostracode fossils identified are as follows:

Ilyocypris gibba Ramdohr

Candona (Candona) parallela pannonica Zalanyi

Candona (Candona) decimai Freels

Candona (Candona) altoides Petkovski

This zone is overlain by silty clay, bluish-gray clay, and then by an unconformably overlying gravelly sandy unit which includes bryozoa and gastropods.

The succession of clay, silty claystone, sand and sandy conglomerate rest upon this zone with coal, and contains very few fossils. Alluvial materials, a thickness of 1 to 2 m, unconformably overlie the zone including fresh-water gastropods .

Borehole No:P-7

It is located to the northeast of Hastane village and between the Sarız river and Saray Hill. (Table 1).

The depth of the borehole is 183.15 m and at the bottom, it begins with conglomerate, which lies unconformably over the basement, and then overlain by gravelly clay
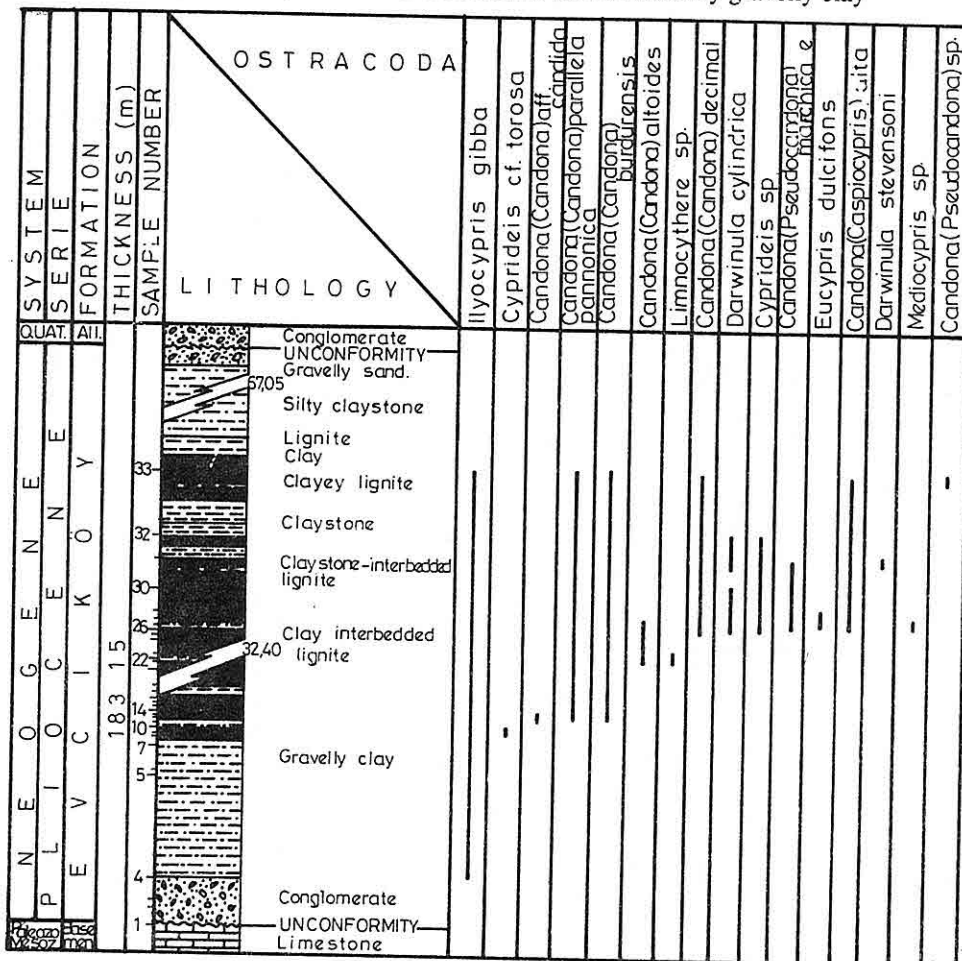
Figure 5. Stratigraphic Columnar Section and Ostracoda Distribution of the P-7 Borehole from Tufanbeyli-Pınarlar Location.

288

Candona (Candona) parallela pannonica Zalanyi

Heterocypris salina salina (Brady)

Candona (Candona) decimai Freels

Candona (Pseudocandona) marchica elbistanensis Hartwig

Darwinula stevensoni (Brady and Robertson)

Darwinula cylindrica Straub

Eucypris dulcifons Diebel and Pietrzenuik
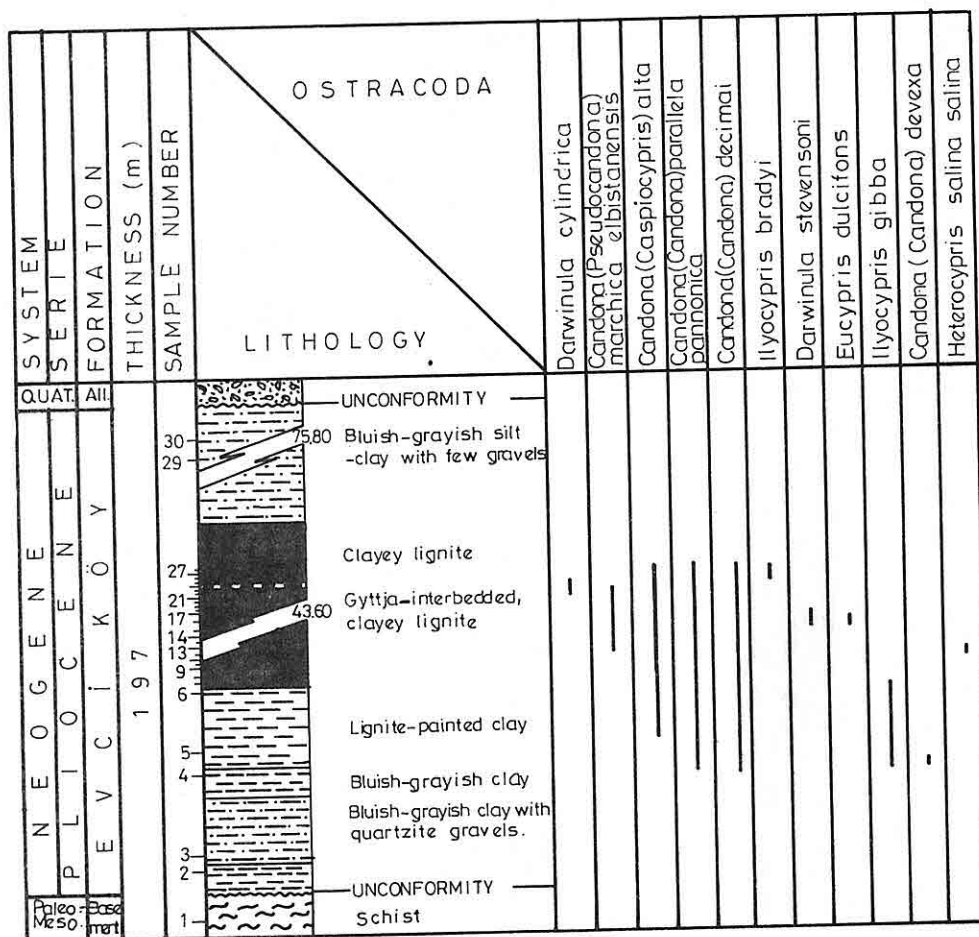
Candona (Caspiocypris) alta (Zalanyi)

Figure 4. Stratigraphic Columnar Section and Ostracoda Distribution of the P-3 Borehole from Tufanbeyli-Pınarlar Location.

287

following fossils were identified:

Candona (Candona) parallela pannonica Zalanyi

Candona (Candona) decimai Freels

Candona (Candona) devexa Kaufmann

Candona (Candona) aff luminosa Bodina

Candona (Candona) altoides Petkovski

Candona (Caspiocypris) aff. alta (Zalanyi)

Candona (Pseudocandona) marchica elbistanensis Hartwig

Heterocypris salina salina (Brady)

Cyprideis (Cyprideis) sohni Bassiouni

Darwinula stevensoni (Brady and Robertson)

Ilyocypris gibba Ramdohr

Gyraulus (Gyraulus) inornatus Brusina

Valvata (Cincinna) sp.

This zone is overlain by clay with lignite traces, sandy, gravelly silt, clayey gravel, silt with sand lenses, gray-colored, fine gravel-included clay-silt and at the top, alluvial material is placed (Figure 3).

Borehole No: P-3

It is located to the east of Hastane village and to the northwest of Tilki Hill in the area under investigation (Table 1).

The borehole is 168.5 m deep at this level, and the following lithologies are observed.At the bottom, down to 168.5, bluish-gray clay with quartzite gravels, bluish clay and lignite-painted clay.These clay rest unconformably upon bluish-gray pellitic schists having a thickness of 13.5 m (Figure 4).

The Ostracoda fossils identified in this zone are as follows:

Ilyocypris gibba Ramdohr

Ilyocypris bradyi Sars

Candona (Candona) parallela pannonica Zalanyi

Candona (Candona) devexa Kaufmann

In additions, various gastropods and charophyte were also found.

Between 94 and 168.5 meters, gyttja-interlaminated, clayey lignite was recovered, the following fossils were identified,
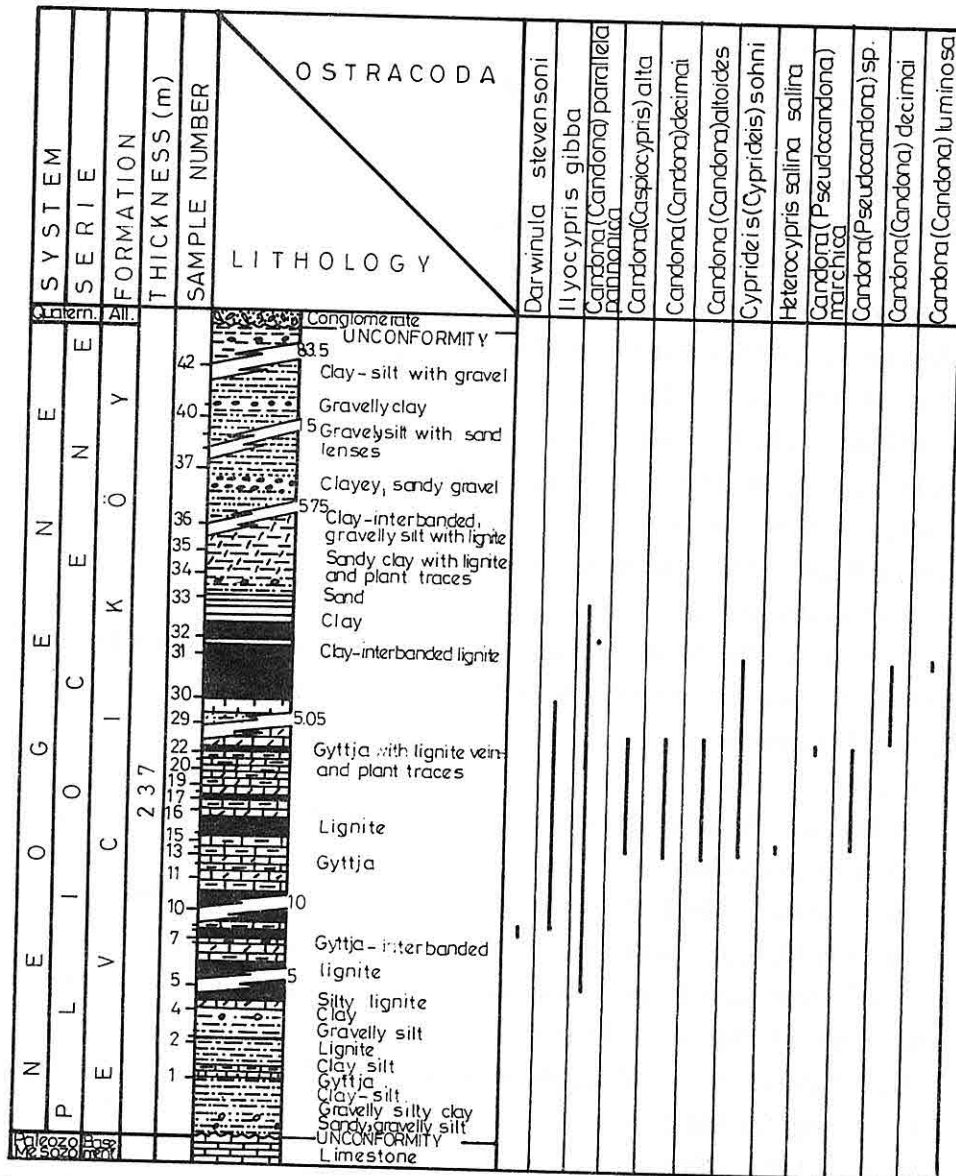
Ilyocypris bradyi Sars

286

Figure 3. Stratigraphic Columnar Section and Ostracoda Distribution of the P-2 Borehole from Tufanbeyli-Pınarlar Location.

Between 223 and 143 m, laminated clay, gyttja-intercalated, beige in color and slightly plant-traced was recovered.

As a result of this paleontological study carried on the zone including coal and gyttja, the

Borehole No: P-2

The coordinates and depth of MTA borehole no:P-2 located to the southeast of Hastane village with the southwest of Tilki Hill and discovered by MTA are given in the Table 1.

This section begins with sandy, gravely zone, which rests unconformably upon Paleozoic-Mesozoic units and continues with lignite-painted clay-silt at a

Figure 2. Generalized Stratigraphic Columnar Section

depth of approximately 228 m and then beige-colored silt including gyttja and coal trace and clay (Figure 3).

Along those ranks, fresh-water gastropods are only observed.

Table 1: Coordinates and Depth of the Boreholes with Abundant Fossils.

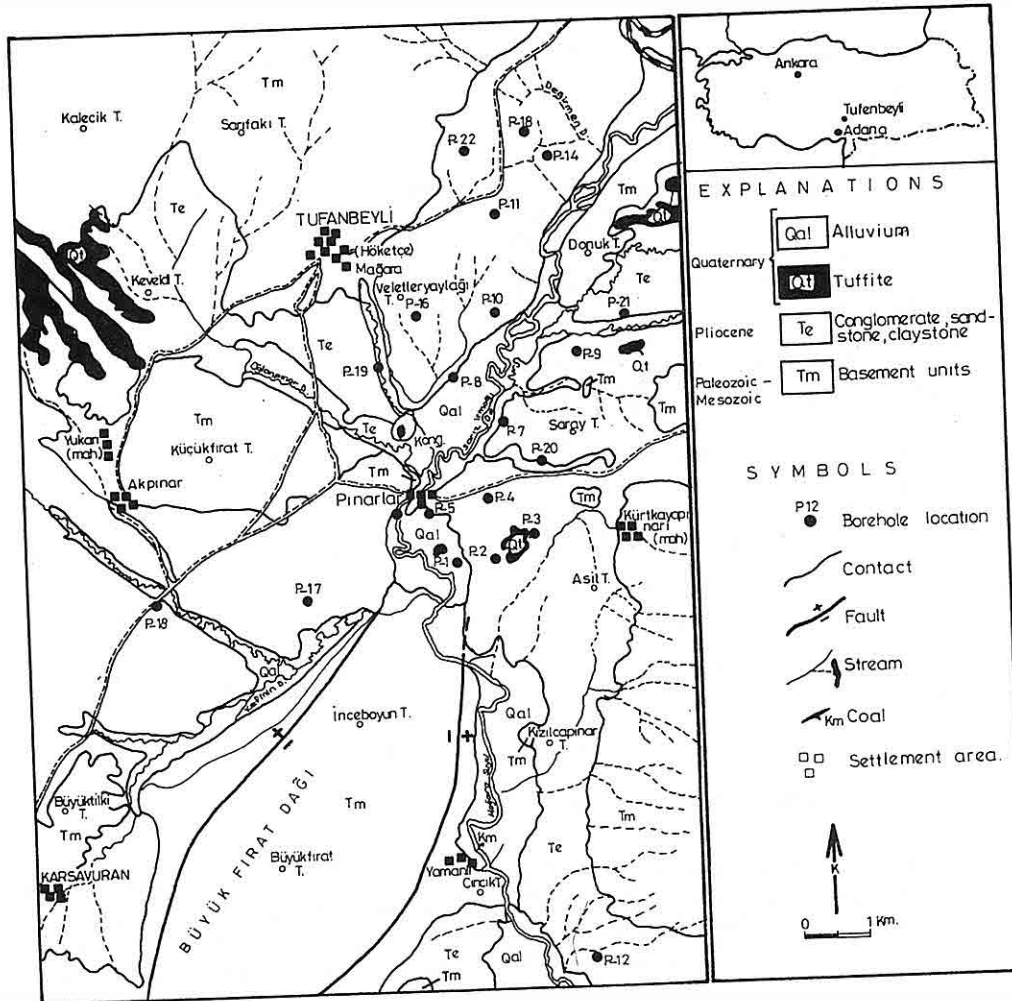| Borehole Number	Borehole Coordinates			Depth of Borehole (m.)
	x	y	z	
P-2	34142.48	58044.28	1377.25	237.05
P-3	34995.98	59014.74	1376.09	197.00
P-7	36171.99	59250.12	1357.42	183.15
P-8	36903.90	58577.71	1358.15	168.35
P-11	39121.00	59408.29	1435.70	201.80
P-14	40095.29	60252.40	1439.42	210.95
P-16	37833.90	58096.60	1427.59	224.65

284

Figure 1. Location and Geological Map of Investigation Area.

283

1. INTRODUCTION

The area under investigation is located approximately 190 km northeast of Adana province, and partly included by 1:25 000 scaled map of Elbistan L 36 a₃, L 36 b₄, L 36c₁ and L 36 d₂.

Blumenthal (1944), Yalçınlar (1955), Demirtaşlı (1967), Özgül et al.(1972 and 1973), Erkan et al., (1978), Metin (1984), Taga (1992), Şafak et al., (1992) and MTA have previously carried out various geologic studies in the study area and its surroundings.The age of units of the area range from Paleozoic to Quaternary. The purpose of this investigation is to delineate the stratigraphic position of clastic units with coal, recovered from 22 boreholes completed by MTA between 1989 and 1990 (Figure 1). The first micropaleontological investigation in the area was, therefore completed achieved just after the environmental interpretation of units including coal, and has been concluded by means of using ostracode and gastropod faunae.

The Evciköy formation described in the study was firstly named by Özgül et al., 1972. The substratum of the formation was identified as Paleozoic and Mesozoic basement units (Figure 2). The upper part, comprising alluvial deposits, represents Quaternary, and the lower part consists of soil materials (Şenol et al., 1992). This unit is overlain by an alternation of sandstone, siltstone and claystone with various sections containing gastropod shells and lignite veins. The uppermost section of the sequence is composed of sandstone and siltstone cemented by carbonate.

2. INTERPRETATION OF BOREHOLES

In the study area, 22 boreholes were completed to discover coals between 1989 and 1990 by MTA (Figure 1). The fossils included by borehole samples recovered from borehole no P-1 to P-20 were identified, and in the present study, only some of them were discussed because of the similarity of the borehole samples. A number of ostracods identified from borehole samples are given in Plate I, II and III.

Those boreholes mentioned above, were shallow (60-250 m) and extended down to Paleozoic and Mesozoic units.

The borehole logs discovered are describe below. They indicate that the relation between the Evciköy formation with abundant fossils and coal intercalation and the basement units and Quaternary age units.

282

MICROPALEONTOLOGICAL INVESTIGATION (OSTRACODA) OF THE PLIOCENE SEQUENCE OF THE TUFANBEYLİ (ADANA) AREA

Atike NAZİK[1], Ümit ŞAFAK[1] and Muzaffer ŞENOL[2]

[1]*Çukurova Univ., Geology Dept., Adana / Türkiye*

[2] *MTA, Adana / Türkiye*

ABSTRACT: *In this study, a micropaleontological investigation was completed on the detrital units which outcropped in the vicinity of the Tufanbeyli area located north of Adana. As a result of the study of borehole samples, Nine genera and 22 species from abundant ostracode fauna, representing Pliocene, which indicates lacustrine features as a result of the study. Gastropods observed together with ostracodes are very abundant long the coal rake and depict a lacustrine-fresh water environment.*

281

Expedition 1947-1948, vol.8, no.4, pp.218-285.

Reiss, Z., Klug, K. and Merling, P., 1961. Recent Foraminifera from the Mediterranean and Red Sea Coasts of Israel. Geol. Surv. Israel, Bull. No 32, pp.27-28.

Yanko, V., 1979. Stratigraphicheskie Complexi Bentosnich Foraminifer (Stratigraphic Assemblages of Benthonic Foraminifera). Geologia i Gidrologia Zapadnoy Chasti Chernogo Morya, Sofia, Academy of Science, pp.82-85.

Yanko, V., 1982. Stratigraphia Verchne Chetvertichnich Otlozeniy Sewero - Zapadnogo Shelfa Chernogo Morya po Bentosnim Foraminiferam (Stratigraphy of the Upper Quaternary Sediments of the North-Western Shelf of the Black Sea on Benthonic Foraminifera). Morskoya Micropeleontologia, Moscow, Nauka, pp.126-131.

Yanko, V., 1989. Chetvertichnie Foraminiferi Uznich Morey SSSR - Ponto - Caspian Region; Classificacia, Ekologia, Istoria Razvitia, Reconstrukcii Paleosredi (Quaternary Foraminifera of the Southern Seas of the USSR - Pontian - Caspian Region; Classification, Ecology, Biostratigraphy, History of Development, Environmental Reconstructions). D.Sc.Thesis, Moscow University, 924p.

Yanko, V., 1991. Stratigraphy and Paleogeography of Marine Pleistocene and Holocene Deposits of the Southern Seas of the USSR. Mem.Ital. Geol.Soc.

Yanko, V., and Troitskaja, T.S., 1987. Pozdnechetvertichnie Foraminiferi Chernogo Morya (Late Quaternary Foraminifera of the Black Sea). Moscow, Nauka, 111p.

Yanko, V., Flexer, A., Kress, N., Hornung, H. and Kronfeld, J., 1992. Benthic Foraminifera as Indicators of Heavy Metal Pollution in Israel's Eastern Mediterranean Margin. French-Israeli Symposium on The Continental Margin of the Mediterranean Sea, pp.73-79.

Walton, W.R., 1952. Techniques for Recognition of Living Foraminifera. Contributions from the Cushman Foundation for Foraminiferal Research, vol.3, no.2, pp.56-60.

in this region. A greater percentage of the assemblage is dominated by the adaptive forms away from the Bosphorous (marine) inlet. By analogy with the Black Sea, the Mediterranean dispersion though being more advanced, probably has not as yet attained its full extent of recovery since the termination of the early Holocene ecological crisis (approximately 8000 years ago).

8. REFERENCES

Abdou, H.F., Samir, A.M. and Frihy, O.E., 1991. Distribution of Benthonic Foraminifera on the Continental Shelf Off the Nile Delta. N. Jb. Geol. Palaont. Mh., No 1, pp., 1-11.

Blanch-Vernet, L., 1969. Contribution a l'etude des Foraminiferes de Mediterranee. Bull. Recl. Trav. Stn. Mar. Endoume, 48, pp.1-281.

Cimerman, F., 1984. Recentne Foraminifere iz Morja Zahodno od otoka Hvara (Srednija Dalmacija) v Luci Aktuopaleontologije, Master's Degree Thesis, Univ. Ljubliana, pp.1-120.

Cimerman, F., and Langer., R., 1991. Mediterranean Foraminifera. Ljubljana, 201p.

Daniels, C.H., 1970. Quantitative Okologische Analyse der Zeitlichen und Raumlichen Verteilung Rezenter Foraminiferen im Limskikanal bei Rovinj (Nordlche Adria). Gottinger Arb. Geol. Palaont., 8, pp.1-109, Gottingen.

Feyling-Hanssen, R.W., 1983. Quantitative Methods in Micropaleontology. NPD - Bulletin no.2, pp.109-126.

Jorissen, F.J., 1987. The Distribution of Benthic Foraminifera in the Adriatic Sea. Marine Micropaleontol., 12, pp.21-48.

Jorissen, F. J., 1988. Benthic Foraminifera from the Adriatic Sea. Principles of Phenotypic Variation, Utrect Micropal., Bull.37, pp.1-174.

Langer, M.R., 1989. Distribution, Diversity and Functional Morphology of Benthic Foraminifera from Vulcano (Mediterranean Sea). Ph.D. Thesis, 115 p., Univ. Basel.

Meriç, E., and Sakınç, M., 1990. Foraminifera: In Late Quaternary (Holocene) Bottom Sediments of the Southern Bosphorous and Golden Horn, 1990, Edit.E.Meriç, pp.13-53.

Mullineaux, L.S., Lohmann, G.P., 1981. Late Quaternary Stagnations and Recirculation of the Eastern Mediterranean: Changes in the Deep Water Recorded by Fossil Benthic Foraminifera. J.Foram.Res., v.11, no.1, pp.20-39.

Moncharmont Zei, M., 1968. I Foraminiferi di Alcuni Campioni di Fondo Prelevati Lungo la Costa di Beirut (Libano). Boll. Soc. Natur. in Napoli, vol. 77, no. 24, pp.3-34.

Olausson, E., 1961. Studies of Deep-Sea Cores: Reports of the Swedish Deep Sea Expedition 1947-1948, v.8, pp.353-391.

Parker, F.L., 1958. Eastern Mediterranean Foraminifera. Reports Swedish Deep-Sea
278

the Mediterranean as a whole, the temperature and salinity gradients are less significant, certainly compared to the gradients within the Black Sea, in regards to restricting the benthic foraminiferal dispersion. Within the Mediterranean Sea, the sea floor is marked by deep basins that serve as geographical barriers against the rapid foraminifera distribution of the shallow water foraminifera. The benthic foraminifera are able to best disperse, upon their arrive from the Atlantic Ocean (Straits of Gibraltar) by migrating along the shallow continious shelf. The well established long shore currents within the basin may help to determine rates of migration; for, it should be easier to migrate with, rather than against, such fixed and relatively strong currents (Fig.1). It may be that the greater diversity in the western Mediterranean ocean and its close similarity to the Atlantic assemblage, is a result of the dispersion - process attaining a greater degree of equilibrium with the Atlantic input source due to their closer proximity. Within the eastern Mediterranean, the difference between the eastern Mediterranean assemblage (as represented by the Israeli coast) and the western assemblage as a whole, may be a result of the, as yet, incompleteness of the progress of population diffusion. A rapid dispersion, as the organisms migrated from the Atlantic Ocean, was assisted by taking a route that is in line with the flow direction of the long shore currents across the north African coast shelf. Likewise the oceanographic pattern may explain the diversity between the Israeli coast and the Bosphorous and Aegean regions. This flow pattern would place the Israeli coastline in closer proximity to the Atlantic inlet source than the northern coast of the eastern Mediterranean (Fig.1). Other factors may locally serve as barriers hinder or diversify the species distribution; but, these should be subordinate effects.

7. CONCLUSIONS

The distribution of shallow benthic foraminiferal populations within the Mediterranean and Black Sea can be affected by a variety of local factors. However, the data presented as representing the different Mediterranean locations, has, in effect integrated a wide variety of local marine conditions. This thereby, takes into consideration much of the differences between sites and minimizes the local marine environmental factors between regions. A very large assemblage difference then still remains between the western and eastern basins, as well as between the southern and northern shelves of the eastern basin. This may be less a function of the variations in marine conditions, than the degree to which a benthic population that has equilibrated with the total recolonizing population undergoing dissemination from the Atlantic Ocean. It is seen (Fig.2) that the population assemblages further from the source are comprised of a larger percentage of adaptive "pioneer" taxa relative to the total population. The Black Sea by comparison has not reattained marine conditions that existed previously during the Pleistocene (Stage 5) (Yanko, 1991). However, the same "Pioneer" forms are dominant
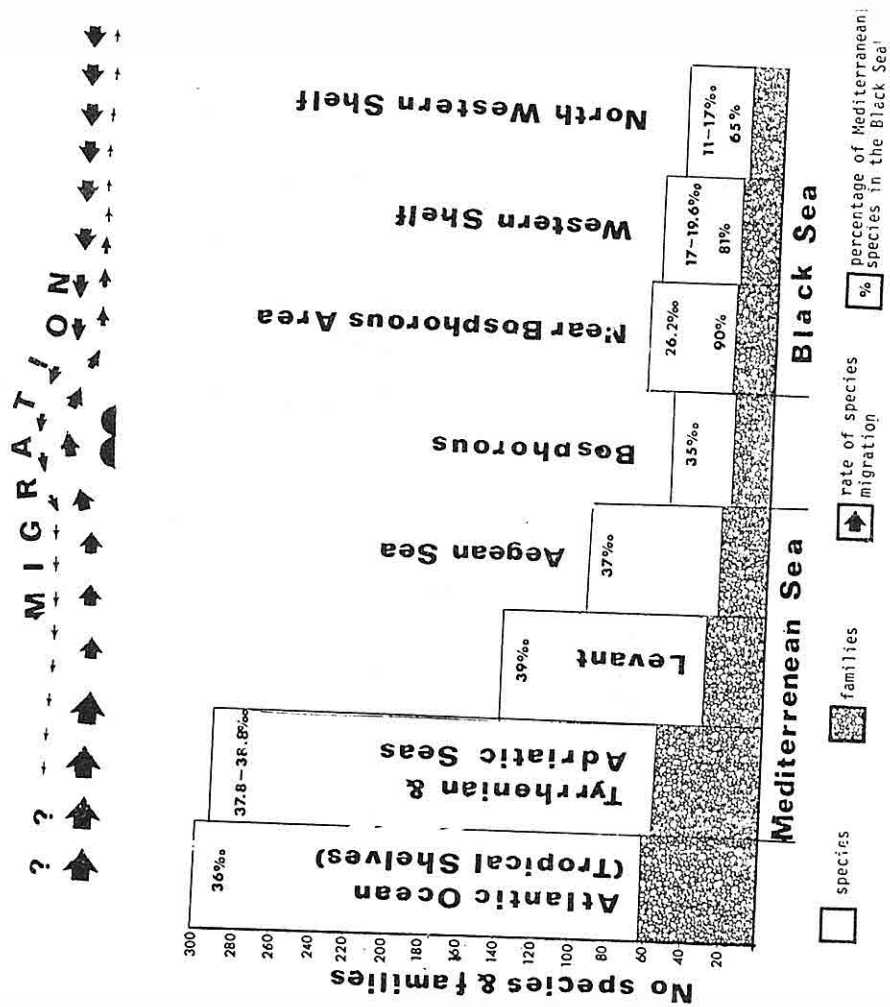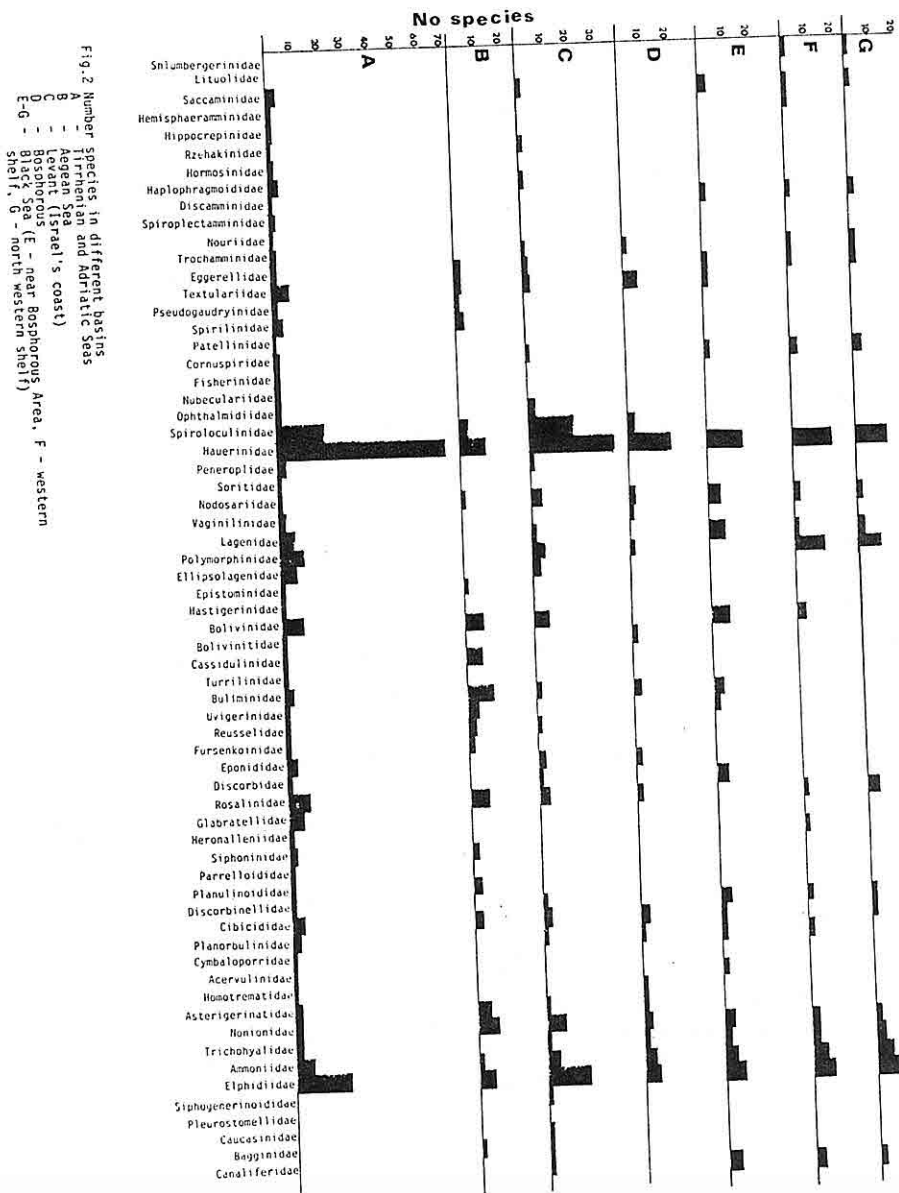
277

Fig.3 Number of benthic foraminifera families and species, and their migration rate and ways in different basins

276

Fig. 2 Number species in different basins
A – Tirrhenian and Adriatic Seas
B – Aegean Sea
C – Levant (Israel's coast)
D – Bosphorous
E-G – Black Sea (E – near Bosphorous Area, F – western shelf, G – north western shelf)

275

benthic assemblage of the Aegean, which is similar to that of the Bosphorous assemblage. The Bosphorous assemblage, which was taken from core data, did not entail a living assemblage. It must be considered to approximate a minimal value of the present day assemblage. This (the Bosphorous) assemblage is richer than that for the Black Sea which shows a geographical population distribution in relation to the Bosphorous inlet (which itself is the sole source for recolonized of the Black Sea by marine fauna). Further along the coast, away from the Bosphorous, the salinity decreases and the benthic foraminiferal populations become poorer in diversity.

The diversity of the foraminiferal species as a function of geography can be best visualized in Figs. 2, 3. These figures present the number of species of shallow water benthic foraminifera that have been found in the various geographic regions .The species diversity is seen to follow a geographical trend.

6. DISCUSSION

The distribution of benthic foraminifera can be influenced by a variety of factors such as temperature, salinity, pollution and oxygen supply of the water, as well as the type of substrate that they colonize. Variations of course do exist along the shelf of the Mediterranean. However, each of the regions discussed in the Mediterranean, are in effect, a compilation of many individual sampling sites representing many ecological habitats. Still the differences between the western and eastern portions of the sea, as well as the differences along the shelves of the eastern basin itself are so great as to make suspect these factors as being the sole or even the primary reason for the magnitude of the diversity difference between inter and infra-basinal assemblages. Rather, another process appears to be of greater importance.

A geographic versus population diversity trend is observed in both the Mediterranean and Black Sea. These are two distinctly different oceanologic bodies of different chemistry and environments; yet, the population distribution within both of these seas may in a sense be regarded as related to a similar process. This process is the, as yet, incomplete population recovery following the ecological crisis that affected (in different degrees) the two water bodies. Both water bodies now appear to be undergoing a marine recolonization. The Black Sea being much less marine in character still serves as a barrier against the less hardly and less adaptive of marine organisms. The more adaptive are represented the Hauerinidae and Elphidiidae families. These have penetrated furthest into the Black Sea from their source of introduction (the relatively shallow Bosphorous (96 m)). Closest to the Bosphorous with its near marine conditions is found the assemblage most similar to that of the eastern Mediterranean (e.g.Aegean). As the marine conditions give way to fresher water conditions fewer benthic foraminiferal forms are able to penetrate at present. The Black Sea is still far from attaining a benthic foraminifera population that is in equilibrium with the eastern Mediterranean's. Within

274

The data base taken from the literature is restricted to shallow benthic foraminifera (approximately 50 m water depth) (a species that were found to exist both at water depths shallower and deeper were also included).

4. MATERIALS AND METHODS

Samples from the eastern Mediterranean (71 samples) were obtained by grab and box core during the summer months of 1986-1991 by workers of National Oceanographic Institute (Haifa) N.Kress and H.Hornung; from the Black Sea (474 samples) by the senior author during 1971-1986.

Benthic foraminifera were studied by standard methods (Feyling-Hanssen, 1983; Yanko & Troitskaja, 1987). The Rose Bengal dye (Walton, 1952) was used to distinguish between dead and living specimens at all stations in the Black Sea. The Israeli study was mainly based upon surface cores collected a few years previously, which did not contain living material. 5 g dry samples (Israel's eastern Mediterranean) and 100 g (the Black Sea) were used. All numerical characteristics of foraminifera are normalized to a 5 g mass of sediment. When possible 300 specimens of foraminifera from the >0.125 mm fraction were counted for each sample. Statistical analysis of 30 specimens of each investigated species was carried out to estimate the variation of foraminiferal test sizes. In certain cases when the number of specimens was less than 300 (for example, at the sites 1 and 4 in the Israel's offshore), the number of each species specimens was normalized to 300.

5. RESULTS

A location map is presented in Fig.1 from which the major areas and sampling sites for the Mediterranean and Black Sea are presented. Included on this map are the major flow directions of the currents in the basins (included in this in the SW-NW surface current direction at the entrance to the Adriatic Sea). The salinity of the Mediterranean varies from west to east (37%o) to (39%o) which is slightly higher than the Atlantic water (35%o). Four sites were sampled in the Black Sea. The salinity into the Black Sea decreased from the Bosphorous northeastwards.

The results of the population distribution, at the family and the species level, of the shallow water (0-60 m) benthic foraminifera from the western Mediterranean, eastern Mediterranean, Bosphorous, Aegean Sea, and Black Sea is represented on Fig.2. It can be seen that in all cases, two families Hauerinidae and Elphidiidae dominate. The eastern Mediterranean is represented by distinctly fewer species than the western. The western basin is most similar (57 families and 285 species) to the Atlantic Ocean assemblages (61 families and at least 300 species) (Michalevich, 1982). The Atlantic Ocean is the only possible source for the foraminiferal reentrance into the Mediterranean. Within the eastern Mediterranean the Israeli coast is richer than the
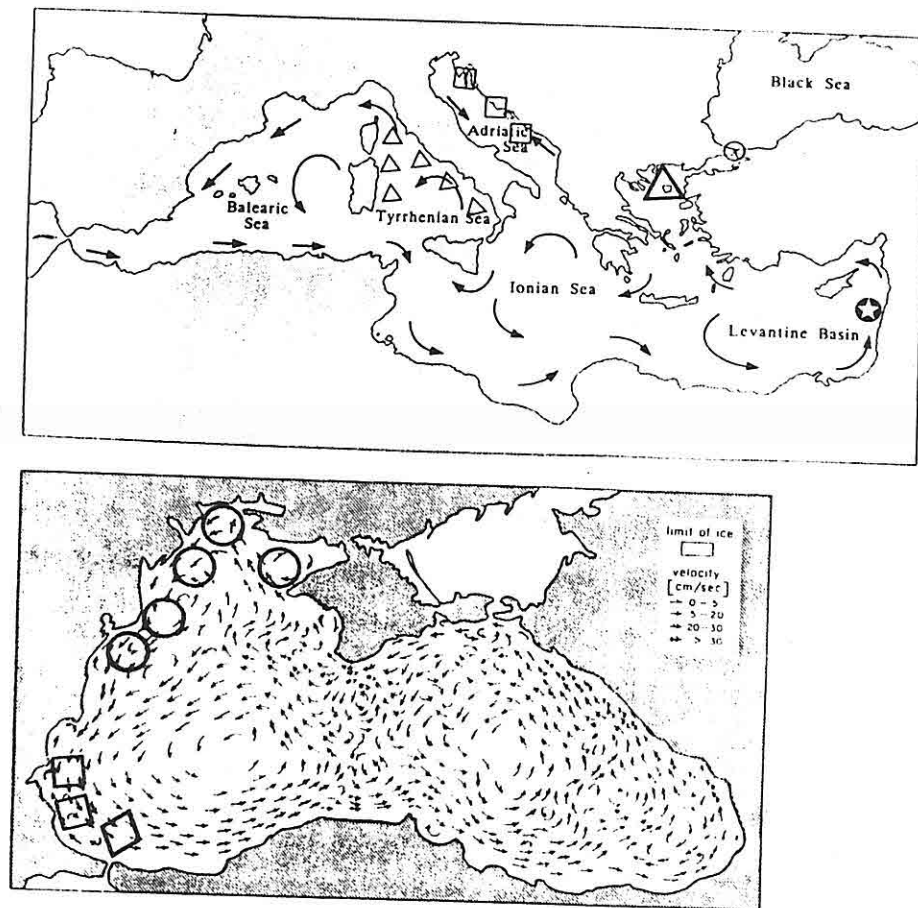
273

Fig.1 Current systems (after Cimerman, 1991 and Zenkevich, 1963;
Shimkus & Trimonis, 1974) and location map in the (A)
Mediterranean Sea(), (B) Black Sea

A) ☐ Adriatic Sea (Cimerman, 1991)

    △ Tirrhenian Sea (Cimerman, 1991)

    ▲ Aegean Sea (Parker, 1958)

    ✪ Levant (Yanko et al., 1992)

    ○ Bosphorous (Meric & Sakinc, 1990)

B) ◯ north western shelf (Yanko, 1989, 1991)

    ☐ western shelf (Yanko, 1989, 1991)

    ◇ near Bosphorous area (Yanko, 1989, 1991)

Mediterranean as well as the Bosphorous. To date the preliminary studies of Parker (eastern Mediterranean and Aegean Sea, 1958), Moncharmont Zei (Lebanon's shelf, 1968), Abdou et al. (continental shelf off the Nile Delta, 1991) and Meriç and Sakınç (Bosphorous, 1990) remain the most detailed references. Detailed environmental and taxonomic investigations of the western Mediterranean foraminifera have been carried out by many authors. The most comprehensive modern information is found in the research of Blanch-Vernet (1969), Daniels (1970), Cimerman (1984), Jorissen (1987, 1988): Langer (1989) and Cimerman and Langer (1991).

For a period of 20 years prior to this work, extensive background studies on present and Quaternary benthic foraminifa (taxonomy, morphology, density, diversity, etc.) had been carried out by the senior author in the Black sea (Yanko, 1979, 1982, 1989 , 1990, 1991: Yanko & Troitskaja, 1987). The environments that were studied here included deltas, open and closed lagoons, bays, and shelf extending from 0-220 m. The bottom water salinity ranged from 1-26%o.

In the Black Sea living benthic foraminifera are distributed to a maximum water depth of 220 m. Foraminifera are not found beyond this depth, in contrast to the Mediterranean, due to the continuous presence of H_2S in the water.

3. SAMPLING AREA DESCRIPTION

With the exception of the Black Sea and the Israeli coast, the other comparative data has been taken from the literature. Therefore, no further description will be given here for these sites (Fig.1 A,B).

Israel's Mediterranean coast (Fig. 1A). Foraminifera were collected from four sites, at a depth interval of 6-50 m. Site 1 (6 stations) is situated off Hadera (24 m water depth). Site 2 (2 stations) was taken at the entrance to Haifa Harbour (6-12 m water depth). Site 3 (4 stations) is located off the beach of Nitzanim (20 to 50 m water depth). Site 4 (6 stations) is situated off Palmachim (20-50 m water depth). Salinity at all of the sites was constant, averaging 39%o. Salinity of the western Mediterranean varies between 37.8%o and 38.1%o (Tyrrhenian Sea), 38.5-38.8%o (Adriatic Sea). The salinity of the Bosphorous is 35%o.

The Black Sea. Surface material was collected by grab and box-cores from selected areas (Fig. 1B). The north-western shelf is represented by 350 stations (3-70 m water depth, salinity 11-18.6%o). 134 stations were taken along the western shelf (8-70 m water depth, salinity 17- 19.6%o). 10 stations were taken at sites located in the vicinity of the area near to the Bosphorous (100-120 m water depth, salinity 26.2%o). Despite the greater depth here, we decided to include these stations for comparison. This site demonstrates the primary influence of salinity on the benthic foraminiferal distribution. Shallower depths are within Turkish territorial waters and could not be sampled at that time.

1. INTRODUCTION

After the Last Glaciation, a drastic oceanographic change affected both the Mediterranean and Black Sea. The Black Sea received increased discharge from by the major rivers that drain central Europe. This significantly lowered the salinity and destroyed its meromictic structure. This lowering of salinity resulted in a major ecological crisis for many marine organisms (e.g. ostracods, molluscs, foraminifers). For example, a near total extinction took place of the Black Sea's shallow benthic foraminifera (Yanko, 1989, 1991). Likewise, the Mediterranean Sea was affected by the sea level changes and the increased fresh water in flow. A meromictic state was created. Circulation was impeded. Low salinity surface water prevented the reoxygenation of the deep water which became anoxic (Olausson, 1961). This state is strikingly denoted by the creation of sapropels. The sapropels are found almost exclusively in the eastern Mediterranean, though, some evidence exists for periods of reducing conditions in the deep western Mediterranean as well. The periods of Mediterranean stagnation were also periods of ecological stress; though, the extent of crisis is less well known and perhaps less severe than that which transpired in the Black Sea. Here too are recorded changes in the benthic foraminiferal populations. Changes in faunal assemblages occurred for deep water benthic foraminifera in response to oscillating oxic-anoxic-oxic conditions. It was noted though that the recovery was relatively slow. The eastern Mediterranean, as reflected in the deep water benthic foraminifera, has not, even today, recovered from the last stagnation (sapropel event, S_1) of about 8000 years ago (Mullineaux & Lohmann, 1981). Relatively little data is available for modern shallow (<60 m) benthic foraminifera from the Mediterranean as a whole. Less is known about earlier benthic foraminiferal populations (such as during formation the periods of sapropel formation).

The present work presents a summary of the published data as well as more recent data in an attempt to synthesize a model for understanding the present distributions of shallow benthic foraminiferal populations both in the Mediterranean and Black Seas. The study intends as a first step to consider some basic questions of today's Levant benthic foraminiferal distribution. A comparative distribution study with the rest of the Mediterranean, coupled with an understanding of the oceanographic processes that led to ecologic stresses at the beginning of the Holocene, may provide insight into the migration pathways into the eastern Mediterranean and Black Sea by benthic foraminifera.

2. PREVIOUS STUDIES

With the exception of a short paper by Reiss et al., (1961) and Yanko et al., (1992) no information is available on benthic foraminifera of the Israeli offshore.

Also there is only limited information concerning benthic foraminifera of the eastern

270

THE RATE OF RECOLONIZATION IN THE MEDITERRANEAN SEA FOLLOWING THE TERMINATION OF THE S_1- SAPROPEL ECOLOGICAL CRISIS

V.YANKO, J. KRONFELD and A. FLEXER

Dept. of Geophysics and Planetary Sciences, Tel Aviv University, Ramat Aviv 69978, Tel Aviv, ISRAEL

ABSTRACT : *Mediterranean sapropels are relics of the anoxic conditions that deliterously affected the marine fauna. Following the last sapropel event, S_1, recolonization commenced, with a reintroduction of marine species from the Atlantic Ocean. By comparing modern benthic foraminiferal populations, it appears that the western Mediterranean has achieved a greater degree of equilibrium with the Atlantic source than has the eastern Mediterranean. Moreover, in the eastern Mediterranean, the south coast of the Levant Basin has attained a greater degree of recovery, as it is closer in line with the long shore current to the inlet source, than has the northern part of the eastern Mediterranean. The dispersion recovery model for the Mediterranean following the last ecologic crisis is in agreement with the recovery model proposed for the Black Sea.*

269

EPDC, 1983. *Feasibility Report on Beşkonak Hydroelectric Power Development Project:* DSİ, Ankara.

Eroskay, S.O., 1968. *Köprüçay-Beşkonak Rezervuarı Jeolojik İncelemesi,* EİE Rapor No: II-06-5, Ankara, 80s, (in Turkish).

Günay, G., 1981. *Manavgat Havzası ve Yakın Dolayının Karst Hidrojeolojisi İncelemesi* H.Ü. Müh. Fak. Doçentlik Tezi, Ankara, 185s,(yayımlanmamış), (in Turkish).

Milanoviç, P.T., 1981. *Karst Hydrogeology: Water Resources Publication,* 433p., USA,

4. CONCLUSIONS

Karstification in the Taurus Mountains has started in Miocene and developed naturally during Pliocene and Pleistocene (Eroskay,1968). However, the paleokarstic features around Seydişehir area in the central part of the Taurus region indicates the presence of karstification before Miocene.

The Köprüçay conglomerate is of Lower-Middle Miocene. Following the karstification started at the surface during Upper Miocene, deep karst has developed during Pliocene and Pleistocene due to the tectonic movements resulted from faulting and suitable climatic conditions.

Existance of Miocene-aged sediments (i.e., the Köprüçay Conglomerate) at Bozburun mountain at an elevation of 2500 m indicates the order of epiorogenic movements taken place in the region.

The position of the one of the most important faults, the Pliocene-aged Kırkkavak fault (Fig. 1), has caused karstification penetrating great depths within the Köprüçay conglomerate which has been karstified during the Upper Miocene.

As the sea has regressed about 100 m during Gunz, Mindel, Riss and Wurm at Pleistocene, the conglomerates which have been thrown to lower elevations by the Kırkkavak fault are continuously karstified.

Thus, karstification has developed over 200 m bsl. since the conglomerates are very thick and underlain by limestone units; the epirogenic movements were very intensive; the Kırkkavak fault played important role in the hydrogeology of the region; regression of the sea during Wurm and a lower groundwater table than the river level.

The karstification depth of Oymapınar dam site, only 30 km east of Beşkonak dam, is 70 m bsl. This is because of the impervious units that underlie the relatively thin karstic unit. Whereas, the conglomerates in the Beşkonak dam site have thickness of more than 1000 m (Eroskay, 1968) and underlain by another karstic unit, a Cretaceous limestone.

5. REFERENCES

Değirmenci, M., Günay, G., 1986. Pre-Dye Test Karst Hydrogeological Investigations in Beşkonak Dam Site: HÜ/UNDP Project (TUR/81/004), Technical Report No: 86/04, 35p, Ankara.

Değirmenci, M., 1989. Köprücay Havzası ve Dolayının (Antalya) Hidrojeoloji İncelemesi H.Ü. Fen Bilimleri Enstitüsü Doktora Tezi, 375s, Ankara (yayımlanmamış), (in Turkish).

Değirmenci, M., Günay, G., 1990. Analysis of Hyrologic Relations Between Eğirdir-Beyşehir-Suğla Lakes Systems and Adjacent Basins by Means of Remote Sensing Techniques; (S Turkey): Environmental Geology and Water Sciences, USA, (in press).

EİE, 1973. Köprücay-Beşkonak Bent Yeri ve Enjeksiyon Perde Güzergahları Mühendislik Jeolojisi İncelemesi , EİE Yayın No. 73-17, Ankara, 86p., (in Turkish).

The number of tests conducted at various elevations (zones of 2 m, above 10 l) and their percentages are given in Figure 8. The figure shows that a significant part of the water loss is of the 2nd group, that is the water loss under zero pressure, even at these few boreholes that have depths of greater than 150 m bsl. Based on these observations, however, one can not conclude that karstification becomes more intense at depths below 150 m bsl because of the limited numbers of boreholes investigated. On the other hand, it will also be erroneous to conclude that karstification is stoping below 100 m bsl. or the karstification depth is 100 m bsl.
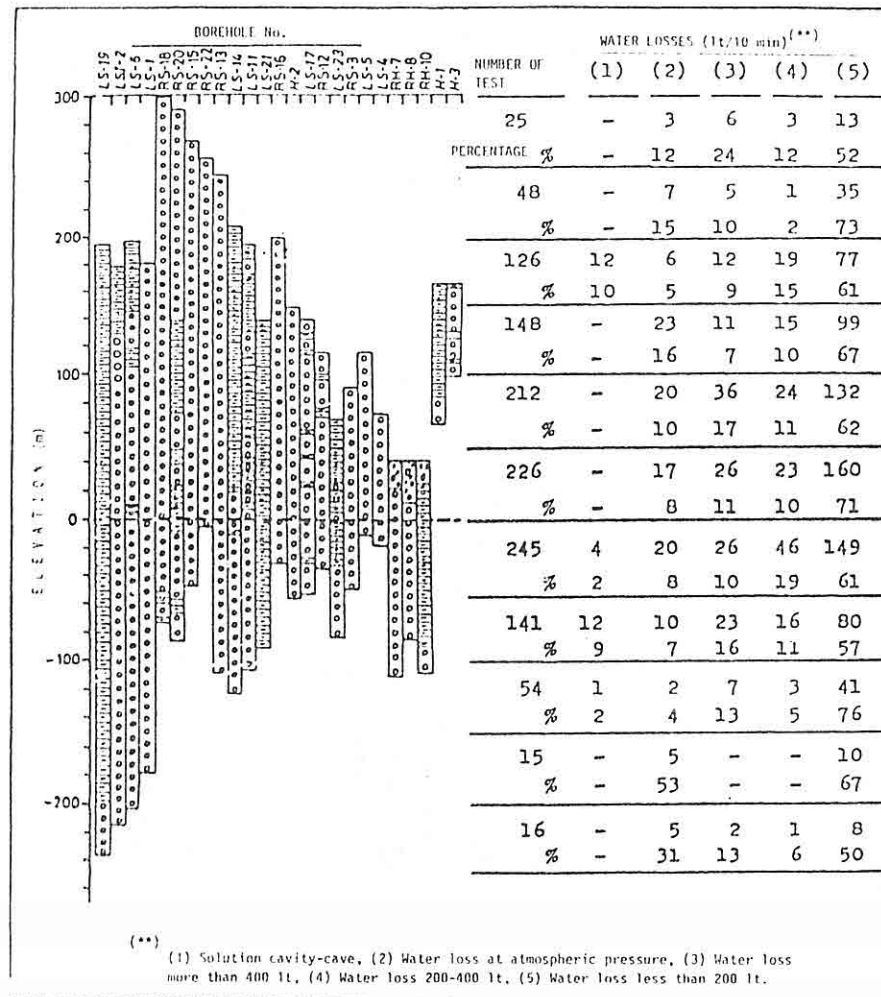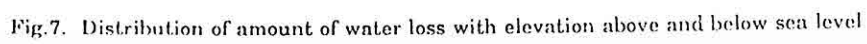

NUMBER OF TEST	WATER LOSSES (1t/10 min)[**]				
	(1)	(2)	(3)	(4)	(5)
25	–	3	6	3	13
PERCENTAGE %	–	12	24	12	52
48	–	7	5	1	35
%	–	15	10	2	73
126	12	6	12	19	77
%	10	5	9	15	61
148	–	23	11	15	99
%	–	16	7	10	67
212	–	20	36	24	132
%	–	10	17	11	62
226	–	17	26	23	160
%	–	8	11	10	71
245	4	20	26	46	149
%	2	8	10	19	61
141	12	10	23	16	80
%	9	7	16	11	57
54	1	2	7	3	41
%	2	4	13	5	76
15	–	5	–	–	10
%	–	53	–	–	67
16	–	5	2	1	8
%	–	31	13	6	50

[**]
(1) Solution cavity-cave, (2) Water loss at atmospheric pressure, (3) Water loss more than 400 1t, (4) Water loss 200-400 1t, (5) Water loss less than 200 1t.

Figure 8. The number of tests conducted at various elevations and their percentages.

266

Fig.7. Distribution of amount of water loss with elevation above and below sea level

265

1. Solution cavity,cave, 2. Water loss at atmospheric pressure, 3. Water loss more than 400 lt/10 min., 4. Water loss 200-400 lt/10 min., 5, Water loss less than 200 lt/10 min., 6. The first 10 m zone from surface that pressure test could not been performed due to intensive karstification.
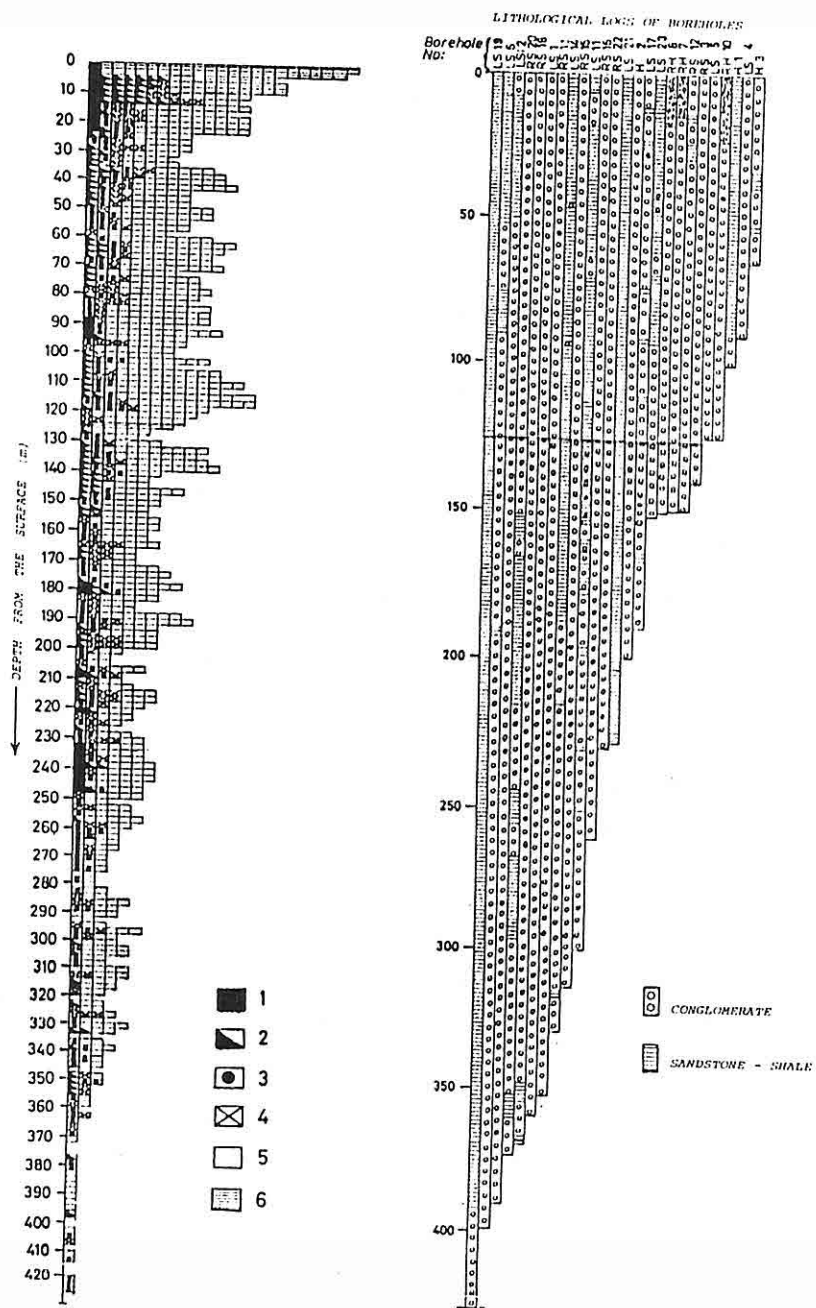
Fig. 6. Variation of karstification by depth according to the pressure test results carried out in the boreholes drilled at dam site and near vicinity

simplify the evaluation and provide a better understanding in application.

1st group: Large solution cavities and caverns determined in boreholes; lugeon test could not be performed.

2nd group: Karstic zone with very high permeability. The capacity of the voids is bigger than the inflow through the well, thus the water escapes under pressure of zero.

3rd group: Zones leaking water more than 400 l, which corresponds to 20 Lu.

4th group: Zones leaking water between 200 and 400 l (10-20 Lu).

5th group: Zones leaking water less than 200 l (1-10 Lu).

6th group: Weathering zone at the surface; soil cover; no tests conducted.

3.4. Evaluation

1) The total steps (zones of 2 m in the borehole that was tested each time) that were used in this evaluation is 1320 and they can be grouped as follows.

1st group	2nd group	3rd group	4th group	5th group	6th group	Total
29	118	154	151	804	64	1320
2%	9%	12%	11%	61%	5%	100%

2) If the 1st, 2nd, 3rd, 4th and 6th groups are considered as pervious and karstic zones, then, of these, the 1st, 2nd and 6th groups constituting 41% of the total can be evaluated as intensively karstified zones. This figure is 27% for the depths below 40 m.

3) Although the depths of the boreholes used in the evaluation are not the same, it is possible to conclude that the water loss, and thus, the karstification decreases with depth as shown in Figure 6.

The relation of karstification with depth was evaluated for a depth of 64 m (all boreholes reached this depth) was expressed mathematically as $\varepsilon = 19.18 \, e^{-0.03H}$, for which the correlation coefficient is found to be 0.81.

In the expression given above, ε : karstification coefficient and, H: depth from the surface (m). This equation has shown that the karstification at the zone 0-10 m from the surface is five times of that seen in depths about 64 m. For a depth of 100 m this expression becomes $\varepsilon = 11.94 \, e^{-0.02H}$ and the releated correlation coefficient is 0.66. For a depth of 150 m it is $\varepsilon = 8.75 \, e^{-0.01H}$ and a smaller correlation coefficient of 0.56.

Distribution of amount of water loss with elevation above and below sea levels is given in Figure 7. As it is seen from the figure, karstification has developed also at elevations 220 m below the sea level in the region. According the Figure 7 the water loss decreases at depths below 100 m bsl. But, the small number of the boreholes with such depths must be taken into consideration during interpretation. In this evaluation, 25 boreholes are used, and only 4 of these have depths below 150 m bsl.
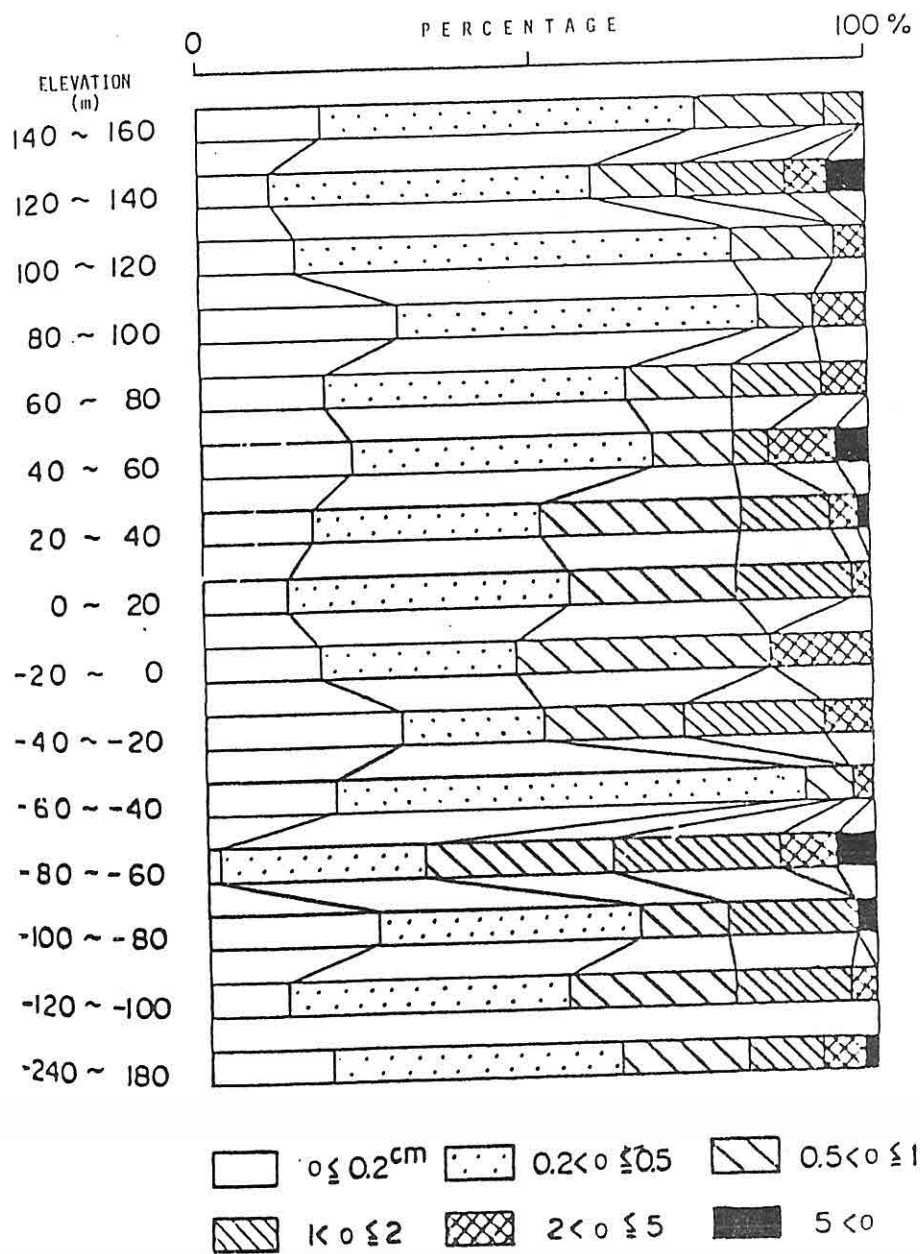
Fig. 5. The distribution of fracture and solution channel oppenings (O) versus elevation (after EPDC, 1983).
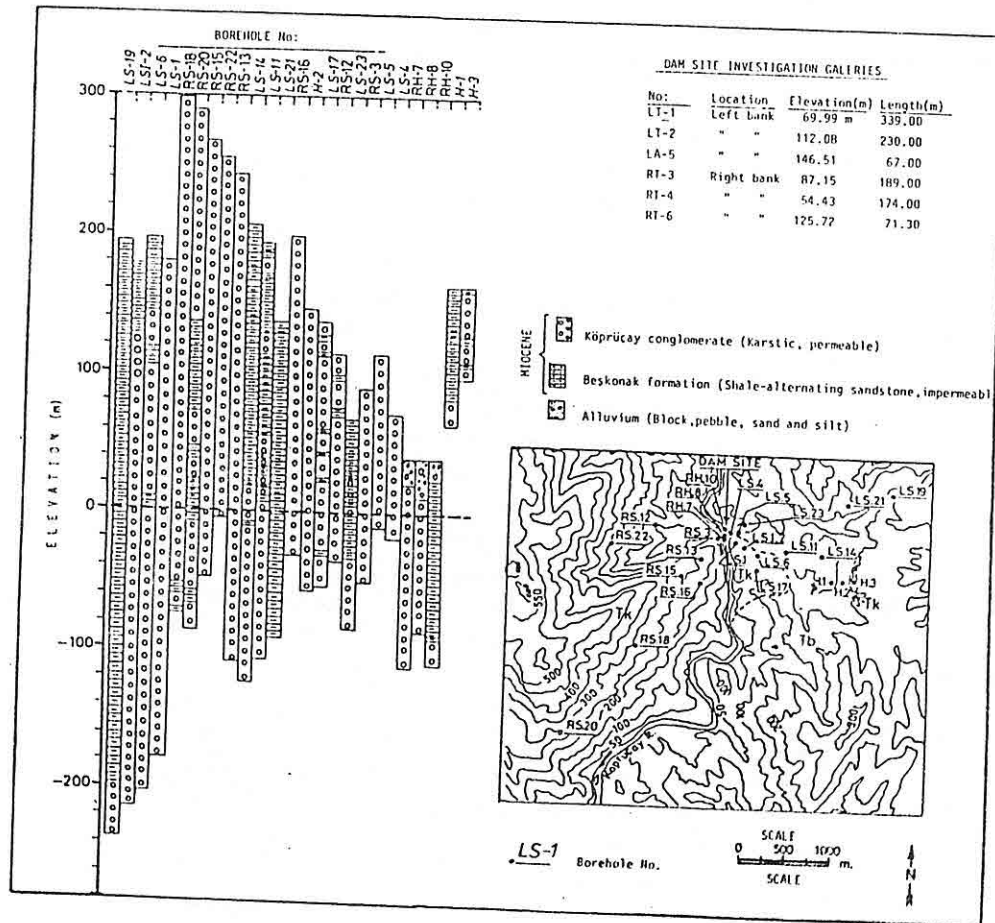
Figure 4. The locatiton, logs and elevation-depth relations of the boreholes at the Beşkonak dam site and vicinity (drilled and pressure test performed by EİE, 1973).

(lugeon) that were carried out in 25 boreholes drilled at the dam site and its near vicinity with depths ranging between 40 and 300 m were evaluated (Fig. 6). Lugeon tests are realized in each 2 m of the borehole. For this reason, the unit termed as water loss, in 10 minutes in liters for each 2 m was used in evaluation.

According to the results of the tests, the water losses were divided into 6 groups to

Fig. 3. Groundwater level observations in Kuruköprü cave and RB-1 Borehole

(1) Groundwater level (28 th July 1987)
(2)   "   "   (1 st February 1988)
(3)   "   "   (25 th   )
(4) Borehole log (conglomerate)
(5) Maximum pressure in pressure test
(6) Lugeon values (Lu)
(7) Groundwater level during the pressure test (23th June 1988)
(8) Water level of Köprüçay river
(9) Depth from the surface (m)
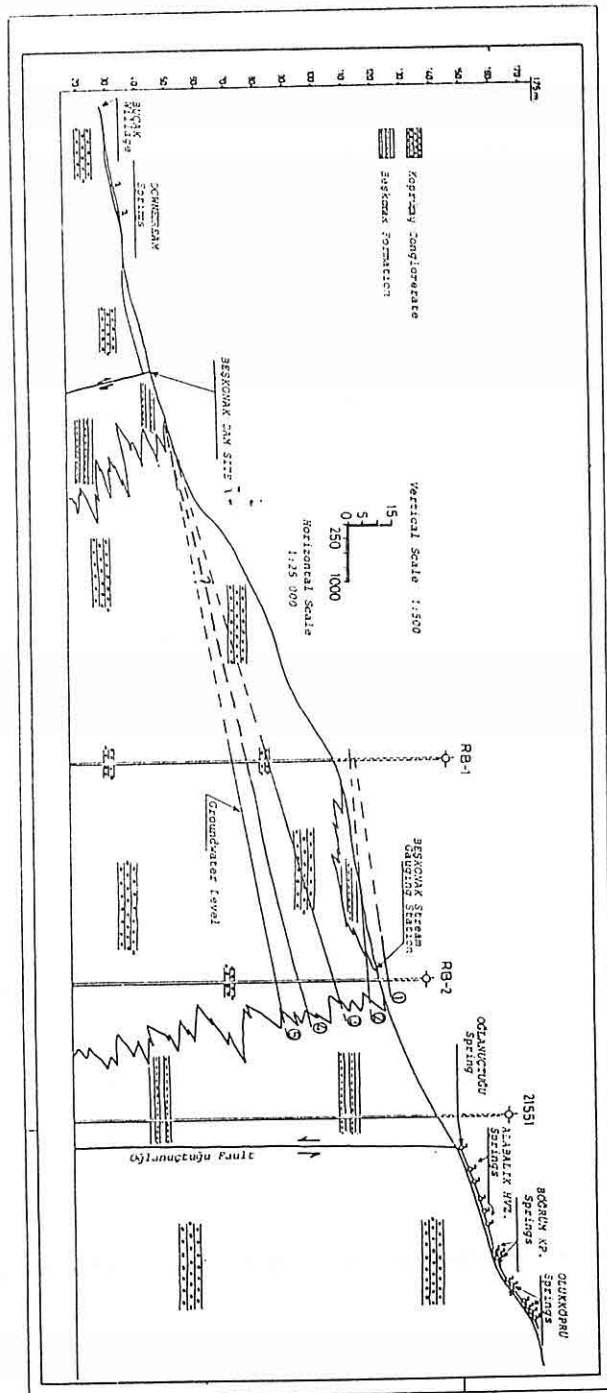
Fig. 2. Geological cross-section along Köprüçay river showing the groundwater-river relationship

1, 2, 3, 4, 5, indicate groundwater levels measured at different times: (1) December 1985, (2) April 1985, (3) May 1985, (4) July 1985, (5) October 1985

3. KARSTIFICATION AT DAM SITE AND ITS VICINITY

The right bank of the dam site is covered completely by conglomerate.Whereas the conglomerates outcrops only over a strip along the river with a width of 200 m on the left bank. Further inland on the left bank, the impervious Beşkonak Formation outcrops which overlies the conglomerate unit (Fig. 1).

Karstification in the region has been developed especially along the faults, cracks, fissures and joint systems. Solutional structures that are exist within the valley at the dam site indicate that the karstification has also developed along the bedding planes. Moreover, four caves that have been developed along the bedding planes at the downstream area of the damsite can be considered as an evidence for the karstification along bedding planes in the region.

3.1. Type, Size and Distribution of Karstification

Evaluation of karstification has been achieved by analyzing the data obtained from the galleries and boreholes drilled by the Electrical Power Resources Survey and Development Administration/EIE, 1973, (Fig. 4).

Based on the results of lugeon tests carried out in the boreholes and observations in the galleries, the following conclusions were made concerning the type, size and distribution of karstification in the region.

3.2.Size of Solution Cavities

The relation between elevation and the width of the cracks and cavities that were determined within the observation boreholes drilled at the dam site by EİE (1973) is shown in Figure 5. The average opening of the solution cavities is 0,9 cm, a maximum width of 4 m was found in LS-11 borehole at an elevation of 68 m below the sea level. The majority of the cracks have an opening of 0.2-0.5 cm and constitue 42% of the total measured samples. Cracks with an opening of 5 cm is only 1% of the total (EPDC, 1983).

The study carried out in the galleries revealed that most of the cracks, solution canals and cavities are filled with clay and calcite aggregate. The average opening of the cracks an solution canals determined in the galleries is about 1.1-3.3 cm. The maximum opening is 80 cm (LT-1, 46th m). 70% of the cracks have an opening of smaller than 2 cm. Openings more than 10 cm are observed in 7% of the total cracks. Average opening that is determined in large cavities is about 26-60 cm. The maximum size is about 150*300 cm (RT-4, 43rd m) and 58% of them have an opening between 10-50 cm while only 5% of the total has openings larger than 100 cm.

3.3. Karstification Depth

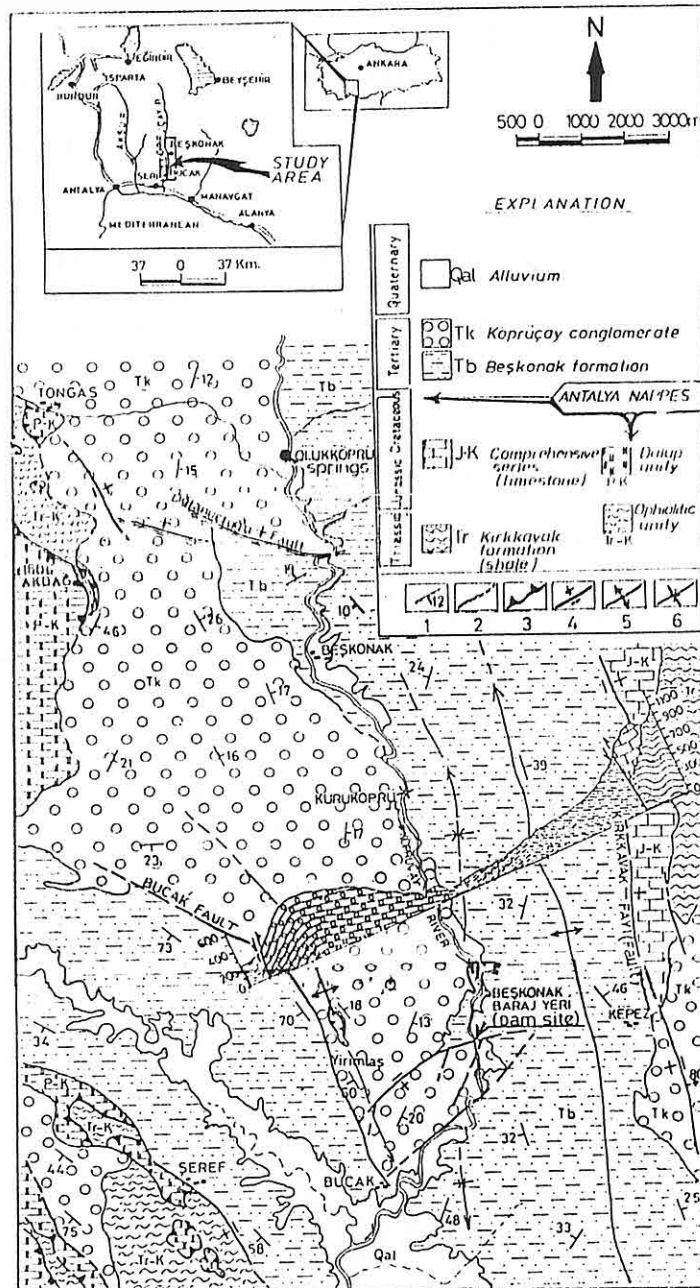In order to determine the variation of karstification with depth, water pressure tests
258

1. Strike and dip of bed, 2. Lithological boundary, 3. Overthrust, 4. Fault, 5. Anticline, 6. Sycline

Fig. 1. Geological map of the Beşkonak dam and its vicinity

257

1. INTRODUCTION

Beşkonak dam and hydroelectric power plant are planned to be constructed on the Köprüçay river, 40 km east of the Antalya city (Fig. 1). The dam site is situated in the most imported karst region of Turkey, namely, Western Taurids Karst Area. Three major problems associated with the dam construction in karst terranes are present in the study area: 1) water losses, especially in the dam site and its vicinity, 2) the grouting curtain planned to be build in order to prevent these water losses and, 3) surface water-ground water relations in the area. Within the content of this study, especially in the dam site and its vicinity, the type, dimension, distribution, and depth of karstification developed in conglomerates have been investigated by means of Lugeon tests and observations and inspections in the galleries and by caving studies .

2. KARSTIFICATION IN BEŞKONAK DAM RESERVOIR AREA AND ITS VICINITY

The left bank of the reservoir area is completely covered by the impervious Beşkonak Formation and thus no karstification has developed here. On the other hand, the Köprüçay conglomerate which outcrops on the right bank (Fig. 1) is composed by limestone gravels within a carbonate matrix and is highly karstified along faults, cracks and joint sets.

At the northern end of the reservoir area, Olukköprü karst springs emerge from the conglomerates with a discharge rate of more than 30 m^3/s even during the most dry season. Within the conglomerates that outcrop at the north and northwest part of the springs, typical joint systems have developed with openings ranging from the order of decimeter to one meter and with a mean strike of N25W. A rough topography resembling a forest of stones has been developed in the region as a result of the karstification processes along these mostly vertical joint systems (Photo 1). Apparently, the karstification is not limited at the surface, it may continue at great depths under the ground. Field observations and analyses of the joint systems suggest that Olukköprü springs discharge along these joint systems. Existence of the 530 m long Kuruköprü cave around the central part of the reservoir area is another typical example for karstification in this region.

Based on 3 years-long water level observations made within the boreholes RB-1 and RB-2, which are drilled at the right bank of the river in the reservoir area, the water table rises to about 5-10 m above the river during rainy seasons and declines down to about 35-40 m below the river level during dry seasons (Fig. 2). Consequently, a karstification zone has been developed at the fluctuation zone of the water table of 40-50 m. This can also be seen from the water pressure tests (lugeon) carried out at the boreholes RB-1 and RB-2. Kuruköprü cave, located near borehole RB-1 is an active cave developed within the mentioned karstic zone (Fig. 3).

256

KARSTIFICATION AT THE BEŞKONAK DAM SITE
AND RESERVOIR AREA

M. DEĞİRMENCİ

Cumhuriyet University, Environmental Engineering Department, Campus 58140
Sivas / Türkiye

ABSTRACT : *Beşkonak dam and hydroelectric power plant are planned to be constructed on the Köprüçay river, 40 km east of the Antalya city. In the dam site and reservoir area, Köprüçay conglomerates of Miocene age and Beşkonak Formation alternating with each other horizontally and vertically crop out. Köprüçay conglomerates with the components of limestone fragments and carbonate texture are, karstic and permeable, whereas, the Beşkonak Formation is impermeable.*

At the northern edge of the reservoir area, Olukköprü karst springs with a minimum discharge of 30 m³/s take place. These springs discharge mostly through vertical and subvertical joint systems. As a result of intensive superficial karstification developed along the joint systems in the area, the terrain reveals a view of columns of rocks; the so called "fairy chimneys" structures. Apart from the superficial karst features, Olukköprü springs represent a large and continuos system of underground solution cavities. In the Köprüçay basin, numereous karstic features such as dolins, sinkholes and caves developed within the conglomerates have been determined. Within the reservoir area, Kuruköprü cave with a length of 530 m, can be named as a typical example of these caves developed within the conglomerates. In some parts of the reservoir area, where the ground water level is lower than the surface river elevation, a highly developed karstification zone is present within the fluctuation range of groundwater occurring between the depths of 40-50 m.

The above mentioned Kuruköprü cave is an active cave developed in this fluctuation zone in the dam site and its vicinity, solution conduits developed along the system of mostly vertical fractures and joints are interconnected, thus, giving rise to a 3 dimentional conduit network. On the other hand, majority of these conduits have clay and calcite filling materials. The karstification in the dam site varies with depth exponentialy. Avaliable data suggest that karstification in the study area has a vertical extention as deep as -220 m.

255

Bernard, A.J., 1971. Metallogenic Processes of Intra-Karstic Sedimentation: 8.Int.Sed.Congress, Ores in Sediments, Heidelberg, 43-58.

Bernard, A.J., 1977. Quelques réflexions sur la genèse de gisements du type de Mississipi. Sciences de la terre, 21(3), 271-302, Nancy.

Church, T.M., 1979. Marine barite-occurence and origine. In marine Minerals, 6. Review Mineralogy. Min.Soc.Amer.Ribbe(Ed.).

Cadek, J., Matkovsky, M., Sulcek, 2., 1968. Geo-chemical significane of ore components:XXIII Int.Geo.Congress, 6. 161-168.

Çevrim, M., Echele, W., 1987. Ayhan, 1987'ye cevap. Türkiye Jeoloji Bült. 30, 84-86, Ankara.

Ginsbourg, I.I., 1986. Karst und Erzbildung:Zeitschr. F.Angew Geol., 12, 2, 67-71.

Gözübol, A.M., Gürpınar, O., 1980."Kahramanmaraş Kuzeyinin Jeolojisi ve Tektonik Evrimi". Türkiye 5.Petrol Kong. 5, 21-29, Ankara.

Haynes, S.L. and Mostaghel, M.A., 1982. Present-day precipitation of Head and zinc from ground-waters. Min.Dep., 17,213-228.

Lange, S., Chaudhuri, S. and Clauer, N., 1983. Strontium isotopic Evidence for the Origin of Barites and sulfides from the Mississipi Valley-Type Ore Deposits in Southeast Missouri. Econ. Geol. 78, 1255-1261.

Önalan, M., 1986.Kahramanmaraş Tersiyer İstifinin Sedimanter özellikleri ve Çökelme Ortamları. İ.Ü.Yerbilimleri derg.5/1-2, 39-78, İstanbul.

Önalan, M., 1988.Kahramanmaraş Tersiyer Kenar Havzasının Jeolojik Evrimi. Türkiye Jeoloji Bült.31., 1-10, Ankara.

Sungurlu, O., 1972. Gölbaşı-Gerger Arasındaki Sahanın Jeolojisi. T.P.A.O.No:802 (Rapport inedit), Ankara.

Tischendorf, G., 1963. Veber SrSO4 Von Baryt als ein Kriterium füı dessen Bildungsbedngungen. Symp. of the Origin of Posmamatic Ore Deposition, 225-229.

Yıldırım, M., 1989.Kahramanmaraş Kuzeyindeki (Engizek-Nurhak Dağları)Tektonik Birliklerin Jeolojik, Petrolojik İncelemesi. Doktora Tezi. İ.Ü.Fen bilimleri Enstitüsü, 3055, İstanbul.

Yiğitbaş, E.1989.Engizek Dağı(Kahramanmaraş) dolaylarındaki Tektonik Birliklerin Petrolojik İncelemesi. Doktora Tezi, İ.Ü. Fen Bilimleri Enstitüsü. 34, İstanbul.

Yılmaz, Y., Gürpınar, M.A., Kozlu, H., Yıldırım, M., Yiğitbaş, E., Genç, C., Keskin, M., 1985. Maraş kuzeyinin Jeolojisi(Engizek-Berit-Nurhak-Binboğa-Andırın Dağları). TPAO, No:2028, 161 S(Rappor inédit), Ankara.

Yılmaz, Y. and yiğitbaş, E., 1990. The tectonic setting and geological significance of the different ophiolitic and metomorphic units of SE Anatolie,8. Petrol kongresi, 12, 23-24, Ankara.

254

de galène (se trouvant au centre) au minerai oxydé de composition smithsonit+anglésite+serusite±limonite. Cette observation a été verifiée également au microscope métallographique et à la microsonde.

La recherche nous amenera à determiner les réserves exploitables régionales du minerai et attribue des modèles de genèse aux diverses minéralisations. Elle permettra ainsi de réaliser des contributions très importantes à la métallogénie de Pb-Zn en général.

11. REMERCIEMENT

12. REFERENCES

Akçakoca, A.B., Bahçeci, A., 1972. Berit Dağı ve Yöresindeki Demir Prospeksiyonunun Jeolojik Raporu. MTA Enst.(Rappor inédit), Ankara.

Anıl, M., 1989. Les gisements de barytine et la minéralisation plombo-zincifère de la région de Kahramanmaraş. Geosound, 17 bis, 161-173., Lefkoşa.

Anıl, M., 1990. Pozantı-Karsantı, Mersin ve Kızıldağ(Hatay) Ofiyolitlerindeki Bazı Kromit Yataklarının Morfolojik-Yapısal ve Jenetik Özellikleriyle Akdeniz Bölgesindeki Benzer Kromit Yataklarının Karşılaştırılması. Doğa, 14, 645-675, Ankara.

Anıl, M., 1992. Engizek(Kahramanmaraş Kuzeyi) Baritli-Kurşun ve Çinko Yataklarının Jeolojik, Metalojenik ve Ekonomik İncelemesi: Tübitak, YBAG-0005 (Rapport inedit), Ankara.

Ayhan, 1983. Aladağ(Yahyalı-Çamardı)Yöresi Karbonatlı Kurşun-Çinko Yatakları. T.J.K Bült. 26, 107-116, Ankara.

Ayhan, A., 1984. Genetic comparison of lead-zince de deposits of Central Taurus. Geology of the Taurus Belt, 335-342, Ankara.

Ayhan, A., 1987. Aladağlarda Paleokarstlaşmaya Bağlı Pb-Zn Mineralizasyonu (Tartışma ve Yanıt). Türkiye Jeoloji Bült. 30, 81-84, Ankara.

Barnes, H.L., 1979. Geochemistry of Hydrothermal Ore Deposits. Holt Rinehart and Winston, New York.

Baydar, O., 1989. Berit, Kandil Dağları(Kahramanmaraş) ve civarının Jeolojisi. Doktora Tezi. İ.Ü.Fen bil.Enst., İstanbul.

Berger, B., 1985. Les gisements de barytine-pyrite-oxyde de fer de la région de Santa-Anna (Alpes Apuanes, Toscane, Italie). Thèse, I.N.P.L.-C.R.P.G., 264 P, Nancy.

Dans la mine de Masat et le secteur d'Olukbaşı-Pınarlar on observe en plusieurs endroits la galène, la sphalérite et la baryte déposés dans les filons et poches. L'origine du minerai pourrait se trouver dans le magmatisme acidique de la région voisine où la galène, la sphalérite, la pyrite et la barytine sont produites par les activités hydrothermales. Le volcanisme tertiare est vraissemblable la source de ces activités. Les fractures et les cavités déja présentes ont dû être comblées grâce aux solutions hydrothermales classiques. Ayhan(1984), Çevrim(1986), proposent un modèle similaire de genèse pour la minéralisation primaire sulfurée de Pb-Zn-Ba.

*Le modèle d'oxydation et de l'altération météorique.

Après mise en place du minerai sulfuré dans les zones fracturés des roches encaissantes une altérat ion météorique bien poussée aurait dissout le minerai sulfuré. Le problème du transportet de la dissolution de Pb-Zn-Ba divers discutés par auteurs (Ginsbourg, 1966; Cadek et al., 1968; Roberts, 1967; Bernard, 1971-1977; Barnes, 1979; Haynes et Mostalegel, 1982). Selon ces auteurs les Pb-Zn peuvent être transportés généralement sous forme d'ions ou absorbés par des matérieux adsorptifs, comme la chlorite, le sulfate, le sulfite, le bisulfite, les complexes organiques et les ions d'hydrogène.

La solution riche en Pb-Zn-Ba est circulée dans les réseaux de fracture de l'encaissant carbonaté permettant une cristalisation du minerai sous la condition suivante:

-Si elle circule dans un milieu réductrice complète, seul l'ion S^{--} est présent, donnera la galène et la sphalérite mais le baryum ne précipitera pas.

-Si elle circule dans un milieu où la réduction est nulle, seul ion SO_4^{--} est présent,donnera alors la barytine et peut-être l'anglésite.

-Si elle circule dans un milieu où la réduction incomplète et les ions SO_4^{--} et S^{--} sont présents, donnera la galène, la sphalérite et la baryte en raison de la faible production d'hydrogène sulfuré mais le zinc sera souvent très mal présenté.

La minéralisation oxydée de la région étudiée a vraissemblablement un caractère supergène et formée par la transformation de minerai sulfuré. Cette transformation se développe sans doute de la façon suivante:

La galène donne l'anglésite en milieux oxydant et la sérusite en milieux très peu reductrice.Les ions de CO_3^{--} y existent toujours. La sphalérite donne facilement la smithsonite pendant cette transformation.

*Le modèle karstique

Un troisième modèle de genèse peut-être proposé pour les minéralisation de la région d'Engizek. On observe frequemment surtout dans les mines contenant du minerai oxydé et carbonaté des remplissages concrétionnés. On constate dans la même zone minéralisée une paragenèse mixte sulfurée-oxydée. On observe parfois à l'oeil nu une transformation

252

1-Minerai oxydé et carbonaté. On y observe souvent une forme de l'entille contenant des lits concentriques.

2-Minerai de smithsonite+anglésite+sérusite montrant une structure en concrétion et mamelonnaire.

3-Transformation en anglésite+sérusite autour d'un cristal de galène

4-Remplissage de barytine (Ba), vraissemblablement dans les cavités de fusion de calcaire. La germination de barytine est légèrement visible autour des cavités qui sont remplies tès souvent d'argile.
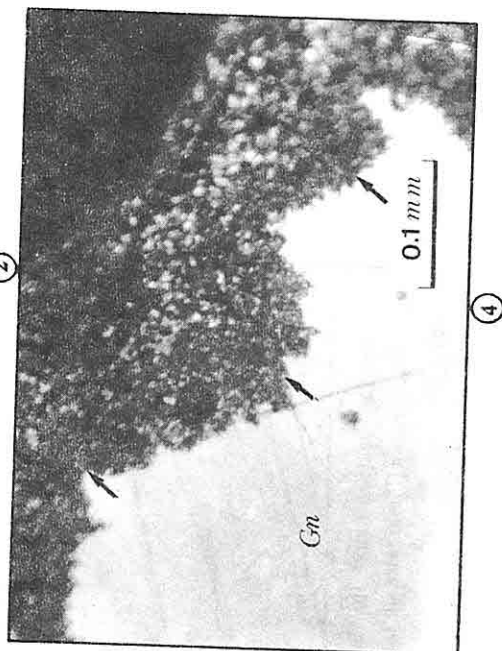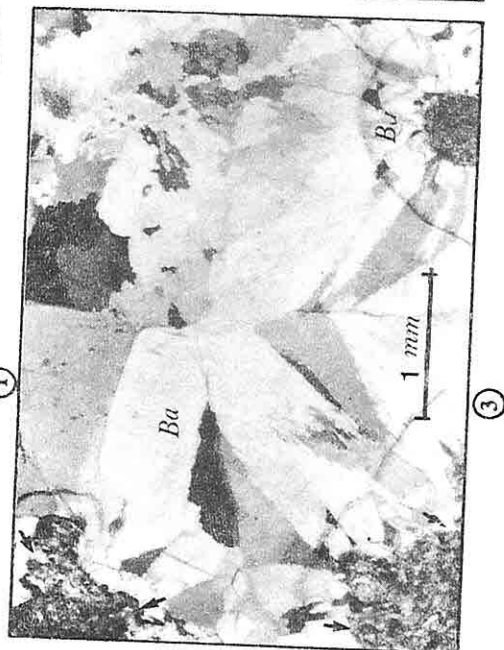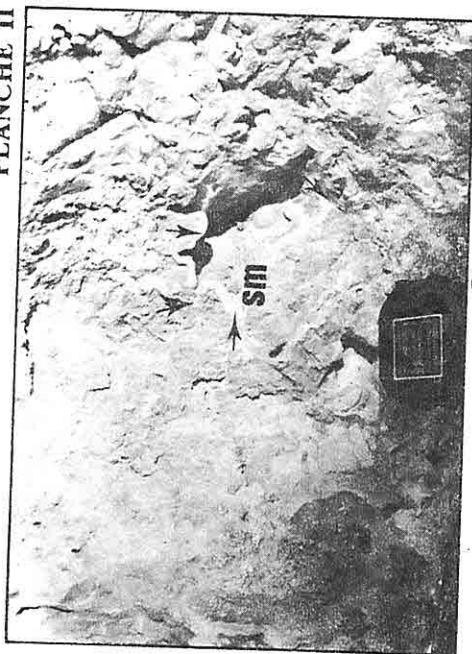
1-Les métamorphites de Malatya constituent souvent des reliefs assez forts (plus de 2500 m). On observe parfois la minéralisation de barytine (Ba) au long de la faille verticale (Photo prise près du sommet de Karataş).

2-La déformation de tectonites harzburgitiques. L'olivine est granulée et l'enstatite est allongée. La serpentinisation se développe en commençant par les fractures de cristaux d'olivine (Microphoto, L.P.).

3-Formation outochtone de Midyat. Le calcaire aux lits minces sub-horizontaux gris-blancheâtre vers le sommet (Photo prise sur la route stabilisée de Bertiz-Kahramanmaraş.

4-Formation outochtone de Beşenli. Elle est caractéristique par sa couleur rougeâtre. Elle est composée de grès, de marne et d'argiles de différentes couleurs(Photo prise près du village de Maksutlu).
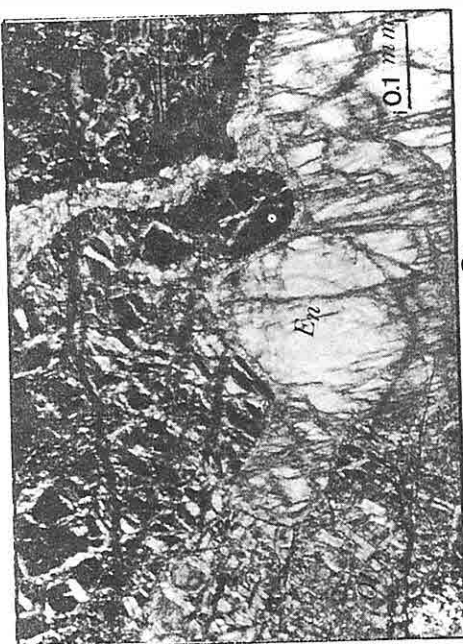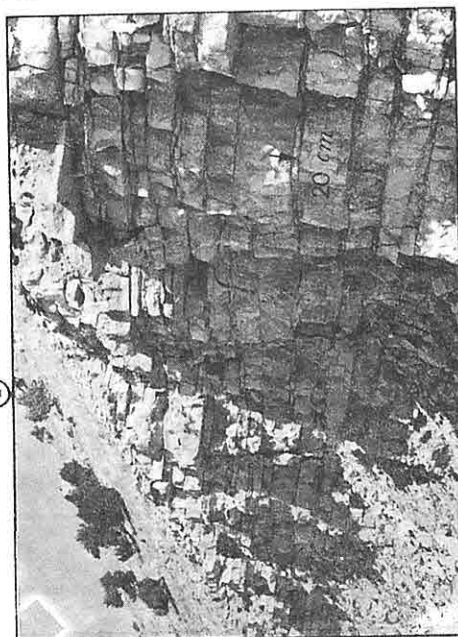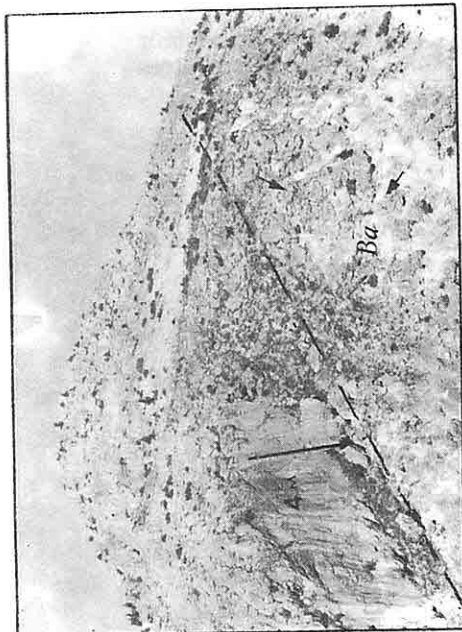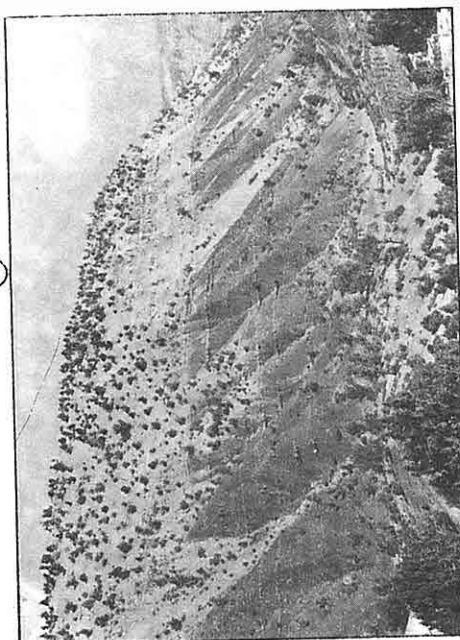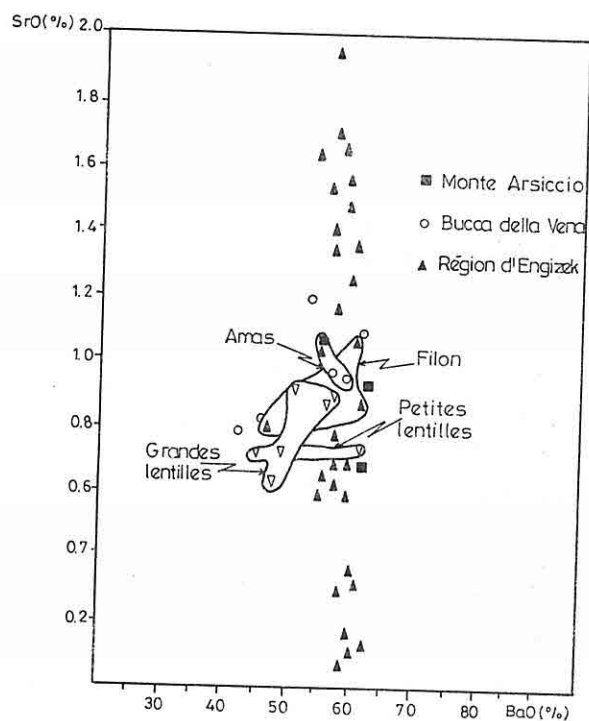
Fig.3. Diagramme SrO=f(BaO) pour le minerai de barytine du secteur d'Engizek (triangles noirs) et comparaison avec celle d'autres regions smilaires (d'après Berger, 1985).
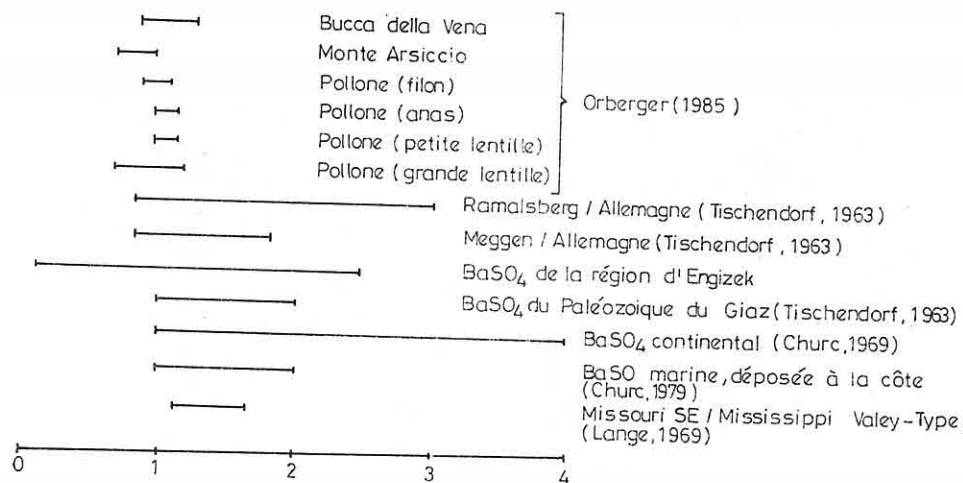

Fig.4. Comparaisons des teneurs en Sr de barytine de la région d'Engizek avec celles des barytines des autres régions.

247

Tableau 2. Analyse au microsonde de galène et de barytine dans le secteur carbonaté d'Engizek (1-41:Galène, 42-68:Barytine).

Numéros des échantillons

Elements	1	2	3	4	5	6	7	8	9	10	11	12	13	14
S	13.43	13.34	13.10	13.27	13.05	12.95	13.28	13.34	13.32	13.22	13.40	13.17	13.68	13.18
Pb	86.56	86.98	86.88	86.14	85.66	87.26	86.10	86.96	86.49	86.28	85.92	86.07	87.49	87.00
Bi	-	0.08	0.24	-	-	-	-	-	-	-	-	-	-	-
Ag	0.06	0.02	-	-	0.10	0.13	-	-	-	0.01	-	-	-	0.11
Total	100.05	100.43	100.22	99.40	98.81	100.33	99.39	99.30	99.81	99.51	99.31	99.23	101.17	100.29

2	15	16	17	18	19	20	21	22	23	24	25	26	27	28
S	13.32	13.21	13.19	9.47	13.18	13.04	12.94	13.26	12.77	13.16	13.23	13.19	13.26	13.22
Pb	86.12	86.08	85.74	85.99	87.69	86.55	85.77	86.96	83.67	86.53	86.44	86.63	84.86	87.03
Bi	-	-	-	0.16	-	-	-	-	-	-	-	-	-	-
Ag	-	-	0.05	-	-	-	0.11	0.25	0.06	0.13	0.04	0.08	-	0.05
Total	99.44	99.29	98.98	95.62	100.88	99.68	98.82	99.46	96.58	99.82	99.71	99.91	97.62	100.30

3	29	30	31	32	33	34	35	36	37	38	39	40	41	
S	13.04	13.00	13.13	13.19	13.17	13.27	13.35	12.98	12.85	13.40	12.90	13.36	13.08	
Pb	85.85	86.75	87.55	85.48	85.18	86.19	87.27	86.67	85.57	86.73	82.05	86.93	86.29	
Bi	-	0.16	-	-	-	-	-	-	-	-	-	-	-	
Ag	-	-	-	-	0.13	-	0.04	0.02	-	0.10	0.14	-	-	
Total	98.90	99.90	100.68	100.17	99.45	99.45	100.83	99.66	98.42	100.23	95.26	100.40	99.37	

4	42	43	44	45	46	47	48	49	50	51	52	53	54	55
Ba	57.57	58.84	58.76	58.58	59.03	85.00	57.52	58.91	57.79	58.28	56.32	58.13	58.56	58.83
S	13.57	13.98	13.47	13.49	13.17	13.97	13.97	13.36	13.48	13.25	13.63	14.09	13.65	13.37
Sr	0.72	0.32	0.19	0.07	0.13	0.93	0.78	0.18	0.63	0.60	2.46	0.35	0.14	0.70
O	28.13	26.86	27.59	27.86	27.67	27.61	28.42	27.55	28.10	27.87	27.60	27.43	27.65	27.84
Total	100.00	100.00	100.00	100.00	100.00	100.00	100.00	100.00	100.00	100.00	100.26	100.00	100.00	100.00

5	56	57	58	59	60	61	62	63	64	65	66	67	68	
Ba	56.83	57.18	56.63	56.81	57.10	57.18	56.84	57.47	57.33	57.41	57.48	57.04	57.91	
S	13.51	13.45	13.45	13.77	13.83	14.06	13.94	13.73	13.69	13.74	13.31	13.55	13.44	
Sr	1.65	1.67	1.73	1.35	1.94	1.47	1.75	1.37	1.52	1.19	1.27	1.41	1.52	
O	28.01	27.70	28.19	28.08	27.13	27.30	27.47	27.43	27.47	27.66	27.94	28.01	27.13	
Total	100.00	100.00	100.00	100.00	100.00	100.00	100.00	100.00	100.00	100.00	100.26	100.00	100.00'	

246

Cameca sous la condution de 15 Kw, 2 Ma et 6s. S, Pb, Bi, Ag dans les cristaux de galène et Ba, S, Sr, O dans les cristaux de barytine ont été recherchés et les résultats sont rapportés dans le tableau 2.

En étudiant ce tableau on peut conclure que la distribution de soufre varie entre 12.90-13.68 % et ceci exprime une décalage étroite. L'argent natif observé en pétite quantité dans les sections polies est ainsi verifiée par la microsonde. La quantité de l'argent varie de 0.04 au 0.16 %. Par ailleur le rappor Bi/Pb ne change pas beaucoup dans le 41 point.

Les analyses dans la phase du cristal de barytine font apparaitre une proportion assez élevée de Ba. On y observe aussi une pourcentage importante (0.07-2.46 %) de Sr. Ces valeurs expriment une substitution considédable entre Ba et Sr.

En utilisant ces valeurs de Sr et Ba la minéralisation barytinefère du secteur d'Engizek a été étudiée dans le diagramme de Ba=f(sr) et comparée avec d'autres régions (Fig.3). On remarque une différence entre les valeurs de Sr du secteur étudié et les minéralisations barytinifères de l'Europe et des Etats Unis. La barytine dans les alges italiens a une valeure en Sr de 0.62 au 1.22 %(Berger, 1985) alors que celle ci-varie de 0.07 au 2.46 % dans la barytine d'Engizek. La comparaison des valeurs en Sr du secteur étudé avec celles des autres régions indique qu'en dehors de Ramelsberg et Continantal elles sont plus ou moins similaires(Fig.4).

10. INTERPRETATIONS ET CONCLUSIONS GENERALES

L'histoire géologique de l'unité allochtone formée des roches métamorphites de Malatya est assez complexe. Cette série métamorphique est constituée à la base de quartzites, phyllites, calcschiste d'age Paléozoique et une couverture composée par des calcaires et des dolomies avec des intercalations de marne et de quartzite d'age Mesozoique au sommêt. Une masse ophiolitique est en contact tectonique avec les roches métamorphites de malatya. Les calcaires non métamorphiques les grès argileux et carbonatés du Crétacé les surmontent. L'unité autochtone est formée par plusieurs formations d'age Tertiaire. Toutes ces formations autochtone sont transgressives et présentent des contacts normaux entre elles.

La minéralisation Pb-Zn-Ba de la région apparait seulement dans les métamorphites de Malatya. Par contre, les corps minéralisés ne sont pas distribués d'une façon systématique par exemple dans un niveau lithostratigraphique préferentiel ou en concordanse avec des couches encaissantes carbonatées. Elle est surtout déposée dans les discontinuités de roches encaissantes soit sous forme de gilons et poches, soit en amas dans les cauités karsttiques. Etude des lames polies au microscope et à la microsonde nous conduisent à proposer trois modèles génétiques:

*Le modèle classique hydrothermal pour la minéralisation sulfurée.

245

plusieurs lames polies où ils sont transformés dans les clivages de galène. On les observent également en alternance avec les lits de smithsonite.

8. ETUDE CHIMIQUE

Les analyses chimiques des échantillons de minerais provenant de différents corps minéralisés indiquées dans le tableau I. La teneur en plomb et en zinc est assez élevée. La densité de barytine est plus de 4.14 gr/cm^2. La teneur moyenne du minerai est favorable pour l'exploitation mais la présence des minéraux sulfurés dans la paragenèse oxydée et carbonatée diminue leurs valeurs économiques.

Tableau 1. Teneurs du minerai en galène, en barytine et en oxydes de Pb-Zn-Ba

1	Numéros des échantillons									
Elemens	1	2	3	4	5	6	7	8	9	10
Pb %	82.80	75.60	65.55	33.70	32.65	6.85	5.16	17.60	5.65	7.13
Zn %	0.32	0.93	0.22	0.40	0.60	0.38	0.41	44.66	47.17	48.66
BaO %	1.40	0.90	15.30	40.20	24.50	55.20	57.60	1.70	2.10	3.10
Cu %	Trace	Trace	Trace	0.01	0.01	Trace	Trace	0.01	0.01	0.01
Ag gr/T	79	85	-	65	39	-	-	55	19	-

2	11	12	13	14	15	16	17	18	19	20	21
Pb %	8.91	8.41	3.68	0.57	16.76	6.16	2.16	3.20	4.10	3.20	4.17
Zn %	46.70	41.09	36.45	49.56	34.70	42.81	59.00	35.50	64.63	60.13	36.50
BaO %	2.85	3.01	3.36	2.98	3.27	-	-	-	-	-	-
Cu %	0.01	0.19	0.99	0.80	1.92	2.93	0.35	1.16	0.23	0.20	1.13
Fe %	5.72	5.42	10.00	1.94	5.27	8.60	7.36	5.22	4.61	3.92	7.14
Cd %	-	0.36	0.27	0.47	0.27	-	-	-	-	-	-
Si %	-	4.84	1.12	0.26	0.66	-	-	-	-	-	-
F %	-	0.020	0.009	0.005	0.10	-	-	-	-	-	-
Cl %	-	0.013	0.008	0.005	0.012	-	-	-	-	-	-
Ag gr/T	-	-	-	-	-	-	-	-	-	-	-

3	MA-90-33	MA-90-16	MA-90-23	MA-90-27	MA-91-10	MA-91-27
BaO	58.96	52.15	48.65	41.19	38.79	59.16
Pb	6.17	7.32	10.42	13.98	11.25	8.51
Zn	0.71	1.26	0.36	0.73	0.95	0.90
d=gr/cm^3	4.32	4.29	4.30	4.13	4.14	4.36

4	MA-91-33	MA-91-40	MA-91-41	MA-91-43	MA-91-4	MA-91-45
BaO	54.17	58.62	59.25	57.36	49.17	52.66
Pb	4.13	3.98	5.27	5.36	5.13	4.22
Zn	0.96	0.71	0.89	0.99	1.42	0.79
d=gr/cm^3	4.32	4.29	4.37	4.40	4.33	4.14
Légende						
1-5 minerai riche en galène; Minerai oxydé; MA-91/92: Minerai riche en barytine.						

9. ETUDE A LA MICROSONDE

Pour l'analyse à la microsonde sont préparées les lames polies du minerai riche en galène et du minerai riche en baryte. Les analyses ont été réalisées à la microsonde de

244

inclusions de sphalérite et de fahlerze. L'argent natif de moins de 10 μ s'observe ravement.L'anglésite (PbCO$_3$) et la sérusite (PbSO$_4$) se rencontrent en bordure des cristaux de galène(Planche I$_1$, Fig.3). La sphalérite constituant un deuxième minéral est assez rare. Elle est en petite plage et très souvent fracturée. Elle présente parfois des inclusions de chalcopyrite distribuées irregulièrement.

La sphalérite est tranformée généralement en smithsonite surtout quand elle est sous forme de cristaux fracturés.

La barytine, le quartz et parfois la calcite constituent la gangue. On constate également des filonnets tardifs de barytine qui traversent le minerai.

*Minerai riche en barytine

Ce minerai est constitué par des rubans et de gros cristaux de barytine. La barytine se présente toujours sous les même faciès aussi bien dans les minéralisations filoniennes que stratiformes. La barytine saccharoide soit caraclasée, soit depourvue de déformation se présente alors en grandes lattes(Planche II, fig.4). Elle présente parois une corrosion de dissolution par l'irrégularité ses bords.

La baryitine contient de la galène de petite dimmension soit en inclusions, soit en filonnets traversant la barytine elle même. Les cristaux de galène sont plus petits (moins de 0,2 μ) que ceux du minerai massif de galénite.

*Minerai oxydé et carbonaté(Smithsonit+Anglésite+Sérusite±Limonite)

Le minerai secondaire oxydé et carbonaté est constitué par une alternance de rubans de smithsonite, d'anglésite et sérusite. La limonite et parfois l'hématite s'associent au minerai surtout entre les rubans. La pyrite est très rarement présente. Ce minéral existant dans la paragenèse primaire est totalement ou partiellement transformé en limonite. On observe de place en place des minéraux argileux qui sont vraissemblablement formés plus recemment.

Le minerai oxydé provenant de mines de Masat et de Karamanlı contient de la galène. Elle s'y transforme en anglésite et sérusite à partir de sa périférie.

La smithsonite est plus abondante dans la paragenèse secondaire et déposée en remplaçant les carbonates de l'encaissant. Elle est souvent en cristaux xènomorphes. Rare cristaux automorphes ne se developpent que dans cavités géodiques. Suivant le degré de la contamination avec le fer, la smithsonite présente un coloration d'aspect zoné. Elle a porfois une structure dentritique entre lits concentriques formés par elle méme. D'autres minéraux du zinc. Comme l'hydrozincite et l'hemimorphite ne s'y observent que rarement.

L'anglésite et sérusite sont moins abondant que la smithsonite. Elles sont souvent sous forme des produits du remplissage. Ces deux minéraux sont nettement observés dans

243

Autres zones minéralisées

On observe encore dans plusieurs endroits du secteur étudié des indices minéralisés en galène, en baryte et à la fois des minéraux oxydés et carbonatés. Tous ces indices se situent aux niveaux très élevés dans la montagne d'Engizek et il n'existe aucune route stabilisée pour l'exploitation à ce jour. Après la première construction d'une route minière dans cette région tous les indices minéralisés peuvent avoir une importance économique.

6. OBSERVATION ET ETUDE MACROSCOPIQUE DU MINERAI

La minéralisation plombifère-zincifère est visible à l'oeil nu. Elle se présente sous forme de lentille, d'amas, filons, remplissages de cavité, bandes, veines dans l'encaissant carbonaté.

On distingue principalement trois types de minerai dans l'ensemble du secteur septentrional de Kahramanmaraş:
*Galénite massive barytinifère (minerai noir)
*Barytine massive avec des filonnets de galénite (minerai blanc)
*Minerai oxydé à smithsonite+sérusite+anglésite (minerai gris)

En plusieurs endroits le minerai a un caractère massif montrant parfois de gros cristaux cubiques de sulfure de plomb. Dans le minerai sulfuré (riche en galénite) la sphalérite est difficilement visible. On observe la barytine et la calcite qui cimentent les autres minéraux constituants.

La barytine massive avec des filonnets de galénite est un minerai caractéristique pour la zone d'Olukbaşı et Çataldere. Ce type minerai a une importance économique grâce à l'extention latérale. Il s'agit d'une minéralisation très riche en barytine (%95) qui est recoupée par plusieurs filonnets de galénite plus ou moins visible à l'oeil nu.

Un troisième type de minéralisation est observe dans le secteur de boyalı, de Kızılkaya et de Karamanlı. Cette minéralisation est complètement différente de deux premières. Il s'agit d'un remplissage de fractures et de cavités montrant souvent une structure en concrétion stalactique (lits concentriques plus ou moins réguliers) ou mamelonnaire avec une coloration grise, jaune, bleue et blanc laiteux(Panche II, Fig.2). Dans ce type de minerai on voit parfois de la galénite au milieu entousé des concrétions de minéraux oxydés comme la smithsonite+anglésite+serusite.

7. ETUDE MICROSCOPIQUE

Etude au microscope métallographique des échantilons permet de distinguer plusieurs types de minerai:

Minerai riche en galénite

Elle est souvent pur est pur et sous forme de grande plage. Elle présente parfois des

242

parfois des lits très minces de lignite.

Bien qu'on sache depuis une cinquantaine d'années l'existence, en plusieurs endroits, de ces minéralisations certaines ont seulement une importance économique relativement récente à cause du mauvais réseau routier. Cette zone minéralisée a une altitude de 1800-2500 m et elle est sous la neige pendant 4 mois par an. Pendant cette période le déplacement est vraiment difficile dans cette région septentrionale de Kahramanmaraş.

Corps Minéralisé

La zone de boyalı et Kızılkaya

Dans cette zone il existe principalement deux mines qui sont actuellement en cours d'exploitation. Au nord du village de Boyalı, on a des affleurements situés paralellement à la ligne de charriage. La minéralisation oxydée et carbonatée est déposée dans les fractures et les cavités karstiques de calcaires métamorphiques et de calcaires dolomitiques. On voit visiblement que le minerai s'est déplacé en suivant les résaux de fracture et les cavités de fusion dans les carbonates(Plance II, Fig.1). On a effectué des travaux miniers par l'intermédiaire d'une entreprise privée. On peut arriver à cette mine par une route stabilisée.

La zone de Çataldere

Cette zone minéralisée est située à 5 km au Nord-Est du village de Kaleköy. Elle a un relief de 2500 m et c'est pourquoi on n'y a pas accès pendant 4 mois en hiver à cause de la neige. Il existe deux tranchées de 3x2x4 m. On y voit une minéralisation de barytine avec des filonnets de galénite. Cette zone minéralisée n'est pas encore liée par une route stabilisée qui permet de réaliser des travaux nécessaires pour la recherche de l'extention du corps minéralisé en Ba-Pb-Zn.

La zone d'Olukbaşı et Eskiyayla

Cette zone est la plus importante zone économique du secteur étudié. On observe en plusieurs endroits des occurences très riches en galénite et en baryytine. Cette zone est située juste à la limite de la faille de Çataldere. On observe en surface une tranche de barytine de 100 m de long sur un largeur de 4 m. Les autres indices ont une distribution irrégulière dans les brèches le long de la faille de Çataldere.

La zone de Karamanlı

Cette zone est située au nord du village de Karamanlı. Elle a été exploitée pendant quelques années par une société privée mais à la suite d'une crise économique cette société a abandonné tous les travaux miniers. Il s'agit d'une minéralisation de smithsonite, anglesite et sérusité déposant dans les fractures des calcaires.

241

Ere	Système	Série	Formation	LITHOLOGIE	MILIEU
CENOZOIQUE	Tertiaire	Qua	Alluvion	Alluvions et terrasses fluviatiles, debris cimentés	
		Miocène	Bertiz	Lita énite-calcaire et shale de couleurs gris -roseverdâtre et brunâtre	BASSIN
			Beşenli	Grès gris, marne, argile avec de couleur bleuâtre -verdâtre, marne rouge-jaune	CONTINENTAL
			Lice	Calcaire crème aux lits gros	VERSANT
		Midyat		Litarènite grise aux extraclastes biomicrite -biosparite	MARGNALE EXTERIEUSE
				Calcaires marneux et argileux jaunâtre, blancheâtre	
		Eocène	Harami lu	Calcaire conglomératique	MARINE PROFONDE
MESOZOIQUE	Crétacé		Metaoph. de Berit	Grès-calcaire à sciste	MARINE PROFONDE
				Harzburgite serpentinisée, gabbro isotropique, lité et dolérite-diabase	MARINE
	Jurassique		METAMORPHITES DE MALATYA	Calcaire dolomitique,	PEU PROFONDE
				Calcaire micritique	
				Calcaire, recristalise aux lits gros	
	Trias			Calcaire greseux,	MARINE
				Grès-calcaires	
				Silt-stone à ciment carbonaté	
PALEOZOIQUE	Permo-Carbonifer			Calcaires recristalisés gris et blanches aux lits gros et moyens	PEU PROFONDE
				Calcaires dolomitiques foncés et bleuâtre aux lits gros et moyens	
	Avant du Permo-Carb			CONTACT NORMAL — Micaschistes quatzeux verdâtre à grenat	PEU PROFONDE

Fig.2. Profil stratigraphique synthétique de la région d'Engizek (Révisé d'après Önalan. 1986; Yıldırım, 1989; Yiğitbaş, 1989).

240

La formation de Bertiz, constituant le niveau supérieur des roches autochtones, affleure dans le village de Bertiz. Elle est composée de membres de Menzelet, Budaklı, Islampınarı, Çukurdere et Alikayası (Önalan, 1986). L'épaisseur de cette formation diminue vers l'ouest. Elle est constituée de litarénite, de calcaire et de shale. Elle a une couleur gris, rose et verdâtre. On lui attribue un âge Miocène inférieur au Miyocène moyen.

Les formations alluvionaires couvrent les plateaux et les vallées. Ces formations sont constituées de débris de métamophites de Malatya, de sable de différentes formations, d'argiles rouge et verdâtre.

4. TECTONIQUE

Les métamorphites de Malatya du secteur étudié ont subi plusieurs mouvements tectoniques et un métamorphisme régional. Dans les formations basales on observe différentes directions de fracturation et des plissements, aussi bien à l'échelle macroscopique, qu' à l'échelle microscopique.

Les métamorphites de Malatya ont été charrié à la fin du Crétacé supérieur sur les roches relativements autochtones. Elles constituent une nappe. On observe principalement deux caractéristiques tectoniques: les charriages et la formation des nappes.

On observe également dans les métamorphites de Malatya plusieurs failles qui sont plus ou moins parallèles l'une à l'autre et orientées très souvent Est-Ouest. Les failles d'Engizek et de Çataldere peuvent être considérées comme les plus importantes de ces failles(Fig.1). On observe aussi des plissements. L'un de ces plissement est situé juste près de la ligne de charriage en commençant au village de Boyalı et se terminant au village d'Hompur. Les métamorphites de Malatya qui ont subi une bousculade du Nord vers le Sud présentent des plissement à l'échelle macroscopique et microscopique. Par ailleurs dans les calcaires métamorphiques(marbres) on voit des anticlinals et synclinals orientés Est-Ouest. L'étude structurale montre que tous ces mouvements tectoniques sont développés à partir du Crétacé supérieur par une bousculade du Nord vers le Sud.

Dans les formations autochtones du secteur étudié ont été repérées des failles réelles et supposées. Sur le terrain, elles sont très peu visibles, et dépourvues de miroirs. Elles sont aussi orientées très souvent Est-Ouest (Fig.1). On observe un anticlinal et un synclinal orientés NE-SW près du village de Kemalli.

La série stratigraphique a été représentée de manière synthétique dans la figure 2 pour démontrer les relations du contact entre la série allochtone et autochtone.

5. DESCRIPTION DES GISEMENTS ET DU MINERAI

Il existe plusieurs indices et corps minéralisés de Pb-Zn-Ba dans la région d'Engizek. Toutes ces minéralisations sont déposées seulement dans les métamorphites de Malatya. Les roches autochtones sont presque stériles sauf quelques petites indices de limonite et

recristalisés. L'étude microscopique de ce calcaire recristalisé montre qu'il s'agit d'une roche métamorphique de paragenèse quartz, grenat, muscovite et minéraux opaques. Cette paragnèse permet de dire que les lentilles appartenant aux métamorphites de Malatya sont certainement placées tectoniquement dans la formation d'Harami.

La formation de Gozlu est en discordance avec les roches métamorphites de Malatya et la formation d'Harami. Elle affleure seulement près de Kızılkaya Tepe. Cette formation est composée des débris de calcaire recristalisé(marbre), de calcaire gris-beige et rougeâtre et de calcaire à nummulite dans une metrixe de shale. On a déterminé des fossiles daré de l'Eocène Moyen (Yıldırım, 1989).

Les autochtones

La moitié du secteur étudié est couvert par des formations autochtones: formation de Midyat, de Lice, de Beşenli et de Bertiz.

La formation de Midyat constituant la base de la couverture autochtone affleure dans une direction Est-Ouest et elle présente un relief assez fort. Sa continuation latérale est recoupée par plusieurs failles. Elle est composée à la base de calcaire biomicritique avec des bancs minces ou moyen dans lequels on observe parfois des nodules de chert. On observe parfois des bancs minces et moyen avec une couleur foncée vers le milieu de la série. Cette formation se termine avec des lits minces (moins de 20 cm) de couleur grise et blanche avec alternance de niveaux de silex(Planche I, fig.3). La formation a une épaisseur de 250-300 m et contient des fossiles d'âge Miocène (Erdoğan, 1975; Önalan, 1986; Yıldırım, 1989; Anıl, 1992).

La formation de Lice affleure l'Anatolie du Sud-Est et est nommée pour la première fois par Schmidt(1958 in Yıldırım, 1989) près de la ville de Lice. Cette formation affleure seulement par de ses deux membres: membre de Tunaboylu et le membre d'Atlık. Cette formation est constituée de calcaire de couleur grise, brunâtre et beige présentant une alternance avec le shale et litarénite. Elle a une épaisseur considérable à l'Ouest de Çağlayancerit par contre vers Ahırdağ elle continue en transition mince sur la formation de Midyat. Önalan(1986) signale des fossiles dans les calcaires extraclastiques qui permettent de les dater de l'Aquitanien-Burdugalien.

La formation de Beşenli est une formation très connue dans la région de Kahramanmaraş. Elle est caractéristique par sa couleur rougeâtre(Planche I, Fig.4). Elle présente une série épaisse qui est composée de grès gris, de marne, d'argiles de différente couleur et de l'alternance de shale-marne. Toutes ces roches peu consolidées se distinguent facilement des autres formations voisines par leurs couleurs frapantes. Cette formation est concordante à la base et passe transitionellement aux formation de Mityat et Lice vers le sommet. Elle est couverte par la formation de Bertiz. Önalan (1986), et Yıldırım (1989) attribuent un âge Miocène moyen-Miocène supérieur.

238

serpentinisée.

*Les minéraux opaques sont plus ou moins observables dans la roche.

Les gabbros à clinopyroxène sont moins abondants que les gabbronorites. Ils sont composés essentiellement de clinopyroxène, plagioclase et de minéraux opaques.

*Le clinopyroxène constitue de 35-45 % de la roche. Il s'agit d'augite qui est d'une part un minéral cumulus d'autre part englobant les plagioclases et les minéraux opaques.

*Le plagioclase est aussi abondant que le clinopyroxène, maclé albite-carlsbad non zoné (An75-85).Il est également un minéral cumulus et post-cumulus

*Les minéraux opaques sont essentiellement interstitiels.

Les gabbros amphibolitiques sont souvent rencontrés dans le secteur étudié. On n'observe ni foliation ni linéation. Il s'agit d'une accumulation d'hornblendes vertes et parfois bleuâtres dans la roche. Ces dernières sont parfois transformées en chlorite. Au dehors du secteur étudié on a déterminé les amphiboles magmatiques (Anıl et Martin, 1992, travaux en cours) dans les gabbros de la région de Kahramanmaraş mais les hornblendes vertes qu'on y rencontre seraient d'origine secondaire bien que les reliques de pyroxène ne soient pas facilement observables. Il ne faut pas oublier par ailleurs que cette zone étudiée est fortement tectonisée et dériverait probablement des gabbros à clinopyroxène ou des gabbros anarthositiques.

Les gabbros noritiques situés au niveau supérieur des cumulats gabbroiques, ont un caractère significatif avec la présence de clinopyroxène ou orthopyroxène ferrifère et minéraux opaques titanifères (titanomagnetite et/ou ilménite; déterminé par microsonde). On observe aussi quelques fois de l'apatite.

*Le clinopyroxène abondant(35 %) est composé d'augite riche en fer, l'orthopyroxène (5-10 %) est composé d'hypesthène riche en fer, Le plagioclase abondant (50 %) frais est maclé d'albite. Les minéraux opaques très abondant(10-15 %) sont la titanomagnetite ou l'ilménite. Ils se présentent en nodules interstitiels et amiboides entourant les pyroxènes ou plagioclases.

Signalons que le massif métaophiolitique de Berit contient pafois des chromites. Il s'agit de deux types de gisement: chromites podiformes en lentilles, filons et poches avec une enveloppe dunitique dans les tectonites harzburgitiques et les bandes riches en chromite dans les lits de dunite.

Autres formations sédimentaires allochtones

Il s'agit de deux formations affleurant au sud de la montagne d'Engizek:Harami et Gozlu. La formation d'Harami est constituée de marne de couleur crème à jaunâtre et beige; de calcaire, de grès carbonaté, de calcaire à chert, de grès turbiditique et de calcaire argileux. Cette formation passe transitionellement aux métamorphites de Malatya. Elle a une épaisseur de 250 m. A la base de cette formation on observe des lentilles de calcaires

237

de gabbros lités, de gabbros amphibolitiques. On distingue par ailleurs de gabbronorite à olivine,de la gabbronorite, des gabbros à clinopyroxène, et des gabbros noritiques dans les different endroits de la région de Kahramanmaraş (Yiğitbaş, 1989; Yıldırım, 1989; Anıl, 1990; Yılmaz et al., 1990).

Les harzburgites sont presque complètement transformées en minéraux de serpentine. Les contacts entre les minéraux constituants ne sont pas visibles à cause de l'intensité tectonique. La roche est fortement fracturée en plusieurs directions et à l'intérieur des fractures on observe parfois un remplissage par des filonnets de gabbro et de pyroxène à texture pegmatitique.

L'étude microscopique de cette roche montre également une déformation à haute température. La granulation est développée dans les olivines de sort que les enstatites sont allongées, bouclées et tordues. La serpentinisation est bien poussée en commençant par des fractures de cristaux d'olivine. Les chrysotiles et lizaradites abondantes sont observables par le méthode optique. L'antigorite est très rare et n'est pas visible au microscope.

Les gabbros massifs et lités sont abondants entre Boyalı et Hompur. Les roches sont également fortement altérées au long de la zone charriée.

Les gabbros massifs surmontent les cumulats ultramafiques dont le passage est souvent tectonique. Le contact entre les gabbros massifs et litées n'est pas aussi bien visible à cause d'un fort broyage.

L'étude microscopique de différents types de gabbros permet de distinguer plusieurs faciès pétrographiques:

- Gabbronorites et Anorthosites
- Gabbros à clinopyroxène
- Gabbros amphibolitiques
- Gabbros noritiques

Les gabbronorites sont des roches mélaà mésocrates, massifs, lités ou rubanés. Elles sont composées principalement de plagioclase, de clinopyroxène, d'orthopyroxène et parfois d'olivine.

*Les plagioclases formant le fond de la texture sont en proportion très variée dans la roche. On observe une accumulation élevée(80-90 %) de labrador dans les niveaux anorthositiques. Ils présentent parfois une deuxième génération tardive constituée par des albites fraiches et de la calcite.

*le clinopyroxène(souvent diopside) représente d'une part un minéral cumulus, maclé ou imbriqué avec l'orthopyroxène et d'autre part un minéral post-cumulus (plus grand que le premier) englobant le plagioclase ou l'orthopyroxène.

*L'orthopyroxène est également un minéral cumulus et post-cumulus. Il s'agit d'enstatite.

*L'olivine est peu abondante comme un minéral cumulus. Elle est souvent non

236

on observe au microscope des micrites fossilifères. Dans les parties supérieures de métamorphites de Malatya les fossiles retrouvés par Yiğitbaş(1989); lui permettent de leur attribuer un âge du Permien au Trias inférieur Jurassique.

*Les roches ophiolitiques

Les métaophiolites de Berit affleurent en plusieurs endroits dans la région de Kahramanmaraş montrant toujours un contact tectonique avec les autres roches. Malgré leur grande extention dans la région on observe seulement une lentille orientée E-W avec une épaisseur de 10 m, au nord du village d'Hompur (Fig.1).

Le massif ophiolitique de la région de Kahramanmaraş est constitué essentiellement de tectonites, de cumulats ultramafiques et mafiques, d'une série volcanique ophiolitique écaillée, de roches volcaniques non ophiolitiques, d'un mini complexe filonien et enfin de roches sédimentaires à la fois détritiques et pélagiques (calcaires détritiques, calcaires siliceux, radiolarites rouges et vertes).

Les tectonites sont formées d'harzburgites déformées à poches ou bandes dunitiques.. Il s'agit d'harzburgites granoblastiques foliées en contraste avec les harzburgites du massif ophiolitique de Hatay.

La composition minéralogique des harzburgites porphyroclastiques et granoblastiques est presque constante. Ces roches sont constituées essentiellement d'olivine, enstatite et chromite (moins de 1 %).On voit localement en petite quantité (2-3 %), du clinopyroxène qui est éventuellement développé de l'orthopyroxène pendant la déformation plastique. La roche est fortement serpentinisée et les cristaux d'olivine sont granulés et parfois recristallisés.

Les cumulats ultramafiques et mafiques sont constitués de dunites massives, de pyroxénolites et de gabbros isotropiques, rubanés et lités. Les cumulats dunitiques sont de couleur noire, verdâtre et recouverts parfois d'une croûte mince (1-5 mm) d'hydroxyde de fer. Dans cette roche, l'olivine est très abondante, toujours transformée en minéraux de serpentine. L'orthopyroxène et les chromites sont peu abondantes. Ces derniers remplissent localement les interstices entre les cristaux d'olivine. Les wehrlites et les lherzolites alternent toujours avec des lits dunitiques ou pyroxénolitiques dans les parties supérieures de la zone dunitique. On observe aussi dans les cumulats une déformation à haute température (granulation, étirement, bande de pliage en extinction roulante)(Planche I, fig.2). On observe également des gabbros isotropiques et lités.

La formation filonienne est constituée principalement par des dykes de dolérite-diabases, des rodingites et par un complexe filonien. Les dykes recoupent toute la masse des cumulats ainsi que des tectonites.

Les roches ophiolitiques affleurant au long de la ligne de charriage du massif de Berit sont constituées essentiellement d'harzburgites porphyroclastiques, de gabbros massifs,

235
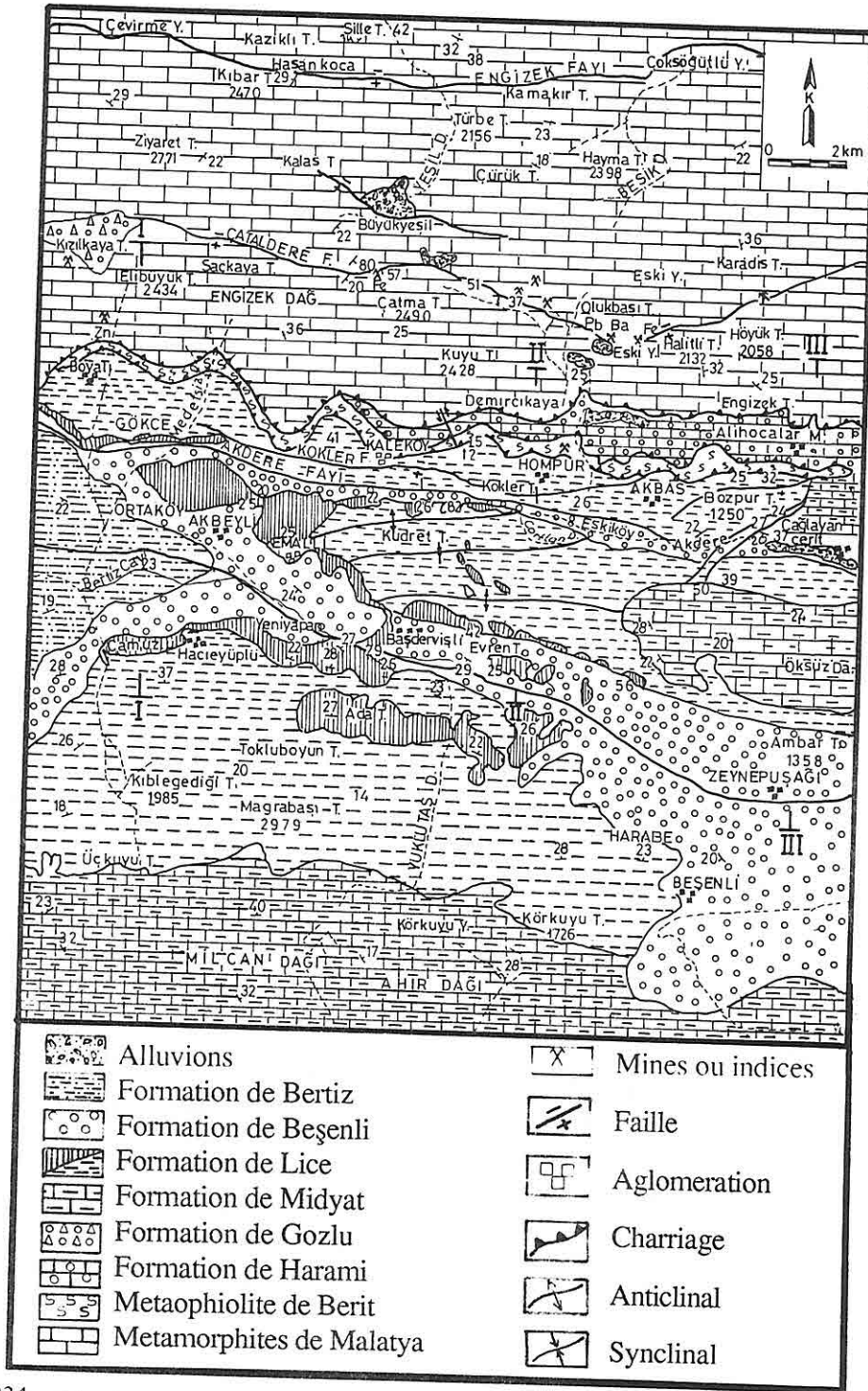
Fig. 1. Carte géologique du secteur étudié (Révisée d'après Önalan, 1986; Yıldırım, 1989; Yiğitbaş, 1989).

amas et en poches (remplissage des zones fracturées) de la minéralisation primaire sulfurée et la nature karstique du piège des minéralisations secondaires.

2. CONTEXTE GEOLOGIQUE DES MINERALISATION Pb-Zn-Ba DU SECTEUR ETUDIÉ

L'unité allochtone est formée de divers groupes lithologiques: près de la moitié du secteur étudié est constituée par les métamorfites de Malatya(Fig.1). Elles constituent des reliefs assez forts(2500m). Elles sont formées de roches carbonatées et silicoalumineuses d'âge paléozoique à la base et de calcaires et dolomies à intercalations de marnes et de quartzites, d'âge mésozoique au sommet. Ces métamorphites sont en contact tectonique avec des roches ophiolitiques également métamorphiques en forme d'une masse étroite allongée Est-Ouest. Les calcaires non métamorphiques, les grès argileux et carbonatés d'âge crétacé et Eocène constituent les autres sous unités des allochtones.

L'unité autochtone est composée de formation de Midyat d'âge Eocène moyen supérieur-Oligocène; de formation de Lice d'âge Miocène qui est en concordance avec la formation de Midyat, de formation de Beşenli et ensuite de formation de Bertiz d'âge Miocène.

Les roches métamorphiques de Malatya présentent du minerai sulfuré en forme de filon, d'amas et remplissage dans les zones fracturées(planche I, fig.1). Les calcaires métamorphiques ont subi une karstification plus ou moins développée; le minerai primaire s'est transformé en minerai oxydé et carbonaté en déposant dans les cavités karstiques après une altération hydrothermale et météorique.

3.DESCRIPTION PETROGRAPHIQUE

Les allochtones

*Roches métamorphiques de Malatya

Le degré du métamorphisme des métamorphites de Malatya varie de la base au sommet. On observe, à la base, des schistes sériciteux et quartzeux, des schistes micacés et de phyllites. Au dehors du secteur étudié, Yıldırım(1989)signale la présence de schistes à grenat .

Les calcaires micritiques et gréseux sont transformés en marbre et calcschiste après un métamorphisme régional. Ces marbres montrent souvent une texture granoblastique et saccaroide et sont essentiellement constitués de calcite(95 %). Les calcschistes sont constitués de 90 % de calcite, 2-15 % de quatz et moins de 3 % de micas généralement chloritisés

Les calcaires recristalisés déposés au sommêt conservent souvent leurs états initials et

233

GEOLOGIC AND METALLOGENIC INVESTIGATION OF THE ENGIZEK CARBONATE PLATFORM, NORTH OF KAHRAMANMARAŞ, TURKEY

ABSTRACT: *The Engizek region consists mainly of two units, which are allochthonous and autochthonous. The allochthonous unit is mainly composed of metamorphic rocks of carbonate and locally of silica-alluminate, such as schist, fillate, calcschist, and quartzite. The tectonic and metamorphic origin of these formations are considerably complex, as the Pb-Zn-Ba minerilization development has taken place within these units. An overlying ophiolitic massive has been thrusted during the period of Upper Cretaceous-Eocene . The autochthonous unit consists mainly of four formations, named as the Midyat, Lice, Beşenli, and Bertiz formations comprising limestone, clayey limestone, sandstone and locally conglomerates. No economic minerilization have been observed within the authocthonous unit.*

In the perspective of the geologic structure, the minerilization in Engizek are mostly observed in the forms of filon, band packed and karstic filling. Mainly three distinct mineralization can be differentiated: Mineralization rich in barite, mineralization rich in galenite, and oxsidized and carbonitized Pb-Zn mineralizations.

Primary mineralization with sulphur have becn deposited along the fractured zones while secondary mineralization with oxides and carbonates have been deposited in the karstic cavities and fractures of carbonate rocks.

1. INTRODUCTION

Dans le district minier d'Engizek, le secteur de Çataldere-Boyalı-Eskiyayla affleurant sur les bordures sud de la montagne d'Engizek a été découvert depuis une vingtaine d'années et a fourni seulement depuis 1986 quelques milles tonnes de minerai sulfuré et oxydé, dont les teneurs en plomb-zinc sont assez élevées((26 à 52 % métal). Parmi plusieurs gisements et indices reconnus, la mine de Boyalı, la mine de Masat et la mine de Karamanlı sont en exploration.Les autres divers indices et occurences ne sont pas exploitable actuellement.

On sait par ailleurs l'importance métallogénique des formations paléozoiques et mésozoique (métamorphiques de Malatya)(Sungurlu, 1972;Akçakoca ve Bahçeci, 1972; Gözübol ve Gürpınar, 1980; Ayhan, 1983, 1984, 1987; Tarhan, 1984-1985; Yılmaz et. al., 1985; Önalan, 1986-1988; Çevrim et al., 1986; Baydar, 1989; Yıldırım, 1989; Yiğitbaş, 1989; Anıl, 1989; Yılmaz ve Yiğitbaş, 1990).Elles représentent un stock métal important, avec près de 500.000 tonnes de plomb-zinc dans l'ensemble de la région d'Engizek(Nord de Kahramanmaraş).

Par la description d'études précédentes, on peut y reconnaitre la nature en filon, en

232

ETUDE GEOLOGIQUE ET METALLOGENIQUE DU SECTEUR SEPTENTRIONAL(PLATEFORME CARBONATÉE D'ENGİZEK) DE KAHRAMANMARAŞ (TURQUİE)

Mesut ANIL

Université de Çukurova, Département de Géologie, Adana-Turquie

RESUME: *L'analyse géologique de la région d'Engizek conduit à distinguer deux unités structurales principales: l'unité allochtone et l'unité autochtone. L'unité allocthone est constituée de roches métamorphiques le plus souvent carbonatées et quelques fois silico-alumineuses(schiste, phyllite, calcsciste, quartzite). L'histoire tectonique et métamorphique de ces formations présentant des zones minéralisées en Pb-Zn-Ba est très complexe. Un massif ophiolitique est charrié sur les métamorphites de Malatya du Crétacé supérieur à l'Eocène moyen. L'unité autochtone comporte essentiellement quatre formations différeents: Midyat, Lice, Beşenli et Bertiz. Toutes ces formations sont composées de calcaires, de calcaires argileux, de grès et parfois de conglomérats. L'unité autochtone ne contient aucune minéralisation économique.*

Dans ce contexte géologique les minéralisations d'Engizek se manifestent en plusieurs endroits sous forme de filons, d'amas, de bandes et de poches karstiques. On peut distinguer essentiellement trois types de minerai: minerai riche en galénite, minerai riche en barytine et minerai oxydé-carbonaté plombo-zincifère.

Le minerai sulfuré primaire est déposé dans les zones fracturées, en revanche le minerai oxydé carbonaté secondaire s'est placé dans les zones karstiques et fracturées surtout au milieu carbonaté.

231

6, 136 pp.

Çapan, U.Z., 1983. Toros Kuşağı Ofiyolit Masiflerinin (Marmaris, Mersin, Pozantı, Pınarbaşı ve Divriği) İç Yapıları, Petroloji ve Petrokimyalarına Yaklaşımlar. PhD Thesis, Hacettepe University.

Çataklı, A.S., 1983. Assemblage Ophiolitique et Roches Associées de la Partie Occidentale du Massif de Pozantı-Karsantı (Taurus Cilicien, Turquie). PhD Thesis, Nancy University, 760 pp.

Matheron, G., 1971. The Theory of Regionalized Variables and its Applications. Centre de Morphologie Mathematique, Fontainbleau, 211 pp.

MTA, 1962. Geological Map of Turkey, Adana region, 1/500000.

Ovalıoğlu, R., 1963. Die Chromerzlagerstätten des Pozantı-Reviers und Ihre Ophiolotischen Muttergesteine. MTA, No: 114, 86 pp.

Rahgoshay, M., and Juteau, T., 1980. The Chromite From the Ophiolitic Massif of Pozantı-Karsantı, Cilician Taurus, Turkey: New Observation About Their Structural Setting and Geochemistry. Proc. Intern. Symp. Metal. Mafic. Ultramafic Complex, Athens, Vol. 1, 114-126.

Rangoshay, M., Juteau, T., and Whitechurch, H., 1981. Kızılyüksek Tepe: Uh Gisement Exceptionnel de Chromite Stratiforme Dans un Complexe Ophiolitique (Massif de Pozantı-Karsantı, Taurus, Turquie). Paris Sc. Academy, No: 11, T.293, 765-770,

Ricou, L.E., Argyriadis, I., and Marcoux, J., 1975. L'axe Calcaire du Taurus, un Alignement de Fenêtres Arabo-Africaines Sous des Nappes Radiolaritiques, Ophiolotiques et Métamorphiques. Bulletin of Soc. Géol. Fr. 17, No: 6, 1024-1043

Tekeli, O., 1980.Toroslarda Aladağların Yapısal Evrimi. TJK Bulletin, No: 23/1, 11-14.

Tekeli, O., Aksay, A., Ertan, I., Işık, A., and Ürgün, B.M., 1981. Aladağ Projesi. MTA, Report No: 6976, 133 pp.

where:

$S^2 (V/D)$ is the variance of actual grades of blocks V within the deposit D

$S^2 (V^*/D)$ is the variance of estimated grades of blocks V within the deposit D

$\overline{\sigma_k^2}$ is the mean kriging variance of the grades of the blocks V

$\overline{\mu}$ is the mean lagrange multiplier obtained in kriging the blocks

The grade-tonnage curve for the actual values is shown in Fig.6.

6. CONCLUSIONS

A geostatistical evaluation of the Kızılyüksek-Yataardıç deposit was carried out using the kriging technique which provides the best linear unbiased estimator of block grades. These improved estimates and the grade-tonnage curves can be taken as a basis for mine planning purposes.

7. ACKNOWLEDGEMENTS

8. REFERENCES

Akın, A.K., 1987. Kızılyüksek-Yataardıç (Karsantı/Adana) ÖİR 634 Nolu Sahanın Maden Jeolojisi Raporu. MTA, 112 pp.

Anıl, M., 1986. Pozantı-Karsantı Ofiyolit Karmaşığı İçinde Seyrek Görülen Tabakalı (Stratiform) Krom Cevherleşmeleri: Tekneli ve Sarıçoban Dere Ocakları. S.Ü., Engineering Faculty, No:2 .

Anıl, M., Billor, Z., and Özüş, S., 1986. Gerdibi-Gertepe-Çataltepe-Çeştepe (Pozantı-Karsantı-Adana) Kromit Yataklarının Jeolojik, Metalojenik ve Ekonomik İncelenmesi. TÜBİTAK, Project No: TBAG-668, 131 pp.

Blumenthal, M.M., 1941. Niğde ve Adana Vilayetleri Dahilindeki Torosların Jeolojisine Umumi Bir Bakış. MTA, Series B, No: 6, 48 pp.

Blumenthal, M.M., 1946. Kilikya Toroslarının Çok Dikkate Değer Bir Parçası (Karanfil Dağ). MTA, No: 2.

Blumenthal, M.M., 1952. Das Taurische Hochgebirge des Aladağ, Neuere Forschungen zu Seiner Geographie, Stratigraphie und Tektonnik. MTA, Series D, No:

kriged to obtain in situ grades and tonnage. The panel size of 50 m was chosen after examination of the average spacing of the drill-holes. The search area contained a volume of dimensions 80x80x20 m. The maximum number of samples involved in estimation was limited to 50.

The grade-tonnage curve for the kriged estimates based on 50x50x3 m blocks is shown in Fig.5. This grade-tonnage curve is the grade-tonnage curve for estimated grades. To obtain an estimate of the grade-tonnage curve for actual grades, permanence of the distribution was assumed and the variance of actual grades was estimated by the
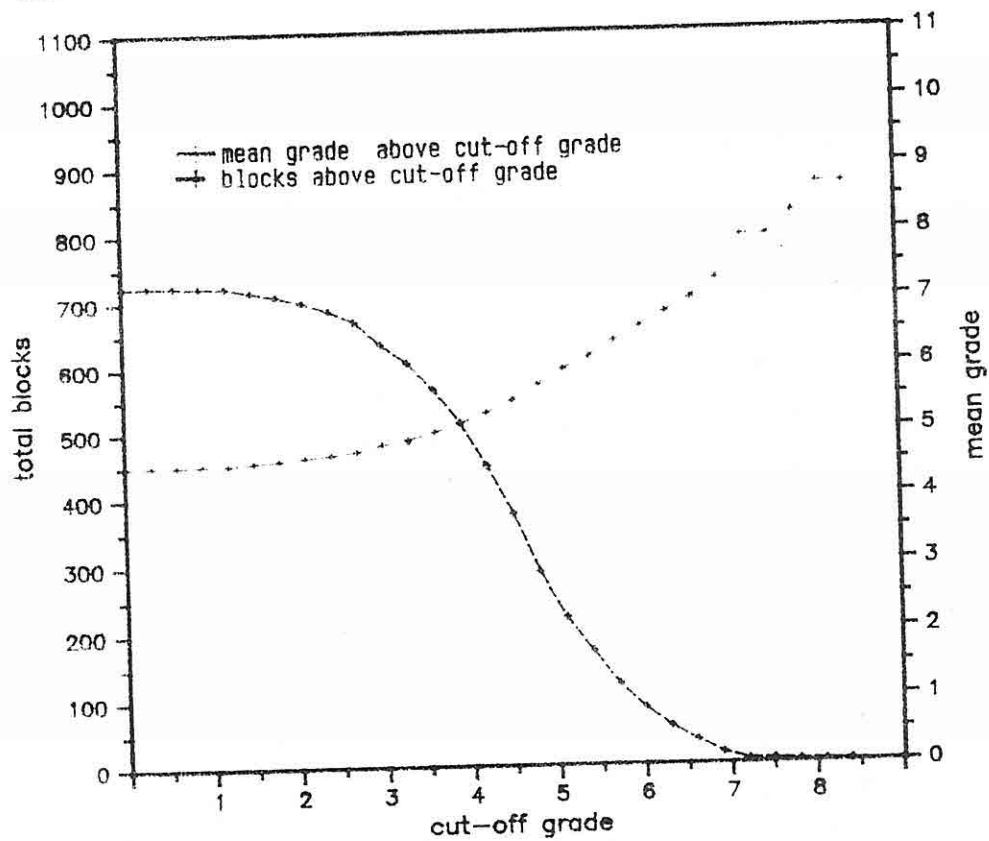
Figure 5.Grade—tonnage curves for estimated values

approximation:

$$S^2 (V/D) = S^2 (V^*/D) + \overline{\sigma_k^2} - 2 \overline{\mu}$$

227

Table 1 : The model validation

Absolute Difference	: 1.62
Difference	: 0.00
Squared Difference	: 6.42
Kriging Variance	: 6.20
Intercept	: 0.12
Slope	: 0.97
Correlation Coefficient	: 0.63

5. BLOCK KRIGING AND GRADE-TONNAGE CURVES

Having modelled the experimental variograms, blocks of dimensions 50x50x3 m were
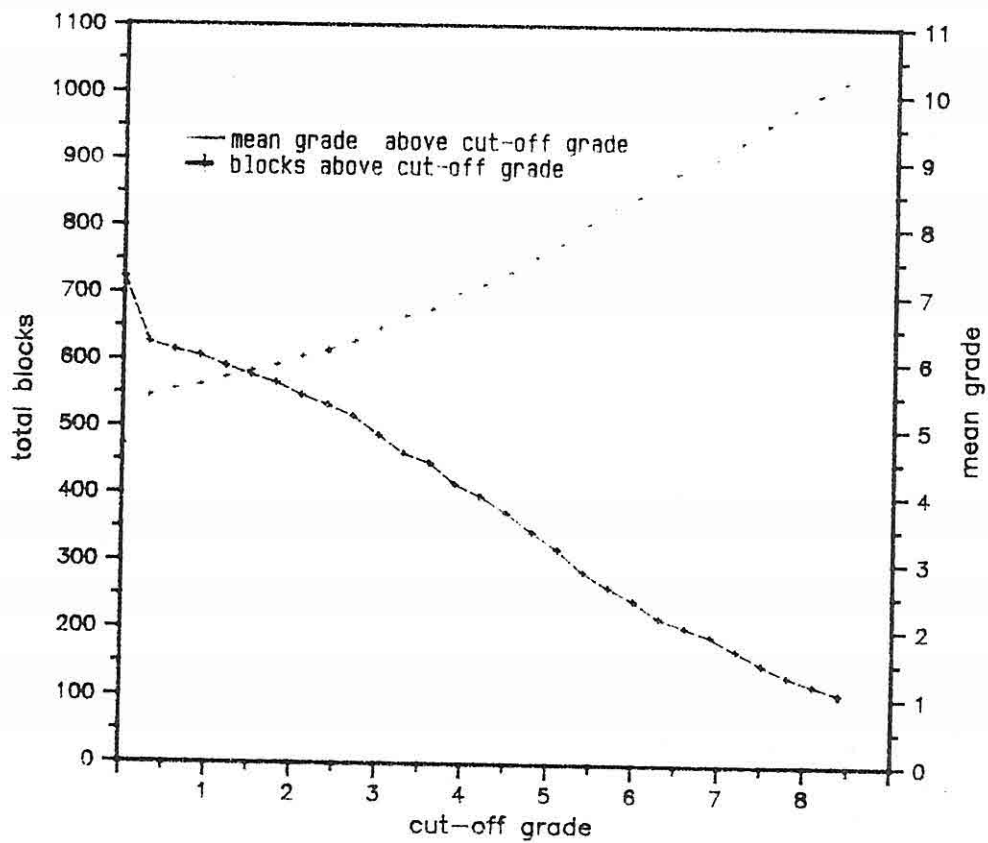
Figure 6.Grade-tonnage curves for actual values

mathematical expression which will best describe the spatial variability of the variables under study.

Experimental variograms representing three main directions namely, strike-plunge, cross-dip, and down-dip directions were calculated and presented in Fig.4. These variograms have a common sill value of approximately 10. The down-dip variogram indicates a nugget variance of 4-5 while the nugget variance of the variograms for the strike-plunge and cross-dip directions is inaccessible due to greater sample spacing, compared with the size of the small scale variability. When assuming the nugget variance in the down-dip direction, the variograms in the strike-plunge and cross-dip variograms appear to have much larger ranges of 100-150 m compared with the range of 20-30 m for the down-dip direction.

The model fitted to the experimental variograms are of simple spherical type with the following expression:

$$\gamma(h) = C_o + C \ (1.5 \ h/a \ (dir.) - 0.5 \ h^3 / a \ (dir.)^3) \qquad \text{for } h \leq a$$
$$\gamma(h) = C_o + C \qquad\qquad\qquad\qquad\qquad\qquad \text{for } h > a$$
$$\gamma(h) = 0 \qquad\qquad\qquad\qquad\qquad\qquad\qquad\quad \text{for } h = 0$$

with the parameters

$$C_o = 4.5$$
$$C = 6.0$$

the ranges in $\begin{bmatrix} \text{strike-plunge} &= 120 \text{ m.} \\ \text{cross-dip} &= 120 \text{ m.} \\ \text{down-dip} &= 30 \text{ m.} \end{bmatrix}$

These model parameters were validated by the kriging back estimation technique. Each data value is removed in turn and estimated from the remaining data.

For conditionally unbiased estimates, the linear regression of actual values on estimated values should be close to the 45° line, i.e., intercept of zero and slope of 1.0. The standard error of estimate of the regression of actual values on estimated values should be approximately equal to the square root of the mean kriging variance and the square root of the mean squared difference between actual grades and estimated grades.

A summary of the results is shown in Table 1.

225

Variable length drillhole samples were composited to give equal 3 m length samples, resulting in 1177 composite samples. The composite size was chosen as close as possible to the average raw sample length whilst minimising the number of raw sample lengths requiring to be split into smaller lengths.

The histogram of 1177 composite samples is given in Fig.3. This shows a low skew distribution with the mean of 4.36, the standard deviation of 3.24 and the coefficient of variation of 0.74.

4. VARIOGRAM ANALYSIS

In geostatistics the tool used to characterise the natural variabilities of a deposit is called the semi - variogram, or variogram, for short. It consists of finding the
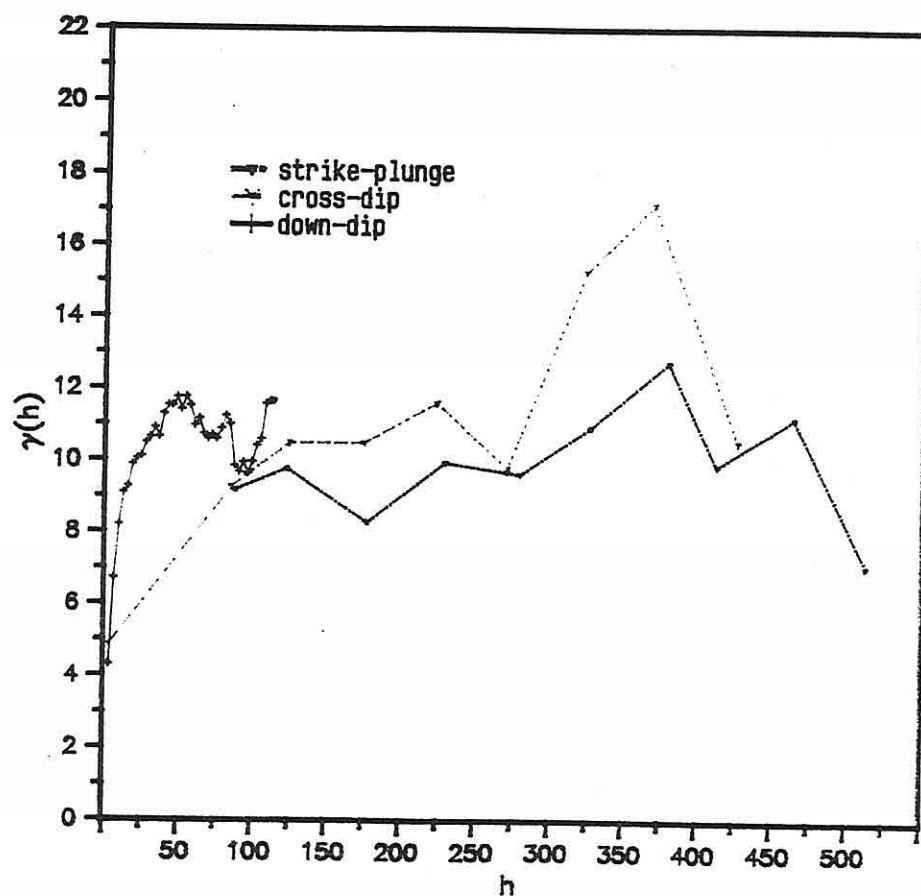
Figure 4.Directional variograms of Cr2O3

224

the top (Çapan, 1983).

The Kızılyüksek-Yataardıç chromium body is located in the lowest part of the cumulative dunites belonging to the peridotitic series (Akın, 1987). The geological map of the study area is presented in Fig.2.

3. DATA ANALYSIS

The data is derived from 26 drillholes distributed over the area. The total depth of the 26 drillholes was 4772 m, the majority of drillholes were approximately 160 m in depth. One of the drillholes was not involved in the calculations, because it is located at the boundry of the panel. The samples were analysed for Cr_2O_3 %, Fe_2O_3 %, MgO %, Al_2O_3 % and SiO_2 %. In this study, the variable under consideration is Cr_2O_3%.

N :1177
mean : 4.36
median : 3.60
min : 0.60
max : 31.76
stdev : 3.24
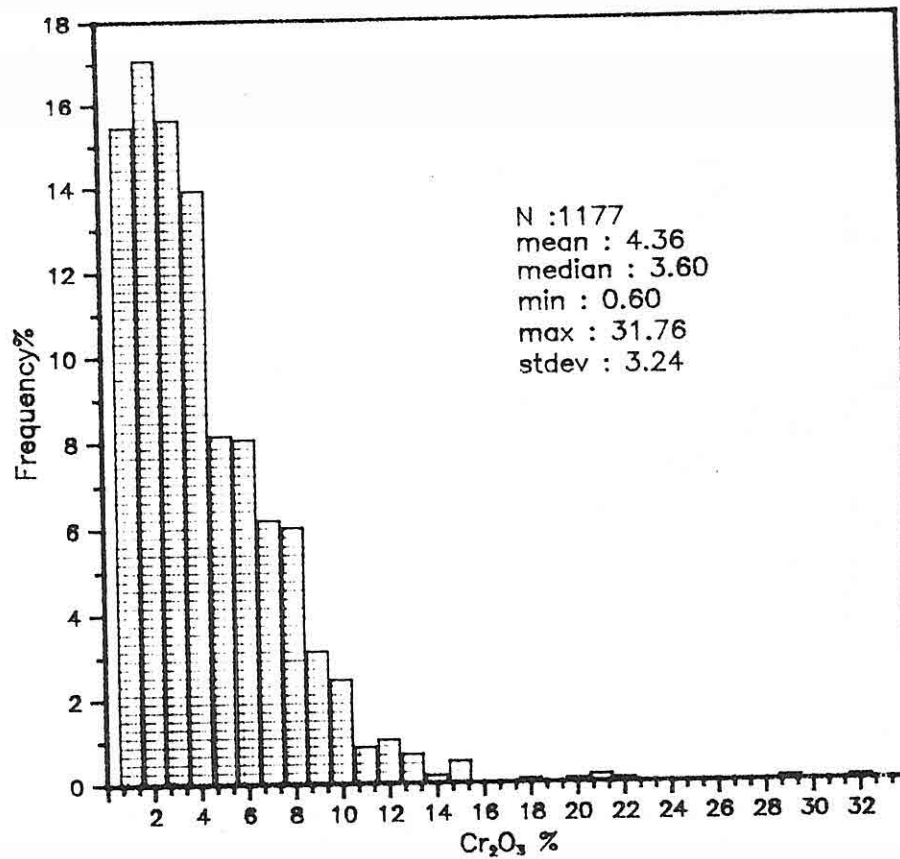
Figure 3.Histogram of the 3m composited samples

223

THE GELOGICAL MAP OF THE AREA
BETWEEN KIZILYÜKSEK & YATAARDIÇ

N

1 km

Alluvion

Debris avalanche

Oligo-Miocene aget rocks

Tourid limestone

OPHIOLITES

Unkown aget unmetamorphic
volcanic & sedimanter units

Harzburgit,dunite, podiform chromite

Dunite & stratiform chromite

Pyroxenites

Gabbronic rocks

Diabase dikes

Chromite mines

Boundry

Approximate boundry

Fault

Approximate fault

Thrust

Breccia

Working deposit

Unworked deposit

Study area

Taken from Akın (1987).

Figure 2 : The Geological Map of the Kızılyüksek-Yataardıç Area

Figure 1 : Regional Geological Setting and Location Map

221
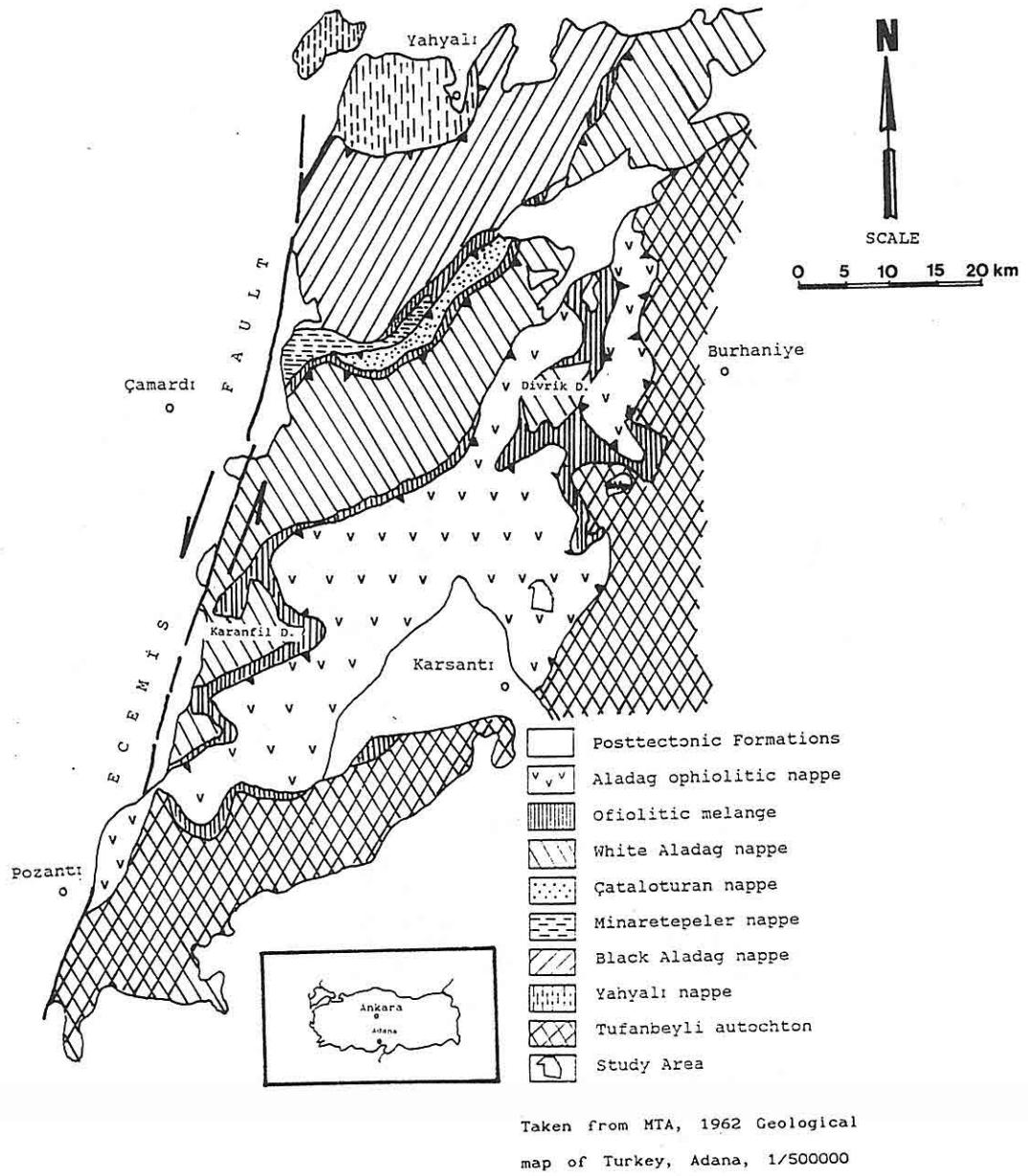
1. INTRODUCTION

In this paper, the ore reserve estimation procedure which was been applied to the data is based on the theory of regionalized variables which has largely developed by Matheron (1971) and is now simply referred to as "geostatistics". Geostatistics offer a practical and reliable estimate which can be fitted into existing evaluation and optimum mine planning methodologies.

The known mineral resources are limited in the world in which we live, principally due to a decreasing of the cut-off grades. For that reason, MTA (Mining Research and Exploration Institute of Türkiye) has started a project which investigates several chromium bodies having the lower grades. In this project the Kızılyüksek-Yataardıç orebody, which is situated 2.5 km NW of Darılık Village in Karsantı (Adana, Türkiye), has been considered, 26 drillholes being bored and the samples analyzed by MTA.

2. GEOLOGY

The Pozantı-Karsantı ophiolitic complex which is found at the Central Taurus ranges, 80 km NW of Adana. The first geological study on the region started with Blumenthal (1941 and 1946). Ovalıoğlu (1963) carried out a detailed geological and petrographic research and the ophiolithes in the complex were first distinguished by Ovalıoğlu (1963). The stratiform chromium mineralizations at the Pozantı-Karsantı ophiolitic complex have been described by Rangoshay and Juteau (1980); Rangoshay et al., (1981). Çataklı (1983?; Anıl (1986); and Anıl et al. (1986) have been identified as an ophiolitic (tholeiitic) volcanic series in the ophiolitic complex. The regional geological setting and location map is given in Fig.1.

The Kızılyüksek-Yataardıç chromium body is located in the Pozantı-Karsantı ophiolitic complex. The orebody belonging to the rocks which were defined as the Pozantı-Faraşa ophiolites by Blumenthal (1952) and later were described as the Aladağ ophiolites by Tekeli et al. (1981).

The Aladağ ophiolites, elongated in NE-SW, has been located over an area of 1600 km² and tectonically overlay the autochton deposits of the Arabian platform (Ricou et al., 1975; Tekeli et al., 1981). The tectono-stratigraphic rocks of the Aladağ ophiolites have been distinguished as autochton, parautochthon, and allochtone by Tekeli (1980) and Tekeli et al. (1981).

The autochton rocks comprises the Cambrian-Eocene age deposits, which are largely observed between Mansurlu-Tufanbeyli in the east of the Aladağ Mountains.

The parautochthon rocks from Upper Devonian to the beginning of Cenonian, consist of the Yahyalı nappe, the Black Aladağ nappe, the Minaretepeler nappe, the Çataloturan nappe, the White Aladağ nappe, and the ophiolitic melange.

The allochthone rocks are represented by the Aladağ ophiolitic rocks, which are composed of the metamorphic series in the basement rocks, and the peridotitic series at

220

A GEOSTATISTICAL CASE STUDY OF THE KIZILYÜKSEK-YATAARDIÇ CHROMIUM OREBODY

Cem SARAÇ [1, 2]   and   Erhan TERCAN [1, 2]

[1]Hacettepe Üniversitesi, Mühendislik Fakültesi, Beytepe 06532, Ankara, Türkiye (Permanent Address)

[2]Leeds University, Mining and Mineral Engineering Dept., Leeds, LS2 9JT, England (Present Address)

ABSTRACT: This paper describes an application of geostatistical ore reserves estimation method to the Kızılyüksek-Yataardıç orebody located in Karsantı, Adana. The main purpose of this preliminary study is to obtain improved ore grade estimates for mine planning.

For this purpose, after a preliminary review of available data, the following work was done:

-Basic statistics treatment of data,

-Estimating and modelling the variograms in three dimensions,

-Estimation of the ore grades for three dimensional blocks using kriging,

-Production of the grade-tonnage curves.

219

distribution in Tertiary and Quaternary volcanic rocks from central and Western Anatolia. Proced. of VI. Colloqium on geology of Aegean Region, İzmir.

Irvine, T.N. and Baragar, W.R.A. 1971. A guide to the chemical classification of the common volcanic rocks. Can. Jour. Earth. Scien. 8, 532-548.

JICA and MTA., 1987.The Pre-feasibilty Study on the Dikili-Bergama Geothermal Development Project in the Republic of Turkey. Progress Report II. MTA, Ankara,

Kaya, O., 1979. Ortadoğu Ege Çöküntüsünün (Neojen) stratigrafisi ve tektoniği. TJK Bülteni, C: 22, S: 35, Ankara.

Kaya, O., 1982. Tersiyer Sırt Yitmesi, Doğu Ege Bölgelerinin Yapısı ve Magmatikliği için olası bir mekanizma. TJK, S: 39, Ankara.

Kuna, H., 1960. High alumina basalt. Journal of petrology, 1, 121-145.

Mc Donald, G.A. and Katsura, J., 1964. Chemical composition of Hawaiian lavas, Journal of Petrology, 5, 82-133.

Miyashiro, A., 1975. Petrology and Plate tectonic. Rev., Geophys. Sp. Phys. 13, 94-98.

Öğdüm, F., 1982. Menemen Dumanlıdağ Volkan Konisi ve Kalderasının Jeomorfoloji Dergisi, S: 42-45, Ankara.

Paola, G.M.D., Innocenti, F., 1969. Anadolu çalışma gezisi petrografik rapor. MTA Der. Rap. No (?).Peccerillo, A., Taylor, S.R., 1976. Geochemistry of Upper Cretaceous volcanic rock from the Pontic chainnorthern Turkey, Bulletin volcanologique, 39, 4, 557-569.

Rittmann, A., 1952. Nomenclature of volcanic rocks, Bulletin volcanologique, 12, 75-102.

Savaşçın, M.Y., 1975. Foça yöresi volkanik kayaçlarından sağlanan petrografik jeokimyasal sonuçlar. TÜBİTAK IV. Bilimsel Kong. Tebliğler Kitabı, 273-289.

Savaşçın, M.Y., Dora, O.Ö., 1977. Foça-Menemen yöresi volkanitlerinde piroksenlerin yayılımı ve kristalografik değerleri, TJK Bült. 20, 1, 21-27.

Turgut, S., 1987. Ege Denizi ve Dolaylarının Tektonik Evrimi ve Hidrokarbon Olanakları. Türkiye 7. Petrol Kongresi, 6-10 Nisan 1987, S: 23-35, TMMO Petrol Mühendisliği Odası TPJD, Ankara.

Wu-Liren, Y.S., Xiangsen, Z., Mingzhe, Z., Dahe, X., Zhenhua, L., Sıkun, F., Keqın, X., Huichu, R., 1983. Progress in Researches on Volcanology and Chemistry of the Earth's İnterior in China: XVIII. General Assembly of IUGG, Hamburg, Germany,

217

The volcanism in the survey area is assumed to be originated due to tectonism took place in Anatolian plate which is located between Eurasian and African plates and moves westward relative to the North Anatolian Transform Fault.

By this study it is proved that the volcanism of calc-alkalic character in Aliağa area had started in Lower Miocene and continued intermittently till the end of Miocene Epoche. Another conclusion obtained from this research is that after the cease of volcanism of calc-alkalic character at the end of Upper Miocene the volcanism of alkalic character began in Pliocene.

5. REFERENCES

Aramaki, S., 1963. Geology of Asama Volcano., Japan Fac., Sc. Univ., Tokyo, 14, 233-439.

Cox, K.G., Bell, J.D., Pankhurst, D.V., 1979.The İnterpretation of İgneous Rocks. George Allen and Unwin Ltd, London, 450 pp.

Ercan, T., 1979. Batı Anadolu, Trakya ve Ege adalarındaki Senozoyik volkanizması. Jeo.Müh.Derg. 9, 23-46.

Ercan, T., Türkecan, A., Can, B., Günay, E., Çevikbaş, A., Ateş, M., 1984. Batı Anadolu'da Manisa-Balıkesir Arasındaki Tersiyer Yaşlı Yalancı Bazaltların Özellikleri, Jeo. Müh. Derg. 30-31.

Ercan, T., 1985. Batı Anadolu Senozoyik Volkanitlerine Ait Yeni Kimyasal İzotopik ve Radyometrik Verilerin Yorumu, TJK, Cilt: 28, S: 2.

Ercan, T., 1982. Batı Anadolu Tersiyer volkanitleri ve Bodrum Yarımadasındaki volkanizmanın durumu.

Ercan, T., 1982. Batı Anadolu Genç Tektoniği ve Volkanizması. TJK, s. 4, Ankara.

Eşder, T., 1978. TPAO İzmir Aliağa Rafinerisi. I No'lu sahanın jeolojik raporu, TPAO İzmir.

Eşder, T., 1988. Gümüldür-Cumaovası (İzmir) Alanının Jeolojisi ve Jeotermal Enerji Olanaklarının Araştırılması. Doktora tezi (Basılmamış) İ.Ü. Fen Bilimleri Enstitüsü Jeoloji Mühendisliği Anabilim Dalı , İstanbul.Eşder, T., Yakabağ, A., Sarıkaya, H., Çiçekli, K., 1991. Aliağa (İzmir) Yöresinin Jeolojisi ve Jeotermal Enerji Olanakları, MTA Derg. Rap., Ankara.

Filiz, Ş., 1982. Ege Bölgesindeki Önemli Jeotermal Alanların O_{18}, H_2, H_3, C_{13} İzotoplarıyla İncelenmesi. Ege Üniversitesi Yerbilimleri Fakültesi, Doçentlik tezi (basılmamış).

Gottini, V., 1968.The TiO_2 frequency in volcanic rocks. Geol. Rdsch, 57, 930-935.

Innocenti, F., Manetti, P., Mazzuoli, R., Peccerillo, A., Poli, G., 1977. Ree
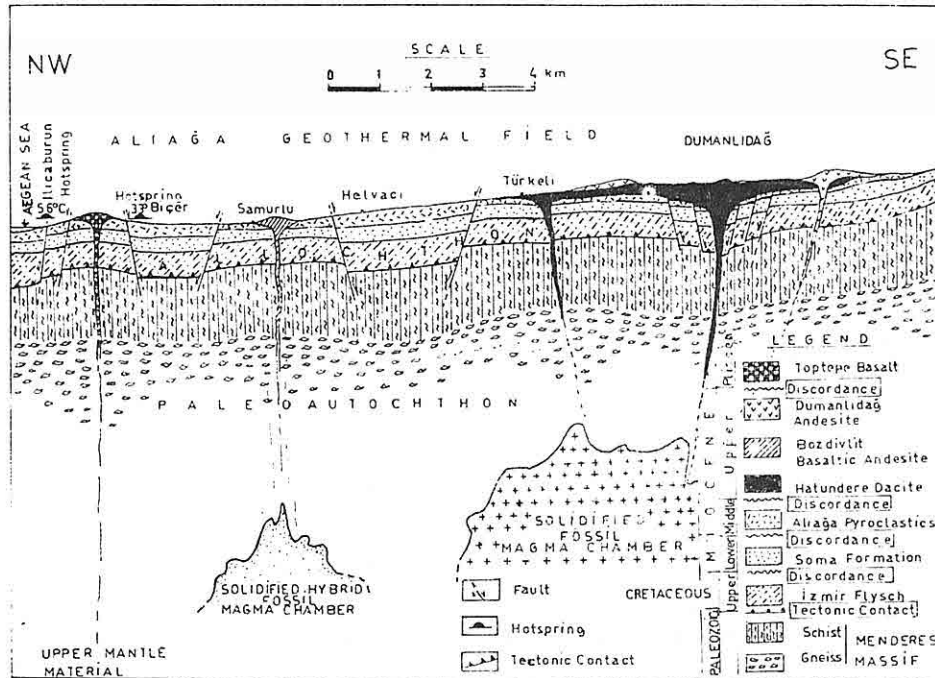
Figure 10. Geological cross-sections of the investigated area (Eşder, 1991).

earth surface through the NE-SW striking oblique faults formed in close association with North Anatolian Transform Fault and cut deeply the crust of the earth. The occurrence of volcanics in NE-SW trends in this area supports the above mentioned assumption (Fig.2). But in contrast, Dumanlıdağ volcanic Complex were formed at the intersection of NE-SW striking oblique fault and NW-SE strike faults. Therefore the older volcanics occur in NE-SW trend whereas the younger ones in NW-SE trend.

In the progressing phases of the expansion the intermixing of the alkalic magmas of mantle origin with the magmas of crust origin the hybrid magmas were formed.

215
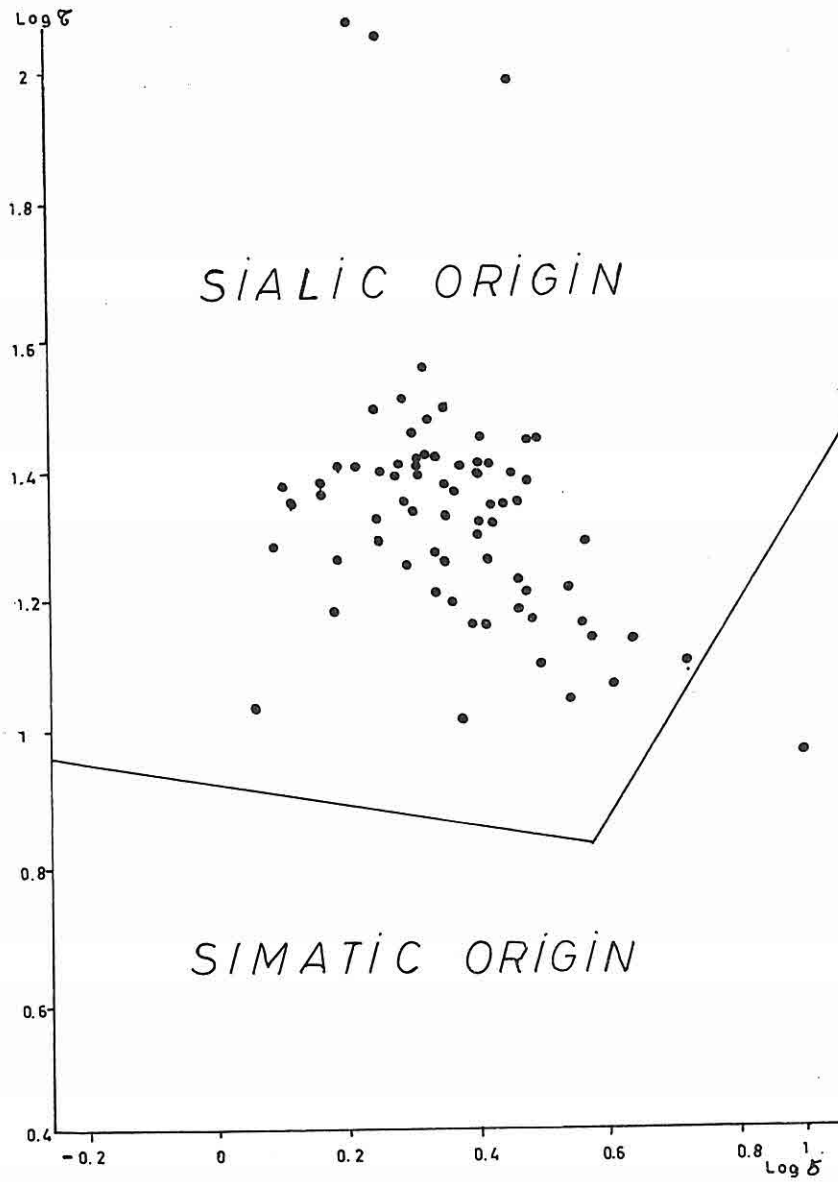
Figure 9. Gottini diagram of volcanics (Eşder, 1991).
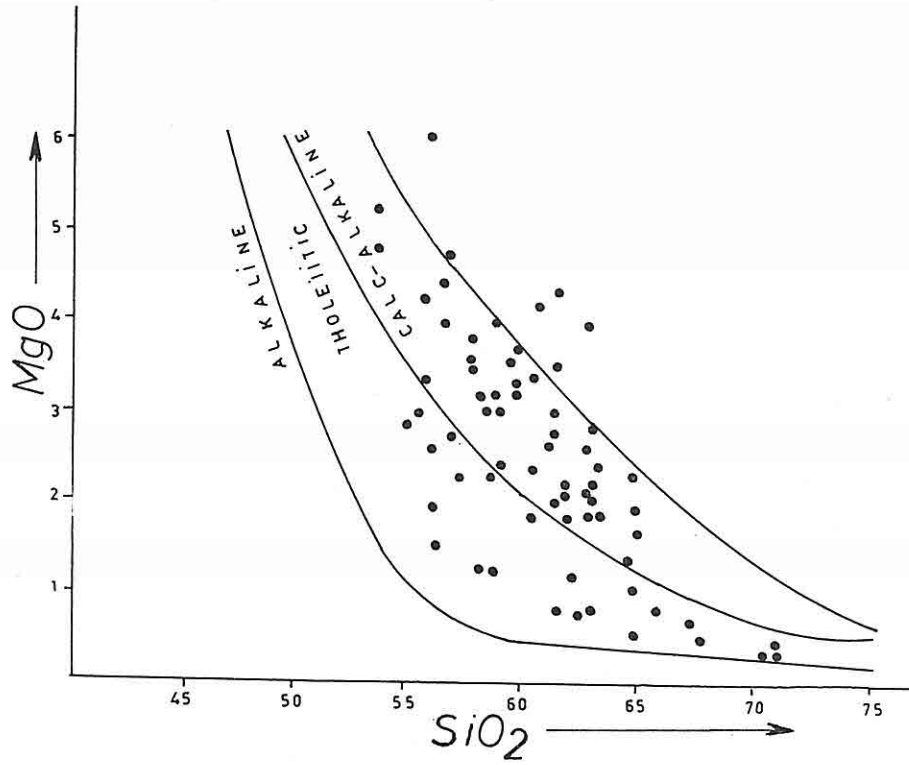
Figure 7. Aramaki diagram of the volcanics (Eşder, 1991).
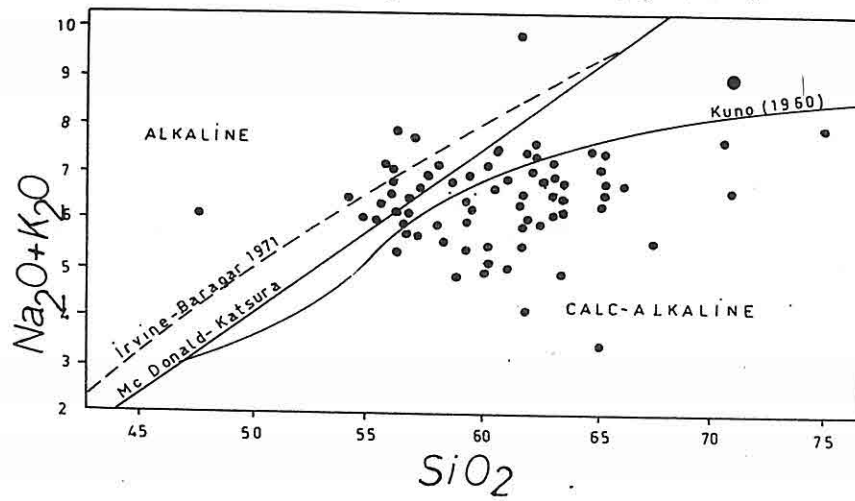
Figure 8. Classification of the volcanics according to alkali-silica content (Eşder, 1991).
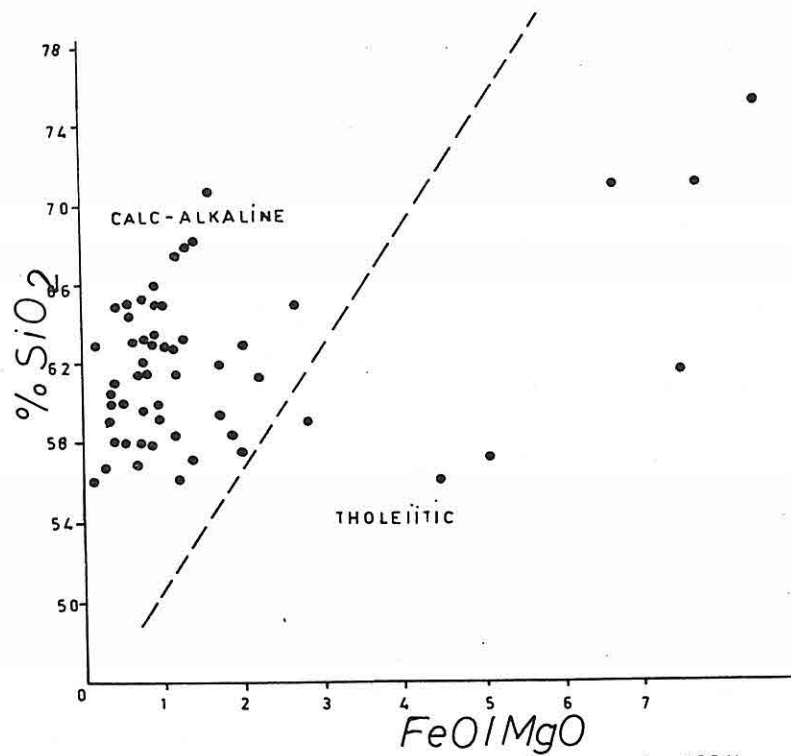
Figure 6 : Miyashiro diagram of the volcanics (Eşder, 1991).

character which later on continued as alkalin volcanism. Aliağa volcanics can be subdivided into calc-alkalic series and sodium series according to Rittmann diagram. In Gottini's diagram it is pointed out, that the volcanics formed in Miocene apoche are of sialic (crust) origin and Toptepe basalts are of simatic (mantle) origin (Fig. 9).

In Aliağa volcanics Rittman index ranges between 1.47 and 3.82 whereas Gottini index ranges between 12.2 and 122.5. Both indices indicate that the volcanic rocks of Miocene age found in the survey area of sialic origin, but the calculated ration of K_2O/Na_2O which ranges between 1.1 and 1.71 shows that these rocks are intracontinental calc-alkalic volcanics (Table-1). In volcanics of Pliocene age Rittman index is found to be 8.09 and Gottini index 7.17. According to this result these rocks are alkalic volcanics.

In this area calc-alkalic magmas which were the cause of the formation of the volcanoes here were formed as a result of the secretion of high amount of heat from mantle into the crust in Miocene which led to the partial melting of the crust. These volcanoes reached the

212

research area. In general, they lie on the tectonic trend which strikes NE-SW. From petro-chemical point of wiew, they differ from other volcanics. They are black and resemble basalts with their cooling columnar joints. The volcanics crop out widely in the area, named as high-K bearing basaltic andesite, trachyandesite and latite. In thin section, the basic plagioclase microlites are disseminated in glassy groundmass. In addition to this, crypto crystals and phenocrysts of pyroxene and olivine are noticed. The olivine grains, which are seen as an assemblage, show serpentinization.

Agglomerates : These are products of an explosive event before the issue of lava from the volcano vent. They are concentrated near the volcano center along the fissures.

Dumanlıdağ Andesites : These rocks crop out widely in the SE part of the survey area in the Dumanlıdağ region. They trend along certain tectonical structures. The volcanic rocks formed as a result of volcanos erupted in Dumanlıdağ and its vicinity buried the older structures towards NW, SE and SW. According to diagrams, they are considered to be high-K bearing andesite. For this reason these volcanics are called high-K containing andesite. The petrographic investigation of this rock revealed the dissemination of plagioclase, amphibole, biotite and pyroxene phenocrysts in a semi-glassy and semi microlitic groundmass. In addition to this, the groundmass and phenocrysts of the rock are seemed to be in equal proportion. Amphibole, opaque minerals, biotite and epidote inclusions are seen in the very large plagioclase grains.

Toptepe Basalts are simatic origin and were formed in the 5 th volcanic phase. Petrochemically and morphologicaly these rocks are completely different from the previously mentioned volcanics. These are situated in the alkalic basalt field of Wu-Liren diagram (Fig. 4). They are located in the shoshonitic basalts area in Peccerillo's and Taylor's diagram (Fig. 5). Thin section studies of these rocks demonstrate the presence of glassy groundmass between olivine crystals and elongated pyroxene microlites. The olivine predominates in the rock composition, but the pyroxene is concentrated in microlites. In the groundmass, chloritized pyroxene are noticed too.

4. ORIGIN AND FORMATION OF VOLCANISM

If one plots the results of chemical analyses of Aliağa volcanics in Miyashori's diagram (Fig. 6), 95 % of these rocks are found to be located in the calc-alkalic field. The samples of basaltic rocks are seen in calc-alkalic region in Aramaki's diagram (Fig. 7). In Irvine-Baragar's, Mc Donald-Katsura's, Kuno's diagram, most of the volcanites take position in calc-alkalic region, only a few of them are seen in alkalic region (Fig. 8).

In general alkalic volcanites and Toptepe basalts are used interchangeably here. In the survey area the volcanic activities started with the eruption of volcanoes of calc - alkaline

211

studies of the tuffs and tuffites showed the distribution of volcanic rock fragments, glass fragments, quartz, plagioclase and K-feldspar phenocrystys in a glassy groundmass. The glass fragments had devitrified, the groundmass is vesicular and kaolinized. The acidic tuffs were accumulated in a lake environment (Fig. 3).

Aliağa pyroclastics formed in the 3 rd phase are approximately 250 m thick and composed of different grain sized white and creamy rhyolitic and dacitic tuffs fragments. Petrographic investigation of the acidic tuff shows the presence of corroded primary quartz, altered K-feldspar, phyllosilicate, crystals, chert, chlorite and sericite fragments in a silisified groundmass. Coarse-grained lava fragments are also noticed in the rock.

Due to extrusive volcanic activities that took place intermittently during the formation of pyroclastics produced pyroxene andesite lava flows inside the Aliağa pyroclastics. The pyroxene lava flows are black and dark grey colored, massive and hard. These intermediate volcanic rocks are made up of plagioclase, pyroxene, amphibole and biotite phenocrysts. The plagioclase shows kaolinization towards the grain edges. Petrographic naming from the same rock specimen proved to be latite in accordance with Peccerillo and Taylor (1976); Cox et al. (1979) and andesite in accordance with Wu-Liren et al., (1983) diagram. Owing to the presence of abundant pyroxene in the sample the rock is called pyroxene andesite.

In the fourth phase, the stretch taking place in Upper Miocene caused tectonic disturbance of the area which led to the formation of Aliağa volcanics covering large area in this region. As a result of extrusive volcanism sialic calc-alkalic type volcanics originated dome and pin shaped structures on the dominant tectonic trend of the area. The petrochemical results of these volcanics are given below from bottom to top;

Hatundere Dacites : overlie Aliağa pyroclastics as thin and thick lava flows. In Peccerillo's and Taylor's, 1976 and Wu-Liren's et al., (1983) diagrams, these rocks are located in the high K-bearing dacite region. The dacites found in this area are assumed to be derived from admixture of granitic and granodioritic magmas with magmas originated in the upper mantle. The microscopic studies of the rock show the presence of unaltered phenocrysts of plagioclase, biotite, amphibolite and pyroxene in a semi-microlitic, semi-glassy groundmass.

Sarıkaya Rhyolites : After the formation of Hatundere dacites, rhyolitic rocks were formed along tectonic trends in separated and restricted zones. These rocks form thin and thick lava flows and dykes. The microscopic studies of these rocks indicate the distribution of phenocrysts in microcrystalline groundmass. Except of plagioclase and biotite phenocrysts, there are glassy fragments in the rock with obscured borders.

Bozdivlit Basaltic Andesites : These volcanic rocks occupy an important part in the

210
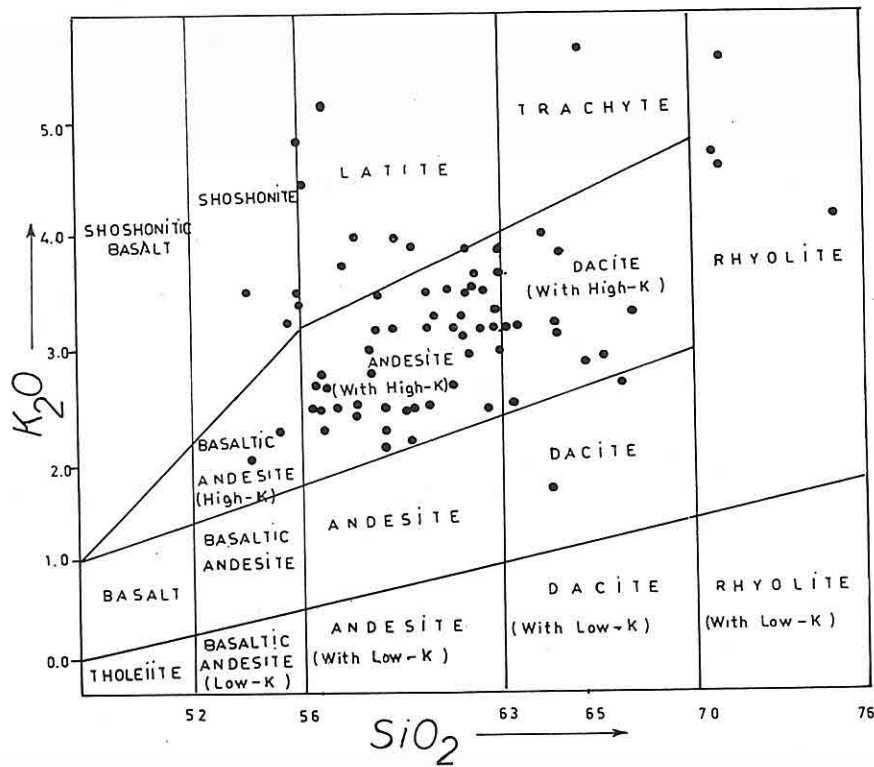
Figure 5. Nomenclature of the volcanics according to Peccerillo and Taylor (1991)

sedimentary rocks were formed. It is approved that these rocks form volcanosedimentary rock sequence constituting the upper levels of Soma Formation (Fig. 3).

III. Volcanic phase ; This phase is mostly of explosive and to a less degree of extrusive character which led to the formation of Aliağa pyroclastics. This volcanic activity took place in Middle Miocene.

IV. Volcanic phase ; It is extrusive character and led to the formation of volcanics which are Sialic calc-alkalic origin. This activity occurred in Upper Miocene. The volcanics, which originated in this period from bottom to the top, are; Hatundere dacites, Sarıkaya rhyolites, Bozdivlit basaltic andesites, agglomerates and Dumanlıdağ andesites.

V. Volcanic phase ; Extrusive eruption of Pliocene Toptepe basalts with shoshonitic character and Simatic origin.

Pyroclastics in the 1 st and 2 nd phase named as acidic tuffs and tuffites. Petrographic
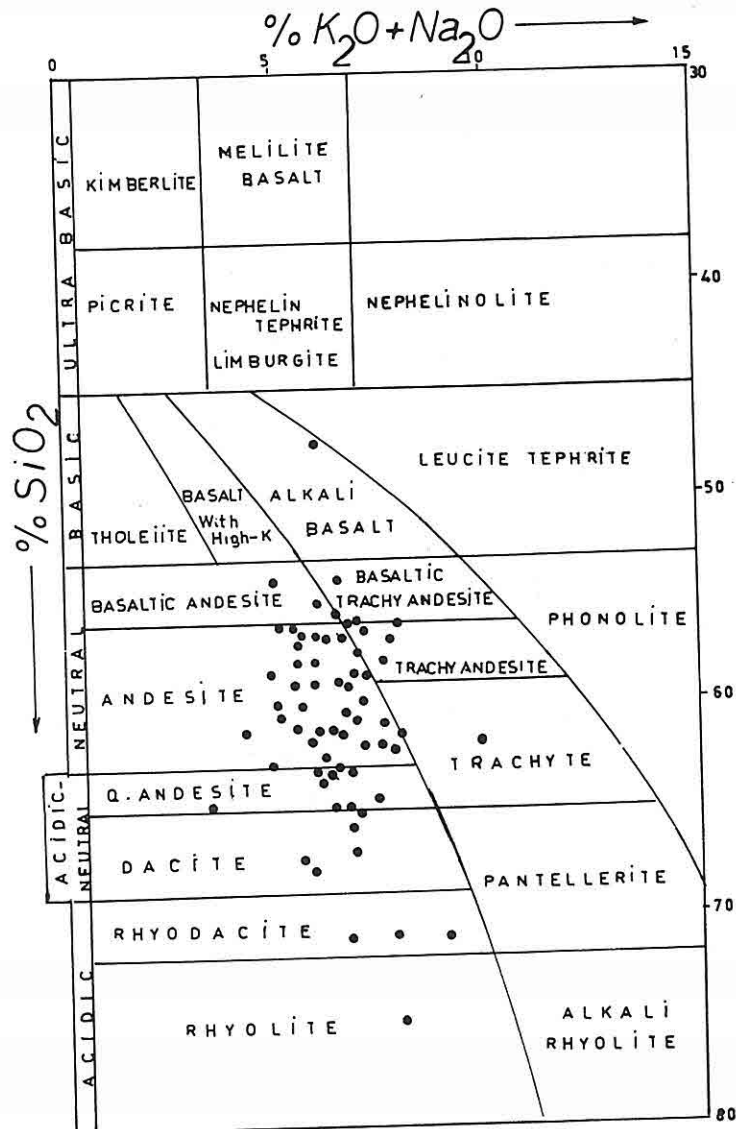
Figure 4: Nomenclature of the volcanics according to Wu-Liren et al., (1983).

1.Volcanic phase ; Began in Lower Miocene as intrusions and explosive (volcanoclastics and carbonatic volcanics) (Turgut, 1987), (Fig. 3).

II. Volcanic phase ; Towards the end of Lower Miocene tuff and tuffite interstratified

TABLE 1. MAJOR ELEMENT CHEMICAL ANALYSES AND VARIOUS PARAMETERS OF THE ALİAĞA VOLCANICS

SAMPLE NO	AY-2	AY-18	AY-26	AY-30	AY-33	AY-36	HS-2	HS-3	HS-5	HS-7	HS-9	HS-15	HS-17	HS-21	HS-37	TE-5	TE-7	TE-15	TE-35	TE-44	TE-47	K-206	K-211	K-214
SiO_2	71.0	61.5	58.0	63.0	64.5	59.0	75.1	60.7	65.0	58.5	71.0	60.0	60.0	63.5	56.0	53.9	56.7	55.6	54.1	60.6	47.6	65.0	61.5	56.0
Al_2O_3	13.2	16.4	15.8	16.3	16.4	16.0	13.0	15.5	15.0	17.0	14.5	15.5	15.0	15.1	17.0	16.8	17.7	15.2	15.7	17.8	13.4	14.0	15.5	13.5
P_2O_5	0.1	0.2	0.3	0.4	0.2	0.3	0.1	0.2	0.4	0.4	0.4	0.5	0.4	0.2	0.3	0.3	0.5	0.5	0.9	0.2	0.6	0.8	0.2	0.7
TiO_2	0.1	0.5	0.9	0.4	0.8	0.6	0.1	0.5	0.4	0.9	0.4	0.5	0.7	0.2	0.7	0.6	1.0	0.5	0.5	0.5	1.2	0.8	0.5	0.8
MnO	0.1	0.1	0.1	0.1	0.1	0.1	0.1	0.1	0.1	0.1	0.1	0.1	0.1	0.1	0.1	0.3	0.5	0.1	0.1	0.1	0.1	0.2	0.1	0.2
Fe_2O_3	3.5	5.4	6.4	4.5	4.8	6.2	2.1	6.5	4.4	6.2	2.0	5.8	6.3	5.5	6.0	7.1	5.0	6.75	7.0	4.9	9.0	6.0	5.5	6.0
FeO	0.1	0.1	0.1	0.1	0.1	0.6	0.1	0.5	0.1	0.9	0.1	0.5	0.4	0.2	0.3	6.4	7.6	8.1	7.3	1.9	9.6	0.2	0.2	0.8
CaO	1.0	5.0	5.7	4.7	3.0	6.0	0.75	6.0	4.4	5.3	1.4	5.15	5.1	4.25	4.55	5.2	2.9	2.95	4.8	4.95	11.0	1.0	4.9	6.45
MgO	0.3	2.8	3.5	2.2	1.3	3.0	0.2	4.2	2.3	1.3	0.4	3.7	3.2	2.4	3.35	3.0	3.6	3.0	2.95	4.0	9.6	1.6	3.0	6.0
Na_2O	3.5	3.0	3.5	3.5	3.5	3.0	3.75	2.6	3.0	3.95	2.25	2.85	3.2	3.6	3.45	3.0	3.6	3.0	2.95	4.0	2.55	1.55	2.95	2.6
K_2O	5.5	3.3	2.4	3.2	4.0	2.5	4.2	2.5	3.85	3.0	4.5	2.2	3.9	2.5	3.5	2.05	2.5	3.3	3.5	3.5	3.55	5.6	2.6	4.45
$C\,O_2$	2.3	2.3	2.4	2.1	0.8	1.0	1.7	4.0	2.35	1.55	0.65	2.15	2.3	2.15	2.65							0.4	2.6	2.7
$Fe\,O$	0.41	0.25	0.66	0.5	0.33	0.41	0.41	0.41	0.28	0.33	0.65	0.5	0.5	0.41								0.58	0.36	0.75
H_2O	1.00	1.22	1.74	1.22	1.24	1.58	1.54	1.2	1.14	1.54	1.66	1.6	1.16	0.9	0.94							1.68	1.14	0.95
PECCERILLO and TAYLOR	RHYOLITE	ANDESITE With High-K	ANDESITE With High-K	DACITE–ANDESITE With High-K	DACITE With High-K	ANDESITE With High-K	RHYOLITE	ANDESITE With High-K	DACITE With High-K	ANDESITE With High-K	RHYOLITE	ANDESITE With High-K	LATITE	DACITE With High-K	LATITE SHOSHONITE	BASALTIC ANDESITE With High-K	ANDESITE With High-K	SHOSHONITE	SHOSHONITE	ANDESITE With High-K		TRACHYTE	ANDESITE With High-K	LATITE SHOSHONITE
COX et all.	RHYOLITE	ANDESITE	ANDESITE	DACITE	DACITE	TRACHY ANDESITE	RHYOLITE	ANDESITE	DACITE	TRACHY ANDESITE	RHYOLITE	ANDESITE	LATITE	DACITE	LATITE	BASALTIC ANDESITE	TRACHY ANDESITE	LATITE	LATITE	TRACHY ANDESITE	HAWAIITE	DACITE	ANDESITE	LATITE
WU LIREN et all.	RHYODACITE	ANDESITE	ANDESITE	ANDESITE Q.ANDESITE	Q.ANDESITE	ANDESITE	RHYOLITE	ANDESITE	DACITE	ANDESITE	RHYODACITE	ANDESITE	ANDESITE	Q.ANDESITE	TRACHY ANDESITE. BASALTIC TRACHY AND.	BASALTIC ANDESITE	ANDESITE	BASALTIC ANDESITE	BASALTIC TRACHY ANDESITE	ANDESITE	ALKALI BASALT	DACITE	ANDESITE	TRACHY ANDESITE. BASALTIC TRACHY AND.
β	2.89	2.14	2.32	2.24	2.62	2.64	1.97	1.47	2.13	3.11	1.63	1.5	2.96	1.81	3.71	2.34	2.72	3.15	3.75	3.20	8.09	2.32	1.91	3.82
$\log \beta$	0.46	0.33	0.36	0.35	0.42	0.42	0.29	0.17	0.83	0.49	0.21	0.17	0.47	0.26	0.57	0.37	0.43	0.50	0.57	0.5	0.91	0.36	0.28	0.58
τ	9.7	26.9	13.6	32.0	25.8	21.7	92.5	23.0	30.0	14.5	122.5	23.5	16.8	115.5	19.3	23.0	14.1	12.2	14.7	27.6	7.17	12.45	25.0	13.6
$\log \tau$	1.99	1.43	1.33	1.5	1.41	1.34	1.96	1.36	1.4	1.16	2.0	1.37	1.22	2.06	1.28	1.36	1.15	1.08	1.17	1.44	0.85	1.09	1.40	1.13
K_2O / Na_2O	1.57	1.1	0.68	0.91	1.14	0.83	1.12	0.96	1.28	0.76	2.0	0.77	1.22	0.69	1.01	0.68	0.69	1.1	1.18	0.87	1.93	3.61	0.98	1.71
K_2O/SiO_2	0.077	0.054	0.041	0.051	0.062	0.042	0.056	0.041	0.058	0.051	0.063	0.037	0.065	0.039	0.062	0.038	0.044	0.059	0.065	0.058	0.075	0.036	0.046	0.079

207

According to the data obtained from Foça-1 offshore drillhole drilled in NW (in Aegean Sea) Soma Formation consists of Lower Miocene volcanic and evaporitic rocks. The rocks belonging to this unit rest on İzmir Flysch. The drill hole data indicate that there are 500 m thick volcanoclastics in the lowermost part of the section. In the middle of the section there are 400 m thick carbonatic volcanics and a 400 m thick anhydrite bed in the upper part of the section. This sequence is overlain by 150 m thick sandstone and mudstone. There is 170 m thick yellowish grey limestone and clayey limestone over the above mentioned level. The last one overlain by 200 m thick tuff and tuffite interstratified with mudstone and claystone. The total thickness of the last three sequences is 520 m and this equals to the thickness obtained by geological work in the area. These data indicate the existence of different facies in the Aegean Sea and on the continental part during Lower Miocene.

The Aliağa pyroclastics formed in Middle Miocene lie over Lower Miocene sediments disconformably. These rocks grade verticaly into bio-micritic Çamdağ limestones.

The Çamdağ limestone indicates a nonvolcanic period in Middle Miocene, Later Çamdağ limestones were buried under Upper Miocene volcanics which started with the eruption of Hatundere dacitic rocks (Fig. 2, 3).

In this area Toptepe basalts were formed in Pliocene, but alluvium and taluses were accumulated in Quaternary.

3. VOLCANISM

For petro-chemical investigations, analyses of 77 volcanic rock specimens were performed in MTA Laboratories (Table I). In addition, detailed petrographic investigations of the same samples were carried out. Peccerillo and Taylor (1976) and Wu-Liren et al. (1983) diagrams were used to classify the different types of volcanic rocks (Figure 4, 5). Naming done according to the above diagrams showed the occurrence of acidic rocks like rhyolite-rhyodacite, high amount-K bearing dacite, quartz andesite, andesite with high K content, basaltic andesite latite and shoshonite. Besides, trachyandesite, basaltic trachyandesite and alkalic basalt type rocks are found in the area.

In the studied area, the volcanic rocks of different ages and types crop out on both the NE-SW trending tectonic structure which intersects the above one and trends NW-SE direction.

Miocene and Pliocene volcanic activity is divided into five phases. The volcanic rocks produced by this activity are studied and identified in accordance with their positions and order of formation within the general stratigraphy of the area.

206

ERATHEM	SYSTEM	SERIES	STAGE	SUB STAGE	FORMATION	MEMBER	SYMBOL	COLUMNAR SECTION	LITHOLOGY
							Qaly		— DISCORDANCE — ALKALI BASALT
				PLIO CENE		TOP.T BASALT	Tβ		— DISCORDANCE — ANDESITE WITH HIGH (K)
						DUMANLIDAĞ ANDESITE	Tand		TRACHY ANDESITE, AGLOMERATE–DIKES
							Tagl		AGLOMERATE
			UPPER	ALIAĞA VOLCANICS		Bozdivlit Basaltic Andesite	Tba		LATITE–BASALTIC ANDESITE, ANDESITE WITH HIGH (K)
						Sarıkaya Rhyolite	Tryl		RHYOLITE AND LATITE, DACITE ANDESITE DIKES
C A I N O Z O I C	T E R T I A R Y	N E O G E N E — M i o c e n e				HATUNDERE DACITE	Tdst		D A C I T E — DISCORDANCE —
			MIDDLE			Camdağ Limestone			LIMESTONE (Lacustre)
					ALIAĞA PYROCLASTICS		Tap		TUFF INTERCLATION WITH PYROXENE ANDESITE — DISCORDANCE (NW) SIDE
			LOWER	SOMA FORMATION			Ts(2)		SILTSTONE CLAYSTONE AND TUFF INTERCLATION
									LIMESTONE, LIMESTONE WITH CLAY
									SANDSTONE AND SILTSTONE INTERCLATION — Well of FOCA-1 (SE) SIDE
						ANHYDRIDE	Ts(1) anh		CLAYSTONE MUDSTONE, MARL, SILTSTONE;
						VOLCANICS WITH CARBONATE	vkl		CONGLOMERATE
						PYROCLASTICS			SILTSTONE, CLAYSTONE WITH LIGNITE — DISCORDANCE —
MESOZOIC	CRETACEOUS	SANTONIAN-MAASTRICHTIAN		İZMİR FLYSCH	KÜif	ALLOCHTHON			FLYSCH WITH RECRYSTALLISED LIMESTONE EXOTIC BLOCK.

Figure 3. Generalized columnar section of the investigated area.

by yellow and beige limestone, clayey limestone, mudstone, claystone and tuffite interlayered rocks. The upper part of Soma Formation is formed of alternating sedimentary rocks and volcanoclastics.

205

Figure 2. The geologic map of the Aliağa (İzmir) area (Eşder, 1991).

Geologically the area is located NW of the İzmir-Ankara Suture Zone. The area specifically is situated in the SE part of the geologic structure that strikes NE-SW which dips together with the basement towards the Aegean Sea.

Several geologist have conducted important geological work on the Neogene magmatic evolution of the NW Anatolia on the basis of tectonic events (Paola,1969; Savaşçın,1975; Innocenti et al., 1977; Savaşçın and Dora, 1977; Eşder, 1978; Ercan, 1979; Kaya, 1979; Ercan, 1982a; Ercan, 1982b; Kaya, 1982; Filiz, 1982; Öğdüm, 1982; Ercan et al., 1984; Ercan, 1985; Jica and MTA, 1987; Eşder, 1988).

The volcanic rocks of different ages and types cover 3/4 of the area. The volcanics are classified according to the order of formation into phases and the volcanostratigraphy and petrologic characteristics of them have been studied. Taking into consideration the geological events of the area the past volcanic activities can be related to the neotectonic events.

2. THE STRATIGRAPHICAL GEOLOGY OF THE AREA

The Paleozoic metamorphics of the Crystalline Menderes Massife do not crop out in this area. The paleo-autochthonous metamorphic sequence forms the basement in Western Anatolia. This sequence consists of different schists in the uppermost parts of the Massif and of gneisses towards the core (Fig. 10).

The İzmir Flysch which was formed in Upper Santonian-Lower Maastrichtian had moved from NW towards SE and rested on the Menderes Massif as allochthonous between Paleocene and Lower Lutetian (Eşder, 1988).

The İzmir Flysch crops out at about 500 m above sea level in the SE part of the research area. The Flysch was intercepted at 2100 m below sea level according to data obtained from Foça-1 offshore drill hole at the Aegean Sea (Turgut, 1987). The flysch in the area is of epiclastic character and generally composed of interbedded turbidite and olistostromal layers (Fig. 2).

Triassic and Jurassic recrystallized limestones lie on the uppermost part of this sequence discordantly (Fig. 3). There is a big stratigraphic gap between Paleozoic and Neogene in this area.

There is an angular unconformity between İzmir Flysch and Lower Miocene aged sedimentary rocks and older volcanics. Neritic, lacustrine and volcano-sedimentary sequences of Lower Miocene age are called Soma Formation.

The sequence is divided in two units (Fig. 3). The Lower part of this formation is composed of conglomerate, claystone, mudstone, siltstone and sandstone beds. The upper part of it ends with micritic marl beds. In the NW part the micritic marl is overlain

203

1. INTRODUCTION

The geological work was conducted in the Aliağa (İzmir) area located in Western Anatolia between Menemen, Yuntdağ and Foça (Fig. 1).
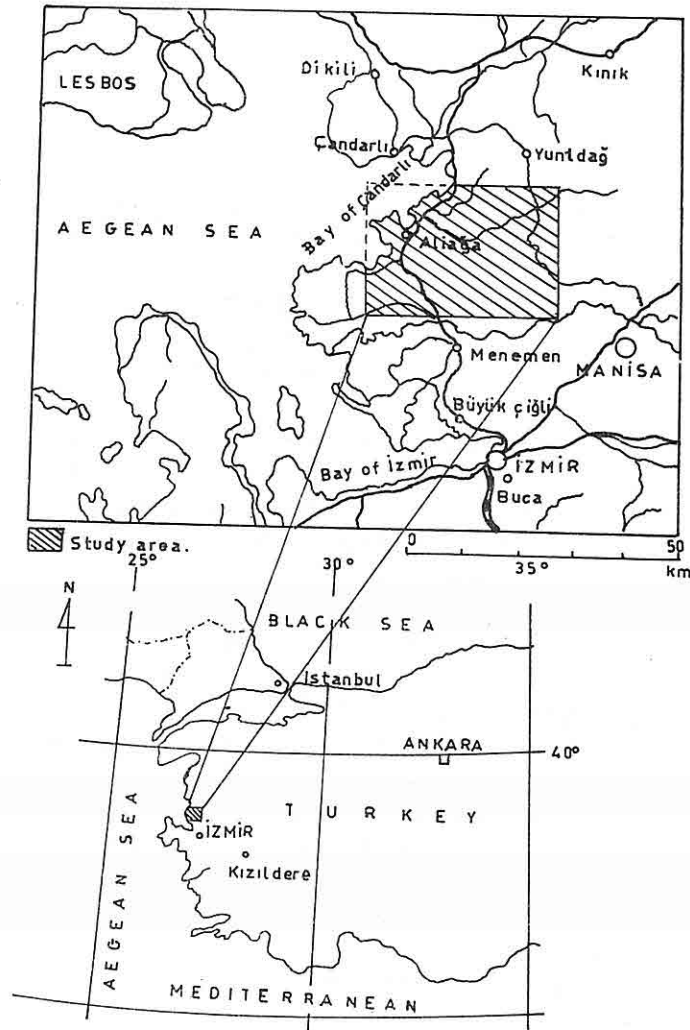
Figure 1. Location Map.

An area of 650 km² was studied in detail and geological map with a scale 1/25 000 was performed. During this work the volcanostratigraphy and geothermal potential of this region were investigated in detail.

202

THE GEOLOGY AND PETROLOGY OF THE NEOGENE AGED VOLCANIC ROCKS OF ALİAĞA (İZMİR) AREA

Tuncer EŞDER

General Directorate of Mineral Research and Exploration Regional Branch Office of İZMİR, PK. 1, 35042 Bornova/İZMİR/TURKEY

ABSTRACT : *Field work was carried out in Aliağa (İzmir-Turkey) area which is situated in Western Anatolia, NW of the İzmir-Ankara Suture Zone with the aim of compiling knowledge on the geology, volcanology and geothermal potential of this area.*

The oldest rock unit of the area is İzmir Flysch of Cretaceous age which overlies the Menderes Massif as allocthonous cover.

The rocks of Lower Miocene age are volcanic, evaporitic and lacustrine deposit at the Aegean Sea side of the area. In the Aliağa area they have lacustrine and volcanosedimentary character. The above mentioned rocks are summarized lithologically to The Soma Formation. This Formation is buried under pyroxene andesite lava interstratified with Aliağa pyroclastics of Middle Miocene age. This unit grades into Çamdağ limestones of the same age.

The rocks of calc-alkalic and alkalic volcanic character were formed during the ent.ı ⹂ Upper Miocene and Pliocene. These rocks are grouped together to the Aliağa volcanics.

In the studied area the sialic calc-alkalic volcanism started in Lower Miocene and continued intermittently during Middle-Lower Miocene. The volcanic activities continued in Pliocene and ended with the formation of so called Toptepe basalts which are of Simatic origin and of basic alkalic character.

After dividing the volcanic rocks into five different phases, their petrology, formation, origin and stratigraphy were studied. Neither calc-alkalic nor alkalic volcanism are assumed to have any association with a subduction zone. The volcanics in the research area are considered to be formed as intracontinental volcanics in the NW part of the Anatolian plate which is located between the Eurasian and African plates and moves Westward relative to the North Anatolian Transform Fault.

The calc-alkalic and alkalic volcanism in the research area are thought to be related to expansional tectonic regime which was active from Lower Miocene up to Quaternary.

201

which were also responsible for the formations of other carbonate clay minerals at the same levels.

3) The formation of Pirrsonite has affected largely the changements of physicochemical parameters, mostly a_{CO2} and temperature and also m_{CO2}. The changements of these parameters have resulted in transformations, mostly to Nahcolite ($NaHCO_3$), Gaylussite ($Na_2CO_3.CaCO_3.5H_2O$), Thermonatrite ($Na_2CO_3.H_2O$) and Calcite.

4) Trace element contents have been analyzed and it was determined at the high levels of Cl, Br, F and B which were indicated to volcanic origin.

5)The XRD, DTA and SEM characteristic of Pirrsonites have been defined.

6) Na/Ca ratio had been increased very fast and for this reason Pirrsonite formation had cut down suddenly; trona accumulation had started. This ratio had been protected from the changements in two large periods, resulting in two thick trona levels. At the last stage of deposition, as a result of increasing of HCO_3 contents in the solutions, Nahcolites have been deposited.

8. REFERENCES

Bradley, W. and Eugster, H. P., 1969. Geochemistry and Paleolimnology of Trona Deposits and Associated Autogenic Minerals of Green River Formation of Wyoming U. S. Geol. Sur. Prof. Pp.469 B.71p.

Eugster, H. P., and Smith, G. I., 1965. Mineral Equilibra in Searles Lake Evaporites California. Journal of Petrology Vol.6. Part 3.

Gündoğdu, N., Tenekeci, Ö., Öner, F., Dündar, A. ve Kayakıran, S., 1985. Beypazarı Trona Yatağının Kil Minerolojisi: Ön Çalışma Sonuçları. II.Ulusal Kil Sem.

Helvacı, C., İnci, U., Yağmurlu, F ve Yılmaz, H., 1989.Geologic Framework of the Beypazarı District and Neogene Trona Deposits, Turkey. Doğa Bilim Dergisi, 13.

Helvacı, C., Yılmaz, H., Yağmurlu, F. ve İnci, U., 1989. Beypazarı Yöresinde Trona İçeren Neojen Tortullarının Stratigrafisi, 5. Müh. Haf. Bil. Öz.

Suner, F., 1989. Beypazarı Trona Yatakları, Doktora Tezi, İTÜ Fen Bil. Ens.

Suner, F. ve Çoban, F., 1989. Beypazarı (Ankara) Trona Havzasında Pirsonit ve Dolomitlerin Mineralojik-Jeokimyasal İncelenmesi, A.Acar Jeo. Sim. Bil. Öz.

Figure 8. The formation paths of Pirrsonite and other carbonates observed in Beypazarı
Trona Deposits

a_{CO_2}, from Gaylussite, other Ca-Na double carbonate hidrated.

2) Pirrsonites have been formed as small and pseudohegsagonal crystals as a result of the rapid changements of physicochemical parameters of depositional conditions. The filling of volcanic outcrops had also affected these deposition and formation parameters

Nahcolites had been formed in upper levels of trona horizons. The general deposition steps and products are summarized in Figure 8.
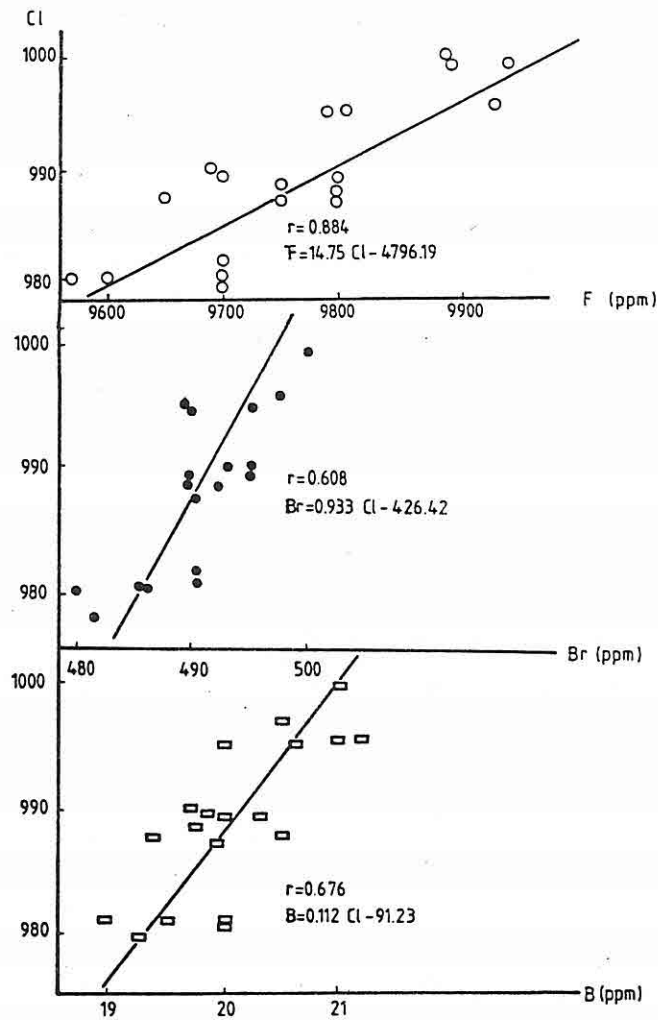
Figure 7. The correlation coefficients and lines of Cl versus F,B,Br

7. CONCLUSIONS

In this study, Pirrsonite has been examined at the first time. The determined conclusions obtained from mineralogical, petrological, chemical studies have been summarized as follows:

1)The mineral had been formed during the beginning period of deposition from the partly Ca-rich solutions not only primarely but also secondarely, depending on

198

Table 1. Statistical Parameters of Trace Elements observed in Pirrsonite

	X	S	S_H	M_i	M_o	S_k
K	38.9	1.66	1.74	38.33	38.39	-0.05
Mg	4165	162.1	170.6	4166.6	4169.9	-0.05
Ba	349.5	11.17	11.75	346.25	339.75	0.82
Rb	31.3	1.92	2.03	31.2	31.0	0.147
Cs	331.5	2.82	2.96	331.4	330.42	0.364
Si	189.0	23.0	24.43	188.0	186.0	0.123
Cl	998.0	71.41	75.17	987.2	985.8	0.29
P	115.5	2.44	2.56	115.33	114.99	0.198
Al	168.6	4.43	4.66	168.86	169.37	-0.163
Ti	54.6	1.26	1.32	54.62	54.67	-0.05
Li	5.2	0.44	0.46	5.2	---	---
F	9780	105.4	110.9	9775	9765	0.135
I	3365	115.21	121.28	3350	3320	0.37
SO4	4745	107.12	112.75	4744.4	4743.3	0.015
B	20.05	0.804	0.847	19.90	19.6	0.53
Br	491	6.63	6.98	491.8	493.43	-0.35

6. PHYSICO-CHEMICAL CONDITIONS OF PIRRSONITE FORMATION

Pirrsonite is a mineral that can be transformed to other similar carbonate minerals easily because of physico-chemical parameters, mostly of a_{H2O}, a_{CO2}, m_{CO2} and temperature. This mineral, according to ion and Eh-pH levels and concentrations, can form from Gaylussite, Nahcolite, Trona, Thermonatrite, Thenardite primarely and secondarely. If there are not any other salts in environment, Pirrsonite can precipitate around 40° approximately. The temperature may decrease depending on the presence and concentration of other salts, such as Burkeit and Thycite. In other words, Pirrsonite formation, as a result of the presence of salts, depends on low a_{H2O} and temperature, generally. In Beypazarı Basin, this deposition with illite- smectite- dolomite- calcite dominant paragenesis, had been formed in low diagenetic conditions and temperature and also from poor salty solutions in limited periods. The solutions which responsible for the formation of Pirrsonite were rich of Ca in the beginning period of filling of the paleolake; forming calcite and dolomite, depending on Ca/Mg ratio at the bottom of Hırka Formation. As a result of the filling of the lake with Na-rich volcanic material and solutions, Pirrsonites had been deposited in limited period because of the increasing of Na concentration in solutions from which thick trona seams had been precipitated. At the last stage of evaporation and as a result of the increasing rate of HCO_3 in solutions and also lower temperature,

As shown in Figure 5., the decomposition of the mineral has been determined at 377°C and 428°C; in two steps. The dehydration has observed at 198°C.
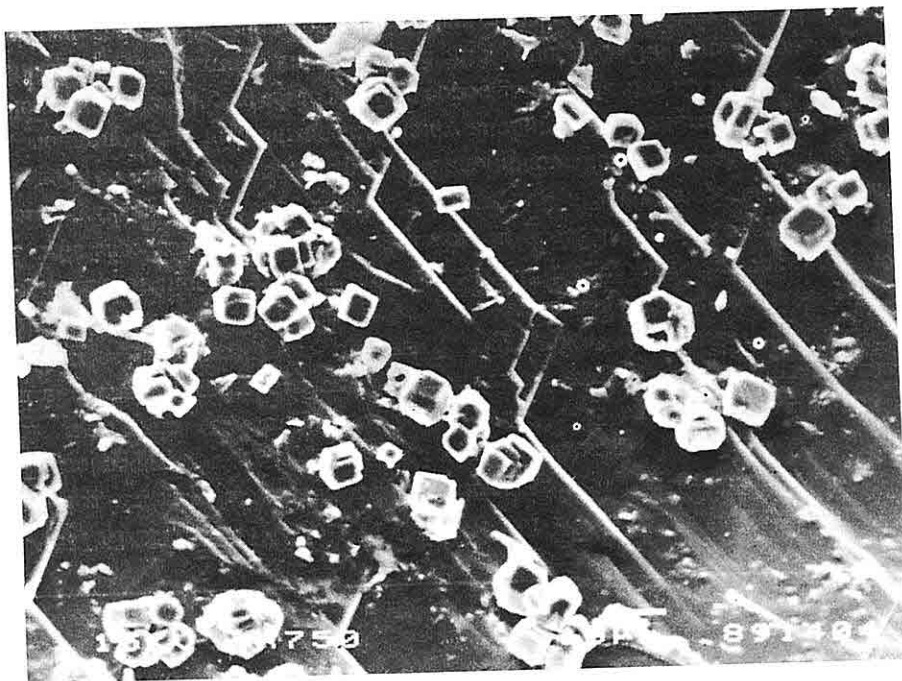
Figure 6. Scanning Electron Microphoto of Pirrsonites on Claystone.

5. GEOCHEMICAL STUDIES

The major and trace element contents of pure Pirrsonite specimens have been determined using different analitical methods. The data getting these studies have been evaluated statistically and obtained statistical parameters which are shown in Table 1.

The most important point of the results was that the trace element contents of Pirrsonites were approximately the same from one specimen to another. As a result of this situation, the coefficient skewness was very low generally and the distribution character has observed as normal Gausian Distribution. The standart deviation of the speciments were also determined as low or very low because of the mentioned properties of Pirrsonite analyses.

The other important point, was that volatile elements such as Cl, Br, F and B were present in Pirrsonites indicating volcanic effect and the precence of circulating water within the rocks.

196
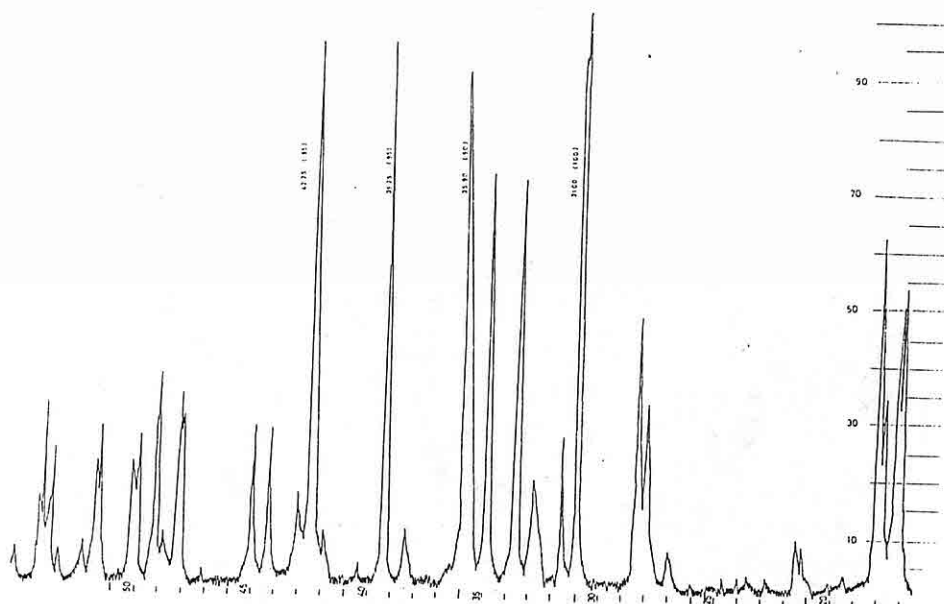
Figure 4. The XRD difractogramme of Beypazarı Pirrsonite; Cu (Ni) K_c
n= 1.54378; (20mA x 40kV); 2θ= 1°/1 sec. operating conditions.
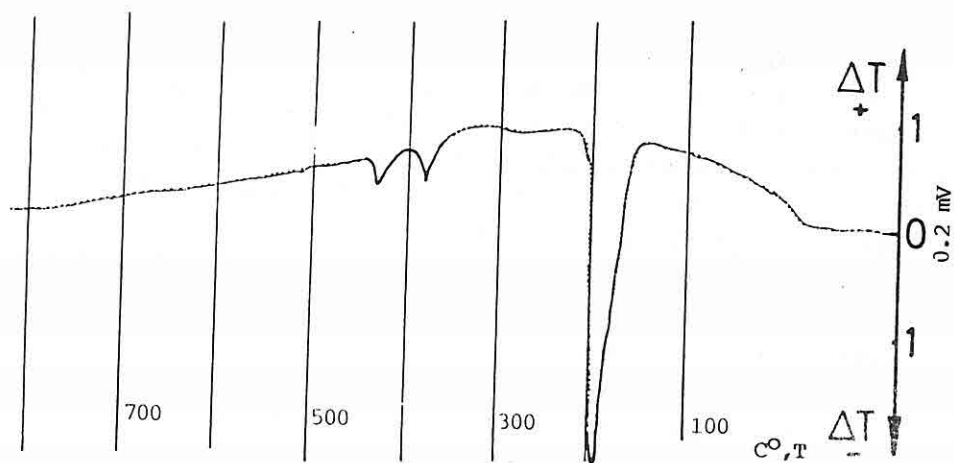
Figure 5. DTA curve of Pirrsonite. Pt-Pt/Rh thermoelement, 10°/sec
heating rate; 2.5 mm/sec. recording rate, normal atmosphere   195
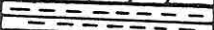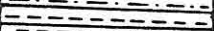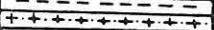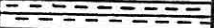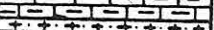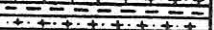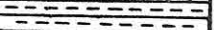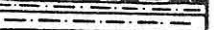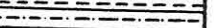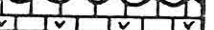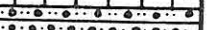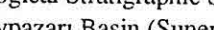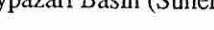
STRATIGRAPHIC SEQUENCE SHOWING TRONA
AND PIRRSONITE OCCURENCES IN BEYPAZARI BASIN

U. SYSTEM	SYSTEM	PERIOD	EPOCH	NAME	THICK (m)	LITHOLOGY	EXPLANATIONS
C E N O Z O I C	T E R T I A R Y	N E O G E N E	M I O C E N E	K.DOR.	40-80		Claystone , Marl
							Chert bearing dolomitic limestone
				H I R K A	250-350		Claystone
							Bituminous Shale
							Claystone
							Tuffite
							Claystone
							Bituminous shale
							Marl
							Tuffite
							Soda (Trona)
							Soda (Trona)
				C O R A K L I	100		Bitu.Shale,Clayst.,Pirrsonite Limestone , Dolomite
							Coal
							Bituminous Shale
							Coal
							Conglomerate
	PALEOGENE	EOCENE			100-150		Volcanic material bearing limestone
							Conglomerate

Figure 3. Geological Stratigraphic Section of Cenozoic Sequences of
Beypazarı Basin (Suner and Çoban, 1989)

The other investigation way of Pirrsonites was XRD method. The XRD pattern is shown in Figure 4. It must state that some of the peaks of Pirrsonite mineral are the same with those of Gaylussite and Trona partly. For this reason, the data of XRD must be interpreted carefully. The DTA studies were the other way of research for Pirrsonites of Beypazarı. These studies were very useful for making distinction between Pirrsonite and Gaylussite because of an exothermic reaction around 300°C. The DTA curve of the Beypazarı Pirrsonite is given in Figure 5.

Scanning Electron Microscopy (SEM) study was the other investigation way and it was very useful to determine the crystal shape and morphology of Pirrsonite and also other minerals.

194
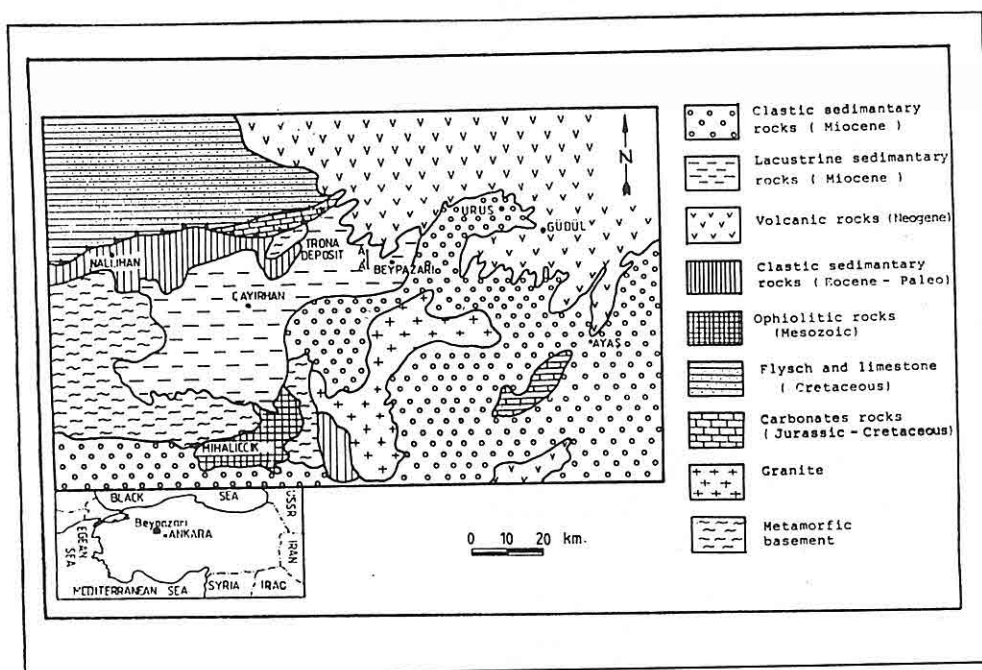
Figure 1. Geological Map of Beypazarı Basin (Helvacı et al., 1989)

a   b
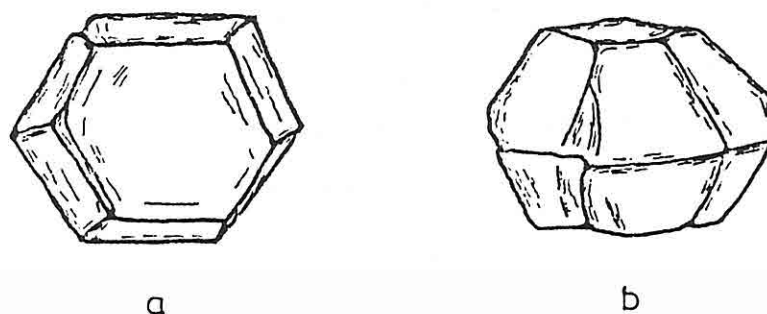
Figure 2. Pseudohegsagonal crystals(Orthorombic) of Pirrsonites

As a result of microscopic studies it was also determined that the single and double nicol optical properties of this mineral were very similar to those of trona ($Na_2CO_3.NaHCO_3.2H_2O$). For this reason, it was difficult to identify easily these two minerals using only microscopic studies.

193

1. INTRODUCTION

Pirrsonite, a rare forming mineral, had been found in Green River Formation (Bradley and Eugster, 1969) and in the muds of Searles Lake (Eugster and Smith 1969) with Trona and other evaporative minerals. In Türkiye, the mineral has been discovered in the second largest Trona Deposits of the world in Beypazarı, the province of Ankara. The mineral had been deposited very scatteredly at the lower parts of trona seams in Hırka formation, showing an association of carbonate laminated limestones, dolomites and claystones. Bituminous shales and tuffs tuffites were the other important rocks. The aim of this study is the evaluation of this mineral and the determination of the periods of Pirrsonite formation physico-chemically by taking into account of experimental data.

2. STRATIGRAPHY

Pirrsonnites have been found within volcano-sedimentary Hırka Formation which has overlaid Çoraklar Formation and was overlaid by Karadoruk Formation (Suner 1989; Helvacı et al., 1989; Suner and Çoban, 1989). All these formations (sequences) were Miocene aged and had been deposited conformably in this period. Pliocene sequences have overlaid with unconformably the Miocene sequences. The thickness of Miocene sequences were very different and have ranged from 60m to 350m. The main lithologic assemblage has been determined as claystone + bituminous shale + tuffite and trona, the main evaporative mineral of the Beypazarı Basin (Gündoğdu et al., 1985). Pirrsonites have been discovered in the lower part of the lower Trona Horizon in Hırka Formation, especially over the level where bituminous shales were common, with claystones and dolomites or dolomitic claystones.

3. MATERIAL AND METHOD

Pirrsonites have been collected from the part of the lower trona horizon and the mineral has been studied under the binocular microscope and prepared for analizing. The chosen specimens have been investigated by XRD, DTA, SEM techniques and analyzed wet chemical, gravimetrical, colorimetrical and spectrographical methods.

4. MINERALOGICAL STUDIES

Pirrsonites have been studied macroscopically and the dimensions of the mineral have been determined. The measured dimensions were not more than 4 mm and there were not big difference in crystal dimensions. Their colors were white and grayish-white ; they have exhibited disseminated structure in host rocks. In most specimens idiomorphic and well-crystallized pirrsonites have been seen. Pseudohegsagonal system were very common while pirrsonites have crystallized in orthorombic system. Piroelectricity was the other observed property of this mineral.

192

MINERALOGICAL AND GEOCHEMICAL PROPERTIES OF TURKISH PIRRSONITES

Yılmaz BÜRKÜT and Fikret SUNER

Technical University of İstanbul, Mining Faculty İstanbul-TÜRKİYE

ABSTRACT: *Pirrsonite is a rare-forming carbonate mineral. This double salt ($Na_2CO_3.CaCO_3.2H_2O$) has been found sporadiccally in Beypazarı Basin (Ankara), as a secondary mineral. In this study, the mineralogical and geochemical properties of Pirrsonites, in Miocenous volcano-sedimantary sequences, associated with dolomites and claystones, have been determined and the formation conditions have been discussed. The idiomorphous crystals and disseminated structures of Pirrsonites have been investigated using XRD, SEM and DTA methods. The trace element contents, phase relations and mineral paragenesis have been determined. According to the data and their stratigraphic positions and horizontal-vertical distributions, it was thought that this mineral had been formed under the effect of low temparature and high Ca^{++}/Na^{+} concentration.*

191

Symposium on Salt (vol. 1): Cleveland, Northern Ohio Geol. Soc., p. 151-159.

Nemec, D., 1975. Genesis of tourmaline spots in leucocratic granites: N. Jb. Miner. Mh., v. 7, p. 308-317.

Nicholson, P.M., 1980. The geology and economic significance of the Golden Dyke Dome, Northern Territory, in Ferguson, J. and Goleby, A.B. (eds.), Proceedings of International Uranium Symposium on the Pine Creek Geosyncline: Vienna, International Atomic Energy Agency, p. 319-334.

Plimer, I.R., 1980. Exhalative Sn and W deposits associated with mafic volcanism as precursors to Sn and W deposits associated with granites: Mineral. Deposita, v. 15, p. 275-289.

_____, 1986.Tourmalinites from the Golden Dyke Dome, northern Australia: Mineral Deposita, v. 21, p. 263-270.

_____, 1987. The association of tourmalinite with stratiform scheelite deposits: Mineral Deposita, v. 22, p. 282-291.

_____, 1988. Tourmalinites associated with Australian Proterozoic submarine exhalative ores, in Friedrich, G.H. and Herzig, P.M. (eds.) Base Metal Sulfide Deposits: Berlin, Springer-Verlag, p. 255-283.

_____, and Lees, T.C., 1988. Tourmaline-rich rocks associated with the submarine hydrothermal Rosebery Zn-Pb-Cu-Ag-Au deposit and granites in western Tasmania, Australia: Mineral. Petrol., v. 38, p. 81-103.

Raith, J.G., 1988.Tourmaline rocks associated with stratabound scheelite mineralization in the Austroalpine Crystalline Complex, Austria: Mineral. Petrol., v. 39, p. 265-288,

Reed, B.L., 1986. Descriptive model of Sn greisen deposits, in Cox, D.P. and Singer, D.A. (eds.), Mineral Deposit Models: U.S. Geol. Survey Bull. 1693, p. 70.

Robinson, G.D., Healey, K., and Kelly, V.C., 1988. Use of tourmaline in stream sediments to detect submarine exhalative sulfide deposits: example from central Virginia, U.S.A.: Appl. Geochem., v. 3, p. 225-230.

Robinson, G.D., 1989. Stream sediment tourmaline geochemistry in massive sulfide exploration: an example from Virginia, U.S.A.: Jour. Geochem. Explor., v. 34, p. 173-188. .

Shcherba, G.N., 1970. Greisens: Internat. Geol. Rev., v. 12, no. 2, p. 114-150, and no. 3, p. 239-255.

Slack, J.F., 1982.Tourmaline in Appalachian-Caledonian massive sulphide deposits and its exploration significance: Trans. Inst. Min. Metall., Sect. B, v. 91, p. B81-B89.

_____, 1984. Herriman, N., Barnes, R.G., and Plimer, I.R., Stratiform tourmalinites in metamorphic terranes and their geologic significance: Geology, v. 12, p. 713-716. .

United Nations Development Programme, 10. 1974. Sinancılar arsenic area (anomaly No.44), in Mineral exploration in two areas, Turkey, Technical report 4, Detailedinvestigations of geochemical anomalies (DP/UN/TUR-72-004/4): New York, United Nations, p. 40-44,

190

Edwards, A.B., 1936. On the occurrence of quartz-tourmaline nodules in the granite of Clear Creek, near Everton: Proc. Roy. Soc. Victoria, v. 49, Pt. 1, p. 11-16..

Ethier, V.G., and Campbell, F.A., 1977. Tourmaline concentrations in Proterozoic sediments of the southern Cordillera of Canada and their economic significance: Can. Jour. Earth Sci., v. 14, p. 2348-2363.

Fleischer, R., and Routhier, P., 1973. The "consanguineous" origin of a tourmaline-bearing gold deposit: Passagem de Mariana (Brazil): Econ. Geol., v. 68, p. 11-22..

Foshag, W.F., 1921.The origin of the colemanite deposits of California: Econ. Geol., v. 16, p. 199-214.

Helvacı, C., 1984. Occurrence of rare borate minerals: veatchite-A, tunellite, terrugite and cahnite in the Emet borate deposits, Turkey: Mineral. Deposita, v. 19, p. 217-226.

Ketin, I., 1983. A general look at the geology of Türkiye: Istanbul Technical University Foundation, Book Publication No: 32, 595 p. (in Turkish).

Konak, N., 1985. A discussion on the core-cover relationship on the basis of recentobservations (Menderes Massif): Abstr. of the Geol. Congress of Türkiye, p. 33,

_____, 1987. Akdeniz, N., and Öztürk, E.M., Geology of the south of Menderes Massif, in Guide Book for the Field Excursion along western Anatolia, Turkey (IGCP Project N.5, Correlation of Variscan and pre-Variscan events of the Alpine-Mediterranean mountain belt; Field Meeting, Turkey, September 13-19, 1987): Ankara, MTA General Directorate, p. 42-53.

Koval, P.V., Zorina, L.D., Kitajev, N.A., Spiridonov, A.M., and Ariunbileg, S., 1991. The use of tourmaline in geochemical prospecting for gold and copper mineralization: Jour. Geochem. Explor., v. 40, p. 349-360.

Kun, N., 1976. A geological and petrographical examination of the vicinity around Nebiköy-Kafaca and Kavak villages (Yatağan): M.Sc. thesis, Ege University Faculty of Science, Geology Dept., İzmir, (in Turkish).

Ito, T., and Plimer, I.R., 1987.The significance of tourmaline in the stratiform Dome Rock deposit, Australia: Mining Geol., v. 37, p. 403-418.

McArdle, P., Fitzell, M., Oosterom, M.G., O'Connor, P.J., and Kennan, P.S., 1989. Tourmalinite as a potential host rock for gold in the Caledonides of southeast Ireland: Mineral. Deposita, v. 24, p. 154-159.

Mittwede, S.K., 1984a. Significance of tourmaline compositions from the Inner Piedmont geologic belt of South Carolina: Southeastern Geol., v. 24, p. 207-210. .

_____, 1984b. Tourmalinite, anomalous tourmaline concentrations, and iron formation as exploration guides in northwestern Cherokee County, South Carolina: South Carolina Geol., v. 27, p. 6-12,

_____, 1985. Geochemical and mineralogical anomalies in the Thicketty Mountain area, Cherokee and Spartanburg Counties, South Carolina: South Carolina Geol., v. 28, p.7-10.

Muessig, S., 1965. Recent South American borate deposits, in Rau, J.L. (ed.), Second

5.ACKNOWLEDGMENTS

6.REFERENCES

Allard, G.O., and Carpenter, R.H., 1988. Mineralogical anomalies in metamorphosed terrains; a neglected but promising exploration tool, in International Conference-- Geochemical Evolution of the Continental Crust, Abstracts Volume: Pocos de Caldas, Brazil, p. 229-236. .

Alonso, R.N., Helvacı, C., 1988. Sureda, R.J., and Viramonte, J.G., A new Tertiary borax deposit in the Andes: Mineral. Deposita, v. 23, p. 299-305.

Appel, P.W.U., 1985. Stratabound tourmaline in the Archean Malene supracrustals, West Greenland: Can. Jour. Earth Sci., v. 22, p. 1485-1491.

_____, 1986. Stratabound scheelite in the Archean Malene supracrustal belt, West Greenland. Mineral. Deposita, v. 21, p. 207-215.

Başarır, E., 1970. The petrology and geology of the eastern flank of the Menderes Massif on the east of Lake Bafa: Scientific Reports of the Faculty of Science, Ege University, No: 102, 44 p., (in Turkish).

Benvenuti, M., Lattanzi, P., and Tanelli, G., 1989. Tourmalinite-associated Pb-Zn-Ag mineralization at Bottino, Apuane Alps, Italy: Geologic setting, mineral textures, and sulfide chemistry: Econ. Geol., v. 84, p. 1277-1292.

Boyle, R.W., 1971. Boron and boron minerals as indicators of mineral deposits, in Boyle, R.W. and McGerrigle, J.I. (eds.), Geochemical Exploration, Proceedings, 3rd International Geochemical Exploration Symposium, Toronto: Can. Inst. Min. Metall., Spec. Vol. 11, p. 112.

Chamberlain, R.T., 1912. The physical setting of the Chilean borate deposits: Jour. Geol., v. 20, p. 763-768.

Dağ, N., 1991. Mineralogical and geochemical investigation of Gördes pegmatoids (Menderes Massif): Dokuz Eylül University Institute of Science and Engineering, Research Papers No:FBE/JEO-AR-89-171, İzmir, 19 p.. .

_____, and Dora, O.Ö., 1991. Gördes (Menderes Massif) pegmatoids: Geol. Bull. of Turkey, v. 34, p. 1-8. (in Turkish).

Dietrich, R.V., 1985.The Tourmaline Group,: New York, Van Nostrand Reinhold Co., 300 p.

Dixon, C.J., and Pereira, J., 1974. Plate tectonics and mineralization in the Tethyan Region: Mineral. Deposita, v. 9, p. 185-198.

Dora, O.Ö., Kun, N., and Candan, O., 1992. Metamorphic history and geotectonic evolution of the Menderes Massif, in Savaşçın, M.Y. and Eronat, A.H. (eds.), IESCA 1990Proceedings, International Earth Sciences Congress on Aegean Regions:İzmir, v. II, p. 102-115.

exhalative processes took place, thereby raising the exploration interest in an area." (Plimer, 1988, p. 280).

Likewise, the tourmalinite near Karahayıt village (#1 above), and the along-strike iron showings, should be considered encouraging indicators of mineralization and the area a prime exploration target for metallic resources.

The boron concentrations represented by the tourmaline disseminated in mica schist, paragneiss and the felsic gneiss unit described above (#2 and #3) are apparently not anomalous and may simply reflect normal B abundances in sediments or magmas.

The quartz-tourmaline nodules and the possibly related massive lenses within the felsic gneiss basement (#4 above) formed via metamorphic processes, metasomatic processes or both. The massive lenses formed within zones of weakness and exhibit evidence of shearing. Both the source of boron and the concentration processes being enigmatic, it is unclear whether or not the nodules and massive lenses have any significance for exploration. It is suggested that where such tourmaline concentrations are abundant, the lithogeochemistry of the felsic gneiss basement unit be studied carefully, with attention especially given to possible concentrations of volatiles and metals. Movement of large amounts of volatiles (such as B) may indicate favorability for mineralization; that is, movement and concentration of metals may have accompanied B metasomatism.

Although tourmaline associated with pegmatitic granitic rocks is sometimes gemmy, because of their color, the tourmaline crystals that occur in pegmatoids of the Kula and Gördes areas (#5) are not suitable for use as gem material. However, the tourmaline maybe useful as an indicator mineral for Be-mineralized pegmatoids. According to Dağ and Dora (1991), the tourmaline-bearing E-W-oriented pegmatoids in the central and northern parts of the Menderes Massif may contain reserves of approximately 2000 tons of beryllium which could be a by-product of muscovite and feldspar mining.

The tourmaline-bearing intrafolial pods or segregations, such as those observed along Gökçay near Bucakbelen (#6), are simple "sweat-outs" produced during regional metamorphism. There is no evidence to suggest that such occurrences have importance for exploration.

Although there is no known mineralization directly related to the occurrence of tourmaline in sheared granitic gneiss near Eskihisar (#7), nearby up-section within another fault zone weak copper mineralization has been observed. The normal faults of the Aydın-Salavatlı geothermal area should be considered prospecting targets with low to moderate potential.

For the Sinancılar tourmaline occurrence (#8), we suggest that more detailed sampling be done along the W-SW side of the granitic body, and that analyses include determinations of Sn, W, Mo, Ta, Nb and possibly U, Th and REE. If the results of such analytical work are encouraging, trenching and possibly drilling will be necessary as exposures are limited. Fluid-inclusion work would be helpful in determining conditions under which the Sinancılar mineralization formed.

Detailed stream-sediment sampling and soil-rock sampling traverses showed very low As and Ag values and no detectable Au.

Nevertheless, exposures along the Sinancılar-Bayındır road on the W-SW margins of the granitic body have many aspects which commend a comparison to greisenization, "a high-temperature (500-300°C), complicated post-magmatic transformation of rocks under the influence of the acid residual solutions, high in silica and volatile constituents, connected with intrusions of granitoids." (Scherba, 1970, p. 114). Scherba described greisens as follows:

> Greisens are metasomatic rocks, essentially quartz-mica by
> composition, often with topaz, fluorite, tourmaline, feldspar, and
> ore minerals, formed from granite and other rocks by action of
> high-temperature pneumatolytic-hydrothermal solutions, high in
> fluorine, chlorine, and water. (p. 114)

In addition, the descriptive model for Sn-greisen deposits of Reed (1986) is an excellent outline to which the Sinancılar occurrence can be compared. Many aspects of the geological setting and mineralogy of the Sinancılar occurrence are consistent with Reed's greisen model.

First, the Sinancılar gangue and ore mineralogy are consistent with typical greisen mineralogy. The predominant gangue minerals within the mineralized zones are quartz, tourmaline and mica. Fe, Cu and As(?) sulfides are present and apparently formed more-or-less coevally with tourmaline. Also, fluorite and torbernite(?) were identified in at least one specimen. Second, the geological context is appropriate for greisen formation. According to Scherba (1970) and Reed (1986), greisens occupy apical parts/cupolas of granite massifs or occur along the margins of granitoids, and greisenization generally is imposed onto contact-metamorphosed rocks. Both of these conditions are satisfied at the Sinancılar occurrence.

4. IMPLICATIONS FOR EXPLORATION AND FURTHER STUDY

Tourmalinite, as described above, is associated with many types of metallic mineral deposits, including those of Au (Fleischer and Routhier, 1973; Plimer, 1986; McArdle et al., 1989), W and Sn (Plimer, 1980, 1987; Appel, 1985, 1986; Raith, 1988), Pb-Zn-Ag (Ethier and Campbell, 1977; Benvenuti et al., 1989), Zn-Pb-Cu-Ag-Au (Plimer and Lees, 1988), Cu (Slack, 1982), and Cu-Co (Ito and Plimer, 1987). Therefore, this minor but significant rock type, by virtue of its spatial relationship with such mineralization, should be considered an important exploration guide.

As pointed out by Plimer (1988, p. 280), "Although tourmalinites can be the host for or are intimately associated with exhalative mineralization, they need not be associated with mineralization." Plimer also noted that the tourmalinites in Australia are most commonly immediately above or stratigraphically equivalent to exhalative mineralization. He further commented that while "no rigid facies relationship between tourmaline-rich rocks and mineralization can be established, their presence indicates that
186

metamorphism. Where exposed on the Alaşehir-Kula road at Selce village, the tourmaline-bearing pegmatoids occur within metavolcanic rocks (leptites) and, locally, there is evidence of migmatization and a lithologic transition to gneiss and schist. It is likely that the pegmatoids, characterized by diffuse contacts rather than by sharp igneous contacts, formed under temperature and pressure conditions that led to migmatization.

6) Black tourmaline occurs in subhedral to anhedral crystals or clots, with quartz, as intrafolial pods or segregations within garnet-quartz-mica schist. We have observed this mode of occurrence along Gökçay, near Bucakbelen village (Muğla-Yatağan).

This is probably a very common mode of tourmaline occurrence in the MM as it is in many metamorphic terrains. During metamorphism, volatiles such as B are easily mobilized and silica seems to be ubiquitously available. Under elevated temperature and pressure conditions, excess silica and volatiles may "sweat out" or be laterally secreted along existing foliation planes or zones of weakness. We envision the Gökçay occurrence as having formed in this manner.

7) Near Eskihisar (Aydın-Sultanhisar) on Bayazık Tepesi, approximately 1-cm-thick, poorly defined bands of anhedral to subhedral black tourmaline crystals occur locally within strongly sheared granitic gneiss. Microcline, quartz and muscovite are the main constituents of this gneiss, but biotite is also present. This tourmaline occurrence is within a normal fault zone; the texture of the rocks should probably be termedprotomylonite or mylonite gneiss. Approximately 100 m upslope, still within the fault zone, undeformed tourmaline-bearing granitic pegmatite dikes transect metavolcanic rocks (leptites). Here, the tourmaline occurs in black euhedral to subhedral crystals, 2-7 mm in cross-section. It is possible that these pegmatite dikes had their source in the underlying sheared granitic gneiss. Movement along the fault zone may have induced melting which resulted in the emplacement of the dikes.

8) Along the Sinancılar - Bayındır road between Sinancılar village (İzmir-Kemalpaşa) and Ovacık Yayla, black tourmaline occurs in narrow (0-3 cm) veins, joint- and fracture-fillings, in irregular layers of massive, sulfide-bearing quartz-tourmaline rock, and with quartz, mica and sulfides as country-rock replacements. These occurrences are at the margins of an unmetamorphosed, post-kinematic, fine- to medium-grained biotite granodiorite body and associated sills and dikes. Andalusite hornfels also reportedly occurs in the contact aureole of this granitic body (UNDP, 1974). This granitic body is believed to be of Miocene age and intruded gently to moderately N-dipping schist and quartzite of probable late Paleozoic age which have been assigned to the Ovacık Formation (UNDP, 1974).

The UNDP (1974) performed an investigation of the Sinancılar arsenic anomaly during which a small (20-m-long) Pb-Zn-Cu mineralized area was discovered in Küçükköy stream, 1.5 km NE of Ovacık Yayla. Although this mineralization was deemed economically insignificant and no further work was recommended, the weak arsenic anomaly farther north remains a "teaser" for explorationists. The results of the UNDP effort to follow up stream-sediments arsenic anomalies were discouraging.

185

pyrite) are generally present. In fact, most of the nodules at the Irmadan locality are of pale, rusty pinkish or reddish color, reflecting the oxidation of iron.

Although these quartz-tourmaline nodules are of great interest, their occurrence is not unique. Similar nodules have been described previously by Edwards (1936, and references therein) from Australia, and by Nemec (1975) from Czechoslovakia. In both of these cases, the nodules occurred in leucocratic granites and it was believed that the nodules formed by metasomatic replacement of granite. Nemec (1975) likened the origin of "tourmaline spots" in granites to the development of the quartz-tourmaline facies of greisens and supposed that the B was imported from outside.

The massive lenses of tourmaline mentioned above have only been observed by us at one locality, between the Labranda ruins and Kargıcak village, ENE of Sarıkaya village. These lenses are mainly tourmaline with some quartz, and are apparently sheared and formed in zones of weakness. They are aligned, as are the abundant quartz-tourmaline nodules, N to N10°E, parallel to a weak lineation defined by elongated potassium feldspars. At this locality and to the north, tourmaline also occurs within narrow veins, as fracture fills, and within light-colored granitic dikes/veins.

In the southern part of the MM, the metasomatic process that led to the formation of the quartz-tourmaline nodules and massive lenses was apparently of large scale; the vast area that was affected by this enigmatic process attests to this. Reheating and circulation of fluids may have been induced during a regional metamorphic event. The process that mobilized the B necessary to form the quartz-tourmaline eyes likely also mobilized the B necessary to form the nearby massive lenses.

The formation of these quartz-tourmaline nodules involved movement of large amounts of B, maybe over relatively long distances. It is possible that the B had an external source. On the other hand, the B may have been concentrated in the granite precursor of the felsic gneiss basement unit, at least in its upper parts, and simply concentrated by a poorly understood metasomatic process. What caused nucleation and subsequent formation of the quartz-tourmaline nodules is unknown.

5) Euhedral crystals, some very large, of black tourmaline occur within pegmatoids and pegmatites in the area of Kula and Demirci-Gördes. Dağ (1991) and Dağ and Dora (1991) have discussed these rocks in some detail, so the reader is referred to those papers for more information.

These pegmatoids, possibly better described as leucosomes, are of fairly simple mineralogy, with quartz, feldspar and tourmaline as major constituents. Biotite is present locally. Dağ and Dora (1991) reported that the tourmaline in the pegmatoids of the Gördes area is dravite (Mg-rich), but presented no optical or geochemical data to support this identification. If this determination is correct, this is indeed an unusual paragenesis as tourmaline in granitic pegmatites/pegmatoids is typically of the schorl (Fe-rich) species.

On the basis of field observations, we conclude that the tourmaline-bearing pegmatoids described above formed by partial melting during high-grade regional

184

migmatite and granitic dikes within the "transition zone" between the felsic gneiss basement and the overlying mica-quartz schist. Konak et al. (1987) also noted tourmaline as a common mineral phase in the various units within the Çine Group. In the highway section at Irmadan Mahallesi (Muğla-Yatağan), Kun (1976) described the occurrence of a deeply weathered, 1.5-m-thick unit of tourmaline-rich quartz-mica schist. Within this unit occur abundant 2-3-cm-long, euhedral, black tourmaline crystals. Using optical and XRD methods, Kun (1976) identified the tourmaline of this schist to be schorl.

With the exception of the Irmadan locality, these aforementioned rocks do not apparently contain anomalous concentrations of tourmaline. The tourmaline-rich schist at Irmadan may have formed by remobilization of B from the underlying felsic gneiss basement unit.

3) Black tourmaline in weakly concentrated, fine- to medium-grained, anhedral to subhedral crystals occur within the vast felsic gneiss unit that is considered to be the oldest unit of the Menderes crystalline sequence. Excellent exposures of this mode of tourmaline occurrence are present near Irmadan Mahallesi and between the Labranda ruins and Kargıcak village.

Previously, Konak et al. (1987) described augen gneisses of granitic origin of the Çine Group. These gneisses represent the core of the MM. These granitic gneisses consist essentially of quartz, feldspar, white mica and some biotite. Minor constituents include tourmaline, apatite, zircon, rutile, and opaque minerals.

This mode of tourmaline occurrence does not seem to reflect an anomalous concentration of B in the paleoenvironment. Because granitic magmas are typically relatively enriched in B, this sort of weakly concentrated or disseminated tourmaline is probably in no way unusual. However, quantitative petrographic studies of many specimens of this gneiss may show that the B concentration is anomalous and that the granitic precursor was a "specialized" granite, enriched in volatiles and metals.

4) In the highway section at Irmadan Mahallesi and in exposures between the Labranda ruins and Kargıcak village, black tourmaline occurs in eye-shaped concentrations or nodules and in massive lenses (the latter in zones of weakness) within the felsic gneiss basement unit. Kun (1976), Konak (1985), and Konak et al. (1987) mentioned the tourmaline at these occurrences, the latter authors describing "tourmalines that are aligned radially and flocs of interesting shapes where they become denser" (p.44). In characterizing the augen gneiss of granitic origin in which these modes of tourmaline occurrence are found, Konak (1985, p. 33) reported the presence of a "tourmaline balled leucocratic phase in the contact aureoles." It is obvious to us these descriptions apply to the nodules that we have observed and describe below.

In longitudinal section, as they typically appear in outcrop, these tourmaline concentrations are roughly eye-shaped, but in toto these concentrations are spherical, ellipsoidal or discoidal nodules. They consist mainly of tourmaline and quartz but, at the Irmadan locality, euhedral cubes (up to 2 mm) of oxidized sulfides (probably

To the north and south, the tourmalinite gradually passes into schist and micaceous quartzite. The tourmalinite continues for an unknown distance to the west and, to the east, only thin discontinuous layers occur within the enclosing schist-quartzite unit. Away from the hillock, the tourmalinite increases in content of quartzofeldspathic minerals and passes imperceptibly into schist and quartzite. Locally, distinct angular (sedimentary) quartz grains and tourmaline-rich rip-up clasts are present.

Obviously, an incredible amount of boron in tied up in a tourmalinite occurrence such as that near Karahayıt. For the depositional environment for tourmalinite, there are only two viable possibilities: either tourmalinites are deposited as volcanogenic chemical sediments (exhalites), or they form by metamorphism of evaporitic borate deposits (Slack et al.,1984). Slack (1982) pointed out that ancient evaporitic terrains are generally marked by an abundance of diagnostic minerals such as anhydrite and scapolite. Therefore, "these minerals, and related chemical signatures, allow identification of evaporitic environments even where post-depositional deformation and metamorphism obscure primary sedimentary features" (Slack, 1982, p. B86). Since most borate deposits are considered to be related to volcanic sources/activity (Chamberlain, 1912; Foshag, 1921; Muessig, 1965; Helvacı, 1984; Alonso et al., 1988), any occurrence of tourmalinite is, either directly or indirectly, volcanogenic and, more specifically, related to volcanic vents, fumaroles or thermal springs.

Based upon these data and observed field relationships, we conclude that the precursor for the tourmalinite - B-rich chemical sediments or exhalites- which likely issued from a volcanic vent/fumarole, was probably deposited into seafloor depressions. The lateral continuity of extremely fine-scale tourmaline and quartz laminae on the hillock indicates a quiescent depositional environment. Because the tourmalinite is almost massive tourmaline locally, that part of the depositional system was probably near the source. The more-distal, lateral equivalents, however, are richer in quartzofeldspathic (arenaceous) material and reflect a more active depositional environment. In these distal facies, bedding and/or lamination tend to be less continuous, that is, more disrupted. It is also in these more-distal parts that the rip-up clasts and distinct angular quartz grains occur.

Interestingly, at least two iron-ore showings are present along strike in approximately the same structural-stratigraphic position (Başarır, 1970). According to Başarır, these hematitic iron ores are probably of sedimentary origin. During our field work, a fragment of magnetite-rich float material resembling iron-formation was found near the cemetery at Karahayıt village.

We suggest that both the Karahayıt tourmalinite and the along-strike iron ores resulted from volcanogenic exhalative activity.

2) Black tourmaline in <1 mm-3 cm-long, euhedral to anhedral crystals is disseminated within various lithostratigraphic units, especially mica schist and paragneiss, in the southern part of the Menderes Massif.

Başarır (1970) reported tourmaline as an accessory mineral in fine-grained gneiss,

182

Turgutlu (Ketin, 1983). Dixon and Pereira (1974) considered the MM to be one of a number of "Zwischengebirge", essentially microcontinental blocks, "made up of pre-Mesozoic basement rocks having some of the characteristics of the cratons, but displaying evidence of Alpine tectonic and magmatic involvement" (p. 187).

It is not an object of this paper to review the geology and structure of the MM, so the reader is referred to Konak et al. (1987) and Dora et. al. (1992) for cogent summaries. However, the major lithostratigraphic units of the MM must be described if the tourmaline occurrences discussed herein are to be understood in context.

A felsic gneiss unit, previously described as augen gneiss, migmatite, granitic gneiss and core gneisses, is considered to be the oldest lithostratigraphic unit in the MM (Dora et al., 1992) and, therefore, is believed by us to be basement to the rest of the rock units in the MM. At the southern end of the MM, where much of the current research was done, this granitic core unit is overlain by a transition zone of fine-grained gneiss/migmatite/granitic gneiss/ gneissic granitic "dike" (sill or leucosome?), then successively by mica - quartz schist, garnet - quartz - muscovite schist (with marble lenses), chloritoid schist, muscovite-quartz schist (or mica quartzite), a repeating series of quartz schist-calc schist-chlorite schist-metaconglomerate-phyllite - marble, phyllite and marble (Başarır, 1970). Many of the tourmaline occurrences described herein are present within the felsic gneiss unit and the overlying mica-quartz schist unit.

3. MODES OF TOURMALINE OCCURRENCES

1) Başarır (1970) described tourmaline zones or bands within his biotite-quartz schist unit, southwest of Karahayıt village (Muğla-Milas) and approximately 2 km east of Bafa Gölü. The maximum thickness of these zones was reported to be about 100 m (Başarır, 1970). We have found these zones/bands to be tourmalinite, a stratabound and/or stratiform laminated quartz-tourmaline rock containing ≥ 15-20% tourmaline by volume (Nicholson, 1980; Slack, 1982). Tourmalinites have been described from many places, including Australia (Plimer, 1988), Austria (Raith, 1988), Brazil (Fleischer and Routhier, 1973), Canada (Ethier and Campbell, 1977), Greenland (Appel, 1985), Italy (Benvenuti et al., 1989) and the USA (Slack, 1982; Mittwede, 1984b). The reader is referred to Slack et al. (1984) for a succinct review of stratiform tourmalinites in metamorphic terranes and their geologic significance.

The tourmalinite at the Karahayıt locality occurs as locally significant but discontinuous lenses or intercalations within mica-quartz (± garnet)schist that grades into micaceous quartzite. The most significant outcrop of tourmalinite is on a hillock about 1 km southwest of Karahayıt village, on the west side of Yatakyeri stream and about 100 m west of the village road. There, black or very dark brown tourmaline and quartz occur together in an extremely finely laminated rock. Locally the tourmalinite is virtually massive tourmaline with some irregular quartz veinlets. No other minerals have been identified on the hillock except very minor sulfides.

181

1.INTRODUCTION

Tourmaline, a complex borosilicate mineral, is the most common boron mineral in crystalline rocks and is also one of the dominant, non-opaque heavy-mineral species in recent and ancient sediments and sedimentary rocks. Recently, an entire volume about the tourmaline group was published (Dietrich, 1985), and the reader is referred to that valuable sourcebook for a discussion of the physical and chemical properties, occurrences, geneses and significance.

Boyle (1971) noted that boron and boron minerals, because they are widely diffused in many types of mineral deposits, can be used as indicators of mineralization. As practical applications of this, Slack (1982), Mittwede (1985) and Robinson et al. (1988) suggested that identification of anomalous concentrations of tourmaline in samples of panned stream sediment might be a useful tool in exploration programs designed to locate metallic ore deposits. Furthermore, the chemical composition of tourmaline can be used in metallogenetic analysis and may be a sensitive and reliable guide to the location of submarine exhalative sulfide deposits (Slack, 1982; Mittwede, 1984a; Robinson, 1989; Koval et al., 1991).

Tourmaline as well as many other minerals, such as spessartine, gahnite, lazulite, hogbomite, are due to hydrothermal enrichment ± metamorphic recrystallization at/near volcanic centers and have been considered "mineralogical anomalies" (Allard and Carpenter, 1988). Because they form by metamorphism of hydrothermal alteration assemblages, these mineralogical anomalies can be important exploration tools for metallic mineral deposits in metamorphosed terrains. Tourmalinite, a laminated or banded quartz-tourmaline rock, can be a particularly valuable exploration guide for metallic mineral deposits as well as a distinct marker unit during field mapping in multiply deformed, highly metamorphosed terranes (Slack, 1982; Slack et al., 1984).

The purpose of this paper is to present the first general synthesis of the modes of tourmaline occurrences in the Menderes Massif, western Anatolia, Türkiye. This paper is based upon our field observations, literature research and interpretations. A paper of this length cannot be considered comprehensive, but an effort has been made to review the main types of tourmaline occurrences with particular attention given to those types that have significance for mineral exploration. Figures have been omitted so that descriptions, interpretations and pertinent references can be presented. Although some of the conclusions may be premature, this work provides a starting point for future investigations. The results of in-progress analytical work will shed light on the problems at hand, especially those concerning petrogenesis and implications for exploration.

2. REGIONAL GEOLOGY

The Menderes Massif (MM), an internal basement massif in western Anatolia, is one of the largest metamorphic massifs in Türkiye, measuring roughly 200 km N-S between Simav and Muğla, and approximately 150 km E-W between Denizli and

180

MODES AND IMPLICATIONS OF TOURMALINE OCCURRENCES IN THE MENDERES MASSIF, WESTERN ANATOLIA, TÜRKİYE

Steven K.MITWEDE[1], Cahit HELVACI[2], İsmail Hakkı
KARAMANDERESİ[3] ,Nejat KUN[2] and Osman CANDAN[2]
[1]McCracken and Associates, P.K. 207, 06443, Yenişehir, Ankara
[2]Dokuz Eylül University, Bornova-İzmir
[3]MTA Ege Bölge Müdürlüğü, Bornova-İzmir

ABSTRACT: *Tourmaline, specifically of the schorl (Fe-rich)-dravite (Mg-rich) series, is abundant in rocks of the Menderes Massif of western Anatolia and has at least eight modes of occurrence, some of which are genetically related, spatially related, or both. In this region, the modes of tourmaline occurrence include the following:*

1) as tourmalinite (stratabound and/or stratiform laminated quartz-tourmaline rocks containing ≥ 15-20% tourmaline by volume) - as locally significant but discontinuous lenses or intercalations within mica-quartz (± garnet) schist; 2) as euhedral to anhedral crystals disseminated within mica schist or paragneiss; 3) as weakly concentrated, fine- to medium-grained, anhedral to subhedral crystals within the vast felsic gneiss unit that is considered to be the oldest unit of the Menderes crystalline sequence; 4) as eye-shaped concentrations/nodules and in massive lenses (the latter in zones of weakness) within the felsic gneiss unit; 5) as euhedral crystals, some very large, in pegmatoids(leucosomes) and pegmatites; 6) as subhedral to anhedral crystals or clots, with quartz, as intrafolial pods or segregations within garnet-mica schist; 7) in bands of anhedral to subhedral crystals within strongly sheared granitic gneiss; 8) as joint- and fracture-fillings, with quartz in veins or layers, and as country-rock replacements accompanying sulfide mineralization near the margin of unmetamorphosed, post-kinematic granite.

These modes of tourmaline occurrences all reflect particular petrogenetic conditions. Some indicate anomalous concentrations of B in the depositional environment (e.g. tourmalinite = volcanogenic chemical sediments/exhalites), while others may simply represent normal B abundances in sediments or magmas (#2, #3). Numbers 4-7 reflect B concentration by metamorphic/metasomatic processes, although in these, too, B may have been anomalously abundant in the paleoenvironment. Number 8 is related to B-enriched, late- or post-magmatic/residual or hydrothermal fluids associated with emplacement of granitic rock. The genetic implications of these types of occurrences may have great significance in mineral exploration and studies of petrogenesis.

Diagrams for the Tectonic Interpretation of Granitic Rocks. J.Petrol., 25, 956-983.

White, A.J.R. and Chappel, B.W., 1977.Ultrametamorphisim and Granitoid Genesis. Tectonophysics, 43, 7-22.

Yılmaz, S., 1991.Hekimhan-Hasançelebi (KB Malatya) Yöresi Jeolojisi ve Magmatitlerin Mineralojik-Petrografik ve Jeokimyasal İncelenmesi. Yüksek Lisans Tezi. Cumhuriyet Üniv., 256s, 2 Ek, (Yayınlanmamış).

Yılmaz, S., Boztuğ, D. ve Öztürk, A., 1991. Hekimhan-Hasançelebi (KB Malatya) Yöresinin Stratigrafisi ve Tektoniği. C.Ü. Müh.Fak.Dergisi Seri-A, Yerbilimleri, 8/1, 1-18.

Yılmaz, S., Boztuğ, D. and Öztürk, A., 1992. The geological setting, Petrographical and Geochemical Characteristics of the Cretaceous and Tertiary Magmatites in the Hekimhan-Hasançelebi Area, NW Malatya, Türkiye. International Workshop: Work in Progress on the Geology of Türkiye, Keele-England, Abstr., p.81.

177

7. REFERENCES

Barton,M.D., Ilchik,R.P. and Marikos,M.A., 1991. Metasomatism. In Kerrick, D.M. (ed.), Contact Metamorphism, Reviews in Mineralogy, V.26, Mineralogical Society of America, 321-350.

Boztuğ, D. ve Yılmaz, S., 1992. Konukdere Metasomatitinin (Hekimhan-Hasançelebi, KB Malatya) Petrolojisi. Türkiye Jeoloji Kurultayı-1992 Bildiriler Bülteni (submitted).

Chappel, B.W. and White, A.J.R., 1974. Two Contrasting Granite Types. Pacific Geology, 8, 173-174.

Debon, F. and Le Fort, P., A ., 1982.Chemical-Mineralogical Classification of Common Plutonic Rocks and Associations. Royal Soc.of Edinburgh Transaction, 73, 135-149.

Deer,W.A., Howie, R.A. and Zussman,J., 1962. An Introduction to the Rock Forming Minerals. Longmans, London, 528 p.

Evensen, N.M., Hamilton,P.J. and O'Nions,R.K., 1978. Rare Earth Abundances in Chondritic Meteorites. Geochim. Cosmochim. Acta, 42, 1199-1212.

Govindaraju, K., 1989. Compilation of Working Values and Sample Description for 272 Geostandards. Geostandards Newsletter, 13, 1-113.

Henderson, P. General Geochemical Properties and Abundances of the Rare Earth Elements. In Henderson, P. (ed.), 1984. Rare Earth Element Geochemistry, Developments in Geochemistry 2, Elsevier, 1-32.

İzdar, E. ve Ünlü, T., 1977. Hekimhan-Hasançelebi-Kuluncak Bölgesinin Jeolojisi. Ege Bölgesi Jeolojisi VI. Kollokyumu, Dokuz Eylül Üniv., İzmir-Türkiye, 303-329.

Mariano,A.N., 1989. Economic Geology of Rare Earth Elements. In Lipin, B.R. and McKay, G.A., (eds.), Geochemistry and Mineralogy of Rare Earth Elements. Reviewes in Mineralogy, V.21, Mineralogical Society of America, 309-337.

Neary, C.R. and Highley, D.E., 1984.The Economic Importence of the Rare Earth Elements. In Henderson, P. (ed.), Rare Earth Element Geochemistry. Development in Geochemistry 2 Elsevier, 423-466.

Özer,T. ve Kuşçu,A.E., 1982. Malatya-Hekimhan-Deveci Demir Yatağı Jeolojisi ve Rezerv Raporu, MTA Raporu, (Yayınlanmamış) .

Pearce, J.A. and Cann, J.R., 1973. Tectonic setting of Basic Volcanic Rocks Determined Using Trace Element Analysis. Earth Planet. Sci.Lett., 19, 290-300.

Pearce,J.A., Alabaster,T., Shelton,A.W. and Searle,M.P., 1981. The Oman Ophiolite as a Cretaceous Arc Basin Complex: Evidence and Implications. Phil. Trans. R.Soc., A-300, 299-317 .

Pearce, J.A., Harris,N.B.W. and Tindle,A.G., 1984.Trace Element Discrimination

from low grade iron mineralization does not have any significant REE$_{CN}$ enrichment (Fig.5), with lower values than those of scapolite and garnet fels. Such a behaviour of REE in a hydrothermal environment, including altogether the silicate, oxide and sulphide phases, is considered as a normal case due to preferred migration of the REE into silicate rather than oxide or sulphide minerals (Henderson, 1984). Sample BLÖ-11, a representative specimen for the biotite rich veins, shows more or less the same LREE$_{CN}$ pattern with that of sample 10 taken from the iron mineralization but differs from that by its lower values of HREE$_{CN}$ pattern (Fig.5).

5. CONCLUSION AND DISCUSSION

The preliminary data on the REE contents of the rock samples of the Konukdere metasomatite may suggest that the possible REE potential is restricted to the scapolite fels, scapolite-pyroxene fels and garnet fels rocks rather than low grade iron mineralization and biotite rich vein occurences, even though the REE contents of the former group are 3 to 5 times higher than that of crustal abundance level (Neary and Highly, 1984). This low grade REE concentration in these rocks can be improved a little by the monomineralic nature, i.e.scapolite fels, of host rocks. As a monomineralic source for REE, some apatites associated with alkaline igneous complexes can be considered as commercial when the grade of REO is about 0.85 % (Neary and Highly, 1984). However, the grade of REE ore reserves varies markedly depending on the type of deposit. For instance, the high grade primary bastnasite deposit at Mountain Pass averages 7 % REO, but in some heavy mineral placer deposits the grade of REO may be as low as 300 ppm, just little above crustal abundance levels (Neary and Highly, 1984), since, the constituent minerals have already been liberated by natural processes. Because of the near monomineralic nature of the scapolite fels and garnet fels rocks from the Konukdere metasomatite, a detailed study of these rocks may provide more meaningful and useful data as to the REE potential of the Konukdere metasomatite.

6. ACKNOWLEDGEMENT

The REE contents (Table 4) of the rock samples from the Konukdere metasomatite have been normalized to chondrite values (Evensen et al., 1978). Figure 5 shows the chondrite normalized spider diagram of REE contents of these samples. Clearly, the scapolite fels and scapolite-pyroxene fels types of rocks possess an enrichment of approximately 100 to 350 times in $LREE_{CN}$ (chondrite normalized light rare earth elements) such as La and Ce. These rocks also represent an enrichment of 15 to 40 times in $HREE_{CN}$ (chondrite normalized heavy rare earth elements). The actual content of La and Ce varies from 30 to 80 ppm and 70 to 190 ppm, respectively (Table 4). The REE_{CN} pattern of the rock specimen BLÖ-8, a representative sample of the garnet fels dikes, is similar to the scapolite fels and scapolite-pyroxene fels, although, its $LREE_{CN}$ values are slightly lower (Fig.5). On the other hand, as clearly seen in Figure 5, the garnet fels sample has a conspicuous Eu_{CN} enrichment of approximately 150 times, although its actual Eu content is only 8.8 ppm (Table 4). Sample BLÖ-10, taken

Table 4. INAA results of the rock samples from the Konukdere metasomatite.

Table 4. INAA results of the rock samples from the Konukdere metasomatite

	BLÖ-1	BLÖ-2	BLÖ-3	BLÖ-4	BLÖ-5	BLÖ-6$_1$	BLÖ-6$_2$	BLÖ-7	BLÖ-8	BLÖ-9	BLÖ-10	BLÖ-11
La	80	33	53	37	50	36	48	32	27	54	14	12
Ce	190	69	93	100	99	100	92	82	110	76	27	22
Nd	73	23	22	42	27	44	28	38	69	16	6	5
Sm	13	4.3	5.0	8.7	5.1	8.6	4.7	6.7	14	2.8	0.8	0.8
Eu	3.9	1.0	1.5	2.1	1.6	2.2	1.7	1.6	8.8	1.0	0.5	0.4
Tb	2.3	0.5	0.8	1.6	0.5	1.7	0.9	0.5	1.6	0.7	0.5	0.5
Yb	7.18	2.62	3.39	5.77	3.62	5.83	2.92	4.41	4.42	1.82	0.90	0.36
Lu	1.05	0.39	0.47	0.85	0.59	0.90	0.50	0.81	0.62	0.29	0.18	0.08
Ta	3	3	2	4	3	5	2	4	1	2	1	5
Au	5	6	5	6	5	5	11	5	6	5	5	10
Ag	5	5	5	5	5	5	5	5	5	5	5	5
As	5	5	7	2	6	2	7	3	35	7	8	7
Br	22	27	26	29	21	29	23	23	1	1	6	1
Cs	2	4	10	2	13	2	2	2	2	2	2	4
Hf	9	7	5	9	8	9	5	16	4	4	2	1
Ir	5	5	5	5	5	5	5	5	5	5	5	5
Sb	1.6	2.6	1.1	1.4	0.9	1.4	0.7	1.3	2.0	4.5	2.0	6.6
Sc	8.4	4.7	13	4.4	6.9	4.4	16	6.2	15	3.1	12	3.5
U	10	8.7	7.4	7.2	7.0	7.7	6.8	14	64	5.9	4.9	0.5

- Au and Ir elements are given in ppb, the others are in ppm.

174

and later the replacement of Fe and Mg by Ca as shown in Figure 4. Excess Ca generated during these transformations can help from the associated garnet and clinopyroxene (Barton et al., 1991).

4. PRELIMINARY REE RESULTS

As mentioned earlier, some geological environments similar to that of the Hekimhan-Hasançelebi area, e.g. Bayan Obo region in the N China (Neary and Highley,
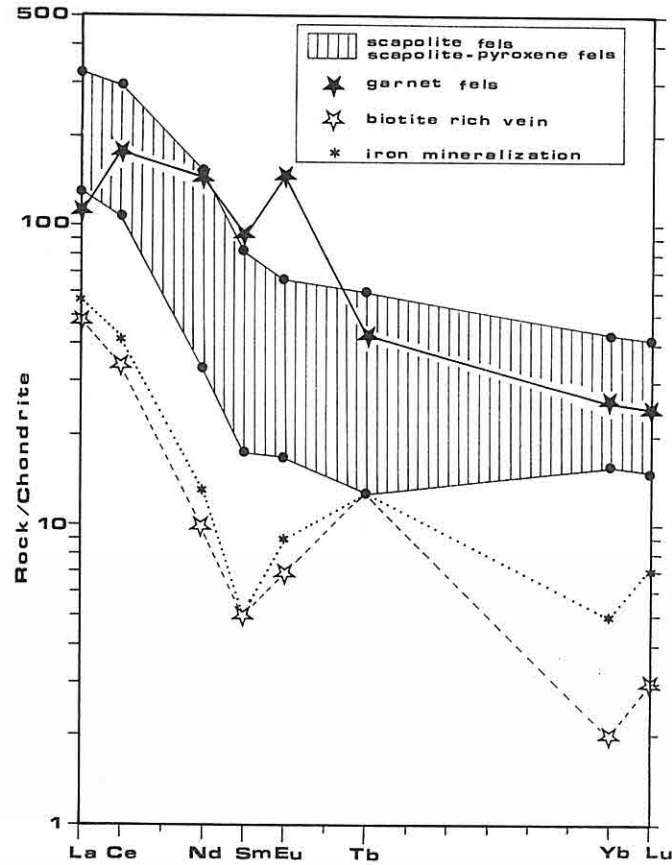
Figure 5. The chrondite (Evensen et al., 1978) normalized distribution pattern of the REE contents of the rock samples from the Konukdere metasomatite.

1984; Mariona, 1989), are associated with REE mineralization. The rare earth oxide (REO) content may range from 1 to 6.19 % however, high grade areas may contain up to 10 % REO in the Bayan Obo region in N China.

Table 3. (continuing)

Sample	Coordinates																									
SY-79	37°50'32" E, 38°53'07" N	47.81	14.68	7.54	0.10	4.86	9.82	2.77	1.48	1.05	0.34	8.09	98.54	48	526	674	27	168	32	27	90	16	242	28	25	132
SY-109	37°54'19" E, 38°52'58" N	47.75	13.96	8.31	0.11	4.29	6.81	2.58	4.26	2.01	0.75	7.33	98.16	116	600	940	26	315	32	38	252	19	91	16	32	208
SY-127	37°50'55" E, 38°57'02" N	41.77	14.66	10.34	0.31	3.00	11.43	3.54	2.71	0.99	0.51	9.72	98.98	65	815	1050	26	162	33	64	106	16	nd	22	28	124
SY-234	37°54'19" E, 38°53'18" N	46.65	16.40	12.08	0.10	3.00	5.29	2.56	1.42	1.82	0.41	8.37	98.10	60	378	555	27	213	49	31	115	19	38	16	24	198
SY-275	37°53'16" E, 38°53'49" N	48.35	16.73	8.26	0.16	1.21	6.67	4.46	3.05	1.18	0.26	8.18	98.51	59	624	904	26	281	60	59	175	19	nd	11	32	126
SY-276	37°51'54" E, 38°53'35" N	54.14	18.13	7.43	0.16	0.92	2.45	3.71	5.12	0.38	0.13	6.02	98.59	137	64	1043	25	421	89	43	120	30	nd	nd	31	52
SY-278	37°51'58" E, 38°53'58" N	53.32	16.86	9.34	0.10	0.84	2.94	3.96	3.85	0.71	0.21	6.26	98.39	108	7	901	26	329	62	34	124	25	24	nd	26	81
SY-403	37°48'01" E, 38°56'33" N	44.85	14.26	8.17	0.14	5.40	10.50	1.75	3.34	1.04	0.36	9.39	99.20	101	481	729	26	132	26	29	69	15	71	26	28	131
SY-406	37°47'16" E, 38°56'28" N	49.71	18.25	6.88	0.16	2.25	8.38	3.17	3.19	1.25	0.31	5.54	99.09	45	172	627	26	185	30	35	72	11	36	17	28	141
SY-407	37°46'16" E, 38°55'56" N	44.80	14.17	10.45	0.15	6.01	5.90	2.22	3.46	1.81	0.49	8.59	98.05	112	447	961	26	200	32	34	88	15	nd	21	33	196
SY-410	37°48'24" E, 38°56'22" N	42.63	14.50	8.06	0.27	4.72	10.81	3.16	2.58	1.10	0.31	9.95	98.09	129	591	1522	27	169	28	36	111	18	39	23	36	133
SY-654	37°54'14" E, 38°56'28" N	41.81	13.38	9.97	0.15	5.76	11.92	2.10	2.48	1.47	0.43	8.13	98.10	70	463	631	27	168	30	40	90	nd	90	34	50	170
KARADERE																										
SY-118	37°51'08" E, 38°54'50" N	46.62	3.02	4.38	0.10	24.85	17.62	0.06	0.05	0.06	0.01	2.46	96.77	32	nd	139	27	nd	17	21	62	nd	3484	60	36	47
SY-119	37°51'29" E, 38°54'50" N	46.04	3.88	5.20	0.14	23.74	16.90	0.04	0.05	0.05	0.01	3.50	99.05	13	nd	138	27	nd	17	22	67	nd	3614	50	24	46
SY-155	37°53'57" E, 38°54'05" N	39.13	6.60	16.65	0.26	25.34	7.44	0.27	0.05	0.30	0.02	4.97	101.06	8	nd	137	27	nd	17	22	91	nd	2356	101	51	70
SY-187	37°51'00" E, 38°49'36" N	36.04	1.67	13.19	0.23	33.71	0.35	0.01	0.01	0.01	0.01	15.27	100.23	29	nd	152	27	nd	17	21	76	nd	2952	164	34	30
SY-238	37°53'14" E, 38°54'30" N	47.87	2.16	4.68	1.15	25.33	16.61	0.03	0.01	0.03	0.01	3.85	100.88	30	nd	147	27	nd	17	22	63	nd	3617	48	22	38

- Major and trace elements are given in weight percent and in ppm, respectively.
- tFe$_2$O$_3$ represents the total iron oxide as ferric iron.
- LOI represents the loss on ignition.
- nd, not determined.

Table 3. Wholerock major and some trace element chemical analysis results of the rock samples from the Konukdere metasomatite and parent rocks.

Rock Sample	Geographic Coordinates	SiO_2	Al_2O_3	tFe_2O_3	MnO	MgO	CaO	Na_2O	K_2O	TiO_2	P_2O_5	LOI	Total	Rb	Sr	Ba	Y	Zr	Nb	Pb	Zn	Th	Cr	Co	Cu	V
BLÖ-1	37°52'46" E, 38°55'12" N	55.02	15.87	1.81	0.05	2.93	7.72	6.26	2.37	1.16	0.02	5.07	98.28	61	424	939	25	359	55	25	61	27	nd	26	30	123
BLÖ-2	37°52'50" E, 38°55'15" N	51.89	14.66	2.90·	0.06	4.72	8.82	4.88	2.13	0.37	0.15	7.95	98.53	45	308	469	26	314	42	26	81	35	21	21	28	60
BLÖ-3	37°52'49" E, 38°55'17" N	53.41	16.74	2.00	0.03	4.03	7.61	8.17	0.55	1.24	0.28	4.58	98.64	43	540	349	26	240	36	29	77	18	24	34	30	140
BLÖ-4	37°52'45" E, 38°55'20" N	55.00	14.21	2.04	0.05	4.17	8.60	6.06	1.58	0.61	0.02	6.52	98.86	59	396	745	26	455	59	24	61	33	nd	29	30	79
BLÖ-5	37°52'48" E, 38°55'34" N	55.54	16.38	2.21	0.04	3.38	5.85	8.16	0.97	0.80	0.23	5.65	99.21	31	288	368	26	356	50	25	78	21	24	30	28	97
BLÖ-6$_1$	37°52'56" E, 38°55'21" N	51.93	14.20	2.03	0.07	1.95	10.91	5.87	1.27	0.55	0.15	9.38	98.31	51	392	317	26	341	44	29	56	24	20	20	26	77
BLÖ-6$_2$	37°52'56" E, 38°55'21" N	54.81	15.74	1.75	0.03	4.42	8.66	7.71	0.83	1.03	0.26	3.80	99.04	44	470	420	26	212	31	26	122	34	33	34	26	122
BLÖ-7	37°52'54" E, 38°55'41" N	53.11	14.64	2.17	0.04	5.63	9.12	5.55	1.26	0.42	0.06	6.18	98.18	56	333	453	26	705	55	25	77	25	19	19	25	64
BLÖ-8	37°51'10" E, 38°56'30" N	35.99	9.12	16.33	0.16	27.47	0.76	0.22	1.01	0.46	0.22	2.36	94.10	35	nd	193	27	43	22	31	5	39	195	33	23	109
BLÖ-9	37°51'53" E, 38°56'29" N	55.52	17.52	0.99	0.08	1.05	8.02	6.18	2.65	0.27	0.03	7.90	100.21	80	193	581	27	264	18	28	58	17	nd	23	27	48
BLÖ-10	37°52'30" E, 38°56'17" N	37.47	11.02	34.47	0.03	5.04	3.73	2.74	2.99	0.78	0.07	2.03	100.37	65	nd	325	31	31	58	25	58	nd	nd	17	28	149
BLÖ-11	37°53'02" E, 38°56'26" N	40.82	9.67	11.86	0.05	20.06	4.37	0.11	5.13	3.23	0.02	6.12	101.44	230	nd	846	26	76	24	25	73	2	91	29	29	307
HASANÇELEBİ																										
SY-17	37°50'00" E, 38°55'22" N	65.76	15.94	1.42	0.11	0.14	0.85	8.89	0.44	0.65	0.02	2.38	96.60	12	276	846	27	1143	102	33	56	106	16	39	39	63
SY-19	37°50'17" E, 38°55'14" N	65.19	18.32	0.82	0.07	0.87	0.81	5.09	7.34	0.71	0.03	0.72	99.97	108	275	2003	26	652	70	31	38	57	67	35	35	80
SY-20	37°50'42" E, 38°55'18" N	61.99	16.92	1.32	0.03	1.39	4.44	5.18	5.60	1.09	0.05	1.18	99.19	85	425	2651	26	418	53	32	23	135	27	27	27	113
SY-21	37°50'32" E, 38°55'17" N	70.70	15.38	1.68	0.02	0.04	0.69	9.05	0.26	0.52	0.03	0.77	99.14	nd	66	233	25	1582	156	38	124	72	135	72	33	69
SY-22	37°50'24" E, 38°55'13" N	66.11	15.56	0.82	0.01	0.43	0.88	3.56	8.09	0.47	0.03	2.55	98.51	120	87	1352	25	929	109	30	70	nd	nd	33	30	62
SY-23	37°50'29" E, 38°55'07" N	65.66	15.46	0.89	0.02	0.04	0.54	3.05	8.98	0.66	0.04	2.82	98.16	109	80	1603	25	1075	125	37	67	nd	nd	29	29	75
SY-25	37°50'45" E, 38°55'00" N	62.03	17.76	0.92	0.01	0.04	1.57	6.95	3.64	0.76	0.17	2.89	96.74	61	525	2411	26	272	50	34	66	28	13	31	31	80
SY-120	37°51'40" E, 38°54'47" N	63.52	17.03	0.58	0.04	0.09	2.50	4.48	7.03	0.71	0.03	2.69	98.70	83	478	3606	26	368	50	28	24	28	28	13	28	77
SY-361	37°49'38" E, 38°55'13" N	67.31	16.97	1.08	0.02	0.04	0.80	5.00	6.80	0.56	0.12	0.69	99.39	132	56	1041	26	228	67	32	43	24	39	28	39	69
SY-362	37°49'43" E, 38°55'14" N	65.40	15.47	1.08	0.02	0.42	1.55	4.39	6.84	0.47	0.13	2.69	98.46	214	63	1303	25	399	61	29	36	39	20	32	39	64
SY-450	37°48'57" E, 38°55'14" N	63.80	15.54	1.29	0.02	0.28	3.45	3.81	6.41	0.65	0.17	2.87	98.29	119	165	1205	26	383	52	31	72	41	10	20	80	80
BAHÇEDAM																										
SY-52	37°52'37" E, 38°54'00" N	44.82	15.99	9.52	0.32	0.62	10.51	3.07	2.19	1.84	0.43	9.61	98.97	58	622	696	27	181	40	34	52	8	23	36	36	203
SY-61	37°51'06" E, 38°54'18" N	51.18	15.78	8.99	0.28	1.06	4.46	4.39	3.47	1.16	0.37	7.79	98.84	95	58	572	26	287	59	31	93	nd	nd	26	26	123
SY-62	37°50'35" E, 38°54'17" N	49.46	15.25	10.65	0.40	1.39	4.60	4.76	2.69	1.19	0.37	7.52	98.28	83	nd	379	26	263	61	32	67	13	nd	21	21	128
SY-64	37°50'27" E, 38°53'38" N	40.45	14.59	10.72	0.39	3.52	12.26	3.23	0.70	1.60	0.42	12.00	100.60	78	120	249	26	144	35	31	91	nd	91	11	26	177

(Boztuğ and Yılmaz, 1992). Such a normalization (Fig. 2), for the major elements, shows that during the metasomatic transformation, the Karadere ultramafite has been depleted of considerable Fe, Ca, Mg, and Mn, and enriched in Si, Al, K, Na, Ti and P. The Bahçedam volcanics also lost Fe, Mn, Ti and P, and gained Si and Na. As for the Hasançelebi pluton, it has lost K and Si, but gained Ca, Mg, Mn and some Na and P (Fig. 2). The trace element normalization diagram (Fig. 3) shows that the Karadere ultramafite has lost Co, Cu and Y, and gained Sr, Zr, Th, Rb, Ba, Nb and V. The Bahçedam volcanics have lost Rb, Ba, Pb, Zn, Cu and V, but gained Zr, Th and Co; the Hasançelebi pluton has yielded Rb, Ba, Th, Zr, Nb, Pb, Co and Cu to the environment, whereas it has gained only Sr and V (Fig. 3).

So far, all mineralogical and geochemical data (Boztuğ and Yılmaz, 1992), summarized here, indicate that the Konukdere metasomatite is product of the Na (-Ca) and Ca-types
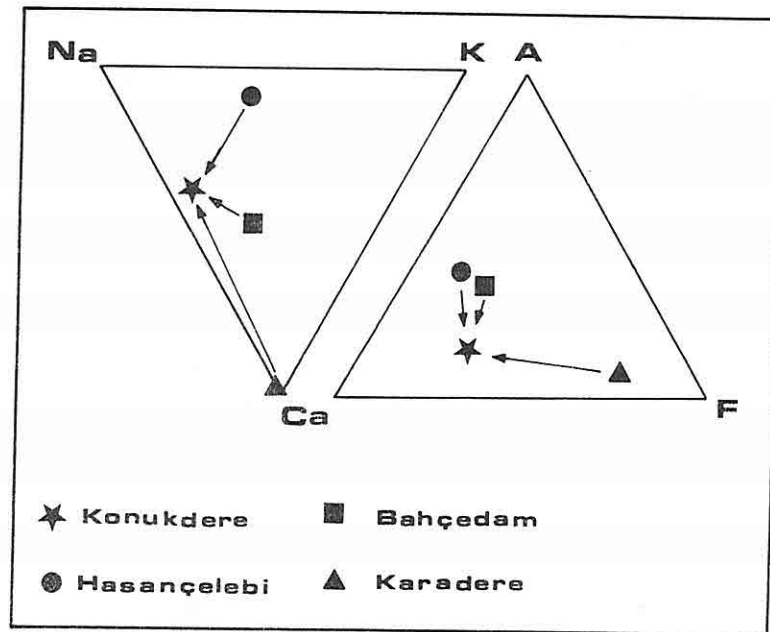
Figure 4. The positions of the Konukdere metasomatite and parent rocks in the molar proportions of Na-K-Ca and ACF triangular diagrams (Boztuğ and Yılmaz, 1992).

of metasomatism (Barton et al., 1991). The main mineralogical characteristics of such a metasomatism are the transformation of albite and anorthite into marialite and meionite with addition of NaCl and CaCO3, respectively (Deer et al., 1962). The principal geochemical transformations include firstly the replacement of Ca or K by Na, 170
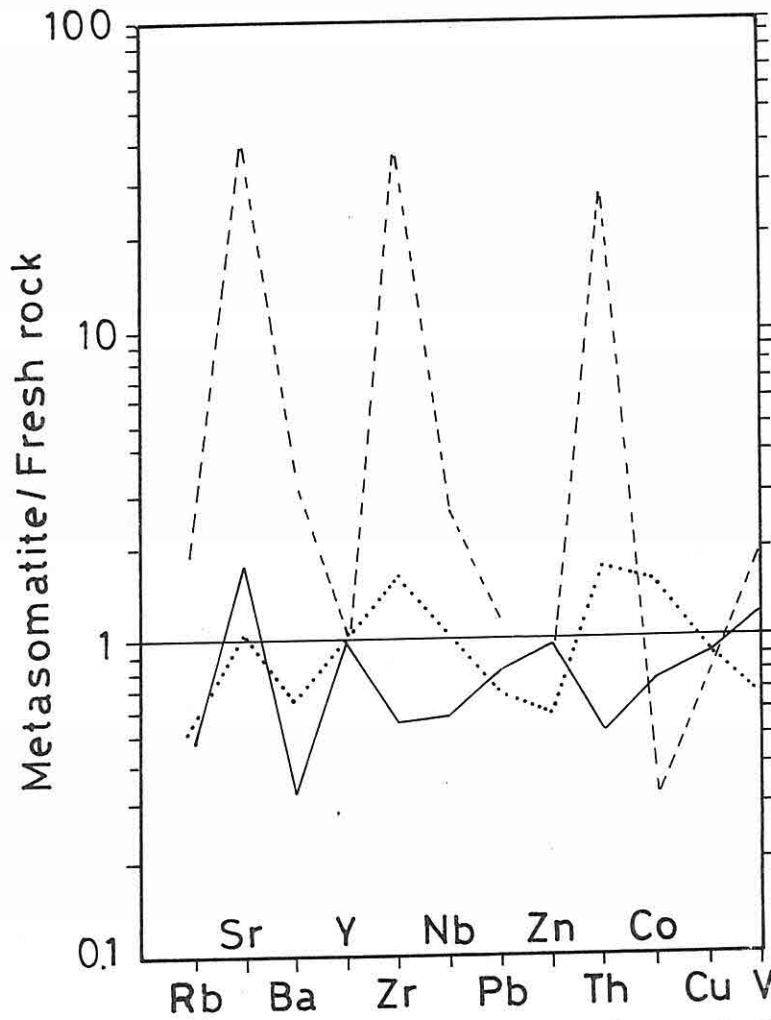
Figure 3. Some trace elements of the Konukdere metasomatite normalized to fresh rocks (Boztuğ and Yılmaz, 1992) (See Fig.2 for location/explanation).

magnesioferrite/magnetite, marialite, and phlogopite (Table 2). Sample BLÖ-11, taken from a biotite rich vein, consists mainly of vermiculite, biotite and phlogopite (Table 2). The vermiculitization of this sample can be considered to be related to the hydrothermal activity which formed the wairakite and analcime found in the scapolite fels rocks (Boztuğ and Yılmaz, 1992).

The major and trace element contents of the most common rock types, e.g. scapolite fels, of the Konukdere metasomatite and parent rocks (Table 3) have been evaluated by means of normalization of metasomatite to the fresh rock for each major and trace element

Table 2. XRD mineralogical compositions of the rock samples from the Konukdere metasomatite.

Rock Sample	Mineralogical Composition
BLÖ-1	marialite + augite + diopside
BLÖ-2	marialite + mizzonite + meionite + calcite + wairakite ± analcime ± andradite ± schorlomite
BLÖ-3	marialite ± wollastonite ± piedmontite(?)
BLÖ-4	marialite + diopside ± nyerereite ± quartz
BLÖ-5	mizzonite + meionite + analcime
BLÖ-6_1	marialite + quartz + andradite + schorlomite
BLÖ-6_2	diopside + augite + hyperstene + marialite ± analcime
BLÖ-7	marialite + augite + diopside + calcite
BLÖ-8	uvarovite + hydrogrossularite + andradite + jacobsite/magnetite
BLÖ-9	calcite + albite + andesine + Na-zippeite(?)
BLÖ-10	magnesioferrite/magnetite + marialite + phlogopite ± brunogeierite(?)
BLÖ-11	vermiculite + biotite + phlogopite ± calcite

- See Table 3 for the geographic locations of the rock samples.
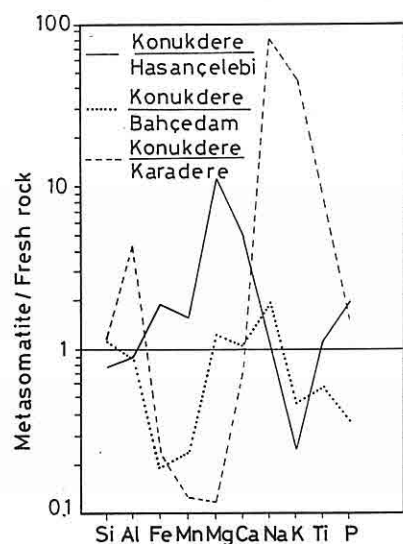
Figure 2. Major element oxide distribution pattern of the Konukdere metasomatite normalized to fresh rocks (Boztuğ and Yılmaz, 1992).

168

the south of the Hasançelebi railway station (Fig.1). The Konukdere metasomatite consists mainly of complex of vein rocks whose thicknesses range from 0.5 to 5 m and even sometimes 10 to 15 m.

The most common rock types among these purely metasomatic veins are scapolite fels, scapolite-pyroxene fels, pyroxene fels, and rarely garnet fels and biotite. Other rock types showing slight metasomatic affects are minette, kersantite, porphyritic syenite and altered aplitic vein rocks (Yılmaz et al., 1992). Scapolite minerals, found in scapolite fels type of rocks, are seen as euhedral, neddle like prisms and radial nodules with crystal lengths from 5 to 10 cm and even at certain localities 15 to 20 cm. The neddle-like prims are 2-3 to 10 mm thick. As pointed out by earlier workers (İzdar and Ünlü, 1977; Özer and Kuşçu, 1982), these fels type rocks are associated with stockwork vein, dyke, massive and disseminated types of pneumatolytic-hydrothermal iron mineralization. The massive iron oxide mineralization, in Karakuz area, also contains minerals indicating hydrothermal activity, e.g. barite, quartz and calcite.

3. MINERALOGY AND PETROLOGY OF THE KONUKDERE METASOMATITE

As mentioned above, the most common rocks in the Konukdere metasomatite are scapolite fels, scapolite-pyroxene fels, pyroxene fels and rarely of garnet fels and some biotite rich veins. Clearly, these rocks are unusual and uncommon and that is why we have studied these rocks in detail by means of their mineralogy, major and some trace and also REE geochemistry. Other, less unusual, rocks such as minette, kersantite, porphyritic syenite and aplites, representing a slight metasomatism, have been excluded from this study.

Table 2 shows the main constituent of the scapolite fels and scapolite-pyroxene fels types of rocks to be marialite (Na-scapolite). In addition to marialite, some rocks also contain meionite (Ca-scapolite) and mizzonite (Na-Ca scapolite). Apart from the scapolite group minerals, other constituents present such as calcite, wairakite and analcime suggest low temperature hydrothermal alteration. The major minerals of the pyroxene fels, seen as an ultramafic vein rock in the field, are diopside, augite, hypersten, ±marialite and ±analcime (BLÖ-6$_2$, Table 2). The garnet fels consists of euhedral, reddish brown garnet grain sizes from 3-5 to 8-10 mm in hand specimen. XRD mineralogical study shows the mineralogy of the garnet fels to be uvarovite, hydrogrossularite and andradite with lesser jacobsite/magnetite (BLÖ-8, Table 2). XRD study of sample BLÖ-10, taken from a massive iron oxide mineralization zone, about 3 km SW of Hasançelebi (Fig. 1), shows that the major constituents are

167

Table 1. The comparision of chemical analysis of some rock standarts from CRPG. (1) represents the observed values in the Cumhuriyet University, (2) shows the published values by Govindaraju (1989).

	MAN (1)	MAN (2)	DRN (1)	DRN (2)	BEN (1)	BEN (2)
SiO_2	65.88	66.60	52.12	52.85	38.30	38.20
Al_2O_3	18.16	17.62	16.54	17.52	9.93	10.07
tFe_2O_3	0,24	0.47	10.55	9.70	12.05	12.84
MnO	0.04	0.04	0.23	0.22	0.19	0.20
MgO	0.02	0.04	4.82	4.40	12.94	13.15
CaO	0.83	0.59	6.82	7.05	13.87	13.87
Na_2O	5.73	5.84	2.73	2.99	3.43	3.18
K_2O	3.09	3.18	1.65	1.70	1.46	1.39
TiO_2	nd	0.01	1.13	1.09	2.59	2.61
P_2O_5	1.26	1.39	0.23	0.25	1.05	1.05
Rb	4304	3600	66	73	43	47
Sr	36	84	349	400	1244	1370
Ba	nd	42	462	385	911	1025
Y	1	1	27	28	27	30
Zr	34	27	116	125	238	265
Nb	174	173	19	8	66	100
Pb	49	29	34	55	23	4
Zn	229	220	123	145	99	120
Th	4	1	7	5	10	11
Cr	38	3	13	42	340	360
Co	1	1	37	35	54	61
Cu	147	140	45	50	49	72
V	29	5	143	220	263	235

- Major and trace elements are given in weight percent and in ppm, respectively.

Hasançelebi pluton. The Hasançelebi pluton is mainly syenite, quartz-syenite and rarely monzonite and quartz - monzonite (Yılmaz et al., 1992). According to the major element geochemistry (Yılmaz et al., 1992), the Hasançelebi pluton is an alumino-cafemic (ALCAF), alkaline oversaturated (ALKOS) (Debon and Fort, 1982), felsic-I type (Chappel and White, 1974; White and Chappel, 1977) intrusive. Some tectonic classification diagrams, based on the trace elements such as Y, Nb and Rb, point to a within plate origin (WPG) (Pearce et al., 1984) for the Hasançelebi pluton. As for the Konukdere metasomatite, the best outcrops are seen around Konukdere village to

166
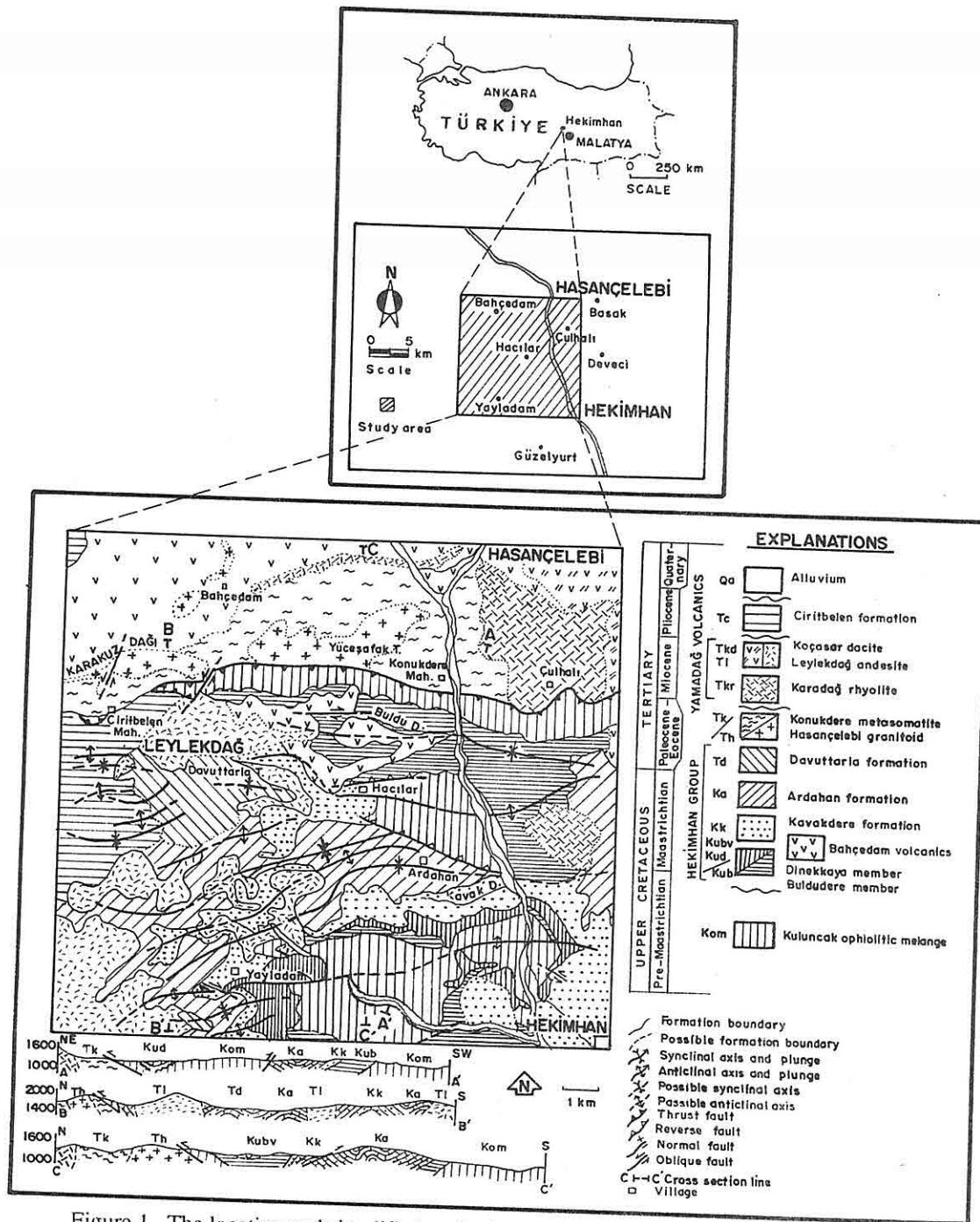
Figure 1. The location and simplified geological map of the Hekimhan-Hasançelebi area (Yılmaz et al., 1991).

165

1. INTRODUCTION

There is a widespread contact metasomatic zone between the Hekimhan and Hasançelebi towns of Malatya province in Central-Eastern Anatolia. The metasomatic rocks, recently named the Konukdere metasomatite (Yılmaz, 1991 and Yılmaz et al., 1991) are also associated with extensive iron mineralization (İzdar and Ünlü, 1977). A petrological study has concluded these rocks are the product of Na (-Ca) and Ca-types of metasomatism (Boztuğ and Yılmaz, 1992). By taking into account the REE occurences in similar geological environments (Neary, 1992 and Mariano, 1989), some 12 rock samples, collected from the Konukdere metasomatite have been analysed by XRD and INAA methods to determine their mineralogical compositions, REE and some trace element contents, respectively, in the Univ. of Nevada-Reno, USA. Major and some trace element geochemical analyses of the Konukdere metasomatite and parent rocks have been completed (Boztuğ and Yılmaz, 1992) using CRPG (Govindaraju, 1989) rock standarts (Table 1) in the Mineralogical-Petrographical and Geochemical Research Laboratories (MIPJAL) of the Dept. of Geological Engineering of Cumhuriyet University in Sivas using Perkin-Elmer Atomic Absorption Flame Spectrophotometer and Rigaku-3270-E(WDS) X-Ray Fluorescence Spectrometer instruments.

The principal aim of this paper is to represent the preliminary results on the REE potential of the Konukdere metasomatite.

2. GEOLOGICAL SETTING

The Konukdere metasomatite has developed in the contact zone of the Palaeocene(?) Hasançelebi pluton which intrudes the Karadere ultramafite of the pre-Maastrichtian Kuluncak ophiolitic mélange and the Maastrichtian Bahçedam volcanics (Yılmaz et al., 1991) (Fig. 1). The Karadere ultramafite consists mainly of wehrlite, pyroxenite, serpentinizated ultramafite and serpentinites. The transformation of the Karadere ultramafite into the scapolite fels of the Konukdere metasomatite by the intrusion of porphyritic syenite dikes belonging to the Hasançelebi pluton is well exposed around Ciritbelen village located to the south of Karakuz mountains (Fig.1). The alkaline Bahçedam volcanics are composed of tephrite - basanite, trachy - basalt, basaltic trachy-andesite and trachy-andesite on the basis of major element geochemical nomenclature (Yılmaz et al., 1992). Ti-Zr-Y and Ti-Zr-Sr triangular diagrams (Pearce and Cess, 1973; Pearce et al., 1981) show both of the within plate and arc characters for these basaltic rock (Yılmaz et al.,1992). Some parts of the Bahçedam volcanics, particularly those of the N Karakuz mountains and W Bahçedam village, are converted to scapolite fels type rocks of the Konukdere metasomatite due to intrusion of

164

PRELIMINARY RESULTS ON THE REE POTENTIAL OF THE KONUKDERE METASOMATITE, HEKİMHAN-HASANÇELEBİ AREA, NW MALATYA, CE ANATOLIA, TÜRKİYE

D. BOZTUĞ[1], L.T. LARSON[2] and A. ÖZTÜRK[1]

[1] *Dept. of Geological Engineering, Cumhuriyet Univ., 58140 Sivas, Türkiye.*
[2] *Dept. of Geological Sciences, Mackay School of Mines, Univ. of Nevada Reno, 89557 USA.*

ABSTRACT: *There is a widespread contact metasomatic zone developed around the Palaeocene(?) Hasançelebi pluton which intrudes the Karadere ultramafite of the pre-Maastrichtian Kuluncak ophiolitic mélange and the Maastrichtian Bahçedam volcanics. The Karadere ultramafite consists of wehrlite, pyroxenite, serpantinizated ultramafics and serpentinites. The Bahçedam volcanics, with an alkaline affitinity, are composed of tephrite basanite, trachy-basalt, basaltic trachy-andesite and trachy-andesite. As for the Hasançelebi pluton, it comprises mainly syenite, quartz-syenite and rarely monzonite, quartz-monzonite all of wich are ALKOS, felsic-I type and WPG in character. The metasomatic rocks, recently named the Konukdere metasomatite, are composed of scapolite fels, scapolite-pyroxene fels, garnet fels, biotite rich veins, lamphrophyres (minette, kersantite), porphyritic syenite and aplitic veins. Characteristic minerals, found in the fels type rocks, are marialite (Na-scapolite), mizzonite (Na-Ca scapolite), meionite (Ca-scapolite), diopside, augite, uvarovite, andradite, hydrogrossularite, jacobsite/magnetite, schorlomite, wairakite, analcime, biotite, phlogopite, vermiculite and calcite. The Konukdere metasomatite is a product of Na(-Ca) and Ca-types of metasomatism. Scapolite fels and scapolite-pyroxene fels rocks show enrichment of 100-350 times in $LREE_{CN}$, and 15-40 times in the $HREE_{CN}$. Garnet fels is enrichment 110-180 and 25 times in the $LREE_{CN}$ and $HREE_{CN}$, respectively, with a conspicuous positive Eu anomaly. Rock samples, taken from both the iron mineralization and biotite rich veins, do not have any significant REE_{CN} pattern, however, and always provide low values relative to those of other metasomatite samples. We conclude that it is necessary to study the scapolite fels and scapolite-pyroxene fels in detail in order to obtain more meaningful and useful data on the REE potential of the Konukdere metasomatite.*

163

Laboratory. *Dowdon, Hutchinson and Ross, Stroudsburg: 665-670*

Goedicke, T.R., 1976. Sagebiel, S., Sediment movement in Lebanese Submarine Canyons. *Acta Adriatica, 18:117-128.*

Goldsmith, V., Golik, A., 1980. Sediment Transport Model of the Southeastern Mediterranean Coast. *Mar. Geol., 37:147-175.*

Gvirtzman, G., Buchbinder, B., 1978.The Late Tertiary of the Coastal Plain and Continental Shelf of Israel and Its Bearing on the History of the Eastern Mediterranean. In: Hsu, K.J. et al. (eds.), Initial Repts. of the Deep Sea Drilling Project, Washington, 42: 1195-1222.

Hall, J.K., 1976. Seismic Studies: Haifa Bay-Summary Report. Isr. Geol. Surv., UN/UNDP-GSI Offshore Dredging Project, Field Rep. 1/76, 106p.

Hall, J.K., 1983. Ben Avraham, Z., Shamai, E., Bathymetric Map off Southern Lebanon, 1:100,000, 25m Contour Interval. Unpublished.

Issar, A., 1972. Kafri, U., Neogene and Pleistocene Geology of the Eastern Galilee Coastal Plain. Isr. Geol. Surv., Bull. 53, 17p.

Kafri, U., 1974. The Geological Map of Israel. Sheet I-IV, Nahariya, 1:50,000 Scale. Isr. Geol. Surv.

Kafri, U.and Ecker, A., 1964. Neogene and Quaternary Subsurface Geology and Hydrology of the Sevulun Plain. Isr. Geol. Surv., Bull. 37, 13p.

Mart, Y., 1989. Sediment Distribution in Akhziv Canyon off Northern Israel. Geo-Marine Letters, 9:77-83.

Mero, D., 1983. Subsurface Geology of Western Galilee and Zevulun Plain. TAHAL Consulting Eng. Ltd., Rep. 04/83/48, 45p.

Neev, D.and Bentor, 1960. Y.K., The Continental Shelf of Israel, Isr. Geol. Surv., Bull. 26:25-41.

Neev, D., Almagor, G., Arad A., Ginzburg, A., Hall, J.K., 1976. The Geology of the Southeastern Mediterranean. Isr. Geol. Surv., Bull. 68, 51p.

Nir, Y., 1973. Geological History of the Recent and Subrecent Sediments of the Israel Mediterranean Shelf and Slope. Isr. Geol. Surv., Rep. MGI/2/73, 179 p.

Ron, H., 1984. Paleomagnetic Investigation of the Fault Structure of the Galilee, Northern Israel. M.Sc. Thesis, Hebrew Univ., Jerusalem, Israel, 102p. (in Hebrew, Engl. Abst.).

Spanier, E., Tom, M., Galil, B.S., 1991. Preliminary ROV Study of the Epibenthic Megafauna at Akhziv Canyon, Mediterranean Coast of Israel. In: Mart, Y., Galil, B.S. (eds.), The Mediterranean Continental Margin of Israel, Abst. of 3rd Annu. Symp., 3p.

161

3. REFERENCES

Almagor, G., 1976. Physical Properties, Consolidation and Slumping Processes in Recent Marine Sediments in the Mediterranean Continental Slope of Southern Israel. Isr. Geol. Surv., Rep. MG/4/76, 132 p. (in Hebrew, Engl. summary) .

Almagor, G., 1990. Effects of Earthquakes on Sediments of the Israeli Continental Margin- Stage 5: Akhziv Canyon. Isr. Geol. Surv., Rep. GSI/20/90, 3p.

Almagor, G., Hall, J.K., 1980. Morphology of the Continental Margin of Northern Israel and Southern Lebanon. Isr. J. Earth Sciences, 29: 245-259

Almagor, G., Hall, J.K., 1984. Morphology of the Mediterranean Continental Margin of Israel. Isr. Geol. Surv., Bull. 77, 31p.

Almagor, G., Wiseman, G., 1977. Analysis of Submarine Slumping on the Continental Slope of the Southern Coast of Israel. Marine Geotechnology, 2:349-388.

Carlisle, D.H., 1965.A Continuous Seismic Profiling Survey off the Coast of Lebanon. M.Sc. Thesis, Mass. Inst. Tech., USA, 138p.

Dubertret, M.L, 1951-1961.Carte Geologique du Liban-Tyr, Saida, Beirut, 1:50,000, Ministere.des Travaux Public, Beirut, Liban.

Eitam, Y., 1988. The Shallow Structure and the Geological Processes of the Inner Shelf of Northern Israel in the Late Pleistocene. Ph.D. Thesis, Tel Aviv Univ., Israel, 100p.
Freund, R., 1970. The Geometry of Faulting in the Galilee. Isr. J. Earth Sciences, 19:117-140.

Frydman, S., 1988. Talesnick, M., Almagor, G., Wiseman, G., Simple Shear Testing for the Study of the Earthquake Response of Clay from the Israeli Continental Slope. Marine Geotechnology, 7:143-171.

Garfunkel, Z., Almagor, G., 1985. Geology and Structure of the Continental Margin of Northern Israel and the Adjacent Part of the Levantine Basin. Mar. Geol., 62:105-131

Garfunkel, Z., Almagor., 1987.Active Salt Dome Development in the Levant Basin, Southeast Mediterranean. In: Lerche, I, O`Brien, J.J. (eds.), Dynamical Geology of Salt and Related Structures. Academic Press: 263-300.

Goedicke, T.R., 1972. Submarine Canyons on the Central Continental Shelf of Lebanon. In: Stanley, D.J. (ed.), The Mediterranean Sea, a Natural Sedimentation
160
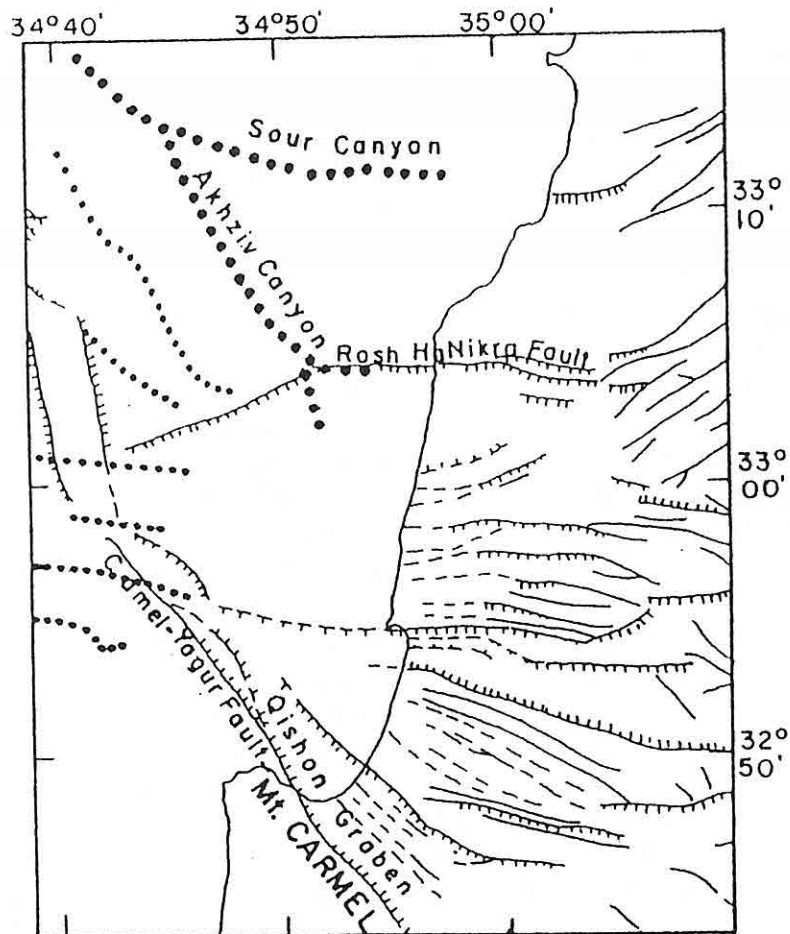
Figure 2. Fault pattern of the western Galilee and its offshore. For sources see references (Almagor, 1980; Garfunkel, 1985; Garfunkel and Almagor, 1987; Freund, 1970; Ron, 1984; Kafri and Ecker, 1964; Issar and Kafri, 1972; Kafri, 1974; Mero, 1983; Hall, 1976).

2. ACKNOWLEDGEMENTS

159

A preliminary foraminiferal study carried out on the 2.4m long topmost section of a finely layered core retrieved from the similar continental slope off Acre at 600m depth showed that the sediment is young, most probably less than 2 000 years old (B. Luz-personal communication).

Occasional sliding of intact large sediment chunks occur. The 1.5 km wide, 80 m high hill that blocks the canyon thalweg at 2835N/1475E (Fig.1) is probably such a slab. The slumping, though frequent, is episodic and must be related to weak earthquake tremors that readily affect the sediment slopes in the area (Almagor, 1976; Almagor and Wiseman, 1977; Frydman et al., 1988). The steep walls of the canyon are especially susceptible to slumping. Almagor and Wiseman, 1977, showed that sediment slopes as steep as 20-22. off southern Israel are stable, and geotechnical studies that are presently carried out by the author and his associates aim to investigate the slope stability in the study area as well.

The active intense faulting of the western Galilee trends in an E-W direction (Freund, 1970; Ron, 1984 among others). Whereas these faults are sharply expressed inland as morphologically fresh narrow latitudinal grabens, this piano-keys-like morphology in the coastal zone can be inferred from the interpretation of shore-parallel seismic reflection lines, and by the thickness of the Pliocene-Quaternary sediments (Kafri and Echer, 1964; Issar and Kafri, 1972; Kafri, 1974; Mero, 1983), (Fig.2). Except for the prominent Rosh HaNikra and Yagur-Carmel faults, and the fault that delimits the northern side of the Qishon Graben, the westward extensions of these faults cannot be or are hardly identified on most of the single channel seismic profiles that were collected off northern Israel. The Carmel and Rosh HaNikra faults, which converge at a zone located some 20-25 km offshore, delimit the seaward extension of the Western Galilee Graben (Garfunkel and Almagor, 1985; Hall, 1976).

The seaward extension of the Rosh HaNikra Fault has in part captured the upper section of the Akhziv Canyon causing its major tributary to deflect from its perpendicular-to-slope NW course and incise its way landwardly (Figs.1, 2). Although the directions of the two heads of this tributary suggest that they are the submarine extensions of the Betzet and Keziv streams, no supportive evidence exists, and the morphology that is hidden underneath the shelf is presently unknown. The author suspects that the Akhziv Canyon does not at all relate morphologically to any of the westward flowing coastal streams. Further seaward the Rosh HaNikra Fault is expressed in the seismic profiles by the shape of the unconformity surface between the Upper Miocene and the Pliocene-Quaternary sediments (Reflector M),(Garfunkel and Almagor, 1985).

It should be noted that the Lebanese submarine canyons (Carlisle, 1965; Goedicke, 1972) seem to be also fault-controlled. They begin opposite the major Lebanese rivers, which are controlled by faults in a WSW direction (Dubertiet, 1951, 1961), and run in the same direction.

158

consolidation is dependent on the sedimentary overburden that rested on them. Ten short gravity cores, 0.4 to 2 m in length (Nir, 1973), and a suite of 22 piston cores, 1.5 to 6m in length, that were retrieved from within the canyons and its margins (Almagor, 1990) neither encountered a rocky bedrock nor contained rocky pebbles. X-radiographs of the cores reveal that in general the continental shelf and upper slope sediments are extensively bioturbated displaying a homogeneous "cloudy"-looking structure with faintly observed lamination and occasionally containing tracks of burrowing animals. Spanier et al., 1991, who photographed the upper head of the canyon, also report that the bottom is "extensively bioturbated by megafaunal species". Common occurrences of gas within the sediment cores also indicate faunal prolifiration within the bottom sediments. The cores recovered from the canyon, and those from its sloping margins contain large sections with slump structures, and still larger proportions of fine, usually inclined layered sediments. Examination of core samples show that these layers grade from fine sand to fine clayey particles. A series of towed video transects that were carried out across the canyon at depths of 30 to 300 m also showed that the canyon and its walls are entirely covered by uniform fine-grained sediments (Mart, 1989).

The canyon thalweg is floored with crushed organogenic (shelly) material of sand and pebble sizes, which were recovered during coring. Cobble-sized fragments 1-5 cm in diameter, scattered along the canyon walls in several places, were photographed (Mart, 1989). These cobbles could either be rocky fragments originating from the Pleistocene kurkar rocks of the continental shelf, or mud fragments from the canyon's floor or walls that subsequently slumped down similar to the mud balls reported by (Goedicke, 1972) in the Beirut Canyon.

The sediments and their structural patterns suggest intensive mass transport over the continental slope and within the canyon. Swift alongshore currents over the shelf (Goldsmith and Golik, 1980) transport large quantities of sand and pebble-sized organogenic material that is largely eroded from the Pleistocene kurkar floor of the shelf. Large exposed rocky areas on the shelf are indicative of these currents (Eitam, 1988). These sediments are trapped by the Akhziv Canyon, which deeply incised the shelf, and are transported to the deep sea. Frequent failures of the steep canyon walls result in massive slumping of large quentities of sediments into the canyon. These sediments are further transported downstream by density currents. The inclined finely layered sediments within the canyon as well as the 10 m thick nepheloid layer over the bottom that was observed by Mart, 1989, are indicative of this mass transport. Slumping also occurs on the undisturbed continental slope to the sides of the canyon. The absence of large slump scars of the type recorded off southern Israel (Almagor and Wiseman, 1977) proves that usually thin sediments slabs slump, and that in the process they completely disintegrate and flow downslope. Large masses of sediments are, however, thus transported.

157

The weaker influence of the Nile-derived sedimentation north of the Carmel promontory and Haifa Bay (Neev and Bentor, 1960), and the differential uplift of the Sinai-Israel-Lebanon versus the subsidence of the southeastern Mediterranean basin, which progressively accentuates northwardly, since Tertiary times (Gvirtzman and Buchbinder, 1978) have led to the build up of a narrow, steeply sloping continental margin off northern Israel and Lebanon relative to that off southern Israel and northern Sinai. Off northern Israel, the contiental shelf, with a slope of less than 0.5. ends with a sharp break at a water depth of 70-80m, located 10-14km offshore. The continental slope, which faces roughly a N60 °W direction, is about 5km wide, and deepens to a depth of 1,150m. The average gradient is 6-8. while the steepest gradients of the slope reach 8-14., occuring at water depth of 500-600m. The continental margin progressively narrows and deepens northward, and north of Beirut forms a 2.5-5km wide strip sloping at 8-14. in average to 1,500m depth, attaining maximal slopes of 17-28. (Carlisle, 1965; Goedicke, 1972; Goedicke and Sagebiel, 1976; Hall et al., 1983). The slope is further accentuated by large scale slumping of large sediment blocks that takes place particularly along the entire lower continental slope from Caesarea in central Israel to Tyre (Sour) in southern Lebanon (Garfunkel and Almagor, 1985; 1987)

Akhziv Canyon (Fig.1) is the southernmost submarine canyon in a system of some 9 large canyons that deeply incise the entire northern Israel-Lebanon margin up to Beirut (Carlisle, 1965; Hall et al., 1983). It deeply (300-550 m) and widely (6.5km) carves its way along a distance of nearly 10km into the continental shelf. Its major head starts at a water depth of about 50m some 3.2 km offshore. Its major tributary sinuously trends in a nearly N-E direction along a distance of about 11.5 km to a depth of 600 m, where it adopts a broadly NW direction to 950 m depth and then runs northwardly until it loses its identity over the adjacent deep sea Levant Platform. A second head, which also starts on the continental shelf some 8 km off Gesher Haziv, trends in a northward direction and joins the canyon after some 5 km at a depth of about 700 m. Other tributaries which originate on the canyon's northern flank trend in a general E-W direction for distances of 4 to 7 km, while those that originate on its southern flank travel for 5 to 8km at N and NW directions. A slopes map prepared by J.K. Hall shows that the thalwegs of the canyon tributaries attain slopes that are generally less than 10., but the deeper parts of the canyon walls are appreciably steeper with common inclinations of 15 to 30 that occasionally reach 40.

The sediments and the pattern of sedimentation have essentially been the same since early Pliocene times (Gvirtzman and Buchbinder, 1978). Their accumulation along the northern Israel-southern Israel coast has created the present continental terrace which is about 1km thick (Garfunkel and Almagor, 1985). It is therefore assumed that the canyon cuts its entire way into essentially unindurated sediments, whose state of

156
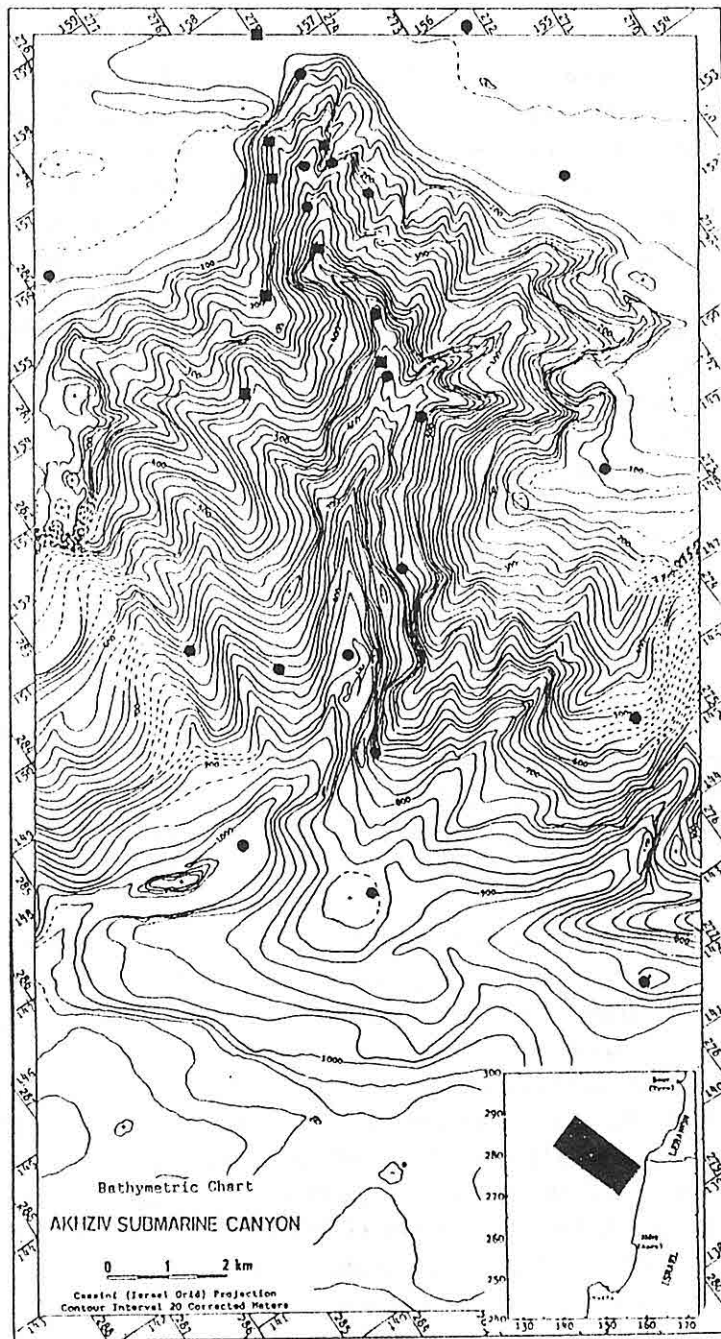
Figure 1. Batymetric map of the submarine Akhziv Canyon off northern Israel. Dots denote piston samples collected during the present study, squares denote gravity cores collected by Nir (1973).

155

1. INTRODUCTION

The existing bathymetric map of the continental margin off northern Israel and southern Lebanon (Almagor and Hall, 1980; 1984) was prepared based on data collected throughout several continuous seismic exploration surveys in the area. These data were assembled at different times and using various equipment and navigational systems. Therefore, even though much effort was made to reliably correlate data of various sources, mismatching of the data and little coverage of certain areas unavoidably resulted in inaccuracies. The need for accurate coring in the morphologically highly rugged terrain of Akhziv Canyon, that was carried out within the framework of the study on the earthquake effects on the sediment slopes and on the sedimentological processes within the canyon area, necessitated the preparation of an accurate bathymetric map.

The R/V "Shikmona" mapped the area using a computerized system that was built and operated by the Israel Oceanographic and Limnological Research, Ltd. This system included a Raytheon echo-sounder and a Motorolla Mini-Ranger navigation system. The boat sailed at a criss-cross pattern in lines along and across the axis of the Akhziv Canyon. The lines were generally 500m, sometimes 1000 m apart as was dictated by the complexity of the submarine topography and the distance limitations of the navigational system. The accurately-navigated bathymetric data were presented as depth points on a 1:10 000 scale trackline map which served as a basis for the preparation of a 1:250 000 scale, 10m contour interval bathymetric map. Fig.1 presents the map, its size reduced to a 1:500,000 scale. A future effort to combine the present and old data will result in a still more accurate map.

The present margin of the southeastern Mediterranean is largely the product of the accumulation of Nile-derived sediments that were transported by the counterclockwise contour current system off the shore of northern Sinai, Israel and Lebanon (Neev et al., 1976; Almagor, 1976). These sediments are predominantly silty clays characterized by their high montmorillonite content (60-80%), some kaolinite (20-40%), low illite content (less than 15%), and low carbonate content (0-60%) (Almagor,1976; Nir, 1973). In the study area the continental margin sediments accumulated since early Pliocene times attain a thickness of up to 1000 m (Almagor and Hall, 1984; Garfunkel and Almagor, 1985). Except for a thin veneer of modern Nile-derived fine-grained sediments, the uppermost sediments of the continental shelf are essentially fossilized dunes made of carbonate - cemented quartz sandstones (locally termed "kurkar") that were formed when it was exposed during the low stand of the sea level at approximately -120 to -130m during the Last Glacial (Neev et al., 1976). Off northern Israel, where no steady supply of quartz sands from the south exists, the kurkar rocks are nearly purely calcarenites, mostly made of reworked crushed shells, and the unconsolidated sediments contain large proportions of organogenic material eroded from these rocks (Neev el al., 1976; Eitam, 1988).

154

THE AKHZIV SUBMARINE CANYON, NORTHERN ISRAEL MARGIN: MORPHOLOGY, STRUCTURE AND PROCESSES

G. ALMAGOR

Geological Survey of Israel, 30 Malkhe Israel Street, Jerusalem 95501, Israel

ABSTRACT : *Akhziv Canyon is the southernmost submarine canyon in a system of some 9 large canyons that deeply incise the entire southern Lebanon continental margin. The canyon is fault-controlled, and runs diagonally across the 6-8.-steep continental slope. The canyon serves as a conduit for massive sediment transport to the adjacent deep Levant Platform. The sediments are: (1) shelf sediments trapped at the canyon heads, and (2) from the steep canyon walls which fail and slump into its thalweg. The sediment transport is episodic, and is believed to be earthquake-induced.*

153

structure of the Troodos dyke complex: In, J. Malpas, E. M. Moores, A. Panayiotou, and C. Xenophontos, eds., Ophiolites, Oceanic Crustal Analogues, Proceedings of the Symposium "Troodos 1987", The Geological Survey Department, Nicosia, Cyprus, p. 27-35.

Parrot, J.-F., 1980. The Baer-Bassit (Northwestern Syria) ophiolitic area: Ofioliti, v. 2, p. 279-295.

Poisson, A., 1977. Recherces géologiques dans les Taurides occidentales (Turquie): Thèse de Docteur des Sciences, Université de Paris-Sud, Orsay, 795 pp.

Reuber, I., 1984. Mylonitic ductile shear zones within tectonites and cumulates as evidence for an oceanic transform fault in the Antalya ophiolite, SW Turkey, In, Dixon, J.F. and Robertson, A.H.F., (eds.), The Geological evolution of the Eastern Mediterranean, Geological Society Special Publication,17, pp. 319-334.

Ricou, L.-E., Argyriades, I., and Marcoux, J., 1975. L'axe calcaire du Taurus, un alignement de fenetres arabo-africaines sous des nappes radiolaritiques et metamorphiques: Bull. Soc. Geol. France, v. 17, p. 1024-1043.

Rowland, J.C. and Dilek, Y., 1992. Rifting and passive margin evolution via asymmetric extension in Mesozoic southern Turkey and analogies with Atlantic margins, Geol. Soc. America Abstracts with Programs, v. 24, p. 71.

Robertson, A.H.F. and Dixon, J.E., 1984. Introduction: aspects of the geological evolution of the Eastern Mediteranean: In, Dixon, J.F. and Robertson, A.H.F., (eds.), The Geological evolution of the Eastern Mediterranean, Geological Society Special Publication 17, p. 1-74.

Şengör, A.M.C., 1984. The Cimmeride Orogenic system and the tectonics of Eurasia: Geological Society of America Special Paper 195, 82 pp.

Tekeli, O., Aksay, A., Urgun, B.M., and Isik, A., 1984. Geology of the Aladağ Mountains: In, Tekeli, O. and Göncüoğlu, M.C., (eds.), Geology of the Taurus Belt, Proc. Int. Symp., Ankara, Turkey, 1983, p. 143-158.

Yazgan, E., and Chessex, R., 1991. Geology and tectonic evolution of the southeastern Taurides in the region of Malatya: Bull. Turkish Assoc. Petrol. Geol., v. 3, p. 1-42.

151

4. ACKNOWLEDGEMENTS

5. REFERENCES

Blumenthal, M., 1955. Geologie des Holen Bolkardag seiner nordlicher Rondgebiete und westliche Auslaufer: Mineral Research and Exploration Institute of Turkey, Ankara Special Publication, Ser. D, No. 7, 169 pp.

Brunn, J.H., Dumont, J.F., De Graciansky, P.C., Gutnic, M., Juteau, T., Marcoux, J., Monod, O., and Poisson, A., 1971. Outline of the geology of the western Taurides: In, Campbell, A.S., (ed.), Geology and History of Turkey, Petroleum Exploration Society of Libya, Tripoli, pp. 225-255.

Demirtaşlı, E., Turhan, N., Bilgin, A.Z., and Selim, M., 1984. Geology of the Bolkar Mountains: In, Tekeli, O. and Göncüoğlu, M.C., (eds.),Geology of the Taurus Belt, Proc. Int. Symp., Ankara, Turkey, 1983, p. 125-141.

Dilek, Y. and Delaloye, M., 1992. Structure of the Kızıldağ ophiolite, a slow-spread Cretaceous ridge segment north of the Arabian promontory: Geology, v. 20, p. 19-22.

Dilek, Y. and Eddy, C.A., 1992. The Troodos (Cyprus) and Kızıldağ (S. Turkey) ophiolites as structural models for slow-spreading ridge systems: Jour. Geol., v. 100, p. 305-322.

Dilek, Y., Thy, P., Moores, E.M., and Ramsden, T.W., 1990. Tectonic evolution of the Troodos ophiolite within the Tethyan framework: Tectonics, v. 9, p. 811-823.

Dilek, Y. and Tekeli, O., 1992. Ophiolite geology of the Inner-Tauride belt, S. Turkey, and implications for Mesozoic tectonics of the Eastern Mediterranean Region: Geol. Soc. America Abstracts with Programs, v. 24, p.

Dilek, Y. and Moores, E.M., 1990. Regional Tectonics of the Eastern Mediterranean ophiolites: In, J. Malpas, E. M. Moores, A. Panayiotou, and C. Xenophontos, eds., Ophiolites, Oceanic Crustal Analogues, Proceedings of the Symposium "Troodos 1987", The Geological Survey Department, Nicosia, Cyprus, p. 295-309.

Juteau, T., 1980. Ophiolites of Turkey: Ofioliti, Tethyan Ophiolites, v. 2, p. 199 - 238.

Juteau, T., Nicolas, A., Dubessy, J., Fruchard, J.C., and Bouchez, J.L., 1977. Structural Relationships in the Antalya Ophiolite Complex, Turkey: Possible Model for an Oceanic Ridge, Geol. Soc. America Bull., v. 88, p. 1740-1748.

Kaaden, G. Van der, 1966. The significance and distribution of glaucophane rocks in Turkey: Bull. MTA Enst. (Mineral Research and Exploration Institute of Turkey), Ankara, v. 67, p. 36-37.

Moores, E.M., Varga, R. J., Verosub, K. L., and Ramsden, T. W., 1990. Regional

Anamas-Akseki platforms and their associated continental margin units show a prominent but reciprocal asymmetry reminiscent of conjugate passive margin pairs around the Atlantic Ocean and the offshore territory of northwestern Australia (Rowland and Dilek, 1992).

Rift assemblages in the Antalya Complex include chert, pelagic limestone, mudstone, sandstone, and alkaline lavas ranging in age from Upper Triassic to Upper Cretaceous and locally include serpentinite lenses exposed along fault zones. These rock units indicate deposition and associated volcanism contemporaneous with block faulting and subsidence between the evolving carbonate platforms and their continental margins through much of the Mesozoic. The basement to the rift assemblages is nowhere exposed within the Isparta Angle because they commonly form the structurally lowermost tectonic unit within the Antalya Complex.

Several platform ribbons, locally several km wide, crop out as north-south trending carbonate strips within the Antalya Complex in a close proximity to the Bey Dağları platform. These ribbons contain Upper Triassic to Jurassic neritic carbonates and Jurassic to Maastrichtian neritic and pelagic limestones and have a Paleozoic nucleus. They are interpreted as marginal plateaus fragmented from the autochthonous Bey Dağları platform during rifting (Rowland and Dilek, 1992).

Ophiolites and mantle slabs in the Antalya Complex occur near the apex and/or the western limb of the Isparta Angle and reveal Late Cretaceous igneous ages. The Tekirova ophiolite along the western coast of the Bay of Antalya displays a nearly complete pseudostratigraphy with harzburgites, cumulate and isotropic gabbros, quartz diorites, plagiogranites, dikes, rare pillow-lavas, and ophiolitic debris flow (Figures 1 and 2) (Juteau et al., 1977). A spreading center-transform fault intersection setting has been inferred for the origin of the Tekirova ophiolite (Juteau et al., 1977; Reuber, 1984). The ophiolite complex tectonically overlies one of the platform ribbons (Kemer Limestone) in the west along a steeply to moderately east-dipping reverse fault.

Rock types and structures documented in the region within the Isparta Angle indicate a progressive evolution from continental rifting and passive margin development to ocean basin formation in the Tauride belt during Mesozoic time. Different phases and the mechanics of this evolution are discussed elsewhere (Rowland and Dilek, 1992). The model presented therein suggests that the sharp bend in the Tauride belt marked by the Isparta Angle is a primary feature inherited from and developed during rifting and subsequent diachronous spreading between the two carbonate platforms (Bey Dağları and Anamas-Akseki) that were either part of a much larger platform or two contiguous carbonate banks. This interpretation disregards the possibility of its origin as a tectonically induced bend of a once continuous carbonate platform in the Tauride belt and suggests that the Antalya Complex is a parautochthonous tectonic assemblage that evolved within the Isparta Angle as the southern branch of Neotethys was opening up in the wake of northward travelling continental fragments.   149

isolated diabasic dikes (Dilek and Moores, 1990; Juteau, 1980). Dike intrusions are generally undeformed and retain their igneous textures. The ophiolite is underlain by a metamorphic sole, compoed of amphibolites, quartzites, and marbles, which in turn overlies a melange unit. The melange consists of thick slices of basalts (locally pillowed), radiolarites, and limestones and rests on the Cretaceous limestones of the Bolkar massif. Diabasic dikes intruding the ophiolite and the metamorphic sole do not cut across the melange units and are truncated by the fault(s) beneath the metamorphic sole indicating that their intrusion occurred prior to the emplacement of the ophiolite over the Bolkar massif. These relations and the internal structure and stratigraphy of the Mersin ophiolite are similar to those described for the Aladağ ophiolite to the east. Restoration of the sinistral offset along the Tertiary Ecemis fault and the palinspastic reconstructions thus suggest that the Aladağ and Mersin ophiolites may be the remnants of the same Neotethyan oceanic lithosphere with a root zone to the north (Dilek and Tekeli, 1992). Their geographic and tectonic position directly over the platforms indicates that the ophiolite-laden carbonate platforms underwent rapid uplifting in Cenozoic time following terminal closure of the Neotethys in Miocene time leaving the ophiolite exposures as erosional remnants of the Neotethyan oceanic lithsophere. Pre-emplacement tectonic setting of the Aladağ and Mersin ophiolites with respect to the Alihoca and İspendere-Kömürhan ophiolitic basement and the island-arc system(s) is a significant question, however, for the Neotethyan paleogeography that awaits further investigations in the region.

3. ISPARTA ANGLE: AN OROCLINAL BEND OR A RIFT STRUCTURE

The Mesozoic carbonate platform of the Tauride belt displays a sharp bend and a north-pointing cusp in the west, near the city of Isparta that is known as the "Isparta Angle" in the literature (Figure-1) (Brunn et al., 1971; Poisson, 1977). The western and eastern limbs of the Isparta Angle closely follow the general outline of the Bay of Antalya and consist of the Bey Dağları and Anamas-Akseki platforms, respectively. The region occupying the center of the angle contains continental margin sequences, rift assemblages, mantle peridotites and ophiolite(s), platform ribbons, and Cenozoic flysch and molasse deposits. Mesozoic units are collectively known as the Antalya Complex (Figure-1), which is thrust over the limbs of the Isparta Angle both in the west and the east.

The autochthonous basement consisting of the Bey Dağları (in the west) and the Anamas-Akseki platforms (in the east) includes continuous series of mainly carbonate rocks ranging in age from Upper Triassic to Eocene. However, the internal structure and stratigraphy of these platforms show differences in their rock record starting in Late Triassic time indicating different sedimentation patterns and paleogeography after the initial rifting in the Tauride belt (Rowland and Dilek, 1992). The Bey Dağları and the

148

İspendere-Kömürhan ophiolite duo might have constituted a Late Jurassic to Early Cretaceous oceanic basement on which an early Late Cretaceous island-arc was constructed in the Neotethys.

The evolutionary path depicted for the İspendere-Kömürhan ophiolites is analogous to that outlined for the Alihoca ophiolite to the west and has two important implications for the Neotethyan geology. One implication is that there was oceanic crust generation and thus seafloor spreading in the Neotethyan branch that developed north of the carbonate platforms and metamorphic massifs in Late Jurassic to Early Cretaceous time. This timing precedes the evolution of oceanic crust generation in the southern branch of the Neotethys that evolved between Afro-Arabia to the south and the platforms to the north. The second implication suggests that a convergent margin tectonics and island-arc development must have occurred in Cretaceous time within the Neotethyan domain immediately north of the Afro-Arabia derived continental fragments. During this period previously formed ophiolites were emplaced in a supra-subduction zone setting to form an oceanic basement for the island-arc system(s) in the Neotethys. The important question to be addressed is the polarity of the inferred subduction zone within the northern branch of the Neotethys.

The ophiolites that occupy an intermediate geographic position between the inner and outer ophiolite tracts and that rest directly on the platform carbonates include the Aladağ ophiolite (or the Pozant-Karsantı ophiolite in some literature) in the Aladağ Mountains and the Mersin ophiolite along the southern foothills of the Bolkar Mountains (Figure-1). These ophiolites and their parautochthonous basements are separated by the sinistral Ecemis fault (Figure-1). The Aladağ ophiolite forms the structurally highest nappe sheet in the Aladağ Mountains and includes tectonized peridotites, cumulate gabbros, and isotropic gabbros that are intruded at all structural levels by numerous microgabbroic to doleritic dikes (Dilek and Tekeli, 1992; Tekeli et al., 1984). A discontinuous outcrop of a thin metamorphic sole is exposed around the periphery of and structurally below the ophiolite and is locally cut by microgabbroic dikes. The metamorphic sole is in turn underlain by an olistostromal melange consisting mainly of ophiolitic material, clastic rocks, and limestones that unconformably overlies the platform carbonates in the Aladağ Mountains. This melange unit occurs as thin slivers between different nappe sheets in the Aladağ Mountains and displays a locally well-preserved internal stratigraphy composed, from bottom to top, of rudistid, pelagic, and detrital limestones, mudstone, ophiolitic olistostrome, and a block-supported melange. Regional correlations indicate that the melange units exposed beneath the ophiolite complexes in the Inner-Tauride belt show a similar internal structure and stratigraphy and that they represent deposition in a restricted basin developed in front of southward advancing ophiolites (Dilek and Tekeli, 1992).

The Mersin ophiolite south of the Bolkar massif represents a dismembered and deformed suite consisting of serpentinized harzburgites and dunites, layered gabbros, and

they contain layered to isotropic gabbros, hypabyssal intrusions and dikes in addition to their mantle sequences. Most importantly, however, different subunits in these ophiolites are cross-cut by dikes and stocks of various rock types of island-arc affinity indicating that the entire ophiolitic sequence in these complexes underwent magmatic plumbing and igneous underplating in a subduction zone environment subsequent to its generation (Dilek and Moores, 1990).

The Alihoca ophiolite north of the Bolkar Mountains forms a narrow zone of oceanic rocks consisting of peridotites, pyroxenites, cumulate to isotropic gabbros, massive diabase, isolated dikes, and pelagic limestones, and marks a suture zone in the Inner-Tauride belt (Dilek and Tekeli, 1992). The tectonic contact between the ophiolite and the Bolkar massif (a continental fragment consisting of Paleozoic to Mesozoic clastic and carbonate rocks) to the south contains discontinuous exposures of glaucophane-riebeckite bearing metamorphosed mafic and ultramafic rocks (Blumenthal, 1955; Kaaden, 1966). The orientation of stretching lineations in metamorphic rocks and steeply to moderately north-dipping thrust contact indicate a root zone of the ophiolite to the north and thus its southward transport over the Bolkar massif. The Alihoca ophiolite constitutes the basement of the Ulukışla basin in which flysch deposits consisting of ophiolitic olistostromes, turbiditic sandstones, agglomerates, volcanic breccias, tuffs, and shales of Late Cretaceous to Paleocene age (Çiftehan Formation) were deposited (Demirtaşlı et al., 1984). Although no radiometric dates are yet available from the ophiolite, basaltic andesite dikes intruding mantle and crustal rocks of the ophiolite have revealed Neocomian ages suggesting that the Alihoca ophiolite may be as old as and/or older than Early Cretaceous (Dilek and Thy, in preparation). The island-arc tholeiite geochemistry of these dike rocks and the existence to the north of dikes and stocks of microgabbro, diorite, and tonalite intrusions indicate that oceanic lithosphere now represented by the Alihoca ophiolite was possibly situated in the hanging wall of a subduction zone during Cretaceous to early Cenozoic time (Dilek and Tekeli, 1992).

The İspendere-Kömürhan ophiolite complexes occur farther east, between the Pütürge metamorphic massif and the Keban metamorphics (Figure-1), and contain, from bottom to top, polydeformed, amphibolite-grade mafic and ultramafic rocks (Kömürhan) structurally overlain by cumulate and isotropic gabbros, sheeted diabase dikes, and pillow-lavas (İspendere) (Yazgan and Chessex, 1991). K/Ar radiometric dates from the amphibolites in the Kömürhan ophiolite reveal metamorphism ages ranging from 127±14 Ma to 95±9 Ma (Yazgan and Chessex, 1991), suggesting protolith ages older than Neocomian. The İspendere ophiolite is unconformably overlain by a flysch sequence that contains Upper Campanian to Lower Maastrichtian fossils, and both İspendere and Kömürhan ophiolites are in turn intruded by Coniacian to Santonian age granodiorites, tonalites, quartz monzonites, monzodiorites, diorites, and gabbros of an island-arc affinity (Yazgan and Chessex, 1991). These relations suggest, in general, that the

146

Tekirova (Antalya Complex)

Lycian Nappes

Beyşehir Nappes

Troodos

Mersin

? Ali Hoca

Bäer-Bassit

Kizildağ

Pozanti-Karsanti

Ovacik Ophiolite Mélange

İspendere-Kömürhan

Guleman

Gevaş

? Cilo

Shallow water or continental deposit
Unconformity
Pelagic sediments; terrigenous/arc deposits
Pillow and massive lavas
Transitional contact
Dike complex (sheeted and/or unsheeted)
Isotropic gabbro, diorite, plagiogranite

Cumulate rocks; ultramafic-mafic at bottom, felsic toward top

Ultramafic tectonite; peridotite with discontinuous layers of dunite (d) and concentrations of chromite (cr)
Metamorphic sole; commonly 0-200m thick
Tectonic and/or sedimentary mélange
Platform carbonates with crystalline basement

Figure-2: Diagrammatic columnar sections of the eastern Mediterranean ophiolites and their comparison with the expanded ophiolite pseudostratigraphy (after Dilek and Moores, 1990).

section.

Recent structural field studies of the crustal sections in the Troodos and Kızıldağ ophiolites have shown that the internal structure and stratigraphy of these ophiolites are most likely to have developed as a result of tectonomagmatic processes that operated at paleo-spreading centers in the southern Neotethys (Moores et al., 1990; Dilek and Delaloye, 1992; Dilek and Eddy, 1992). Both ophiolites display numerous planar to listric normal faults and structural grabens in their sheeted dike complexes suggestive of tectonic extension along a spreading axis. Complex intrusive relations in their plutonic units indicate recurring and intermittent magmatic activities which alternated and/or had a balanced interplay with amagmatic crustal stretching and thinning. The existence of accommodation zones as detachment surfaces within the lower crustal sequence (Troodos) or at the boundary between the crustal and mantle sequences (Kızıldağ) provide a further evidence for tectonic extension during the evolution of fossil oceanic lithosphere. In the Kızıldağ ophiolite, northeast-trending contacts between the ophiolitic subunits, consistent dike trends, and the inferred paleo-spreading axis are cut and offset by northwest-striking tear faults that are analogous both in size and geometry to the transfer faults on the eastern wall of the Mid-Atlantic Ridge in the TAG area (Dilek and Delaloye, 1992). Transfer faults in modern oceanic crust permit differential extension and rotation between major crustal blocks along the spreading axis, generally are oblique slip in nature, and are sites of off-axis volcanism and hydrothermal alteration (Dilek and Delaloye, 1992 and references therein). These characteristics of transfer faults are similar to those observed and inferred for the tear faults mapped in the Kızıldağ ophiolite and provide further evidence for its paleo-tectonic setting in a spreading center environment (Dilek and Delaloye, 1992; Dilek and Eddy, 1992). The structural architecture and the inferred tectonic evolution of both ophiolites are reminiscent of a slow-spreading ridge system in the southern Neotethys, which evolved immediately north of Afro-Arabia in Mesozoic time (Dilek and Delaloye, Dilek et al., 1990).

Ophiolites of the inner ophiolite tract are in general deformed and metamorphosed, and display an incomplete pseudostratigraphy. The main ophiolite massifs include, from west to east, Lycian and Beyşehir nappes, Alihoca, Pınarbaşı, Ovacık, Guleman, İspendere-Kömürhan, and Gevaş ophiolites, which are commonly associated with underlying metamorphic soles and melanges (Figures 1 and 2). Some of these inner tract ophiolites in the east occur between the metamorphic massifs to the south and the easternmost platforms to the north (i.e., Munzur) and are displaced and translated laterally along the East Anatolian Fault. The Lycian and Beyşehir nappes in the west represent 'decapitated' oceanic lithosphere with extensive peridotite exposures intruded by numerous diabasic to microgabbroic dikes. Crustal subunits are missing in these ophiolites most likely due to their post-emplacement uplifting and subsequent erosion. Towards the east the ophiolites seem to have preserved their subcrustal units better, for
144
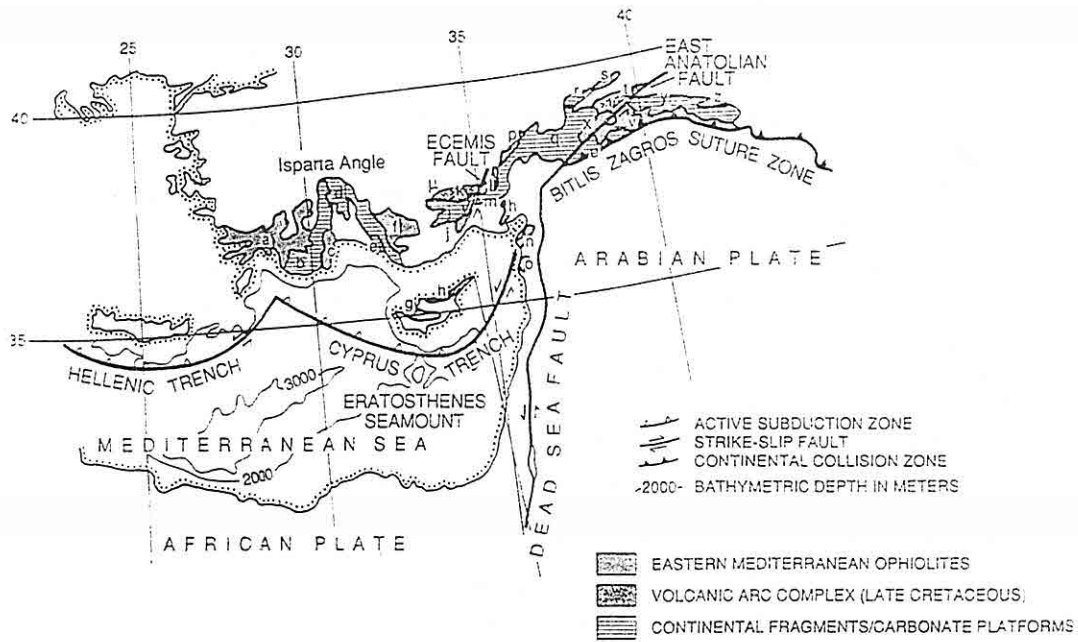
Figure-1: Simplified tectonic map of the eastern Mediterranean region showing the distribution of current plate boundaries, ophiolites, and major tectonic features (modified from Dilek et al., 1990). Key to lettering: (a) Lycian nappes, (b) Bey Dağları platform, (c) Antalya Complex, (d) Anamas-Akseki platform, (e) Alanya massif, (f) Beyşehir nappes, (g) Troodos ophiolite, (h) Kyrenia range lineament-Misis complex, (i) Bolkar massif, (j) Mersin ophiolite, (k) Alihoca ophiolite, (μ) Çiftehan Formation, (l) Aladağ or Pozantı-Karsantı ophiolite , (m) Aladağ platform, (n) Kızıldağ ophiolite, (o) Bäer-Bassit ophiolite, (p) Pınarbaşı ophiolite, (q) Keban metamorphics, (r) Munzur platform, (s) Ovacık ophiolite, (t) Elazığ-Palu nappe/Baskil volcanic arc, (u) Pütürge massif, (v) Guleman ophiolite, (x) İspendere-Kömürhan ophiolites, (y) Bitlis massif, (z) Gevaş ophiolite.

143

1. INTRODUCTION

The Tauride belt in southern Turkey is a significant component of the Alpide orogenic system in the Tethysides (Şengör, 1984) and has developed mostly during Mesozoic and Cenozoic times as a result of amalgamation of a number of metamorphic massifs, carbonate platforms, and oceanic terranes of Tethyan origin (Figure-1). Of particular significance in the architecture of the Tauride belt is the existence of Mesozoic ophiolite complexes with the Neotethyan affinity, which rest tectonically on the platform carbonates (Figure-1). These ophiolites and related tectonostratigraphic terranes generally form two nearly east-west trending, discontinuous linear zones in the southern and northern parts of the belt , although some ophiolite complexes occupy an intermediate geographic position between them (Dilek and Moores, 1990). Timing and the mode of igneous development and tectonic accretion into the Tauride belt of these ophiolite complexes are important subjects of the Neotethyan geology and have strong implications for the Mesozoic and early Cenozoic paleogeography of the eastern Mediterranean region.

This paper presents a synoptic overview of some aspects of the geology of the Tauride belt and outlines some new information and interpretations derived from most recent studies in the region.

2. OPHIOLITE GEOLOGY OF THE TAURIDE BELT

The Neotethyan ophiolites in the eastern Mediterranean region occur in two nearly east-west trending tracts separated by a number of carbonate platforms and metamorphis massifs of the Tauride belt. These platforms (e.g., Bey Dağları, Anamas-Akseki, Aladağ, Tufanbeyli) and metamorphic massifs (e.g., Pütürge, Keban, Bitlis) are underlain by a Paleozoic and older (?) basement and are interpreted to be rifted-off fragments of Afro-Arabia (Figure-1) (Şengör, 1984; Dilek and Moores, 1990; Ricou, 1975; Robertson and Dixon, 1984). In this paper the ophiolites that are exposed to the south of the carbonate platforms and metamorphic massifs are grouped as part of the outer ophiolite tract and those to the north as part of the inner ophiolite tract.

Ophiolite complexes of the outer ophiolite tract display a relatively complete pseudostratigraphy with thicknesses around 5 to 7 km. These ophiolites include the Troodos massif in Cyprus, Tekirova and Kızıldağ ophiolites in southern Turkey, and Baer-Bassit ophiolite in Syria (Figures 1 and 2). The Baer-Bassit ophiolite differs from the others in that it has a metamorphic sole that separates it from the underlying Arabian platform and that it is strongly dismembered by numerous thrust slices, which were probably developed during its emplacement (Parrot, 1980). The Tekirova ophiolite is part of the Antalya Complex, a tectonic assemblage of continental margin and rift units, platform ribbons, ophiolites and mantle slabs. The Antalya Complex as a whole rests tectonically on the Bey Dağları and Anamas-Akseki platforms in the west and east, respectively. The evolution of this assemblage in the Tauride belt is discussed in the next

142

SOME ASPECTS OF THE MESOZOIC TECTONICS OF THE TAURIDE. BELT, SOUTHERN TURKEY

Yıldırım DİLEK

Department of Geology and Geography, Vassar College, Poughkeepsie, New York 12601, U.S.A.

ABSTRACT : *The Tauride tectonic belt in southern Turkey consists of a number of tectonostratigraphic terranes with both continental and oceanic affinity, which evolved and were pieced together through mainly divergent and convergent tectonics within the Mesozoic Neotethyan realm. Whereas rifting and seafloor spreading played an important role during early stages of the evoluton of the Tauride belt as evidenced by the existence of several tracts of ophiolites with ages ranging from Late Jurassic to Late Cretaceous, contraction and associated thrusting, crustal stacking, and magmatic underplating dominated its late-stage evolution in terms of island-arc development, emplacement of ophiolites and nappe sheets, and internal imbrication within its different entities during Late Cretaceous through early Cenozoic time. The Neotethyan paleogeography in the late Mesozoic is envisioned to have included a small ocean basin in the south with an active spreading center system between Afro-Arabia and the carbonate platforms and a wide ocean with island-arc system(s), marginal basins, and continental fragments to the north. Carbonate platforms that constitute the backbone of the Tauride belt seem to have experienced internal rifting as they travelled northwards away from Afro-Arabia during opening of the southern branch of Neotethys.*

141

Ponikarov, V.P., 1988.Explanatory Notes on the Geological Map of Syria, 1967.

Sheleh, F., Les Enclaves Ultramafiques du Basalte du Sud de la Syrie. Thèse Magistère, Universitè de Damas, 159 p.

Witt, G.,Seck, A., 1987.Temperature History of Shoared Mantle Xenoliths from the West Eifel, West Germany: Evidence for Mantle Diapirism Beneath Rhenjsh Massif. J.Petrol, 28, 475-493

Vincent, B., 1987. Etat D'équilibre des Peridotites du Manteau Supéerieur. Application auPlateau du Colorado. Thèse Université Paris VII,

Webb, S.A., Wood, B.J., 1986. Spinel-Pyroxene-Garnet Relationships and Their Dependance on Cr/Al Ratio. Contr. Mineral. Petrol. 92, 471-480

Bilal, A., 1984. Petrology of the Basalt of the Sud of Syria-Fluid Inclusions, 27 ème Inter. Geol. Congres, Moskow.Bilal, A., Etude Géothèrmometrique des Enclaves Profondes Dans la Region de NabiSaleh, Nabi Mata, et Mhailbeh., 1990. Contr 2/90, GORS, 67 p.

Bilal, A., 1991. Moho Depth of the Northern Part of Arab Plate (Syria), Through the Ultrabasic Xenoliths Study,. Symposium, Irbid, Jordan .

Bilal, A. et Touret, J., 1976. Les Inclusions Fluides Dans les Enclaves Cazonalae de Bournac, Massif Central Français. Bull. Soc. Fr.Mineral.Cristallo, 92, 2-3, 134 - 139. Bilal, A. et Touret, J., 1977. Les Inclusions Fluides des Phénocristaux des Laves Basaltiques du Puy Beaunit-Massif Central Français. Bull. Soc. Fr. Mineral. Cristallo. 100, 324 - 328.

Brey, G.P., Nickel, K.G., Kogarkol, L., 1986. Garnet - Pyroxene Equilibria in the SystemCaO - MgO - Al₂O₃ - SiO₂ (CMAS): Prospects for Simplified (T - Independent) Lherzolite Barometry and an Eclogite Barometer. Contr. Mineral. Petrol. 92, 448-454 .

Coleman, R. and McGuire, A.V., 1988. Magma Systems Related to the Red Sea Opening Tectonophysics, 150, 77-100 .

Dawson, J.B., 1940a. Kimberlites and Their Xenoliths. Springer Verlag, 250p., 1980.

Dubertret, L., Sur L'âge du Volcanisme en Syrie et au Liban. C.R.Som. Soc.Geol.Fr, 55-57.

Ghent, E.D., Coleman, R.G., Hardley, D.G., 1980. Ultramafic Inclusions and Host Alkali Olivine Basalts of the Southerncoastal Plain of the Red Sea. Saudi Arabia. Am. J. Sci. 280-A, 499-527 .

Glucklich, M. et Mercier, J.C., 1992. Manteau Superieur VS Manteau Primitif. 14 eme Reunion des Sciences de la Terre, Toulouse, France, p. 69.

Gutmann, J.T., 1986. Origine of Four and Five-Phase Ultramafic Xenoliths from Sonora Mexico. Am. Mineral.71, 1076-1084.

Leyreloup, A., 1973. La Lithologie du Socle Profond enVelay D'après Les Enclave Remontees Par Les Volcans Néogenes, Massif Centtral, Français. Thèse 3eme Cycle, Nantes, 356p.

Nasir, S. and Al-Fuqha, H., 1988. Spinel-Lherzolite Xenoliths from the Aritain Volcano, NE-Jordan. Minerolog and Petrology, 38, 127-137.

Neville, S.L., Schiffman, P., Sadler, P., 1985. Ultramafic Inclusions in Late Liocène Alkali Basalts from Frey and Ruby Mountains, San Bernandino Country, California. Am. Mineral. 70, 668-677.

Nickel, K.G., Phase Equlibria in the System SiO₂-MgO-Al₂O₃-CaO-Cr₂O₃(SMACCR) and Their Bearing on Spinel/Garnet Lherzolite Relationships. N.Jb. Miner. Abh., 155, 259-287.

As the fluid inclusions keep their originality until 60 Km of depth (Bilal, 1978), the lower determined temperature, by geothermometric model, gives with the density of early carbonic inclusions, the thermodynamic conditions and consequently the depth of upper mantle in the studied localities as it is presented in table(3).

Locality	Dj.AL Arabe	AL Mhailbeh	Kadmous	Jubates
TC°Minm	1028	978	1013	956
PKbMinm	11.3	11	10.4	10
Depth Km	39.4	38	35.4	33

Table 3. Depth of upper mantle in the studied localities.

5. CONCLUSION

These results correspond to a rift geothermometre which confirm, so, the riftogenesis of the Syrian fault Fig.3, and suppose a thermal anomaly inviting, thus, more care of this region which could be rich in some liquid and solid gisements.

The thermodynamic conditions in the studied localities allow to follow the oscillations of the upper mantle depth and to more understanding the Arab-African plate tectonic. The depth of upper mantle, after these results, increases towards the South and East, which explain partially, the thinness of the crust in the opposite direction and to explain the changes of the rejection of the Syrian fault and their projection of the orogenesis of Palmyra Chains.

6. REFERENCES

Al Barede, F., 1992. De Quelle Profondeur Proviennent les Basaltes? 14e Reunion des Sciences de la Terre, Toulouse, France, p3.

Al Sharkawi, M., 1982. Lherzolite Xenoliths from the Shihan Basalts-Jordan. Journal of theUniversity of Kuwit (Sciences), Vol 9, no 2, 278-301.

Berger, E. et Vannier, 1984. M., Les Dunites en Enclaves Dans les Basaltes Alcalins des Iles Océaniques - Approche Pétrographique. Bull. Minéral, Vol 107, 5, 649 - 665.

Bergaman, S. and Dubessy, J., 1984. CO_2-CO Fluid Inclusions in a Composite PéridotiteXenolith: Implications for Upper Mantle Oxygen Fugacity. Contr. Mineral. Petrol., 85, 1-13.

Bertrand, P. et Mercier, J.C., 1986. The Mutual Solubility of Coexisting Ortho and Clinopyroxene: Toward an Absolute Geothermometre for the Natural System? Earth and Planetary Sciences Letters, 76, 109-122.

Bilal, A., 1978. Les Inclusions Fluides des Roches de la Croûte Continentale Inférieure et du Manteau Supérieur - Implications Géotectoniques. Thèse Doctorat D'état ès Sciences, Université Paris VII, 311 p.
138
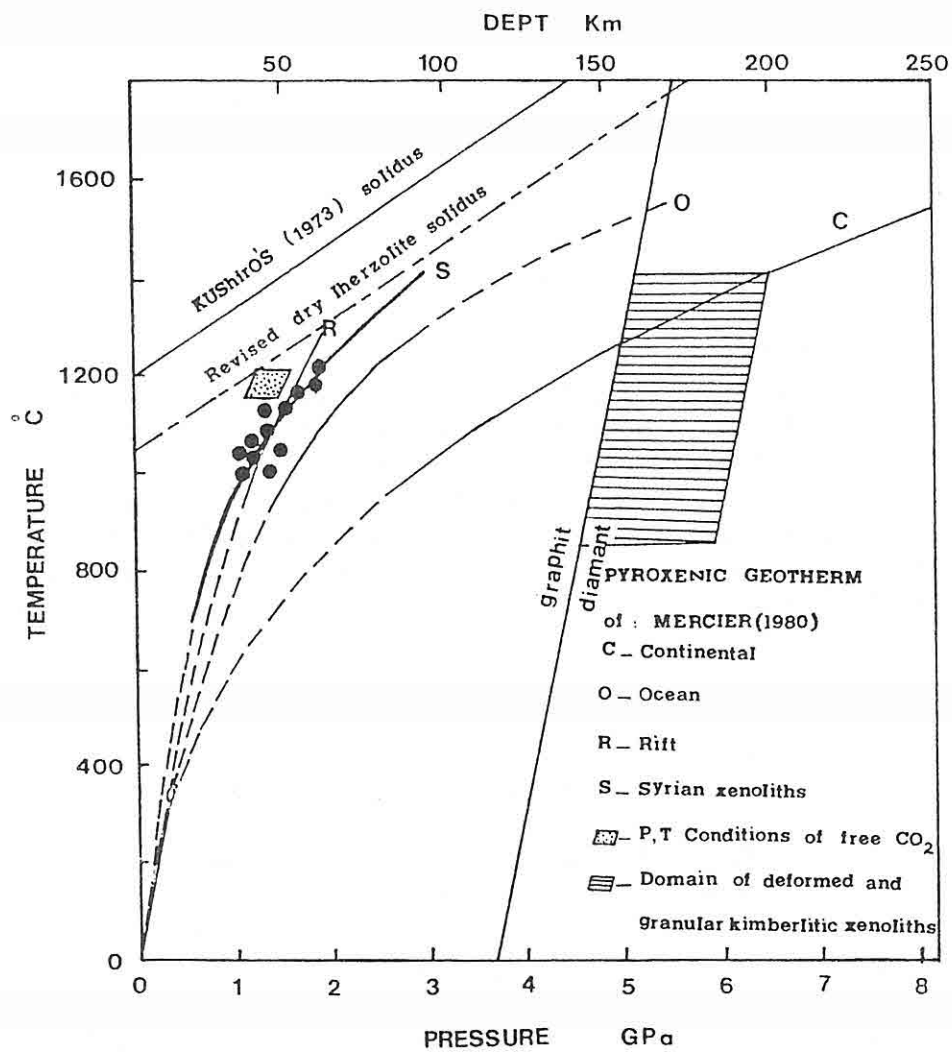
Fig 3. Different geothermometric models and position of Syrian xenoliths.
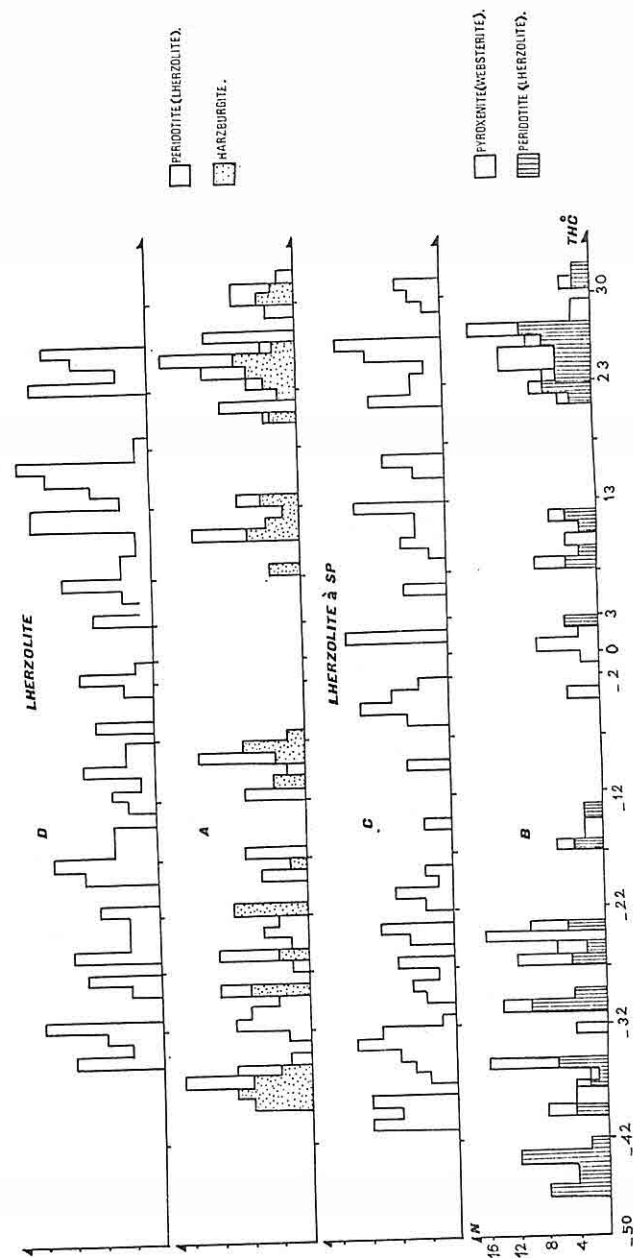
Fig 2. Homogenization temperature histograme of early carbonic inclusions.

136

-Early generation where the homogenization changes in relation with locality and petrographic type Fig(2);

-Late generation, the same in all localities and result from the contamination by the volcanic gas (Bilal and Touret ,1976, 1977).

Table (2) presents physio - chemical variations (Th: homogenization temperature, Tf: fusion temperature) of early carbonic inclusions. Fusion temperature is stable at -56.6°C which indicate a pure CO_2.

Locality	Dj.AL Arabe	AL Mhailbeh	Kadmous	Jubates
TF°C	-56.6	-56.6	-56.6	-56.6 à -57
Th°C	-41	-47	-39	-35
D g/cm³	1.11	1.12	1.1	1.02

Table 2. Physio-chemical variations of early carbonic inclusions.

4. THERMODYNAMIC CONDITIONS

According to the recent data (Al Sharkawi ,1982; Glucklich and Mercier, 1992) the studied xenoliths are a represenative sample of upper mantle (Bilal, 1990) which allows to apply the geothermometric models.

Many geothermometric models are proposed (Brey et al., 1986; Vincent 1987, Webb and Wood, 1986), but the Bertrabd and al model (1986) is the best applied model where the fault ranges from ±1%, which could be negligible for a high temperature (1000°C) as is the case of the upper mantle.

This model is based on the chemical equilibrium between ortho and clinopyroxene using the equation:

$$T_{CMS} = (36273 + 399P)/ [19.31 - 8.314 \ln(K^*) - 12.15(Ca^*_{cpx})^2]$$
where

$$[X^{M2}_{Ca}]_{cpx.CMS} = Ca^*_{cpx} = [X^{M2}_{Ca} / (1 - X^{M2}_{Na})]_{cpx} + [- 0.77 + 10^{-3}T] \cdot [Fe/Fe + Mg)]$$

$$[X^{M2}_{Ca}]_{opxCMS} = Ca^*_{opx} = [X^{M2}_{Ca} / (1 - X^{M2}_{Na})]_{opx}$$

$$K^* = [1 - Ca^*_{cpx}] / [1 - Ca^*_{opx}]$$

Type petrographic	Lherzolite à SP		Webstrite à SP	Basalts		Grenatites
Echantillon	1	14 Th	11	5	10	4
SiO_2	44.43	42.82	49.90	49.83	44.48	37.90
Al_2O_3	1.41	3.07	10.12	16.56	19.34	22.54
Fe_2O_3	1.35	2.17	1.62	3.41	3.24	5.95
FeO	6.92	6.74	4.18	6.93	5.83	8.90
MnO	0.13	0.14	0.15	0.18	0.14	0.54
MgO	43.45	39.96	20.85	5.03	10.98	8.35
CaO	1.01	2.41	11.20	9.08	12.56	6.25
Na_2O	0.08	0.29	0.48	3.37	1.33	0.27
K_2O	0.01	0.13	0.03	1.47	0.11	0.85
TiO_2	0.04	0.35	0.15	2.29	0.42	0.41
P_2O_5	0.01	0.10	0.06	0.36	0.06	0.87
CO_2 tot	0.08	0.40	0.19	0.13	0.09	0.33
H_2O tot	0.77	1.03	0.52	1.16	1.39	6.15
TOT AL	99.68	99.61	99.45	99.80	99.97	88.31

Table 1. Total chemical composition of principal petrographic types.

1-Kadmous, 14Th-Dj.Al Arabe, 4,5,10,11-Mhailbeh
(Analyse de C.R.P.G., Nancy, France)

The olivine is forsterite at a rate of 90-93%, and exists in contact with orthopyroxene (enstatite) which is changed in situ, to diopside by coronetic reaction with spinel and clinopyroxene. This later is diopside, while spinel, which could be green, brown or chestnut, takes different shapes: In inclusions or in thin interstice plates, it can also fill the mineral fractures especially olivine and orthopyroxene.

Table(1) shows global chemical composition of studied types and carrier rock. The peridotite (samples 1, 14Th) is spinel lherzolite, but sample 1 is more magnesian and differential (poor in Al_2O_3 and CaO) from sample 14Th. The pyroxenite (sample 11) is spinel webstrite, and the basalt indicate high quantity of Al_2O_3, so it is differential alkali basalt and feldspathic. Finally, in garnetite (sample 4) the relation Fe/Mg is over 1 indicating Almandine garnet, which distinguish amphibolitic and granulitic rocks, of the lower continental crust.

These rocks contain many carbonic fluid inclusions which can be distinguished in two generations:

134
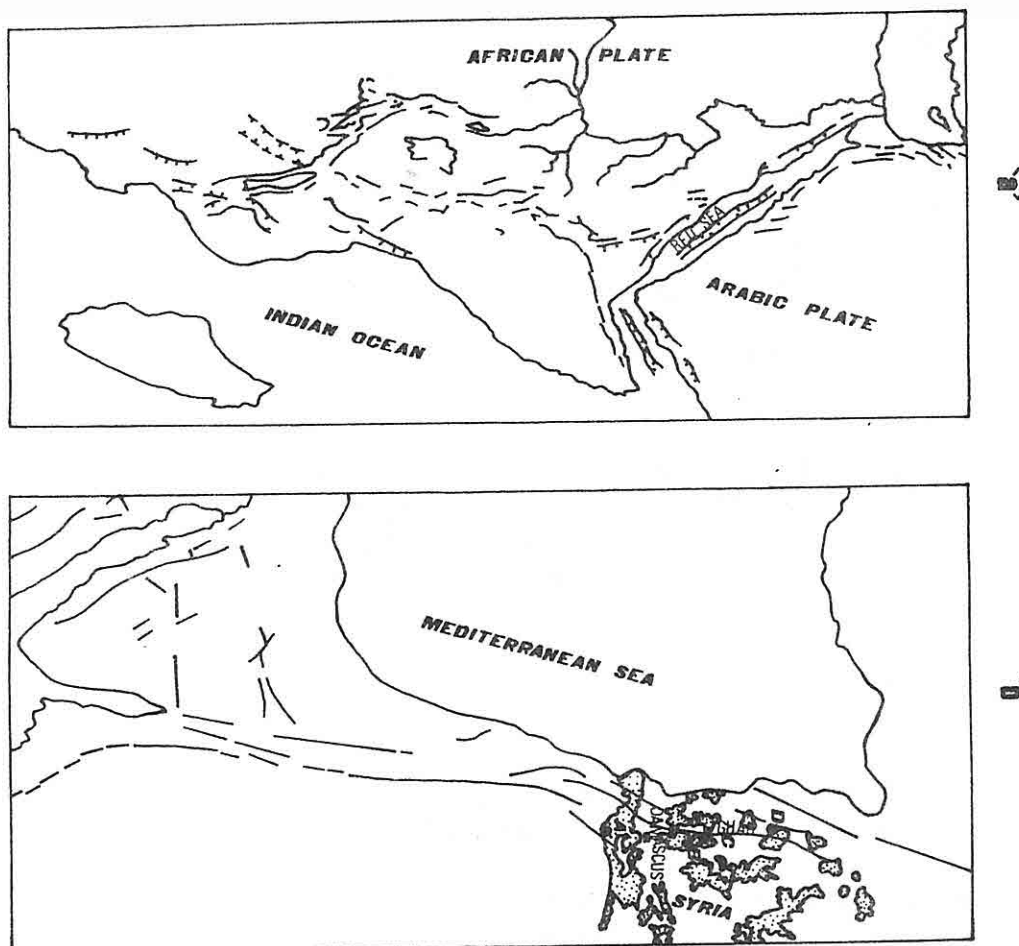
Fig 1. African Rift (a) and Syrian Rift (b) with lava basaltic distribution in Syria.

1. INTRODUCTION

The study of the mantle xenoliths, which arise to the surface by kimberlitic and basaltic lava, increasingly entice geologists attention throught various aspects: Petrology, structurology and geochemistry (Berger and Vannier ,1984; Dawson 1980, Gutmann, 1986; Leyreloup, 1973; Neville et al., 1985; Witt and Seck,1987) in different countries of the world.

More-over the study of the liquid phase enclosed in these xenoliths by studying of fluid inclusions has increased our knowledges on the depth levels, hence more understanding of the geological processes of these levels of lithosphere and particularly the upper mantle.

In the Arab region, the study of the upper mantle xenoliths and its bearing rock, has not begun until the last ten years. In Saudi Arabia (Ghent et al., 1980), in Red Sea (Coleman and McGuire 1988), in Jordan (Berger and Vannier, 1984; Bilal, 1991) and in Syria (Bilal 1984, 1990,1991; Sheleh ,1988).

The aim of this paper is to contribute to the study of the evolution of the lithosphere in the Northern part of the Arab plate and particularly drawing the oscillations of the upper mantle depth and its reflex on the movement of the Arab-African plates.

2. REGIONAL GEOLOGY

Volcanism covers an important portion of Syria. Its age is unknown exactly, but after the previous studies (Dubertret ,1940a; Ponikarov ,1967) are believed to have begun in Secondary (Cretaceous?) and arrived his apex in Tertiary and Quaternary.

The basaltic lava, which represent different petrographic types: Olivine basalt, Hawaiian basalt, mugearite, trachite and basanite, carried to the surface a large quantity of xenoliths of differents geological levels. These xenoliths were observed in the southern of the country from 1977 by the General Establishment of Geology and Mineral Resources team, where a brief petrographic description and chemical analysis have been excuted, but the first serious study has been effected by Sheleh (1988).

The studied localities in this paper are: Djabel AL-Arab in the South, AL-Mhailbeh in the middle and Kadmous and Jubates in the North. All these localities are placed along the grand Syrian Rift which is the northern continuation of the African rift Fig(1).

3. PETROGRAPHIC STUDY AND FLUID INCLUSIONS

The global mineralogical composition of studied xenoliths permits to determine several peridotitic and pyroxenitic types. The studied types are: Lherzolite, spinel lherzolite, harzburgite, wehrlite, websterite and garnetite. All these types are characterized of three principal minerals: Olivine, ortho and clinopyroxene, except garnetite which is composed completely of garnet.

132

LITHOSPHERE EVOLUTION IN THE NORTHERN PART OF ARABIC PLATE (SYRIA)-XENOLITHS STUDY

Ahmad BILAL

Dept.of Geology, Faculty of Sciences, University of Damascus/Syria

ABSTRACT : *The Syrian basalt cover an important part of country which indicates an intense volcanic activity, distributed as parallel lines oriented South-North. The basaltic products are composed of several petrographic types: Olivine basalt, hawaiite, mogerite, trachyte and basanite. They contain various xenoliths: Peridotites, pyroxenites, grenatites, granulites, amphibolites, ...etc. These xenoliths belong to the mantle and they allow the determination of the crust thickness, hence the depth of the upper mantle.*

Tens of samples of ultrabasic xenoliths ascending in basalt have been studied in various locations in Syria: Nabi matta, Tubate, Kadmous and Djabel Al-Arab. It was found out that they reflect a petrographical stability consists in peridotite, pyroxenite, and grenatite rocks which are essentially composed of Olivine, Orthopyroxene, Clinopyroxene, as well as Grenat, Spinelle and Plagioclase as minor minerals, depending on the rock type. Such types contain carbonic fluid inclusions similar to those describe in other regions of the world.

Through the analysis of Orthopyroxene and Clinopyroxene conducted by the use of Bertrabd et al., (1986) geothermometre, subsequent to ensuring that the studied samples belong to the upper mother mantle, and using the density of carbonic fluid, it has been possible to determine the pressure and temperature conditions.

These conditions comply with a rift geotherm and they determine the depth of upper mantle in the studied locations. It changes from North to South and from West to East. As a matter of fact, these results are of great importance for understanding the evolution of the lithosphere of the northern part of the Arabian Plate.

Weaver, C.,E., 1984. Shale - Slate Metamorphism in Southern Appalachians, Elsevier, New York, 235 pp.

Weaver, C.E., and Pollard, L.D., 1973.The Chemistry of Clay Minerals. Devolopments of Sedimentology, Elsevier, Amsterdam, 15, 213 pp.

130

1989). The K_2O content of illite varies between 8.70 and 10.82 % and these values are very close to real illite defined in the literature.

As a conclusion, both chemistry and polymorph types of hydrothermal illites in the study area are unlike to the illites in the Paleozoic rocks. As defined above,Paleozoic aged clays shows different clay mineral paragenesis and their illite polymorph types are different. Neogene aged volcanics and tuffs are not observed in the investigation area. But at near the study area (Hatip), the tuffs include various clay minerals. The illite occurred at the country rocks of ore mineralization is not related to the volcanics. That's why the illites are products of neither degradation nor aggradation of volcanics. They are neoformed minerals have developped by hydrothermal solutions being rich in K cation.

4. ACKNOWLEDGEMENT

5. REFERENCES

Caillere, H., Henin, S.et Rautureau, M., 1982. Mineralogie des Argiles, ın "INRA, Actualites Scientifiques", Masson, Paris.

Çelik, M., Karakaya, N. ve Turan, A., 1991. Erken Paleozoyik Yaşlı Killerin Metamorfizma Özellikleri: Konya Güney-Güney Batısı. VI. Ulusal Kil Sempozyumu 63-73 , Eskişehir.

Chamley, H., 1989.Clay Sedimentology. Springer-Vertlag, Berlin, 623pp.

Closs, M., 1983. Comperative Study of Melange Matrix and Metashale from the Fraciscan Subduction Complex with the Basal Great Walley Sequence, California, Jour. Geol., 91, 291-306.

Inoue, A., and Utada, M., 1983. Further Investigation of a Conversion Series of Dioctahedral Mica/Smectites in the Shinzan Hydrothermal Alteration Area , northeast Japan: Clays and Clay Minerals 31, 401-412.

Larsen, G. and Chilingar, G.V., 1983. Diagenesis in Sediment And Sedimentary Rocks, Elsevier, Developments in Sedimentology, 25B, 572 pp.

Maxwell, D.T. and Hower.J., 1967. High - Grade Diagenesis and Low - grade Metamorphism of the Illite in the Precambrian Belt Series, Amer. Mineral, 52, 5/6, 843-857.

Motorcu, A., 1987. Ladik - Sızma (Konya) Bölgesi Civa Yatakları. S.Ü. Fen .Bil. Enst. Master Tezi , 98 s. (unpublished) .

Nemecz, E., 1981. Clay Minerals, Akademiai Kiado' Budapest, 547 pp.

Thorez, J., 1976. Practical Identification of Clay Minerals. Letotte, Dison 90 pp.

Velde, B., 1985. Clay Minerals: A Physical-chemical Explanation of their Occurrence. Elsevier Amsterdam, 218 pp.

Table 2. Chemical Analysis and Structural Formulae of Pure Illites.

% Oxide	1	2	3	4
SiO_2	63.07	62.53	60.46	61.20
Al_2O_3	24.94	25.09	24.22	24.51
Fe_2O_3	1.25	1.24	3.03	3.04
TiO_2	1.40	1.44	1.47	1.35
K_2O	9.35	9.70	10.82	9.90
Total	100.01	100.00	100.00	100.00
Tetrahedral				
Si	3.86	3.84	3.75	3.79
Al	0.14	0.16	0.25	0.21
Octahedral				
Al	1.65	1.66	1.55	1.57
Fe	0.057	0.057	0.143	0.150
Ti	0.064	0.066	0.071	0.064
Interlayer Cation				
K	0.73	0.74	0.87	0.78
Total Octaeder	5.41	5.42	5.38	5.42
Tetrahedral Charge	0.14	0.16	0.25	0.21
Octahedral Charge	0.59	0.58	0.62	0.58
Calculated Layer Charge	0.73	0.74	0.87	0.89

128
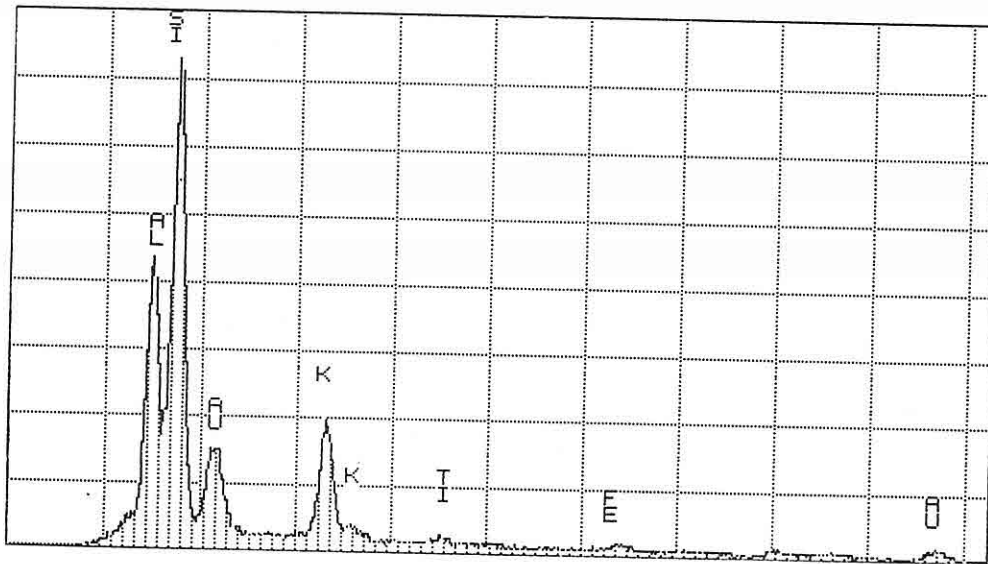
Figure 6. EDX Analysis of high K illite.
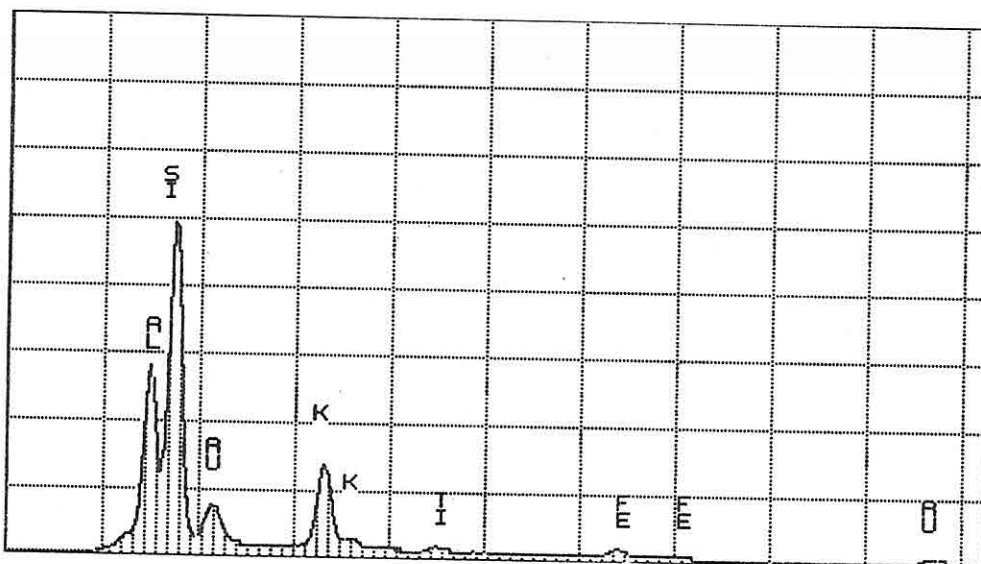
Figure 7. EDX Analysis of low K illite.

127
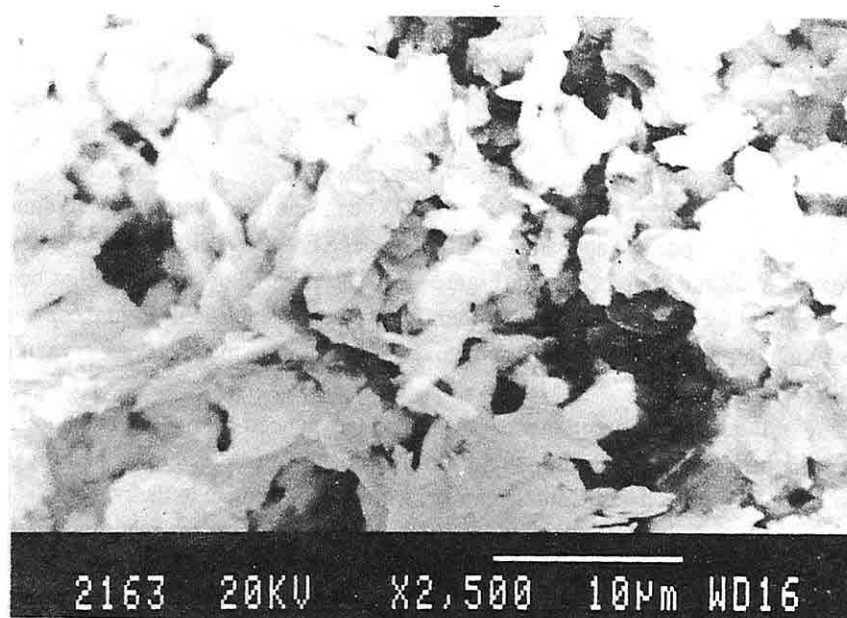
Figure 4. Electron microscope morphology of illites.
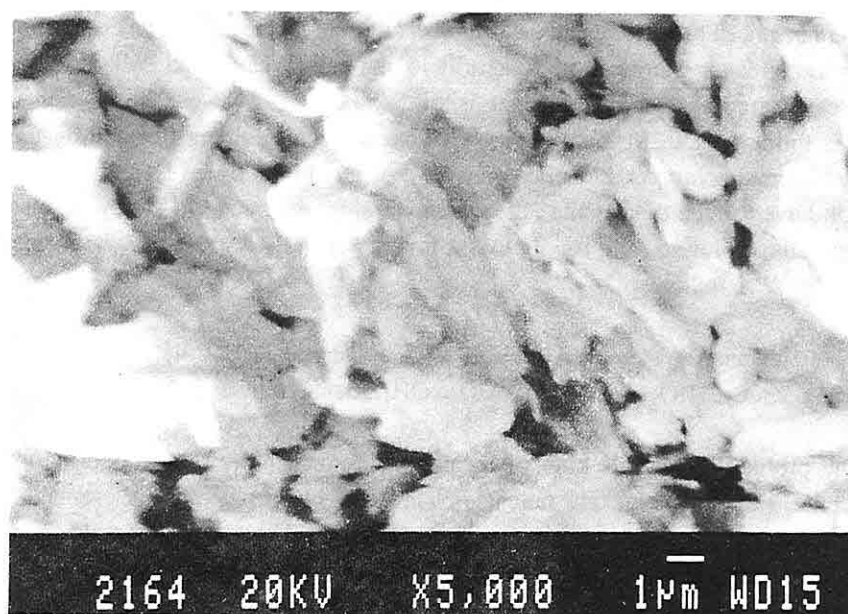
Figure 5. Electron microscope morphology of illites.

126

mica was formed from 1Md illite. In the literature it is pointed that unorganised 1Md illite transforms to 2M mica under condition of presence of sufficient element, heat and pressure (Closs, 1983; Velde, 1985; Larsen and Chilingar, 1983; Weaver, 1984). In these studies, it has been concluded that approximately 1kb pressure and 150-200 °C heat is necessary for this kind of transition. The temperature of hydrothermal solutions caused the formation of mercury deposits in the study area is close to above mentioned temperatures (Inoue and Utada, 1983; Nemecz, 1981).

The appearance and electron diffraction (EDX) analysis of the samples were done by the electron microscope. The appearance of illite under SEM are as elongated crystals, detritic appearance has not been observed (Figure 4,5). The EDX analysis of illite has been done and chemical formulae of analyzed minerals have been established (Figure 6,7 and Table 2). In the arragement of mineral formulae calculations were made eleven oxygen base by finding % oxide.

K are only present between layers of illite, no unbalanced charge has been determined. The structure of illite is quite stable. Illite octahedra in the samples bearing %10 of chlorite in the paragenesis. Contains more Fe but less K relative to the others.

Measured d_{hkl} heights of above mentioned samples are lower than these having high K content. The d_{hkl} heights of these samples which having high K content and high unbalanced charge of octahedra and tetrahedra are much lower (Table 1). After correction relative to the standart patterns,it has been seen that differences between d_{hkl} parameters of samples having high and low K content are about 0.03-0.01 range. Minerals, having high unbalanced tetrahedral and octahedral charge, attract the cation, which equilibrate the unbalanced layer charge, more forcefully to unit cell (Weaver and Pollard, 1973). This causes differences even if d_{hkl} height is low.

It is thought that 2M mica occured as an authigenic mineral formed by means of hydrothermal solutions. 2M mica may have occured in two ways, firstly the solutions might have formed to smectite , then the mineral transformed to 1Md by means of high temperature solutions and finally to 2M mica . Secondly K-mica may be formed from K-feldispar as follow:

$$3K- Feldispar + 2Water ======= K-Mica + 6Quartz + 2K^+ + 2OH^-$$
$$3KALSi_3O_8 + 2H_2O -------- [Si_3AlO_{10}(OH)_2Al_2] K + 6SiO_2 + 2K^+ + 2OH^-$$
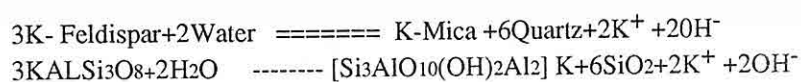
The probability of this kind of formation is much more than trasformation from smectite. The type of smectite may be rich in Al (baydellite) because determined Mg was not found Mg in analysis. This is supported by the observation of no change in peak position of clay size fraction, especially in ethylene glychol and heat threated samples. Microcline found at the whole rock paragenesis show that the solution is rich in K. K took part in the formation of 2M mica by fixation between to smectite layers (Chamley,

125

Table 1. X-ray Diffraction peaks of 2 M Mica.

Low K		High K	
d	rel. I	d	rel. I
		10.0248	100.00
9.8522	100.00	3.3371	94.24
3.3143	75.94	4.9849	25.90
4.9476	33.96	1.9965	24.46
1.9903	25.13	2.5632	19.42
2.5554	17.38	2.9887	16.55
2.9807	16.84	4.2617	14.39
3.1822	16.84	4.4692	14.39
2.8466	13.64	2.3800	13.67
2.7795	13.37	2.7901	13.67
3.4719	13.10	3.2080	13.67
4.4491	12.83	1.5057	13.20
1.3514	9.63	2.1330	12.95
2.4893	8.29	1.6489	12.80
2.1231	8.02	1.3744	11.60
2.4547	7.60	2.8708	11.51
3.7075	7.60	3.4858	11.51
1.3365	7.22	2.4565	10.79
4.2322	7.22	3.7265	10.07
1.4982	7.20	1.3390	10.00
1.6489	7.20	1.3805	9.20
3.8338	7.20	1.5448	8.00
1.9701	6.95	2.2331	8.00
3.8907	6.80	1.4523	7.91
2.3758	6.40	3.8638	7.91
1.5237	6.00	1.3564	6.40
1.7262	5.61		
1.4493	4.81		
1.6872	4.81		
2.2392	4.80		
4.0888	4.55		
2.2751	4.01		
1.8158	4.00		
1.5502	3.60		
2.6890	3.48		

124
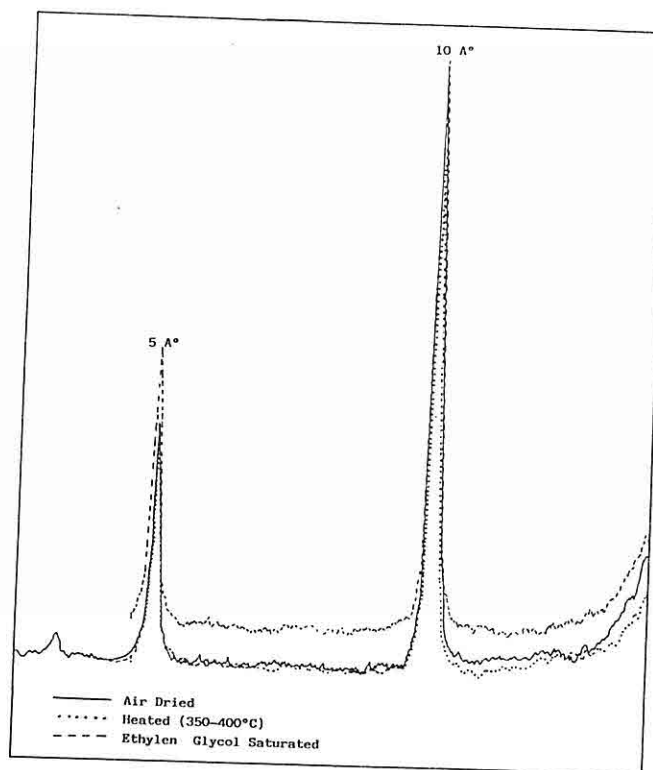
Figure 2. Oriented Clay Size Diffractogram of 2M illite.
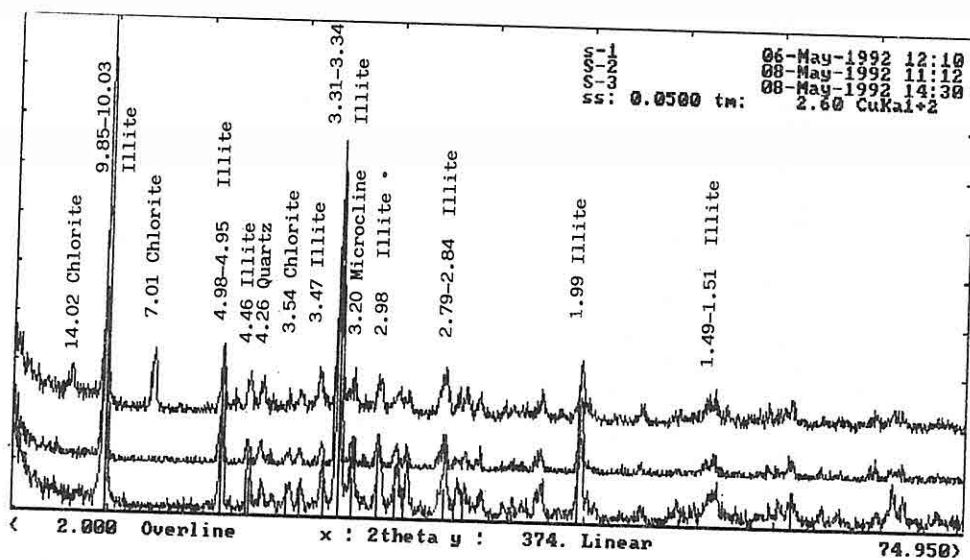
Figure 3. Unoriented Clay Size Diffractogram of Samples (Peak values is in Table 1).

are observed in the study area. Aciddic volcanic rocks widely crop out in the vicinity of Konya (Figure 1). Clay mineral paragenesis of Paleozoic low grade metamorphics rocks consist of illite+chlorite rich in Fe. In addition to main minerals (14C-14V), kaolinite, smectite and(10I-14S) are observed as a degradation product in the investigation area (Çelik et al., 1991).

Neogene aged volcanics are mainly acidic and clay occurrences originated from the volcanics generally are composed of kaolinite , illite, alunite, jarosite, natroalunite and smectite. In addition to clay minerals, polymorphs of SiO_2 such as crysobalite, opal -CT and quartz are found.

Mercury deposits mined in Ladik-Sızma town occurs at the contact of Paleozoic aged schist and limestone and are the most important mercury ore in Turkey. The contact is generally fault controlled (Motorcu, 1987). Low temperature hydrothermal solutions affected the contact and their circulations were retarded by schist.

4. XRD AND SEM ANALYSES

Whole rock and clay mineral analysis of samples taken from mercury deposits were done by X-ray. Collected samples are highly soft, whitish, beige and gray in places and are as few cm wide bands around mercury deposits. The whole rock composition of whitish beige samples is in muscovite+microcline+quartz paragenesis, and of gray samples is in muscovite +microcline+ quartz + chlorite + siderite + calcite paragenesis (Figure 2).

In clay size paragenesis, the whitish ones have only illite, whereas gray ones contain illite+chlorite. But semiquantitavive analysis show that the ratio of chlorite is %10 or less (Figure 2,3). The presence of illite siderite beside chlorite in the above mentioned samples show that there was Fe with solutions. No apparent change in the 10 A° peak of oriented illite have been observed after treating them with ethylen glycol and heat (350-400 °C) (Figure 3). Illite shows good crystallinity. An asymmetry of peaks toward the 11-12 A° has not been observed. This points that the illite+smectite intrerstratification content of illites is very low. The pure illite peaks were measured by analysing unoriented of clay fractions of samples with 0.5°/min accuracy. In the analysis, NaCl standard was used. The illite's peaks were determined by taking diffractions of powder samples of pure illites (Table1). İllite peaks are alike 2M mica peaks given by Thorez (1976). The 2M illite content in the paragenesis is calculated by the following formulae:

%2M=2M/2M+1Md(Maxwell and Hower, 1967) and
%2M=1(025)(2M)*100/[1(112)(1M)] (Caillere et al., 1982).

Peaks of (025) and (112) are calculated from 2.99 and 3.06 A° peaks. 2M mica polymorph conent is determined to be %96. It contains about %4 of 1Md polimorph. 2M

122
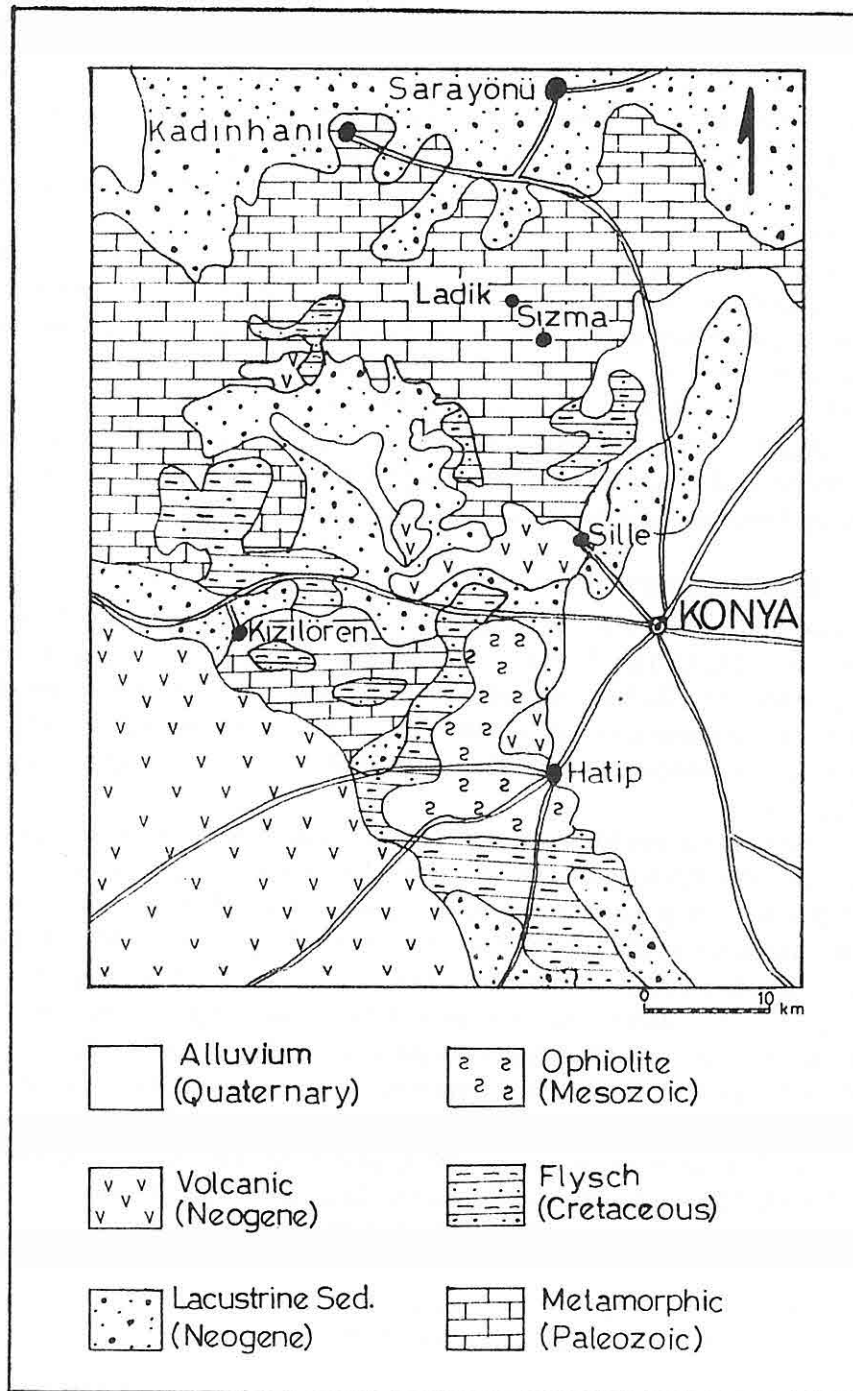
Figure 1. Generalized Geological Map of the Study Area is Simplfield from 1 / 500 000
Scaled Geological Map of Turkey.

1. INTRODUCTION

Investigated clay occurrences are located between Ladik and Sızma towns at the southern part of Sarayönü, Konya (Figure 1). The aim of this investigation is to determine mineralogical and geochemical properties of clay layers formed by hydrothermal solutions around the mercury deposits. Research on secondary hydrothermal alteration in the country rock and its relationship to the ore mineralization is not new. Ore lodes tend to be embedded in highly decomposed country rock, and this has focussed interest on some sort of connection between alteration and mineralization. But there is a few study on this type of clay minerals originated from hydrothermal alteration in Turkey.

Ore minerals, observed at the contact of Paleozoic aged schists and limestones, consist of sulphide minerals such as cinnabar, stibnite, pyrite, tetrahedrite and oxidation minerals(malachite and azurite). Calcite and quartz veins cross the wall rocks and have 20-50 cm thickness. The quartz veins show brecciated structure. Lateral distance of quartz veins is about one to two meters. The clay occurrences at the country rock generally are whitish, and have 2-4cm thickness.

2. ANALYTIC METHODS

Samples were examined by means of optical microscopy, scanning electron microscopy (SEM) and X-ray powder diffractometry (XRD). XRD patterns were obtained using a Philips 1540 and a Siemens D-5000 diffractometer equipped with a generator, Cu radiation, and a graphite monochromator. A scanning rate of 2°/ min was used. The clay samples are 2m fractions separated from samples using by series of centrifugations and sedimentation methods. The type and content of illite polymorphs of war defined by detailed X-ray techniques. Samples of clay were prepared for scanning electron micrography by breaking, them so as to expose fresh surfaces of natural fractures that are characteristic of the minerals . To avoid introducing artifacts, they were not processed further except to sputter them with a thin layer of Au to carry away excess charge from the electron beam . The microscope was equipped with an auxiliary energy-dispersive analytical unit which with element content of illite were estimated. Structural formulae were calculated by normalizing cation analyses to a theoretical structure containing O_{10} $(OH)_2$. All Fe was treated as Fe_2O_3. K was assumed to be nonexchangeable(i.e., fixed in the interlayer of illite layers) cation. X-ray analysis of clay size fraction was done at Hacettepe University while whole rock analysis was made at Laboratories of Etibank Seydişehir Aluminum Institute. Electron microscopy investigation was carried out at TPAO Research Centre laboratory.

3. GEOLOGIC SETTING

Paleozoic aged metasediments and magmatic rocks and Neogene aged acidic volcanics

120

HYDROTHERMAL ILLITE OCCURRENCES AT MERCURY DEPOSITS (SIZMA-KONYA)

Muazzez ÇELİK and Halil BAŞ

Selçuk Univ., Geology Department, Konya / TÜRKİYE

ABSTRACT : *Argillazation was observed at the wall rocks of ore minerallization, as being mainly mercury and low temperature sulphides, formed by means of hydrothermal solutions. Clays are of hydrothermal in origin and generally consist of pure mica and rarely mica+Chlorite paragenesis. The polymorph of mica is 2M and include K in their interlayer. It is determined that micas are rich in K, and K content is equal to charge deficiency of layers. K_2O content of mica varies between 8.70% and 10.80% and they have same the features as potassium mica . The mineral formula of 2M illite is organised as follows;*

$$(Si_{3.81}Al_{0.19}) (Al_{1.61} Fe_{0.101} Ti_{0.066})K_{0.78} O_{10}(OH)_2$$
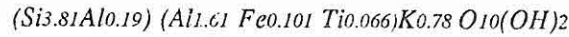
The origin of illite is dependent on two factors. First , Al smectites may be transformed to 1Md illite by fixation of K into present in hydrothermal solutions their interlayer. And then 1Md illite might be aggradated to 2M mica by the effected of temperature. Second factor is alteration of K-feldispar to 2M mica by means of solutions being rich in SiO_2 .

119

of Petroleum Geologists Bulletin, In Press.

Chaimov., T.A., Barazangi, M., Al-Saad, D., Sawaf, T. & Gebran, A., 1990.Crustal Shortening in the Palmyride Fold Belt, Syria, and Implications for Movement Along the Dead Sea Fault System, Tectonics, 9, 1369-1386.

Chaimov., T.A., Barazangi, M., Al-Saad, D., Sawaf, T. & Gebran, A., 1992. Mesozoic and Cenozoic Deformation Inferred from Seismic Stratigraphy in the Southwestern Intracontinental Palmyride Fold-Thrust Belt, Syria, Geological Society of America Bulletin., 104, 704-715.

McBride, J.H., Barazangi, M., Best, J., Al-Saad, D., Sawaf, T., Al-Otri, M. & Gebran, A., 1990. Seismic Reflection Structure of Intracratonic Palmyride Fold-Thrust Belt and Surrounding Arabian Platform, Syria, The American Association of Petroleum Geologists Bulletin, 74, 238-259.

Sawaf, T., Al-Saad, T., Gebran, A., Barazangi, M., Best, J.A. & Chaimov, T.,1993. Structure and Stratigraphy of Eastern Syria Across the Euphrates Depression, Tectonophysics, In Press.

Seber, D., 1993. Barazangi, M., Chaimov, T.A., Al-Saad, D., Sawaf, T. & Khaddour, M., Upper Crustal Velocity Structure and Basement Morphology Beneath the Intracontinental Palmyride Fold-Thrust Belt and North Arabian Platform in Syria, Geophysical Journal International, In Press.

along the southern segment (south of Lebanon) since Miocene time is contrasted with only about 25 km offset along the northern segment in Lebanon and Syria. One reported possible explanation for the difference in the observed offsets in that the Palmyrides absorb this documented difference through shortening. Estimates of crustal shortening along strike of the Palmyrides belt based on balaced cross sections constrained by available seismic reflection profiles, drill holes, and detailed geologic maps give a minimum estimate of about 20 km in the intensely deformed, southwestern segment of the belt (Chaimow et al., 1990). Shortening estimates are much less to the northeast. Clearly this is insufficient to explain the above paradox. Two geologically reasonable alternatives are (1) considerable strike-slip movements exist along the Palmyrides and possibly within the Aleppo region, though displacements can not yet be estimated, or (2) the southern Dead Sea fault segment formerly continued in a NW direction towards the Mediterranean (the Roum fault) and only began to propagate northward in Lebanon and Syria (the Yammuneh and Ghab faults) since about the beginning of Pliocene time. The segment of the fault in Lebanon and Syria is historically a very active seismogenic fault (Ambraseys and Barazangi, 1989).

In conclusion, the evolution of the Palmyrides, an active right-lateral transpressive mountain belt, probably can be traced back as far as the Proterozoic. The present structure of the belt, however, is the results of successive tectonic phases that were dramatically influenced by variations in the sedimentary section and the presence of crustal zones of weakness, and by interactions with nearby plate boundaries.

2. REFERENCES

Al-Saad, D., Sawaf, T., Gebran, A., Barazangi, M., Best, J. & Chaimov, T.,1991. Northern Arabian Platform Transect Across the Palmyride Mountain Belt, Syrian Arab Republic, Global Geoscience Transect 1, Copublished by the Inter-Union Commission on the Lithosphere and American Geophysical Union, Washington, DC, ISBN 0 - 87590 - 778 - 43.

Al-Saad, D., Sawaf, T., Gebran, A., Barazangi, M., Best, J. & Chaimov, T., 1992. Crustal Structure of Central Syria: The Intracontinental Palmyride Mountain Belt, Tectonophysics, In Press

Ambraseys, N.N. and Barazangi, M., 1989.The 1759 Eartquake in the Bekaa Valley: Implications for the Earthquake Hazard Assessment in the Mediterranean Region, Journal Geophysical Research, 94, 4007-4013.

Best, J.A., Barazangi, M., Al-Saad, D., Sawaf, T. & Gebran, A., 1990. Bouguer Gravity Trends and Crustal Structure of the Palmyride Mountain Belt and Surrounding Northern Arabian Platform in Syria, Geology, 18, 1235-1239.

Best, J.A., Barazangi, M., Al-Saad, D., Sawaf, T. & Gebran, A., 1993. Continental Margin Evolution of the Northern Arabian Platform in Syria, The American Association

southwest segment, just east of Lebanon, to 9 km in the northeast segment of the belt (Seber et al., 1993). Neogene and Quaternary basaltic volcanism is widespread in the Rutbah and Aleppo regions but no surface volcanism exists within the Palmyrides.

Bouguer gravity anomalies in central Syria indicate that three is a fundamental difference in the crusts of the Rutbah and the Aleppo regions: the Aleppo crust being denser and/or thinner than the Rutbah crust (Best et al., 1990). This observation could be interpreted, though not uniquely, to suggest that the Palmyrides, which separates these two subprovinces, is the location of a possible Precambrian (Proterozoic?) suture and/or strike-Slip fault zone. This is not a suprising possibility since Proterozoic suture zones are documented in the exposed Arabian shield in western Saudi Arabia. If the above interpretation is valid, then it may explain the subsequent development of the Palmyrides in early Mesozoic time as reactivation of a zone of crustal weakness along the postulated Proterozoic suture zone.

Minor Late Cretaceous uplift marks the first inversion phase of the Palmyride trough. This phase had a direct temporal relationship to the emplacement of ophiolites along the northern and eastern Arabian plate margins. Thus, the inititation of inversion in the Palmyrides, an integral part of the Syrian Arc (which extends from central Syria southward to central Sinai) apparently predates development of the Red Sea/Dead Sea plate boundary and is approximately coeval with the closing of the Neo-Tethys. However, the development of the present-day Palmyrides, mostly in Neogene and Quaternary times, is synchronous with documented intense movements along nearby Arabian plate boundaries, including the development of the Dead Sea transform fault system, the Bitlis suture and the East Anatolian fault, and the Zagros continental collision zone (Chaimov et al., 1992). The northward movement and anticlockwise rotation of the Arabian plate since Miocene time must have played a critical role in the intense inversion of the Palmyrides depression. The above discussion suggests that plate stresses have been transmitted penecontemporaneously for hundreds of kilometers from the surrounding Arabian plate boundaries to the Palmyrides, in the interior of the plate, through the stable northern Arabian platform. Finally, it is tempting to speculate based on limited seismic evidence about the presence of a regional master detachment beneath the Aleppo plateau, either along the basement surface of within the basement, that accommodates some of the convergence along the Bitlis suture in southern Turkey and transmits it farther southwards to the Palmyrides in central Syria. Evidence for this scenario is sparse at the present time.

An important question is the magnitude of shortening along the Palmyra fold and thrust belt, and how this shortening contributes to a better understanding of the kinematics of the nearby plate boundaries. A long-lasting paradox in the literature is the reported major discrepancy in the measured left-lateral offsets along the southern versus the northern segments of the Dead Sea fault system. A well-documented 105 km offset

116
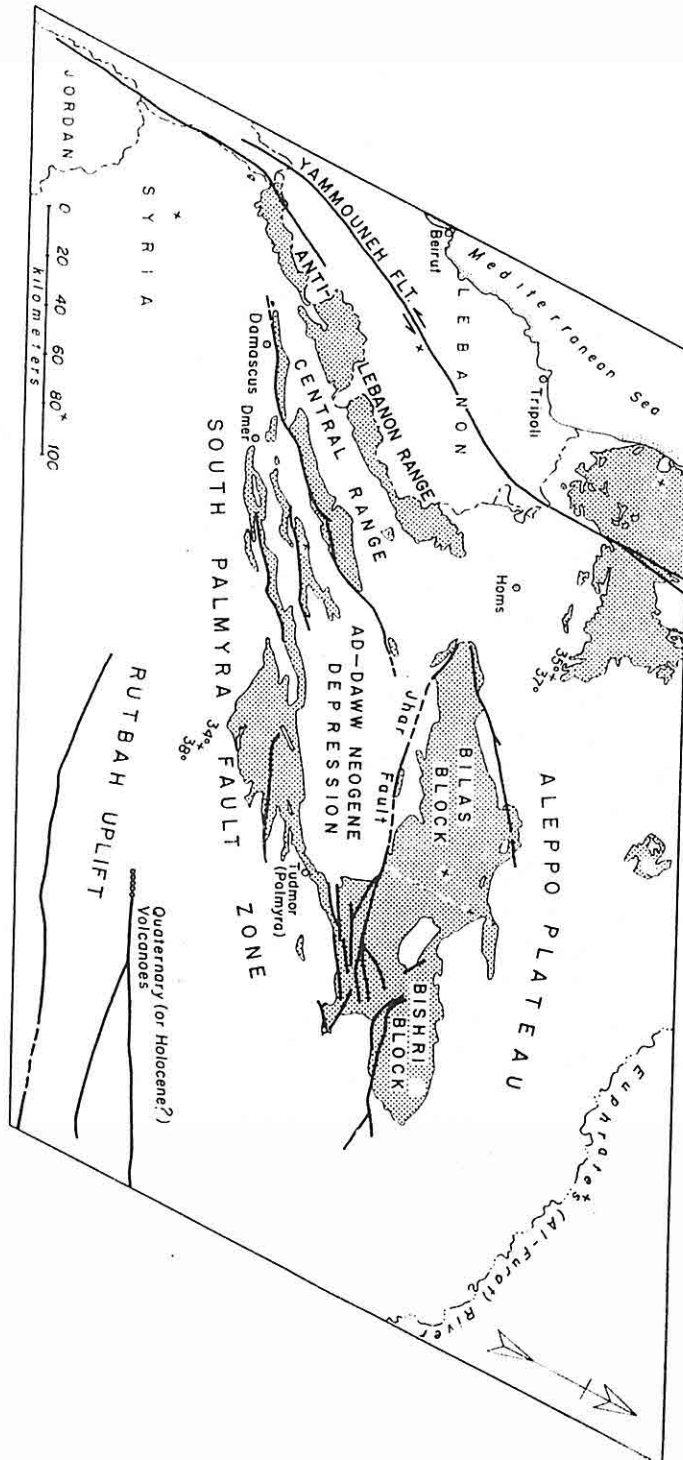
Figure 2-- Simplified geologic map of Palmyrides showing area of Cretaceous outcrop (shaded), major faults, and general tectonic provinces.

115

with the development of Neo-Tethys. The Palmyrides were the site of an aulacogen - type depression in early Mesozoic time that was linked to the Levantine rifted continental margin. Inversion of this depression throughout the Cenozoic, especially in Neogene and Quaternary times, resulted in the present - day Palmyrides. The inversion process involves both shortening by folding and reverse faulting as well as translation and rotation along numerous strike - slip faults. The Palmyrides can be considered as a type example of an intracontinental transpressive mountain belt.

To a first approximation the Palmyrides can be divided into northeast and southwest segments that are separated by the E-W oriented Jhar fault zone. The northeast segment basically consists of broad anticlines, including the Bilas and Bishri blocks, while the southwest segment consists of long linear ridges with a few intervening depressions (McBride et al., 1990; Al-Saad et al., 1991 and 1992). All of these structural elements are bounded by faults of both the reverse and strike-slip types. The most prominent of these faults is the South Palmyra fault zone that approximately defines the southernmost limits of the Palmyrides (Figure 2). Geologic evidence based on morpho-tectonic observations indicate that many of these faults in the Palmyrides have been active during Quaternary time. The occurence of earthquakes along the Palmyrides, though infrequent and relatively small in size, supports the above observation. The focal mechanism of two moderate-sized earthquakes show both reverse and strike-slip components (Chaimov et al., 1990).

Available seismec reflection data indicate that the northeast Palmyrides belt exhibits more symmetrical deformation, with reverse faults along the southern and northern flanks of the belt that dip towards the interior of the belt, whereas the southwest segment exhibits clear asymmetrical deformation with predominantly north dipping reverse faults. Moreover, seismic reflection data suggest that deformation is thick-skinned in the northeast segment in contrast to some locally thin-skinned deformation in the southwest segment, where possible detachment surface(s) exists along the Triassic evaporites. A pervasive regional decollement is not observed, however, in either region. The seismic data also suggest the inversion of some of the Mesozoic rift-bounding normal faults into reverse faults in both segments during Cenozoic time.

The Palmyrides separate the northern Arabian platform into the Rutbah uplift in the south and the Aleppo plateau in the north. The Phanerozoic sedimentary section in these two regions is relatively undeformed; this is in sharp contrast to the intense deformation of the Phanerozoic section, especially the Mesozoic and Cenozoic sections, within the Palmyrides. No foreland basin exists along the margins of the Palmyride belt-the belt is strictly "sandwiched" between the two relatively rigid subprovinces of the Arabian platform. Detailed seismic refraction/wide-angle reflection profiling indicate that depth to Precambrian basement varies from about 5.5 km in the Aleppo region to about 8 km in the Rutbah region. In the Palmyrides, basement depth decreases from 11 km in the

114
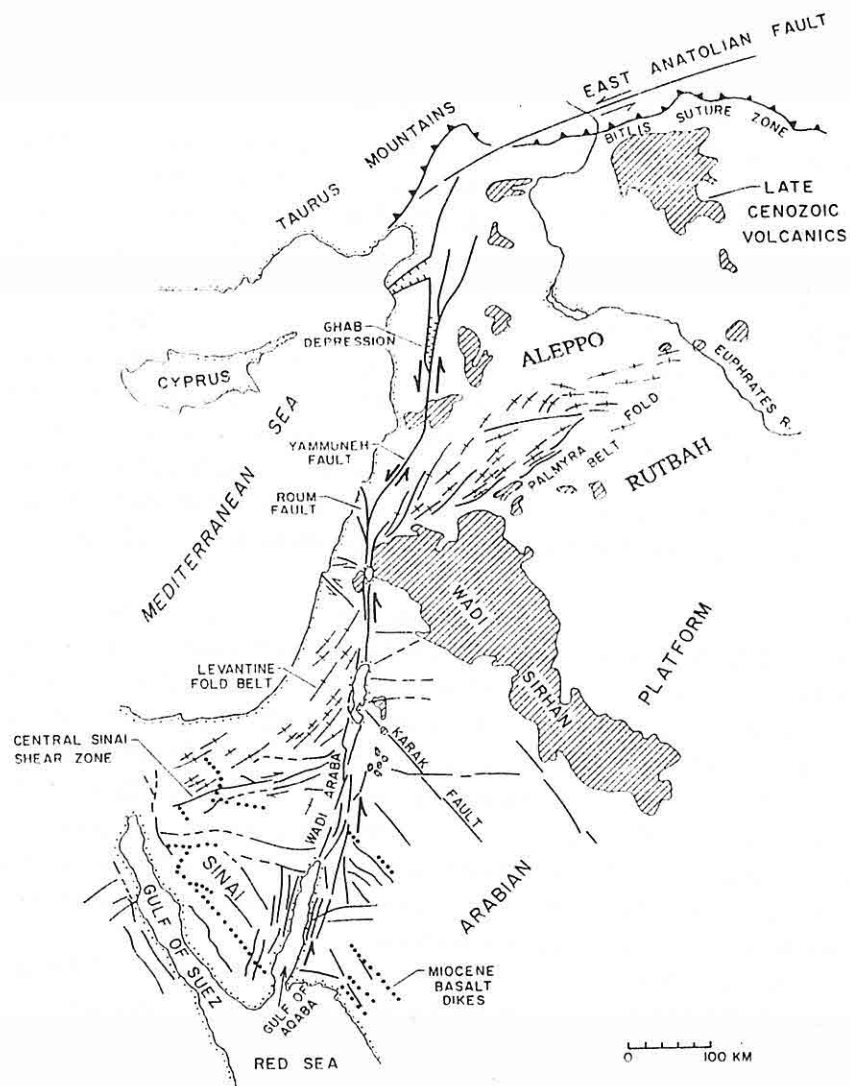
Figure 1--Summary tectonic map of the Dead Sea transform fault system and nearby plate boundaries including the intracontinental Palmyride fold-thrust belt within the north Arabian platform. Shaded areas indicate late Cenozoic volcanic flows.

113

faults. The inversion processes formed at least three structurally distinct crustal blocks within the Palmyrides. The two blocks in the northeast Palmyrides (Bilas and Bishri) consist of broad anticlines that exhibit symmetrical thick-skinned deformation with reverse faults on the southern and northern flanks of the belt, whereas the southwestern Palmyrides consist of long linear ridges with intervening depressions that exhibit clear south vergence and local detachment, probably within Triassic evaporites. Depth to metamorphic basement beneath the Palmyrides increases from 9 km in the northeast to 11 km in the southwest. This is in contrast to a basement depth of about 6-8 km beneath the adjacent stable Arabian platform. A 20-25% estimated shortening across the southwestern Palmyrides has not been sufficient to invert the basement morphology beneath this mountain belt.

Close temporal relations between inversion episodes in the Palmyrides and well-documented episodes of convergence and collision along nearby Arabian plate boundaries suggest that plate boundary stresses are transmitted hundreds of kilometers across the northern Arabian platform to the Palmyrides. Finally, Bouguer gravity observations provide an estimate of crustal thickness of about 38 km beneath the Palmyrides, but also require different crustal properties to the north and south of the Palmyrides. These observations suggest that the Palmyrides occupy the location of a possible Precambrian (Proterozoic?) suture and/or strike-slip fault zone along which the two crustal blocks of northern Arabia were accreted. This possible early history may explain the subsequent development of the Palmyrides in early Mesozoic time as due to a reactivation of a zone of crustal weakness along the postulated Proterozoic suture zone.

1. DISCUSSION

Syria is part of the Arabian plate and surrounded by the Dead Sea leaky transform fault in the west, the Turkish Bitlis suture and the East Anatolian fault in the north, and the foothills of the Zagros folded belt in the northeast (see Figure 1). The Palmyride fold-thrust belt is a relatively modest mountain belt, though it is the most prominent structural feature in central Syria. The Palmyrides is embedded in the northern Arabian platform, is about 400 km in length and about 100 km in width, and strikes in a NE-SW direction. The belt approaches an average elevation of about 1.5 km in the southwest, where it merges with the Dead Sea fault system and associated Lebanon and Anti-Lebanon mountain ranges. Toward the NE the Palmyra belt gradually becomes more subdued with an average elevation that rarely exceeds eight hundred meters, until it intersects with the NW-SE oriented Euphrates graben/fault system (Sawaf et al., 1993).

Geologic and seismic evidence suggests that the northern Arabian platform records the transformation of an east - facing Gondwanaland passive-margin in the early Paleozoic into a west - facing Levantine margin in the Mesozoic. Timing of the margin transformation is inferred to be Triassic in age (Best et al., 1993) and is closely associated

112

STRUCTURE OF THE INTRACONTINENTAL PALMYRIDE MOUNTAIN BELT IN SYRIA AND ITS RELATIONSHIP TO NEARBY ARABIAN PLATE BOUNDARIES

Muawia BARAZANGI[1], Doğan ŞEBER[1],
Damen AL-SAAD[2] and Tarif SAWAF[2]

[1]*Institute for the Study of the Continents and Department of Geological Sciences,
Cornell University, Snee Hall, Ithaca, New York 14853, USA*
[2]*Ministry of Petroleum and Mineral Resources, Syrian Petroleum Company,
Damascus, Syrian Arab Republic*

ABSTRACT : *The intracontinental Palmyride mountain belt strikes NE and is located within the northern Arabian platform. The belt is about 400 km in length and about 100 km in width. Abundant data, including seismic reflection and refraction profiles, drill holes, gravity, magnetics, and geologic maps are used to infer the crustal structure and geologic evolution of this belt.*

The Palmyrides were the site of an early Mesozoic aulacogen-type depression that was linked to the Levantine rifted continental margin in the eastern Mediterranean. Seismic stratigraphic analysis indicates that inversion of the Palmyride depression was initiated in late Cretaceous time, but especially intensified in Neogene and Quaternary times. The inversion process varies considerably along strike and involves both shortening by folding and reverse faulting (including the inversion of some of the Mesozoic rift - bounding normal faults) as well as translation and rotation along numerous strike-slip

111

evolution of the Levantine margin along the eastern Mediterranean. There is at least one exploratory well located on each profile. This gives us a unique opportunity to correlate velocities with geologic formations (Figure 5). Also the velocity models obtained for Profile I and Profile III agree well at the intersection of these two profiles and allow us to correlate each velocity layer from one profile to the other. We have not observed considerable variations in the basement velocities between the Aleppo and Rutbah blocks. Considerable velocity variations, however, are observed in each geologic formation depending on the depth rather than age of the formation.

4. REFERENCES

Abed, A.M., 1985. On the Supposed Precambrian Paleosuture Along the Dead Sea Rift, Jordan, J. Geol. Soc., London, 142, 527-531.

Best, J., Barazangi, M., Al-Saad, D., Sawaf, T. & Gebran, A., 1992. Continental Margin Evolution of the Northern Arabian Platform in Syria, Am.Assoc.Petrol.Geol.Bull., (in press).

Best, J., Barazangi, M., Al-Saad, D., Sawaf, T. & Gebran, A., 1990. Bouguer Gravity Trends and Crustal Structure of the Palmyride Mountain Belt and Surrounding Northern Arabian Platform, Geology, 18, 1235-1239.

Chaimov, T., Barazangi, M., Al-Saad, D., Sawaf, T. & Gebran, A., 1990. Crustal Shortening in the Palmyride Fold Belt, Syria, and Implications for Movement Along the Dead Sea Fault System, Tectonics, 9, 1369-1389.

Husseini, M.I., 1989. Tectonic and Depositional Model of Late Precambrian Arabian and Adjoining Plates, Am.Assoc.Petrol.Geol.Bull., 73, 1117-1131.

Luetgert, J.H., 1988. Interactive Two-Dimensional Ray Tracing/Synthetic Seismogram Package, Unites States Geological Survey, Open-File Report 88-238, Menlo Park, California.

McBride, J.H., Barazangi, M., Best, J., Al-Saad, D., Sawaf, T., Al-Otri, M. & Gebran, A., 1990. Seismic Reflection Structure of Intracratonic Palmyride Fold-Thrust Belt and Surrounding Arabian Platform, Syria, Am.Assoc.Petrol.Geol.Bull., 74, 238-259.

Ouglanov, V. Tatlybayev, M. & Nutrobkin, V., 1974. Report on Seismic Profiling in the Syrian Arab Republic, Unpublished General Petroleum Company Report, pp 73, Aleppo, Syria.
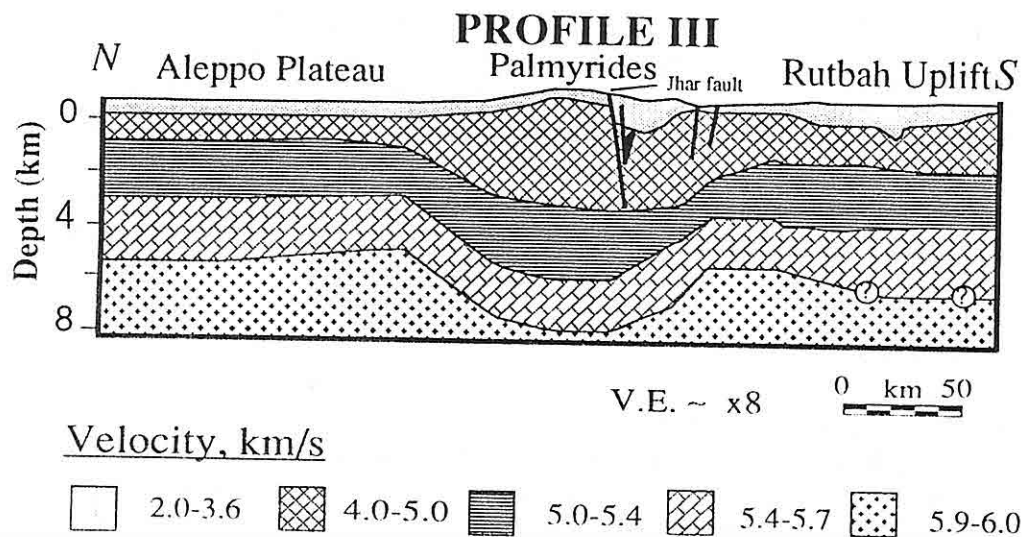
PROFILE III

Figure 4. Interpreted velocity model for Profile I. This profile shows the geometry of the central Palmyrides trough. The major faults are easily identified from the velocity models. In this model each velocity layer does not necessarily correspond to one specific geological formation, since geological formations have different velocities depending on the depth and location, thus they may have different geometries than these velocity layer
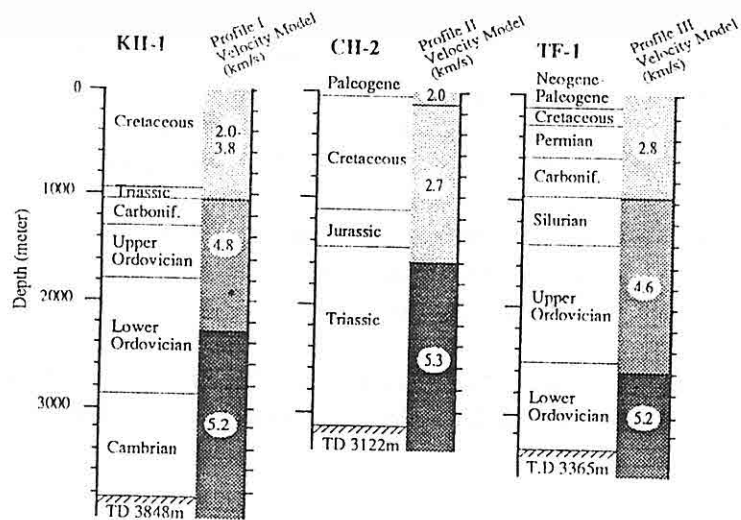
Figure 5. Correlation diagram of velocity models with nearby well information. Locations of the wells are shown in Figure 2. The correlation suggests that, in general, velocities vary with depth and location for the same formations. Same geological formations have different velocities depending on the location.

109
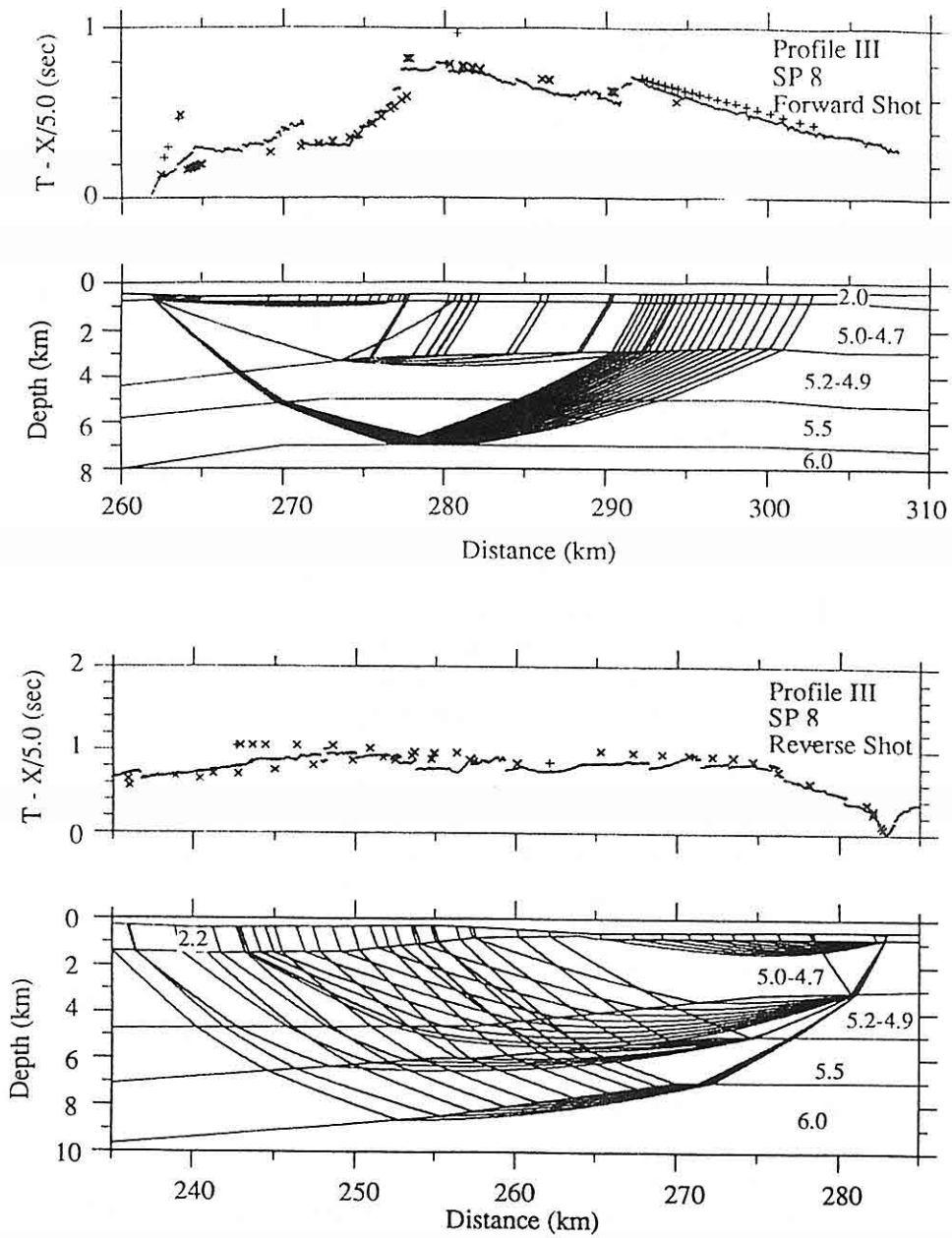
Figure 3. Examples of ray tracings of a reversed refraction line near the Palmyrides-Euphrates transition. The small dots are the actual observations, the crosses are calculated travel times of refracted rays and the pluses are calculated travel times for wide-angle reflections. Velocity values are in km s^{-1}. Only some sample rays from each layer are shown.

108

Profile I. The bottom layer is the basement. Wide-angle reflections become crucial in identifying the basement along this profile, because these reflections, not the refractions, are usually the first arrivals seen on the records at long offsets in this region. The deepest basement is observed beneath this profile. A sedimentary column, totally 11 km in thickness, overlies the basement in the severely deformed southwestern segment of the Palmyrides. This very thick sedimentary column formed mainly in the Mesozoic as a results of the Palmyrides rifting. Approximately the upper 6 km of sediments in this region is composed of Mesozoic sediments (Best et al., 1992). The remaining part is a combination of Paleozoic and Precambrian sediments. The minimum Bouguer gravity values, with-70 mgal, in the region are also observed in the vicinity of the profile. Modeling of Bouguer gravity anomalies in the Palmyrides also confirm the existence of a very thick sedimentary cover beneath the Palmyrides (Best et al., 1990).

Profile III

Profile III is 380 km long, N-S trending regional profile traversing Syria from Turkey in the north to Jordan in the south. It crosses three major structural units: The Aleppo plateau, Palmyride belt, and Rutbah uplift. Data from 62 different shots, 33 forward and 29 reverse, were analyzed. The final model consists of the five characteristic layers that are also identified in Profiles I and II (Figure 4). A low 2.0-2.8 km s^{-1} velocity layer near the surface is followed by sedimentary layers having velocities of about 4.4-4.5 km s^{-1}; 5.2-5.3 km s^{-1}; 5.4-5.7 km s^{-1} and basement with a velocity of about 6.0 km s^{-1}. Lateral velocity variations are obvious in the model, especially at locations where major faults of the region are crossed. Considerable variations in basement morphology is observed along the profile. The Rutbah uplift also shows considerable variations in basement structure. In the northern portion of the Rutbah uplift, adjacent to the Palmyrides, a basement depth of about 6.5 km is obtained. Ray tracing results from two shot points are shown in Figure 3. Farther south the basement deepens steeply and becomes undetectable because of the absence of the 6 km s^{-1} basement identifying branch in the travel-time observations. This may be due either to decreasing basement velocities towards the south nearing that of the overlying layer, or, more probably, to steep increase in basement depth towards the south.

3. CONCLUSIONS

Interpretation of the seismic refraction profiles indicates that sedimentary rock thickness in the northern Arabian platform in Syria varies from 5.5 km in the Aleppo plateau to 11 km in the Palmyride belt. Despite the crustal shortening since the late Mesozoic a basement trough, filled with 9-11 km thick Phanerozoic sediments, still remains beneath the intracontinental Palmyride fold belt. The obtained geometry of the Palmyride trough supports the idea that rifting in the Palmyrides developed as an aulacogen during the

Profile I

This profile is located in the relatively stable Aleppo plateau. The final model for this profile has a three-layered sequence in the upper 1 km, with increasing velocities from 2.0 to 3.8 km s⁻¹, corresponding to Cenozoic and Mesozoic sedimentary rocks. This sequence was also constrained by the sonic log of the Khanaser-1 well. Even though different geological units are traversed, no lateral velocity variation is observed. The boundary between this three-layered sequence and the underlying layer with a velocity of about 4.8 km s⁻¹ corresponds to the Mesozoic-Paleozoic boundary as inferred from the Khanaser-1 well. Beneath this layer lies another sedimentary layer with a velocity of about 5.2 km s⁻¹, which corresponds to the lower section of the Paleozoic. The Khanaser-1 well bottoms at about 3800 m in the lower Cambrian. The refraction model gives a velocity boundary at about 4000 m, possible marking the base of the lower Cambrian in this region. According to the refraction interpretation, approximately 1.5 km lies between this interface and the top of basement, amounting to a total sedimentary thickness of 5.5 km. The lowest sedimentary layer on top of the metamorphic basement has a velocity of 5.5 km s⁻¹, and is interpreted as early Paleozoic and late Precambrian sediments equivalent or similar to those documented to the south in Jordan (e.g., Abed 1985; Husseini 1989). The deepest boundary on the refraction model represents the sedimentary-metamorphic basement boundary. The basement velocity is 5.9-6.0 km s⁻¹, and the basement depth is about 5.5-6.0 km in this region. An offset in the velocity-depth model beneath the southeastern end of Profile I was interpreted as a fault. Relatively deeper southeastern segment in the section is a clear indication of either a normal and/or a strike-slip fault. Observations based on nearby seismic reflection profiles (Figure 1) and the Bouguer gravity map confirm this interpretation.

Profile II

Profile II is 83 km long, NW-SE trending profile located in the southwestern segment of the Palmyrides. This is the most deformed region in the Palmyrides and shows 20-25% crustal shortening (Chaimov et al., 1990). The upper crustal model includes the same five distinct velocity layers observed in Profile I with some lateral velocity variations. The major mapped faults of the region are also observed in the model. The Cheriffe-2 well located on this profile provides information on near surface rocks. It bottoms at about 3100 m in Triassic rocks. The first layer, with a velocity of about 2.0 km s⁻¹, represents young (Quaternary) and/or surface exposed sedimentary rocks. The second layer, with a velocity of about 2.6 to 3.6 km s⁻¹, corresponds to upper Triassic dolomitic rocks. A much thicker underlying layer with a velocity of about 5.0-5.4 km s⁻¹, corresponds to lower Triassic and late Paleozoic sedimentary rocks as indicated by the Cheriffe-2 well. The fourth layer with a velocity of about 5.4-5.7, km s⁻¹ is probably composed of the early Paleozoic and late Precambrian sedimentary rocks also identified in

106
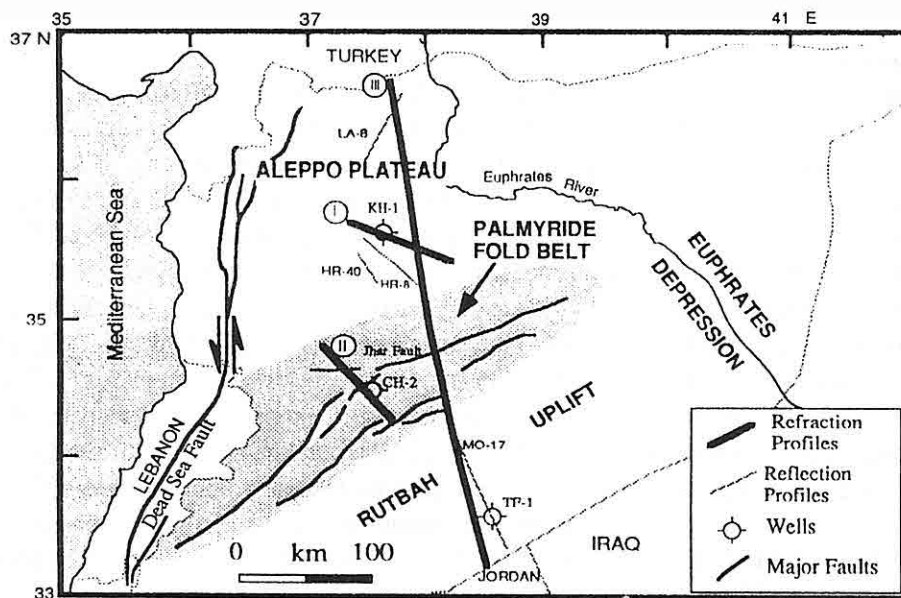
Figure 1. Locations of the seismic refraction and reflection profiles and well information relative to the major tectonic units of the western and central Syria.
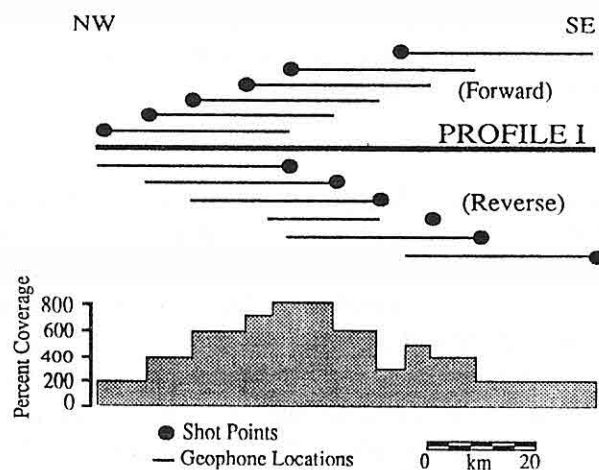
Figure 2. Example of configuration of data acquisition technique. Overlapping forward and reverse shots enable detailed velocity-depth estimation.

1. INTRODUCTION

Geological and structural units of Syria are under an extensive study to understand the evolution of the northern Arabian platform. All existing knowledge about this region has been primarily from surface mapping, exploratory wells, and seismic reflection lines. However, no wells penetrate into the Precambrian basement. The deepest seismic reflector that can provide structural constraints on the older sedimentary rocks in the so-called "D" reflector (McBride et al, 1990), which is most probably the mid-Cambrian Burj limestone. In this study we attempt to explore the nature of the basement and to determine the upper crustal velocities, thicknesses of sedimentary layers, especially those of early Paleozoic and late Precambrian in age, and basement morphology throughout the region. Obtaining the depth to the basement beneath an intracontinental mountain belt is a challenging task. To constrain our results, seismic reflection and well data acquired for hydrocarbon exploration in the region along with Bouguer gravity and surface geology information will be integrated with the refraction data.

The first interpretation of the refraction data was made by the Soviet scientists in 1974 using classical interpretation techniques of refraction data (Ouglanov et al., 1974). However, this interpretation is questionable because of lack of geological information and also lack of computerized techniques at the time of interpretation. There are considerable differences between our interpretation and that of the Soviet scientists. Our results differ substantially especially in thicknesses of sedimentary layers and basement velocity throughout the region, such as the thickness of sedimentary cover in the Rutbah uplift and basement velocities.

2. DATA AND RESULTS

The locations of the three available seismic refraction profiles in the region are shown in Figure 1. The lengths of Profiles I, II and III are 92 km, 83 km, 380 km, respectively. Data from 90 forward and reverse shot points in these three profiles are analyzed. The distance between any given shot point and the last geophone averages about 40 km, ranging from 25 km to 55 km. Geophone spacing for Profiles I and III is 100 m and for Profile II is 150 m. An example of data collection geometry is shown in Figure 2. Overlapping forward and reverse shot points provide up to 8-fold data coverage in some regions, which helps in obtaining reliable and unique velocity-depth models. Average charge size varied from 200 kg to 1000 kg in the Aleppo and Rutbah regions and it was usually twice as large in the Palmyride region, mainly because of a thicker and more deformed sedimentary section.

Interpretation was carried out using a 2-D ray tracing software developed by Luetgert (1988). Approximately 25,000 first arrivals of original, analog, photographic paper records were digizited and interpreted.

GEOMETRY AND VELOCITY STRUCTURE OF THE PALMYRIDE FOLD-THRUST BELT AND SURROUNDING ARABIAN PLATFORM IN SYRIA

Doğan ŞEBER[1], Muawia BARAZANGI[1], Thomas CHAIMOV[1]
Damen AL-SAAD[2], Tarif SAWAF[2] and Mohammed KHADDOUR[2]

[1]Institute for the Study of the Contitents and Department of Geological Sciences,
Cornell University, Snee Hall, Ithaca, New York 14853, USA
[2]Syrian Petroleum Company, Ministry of Petroleum and Mineral Resources, Damascus,
Syrian Arab Republic

ABSTRACT : *A seismic refraction survey was conducted in the northern Arabian platform in Syria in 1972-73 by Syrian and Soviet scientists for the upper part of the crust (<15 km). Seismic refraction data were collected over 9 transects. Data from three transects, i.e., one in the Aleppo plateau, one in the southwestern Palmyrides, and a regional profile traversing Syria from Jordan to Turkey, have been made available and form the refraction database for this study. The data were analyzed using 2-D ray tracing to obtain an upper crustal velocity-depth model in the region. Our results show that high velocity (4-5 km s⁻¹) Phanerozoic sedimentary rocks overlying the metamorphic basement vary in thickness from 5.5 km in the Aleppo plateau to 11 km in the Palmyrides trough. The depth to the basement beneath the Palmyride belt decreases from the southwest (11 km) to the norheast (9 km), suggesting that development of the Palmyrides trough is related to the Levantine margin to the farther west.*

103

Şengör, A.M.C. and Kidd, W.S.F., Post - Collisional Tectonics of the Turkish - Iranian Plateau and A Comparison with Tibet. Tectonophysics 55, 361-376, 1979.

Şengör, A.M.C., Türkiye'nin Neotektoniğinin Esasları. Türkiye Jeol. Kur. Yayını pp.40, 1980.

Şengör, A.M.C. and Yılmaz,Y., Tethyan Evolution of Turkey: A Plate Tectonic Approach. Tectonophysics 75, 181-241, 1981.

Şengör,A.M.C., The Tethyside Orogenic System: An Introduction. In "Şengör, A.M.C.(ed),Tectonic Evolution of the Tethyan Region". NATO, ASI, Series C, 1-22, 1989.

Tatar, Y., Tectonic Structures Along the North Anatolian Fault Zone, Northeast of Refahiye, Erzincan. Tectonophysics 29, 401-409, 1975.

Tatar, Y., Fotojeoloji K.T.Ü. Yayını No 289, 230s., Trabzon, 1978 a.

Tatar, Y., Kuzey Anadolu Fay Zonunun Erzincan - Refahiye Arasındaki Bölümü Üzerinde Tektonik İncelemeler. Hacettepe Üniv. Yerbilimleri Derg., 4, 1/2, 201-236, 1978b.

Tatar,Y., Yıldızeli (Sivas) Kuzeyinde Çamlıbel Dağlarının Tektonik Yapısı. K.T.Ü. Yerbil. Derg., Jeoloji 2/1-2, 1-20, Trabzon, 1982.

Tatar, Y., Yıldızeli Subaşı Köyü Yöresinde Tektonik İncelemeler. Türkiye Jeol. Kurultayı, Bildiriler, 3-15, 1983.

Tatar,Y., Elazığ Bölgesinin Genel Tektonik Yapısı ve LANDSAT Fotoğrafları Üzerinde Yapılan Bazı Gözlemler. Hacettepe Üniv. Yerbilimleri Derg., 14, 295-308, 1987.

Tatar, Y. ve İnceöz, M., Ergani-Çermik-Çüngüş Bölgesinde Kırık Analizi. A.Acar Simpoz.,Ç.Üniv., Adana, 183-190, 1991.

Tokel, S., Doğu Anadolu'da Kabuk Deformasyonu Mekanizması ve Genç Volkanitlerin Petrojenezi. Türkiye Jeol. Kur., Ketin Simpoz., 121-130, 1984.

Turan, M. and Bingöl, A.F., Kovancılar - Baskil (Elazığ) Arası Bölgenin Tectono - Stratigrafik Özellikleri. A.Acar Sempz., Ç.Üniv., Adana, Bildiriler, 213-227, 1991.

Turan, M., Elazığ Civarındaki Bazı Önemli Tetktonik Yapılar ve Bunların Bölgenin Jeolojik Evrimindeki Yeri. S.Erk Semp., Ankara Üniv. 1991 (in press).

Türkmen, İ., Elazığ Doğusunda Çaybağı Formasyonu (Üst Miyosen-Pliyosen?) Stratigrafisi ve Sedimantolojisi. Türkiye Jeol. Bült. 34/1, 45-52, 1991.

Yalçın, N., Doğu Anadolu Yarılımının Türkoğlu-Karaağaç (K.Maraş) Arasındaki Kesiminin Özellikleri ve Bölgedeki Yerleşme Alanları. Türkiye Jeol. Kur., Altınlı Simpoz., 49-56, 6-7 Mart 1979.

Yazgan, E., 1984. Geodynamic Evolution of the Eastern Taurus Region, in "Geology of the Taurus Belt". Ankara, 199-208.

Yılmaz, A., ve Özer, S., 1984. Kuzey Anadolu Bindirme Kuşağının Akdağmadeni (Yozgat) ile Karaçayır (Sivas) Arasındaki Bölümünün Temel Jeoloji İncelemesi ve Tersiyer Havzasının Yapısal Evrimi. Türkiye Jeol. Kur., Ketin Simpoz., 163-174.

Gülen, L., Barka, A. and Toksöz, N., 1987. Kıtaların Çarpışması ve İlgili Komplex Deformasyon: Maraş Üçlü Eklemi ve Çevre Yapıları. Hacettepe Üniv. Yerbilimleri Derg., 14, 319-336.

Hempton, M.R., 1987. Constrains on Arabian Plate Motion and Extensional History of the Red Sea. Tectonics 6, 687-705.

Illies, J.H., 1975. Recent and Paleo-Intraplate Tectonics in Stable Europe and the Rhinegraben Rift System. Tectonophysics 29, 251-264.

Innocenti, F.,Mazuoli, R., Pasquare, G., Serri, G. and Villari, L., 1980. Geology of the Volcanic Area North of Lake Van (Turkey). Geol. Rndsch. 69, 292-323.

İnceöz, M., 1989. Çermik-Çüngüş (Diyarbakır) Arasındaki Bölgenin Tektonik Özellikleri. Y.Lisans Tezi,F.Ü.Fen Bil.Enst., Elazığ, 78 s., (yayımlanmamış).

Jackson, J. and McKenzie, D., 1984. Active Tectonics of the Alpine-Himalayan Belt Between Western Turkey and Pakistan. Geophys.J.R.astr.Soc. 77, 185-264.

Ketin, İ., 1955. Diyarbakır Kuzeybatısında Çermik Bölgesinin Jeolojisi Hakkında. İ.Ü.Fen Fak.Mecm., 3, 155-164.

Ketin, İ., 1983. Türkiye Jeolojisine Genel Bir Bakış. İ.T.Ü.Matbaası, 583s., İstanbul.

Koçyiğit, A., 1983. Doğu Anadolu Bölgesinin Depremselliği ve Gerekli Çalışmalar. Yeryuvarı ve İnsan 8/3, 25-29.

Koçyiğit, A., 1989. Suşehri Basin; An Active Fault-Wedge Basin on the North Anatolian Fault Zone, Turkey. Tectonophysics 167, 13-29.

Kürsten, M., 1980. Zur Geodynamischen Entwicklung des Iran, ein Beispiel Intrakratonischer Struktureller Vorgaence. Geol. Rndsch. 69, 22-40.

Mattauer. M., 1980. Les Deformations des Materioux de l'ecorce Terrestre. Hermann, Paris, pp.492.

Michard, A., Whitechurch, H., Ricou, L.E., Montigny, R.and Yazgan, E., 1984. Tauric Subduction (Malatya-Elazığ Provinces) and its Bearing on Tectonics of the Tethyan Realm in Türkiye. In "The Geol. Evol. of the Eastern Mediterranean, Geol. Soc. Spec. Publ.17, London", 361-375.

Perinçek, D., 1979. The Geology of Hazro - Korudağ - Çüngüş - Maden - Ergani - Hazar - Elazığ - Malatya Area. Guidebook, Türkiye Jeol. Kur. Yayını, 33 s.

Perinçek, D. ve Özkaya, İ., 1981. Arabistan Levhası Kuzey Kenarı Tektonik Evrimi. Hacettepe Üniv.Yerbilimleri Dergisi, 8, 91-101.

Perinçek, D., Günay, Y. ve Kozlu, H., 1987. Doğu ve Güneydoğu Anadolu Bölgesindeki Yanal Atımlı Faylar ile İlgili Yeni Gözlemler. Türkiye 7. Petrol Kongresi.

Sungurlu, O., Perinçek, D., Kurt, G., Tuna, E., Dülger, S., Çelikdemir, E., ve Naz, H., 1985. Elazığ - Hazar - Palu Alanının Jeolojisi. Petrol işl. Gn.Mdl. Derg., 29, 83-191.

Şaroğlu, F.ve Yılmaz, Y., Doğu Anadolunun Neotektoniği ve İlgili Magmatizması. Türkiye Jeol. Kur., Ketin Simpoz., 149-163, 1984.

Şaroğlu, F.and Yılmaz, Y., Doğu Anadolu'da Neotektonik Dönemdeki Jeolojik Evrim ve Havza Modelleri. Maden Tetkik ve Arama Derg.,107, 73-94, 1987.

7. REFERENCES

Aksoy, E., 1988. Van İli Doğu-Kuzeydoğu Yöresinin Stratigrafisi ve Tektoniği. F.Ü. Fen Bil. Enst., Doktora Tezi, 171s., Elazığ(yayımlanmamış).

Aksoy, E., ve Tatar, Y., 1990. Van İli Doğu-Kuzeydoğu Yöresinin Stratigrafisi ve Tektoniği. Doğa. Tr .J. of Engin. and Environmental Sciences 14, 628-644.

Aktaş, G. and Robertson, A.H.V., 1984. The Maden Complex, SE Türkiye: Evolution of a Neotethyan Active Margin, in "The Geol. Evol. of the Eastern Mediterranean, Geol. Soc. Spec. Publ.17, London", 375-403.

Aktürk, A., 1985. Çatak - Narlı (Van) Yöresinin Stratigrafisi ve Tektoniği. F.Ü. Fen Bil. Enst., Doktora Tezi, 187s., Elazığ, (yayımlanmamış).

Altıner, D., 1989. Arabian Platform Margin, SE Anatolia, In "A.M.C.Şengör (ed), Tectonic Evolution of the Tethyan Region. Nato ASI, Series, Series C, vol.259, 117-129.

Arpat, E., ve Şaroğlu, F., 1975. Türkiye'de Bazı Önemli Genç Tektonik Olaylar. Türkiye Jeol. Kur. Bült. 18, 91-101.

Barka, A.and Gülen, L., 1987. Age and Total Displacement of the North Anatolian Fault Zone and Its Significance for the Better Understanding of Tectonic History and Present Day Dynamics of the Eastern Mediterranean Region. M.Tokay Geology Sympoz., Middle East Tech.Univ., Abstracts, p. 57, 11-13 Nov.

Barka, A.A., Toksöz, M.N., Gülen, L. ve Kadinsky-Cade, K., 1987. Kuzey Anadolu Fayının Doğu Kesiminin Segmentasyonu, Sismisitesi ve Deprem Potansiyeli. Hacettepe Üniv. Yerbil.Derg.14, 337-352.

Baştuğ, C., 1980. Sedimentation, Deformation and Melange Emplacement in the Lice Basin, Dicle-Karabegan Area, SE Turkey. Dissert., METÜ, Ankara, pp.282, (unpublished).

Bektaş, O., 1981. Kuzey Anadolu Fay Zonunun Erzincan Tanyeri Bucağı Yöresindeki Jeolojik Özellikleri ve Ofiyolit Sorunları. K.T.Ü. Yerbil. Fak. Yayını No 32, 196s.,

Bingöl, F., 1984. Geology of the Elazığ Area in the Eastern Taurus Region. In "Geology of the Taurus Belt", MTA, Ankara, 209-217.

Brinkmann, R., 1976. Geology of Türkiye. Elsevier, 158pp.

Dercourt, J., Zonenshain, P.L., Ricou, L.E., Kazmin, V.G., LePichon, X., Knipper, A., Grandjacquet, C., Shortshikov, I.M., Geyssant, J., Lepvrier, C., Perchersky, D.H., Boulin,J. Sibuet, J.-C., Savostin, L.A., Sorockhtin, O., Westphal, W., Bazhenov, M.L., Lauer, J.P., and Biju-Duval, B., 1986. Geological Evolution of the Tethys Belt from the Atlantic to the Pamirs Since the Lias. Tectonophysics 123. 241-315.

Dewey, J.F., Hempton, M.R., Kidd, W.S.F. Şaroğlu, F., and Şengör, A.M.C., 1986. Shortening of Eastern Anatolia, A Young Collision Lithosphere, in "The Neotectonics of Eastern Anatolia, A Young Collision Zone, Collision Tectonic", Geol. Soc. Publ., 19, 3-36.

Ercan, A., D. 1979. Anadolu Fayı Üzerinde Küçük Deprem Çalışmaları. Yeryuvarı ve İnsan. 4/1, 21-30, Ank.

regime in these times. E-W trending and N dipping thrusting affected also Lower Pliocene beds. Fold axes in this area trend also E-W (Tatar, 1982; Tatar, 1983; Yılmaz and Özer, 1984).

6. DISCUSSION AND CONCLUSION

According to the plate tectonics, mountain building results from the convergence and collision between any two plates. The direction of the plate movements is of prime importance for the trends of the resulting orogenic lines. The expected horizontal direction of the plate movement must normally be perpendicular to the trends of the main orogenic lines. In some orogenies of the World, e.g. in the Andes, this geometric relation seems not to be complicated, and rather simple to explain. But in the Alpine-Himalayan belt with many mega curvatures it is rather complicated and uneasy to understand.

The difficulty mentioned above is also valid for the region around the northern and northeastern border of the Arabian plate. If we consider the orogenic trends in E and SE-Türkiye, we come to the conclusion that the direction of the movement of Arabian plate must have been due nearly N;but the consideration of the trends in Zagros region suggests approximately a NE direction for the same movement during the Alpine mountain building.

To overcome this difficulty, some authors tried rotational stress field models. Illies (1975) suggests such a model for the Middle East region. According to this model, the direction of the movement of the Arabian plate has episodically rotated from NNW (40 ma ago) to NE (20 ma ago) and its recent position is towards NW. Illies also emphasizes the role of microplate rotations during the evolution of the Alpine mountain system in the Mediterranean region. Bektaş (1987) assumes a NNE direction in Upper Cretaceous-Eocene period, and a change to NNW after Eocene, relying rather on very local structural data. In another model published by Roy. Soc. London (Mattauer, 1980), a continious sinistral rotation of the Arabian plate from NNE to NNW by the angle of about 6 was proposed, and held responsible for the opening of the Red Sea. These proposals howewer seem not sufficiently supported by field evidence.

The very briefly discussed data in the present paper indicate approximately a N direction for the movement of the Arabian plate during the shrinkage and closure of Neotethys in E and SE Türkiye within the time interval between Upper Cretaceous and Upper Miocene to Early Pliocene. In this region, no convincing field data was found supporting any notable change in the direction of the movement of the Arabian plate within this geological time span. This conclusion however is also subject to further discussion. The on-going northward movement of the Arabian plate seems evident in the seismo-tectonic activities along the North Anatolian and East Anatolian fault zones, and even along the Bitlis suture zone (Dewey et al., 1986; Barka and Gülen, 1987; Koçyiğit, 1983-1989; Brinkmann, 1976).

5. DATA FROM SİVAS-YILDIZELİ AREA

The Central Anatolian ophiolite thrust, an ophiolite obduction, extends from Erzincan westwards through Sivas area and can be traced as far as Yozgat, a city nearly 150 km east of Ankara. The thrust faults in this thrust belt strike E-W and dip due N. Field mapping on this important tectonic zone revealed interesting data about the Late
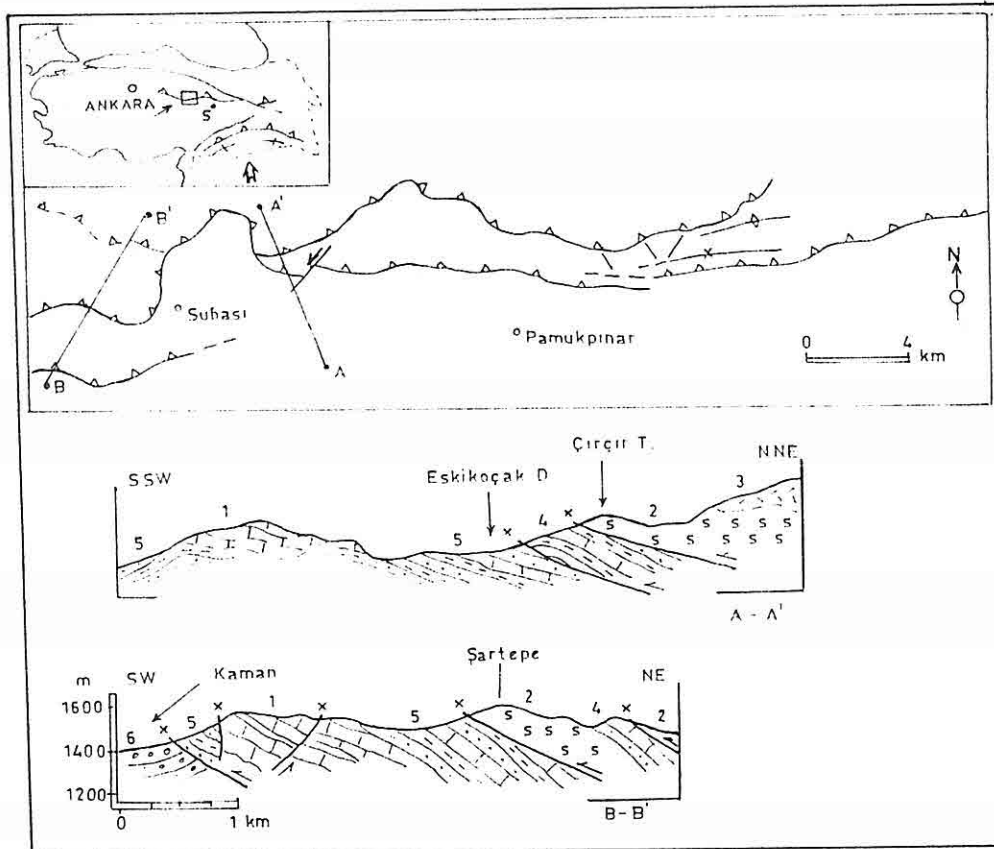
Figure 7. The Yıldızeli segment of the Central Anatolian ophiolite thrust zone (Tatar, 1982; Tatar, 1983; Yılmaz and Özer, 1984). The traces of the geological cross sections A-A' and B-B' are shown on the map. 1: Akdağ metamorphics (Paleozoic), 2: Serpentinite and 3: Diabase(Pre-Upper Cretaceous), 4: Flysch (Upper Cretaceous), 5: Flysch (Paleocene-Eocene), 6: Conglomerate (Pliocene).

Alpine tectonic movements in Anatolia. Olistoliths of ophiolitic composition are found in Upper Cretaceous and in Eocene sediments, indicating a N-S compressional

98
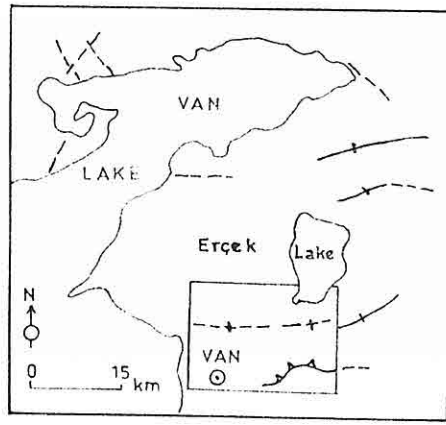
Figure 5.   Location of the study area in Van region (Aksoy and Tatar, 1990), and the trends of the folds and thrust faults in this area.
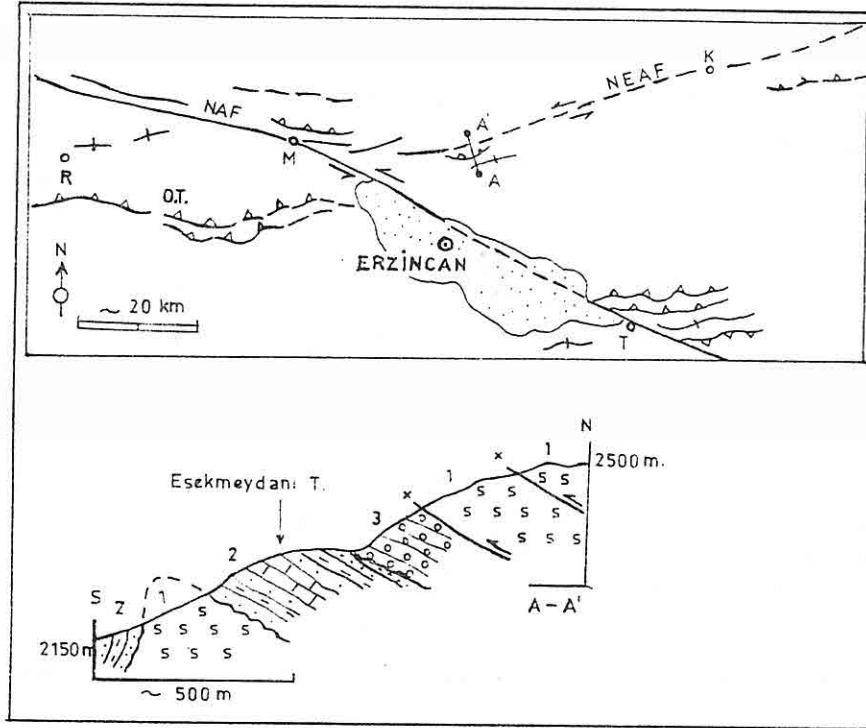
Figure 6. The main neotectonic structures in the vicinity of the city of Erzincan (simplified from Tatar, 1978b).NAF: North Anatolian fault, NEAF: Northeast Anatolian fault, OT: Central Anatolian ophiolite thrust. K: Karakulak, M:Mihar, R: Refahiye, T: Tanyeri. The trace on the cross section A-A' is shown on the map. 1:Serpentinite (?Paleozoic) 2: Limestones and clastics (marine Miocene), 3: Conglomerates (Pliocene).Late Miocene-Pliocene times (Tatar, 1978; Bektaş, 1981; Tatar, 1975; Barka et al., 1987; Tatar, 1982; Tatar, 1983;,Yılmaz and Özer, 1984 and Fig.6).

97
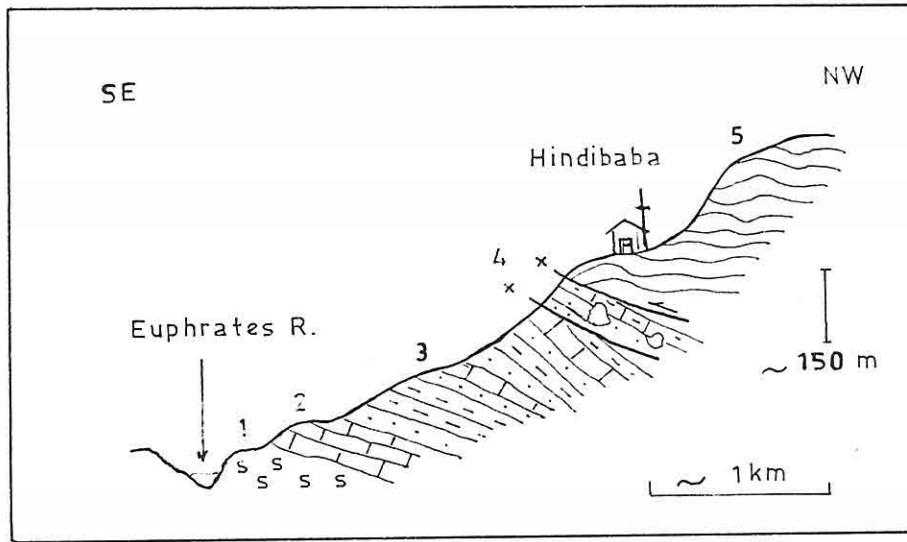
Figure 4. Geological cross section 6 km east of Karakaya dam site, via Hindibaba village (schematically drawn in the field). 1- Koçali complex;(ophiolitic melange emplaced in Upp. Cretaceous), 2- Fırat Formation of Midyad Group (Eocene-Miocene limestone) 3-Lice Formation (Lower Miocene flysch-like facies), 4- Çüngüş Formation (Lower Miocene, wild flsch),5-Pütürge metamorphics (Paleozoic-Mesozoic). Arrows indicate the thrust direction (Tatar, 1991; and see Photo 12 in İnceöz, 1989).

3. DATA FROM VAN AREA

The dissertation work we have carried out in Van district (Aksoy,1988) has revealed that the upper limit of the age of Kırkgeçit Formation is not Oligocene, but it extends to the Lower Miocene. This formation contains olistolithic blokcs of Seske limestone, the age of which is Late Paleocene-Early Eocene. The existence of these blocks indicate a compressional regime during Oligocene and Early Miocene times. Fold axes and thrust faults of post-Early Miocene age in this area also strike nearly E-W and the thrust faults dip due N (Aktürk,1985; Aksoy,1988, Aksoy and Tatar,1990; and Fig.5).

4. DATA FROM ERZİNCAN AREA

The Erzincan area has an interesting, 110^0-striking segment of the active and dextral North Anatolian fault zone with excellent outcrops of the main fault and other related structures (Tatar, 1978; Bektaş, 1981). The starting age of this large fracture zone seems very likely to be Upper Miocene, perhaps Lower Pliocene. Its total horizontal offset is estimated to be about 50 km. Folds and N-dipping thrust faults in Early-Middle Miocene and even Pliocene deposits must be genetically related to the wrenching along the fault. We find field evidence (such as the E-W trending tectonic melange zones and main structures of Upper Cretaceous and younger ages) suggesting roughly a N-S compression in Upper Cretaceous-Paleocene, and also in

96
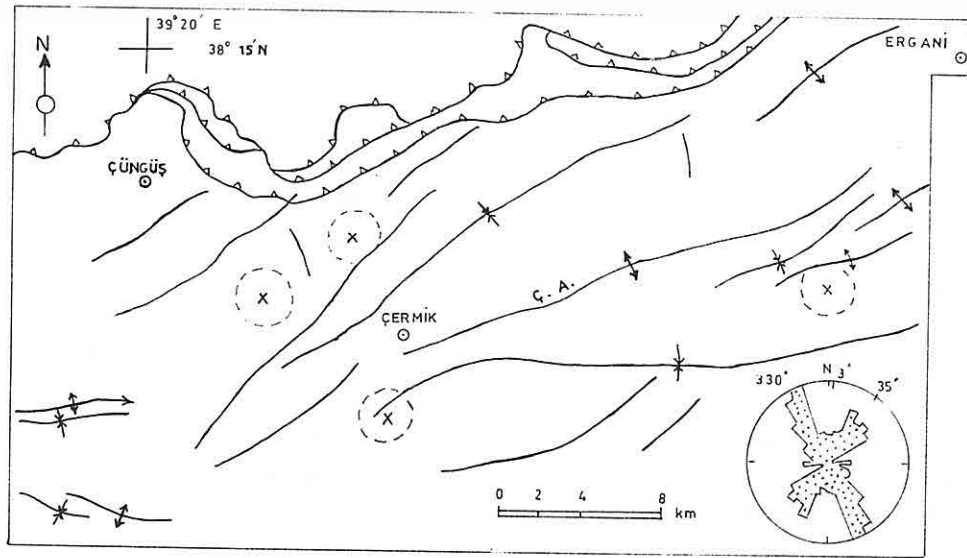
Figure 3. The result of the fracture analysis in the area around the town Çermik (for location see fig.2). The dashed circles show the localities where strikes of the fractures were measured. The rose diagram to the right below was prepared using all the measured strike values. The interpretation of the rose diagram suggests approximately a N-S compression responsible for the formation of the fractures. The thrust faults seen on the map between Çüngüş and Ergani are parts of the Bitlis thrust zone. The structural base map from (Sungurlu et al., 1985), data for the fracture analysis from (Tatar et al., 1991). Ç.A.:Çermik Anticline.

1991; Tatar, 1987). It has a length of about 100 km and it trends nearly 75°. Beside Middle Eocene-Upper Oligocene, this folding included also Upper Miocene, and eventually Plio-Quaternary strata (Tatar, 1978; Türkmen, 1991). Especially the youngest deformations about 10 km to the west of Palu (Fig.2) are interpreted as produced by wrenching along the East Anatolian fault zone (Tatar, 1987).

The East Anatolian fault zone is a sinistral active fault zone which was initiated in Late Miocene-Early Pliocene, and has a total offset of about 20km (22 near Göynük, 18 near Gölbaşı, 15 SW of Hazar Lake at Euphrates River, about 25 near Maraş; see Dewey et al., 1986; Arpat and Şaroğlu, 1975; Ercan, 1979; Yalçın, 1979; Perinçek et al., 1987).

The Ovacık fault zone is also a sinistral and active strike-slip fault zone. It has a trend parellel to the East Anatolian fault zone, and its origin seems to be common with the origin of the latter one. Field data is insufficient yet to make a clear picture of it (Tatar, 1987).

95
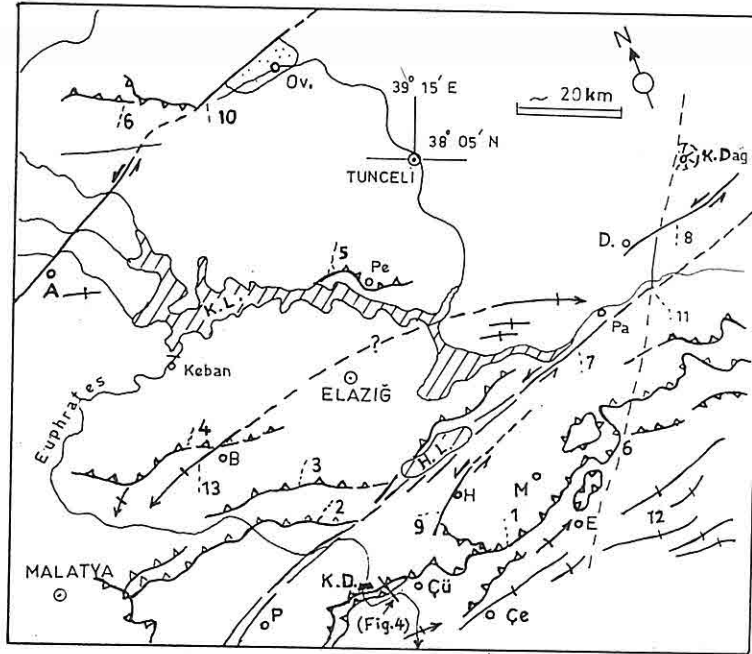
Figure 2. Main tectonic lines in Elazığ area (redrawn from Tatar, 1987 with simplifications). 1-Bitlis thrust belt, 2-İspendere thrust, 3- Kömürhan thrust, 4- Baskil thrust 5- Pertek thrust, 6- Kemaliye-Ovacık thrust, 7- East Anatolian fault, 8- Demirci fault, 9- Hazar fault, 10-Ovacık fault, 11-Korucadağ, 12-Border folds. Abbrevations-A: Ağın, B:Baskil, Çe:Çermik, D:Demirci E:Ergani, H:Hazar village, H.L:Hazar Lake, K.D:Karaya Dam K.L:Keban Lake, M:Maden, Ov:Ovacık, Pa:Palu, Pe:Pertek.

formed as a result of the continental collision in Late Miocene - Early Pliocene. Along this thrust zone southward displacement rates have been found as large as 20 km (Ketin, 1983).

In the area to the north of the Bitlis thrust there is a series of smaller, again E-W trending and N dipping thrust faults, the age of which are getting younger from N (Upp. Cretaceous) to S (Mio-Pliocene). These structures are described elsewhere (Tatar, 1987; Bingöl, 1984 see also Fig.2).

The fold axes to the south of the Bitlis thrust zone are more or less parallel to the strike of the main thrust. Tear faults and systematic joint sets in genetic relationship to the folding are not seldom in the area (Tatar and İnceöz,1991; Bingöl,1984; Ketin,1983). The age of folding is also Late Miocene-Early Pliocene. The tightness of the folding increases as one approaches to the thrust zone and vice versa. Some of the folds near the thrust zone are south vergent (Ketin, 1983; Tatar,1978; Türkmen, 1991).

In the area north of the Bitlis thrust,fractures are dominating, but there are also fold structures of which the "Baskil - Palu anticline" is a noteworthy example (Turan,

94
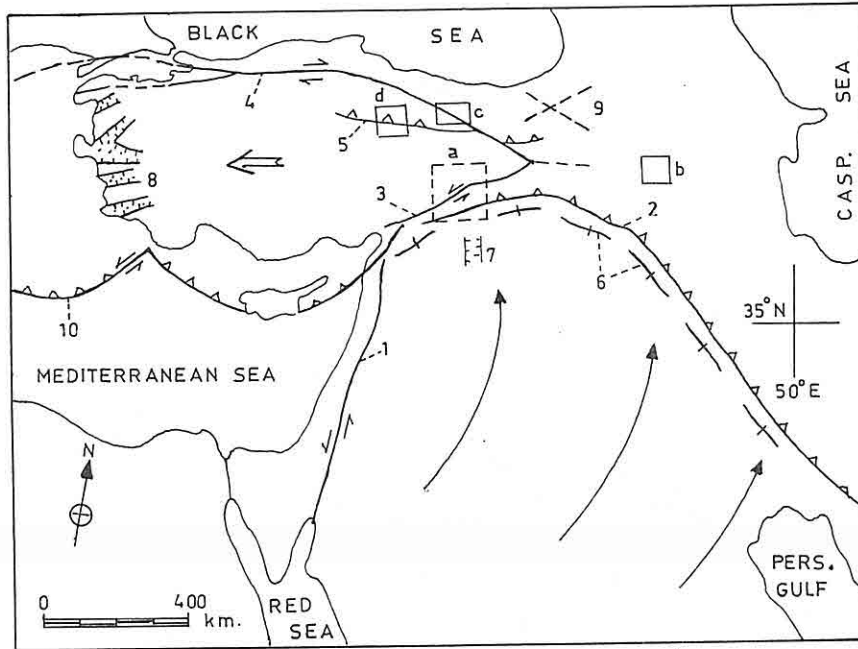
Figure 1. Location map showing the considered areas and some neotectonic lines in the Middle East. 1-Dead Sea fault zone, 2- Bitlis-Zagros suture zone, 3-East Anatolian fault zone, 4- North Anatolian fault zone, 5-Central Anotalian ophiolite thrust, 6- Border Folds, 7- Karacalıdağ graben, 8- West Anatolian grabens, 9- Fracture system in Eastern . Pontids, 10- Hellenic trench.Drawn by the author using some data from (Şengör, 1980; Mattauer, 1980). (a) Elazığ area, (b)Van area,(c) Erzincan area, (d) Sivas-Yıldızeli area. Arrows indicate the rotational direction of the arabian plate motion (see Fig.6.7 in Mattauer, 1980).

Eastern Anatolian fault zone, and the Ovacık fault zone are prominent structures which can all be studied in the vicinity of Elazığ. For the tectonic setting of the E and SE Anatolian fold- and thrust belt the reader should refer to other publications (e.g. Şengör, 1980; Şengör and Yılmaz, 1981; Ketin, 1983; Brinkmann, 1976).

The well-known E-W trending and N dipping Bitlis thrust (suture) zone, in a more regional sense Bitlis-Zagros suture zone, which separates the eastren part of the Taurus chain from the Border Folds, that is from the foreland flexural basin, has an important segment in this area. The so called "double-thrust" crops out very spectacularly for example at the village of Hindibaba, halfway between the town Çüngüş and the Karakaya dam site (Tatar, 1987 and Figures 2, 3, 4). The thrust zone was

93

1. INTRODUCTION

The interpretation that the movement of the Arabian peninsula played an important role on the Alpine mountain building in Türkiye and in Iran was considered in the geological publications, issued at least in the last few decades by many scientists who worked in Türkiye and in the Middle East (e.g. Perinçek,1979; Kürsten, 1980; Innocenti et al., 1980; Perincek and Özkaya, 1981; Aktaş and Robertson, 1984; Michard et al., 1984; Şaroğlu and Yılmaz, 1984; Dewey et al., 1986; Barka and Gülen, 1987; Şaroğlu and Yılmaz 1987; Altıner, 1989; Turan, 1991). The importance of movement of the Arabian plate was emphasized also in many recent review papers (e.g Perinçek and Özkaya, 1981; Turan, 1985; Illies, 1975; Şengör and Kidd, 1979; Şengör, 1980; Şengör and Yılmaz, 1981; Jackson and McKenzie, 1984; Tokel, 1984; Yazgan, 1984; Dercourt et al., 1986; Gülen et al., 1987; Hemton, 1987). But the question of the exact direction of the movement during the shrinkage and closure of Neotethys in this region remains unexplained.

Though many earth scientists, have carried out many investigations in the huge Alpine-Himalayan belt for the last 200 years, there are still many geological problems that have not been satifactorily explained. One example of such problems is how large curvatures, such as the one in the Carpathians or Macran-Sülaiman Range, have been formed. Another example of such geotectonic curvatures is the northern and northeastern boundary of the Arabian plate. The main tectonic lines of the Alpine structures in E and SE Anatolia strike roughly E-W, whereas they trend NW-SE in the Zagros region. It is assumed that both structures resulted from the movement of the Arabian plate during the Alpine period. However, it is difficult to find a reasonable explanation to the question how movement of the same plate could produce both E-W and NW-SE striking orogenic lines which appear to be continuation of each other.

This paper aims at the interpretation of some Alpine structures in E and SE Türkiye in relation to the geodynamics, especially as they relate to the direction of the Arabian plate motion. Introductory regional geologic descriptions are not included here because of limited space. There are however other publications which the reader could refer to (e.g. Şengör,1980; Şengör and Yılmaz, 1981; Ketin, 1983; Brinkmann, 1976).The local field data discussed here have been collected since 1970 through the author's own fieldwork, and fieldwork with his students. The areas under special consideration in this paper are (a) Elazığ area, (b) Van area, (c) Erzincan area, and (d) Sivas-Yıldızeli area (Fig.1).

2. DATA FROM ELAZIĞ AREA

As it has been discussed in some previous papers (Tatar, 1987; Tatar and İnceöz, 1991), the area around Elazığ has abundant outcrops of tectonic and especially neotectonic features of both E and SE Anatolia. Border Folds, Bitlis suture zone,

92

ON SOME TECTONIC STRUCTURES IN E AND SE TURKEY AND THEIR SIGNIFICANCE TO THE GEODYNAMICS OF THE ARABIAN PLATE

Yusuf TATAR

Fırat Üniversitesi Mühendislik Fakültesi, Elazığ/TÜRKİYE

ABSTRACT : *North-northwestward movement of the Arabian peninsula has played a determining role on the evolution of the Alpine orogenic system in Türkiye and in Iran. However, the direction of the Arabian plate convergence and its variation during the closure of Neotethys in the region of Türkiye and Iran still remain poorly understood. Some recently collected tectonic field data from certain areas of E and SE Türkiye; are reviewed in search of a new interpretation to this problem.*

The geometric-mechanical and age-related data on the studied structural elements indicate a compressional regime for E and SE Anatolia directed N-NNW. It is obvious that this compressional regime, beginning in Late Cretaceous and extending to the Late Miocene with at least some reactivations in Pliocene originated from the motion of the Arabian plate. Recent seismo-tectonic activities along the major strike-slip faults in Anatolia indicate that the northward movement of the Arabian plate still continues. In the considered areas no remarkable field evidence was found, indicating a notable change in the direction of the motion of the Arabian plate within this geological time interval. This conclusion, however, is open to further discussion.

91

Romana, M., 1985. New Adjustment Ratings for Application of Bieniawsk Classification to Slopes. Int. Symp. on the Role of Rock Mechanics. Zacatecas. pp 49-53.

Shamburger, C.H., Patrick, D.M. and Lutter, R. J., 1975. Survey of Problem Areas and Current Practices. National Technical Information Service, U.S. Deparment of Commerce Springfield, VA. 22161.

Steffen, O.K.H., 1976. Research and Development Needs in Data Collection for Rock Engineering. Proc.Symp. on Exploration for Rock Engineering. Balkema-Rotterdam. vol. 2, pp 95-104.

Yılmazer, İ., 1991. An Approach to Construct Ground Water Recharge Area Boundary Over a Stratified and Tilted Geological Unit (in Turkish). Symposium Upon Precipitation, Flooding and Landslide, Ankara.

Yılmazer, İ., 1992. Hidrojeolojik Araştırmalarda Yükseklik ve Süreksizlik Etkenleri. 3.Ulusal Mühendislik Jeolojisi Sempozyumu, Çukurova Üniversitesi, Türkiye, (In Turkish).

Yılmazer, İ. and Erhan, F., 1991. Engineering Geology of the TAG Motorway: Section 3, Dar al Handasah, (unpublished report)

Yılmazer, İ. and Demirkol, C., 1992. About the Geology of the Nurmountain Range (NMR). 1st Int. Symp. on East - Mediterranean Geology. Çukurova University-Turkey, (in press)

Yılmazer, İ., İşler, F., and Duman, T., 1992. Metamorphism in the Nurmountain Range and its Effect on Engineering Geology of the Region. 1st. Int. Symp. on East - Mediterranean Geology. Çukurova University, Turkey.

Zika, P., 1990. Engineering Geological Evaluation of the Rock Cuts Stability Along the D1 Highway. IAEG Congress. Balkema-Rotterdam.

orogenic movements, and degree of metamorphism. Burial metamorphism has improved engineering properties of the Dhm appreciably. In the surrounding area, instead of metamorphic rock names, sedimentary rock names have been used incorrectly by some other previous investigators. It is obvious that a proper usage of geological terms allows easy and more accurate recognition of actual ground condition, review of past experiences, and sound engineering judgement.

Stability of embankments and foundations over such metamorphic terrains could be easily performed. But, numerous engineering geological factors besides cost, have to be taken into account to design cut slopes. Surface and subsurface geotechnical investigations may not be adequate especially in the tectonically disturbed units(Dh, Kb, and Kp) which constitute ≈80% of the study area. In addition past experience and sound engineering judgement prior to design may contribute greatly. Potentially unstable grounds should be eliminated at the route location phase. Stabilization; principally removal of the driving forces, increasing toe restraint and effective drainage could essentially be achieved by executing a detailed and continuous engineering geological study at every stage of a design.

5. ACKNOWLEDGEMENT

6. REFERENCES

Bieniawski, Z.T., 1979. The Geomechanics Classification in Rock Engineering Applications. Proc. 4th Int. Cong. Rock Mech., ISRM, Montreux, v. 2 pp 41-48.

Bieniawski, Z.T., 1989. Engineering Rock Mass Classifications. A Complete Manual for Engineers and Geologists in Mining, C.v.l, and Petroleum Engineering.John Willey & Sons, New York, 251 p.

Erhan, F., Yılmazer, I., and Duman, T., 1992. Mühendislik Çalışmalarında Süreksizlik Araştırmalarının Önemi. 3.Ulusal Mühendislik Jeolojisi Sempozyumu, Çukurova Üniversitesi,Türkiye, (In Turkish).

Ertunç, A., Yılmazer, İ., and Kaya, Ş., 1992. Yarma Yamaç Tasarımı ve Kinematik İnceleme. 3.Ulusal Mühendislik Jeolojisi Sempozyumu, Çukurova Üniversitesi, Türkiye, (In Turkish).

Hendron, H.J., Jr., Mesri, G., Gamble, J.C., and Way, G., 1970. Compressibility Characteristics of Shales Measured by Laboratory and Insitu Tests. Determination of the Insitu Modulus of Deformation of Rock, STP 477, Amer. Soc. for Test. and Mat., Philadelphia, Pa., pp. 137-153.
88

1985, suggested Slope Mass Rating (SMR) which is based upon RMR method proposed and then developed by Bieniawski, 1979 and 1989. The SMR is more applicaple to tectonically disturbed and stratified units.

Thick (>20 m) colluvial deposits accumulated over hill slopes, form a common type of unstable areas. Weathered blanked of phyllite, calcschist, and outsloping Mib levels are also susceptible to slide at many localities.

Table 1. Common discontinuity types and attitudes in the prevailing geological units.

DISCONTINUITY TYPE	GEOLOGICAL UNITS						
	Mib	Kp	Kbc	Kbs	Dhm	Dhl	Kbp
BEDDING	16/205	70/200	26/230	----	35/270	22/275	----
	45/185	68/160	30/245	----	40/345	38/330	----
JOINTS							
Conjugate	38/320	78/168	75/340	55/335	68/047	56/141	55/248
	78/087	70/080	80/140	63/035	72/231	50/238	30/125
Compressional	25/254	75/124	----	50/272	82/314	58/066	62/283
Tensional	78/320	85/295	85/320	60/005	86/209	85/005	63/004
SCHISTOSITY	----	----	----	----	40/320	55/315	----
FAULTS							
Normal	75/153	56/358	----	----	75/035	65/300	----
Reverse	----	----	58/270	55/280	65/275	70/259	----
Thrust	----	----	44/245	45/230	40/295	40/278	----
SHEAR PLANE	----	----	----	20/235	37/300	----	----

4. CONCLUSIONS AND RECOMMENDATIONS

Engineering of the surrounding area along the most diffucult portion of the Tarsus-Adana-Gaziantep Motorway (TAGM) in Southern Turkey, has been studied. The Engineering desing of a motorway, particularly over a highly dissected and rugged topography such as the Nur Mountain Range (NMR) is dependent on a sound understanding of stratigraphy, structural geology, and hydrogeology.

Engineering characteristics of the geological units show great variation from place to place depending upon the associated structural elements, hydrogeological features and rock types. These have been influenced by the mode of deposition or emplacement,

(a)

Magnitude				
Number	MS 5.	MS 6.	MS 7.	MS 8
4.2 45	21	2	0	

(b)
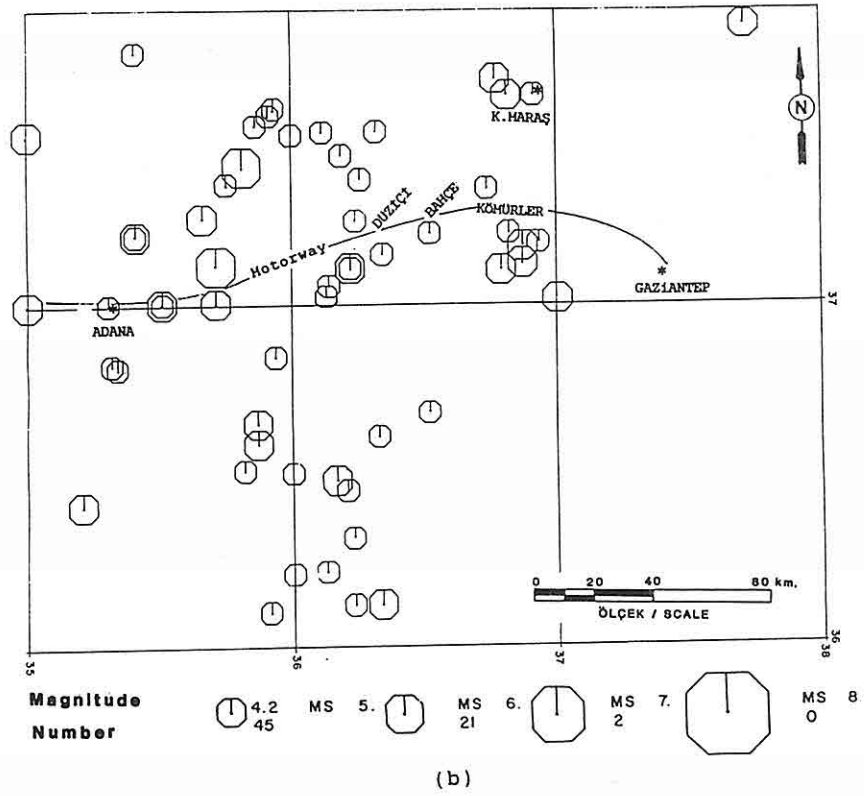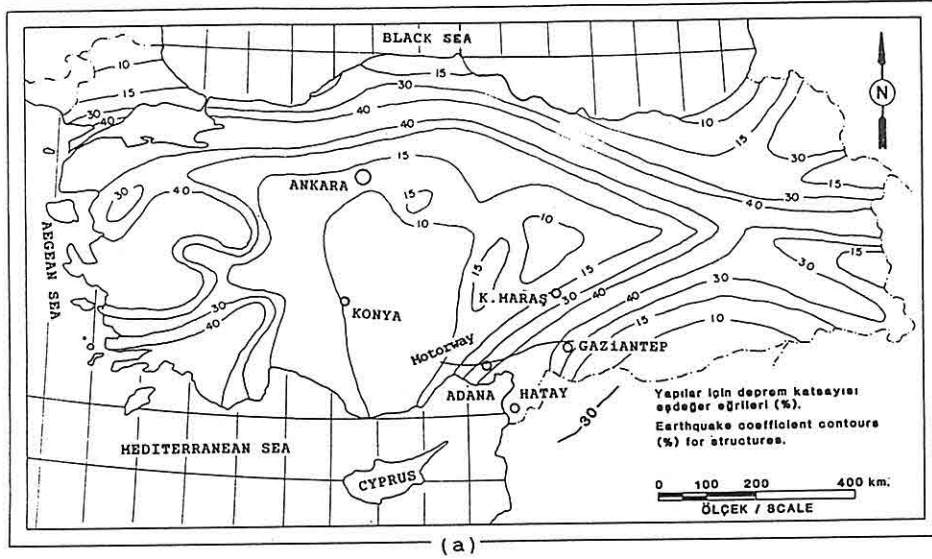
Figure 4: Seismicity in the Adana-Gaziantep region (Yılmazer and Erhan, 1991).

86

figures presenting comparative engineering properties of different rock types. Hendron et al. (1970) have studied compressibility characteristics of shales. The in situ static rock modulus ($Er \approx 10^{-5}$) of shale is much less than that of slate ($Er > 10^{-7}$) in the study area. However, some researchers call slate as shale because of its fissile character at the surface due to stress relief (J. Gallerany, 1989, personal commun.)

Low to medium grade burial metamorphism (green schist facies) has increased the strength of the flyschlike sedimentary rocks of Paleozoic age appreciably (Yılmazer et al., 1992). The main rock types are metagreywacke, metaquartzite, slate, phyllite, sericite schist, hematite schist, mica schist, chlorite schist, and metaconglomerate along the mountain range. Rock strength varies from moderately weak to very strong where far away from the main thrust zones. Bedding planes are locally obscure because of amalgamation due to high temperature and pressure exerted during burial metamorphism. No planar or slickensided fault planes could be observed. However, thick deformation zones formed along the major thrusts which trend basically NNE-SSW. Discontinuities are mainly discontinuous because of intense folding which has appreciably increased the overall cut slope stability. But, major fault zones have been intensely to highly altered and weathered which adversely affects ground stability. Most of these zones have been detected by surface geological investigation and then proved by deep excavation and/or drilling where suspicious.

A few thousand discontinuity measurements have been taken along the motorway to enable the execution of kinematic analyses and to describe subsurface geological conditions (Erhan et al., 1992). Each data point has been described in terms of discontinuity type, attitude, space, aperture, water condition, infill, discontinuity strength, rock substance strenth, weathering and alteration, slaking, and discontinuity types. Common discontinuity types and attitudes with relevant geological units are given in Table 1. The rational numbers indicate dip amount and dip direction respectively.

Special effort has to be made to design high (>25 m) cut slope faces in such stratified, faulted, and jointed lithological units. The region besides its complex geology, is seismically very active (Fig. 4). The past 100 year earthquake records are presented to give idea about the seismicity of the region. Zika, 1990, emphasized the signifiance of natural slope condition on the design of cut slope for a particular site. Naturally formed steep slopes, in the delineated area, are mainly the result of inslope contidion and lithological resistance to erosion. Cut slope stability analysis was performed kinematically. Numerical analyses such as Modified Bishop Method were also utilized. Stability of cut slopes is mainly governed by discontinuities, hydrogeology and rock mass quality rather than rock substance strength parameters. Therefore, engineering geology description sheets for each cut have been prepared in detail. Typical forms are presented in Ertunç et al.,(1992) and Steffen (1976). Moreover , Romana,

85

ASYMMETRICAL DEPOSITIONAL BASIN

SEDIMENT INFLUX

	COMMON	MINERALS
MAINLY FROM Dhm	Kbp	

QUARTZ, ALBITE, OLIGOCLASE, ORTHOCLASE,
MUSCOVITE, CHLORITE, BIOTITE,
CALCITE, SERICITE, DOLOMITE, AMPHIBOLE, ...

MAINLY ILLITE IN Plg

OLIVINE, PYROXENE,
ANTIGORITE, CHRYSOTILE,
CHROMITE, MAGNETITE, ...

SMECTITE IN Plg

SE

1250

1000

750

500

SEE NW

NWW
KIMARCIK HILL

Dhm

Dhl

Kbs

Dhm

GARIPARDIC HILL
Dhl

Kbs

Qc/Plg

Qs

KARÖLMEZ HILL

Kbp

Kbp

0 250 500 1000 m
SCALE

TOPOG. ELEVATION ABOVE MEAN SEA LEVEL, M.
1250 1000 750 500

8

Figure 3. Illustrating effect of thrust zone on the formation of asymmetrical depositional basin.

Figure 2. Illustrating a naturally stabilized old landslide.

83

good quality chlorite schist, hematite schist, and slate dominate and their fresh levels are strong to very strong. However, Dhmp and the other Dhm beds neighbouring the major fault zones have poor to medium quality rocks. Extremely weak rocks are exposed or encountered during subsurface investigation adjacent to the thrust zones. Almost all of the active and potential landslides naturally formed and being formed, are located adjacent to major fault zones. In addition, thick Qy and Qc materials have accumulated and stratified over the hillslope of very high mountains. These have created and continuing to create huge unstable masses. The combined effects of faults, groundwater, and geomorphologically very high mountains have caused the formation of huge slide masses (>2 million m^3). One of them is shown in Fig.2. Slide morphology is very distinct. The maximum preserved thickness is 60 m. The river has been shifted about 300 m northward. Many of them have been naturally stabilized. However, they are ready to be reactivated when resisting forces are reduced, driving forces increased, and/or groundwater level increased. As it is clear, various stabilization measures regardless of cost can be implemented if geological models of the actual ground condition are fully understood.

Plg, as described above, is a Plio-Quaternary aged intermountain basin deposit. Therefore, its engineering properties are determined by the lithological properties of the source rocks and its location in the basin (Fig. 3). As shown in Fig. 3, an asymmetrical basin has formed. The Eastern side is bounded by Kbp whereas the western side is bounded mainly by Dhm and Dhl. The Kbs underlies the unit adjacent to thrust, where concretioned and fissured CH material formed at the bottom zone. A huge sediment influx has produced a relatively thick sedimentary succession over the CH material zone. Sorting is not good. However, coarse grained levels along the coast, pass transitionally into fine grained levels toward the basin. On the other side, the Kbp has supplied a small quntity of sediments because of its massive to thick layered engineering properties and its smaller erosional surface A swampy ground prevails along the long axis of the asymmetrical basin and closer to the Kpb mountain range. The Qs is characterized by fully saturated CH-MH material.

Medium quality and moderately strong peridotite constitutes the majority of the Kbp. Very strong chromite and very weak serpentinized peridotite zones are also present, but to a lesser extent. Layering and joint systems are well developed. Consequently, kinematic analysis is one of the best methods to design cut slopes in such units.

Identification of major rock types (igneous, metamorphic, and sedimentary) and their interrelationships are very important in geological and geotechnical investigations. A massive and amalgamated slate is always better than shale which is readily susceptible to slaking and swelling (Shamburger et al., 1975). They have described geology, mineralogy, and engineering properties of shales from different parts of the world in detail. Furthermore, numerous related books and periodicals include tables and

82

3. ENGINEERING GEOLOGY

Detailed engineering geological investigations which proceed stratigraphical, structural, and hydrogeological study, form an essential basis in selecting proper motoway elements and to implement effective design practices. Numerous drilling and treching were done especially where the surface geology was not obvious and/or to define engineering parameters of lithological units to execute railway and motorway design.

The Qt becomes more fine grained with distance from the toe of the NMR. Soft CH material becomes the main constituent in pond deposits. The uncorformity plain between Mib and Qt is generally slippery because of the relatively impervious character of the underlying unit. Dense to very dense levels are observable especially along the immediate toe of the NMR.

The Mib contains extremely weak mudstone layers to moderately strong sandstone layers. Rock mass quality can be described as poor and very poor along fault zones. The Kpv comprises deformed spilitic basalts which are in places highly altered and/or weathered. The Kpl is characterized by moderately strong limestone blocks, bedchunks, and huge slabs in a chaotic mixture. Faults, shear zones Kpv-Kpl contacts and other discontinuities are easily perceptible due to color contrast.

Conglomerate and sandstone levels of the Kbc are well cemented by $CaCO_3$ which increased the strength appreciably. Excavation requires blasting and fragmentation. About 80% of the unit comprises strong to moderately strong lithologies. Mudstone levels can be classified as weak rocks. Bedding planes are rough, irregular, and often obscure due to sedimentary transition.

Kbs has been deformed extensively along tectonic zones and emplaced tectonically. Both upper and lower contacts are thrust faults. Hence, closely spaced shear planes and fractures are common features and the rock has poor to very poor quality. Active but shallow seated slides are situated only along fault zones. Elsewhere, it forms stable grounds due to its massive appearance, impersistent discontinuities, and impervious character. Moreover, the weathered and destressed surface part is being eroded and washed away without giving rise to the accumulation of unstable masses (Qc).

The Dhl, where represented by thick tectonic slabs, appears as a relatively high altitude landform. Except for the calcschist levels, the majority of the unit comprises strong rocks. The unit along the eastern tectonic zone, has been silicified at many locations. Silicification has made the unit massive, hard, and brittle. It is being quarried as a source of sand along the eastern toe of the NMR for over 50 km. High hardness (4-7), non-reactivity, very low porosity (<5%), and angular shape are its favorable properties as sand.

The Dhm is a very thick metamorphic unit. Regional metamorphism has increased its rock mass quality and rock substance strength considerably. Levels of

appreciably high. Discontinuities are basically smooth and slickensided. Rock substance property of the Dhl is quite high and the stronger portions are being used as good qualty aggregate source. Shear zones, calcschist levels, and phyllite levels control ground stability in the Dhl. Silicification along the eastern boundary of the NMR has created silicified dolomitic limestone which is massive but extremely brittle and being quarried as a sand source by nearby dwellers. Excluding phyllite levels and away from the major fault zones, moderately weak to strong rocks constitute the essential part of the Dhm. A 5 km long and open sided railway tunnel throughout the unit, has stood stable for over 65 years. The Kbp has very widely spaced shear zones which are mainly serpentinized. It includes medium to closely spaced joints and medium thick layers and transits into serpentinite where approaching major thrust zones.

2. HYDROGEOLOGY

Ground stability is greatly affected from the presence of water. Hence seeps, springs, streams, water supply wells, and swamps have been mapped and investigated in detail. Discharge rates of springs and stream have been recorded at predetermined intervals.

Faults, bedding planes, and folding can control the distribution and movement of both groundwater and surface water to a certain degree. The TAGM alingment is located along the Horu valley which drains very high and steep hillsides. Therefore, In addition to the conventional hydrogelogical methods some site specific methods (Yılmazer 1991 and 1992) were also adopted.

Permeability of fresh Mib, Dhm, and Kbs-Kbp is very low ($<10^{-6}$ cm/sec) because of a very high percentage of clayey rock levels, metamorphism, and crystallinity respectively. Coarse grained Mib levels, postorogenically deformed zones in Dhm, and Dhl have relatively higher permeability.

The Kp is a chaotic mixture of different lithologies which are diverse in origin. Therefore, its hydrogeological properties show great variation from place to place. The Dhl has noticeably high ($>10^{-2}$ cm/sec) secondary permeability.

A shallow groundwater condition prevails in an extensive part of the Plg area. Marshy to swampy grounds have formed at many localities in the Plg.

Seeps and springs are clustered along fault zones. They are the main causes of active and potential slides particularly in the Qc. The Horu Creek and some of its tributaries are perennial with varying discharge rates from 2 lt/sec to 20 lt/sec during the driest period. Due to the NW- dipping monoclinal structure of the NMR, western side streams are all perennial whereas eastern side rivers are seasonal (intermittent). Seeps and springs are also densely distributed over the western side.

Figure 1. Location and accessibility map.

1. INTRODUCTION

Engineering geology of a site is mainly governed by stratigraphy, structural geology, and hydrogeology of the surrounding area. Therefore, prior to engineering design, each of these subjects should be studied and reviewed in detail. The delineated area is situated along the stretch between stationings KM 190+000 - 240+000 (Fig.1).

The Nurmoutain Range (NMR) exhibits distinct monoclinal structures (Yılmazer and Demirkol, 1992). The motorway crosses the NMR between the towns of Düziçi, Bahçe, and Kömürler. Tunnels and viaducts are essential elements of the motorway along this stretch because of the highly dissected and the rugged topography and the presence of potentially unstable grounds.

Geological units from west to east are; Plio-Quaternary aged terrestrial deposits (Qt), Upper Miocene aged detrital sequence, conglomerate to claystone (Mib), tectonosedimentary deposits (Kp) along the border zone of the Upper Cretaceous aged ophiolitic melange (Kb), about 350 m thick conglomerate-siltstone alternation (Kk), structurally 1.5 km thick serpentinite (Kbs), Devonian aged recrystallized dolomitic limestone (Dhl), Metadetritics (Dhm) comprising mainly schist, phyllite, slate, metaquartzite, and metaconglomerate alternation, silicified dolomitic limestone (Dhl), serpentinite (Kbs), Peridotite (Kbp), and Plio-Quaternary lake-pond deposits (Plg). Recent deposits such as Alluvium (Qa),Colluvium (Qc), and Talus (Qy) have significant extents on both sides of the NMR.

Site-specific hydrogeological features in the corridor greatly influenced the design of the motorway elements. Seeps, springs, shallow groundwater conditions, swampy and marshy grounds, and streams could have been detailed out by surface geological inspection and the review of all written information and local knowledge. Interrelationships between groundwater and surface water conditions and the influence of major discontinuities in hydrogeology have also been investigated deliberately.

The Qt is characterized by dense to very dense GM-SC and locally ML-CH materials. The Mib consists of extremely weak mudstone to moderately strong sandstone layers. Its contact with the underlying Kp is mainly tectonic. Numerous active and potential landslides are observable along this contact. Megaolistoliths of limestone (Kpl) which are being quarried as crushed rock, have moderately weak to strong property. Deformed spilitic basalts (Kpv) have strength varying from very weak to moderately strong. The Kk has medium to good quality. Massive to thick bedded conglomerate levels constitute the majority of the unit. The tectonic contact with the underlying Kbs is exposed at several locations. Abrupt changes in vegetation and the presence of springs, seeps, and/or wet ground condition make this boundary distinct. The Kbs comprises extensively sheared and intensely fractured serpentinites. The end bearing capacity is

78

ENGINEERING GEOLOGY OF THE DÜZİÇİ-KÖMÜRLER REGION

İlyas YILMAZER[1], Aziz ERTUNÇ[2] and Ferudun ERHAN[1]
[1] *Dar Müh. Müş. A. Ş., Adana / TÜRKİYE*
[2]*Çukurova University, Engineering Faculty, Adana / TÜRKİYE*

ABSTRACT: *A 30 km long portion of the Tarsus - Adana - Gaziantep motorway (TAGM) crosses the Nurmountain Range (NMR) between the towns Düziçi and Kömürler. It is the most difficult stretch of the TAGM. A proposed railway alignment which is subparallel to the motorway , will take place in the same corridor. The Design of such large engineering structures has to follow comprehensive engineering geological and geotectonical investigations. The NMR forms a topographical obstacle (>1000 m) between the Çukurova and Hatay-Gölbaşı Basins (<500 m). The presence of varous lithological units, numerous structural elements, and very high seismicity have created a complex engineering geology. Since every geological event undergoes a definite system, available engineering features can be assessed by detailed surface and subsurface investigation, past experience, and engineering judgement.*

Colluvium, talus, and alluvium constitute an essential part of the recent deposits which have very wide spectrum of soil properties. Terrace and Lake deposits crop out respectively at far western and eastern parts. They behave as soil and in places poorly cemented very weak rock. A flyschlike Miocene unit overlies a tectono sedimentary unit cosisting largely of deformed spilitic basalts and locally strong limestone blocks. Serpentinite of poor quality rock type thrusted medium to good quality recrystallized limestone and metadetritics. Moderately strong, medium widely jointed, and in places layered peridotite is exposed in eastern part of the study area.

Tectonic contacts between successive units and in each unit, are well developed. Monoclinal structures such as recumbent folds and high angle thrusts which are striking NEN-SWS and dipping NWW,are also clearly perceptible. The Geomorphology and hydrogeology of the area are greatly influenced by those structural and tectonic features. A discontinuity survey over such a rugged and highly dissected morphology, enables investigators to predict. and recognize a three-dimensional picture of subsurface geologic conditions. To be acquainted with these features helps to locate engineering structures properly and/or to find satisfactory solutions to the engineering problems at the right time.

77

M.T.A., 1975. Geological map of Turkey, scale 1/500,000, Hatay Sheet, Maden Tetkik Arama Enstitüsü, Ankara.

Miller, D.M. and Oertel, G., 1979. Strain Determination from the Measurement of Pebble Shapes: A Modification. Tectonopysics 55, T11-T13.

Oertel, G., 1983.The Relationship of Strain and Preferred Orientation of Phyllosilicate Grains in Rock- A Review. Tectonophysics 100, 413-447.

Oertel,G. and Reymer, A.P.S., 1992. Pertubation of strain and rotation in a nodular slate. Jour. of Structural Geology 14 ,257-269.

Shamburger, J.H., Patrick, D.M., and Lutter, R.J., 1975. Design and Construction of Compacted Shale Embankments. Federal Highway Administration Offices of Research and Development, Washington D.C. 28590.

Swanson, M.T., 1992. Late Acadian-Alleghenian Transpressional Deformation : Evidence from Asymmetric Boudinage in the Casso Bay Area, Coastal Maine. Jour. of Structural Geology 14, 323-341.

Ünalan, M., 1986. Amanos Dağlarındaki Alt Paleozoyik Çökellerinin Çökelim Ortamları ve Bölgenin Paleocoğrafik Evrimi, Bulletin of the Geological Society of Turkey, v.29, No. 2, 49-63. (In Turkish).

Wheeler. J.,1986. Average Properties of Ellipsoidal Fabrics: Implications for Two-and Three-Dimensional Methods of Strain Analysis. Tectonophsics 126, 259-270.

Wınkler, H.G.F., Petrogenesis of Metamorphic Rocks. Springer-Verlag NewYork Inc. 334p, 1976.

Yalçın, N., 1980. Amanosların Litolojik Karakterleri ve Güneydoğu Anadolu'nun Tektonik Evrimindeki Anlamı , Bulletin of the Geological Society of Turkey, v.23, 21-30, (In Turkish).

Yılmaz, Y., Demirkol, C., Gürpınar, O., Yalçın, N., Yetiş, C., Yiğitbaş, G., Günay, Y., and Sarıtaş, B., 1984 . Amanos Dağlarının Jeolojisi ve Stratigrafisi , İ.Ü. Müh.Fak. Döner Sermaye İşletmesi , 227s, İstanbul, (In Turkish).

Yılmazer, İ., Erhan, F., Aytekin, E. ve Duman, T.Y., 1992a. Mühendislik Çalışmalarında süreksizlik araştırmalarının önemi, Mühendislik Jeolojisi Sempozyumı bildiri özetleri, Çukurova Üniv. Adana, (In Turkish).

Yılmazer, İ., Ertunç, A. and Erhan , F., 1992b. Engineering geology of the Düziçi-Kömürler region. 1st Int. Symp. on East - Mediterranean Geology. Çukurova University-Turkey, (In press).

problematic zones into consideration.

5. CONCLUSION AND RECOMMENDATION

Metamorphism of sedimentary rocks, especially pelitic types, creates an appreciable increase in strength. Detrital rocks, such as claystone, shale, siltstone, mudstone and sandstone mostly have grain type cement and they alter into slate, phyllite, metagreywacke, and schist depending on the degree of metamorphism and chemical composition of the their sedimantary equivalents. Strength parameters of these metamorphic rocks are generally higher than that of the original sedimentary rocks. Examples can be extended simply by field observation . A marble usually has higher quality than limestone or other carbonates. Permeability decreases with metamorphism. Thus, weathering is not effective especially away from the shear zones that favours stability.

Preferred orientation of flaky, platy, prismatic and ellipsoidal minerals and /or grains by the regional metamorphism creates unisotropy. Such unisotropy can only be important to describe rock substance strength directionwise rather than rock mass property.

Strength of weak igneous rocks, such as a kaolinized granite through weathering or hydrothermal alteration , may improve with metamorphism. However, strong and massive igneous rocks (such as fresh andesite, peridotite and granite) may become weaker due to preferred orientation of minerals and formation of talc and serpentine type minerals especially in mafic rocks. Metasomatism (hydrothermal alteration) of ultrabasic rocks yields serpentinite which is a poor quality rock.

It can be recommended that the main rock (sedimentary, igneous and metamorphic) types have to be identified properly even at the prepreliminary phase of large engineering structure projects.

6. ACKNOWLEDGEMENTS

7. REFERENCES

Dean, W.T and Monod, O., 1984. An interpretation of Ordovician Stratigraphy in the Bahçe Area, Northern Amanos Mountains, South Central Turkey. Geol. Mag. 122, (1), 15-25.

Demirkol, C., 1988 . Türkoğlu (K.Maraş) Güneybatısında Yer Alan Amanos Dağlarının Stratigrafisi ve Yapısal Jeolojisi , Ç.Ü. Araştırma Fonu I. Bilim Kongresi Bildirileri, Cilt 1, Adana,(in Turkish).

Hunt, R.E., 1986. Geotechnical Engineering analysis and evaluation. McGraw Hill, Inc.

firm texture, hence causes an appreciable increase in strength. Schistose texture is comman in regional metamorphic rocks. But it is not persistent as the other discotinuities such as beds, faults, layers and shear zones. Most of the schistose rocks have massive appearance due to amalgamation by metamorphic processes.

Geomorphology of the area reflects the difference in strength and resistance of sedimentary and metamorphic units. The highest hills (2000m) are made of Dhm whereas Mib forms lower altitudes (700m). The Mib is much prone to weathering and mass wasting processes. Thick slope wash deposits (Qc) are accumulated along toe of hills and over hillsides. The Qc is generally characterized by CH material. About 80% of slope wash deposit derived from Dhm consists mainly of gravelly-silty and clayey gravelly material (Qt). The Qt can be utilized as good quality fill material. High shear strength and free draining material can also be obtanined.

Fault zones which have formed before metamorphism could be amalgamated or recemented with minerals to yield good quality rocks when subjected to high T-P and hydrothermal activites. Post - metamorphic faults may produce extremely weak and well sheared zones only in weak rocks such as phyllite, calcschist, and talcschist. However, faults are so effective in detrital rocks. Thick fault gouge, breccia and mylonite may form during and after faulting. CH-MH material is essential constituent in such shear zones. The other discontinuities become impresistent with increasing T-P condition . Particularly bedding planes become discontinuous when tight and drug folds are forming. High T-P cause semi -plastic behaviour which is particularly important along hinges to prevent intense fracturing and form minerals, generally quartz and calcite, in open discontinuities. Sausage structures and boudins may make weak layers impersistent and bedding planes rough and irregular.

Oxygenated groundwater is the main agent in chemical reactions (Oxidation processes) which deteriorate rock quality. Many of aquifers become aquifuge throughout the metamorphism. Thus, metamorphic rocks impede downward percolation of surface water. However, postorogenic movements have caused some superimposed disturbances along the previously formed thrust zones under low T-P conditions. Such zones gained relatively higher secondary permeability. About 5.5 km long and approximately 70 years old railway tunnel is still under use without treatment and dry except the northern and portion which has been located a few meters below the bedrock surface. However, numerous seeps are observable in a few hundred m long tunnels constructed throughout the sedimentary units.

Main shear zones in terrains which have been subjected to tectonic movements and suffered from erosion for longer periods can easily be recognized. Such weaker zones commonly form saddles, gullies, toe of cliffs end other depression like morphologies. Such zones can be mapped by geomorphological study, areal photography study and geological survey. Then , engineering structures can be located properly by taking such

74

Figure 3. Deformation modulus-uniaxial compressive strength of different rock types
(after Hunt, 1986).
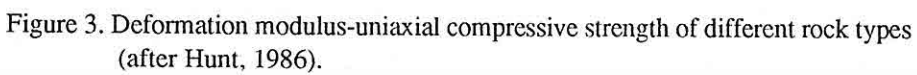
Claystone, mudstone and siltstone (Mib) : They are slightly to highly slakable. Clay minerals (mainly illite), quartz and feldspars are essential constituents . When exposed to atmospheric conditions, their engineering properties deteriorate rapidly due to high clay content and poor grain type cement.

Sandstone and Conglomerate (Mib) : Cement is grain type. Durability depends on clay content in the cement. Grains (coarse sand- gravel) are subrounded to rounded and approximately 95% derived from the Dhm and Dhl. Quartz, albite, orthoclase, tiny muscovite grains and clay minerals constitute majority of the cement.

Phyllite (Dhmp) : Fresh ones are durable. Weathering is effective down to 10 m below the ground surface and relatively deeper along the shear zones. Quartz, feldspar, micas and in places talc are main constituents. Micas and feldspars are altered into clay mineral (mainly illite) in weathered and altered levels. Such zones have a high slaking property.

4. ROCK PROPERTIES

Engineering properties of detrital rocks generally improve through metamorphism (Fig. 3). Detrital rocks form by physical and chemical processes of open-system which is characterized by the mobility of interstitial fluids till the diagenesis stops. At this point intercommunicating pore spaces are closed up and reactions of closed system start to create a metamorphic suit (Winkler, 1976).

Clay minerals; such as illite, kaolinite, dehydrated hallosite and chlorite in decreasing order, quartz, silt size mica, feldspar, and pyrite, are main constituents of pelitic rocks. Irregular mixed-layer illite/montmorillonite alter into Al-rich chlorite, illite, quartz and water throughout the diagenesis . However , the new assemblage is not stable. The above reaction is reversible under atmospheric conditions or very susceptible to weathering and chemical reactions. Such rocks used as fiil material in embankments , usually creates settlement and/or slope failure (Shamburger et al., 1975).

Beyond the diageneis, by the increase of T-P , metamorphism commences and more stable minerals start to form. For instance, kaolinite in the presence of quartz alter into prophyllite (Winkler, 1976). This mineral together with albite produces paragonite or muscovite in the presence of potash feldspar. Mixed-layer clay minerals and smectite yield metamorphic assemblage of paragonite, phengite and chlorite. They new assemblage is more stable than the former. Pyrite in pelitic rocks, recrystallizes into hematite and thus rebound crystals and grains to create hematite schist. Strength of shale is incomparatively lower than that of its metamorphic equivalent schist or slate. Furthermore, some mineral smay persist to stay as they are with increasing degree of metamorphism. But , crystal size increases to yield interlocked texture and smaller specific surface (sericite enlarges into muscovite) and consequent reduction in chemical reaction capacity. Optical continuity of original minerals during over growth yields more

72

ERA	SYSTEM	SERIES	FORMATION	MEMBER	BED	LITHOLOGY	ENGINEERING GEOLOGICAL DESCRIPTIONS
CENOZOIC	QUATERNARY		MADE GROUND (Qm)				Existing road fill, earth dump, reclaimed land areas, and earthfill pond bodies are mapped as Qm. Mainly medium stiff or medium dense.
			COLLUVIUM (Qc)				Basically loose to medium stiff heterogeneous, and incoherent soil mass deposited on and accumulated at the base of slopes. Slide areas are also mapped as Qc.
			TALUS (Qy)				Rock fragments of any size derived from the Dh and accumulated on steep slopes and at the base of cliffs. Angular, loose to medium dense.
			ALLUVIUM (Qo)				Recent coarse to fine unconsolidated sediments deposited in the base of valleys, flood plains, and alluvial fans by creeks, streams, and rivers.
			MARSHY GROUND (Qs)				Marshy ground has formed as a remnant of the Pl-Q lake. Clay content increases away from the adjacent sources. Especially the first 2 m zone has soft ground property.
			TERRACE DEPOSITS (Qt)				The Pleistocene river and other fluvial deposits which were dissected by Holocene rivers are mapped as Qt. Poorly consolidated to weakly cemented by finers. In places it shows GC character.
	TERTIARY	PLIOCENE	GÖL (Plg)				Some narrow lake basins have formed during the Pliocene time which were controlled by tectonic movements and prevailed till the Holocene. Composition and grain size depend on adjacent source rock and distance being transported. Roughly bedded, weakly cemented by finers and occasionally CaCO3. Majority consists of gravelly CH material.
		MIOCENE	BEYAZEV (Mib)				Characterized by the alternation of sandstone, mudstone, siltstone, claystone, fossiliferous mudstone, argillaceous limestone, and shale. It has been intensely deformed by tectonic forces. Discontinuities are well developed. Thick shear zones have formed. Bedding faults are occasionally observable in extremely weak mudstone layers confined competent sandstone layers. Rock substance strength has very wide range, from extremely weak to strong. CL-CH type material exists in most of the discontinuities.
		EOCENE	SAK. (Es)				Medium thick bedded limestone, argillageous limestone, and sandstone-claystone alternation consitutes majority of the unit.
MESOZOIC	CRETACEOUS	UPPER	PINAR (Kp)	LMST (Kpl)			A tectonic assemblage of rock of diverse in origin and geologic age bound in a matrix of mainly spilitic basalt fragments. Some huge slabs (allochton) still preserve their original identities. Some mappable limestone (Kpl) and flysch slabs (bedchunks) are available very close to the mapped area. Limestone bedchunks bear medium quality rock mass property. Volcanics are intensely fragmented but polished surfaces are rarely observable. The areas, consisting of deformed spilitic basalts and autobreccia, are mapped as Kpv.
				VOLC. (Kpv)			
			KARAHASAN (Kk)				Thickly bedded and in places strongly cemented by CaCO3. It can be classified as medium to good quality rock away from tectonic zones. Majority of the unit comprises conglomerate.
			BAHCE (Kb)	SERPENT. (Kbs)			As known it is an alteration product of Mg rich silicate (esp. olv+opx.) rocks. In the study area it has formed along the major tectonic zones (mostly reverse and thrust faults). Hence intensely fractured and locally sheared. Discontinuity planes are smooth and irregular. The Kbs can be classified as poor quality rock with relatively higher bearing capacity. Serpentinized along discontinuities. Hence shear strength along discontinuities was significantly reduced. Chrysolite and chromite are rarely observable. Rock substance strength can be described as moderately strong to strong whereas rock mass quality can be classified as poor to medium quality.
				PERIDOTITE (Kbp)			
PALEOZOIC	DEVONIAN		HORU (Dh)	LMST. (Dhl)			Mostly recrystallized and dolomitized. Tight folding is common. Discontinuities are not persistent. Some alternating calschist and partially phyllite levels constitute very weak zones in the unit. Rock substance strength varies from moderately strong to strong.
				METADETRITICS (Dhm)	SLATE (Dhms)		Dark black color is its characteristic at fresh outcrop. Fissile at surface but massive (amalgamated) just below land surface. It can be classified as good quality rock. Rock substance strength in fresh Dhms is strong.
					PHYLLITE (Dhmp)		It belongs to greenschist facies rocks and carries very weak rock strength along the tectonic zones due to intense deformation, alternation, and weathering. Mica schist are also included in this unit. Adjacent to some thrust zones dolorite (Kd) has intruded through the Dhm. Generally strong but in places hydrothermally altered into very weak rock.
					HEM.SCH. (Dhmh)		Similar to the Dhms strengthwise. The dark brown color is due to presence of iron oxide (hematite). Occasionally it has well developed cleavage and schistosity oblique to bedding planes and perpendicular to the mountain building stresses. Metaquartzite and micaschist constitute significant portion of the unit.
					CHLOR.SCH.		Chlorite schist is a good quality rock. Recrystallization due to metamorphism increased the strength appreciably. Dark green color due to chlorite and presence of large crystals of garnet are its distinguishing features. Metaquartzite and mica schist levels are also present.

Figure 2. Generalized engineering geological columnar section.

elongated pebble shapes (Miller and Oertel, 1979). Oertel and Reymer (1992) have studied perturbations of strain and rotation in nodular slate at three dimensional grid points to recognize episodes of strain. Preferred orientation of phyllosilicate grains could also reflect strain condition (Oertel, 1983). Such detailed investigations can only be performed in metamorphic rocks rather than sedimentary rocks. The recognition of such structural systems and contingent engineering geological features could enable engineers to design appropriately.

2. STRATIGRAPHY

The study area comprises sedimentary, tectonosedimentary, tectonic and metamorphic units. Generalized engineering geological columnar section is presented in Figure.2. Five of the differentiated units are mainly concerned in this paper, namely Upper Miocene aged Beyazev formation (Mib), Cretaceous aged Pınar formation (Kp), Karahasan formatin (Kk) and Bahçe formation (Kb), and Devonian (?) aged Horu formation (Dh). All have tectonic contacts with each other.

The Mib consists mainly of claystone, mudstone, siltstone, calcareous, and fossiliferous mudstone, sandstone, and other detrital rocks in a lesser quantity. Extremely weak to moderately weak layers constitute majority of the unit.

Deformed spilitic basalts, autobreccia, limestones, and some detrital rocks make up the Kp. The main portion has been tectonically emplaced, where the rest deposited tectonosedimentarily. Limestone is stronger than the other components which are very weak to moderately strong.

The Kb comprises peridodite (Kbp) and serpentinite (Kbs) along the motorway. The Cretaceous (?) aged Karahasan formation (conglomeratic sequence) overlies the Kb with a tectonic contact.

The Dh embraces metadetritics (Dhm) and recrystallized and inplaces silicified dolomitic limestone (Dhl). Hematite schist (Dhmh), Chlorite schist (Dhmc), Phyllite (Dhmp), Slate (Dhms) are four distinguished beds in the Dhm. This unit has been described as a sedimentary succession consisting of mainly shale, mudstone, siltstone, sandstone, and conglomerate by Dean and Monod (1984), Yalçın (1980); Yılmaz et al. (1984) and many other former researchers. However, Demirkol (1988) mentioned about cleavage in the Paleozoic unit which has been caused from metamorphism. Yılmaz et al.(1984) described the ophiolite of the study area as metaophiolitic complex and suggested that the metamorphism resulted from thermodynamic processes rather than hydrothermal alteration.

3. PETROGRAPHIC STUDY

Numerous samples were picked up and thin sections have been prepared to define metamorphic facies and to correlate mineral compenents of both Dhm and Mib .

70
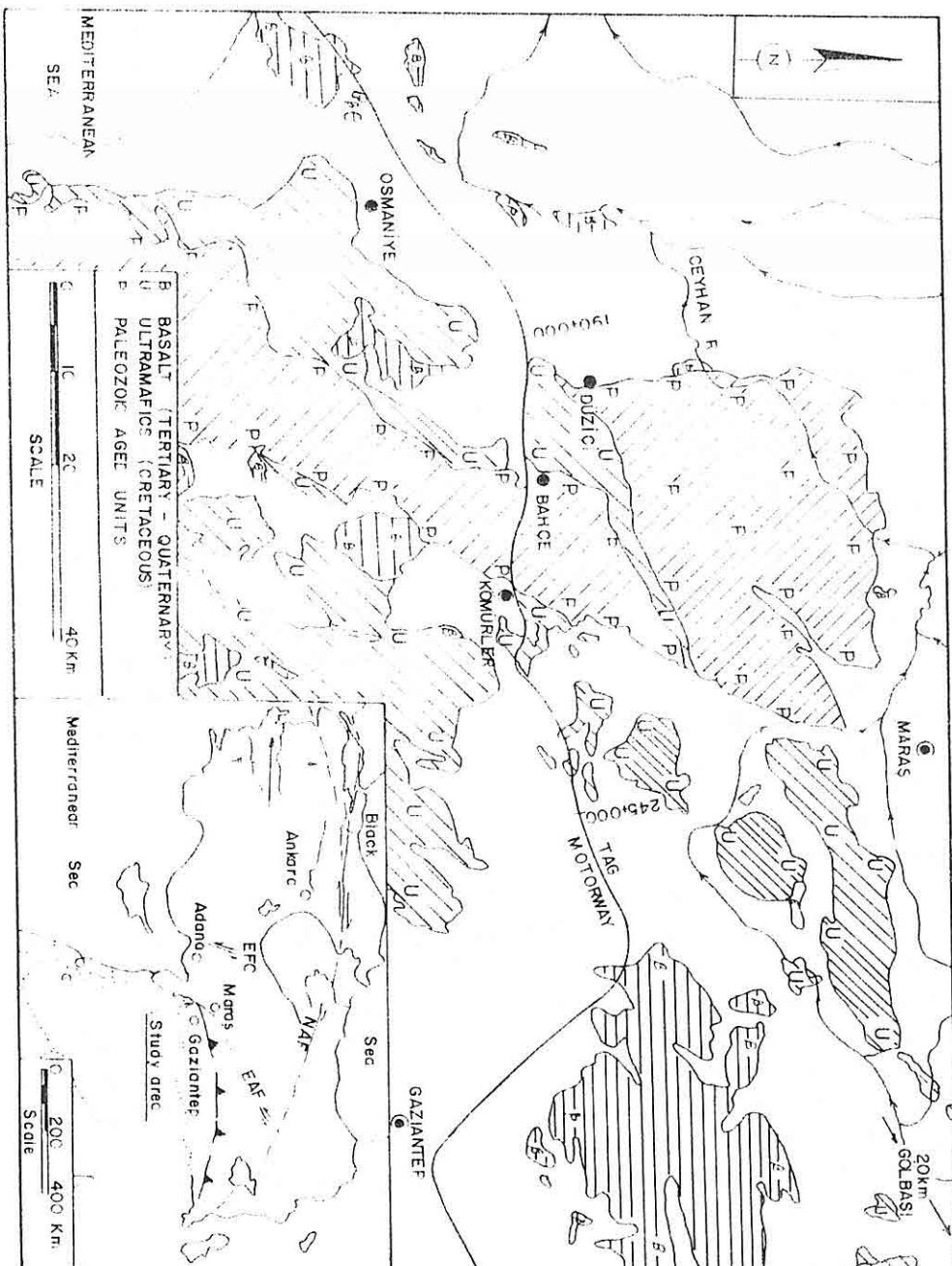
Figure 1. Regional geological map (modified from MTA 1975)

Upper Cretaceous time. At which time, dolerite dikes have intruded parallel to subparallel to the tectonic forces. Fresh sill outcrops are also observable. They do not show any indication of metamorphism and ophitic texture peculiar to them easily distinguishable, particularly in fresh dolerites.

Orginal rock of slate naturally is either shale, claystone or mudstone. Shear strength values of slate are incomparatively higher than that of original sedimentary rocks. Misuse of rock names will definitely misleads investigator and designer of an engineering structure. The following changes which are appreciable from engineering point of view, may develop through metamorphic processes;

-Clay minerals, which are main causatives of ground instability, recrystallize into relatively more stable minerals such as mica minerals, chlorite, chloritoid, pyrophyllite and paragonite.

-Successive layers become amalgamated producing rough, irregular, and/or impersistent bedding.

-All slippery discontinuities with CH material are sealed by means of recrystallization.

-Porosity and permeability become negligible. Metamorphic rocks, in genaral neither store nor transmit water.

-Tight folding and contortion under high pressure and temperature make discontinuities tight and irregular.

Schistosities, in most cases, are discontinuous. Weathering is not much effective on metamorphic rocks and the thickness of weathered zone is less than that of the original sedimentary rocks.

1. INTRODUCTION

The main objective of this paper is to investigate the effects of metamorphism on engineering properties of flyschlike deposits,mainly pelitic rocks. A few km wide zone along the Tarsus-Adana-Gaziantep (TAG) Motorway between the chainages KM 190+000-225+000 (Fig. 1) have been stuidied. Approximately 70 years old railway and a proposed railway alignment take place in the same corridor.

Discontinuity types and their characteristics, affected from metamorphism, have been investigated. Miocene aged detritic rocks (Mib) and Devonian(?) aged metadetritics (Dhm) were studied comparatively from engineering respect. Further information about the engineering geology of the stretch is presented in Yılmaz, et al., (1992a).

Numerous petrographic thin sections have been prepared to compare their mineralogical contents and textures. New mineral assemblage and crystal development, overgrowth, interlocking structures and preferred orientation in Dhm and their influence on engineering properties of rock were studied.

Regional deformation can be recognized by detailed discontinuity survey investigation of boudins (Sawson, 1991), strain analysis of ellipsoidal fabrics (Wheeler, 1986), and

68

METAMORPHISM IN THE NURMOUNTAIN RANGE AND ITS EFFECT ON THE ENGINEERING GEOLOGY OF THE REGION

İlyas YILMAZER[1], Fikret İŞLER[2] and Tameryiğit DUMAN[3]

[1]Dar Müh.Müş.A.Ş.

[2]Çukurova Univ., Engineering Faculty, Adana / Türkiye

[3]MTA Adana District Directory, Adana / Türkiye

ABSTRACT : *Northern middle portion of the Amanos mountains, which is called Nurmountain Range (NMR), has been studied. A metamorphosed clastic sequence (Dhm), thickened by overlapping arrangement of thrust sheets and recumbent folds, is an essential rock unit in the NMR. Structural thickness, in places , exceeds 7 km. Recrystallized dolomitic limestone and serpentinite take place on both sides almost symmetrically. They all trend in the direction of SWS-NEN.*

A proposed railway and a motorway which is under construction cross this mountain range and they are subparrallel to each other. Rock types, as well as stratigraphical features and structural elements, have a great influence on engineering geology. Four beds have been distinguished among the Dhm. These are Chlorite schist (Dhmc), Hematite schist (Dmh), Phyllite (Dhmp), and Slate (Dhms). Metaquartzite, mica schist, porphyroblastic schist, granoblastic schist, and metaconglomerate levels are also observable in the sequence. A Miocene aged flyschlike deposit crops out at far western portion of the study area. The nomenclature was done in relation with type locality and major rock type.

In addition to well developed schistosity and slaty cleavage, the presence of cordierite, sillimenite, prophyllite, andalusite, chlorite, biotite, clinochlore and some other metamorphic minerals indicates that the unit has been subjected to low to medium - grade dynamothermal metamorphism. Age of metamorphism is likely before the emplacement of the Upper Cretaceous ophiolitic melange. However, the unit has undergone orogenic forces which created superimposed schistosity, high angle thrusts, drag folds, well systematized joints, and recumbent folds mainly along the main thrust zones during the

failure occured in land inclined at only 6 degrees.

It is recommended that the liquefaction potential of sand deposits in the Erzincan plain must be accounted for in the general planning and design of construction projects in the region.

6. ACKNOWLEDGEMENTS

6. REFERENCES

Ambraseys, N.N., 1985. ESEE Research Report No:85.5, Engineering Seismology and Earthquake Engineering Section, Imperial College, London.

Berrardi, R., Margottini, C., Molin, D. and Parisi, A., 1991. Soil Liquefaction; Case histories in Italy. Tectonophysics, V.193, No:1-3, p.141-164.

Dowrick, D.J., 1987. Earthquake Resistant Design for Engineers and Architects. A Wiley-Interscien Publication.519p.

Koçyigit, A., and Tokay, M., 1985. Çatalçam (Zevker) - Erzincan arasında Kuzey Anadolu Fay Kusagı'nın Sismo-Tektonik İncelemesi: Bayındırlık ve Iskan Bakanlıgı, Teknik Arastırma ve Uygulama Genel Müdürlüğü, Proje Kod No 82-04-08-00-02, 101 s. (Unpublished-in Turkish).

Seed, H.B., 1987. Design Problems in Soil liquefaction., J.Geotech. Engrg., ASCE, V.113, No:8, p.827-845.

Tutle, M. and Seeber, L.., 1991. Historic and prehistoric earthquake-induced liquefoction in Newburg, Massachusetts., Geology, V.19, p.594-5597.

Tuzcu, G., and Çuhadar, G., 1981. Erzincan Ovası Hidrojeolojik Etüd Raporu.DSI, 71s.(In Turkish).

Vaid, V.P., Fisher, J.M., Kuerbis, R.H., and Negussey, D., 1990. Particle Gradation and liquefaction., J. Geotech., Engrg, ASCE, V.116.
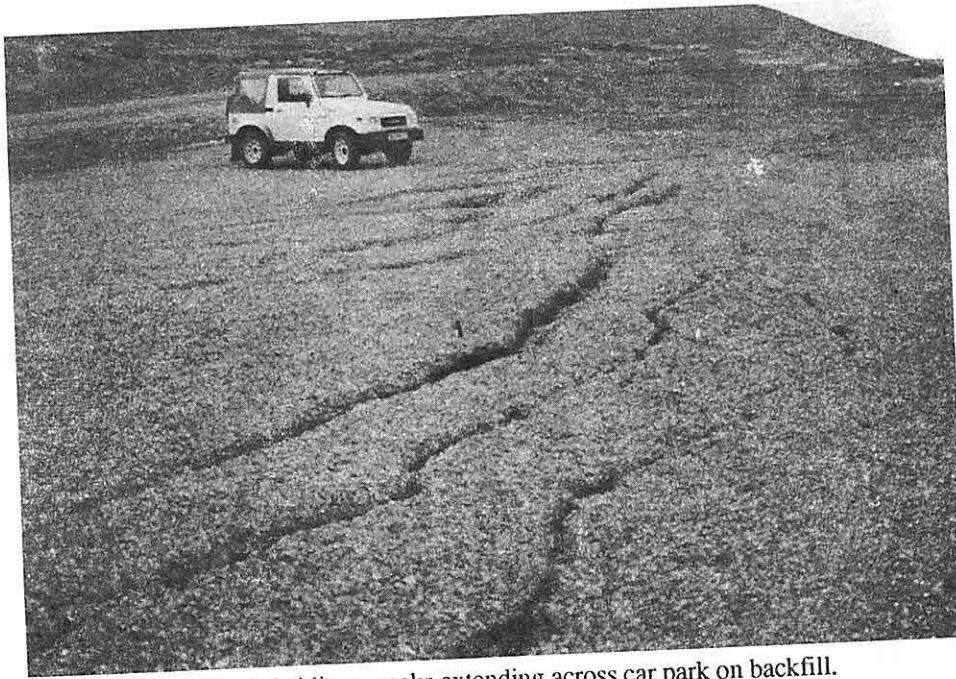
Figure 10. Subsidiary cracks extending across car park on backfill.
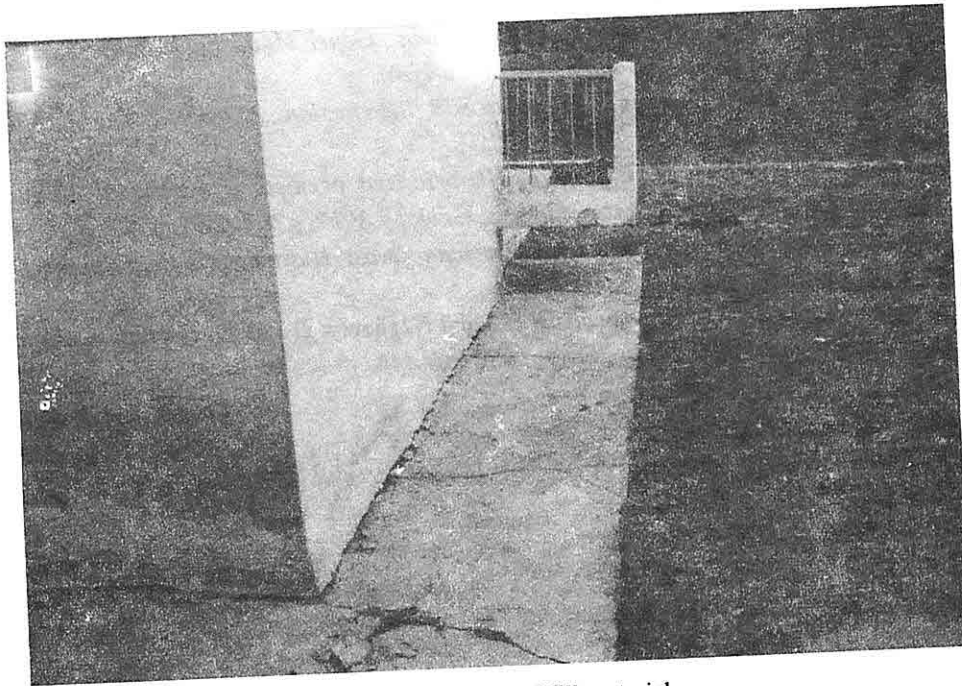
Figure 11. Settlement of fill material.
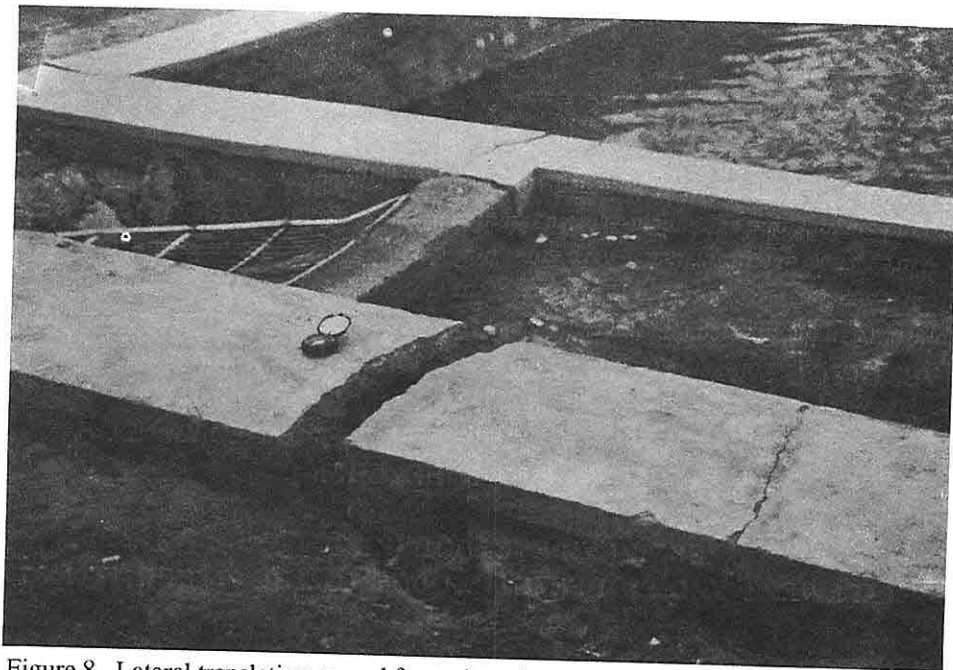
Figure 8. Lateral translation caused fracturing of retaining wall with associated tension crack in backfill.

Figure 9. Large cracks extending across car park.

Figure 6. Railway bending due to settlement of railway embankment.
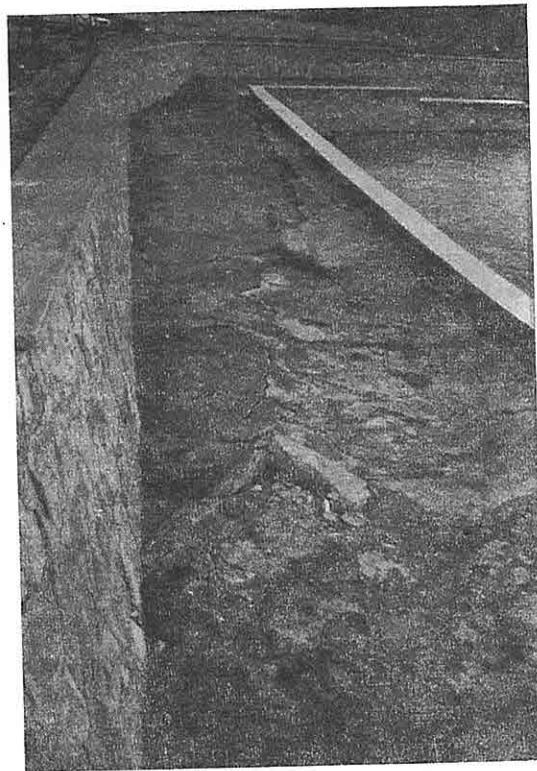
Figure 7. Tilting of retaining wall.

63
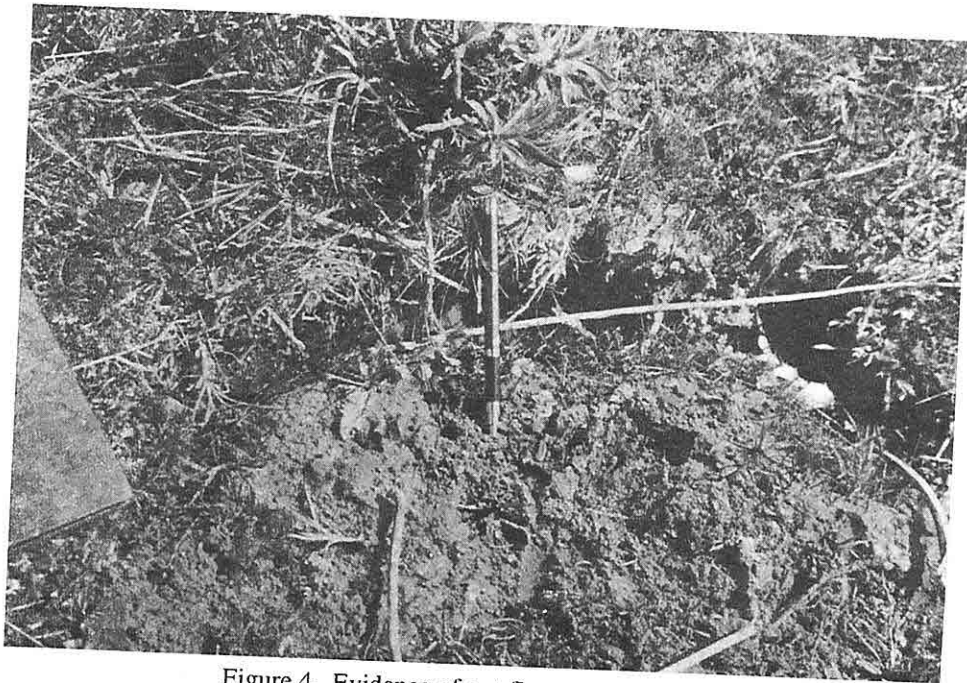
Figure 4. Evidence of out-flow sand and water.
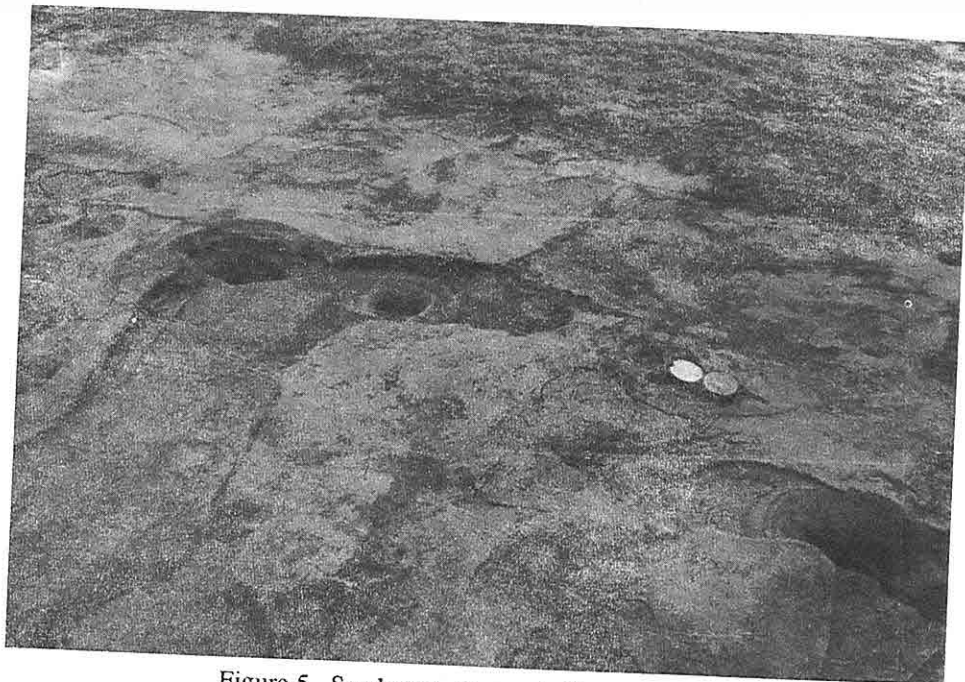
Figure 5. Sand vents surrounded by sand rings.

62

a considerable depth of water accumulated at the site. It is reported that the railway embankment had to be raised by 0.5 m locally and evidence was noted at structural damage to a tunnel through the embankment (Fig. 6).

According to the local people there were numerous other examples of liquefaction following the earthquake although many features were soon destroyed by farming. It was reported that in Uluköy village located 15 km southeast of the epicentre, a number of local houses tilted through an angle of 5 to 10 , and out-flow of sand and water was observed along the small irrigation canal running through the village.

3. SITE 2 EKŞİSU

At Ekşisu, 6 km northeast of the epicentre, natural springs are bottled by the local mineral water company for marketing. Ground water levels are close to the surface. Several retaining walls in the vicinity and the car park suffered major damage during the earthquake due to liquefaction of backfill exerting higher lateral pressure on the walls. Tilting and lateral displacements of walls was associated with severe ground cracking.

Movement of retaining structures occurred over a length of 50 m. Retaining walls which are typically of a 1.5 m high gravity boulderwork structure had their lower sections locally tilted outward (Fig.7). Elsewhere lateral translation caused fracturing of the retaining wall with associated tension cracks in the backfill (Fig. 8).

The major cracks across the car park trended N50° W although this direction probably related local failure mechanisms and topography rather than any association with the North Anatolian Fault which runs close by and with a smilar strikes (Figs. 9 and 10).

4. SITE 3 TANYERİ

The third site is located 45 km southeast of Erzincan, next to the highway between Erzincan and Erzurum, at Tanyeri Railway Station. At this location, compaction of alluvial material used as backfill to the basement of a three storey building occurred causing concern to residents. The ground settled by approximately 10 cm around the building which otherwise showed no significant damage (Fig. 11). According to the residents the 2 m basement is dry and no signs of water outflow were observed. It can be concluded that the settlement was simply the result of ground shaking causing densification of loose backfill.

5. CONCLUSION

Evidence of liquefaction and ground settlement were observed at various locations in the Erzincan plain following the earthquake of March 13th 1992. Liquefaction occured in saturated silty sand, due to increase in pore water pressure. Sand vents sometimes surrounded by sand rings provided evidence of water outflow and numerous ground fractures accompanied the sinking of the ground surface. Some remarkable discrete

61
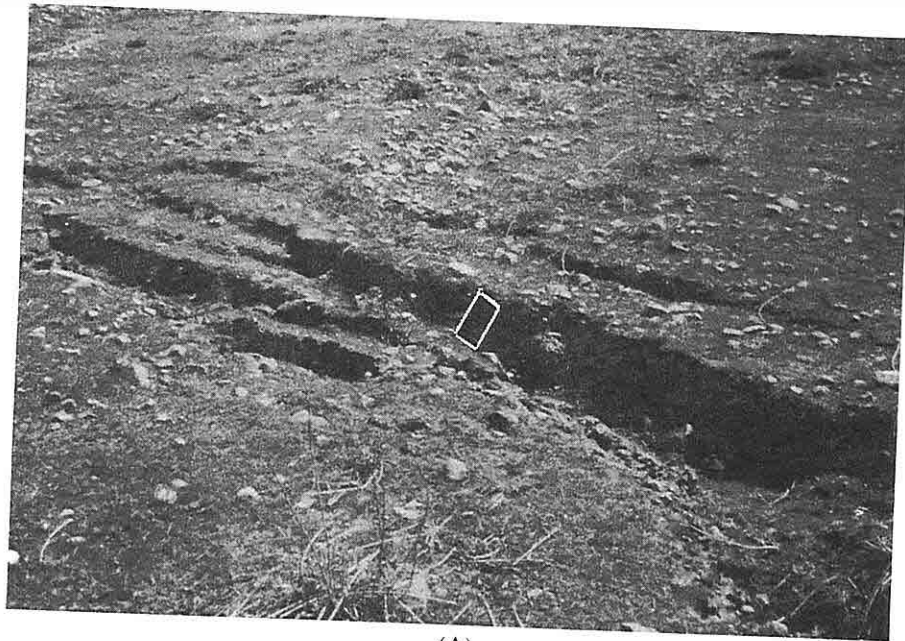
(A)
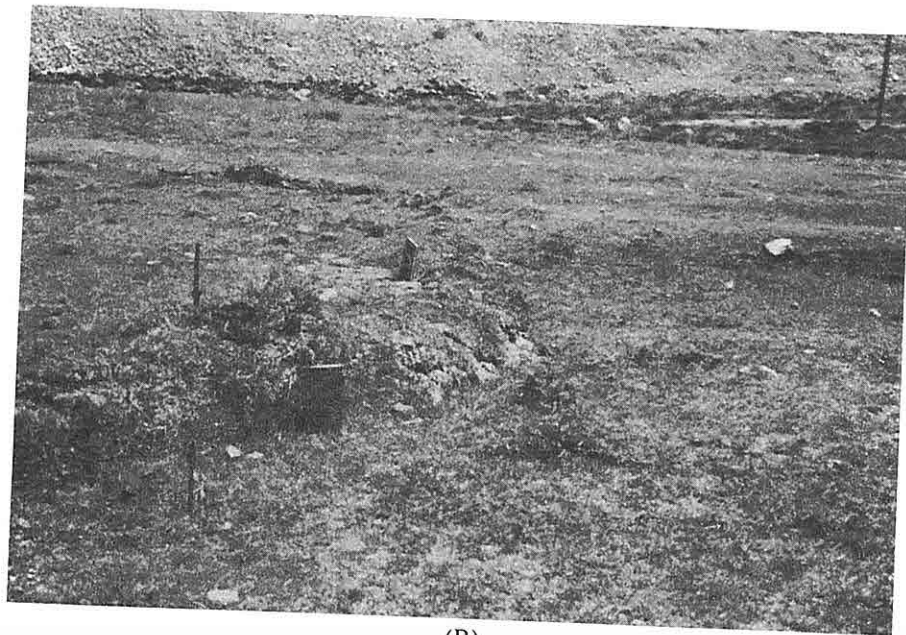
(B)

Figure 3. Discrete slump due to liquefaction. (A) Ground sinking 30cm at rear tension scarp. (B) Ground rising 30 cm at toe.

60
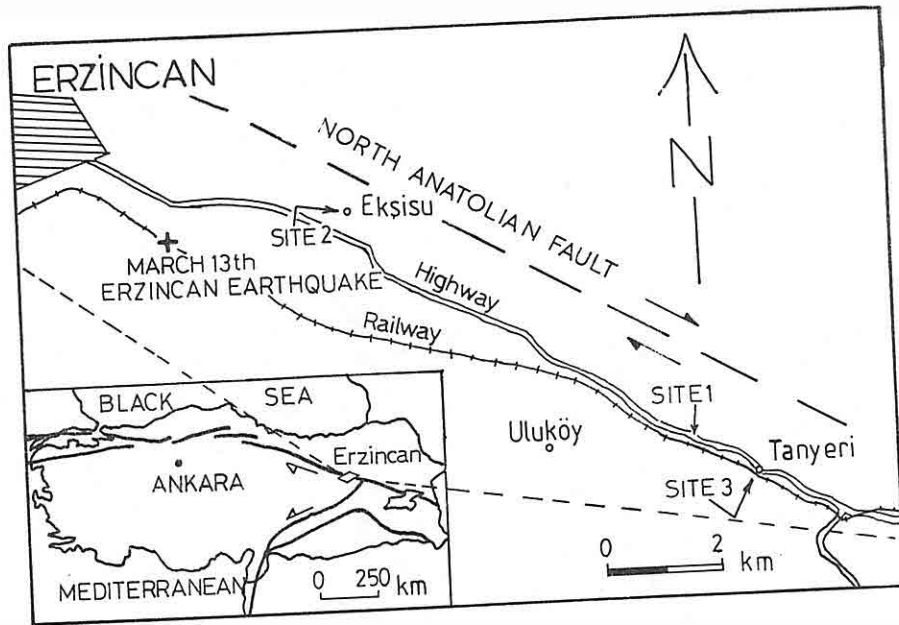
Figure 1. Location map showing 13 March 1992 Erzincan earthquake epicentre, and sites of liquefaction and settlement.

Figure 2. Slumping of highway embankment.

1. INTRODUCTION

The epicentre of Erzincan earthquake 13 March 1992 (Ms = 6.9) was located in the Erzincan plain at 39.705° N latidude, 39.549 ° E longitude and 28 km depth according to the Geological Survey of United States (Fig.1). A maximum acceleration of 0.49g was recorded in the East-West component at the Meteorological Observation Station in Erzincan by the Earthquake Research Department of the Ministry of Public Works and Settlement, Ankara.

It is well documented that under earthquake loading some soils, especially loose sands, may densify, and that, where saturated, pore water pressures may develop causing a total loss in shear strength (see Ambraseys, 1985; Dowrick, 1987; Seed, 1987; Vaid et al., 1990; Berrardi et al., 1991 and Tuttle & Seeber, 1991). Following the Erzincan eartquake, evidence of liquefaction and ground settlement were observed at several sites in the Erzincan plain within 40 km of the epicentre (Fig. 1). The liquefied sites were all underlain by flood plain alluvium which mainly comprises sand, silt and clay with lateral transition into other alluvial deposits of the Erzincan plain, such as river bed and braided river alluvium, and alluvial fans controlled by faults (Koçyigit and Tokay, 1985). Sixty-two boreholes and thirty-four drainage wells were drilled between 1960 and 1971 in the plain by The State Hydraulic Works to a maximum depth of 275 m. The nearest borehole to major liquefied site recorded mainly silty and gravelly sand deposits to a depth of 217 m (Tuzcu and Çuhadar, 1981). No indication is given of in situ density. Artesian wells occur throughou: the Erzincan plain as well as a hot spring close to the recent epicentre.

2. SITE 1, 35 km SW of ERZİNCAN, 5 km SW of AVCILAR

During a reconnaissance survey just after the Erzincan earthquake, several fractures were observed cutting the highway where constructed on alluvial deposits between Erzincan and Erzurum, approximately 35 km southeast of Erzincan. The highway embankment had slumped severely with associated longitudinal cracking (Fig.2) and this is attributed to liquefaction of the weak foundation alluvial deposits. On the south side of the highway, a number of cracks, 5 to 10 cm wide, more than 10 m in length, and trending N45°W, were observed. Similar cracks were also found locally within an area of 2 km^2.

The most remarkable fractures observed occurred between the railway and the highway. One discrete perfectly elliptical slump approximately 11 m in length and 7 m wide was found in ground inclined at only 6 degrees. The ground had simply rotated on an axis sinking 30 cm at the rear tension scarp and rising 30 cm at the toe (Fig.3). Many of the fractures showed evidence of the upwelling of sand as illustrated in Fig.4. Rings of sand 5-20 cm in diameter and 10-20 cm thick formed as a result of upward flowing water were found adjacent to the the railway track (Fig.5). Following settlement of the ground

58

SETTLEMENT AND LIQUEFACTION DUE TO THE MARCH 13, 1992 ERZINCAN EARTHQUAKE

Altay ACAR and Steve R. HENCHER

Dept. of Earth Sciences, The Univ. of Leeds, Leeds-UNITED KINGDOM

ABSTRACT: *Following the Ms =6.9 Erzincan earthquake of March 13, 1992 with its epicentire in the Erzincan plain, evidence of soil settlement and soil liquefaction due to ground-shaking were observed in alluvial areas close to the epicentre.*

Three sites are described where sand boil deposits, ground cracks, sinking of the ground surface and settlement-related damage to buildings and retaining walls were observed. The material that liquefied during the earthquake is a dark grey silty sand.

57

Irvine, T.N. and Baragar, W.R.A., 1971. A Guide to the Chemical Classification of the Common Volcanic Rocks. Canadian J. Earth Sci. 8: 523-548.

Kokubu, N., 1956. Fluorine in Rocks. Geol. Fac. Sc., Kyushu Univ., Series C, Vol. 2, No. 3, 95-149.

Lefevre, C., Bellon, M., and Poisson, A., 1983. Leucitites Dans le Volcanisme Pliocene de La Region d'Isparta, Taurides Occidentales, Turquie, C.R. Acad. Sc. Paris, 297, 11,367-372.

Özgür, N., Pekdeğer, A., and Schneider, H-J., Origine of the High Fluorine Contents in Shallow Aqueous Systems of the Gölcük Area, SW Turkey. Proc. 1st. Internat. Symp. on East Mediterranean Geology, Adana/Turkey, (in press).

Özgür, N., Pekdeğer, A., Schneider, H.J., and Bilgin, A., 1990. Pliocene Volcanism in the Gölcük Area, Isparta/Western Taurides. in: Savaşçın, M.Y. and Eronat, H.H. (eds.): Proc. Internat. Earth Sci. Congr. on Aegean Regions, İzmir/Turkey, IESCA Publ. 2, Vol.II, 41!-419.

Pekdeğer, A., Özgür, N., Schneider, H-J., and Bilgin, A., 1990. High Fluorine Contents in Aqueous Systems of the Gölcük Lake Drainage Area, Isparta/Western Turkey. in: Savaşçın, M.Y., and Eronat, H.H. (eds.): Proc. Internat. Earth Sci. Congr. on Aegean Regions, İzmir/Turkey, IESCA Publ. 2, Vol.I, 160-170.

Poisson, A., Akay, E., Dumont, J.F., and Uysal, S., 1984.The Isparta angle: a Mesozoic Paleorift in the Western Taurides. in: Tekeli, O. and Göncüoğlu, M.C. (eds.): Geology of Taurus Belt, 11-26, Ankara.

indicating a degassing of an open system. Moreover, the relatively high REE contents with a maximum of 0.15 percent can be derived from the occurence of F-apatite (Özgür et al., 1990). The remarkable similarity of the REE patterns suggests a common petrogenic origin for the whole rock spectrum of the volcanic sequence (Özgür et al., 1990; Capaldi et al., 1972).

4. CONCLUSIONS

As a result of formation of the plate tectonic event which is connected with the Afro-Arabian plate being subducted under the Euro-Asiatic plate the volcanism began in central Anatolia in Paleocene continuing up to Quaternary (Ercan, 1986; Innocenti et al., 1975, 1982).

The volcanic activity in the Gölcük area with its Lower Pliocene age represents one of the youngest events in central Anatolia. The development of volcanism which shows a sodic alkaline character may be divided into three stages: tephriphonolites (stage 1), pyroclastic series (stage 2), and trachyandesites and trachytes (stage 3). In accordance with this succession the volcanic rocks indicate a magmatic differentiation suite (Özgür et al., 1990).

By their high F-contents, the volcanic rocks in the Gölcük area are distinguished from the sedimentary rocks which can be lead to different mineral phases as determined in thin sections. There is a close correlation between F and P_2O_5 which indicates that the F-contents in the volcanic rocks are controlled by the mineral phase fluorapatite generally. A remarkable relative F-depletion from the basic towards the acidic rocks shows a trend to increasing degassing during the different stages. The important F portions must be discharged during fumarolic activity.

5. REFERENCES

Capaldi, G., Gasparini, P., Moaura, A., Salvia, E., And Travaglione, O., 1972. Rare Earth Abundances in the Alkaline Rocks from Campania. Earth Planet Sci. Lett. 17: 247-257.

Ercan, T., 1986. Cenozoic Volcanism in Central Anatolia. Maden Tetkik ve Arama Enstitüsü Bull. 107, 119-140.

Flühler, H., Polomski, J., and Blaser, P., 1982. Retention and Movement of Fluoride in Soils. J. Environ. Qual. 11/3: 461-468.

Innocenti, F., Mazzuoli, R., Pasquare, G., Radicati di Brozola, F., and Villari, L., 1975. The Neogene Calkalkaline Volcanism of Central Anatolia: Geochronological Data of Kayseri-Niğde area. Geol. Mag. 112 (4): 349-360.

Innocenti, F., Manetti, P., Mazzuoli, R., Pasquare, G., and Villari, L., 1982. Anatolia and Northwestern Iran. in: Thorpe, R.S. (ed.): Andesites, 327-349.John Wiles & Sons.
54

glassy groundmass. Compared with other volcanic rocks, an important portion of fluorine in the pyroclastic series may also attributed to the glassy groundmass (Flühler et al., 1982), because this rock type contains up to 90 percent glassy groundmass.

F-contents in trachyandesite lavas (stage 3) reach a range from 240 to 3200 ppm and a background value of 1415 ppm, which can be also linked to the various minerals phases, i.e fluorapatite, biotite, hornblende, and pyroxene. The trachyte lavas (stage 3) have
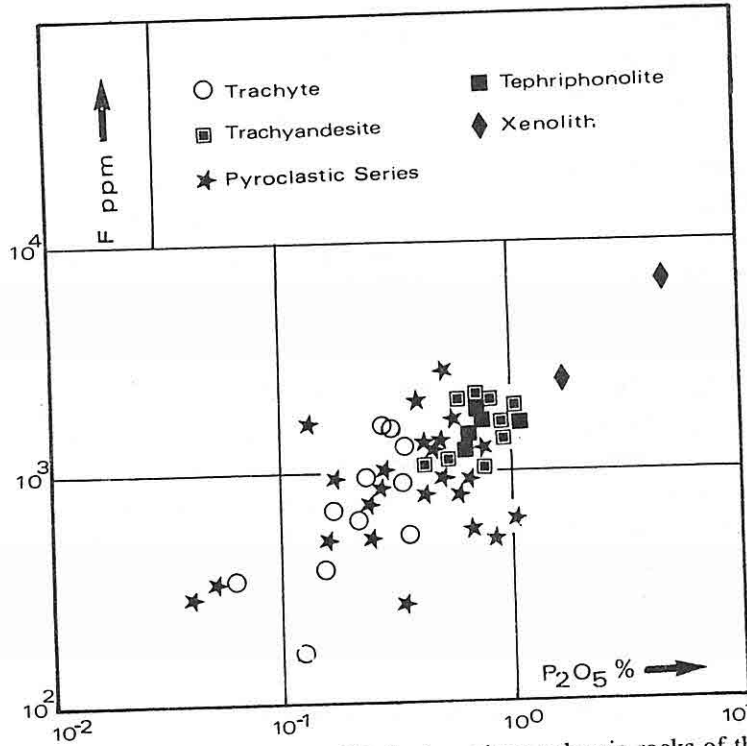
Fig. 4. Close correlation between F and P_2O_5 in various volcanic rocks of the Gölcük area.

fluorine contents in a range from 150 to 2425 ppm and a background value of 933 ppm. These high F-contents may be derived from the above mentioned mineral phases in these rocks.

There is a close correlation between F and P_2O_5 contents in the volcanic rocks generally which can indicate the geochemical role of the microscopically determined fluorapatite as one of the important F-carriers (Fig. 4). Furthermore, F-contents display a depletion from basic towards the acidic rocks as a novelty of our investigations, which is contradictory to a common magmatic differentiation process. It can be attributed to a discharging of fluorine during fumarolic stages subsequent to the volcanic eruptions

53

3. FLUORINE IN VOLCANIC ROCKS

Fluorine contents in the volcanic rocks of the Gölcük area range from 30 to 3200 ppm and show a background value of 1000 ppm (Fig. 3), which can be attributed to different F-bearing minerals, i.e. pyroxene, hornblende, biotite, F-apatite, fluorite, and glassy groundmass, in the volcanic rocks (Özgür et al., 1990).

The xenoliths with their rare occurences have fluorine contents in a range from 1710 to 6750 ppm, which are without relevance for hydrogeochemical problems (Özgür et al., 1990). These high fluorine contents are related to the intensity of the mineral phase of fluorapatite, as observed microscopically (Özgür et al., 1992, inpress).

The tephriphonolite lavas (stage 1) are distinguished by the F-contents in a range
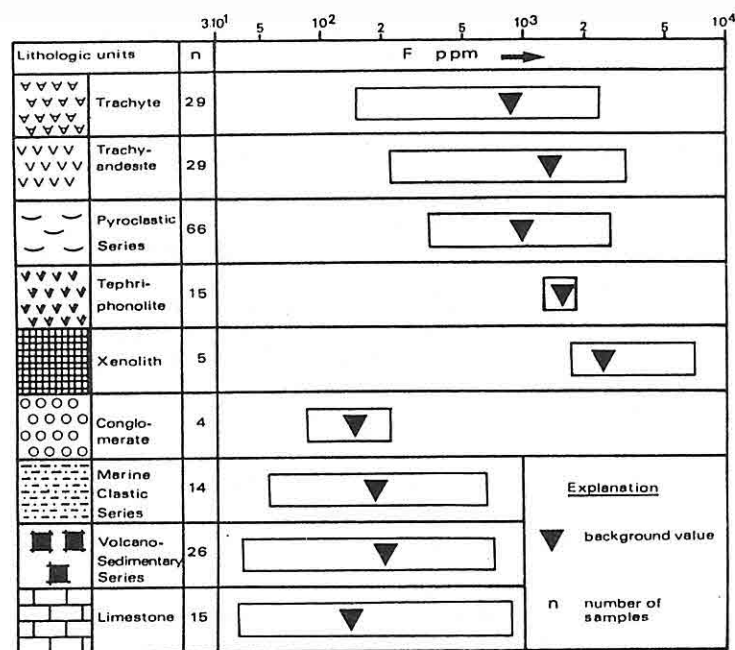
Fig. 3. Range and background values of fluorine in various volcanic rocks of the Gölcük area.

from 1260 to 1820 ppm and a background value of 1635 ppm, which are identical with the fluorine contents of the alkaline phonolite of the African rift systems (Kokubu, 1956). They can be attributed to the mineral phases of fluorapatite, biotite, hornblende, and pyroxene. The pyroclastic series (stage 2) shows fluorine contents in a range from 30 to 2650 ppm and a background value of 1030 ppm, which are identical with the mean value of 1000 ppm of the alkaline pyroclastics (Kokubu, 1956). The F-bearing minerals in the pyroclastic series are F-apatite, biotite, hornblende, pyroxene, fluorite, and

52

1983) and shows an alkaline character (Fig. 2).

The volcanic rocks consist of lava flows and pyroclastic rocks. As a result of the development of the graben systems, the basic tepriphonolite lavas intruded into the space of the recent Gölcük lake accompanied by local eruptions (stage 1) (Özgür et al., 1990). Subsequently, they have been eroded intensively. Around the center of the recent Gölcük caldera, a strong volcanic explosion took place (stage 2). Products of this stage are great masses of friable tuff (150 m), ignimbrite (20 m), and pumice deposition (10 m) dominating the recent landscape. Isolated extrusions of trachyandesites and trachytes have been taken place at various localities in the center and the surrounding area of the caldera (stage 3). They are presented as vents, dikes, and volcanic domes proving that the trachytes are always the latest volcanic event.
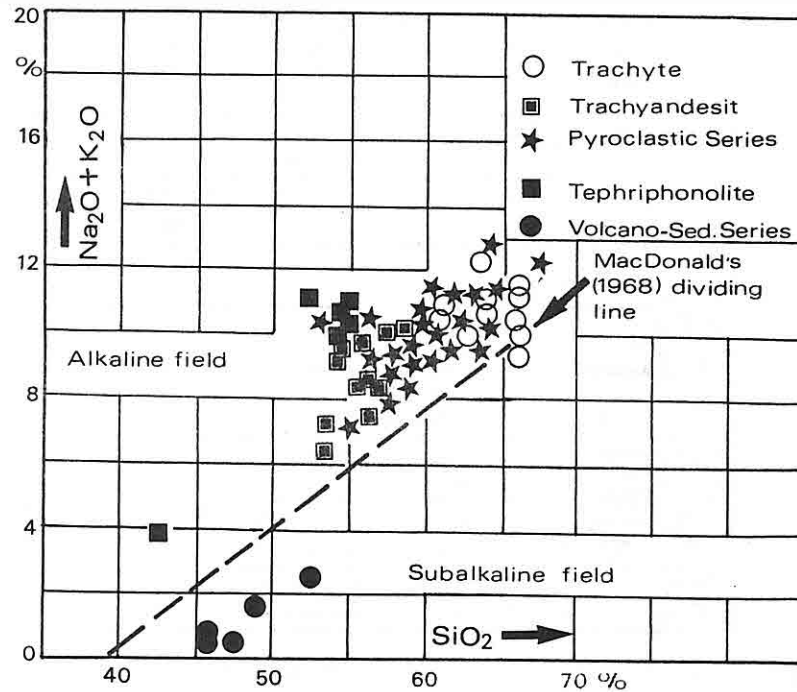
Fig. 2. Alkaline character of the Gölcük volcanic rocks according to the classification schema of (Irvine and Baragar, 1971).

Primarily, the volcanic rocks consist of varying constituents of Na (K)-sanidine, oligoclase, pyroxene, biotite, hornblende, pyroxenitic xenoliths, glassy groundmass, and minor quantities of F-apatite, fluorite , and sphene commonly. Moreover, the tephriphonolite contain augite and nepheline additionally. As F-carrier in the investigated volcanics, pyroxene, hornblende, biotite, F-apatite, fluorite, and glassy groundmass can be considered.

51

1. INTRODUCTION

The Gölcük area, located in the SW part of Isparta (Fig.1), represents a post tectonic Neogene volcanism upon a Mesozoic paleorift (Poisson et al., 1984), the so called Isparta angle between Lycian and Hadim-Hoyran-Beyschir nappes. In central Anatolia, an extensive volcanic activity took place at least as early from Paleocene through Quaternary (Ercan, 1986) as a result of formation of the plate tectonic event which is related to the Afro-Arabian plate being subducted under the Euro-Asiatic plate. The volcanic rocks of the Gölcük area belong to a Pliocene sequence.
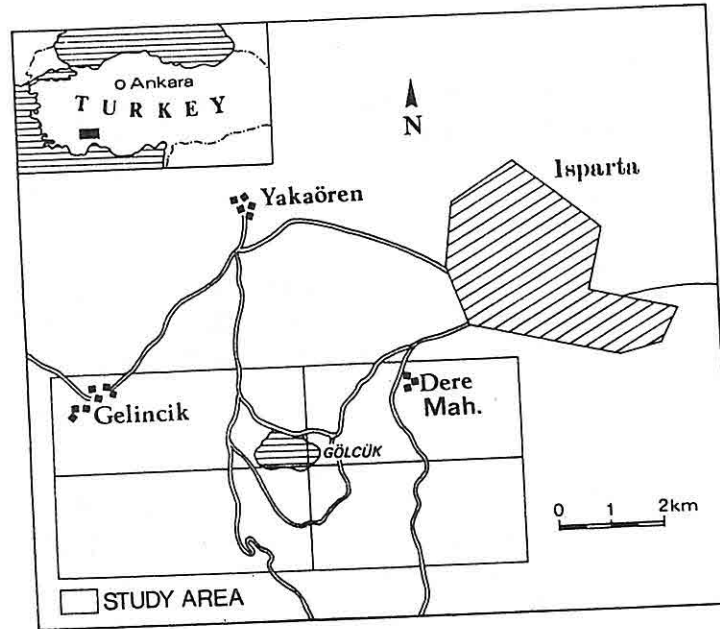
Fig. 1. Location map of the Gölcük area and its environs

The aim of this paper is to elucidate the origin and the distribution of the fluorine contents in various volcanic rocks of the Gölcük area, because the fresh water regime in this area is characterized by unusually high F-concentrations (Özgür et al., in press, 1992).

2. GEOLOGIC SETTING

The Triassic through Upper Cretaceous Akdağ-limestone and the Upper Cretaceous to Lower Tertiary volcano-sedimentary series constitute the basement rocks in the investigated area as allochthonous. They are transgressively overlain by marine clastic series of Eocene and conglomerate of Oligocene age. The volcanic sequence is of Lower Pliocene age (4.07±0.20 to 4.70±0.50 Ma by K-Ar method) (LeFevre et al.,

50

FLUORINE IN PLIOCENE VOLCANIC ROCKS OF THE GÖLCÜK AREA, SW TURKEY

N.ÖZGÜR, A. PEKDEĞER, AND H.J. SCHNEIDER

Institut für Geologie, Geophysik und Geoinformatik der Freien Universität Berlin, Wichernstr. 16, 1000 Berlin 33, Germany

ABSTRACT: *From Paleocene through Quaternary, an extensive volcanic activity took place in central Anatolia which is related to the Afro-Arabian plate being subducted under the Euro-Asiatic plate. The volcanic rocks of the Gölcük area belong to a Pliocene sequence and represent a post tectonic volcanism upon a Mesozoic paleorift in the entire Taurides margin. The investigated area consists of sedimentary and volcanic rocks. As allochthonous, the Triassic through Upper Cretaceous Akdağ-Limestone and the Upper Cretaceous to Lower Tertiary volcano - sedimentary series constitute the basement rocks in the area. The volcanic rocks are tephriphonolite (stage 1), pyroclastic series (stage 2), and trachyandesite with trachyte (stage 3) as vents, dikes, and volcanic domes. They indicate a sodic alkaline character.*

As F-carriers in the volcanic rocks, pyroxene, hornblende, biotite, fluorapatite, and extreme small fluorite crystals can be considered. Additionally, the glassy groundmass can be added to the F-bearing minerals. The fluorine contents in the volcanic rocks show a close correlation with P_2O_5 and are controlled by fluorapatite consequently. Furthermore, it is a novelty that the F-contents display a remarkable depletion from basic towards the acidic rocks which can be linked to discharcing of the F portions during fumarolic stages.

PLATE I
1. Biomicrite with Orbitoides
2. Fossiliferous Intramicrite (Sirtina orbitoidiformis)
3. Biosparite with Intraclast (Dargenioella)
4. Biosparite (Cuneolina)
5. Biomicrite with Mollusca
6. Biomicrite with Intraclast (Laffitteina)
7. Biosparite with Intraclast

300 micron

48
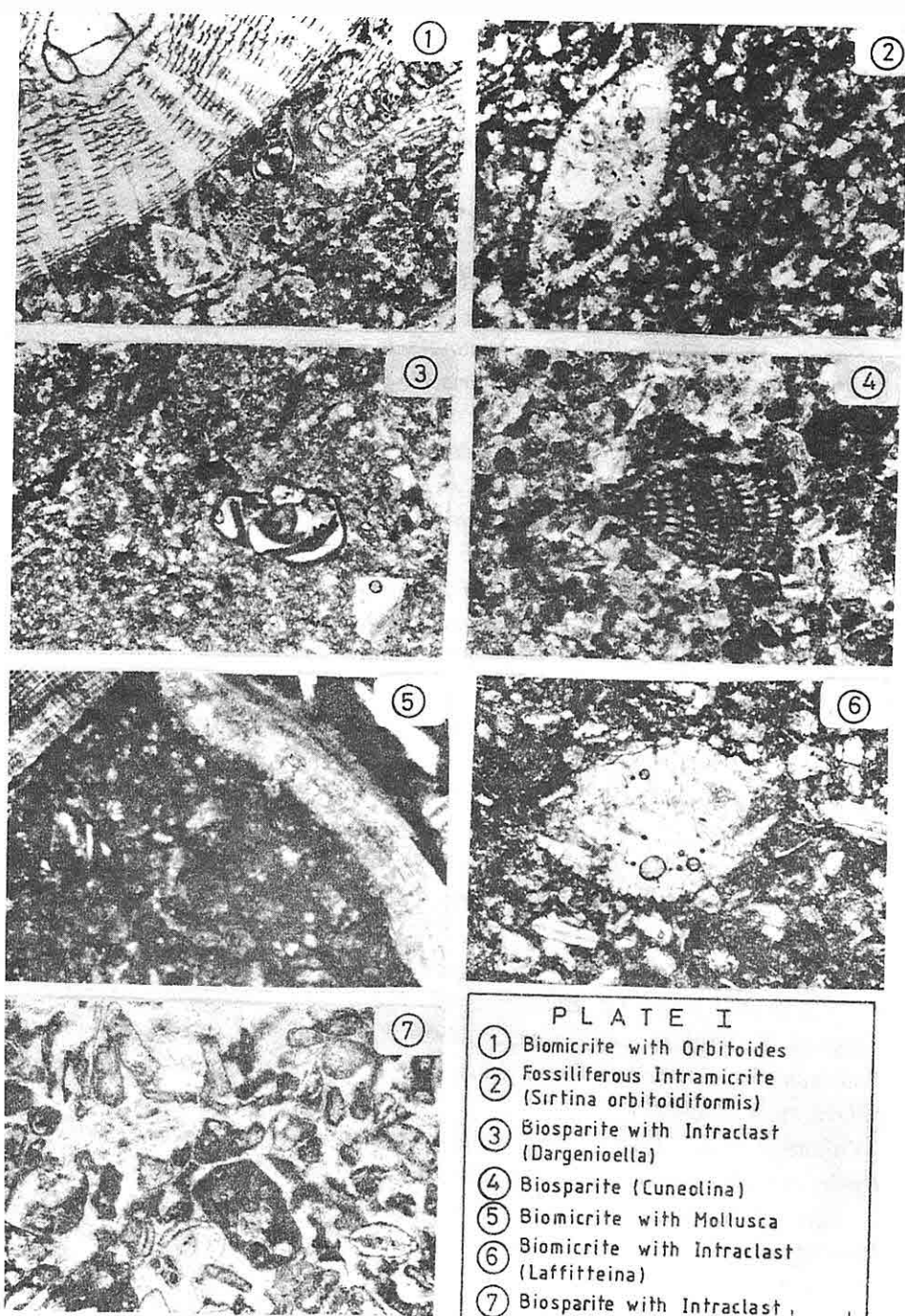
Trace Element Patterns at Anonmarine Cretaceous - Tertiary Boundary, Western Interior, Nature, 307, 224-228.

İnan, N., Kurt, İ., and Demirbaş, M., 1992. Kretase-Paleosen Geçişinde Yeni Paleontolojik Bulgular: İğdir Kireçtaşı (Koyulhisar-Sivas), Abstract of the Geological Congress of Turkey, p.28.

Kyte, F.T., Zhou, Z., and Wasson, J.T., 1980. Siderophile-Enriched Sediments from the Cretaceous-Tertiary Boundary, Nature, 288, 651-656.

Meriç, E., 1985. Loftusia Anatolica Meriç'in Neo-Tetis İçindeki Yayılımı, T.J.K. Bült., 28/1, 11- 19.

Neumann, M., 1958. Revision des Orbitoidés du Crétacé et de l'Eocéne en Aquitaine Occidentale. Mém. Soc. Geol. France, Paris, No 88.

Schmitz,B., 1988. Origin of Microlayering in Worlwide Distributed Ir-rich Marine Cretaceous/Tertiary Boudary Clays, Geology, 16, 1068-1072.

Schmitz, B., Andersson, P., and Dahl, J., 1988. Iridium, Sulfur Isotopes and Rare Earth Elements in the Cretaceous-Tertiary Boundary Clay at Stevns Klint, Denmark, Geochim. Cosmochim. Acta, 52, 229-236.

Serra-Kiel, J., Rabador, A., Samso, M.J., Tosquella, J., 1990. The Biostratigrapy and Environmental Distribution of Benthonic Foraminifera: Introduction to the Early Paleogene of the South Pyrenean Basin, IGCP Project no 286, Early Paleogene Benthol, October, 16-20, 69-74.

Seymen, İ., 1975. Kelkit Vadisi Kesiminde Kuzey Anadolu Fay Zonunun Tektonik Özelliği, Doktora Tezi, İ.T.Ü. Maden Fak. yayını.

Smith, J., and Kyte, F.T., 1984. Siderophile-Rich Magnetic Spheroids from the Cretaceous-Tertiary Boundary in Umbria, Italy, Nature, 310, 403-405.

Tambareau, Y., 1972. Thanétien Supérieur et Illerdien Inferieur des petites Pyrénées du Plantaurel et des Chainoss audois, Trav. Lobor, Univ. Paul. Sabatier, 1/2, Toulouse, p.377.

Terlemez, İ. and Yılmaz, A., 1980. Ünye-Ordu-Koyulhisar-Reşadiye Arasında Kalan Yörenin Stratigrafisi, T.J.K. Bült., 23/2, 179-192.

Toprak, V., Sirel, E., and Özkan, S., 1989. Koyulhisar (Sivas) Dolayında Kretase - Paleosen Geçişi, Akdeniz Üniv., Isparta Müh. Fak. Dergisi, Jeoloji Mühendisliği Seksiyonu, 4, 396-407.

Villatte, J., 1962. Etude Stratigraphique et paléontologie du Montiéen des petites Pyrénées et du Plantaurel, C.N.R.S., Toulouse, p.331.

Yalçın, H., and İnan, N., Tecer Formasyonunda (Sivas) Kretase/Tersiyer Geçişine Paleontolojik, Mineralojik ve Jeokimyasal Yaklaşımlar, Türkiye Jeol. Bült., 35, 1, 1992.

Zhou, L., Kyte, F.T., and Bohor, B.F., 1991. Cretaceous/Tertiary Boundary of DSDP Site 596, South Pacific, Geology, 19, 694-697.

Fig. 3. As a conclusion, MgO in the carbonate fraction, Fe_2O_3, V, Cr, Ni, Zn, Zr, Pb and U concentrations go up and give a peak at the C/T transition or near parts of transition. The differences in the metal element contents are related to the ratio of mafic/felsic minerals in the some stratas of Maastrichtian and Danian. A number of authors (Kyte et al, 1980; Smith et al, 1984; Gilmore et al, 1984; Brooks et al, 1984; Bohor et al., 1986/87; Schmitz, 1988 ; Schmitz et al, 1988; Zhou et al, 1991) suggested that some of the trace elements and especially Ir anomalies were the evidence of meteoridimpact hypothesis of Alvarez et al. (1980). The data in the study area seem to support the asteroid theory. However, detailed clues about C/T boundary will be able to provided by using advanced techniques in the future.

4. ACKNOWLEDGEMENT

5. REFERENCES

Alvarez, L.W., Alvarez. W., Asaro, F., and Michel, H.V., 1980. Extraterrestrial Cause for the Cretaceous-Tertiary Extinction, Science, 208, 1095-1108.

Bohor, B.F., Foord, E.E., Ganapathy, R., 1986/87. Magnesioferrite from the Cretaceous - Tertiary Boundary, Caravaca, Spain, Earth Planet. Sci. Lett., 81, 57-66.

Bozkaya, Ö., and Yalçın, H., 1991.An approach to Upper Cretaceous-Tertiary Transition by Using Clay and Carbonate Mineralogy, Malatya - Hekimhan Province, Eastern Turkey, 7th Euroclay Conference, Dresden, 26-30 August, Proceedings, 1, 141-146.

Brooks, R.R., Reeves, R.D., Yang, X.H., Ryan, D.E., Holzbecher, J., Collen, J.D., Neall, V.E, and Lee, J., 1984. Elemental Anomalies at the Cretaceous - Tertiary Boundary, Woodside Creek, New Zealand, Science, 226, 539-541.

Brönnimann, P., and Wirtz, A., 1962. New Maastrichtian Rotaliids from Iran and Libya, Ecl. Geol. Helv., Spain, 519-528.

Caus, E., and Hottinger, L., 1986. Particularidades de la fauna (macroforaminiferos) del Cretacico Superior Pirenaico, Paleontologia, Evolucio, Spain, 20, 115-123.

Caus, E., 1988. Upper Cretaceous Larger Foraminifera: Paleontological Distribution, Révue Paléobiologie, Geneve, Vol. Spéc. No 2, Benthos 86, 417-419.

Dilley, F.C., 1971. Cretaceous Foraminiferal Biogeography. Faunal Provinces in Space Time, Geological Journal, Special Issue, Proc.of the 17 th International University Geological Congress, No 4, 169-190.

Folk, R.L., 1968. Petrology of Sedimentary Rocks, Hemphill's, Austin-Texas, 170 p.

Gilmore, J.S., Knight, J.D., Orth, C.J., Pillmore, C.L., and Tschudy, R.H., 1984.
46
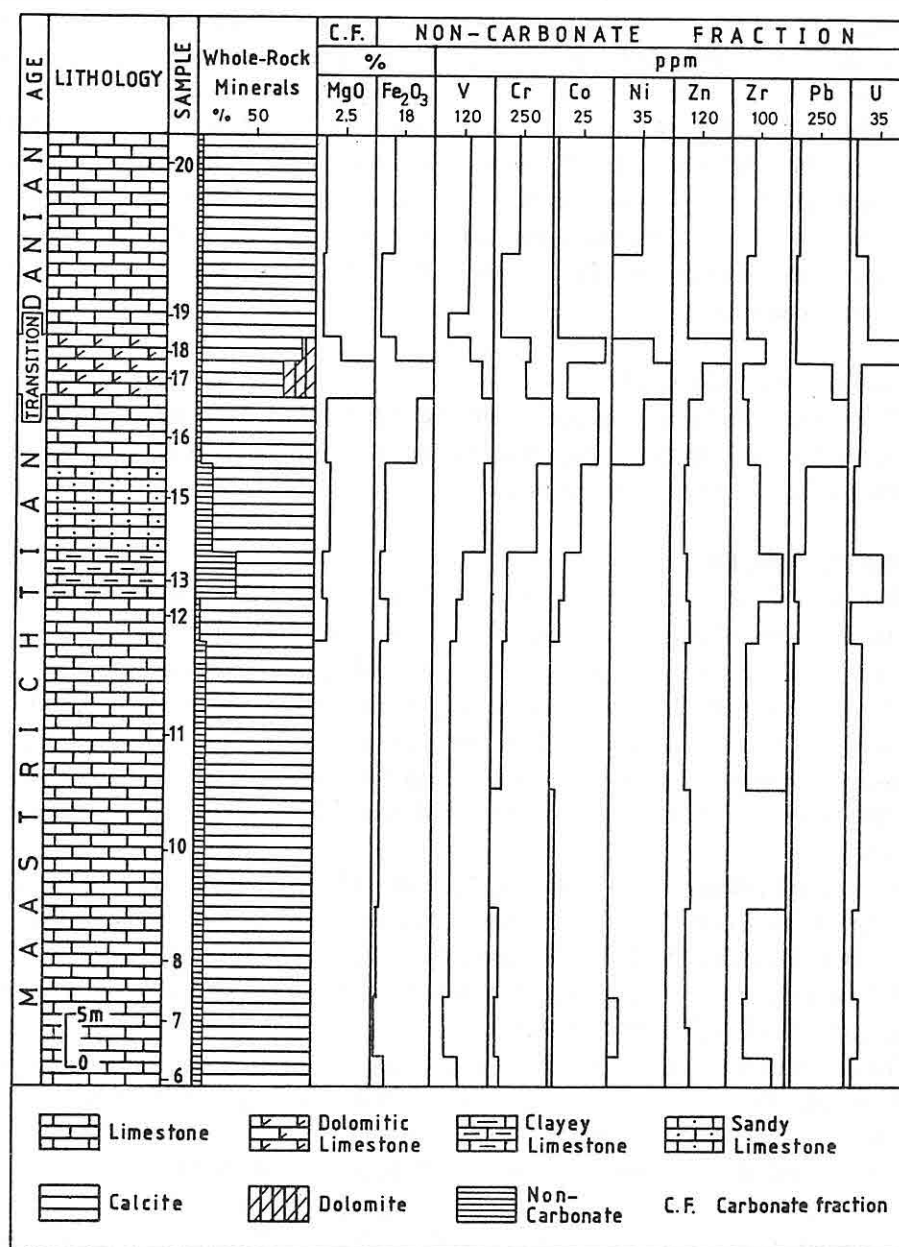
Figure 3. Vertical distribution of major and trace elements at the C/T transition in the Iğdir formation.

3. MINERALOGY AND GEOCHEMISTRY

Carbonate rocks composed of calcite from 62 to 99% in the Iğdir formation. Calcite is unique carbonate mineral in the Maastrichtian and Danian . Dolomite appears at the C/T transition and its amount ranges between 10 and 35%. The importance of this mineral for determination of C/T transition was emphasized at the Hekimhan basin (Bozkaya et al, 1991) and the Tecer formation (Yalçın et al, 1992). Non-carbonate minerals as generally silicates and Fe-oxides are 1 to 38% in the carbonate rocks. The abundance order of these minerals as follow; quartz, K- feldspar (orthoclase and sanidine), epidote (zoisite, clinozoisite), clinopyroxene (augite, diopsite), Fe-oxides (goethite, pyrite), clay (Fe-chlorite, illite, smectite), mica and plagioclase. While all the above minerals have been observed in the Cretaceous series, quartz and K-feldspar were found more than others in the Paleocene. This situation points out that epiclastic transportation is more widespread in the Cretaceous than Paleocene. The amounts of quartz and K-feldspar, particularly goethite increase at the C/T transition. In addition, Fe-chlorite and illite are more abundant in the Cretaceous, simectite in the Tertiary rocks.

On the other hand, chemical analysis results of non-carbonate fractions are given in Table 1 and 2. The vertical distributions of some major and trace elements are presented in

Table 2.Chemical analysis results of carbonate fractions

Sample	Maastrichtian				Transition		Danian	
	CM-12	Cm-13	CM-15	CM-16	CM-17	CM-18	Cm-19	Cm-20
% MgO	1.21	0.76	1.35	1.01	5.14	2.26	0.74	0.99
ppm								
Li	1	1	1	1	1	1	1	1
Na	290	279	312	235	248	268	200	145
K	286	373	335	112	147	220	229	153
Cr	18	9	10	15	16	21	15	21
Mn	78	90	75	67	65	40	30	32
Fe	1546	440	1677	1046	1620	718	505	461
Co	39	31	29	30	24	26	20	27
Ni	237	123	218	197	53	52	62	53
Cu	7	11	5	4	6	6	6	6
Zn	29	73	96	66	60	48	50	47
Sr	1014	1209	959	907	725	887	1028	796
Pb	64	63	57	58	38	37	37	37
%Soluable	96.54	62.02	87.29	96.94	95.56	98.53	98.26	96.07

44

Table 1. Chemical analysis results of non-carbonate fractions.

% Oxide	Maastrichtian									Transition		Danian	
	CM-6	Cm-7	CM-8	CM-10	CM-11	CM-12	CM-13	CM-15	CM-16	CM-17	CM-18	CM-19	Cm-20
SiO_2	51.72	52.93	58.61	77.31	52.05	55.40	61.73	52.15	40.79	36.57	48.92	34.32	53.36
TiO_2	0.77	0.23	0.32	0.40	0.28	0.55	0.83	0.69	0.98	0.75	0.79	0.27	0.88
Al_2O_3	16.56	18.87	19.27	11.54	16.19	17.92	17.42	15.44	12.14	11.54	16.14	9.51	16.45
$Fe_2O_3(+)$	8.18	1.87	2.54	4.25	4.58	9.36	3.52	6.17	26.84	36.11	12.82	4.03	12.82
MnO	0.03	0.01	0.01	0.01	0.01	0.01	0.02	0.01	0.03	0.01	0.01	0.01	0.01
MgO	2.43	2.20	2.71	0.39	1.45	2.11	1.91	1.05	1.24	1.53	2.36	1.71	1.79
CaO	0.77	1.11	1.46	0.53	3.70	1.05	0.60	2.35	0.95	1.07	2.68	10.35	1.70
Na_2O	0.28	0.18	0.17	0.20	0.18	0.24	0.61	0.57	0.23	0.17	0.20	0.14	0.25
K_2O	9.02	8.03	8.76	1.15	8.46	9.78	9.59	8.47	6.62	4.95	6.42	2.83	6.55
P_2O_5	0.04	0.03	0.04	0.14	0.04	0.05	0.03	0.08	0.11	0.14	0.07	0.05	0.05
LOI	8.80	13.70	5.09	3.58	11.70	2.15	2.45	11.70	9.50	6.03	8.10	35.32	5.07
TOTAL	98.60	99.16	98.98	99.50	98.64	98.62	98.71	98.68	99.43	98.87	98.51	98.54	98.93

ppm													
Li			30	37	16		18				21		20
V	113	58	70	69	67	101	117	205	241	207	142	61	152
Cr	111	74	83	19	112	136	136	402	525	265	321	68	228
Co	6	6	6	6	1	8	12	24	39	12	45	4	4
Ni	2	14	2	2	2	2	2	2	39	71	51	2	38
Cu	35	35	32	57	30	32	42	38	32	37	53	32	37
Zn	95	80	82	90	71	89	76	66	71	130	236	68	73
Rb	117	95	99	87	77	102	111	99	56	56	128	69	95
Sr	51	165	111	1916	60	60	111	216	30	15	26	72	15
Y	27	27	27	27	27	27	27	27	27	27	27	27	27
Zr	159	56	71	208	61	102	193	97	59	45	119	70	87
Nb	23	19	20	21	20	20	24	22	21	20	23	20	21
Ba	486	915	654	242	413	706	626	352	250	236	307	208	238
Pb	68	56	50	33	61	91	42	140	503	356	58	53	78
Th	9	7	7	8	2	6	7	9	7	6	2	10	9
U	6	11	6	12	12	3	46	8	16	17	70	18	8

LOI = Loss on Ignition (1000°C), Fe_2O_3 (+) = Total Iron

43

Figure 2. Lithological and biostratigraphical column of the Dağönü section in the İğdir
formation

42
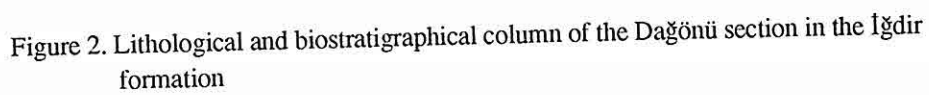
Physical, sedimentological and tectonic changes have never been seen at the C/T transition of the İğdir formation. The C/T transition is firstly detected with fossils (Fig. 2), after that mineralogical and geochemical clues are correlated and interpreted with biostratigraphic results.

Two associations of benthic foraminifers were recognized in the İğdir formation. In the lower part, Association I comprising *Orbitoides medius* (d'ARCHIAC), *Orbitoides apiculatus gruenbachensis* PAPP, *Omphalocyclus macroporus* (LAMARCK), *Hellenocyclina beotica* REICHEL, *Siderolites calcitrapoides* LAMARCK, *Loftusia minor* COX. *Smoutina cruysi* Drooger and *Laffitteina* aff. *marsicana* FARINACCI is present. These fossils indicate the Upper Maastrichtian age at the reefal facies of eastern part of Neo-Tethys (Neumann, 1958; Villatte, 1962; Brönnimann et al., 1962; Tambareau, 1972; Meriç, 1985; Caus et al., 1986; Caus, 1988). Two microfacies such as packed biomicrites and fossiliferous intramicrites were distinguished in these levels of Upper Maastrichtian (plate I, 1-2). Textural nomenclatures were made according to Folk (1968) classification. Microcrystalline calcite matrix is the most dominant orthochem in the carbonate rocks, but recrystallization of sparry calcite cement are also at times common. Packed biomicrites contain abundantly Association I of foraminifers (90 %), whereas it is rare (10 %) in the fossiliferous intramicrites.

Association I of foraminifers are not generally preserved at the C/T transition, which is 5 m in thickness. These beds cover biosparite with about 80-90 % rudist shell fragments and poorly washed biosparite.

Association II of benthic foraminifers including *Dargeniopella sp.* (plate I, 3), *Cuneolina ketini* İNAN (Plate I, 4), *Laffitteina* aff. *Lecalvezae* RAHAGHI, *Idalina* aff. *sinjarica* GRIMSDALE, *Moncharmontia sp.* appears at the beginning of Paleocene. This association is typical by the abundance of *Laffittenia* in the biomicrite with mollusca (Plate I, 5) and biomicrite with intraclast (Plate I, 6). This fossil was supposed as a new species and liken to *L. le calvezae* for the present. The upper facies of Danian consists of biosparite with intraclasts that is associated with foraminifers of Associated II, algae and bryzoa (Plate I, 7).

As a result, the benthic foraminifers of Association I show that the environment is characterized by shallow, warm marine, surrounding of reef and main reef in the subtropical climate conditions (Dilley, 1971). Both the deficiency of algae ratio and sometimes the increasing of sparry calcite cement remind the back of reef environment. The locations of decreasing of Association I foraminifers and increasing of intraclast ratio are considered as tidal environments. *Laffitteina* is the most dominant benthic foraminifer in Association II. This genus points out the restricted shelf-lagoon with high salinity between terrestrial and marine environments (Caus et al. 1986; Serra et al, 1990).

In that case, it exists a marine regression which is converted into back reef and tidal flats in the Maastrichtian, lagoon in the Paleocene.

41

1. INTRODUCTION

The study subject is the İğdir formation, which is located between Reşadiye and Koyulhisar on the Northern Anatolian Fault Zone (Fig. 1). This unit was first described and named by Terlemez and Yılmaz (1980) as İğdir limestone member of Reşadiye formation. They reported that it was deposited in neritic environment in Maastrichtian (Toprak et al, 1989). Also defined the unit as very shallow marine environmental and dated as Maastrichtian. In spite of these ideas, İğdir formation is aged as Upper Maastrichtian-Lower Thanetian by İnan et al.(1992). In the present study, the C/T transition was paleontologically determined and lithological, mineralogical-geochemical differences in this transition are investigated.
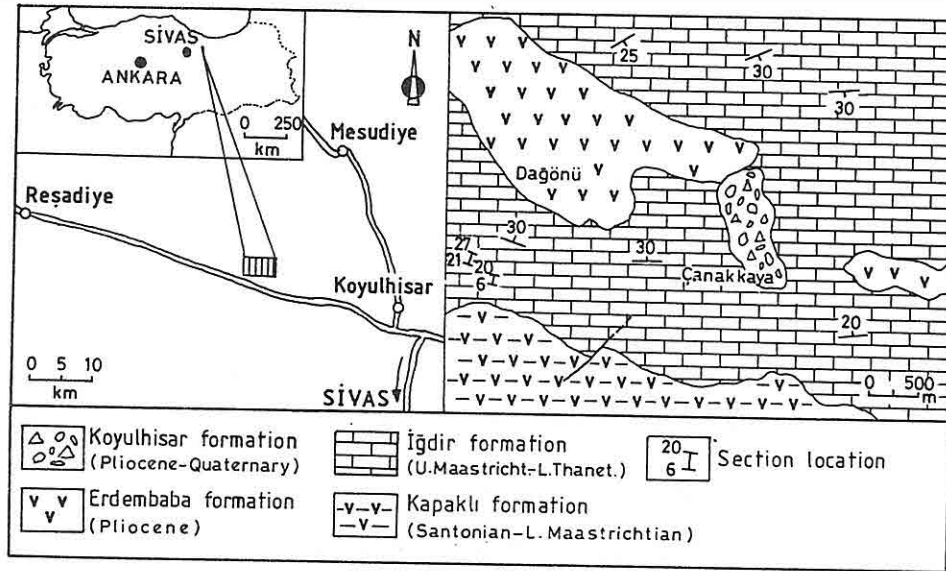
Figure 1. The location and simplified geological map of study area.

2. STRATIGRAPHY AND PALEONTOLOGY

İğdir formation conformably overlies the Kapaklı formation, which is represented by limestone, marl, tuff, agglomerate, sandstone, siltstone, claystone alternations. This unit is Upper Campanian-Lower Maastrichtian age according to Seymen (1975), and Upper Santonian-Middle Maastrichtian age to Toprak et al.(1989). Stratigraphical sequence continues with Gölköy formation of Paleocene age, which is composed of limestone, clayey and tuffaceous limestone, tuffite and sandstone alternations (Motorcu, 1980). However, İnan et al.(1992) stated that Gölköy formation which has vertical and lateral transition with İğdir formation is Danian-Lower Thanetian age.

40

PALEONTOLOGICAL FEATURES AND MINERALOGICAL - GEOCHEMICAL CHANGES OF THE CRETACEOUS / TERTIARY TRANSITION AT THE İĞDİR FORMATION, KOYULHİSAR-SİVAS, TURKEY

Hüseyin YALÇIN and Nurdan İNAN

Cumhuriyet University, Dept. of Geological Engineering, 58140 Sivas / Türkiye

ABSTRACT : *The packed biomicrite with abundantly rudist shell fragments and fossiliferous intramicrites in the Upper Maastrichtian age are placed at the bottom of the İğdir formation, which is formed of completely carbonete rocks. Dolomitic sparites are quite common at the C/T transition. Generally the biosparites including frequently* **Laffiteina** *aff.* **lecalvezae** *of the Danian age are situated at the top of this formation. Typical minerals of the C/T transition are dolomite and geothite; and amounts of MgO in the carbonate fraction and Fe_2O_3, V, Cr, Co, Ni, Zn, Zr, Pb, U in the non-carbonate materials give considerable anomaly.*

39

continental crust. The samples taken from Kaynarca-I well also show similar features towards depth.

6. ACKNOWLEDGEMENTS

We give our thanks to all people who worked at various stages to complete this study and to the M.T.A General Directorate.

7. REFERENCES

Akyürek, A.and Soysal, Y. Kırkağaç, 1978. Soma (Manisa), Savaştepe, Korucu, Ayvalık (Balıkesir), Bergama (İzmir) Civarının Jeolojisi. MTA Rapor No: 6432, Ankara.

Ercan, T., Günay, E., Çevikbaş, A., Ateş,M., Türkecan, A., Can, B., ve Erkan, M., 1984. Dikili-Çandarlı, Bergama (İzmir) ve Ayvalık, Edremit, Korucu (Balıkesir) Yörelerinin Jeolojisi ve Mağmatic Kayaçların Petrolojisi. MTA Rapor No:7601, Ankara.

Ercan, T., Satır,M., Kreuzer, H., Türkecan, A., Günay, E., Çevikbaş, A., Ateş, M., Can, B. 1985. Batı Anadolu Senozoyik Volkanitlerine Ait Yeni Kimyasal İzotropik ve Radyometrik Veriler Yorumu. T.J.K. Bült., 28, 2, 121-137.

Gottini, V. , 1968.The TiO_2 Frequency in Volcanic Rocks. Geol. Rdsch., 57, 930-935.

Irvine, T.N. and Baraagar, W.R.A. 1971. A Guide to the Chemical Classification of the Common Volcanic Rocks. Can. Jour. Earth Scien., 8, 523-548.

Kuno, H., 1960.High-Alumina Basalt. Journal of Petrology, 1, 121-145.

Macdonald, G. A. and Katsura, J.,1964. Chemical Composition of Hawaiian Lavas. Journal of Petrology, 5, 82-133.

Miyashiro, A.,1975. Petrology and Plate Tectonics. Rev. Geophys. sp. Phys., 13, 94-98,

MTA-JICA, 1987.The Pre-Feasibility Study on the Dikili-Bergama Geothermal Development Project in the Republic of Turkey. Progress Report II, MTA, Ankara.

Yılmazer, S., Gevrek, A. İ., Sünger, Z., Çetiner, L., 1990.. İzmir-Dikili-Kaynarca Jeotermal Sahası Kaynarca-I, Derin Jeotermal Sondajı Kuyu Bitirme ve Değerlendirme Raporu. MTA, Ankara .

The chemical analysis of 12 samples from the geothermal area have been done in the laboratory of M.T.A . According to the alcaline-silica diagrams of Irvine and Baragar (1975), Macdonald and Katsura (1964), Kuno (1960) and the SiO_2 - FeO/MgO diagram of Miyoshiro (1975), the andesites are of calcalkaline character. Also Rittmann indice is less than 4.

According to the diagram showing relationships between logarithmic values of Rittmann
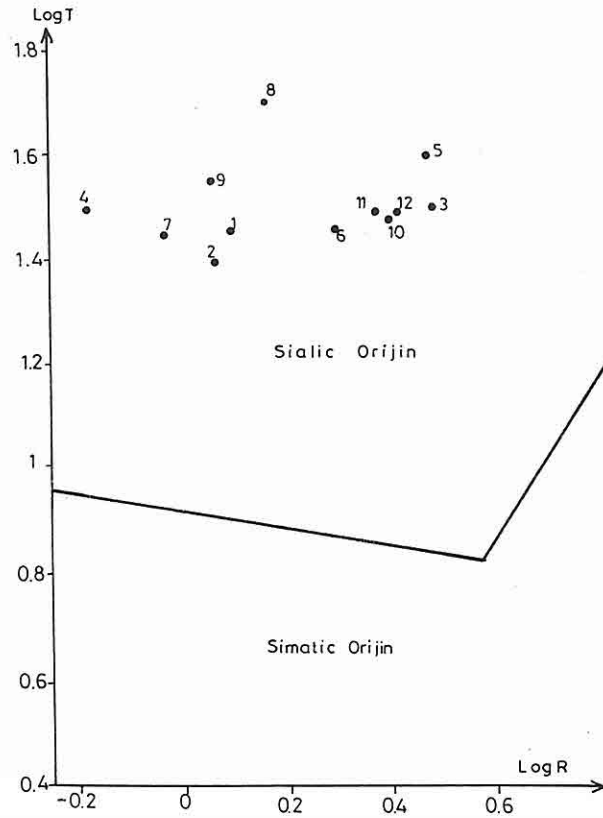
Figure 6. Gottini (1968) diagram of the volcanics

and Gottini indices, the andesites are of sialic origin.

According to geochemical studies of Ercan et al. (1985) on 22 samples outcroping at Ayvalık, Edremit, Dikili, Bergama, Soma, Bigadiç, Kepsut, Sındırgı, Gördes, Demirci, Kula, Denizli and Söke in Western Anatolia, the whole volcanics except Kula and Denizli are of calcalkaline character and have been occured from anatectic melting of the

37

Samp.No.	1	2	3	4	5	6	7	8	9	10	11	12
Depth	K-1050	K-1063	K-113	K-588	K-002	K-753	K-1083	K-1046	K-1047	K-1379	K-001	K-102
SiO_2	62.6	63.4	63.3	66.0	65.0	59.1	63.0	63.5	60.7	59.8	62.9	64.4
Al_2O_3	12.5	10.8	16.0	13.2	16.0	11.2	11.5	14.9	14.7	15.8	15.9	16.3
Fe_2O_3	6.1	5.8	5.2	4.8	4.6	5.8	5.2	4.2	6.3	5.7	5.4	5.5
FeO	4.00	3.45	0.86	1.72	0.57	2.00	3.30	3.16	4.45	2.87	0.86	0.58
MnO	0.1	0.1	0.1	0.1	0.1	0.1	0.1	0.1	0.1	0.1	0.1	0.1
MgO	2.48	2.65	1.22	1.42	1.20	2.60	2.75	1.52	2.65	1.70	2.25	0.92
CaO	3.85	4.40	4.00	2.85	3.40	5.00	4.80	3.20	3.50	4.25	4.80	3.60
Na_2O	0.90	0.90	4.00	0.60	3.90	0.40	0.60	0.90	0.60	3.30	3.40	3.75
K_2O	4.10	3.90	3.60	3.25	3.75	5.80	3.75	4.60	4.00	3.25	3.50	3.70
TiO_2	0.4	0.4	0.4	0.4	0.3	0.4	0.4	0.3	0.4	0.4	0.4	0.4
P_2O_5	0.2	0.3	0.2	0.2	0.2	0.4	0.2	0.2	0.2	0.2	0.2	0.2
A.K.	4.65	7.27	1.83	6.99	0.92	9.50	7.50	6.00	6.77	5.72	1.00	0.95
Bittmann Indice	1.27	1.13	2.84	0.6	2.66	2	0.94	1.47	1.19	2.55	2.39	2.59
Gottini Indice	29	24.75	30	31.5	40.33	27	27.25	46.66	35.25	30.5	31.25	31.37

Table 1. Major element chemical analyses and Rittmann-Gottini index of Kaynarca-I volcanics (Only Sample No: 5 and 11 were taken from out-crop)

between 0.6-2.84. Roughly, if Rittmann indice is less than 4, the lava is of calcalcaline character (Ercan et al.,1984).

According to the diagram showing relationships between logarithmic values of Rittmann and Gottini indices (1968), the volcanics are of sialic origin (Fig.6).

Summarizing the geological data, the volcanic rocks were determined as calcalkaline and of sialic origin.

5. CONCLUSIONS

Kaynarca-I geothermal exploration well was drilled in Dikili-Kaynarca (İZMİR) geothermal area to a depth of 1500m. As a result of the petrographic studies, biotite-hornblend andesite and pyroxene-biotite-hornblend andesite have been confirmed as Yuntdağ-III volcanics. The underlying Demirtaş pyroclastic rocks consist of agglomerates and tuffs. Yuntdağ-I volcanics contain altered andesite.

36
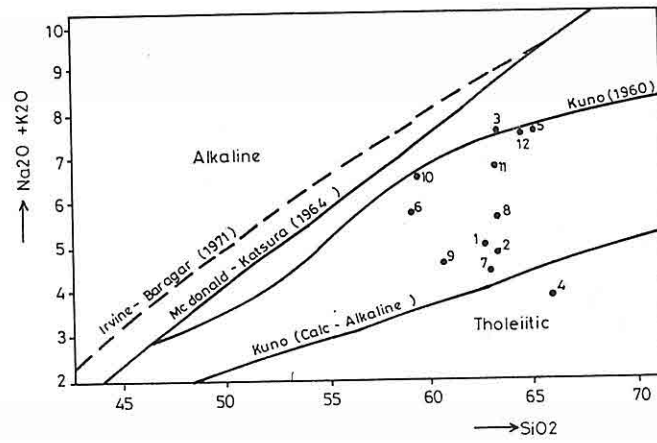
Figure: 4. Classification of the volcanics according to their alkali - silica contents.
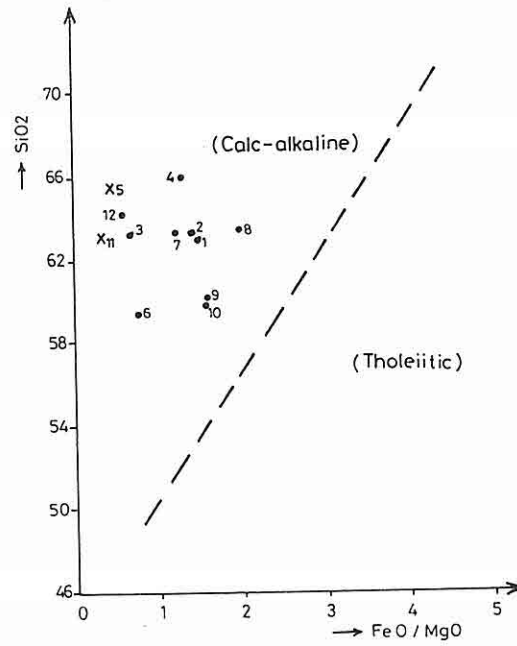
Figure: 5. Classification of the volcanics according to their SiO2 - FeO/ MgO contents.

35

Petrography of Yuntdağ-I volcanics

The petrographic studies of the Yuntdağ-I volcanics were carried out on the samples K-001, K-1047 m, K-1347 m and K-1379 m.

Primary structures of the phenocrystals and the ground-mass are lost in Yuntdağ-I volcanics by tectonics processes and alteration. The ground-mass has been altered into clay minerals, calcite, silica and chlorite. The traces of microlites occasionally can be seen.

The mineralogical composition of altered andesite is given as following :

Plagioclase : 50 % of the thin-section is composed of plagioclase crystals are almost completely altered into calcite, sericite, chlorite and silica with some relicts.

Amphibole : Amphiboles form about 20 % of the thin-section. The subidiomorph or idiomorph crystals have been partly altered into silica and magnetite.

Pyroxene : They only exist in thin-sections of sample K-001m. The subidiomorph or xenomorph pyroxene crystals have been slightly transformed into magnetite along edges.

Biotite : Biotite forms approximately 10 % of the rock. They observed either as phenocrystals or as small crystals. Some of them have been transformed into magnetite along edges or cleavage traces.

Accessory minerals : A small amount of apatite appears as minute six-sided prismatic crystals or short prismatic crystals. Also, there are a few short prismatic zircon crystals.

Magnetite : A small amount of magnetite crystals shaped idiomorph, subidiomorph or xenomorph. Also some of mafic minerals have been partly altered into magnetite.

Secondary silica and secondary calcite : The rocks contain some cracks and fractures which are usually filled with secondary silica or calcite.

4. GEOCHEMISTRY OF VOLCANIC ROCKS

In the geochemistry laboratory of M.T.A chemical analyses have been done on 10 samples which have been taken from Kaynarca-I well and 2 samples which have been collected from outcrops in the study area. The chemical analyses results are listed and Rittmann-Gottini indices are given in Table.1.

The volcanic rocks indicate a calcalkaline character by using the alkaline-silica diagram of Irvine and Baragar (1971), Macdonald and Katsura (1964), Kuno (1960) in Fig.4.

The volcanic rocks were also established as calcalkaline by using the SiO_2-FeO/MgO diagram of Miyashiro (1975) in Fig.5.

They also show calcalkaline characteristic according to Rittmann indice changing

34

3. PETROGRAPHY OF VOLCANIC ROCKS

Mineralogic-petrographic investigations were carried out on samples of Yuntdağ-III volcanics, Demirtaş pyroclastic rocks and Yuntdağ-I volcanics.

Petrography of Yuntdağ-III volcanics

Petrographic studies of Yuntdağ-III volcanics are carried out using samples from different depths (102m, 113m, 167m). They have been classified as biotite-hornblende andesite and pyroxene-biotite-hornblende andesite according to their mineralogical composition.

Plagioclase : 55 % of the thin-section is composed of plagioclase crystals which occur either as phenocrystals or as microlites. The plagioclases are generally subidiomorph, showing zoning, albite twinning and internal alteration by clays. Some of the plagioclase crystals contain amphibole and biotite crystals. Most of them show cracks, sometimes filled by ironoxide. They have andesinitic composition.

Amphibole : Amphiboles forms about 20-25 % of the rock. They occur either as lath-shapped crystals or as small crystals. Amphibole crystals are usually subidiomorph or idiomorph. Most of the amphibole crystals show cracks.They are often surrounded or replaced by magnetite. Also some of them show alteration into chlorite and talc.

Biotite : Biotite forms approximately 7 % of the thin-section. The subidiomorph biotite crystals have been altered into magnetite along edges or cleavage traces.

Pyroxene : A small amount of subidiomorph or idiomorph clinopyroxene crystals are observed in the samples of K-102m and K-167m. Some of them show h'(100) twins and alteration into chlorite and talc.

Apatite : A small amount of apatite exists within plagioclase and biotite as final crystallisation.

Magnetite : The small idiomorph or xenomorph opaque minerals appear in the ground-mass. Also the amphibole and biotite have been partly or completely altered into magnetite.

Ground-mass : The ground-mass is composed of plagioclase microlites, cryptocrystalline mafic minerals and glassy material. It has been generally altered into clay minerals.

Petrography of Demirtaş pyroclastic rocks

The volcanic rock fragments and crystals of quartz, feldspar, biotite, hornblende are observed within a glassy ground-mass of agglomerates. The microcrystalline quartz, feldspar, biotite and opaque minerals are observed within cryptocrystalline ground-mass of tuff samples.

AGE		FORMATION	LITHOLOGY	EXPLANATION
HOLOCENE				Alluvium
N E O G E N E	P L I O C E N E	YUNTDAĞ III VOLCANICS		Sulukaya biotite hornblende andesite
				Kocatepe biotite hornblende andesite
				Çamtepe rhyolite
				Çamtepe biotite dacite
				Dikili biotite hornblende andesite
				Kocaağıl pyroxene hornblende andesite
	M I O C E N E	YUNTDAG II VOLCANICS		Pyroxene andesite
				Hornblende pyroxene andesite
		SOMA FORMATION		Demirtaş pyroclastic rocks
				Felsic pyroclastic rocks dacite ignimbirit
		YUNTDAG I VOLCANICS		Alterated andesite

Figure: 2. Geologic succession of Kaynarca area
(From MTA- JICA 1987)
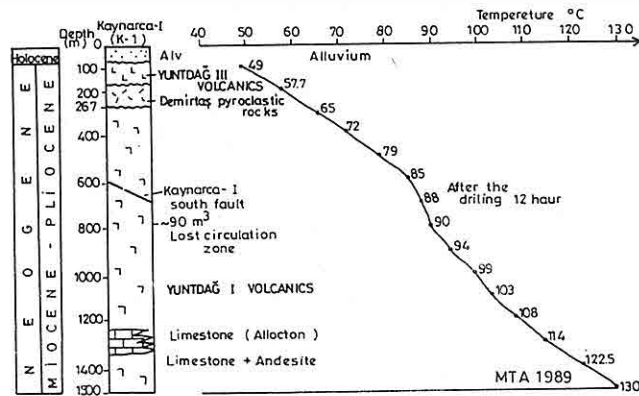
Figure : 3. Geologic column of K-1 hole

32

Figure 1. Location and geological map.

31
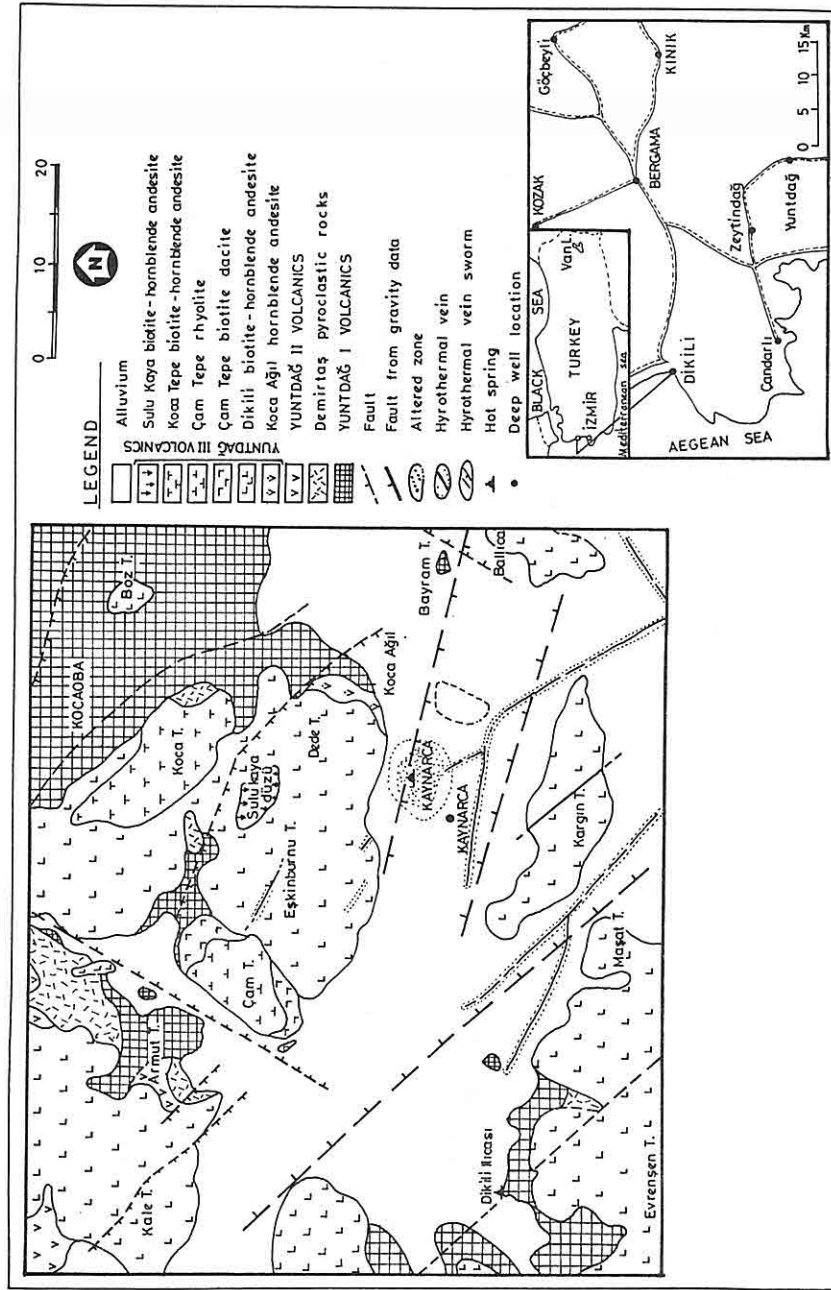
1. INTRODUCTION

The geothermal exploration well with a depth of 1500 m was drilled in Dikili - Kaynarca area, 90 km north of Izmir (Fig. 1). 10 samples were taken from Kaynarca-I and 2 samples were collected from the geothermal area. The petrographic investigation and chemical analyses of total 12 samples have been carried out in laboratories of the Mineral Research and Exploration Institute (MTA).

Field observations have been made by the following authors: Akyürek and Soysal (1978) have made a study of the geology of the Dikili-Kaynarca volcanics with calcalkaline characteristic. Ercan et al. (1984) have described the petrography of magmatic rocks and geology. MTA-JICA (1987) have investigated petrographical and petrochemical features of volcanics.

2. GENERAL DESCRIPTION OF THE ROCKS

The geological map of Dikili-Kaynarca geothermal area has been taken from MTA-JICA (Fig.1, 2). There are andesite, pyroclastic rocks and alluvium in the area. The volcanics, as they show differences in mineralogic composition, structure and alteration productes, were described Yuntdağ-I volcanics, Yuntdağ-II volcanics and Yuntdağ-III volcanics.

Yuntdağ-III volcanics were divided into Koca Ağıl hornblende andesite, Dikili biotite-hornblende andesite, Çam Tepe biotite-hornblende dacite, Çam Tepe rhyolite, Koca Tepe biotite-hornblende andesite and Sulu Kaya biotite-hornblende andesite (MTA-JICA,1987).

Kaynarca-I well has cut altered andesite of Yuntdağ-I volcanics of Miocene-Pliocene age. Demirtaş pyroclastic rocks of Pliocene age and Yuntdağ-III volcanics as Dikili hornblende andesite (Fig.3).

The lithological description of the well sequence is given from top to bottom as follows (Yılmazer et al.,1990):

- Alluvium (0-74 m)= The sediments are composed of clay, sand and volcanic rock fragments.

- Yuntdağ-III volcanics (74-167 m)= The colour of the rocks is grayish brown or reddish brown. The volcanics show cracks and some of them have been altered by secondary silica and clay minerals.

- Demirtaş pyroclastic rocks (167-267 m)= They consist of agglomerate and tuff. The agglomerates are pinkish gray or brownish gray and contain volcanic rock fragments and silica gravels. The tuff consists of very fine particles.

- Yuntdağ-I volcanics (267-1500 m)= The strongly altered andesites are of greenish gray or reddish gray colour. Tectonical senses can be deduced from cracks and fractures in the rocks. The limestone which contains volcanic rock fragments is found between 1262-1315m within Yuntdağ-I volcanics.The limestone is thought to be allochthonous (Yılmazer et al., 1990).

30

PETROGRAPHIC AND GEOCHEMICAL INVESTIGATIONS OF VOLCANIC ROCKS FROM THE BY KAYNARCA - I WELL (DİKİLİ - KAYNARCA - İZMİR)

Ender SARIFAKIOĞLU[1], Servet YILMAZER[1], Ali İhsan GEVREK[2]

[1]*MTA Ege Bölge Müdürlüğü, İzmir / TÜRKİYE*
[2]*MTA Genel Müdürlüğü, Ankara / TÜRKİYE*

ABSTRACT : *Kaynarca-I deep geothermal exploration well has been drilled at Dikili-Kaynarca geothermal area north of İzmir in Western Anatolia.*

Kaynarca-I well has cut Yuntdağ-I volcanics, Demirtaş pyroclastic rocks, Yuntdağ-III volcanics, which are of Tertiary age and alluvium of Quaternary age. Kaynarca-I well hasn't cut Yuntdağ-II volcanics. Yuntdağ-I volcanics are composed of very altered andesite. Demirtaş pyroclastic rocks consist of agglomerate and tuff. Yuntdağ-III volcanics are composed of biotite - hornblende andesite or pyroxene - biotite - hornblende andesite.

According to diagrams, reflecting the chemical analysis, the volcanics show calcalkaline characteristic and sialic origin.

29

of as much as >100 ppm, and even Fatsa at 1 ppm Hg would be deemed anomalous by many explorationists.

Overall, the trace element geochemistry for the 22 prospects/districts shown on Figures 3-11, shows, with local single element and/or single prospect exceptions, a clear epithermal trace element geochemical signature that is very similar to those summarized by Tooker (1985); Berger (1985); Romberger (1986) and many others for epithermal disseminated precious metal deposits of various varieties (volcanic and sediment-hosted) in the western United States, Japan, and elsewhere.

Clearly, amongst those discussed, some prospects are more favorable to and "prospective" of ore grade mineralization than are others and on the basis of surface rock chip geochemistry we would have to assign Örencik, Kurşunlu, Karakaya, Celaller, Gümüşler, Akmaden and possibly Çakmakdere at İvrindi to that group.

5. ACKNOWLEDGEMENT

6. REFERENCES

Berger, B.R., 1985. Geologic-Geochemical Features of Hot-Spring Precious Metal Deposits. in, Tooker, E.W. Ed., Geologic Characteristics of Sediment and Volcanic-Hosted Disseminated Gold Deposits--Search for An Occurance Model: U.S. Geological Survey Bull. 1646, p47-54.

Erler, Y.A., and Larson, L.T., 1990. Genetic Classification of Gold Occurance of he Aegean Region of Turkey. in, M.Y. Savascin and A.H. Eronat, Eds., Proceedings of the International Earth Science Congress on Aegean Regions, 1990, İzmir, Turkey. Vol. 1, p.12-23.

Larson, L.T., 1989. Geology and Gold Mineralization in Western Turkey. Mining Engineering, v. 41, p. 1099-1102.

Larson, L.T. and Erler, A., 1992. Geologic Setting and Lithogeochemical Characterization of two Disparate Precious Metal Prospects, Western Turkey. Journ. Geochem. Expl. v. 35, (in press).

M.T.A., 1979. Turkiye Antimon Envanteri. Ankara, M.T.A. Publication No. 178, 55 p.,

Romberger, S.B., 1986. Disseminated Gold Deposits, in, R.G. Roberts and P.A. Sheahan, Eds., Ore Deposit Models, Geoscience Canada, Reprint Series 3, p. 21-30.

Tooker, E.W., 1985. Discussion of the Disseminated Gold-Ore Occurance Model. in, Tooker E.W., Ed., Geologic Characteristics of Sediment-and Volcanic-Hosted Gold Deposits --Search for An Occurance Model: U.S. Geological Survey Bull. 1646, p.107-150.

Yıldız, M., and Bailey, E.H., 1978. Mercury Deposits in Turkey. U.S. Geological Survey Bull. 1456, 80 p.
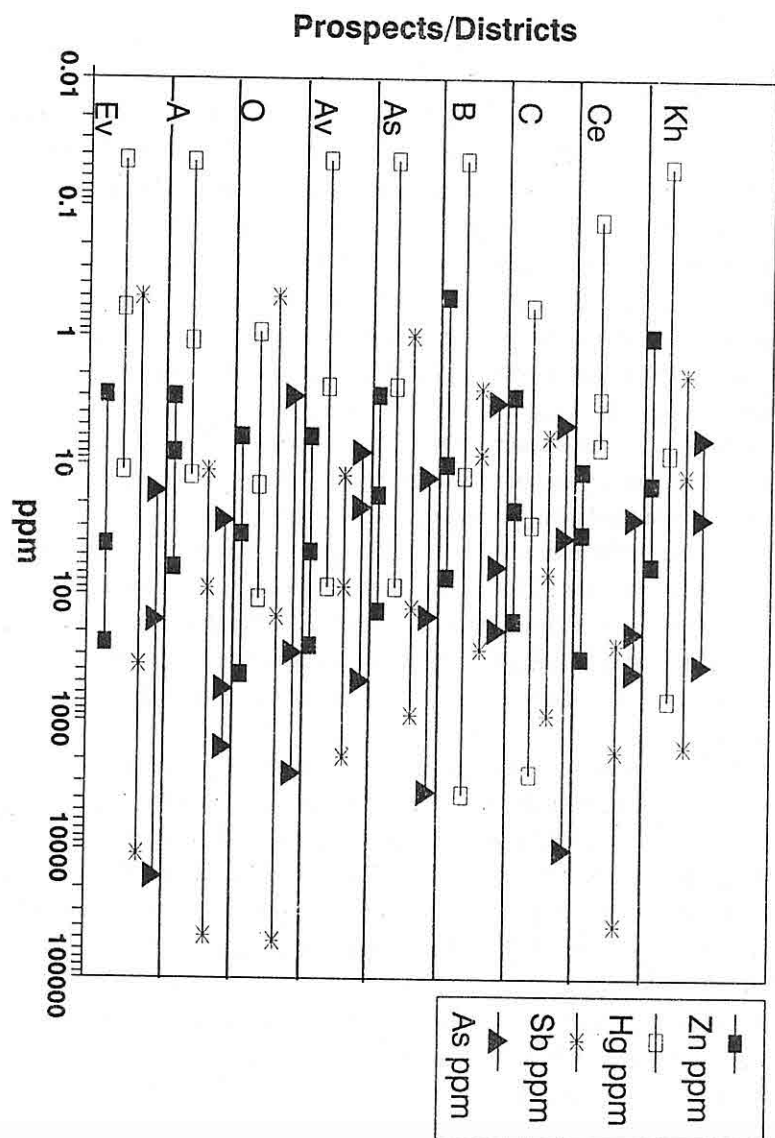
28
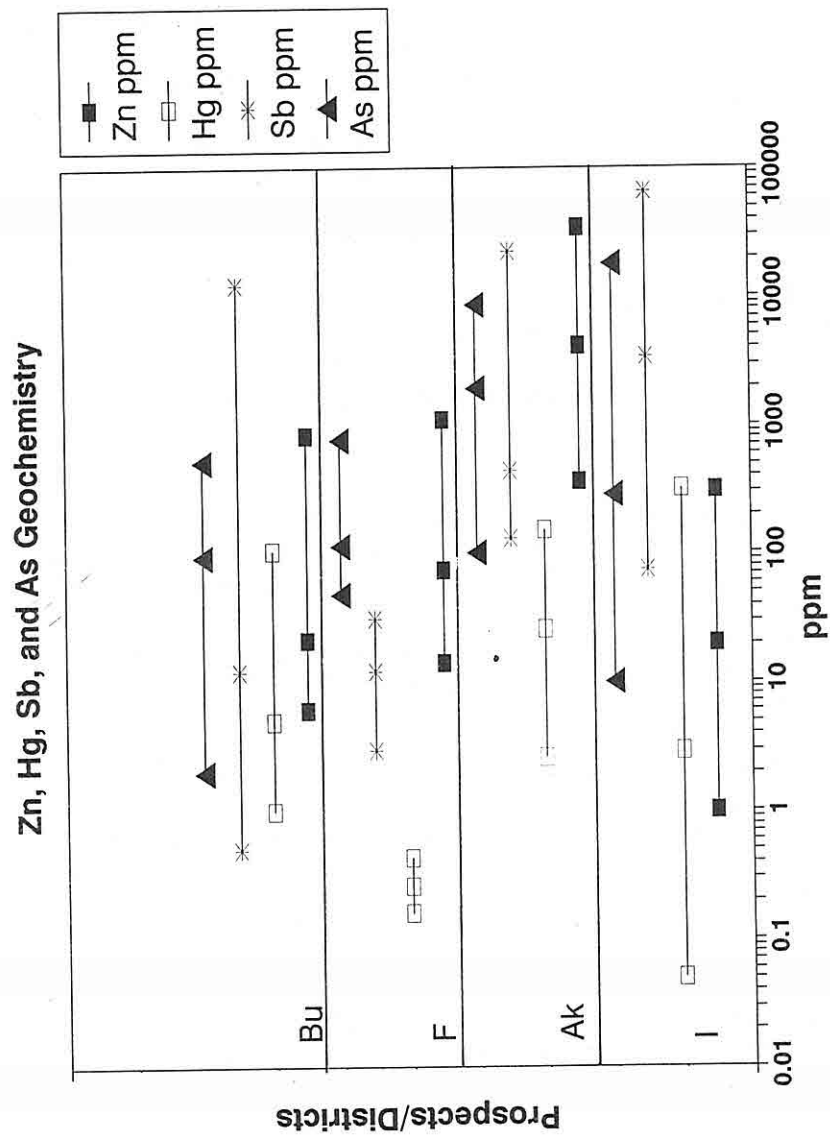
Figure 11. Zn, Hg, Sb and As trace element geochemistry for volcanic-hosted prospects/
districts listed in Figure 10.

27

Figure 10. Au, Ag, Tl and Mo trace element geochemistry for volcanic-hosted prospects/districts. I=Ivrindi; Ak=Akmaden; F=Fatsa; and Bu=Bulancak.

mineralized system--levels at which Hg, Tl and As (+/- Sb) are enhanced and precious metals, if present at all, will increase at depth. In terms of exploration potential based on trace element geochemistry, the Örencik prospect near Dağardı stands out with definitely anomalous median and maximum Au values as well as higher median As and Ag.

Figures 8 and 9 illustrate the trace element geochemistry of the Suluklugölköy district and the Karakaya and Ilıcalar prospects. These are geologically similar in the sense that all are associated with ophiolitic melange but differ one from the other in the apparent structural controls and host rock lithology within which the metal values occur. At Ilıcalar, for example, the rock sampled was paleosinter, whereas at Suluklugölköy both listwaenite and schist and at Karakaya listwaenite at a serpentinite/granite contact was sampled. At Ilıcalar the indicator element signature except for Au and Ag is epithermal with median As greater than 1000 ppm, and Sb ranging as high as 2000 ppm with a median at 300+ ppm. Au and Ag medians, however, are <0.5 ppm with Au being particularly low at but 3 ppb. Thallium, generally at detection limits of 0.25 ppm is locally enhanced to a maximum of 2 ppm and this, plus the very elevated As and Sb values suggest a possible interpretation that the present topographic surface where sampling was done is very high in the system and that at depth precious metal values will improve. This interpretation is strengthened by the anomalous Hg values of as much as 7 ppm. Mercury, a highly volatile element, is frequently at a maximum at higher structural levels in epithermal systems than are the less volatile precious metals. Both Suluklugölköy and Karakaya have excellent high medians and maximum values for the entire trace element suite reported on (except for Hg at Karakaya) with high Au, and Tl values of 10 ppm or more and Ag maximums clearly enhanced at 3 to 10 ppm. Arsenic is very high with medians >1000 ppm. Notable here in contrast to those prospects hosted by metamorphic rocks or the group in melange near Murat Dağı is the low Ag:Au ratio which, using median values, is closer to 1:1 to 2:1. Gold values at Suluklugölköy range very widely from a low of a few ppb to a high of > 20 ppm, a circumstance resulting from the broad range of rock types sampled and the spotty restricted distribution of the precious metal mineralization.

The trace element geochemistry of the vein/stockwork prospects hosted in andesitic to dacitic volcanics is summarized in Figures 10 and 11. All have Au maximum values >1 ppm with all but Bulancak being >10 ppm. Silver maximums are >50 ppm for all prospects but İvrindi. Using medians, the Ag:Au ratios for all of the prospects but İvrindi is 15:1 to 20:1 while İvrindi is but 3:1. Thallium medians are everywhere greater than 2 ppm except for Bulancak where, due to analytical difficulties, only one Tl value was determined. Zinc, and to a lesser extent, Mo values are high with Zn maximums always greater than 200 ppm and often exceeding 1000 ppm while Mo maximums are nearer 100 ppm. Arsenic and Sb (except for Sb at Fatsa) are highly anomalous with maximums in the 1000 to 10,000 ppm range. Mercury is everywhere enhanced (except Fatsa) to levels

25
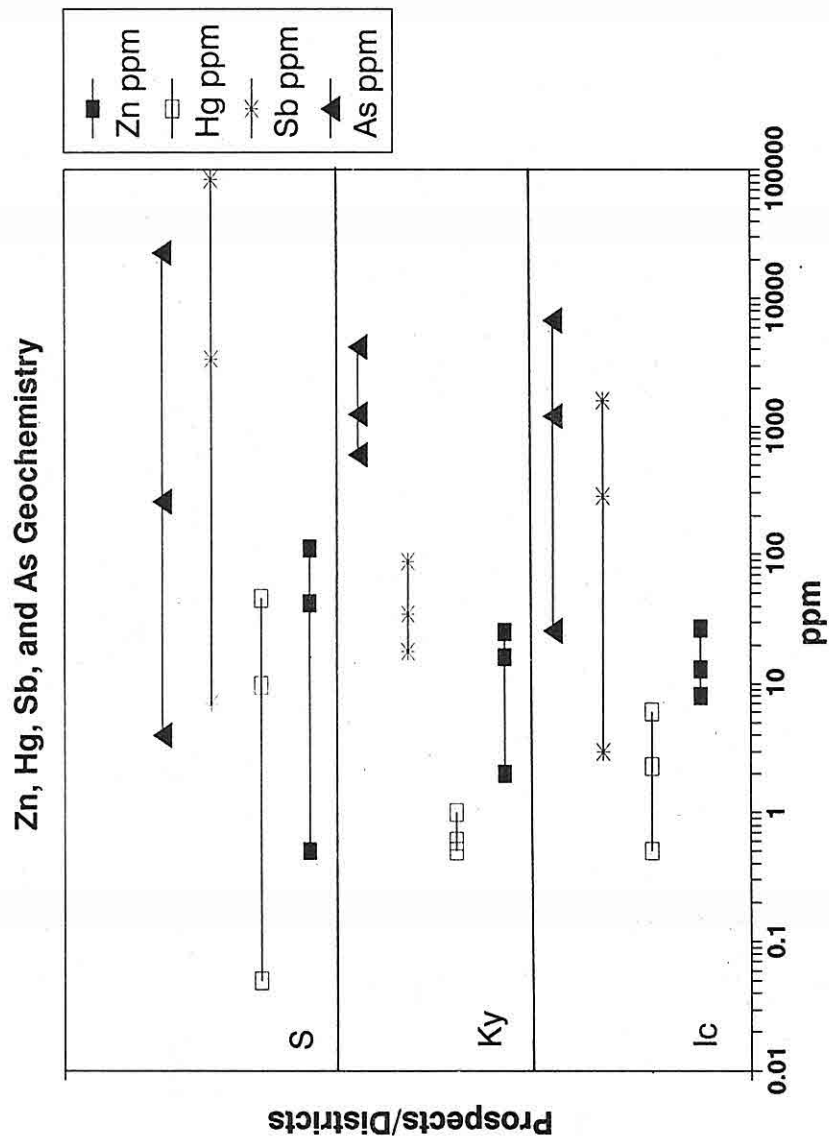
Figure 9. Zn, Hg, Sb, and As trace element geochemistry for melange/listwaenite-hosted prospects/districts listed in Figure 8.

24
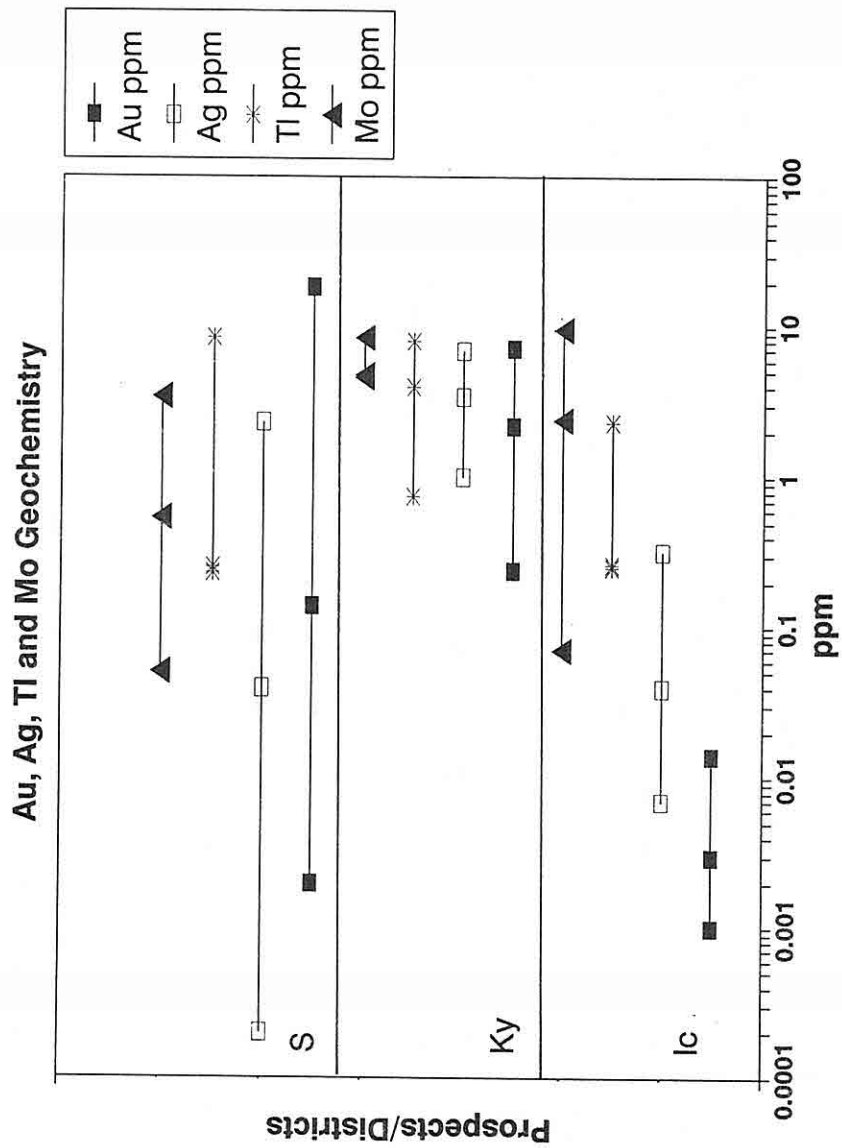
Figure 8. Au, Ag, Tl, and Mo trace element geochemistry for melange/listwaenite-hosted prospects/districts. Ic=Ilıcalar; Ky=Karakaya; and S=Suluklugölköy.

23

are in the 1 to 10 ppm range while corresponding lows are in the 1 to 10 ppb range and medians are (except for Madsan) tightly grouped at 0.1 to 0.5 ppm. Silver (Ag) highs range from 10 to 40 ppm and with (except for Celaller) lows of 0.05 to 0.2 ppm with a fairly tight median at 0.7 to 3 ppm. Ag:Au ratios, using median values, are from a low of about 5:1 at Kurşunlu to as much as 20+:1 at Madsan and Celaller. Figure 3 also shows that despite differences in structural control or type of deposit shown in Figure 2, the Au-Ag-Tl-Mo trace element signatures of Kurşunlu and Emirli (both within the Menderes massif) are remarkably similar. In general, the Ag:Au ratios for deposits within the Niğde massif are 3 or more times higher than those within the Menderes Massif. Figure 4 addresses the same prospects/districts as does Figure 3 but provides lows, highs and medians for Zn, Hg, Sb, and As. Figure 4 makes clear that all the prospects hosted by metamorphic rocks are very antimony and arsenic enriched with maximum values in the 1000 to several thousand ppm range. Mercury, another element typically enriched in epithermal precious metal deposits, has extremely high maximum values in the 80 to 1000+ ppm at all the metamorphic rock hosted deposits. In this group whose trace element geochemistry is summarized in Figures 3 and 4 the Celaller prospect in the Niğde Massif stands out as having extreme As and higher Ag and Tl values as well as having the highest Ag:Au ratio. Not shown in the Figures but evidenced by numerous analyses is that the prospects of the Niğde massif have enhanced Bi values as great as 200+ ppm (the Gümüşler prospect is also high in Te and Se), while in the Kurşunlu prospect in the Menderes massif is selenium enriched to a maximum of 60 ppm with an average of 4 ppm. The silver selenide Naumannite has been observed in polished section in Kurşunlu specimens.

Figures 5, 6, and 7 address the trace element geochemistry of melange hosted prospects/deposits. With the exception of Örencik, median Au and Ag values are 1 to 2 orders of magnitude lower than for metamorphic rock hosted deposits. Au:Ag ratios, using median values, are typically in the 10:1 to 20:1 range. Thallium ranges are very large and maximums in the 100's of ppm are an order of magnitude greater than for metamorphic rock hosted deposits. Molybdenum medians are generally in the 1 to 10 ppm range with most highs in the 10 to 30 ppm range-- values which are quite similar to deposits in metamorphic rocks. Figure 7 shows that for melange-hosted deposits Sb and As maximums are, with some exceptions, extreme at >1,000 ppm and often >10,000 ppm, while medians are in the 50 to 100+ ppm range. Median Hg values range from <1 ppm to >10 ppm with the highest medians and maximums expectably occurring at Baltalı and Çiçeklikayasıtepe both of which are inactive mercury mines. Zn median values are 10 to about 40 ppm, a range similar to that shown by most metamorphic rock hosted dposits. In summary, the epithermal trace element signature, except for anomalous Au and Ag, is present at most of the Murat Dağı area prospects as well as those near Dağardı. A possible interpretation is that the present surface topography represents very high level in the

22

Prospects/Districts

Zn, Hg, Sb, and As Geochemistry

Figure 7. Zn, Hg, Sb, and As trace element geochemistry for melange-hosted prospects/districts listed in Figures 5 and 6 above.

21
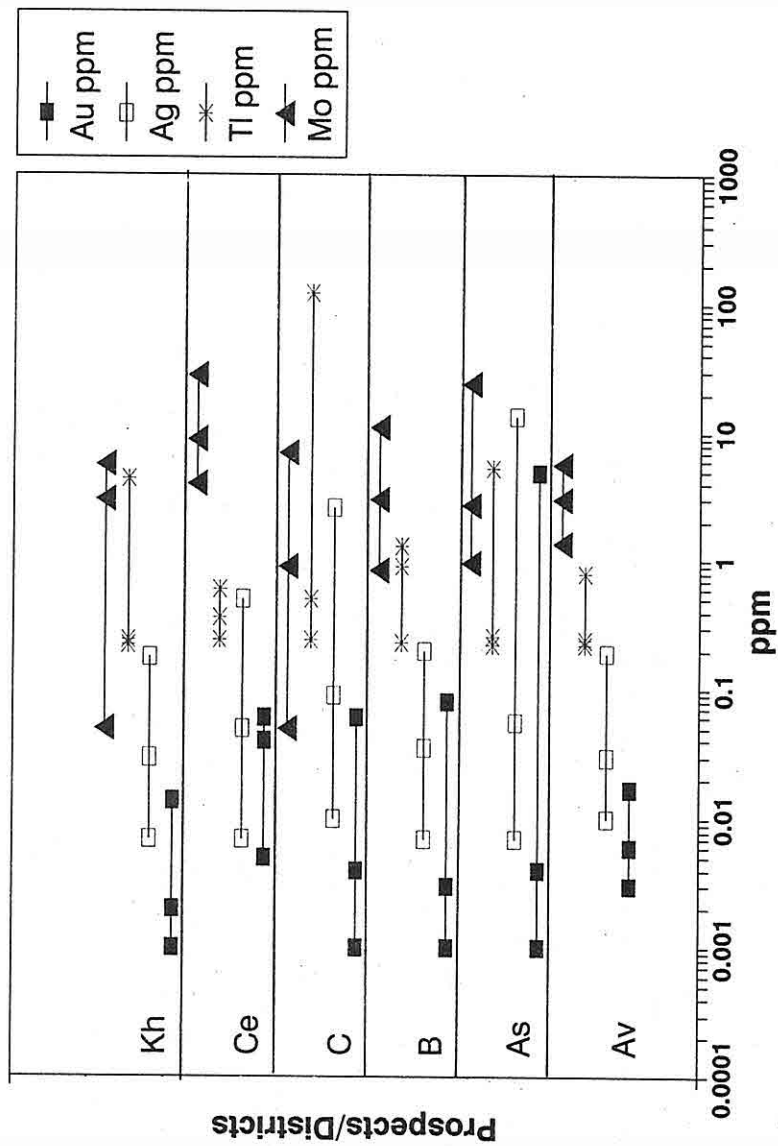
Figure 6. Au, Ag, Tl, and Mo trace element geochemistry for melange-hosted prospects near Murat Dağı. Av=Avdantepe; As= Arsaktepe; B=Baltalı; Ç = Çiçeklikayasitepe; Ce=Cebrail; and Kh=Karacahisar.

20
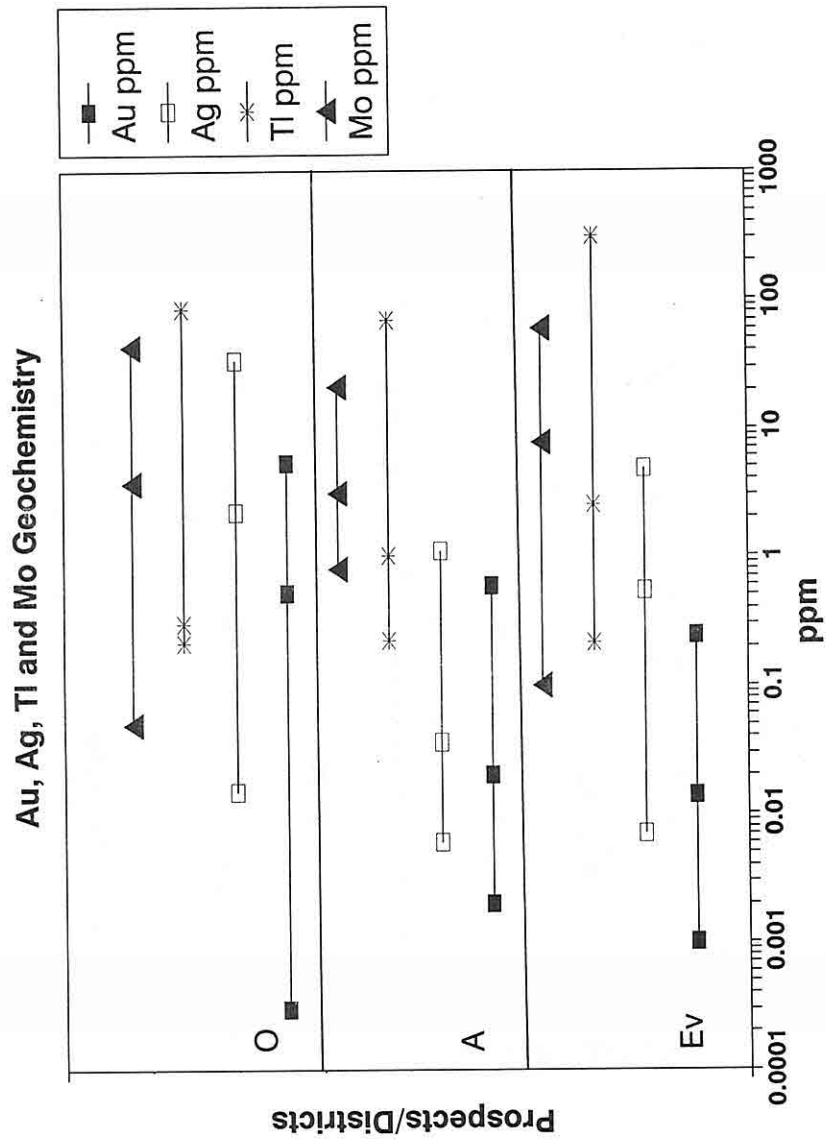
Figure 5. Au, Ag, Tl, and Mo trace element geochemistry for melange-hosted prospects near Dağardı. Ev= Evciler, A=Arıklar, and Ö=Örencik.

19

Figure 4. Zn, Hg, Sb, and As trace element geochemistry for metamorphic rock hosted prospects. Abbreviations for prospects as in Figure 3.

18

Figure 3. Au, Ag, Tl, and Mo trace element geochemistry for metamorphic rock hosted prospects. K=Kurşunlu; E=Emirli; Bl=Beril Cl=Celaller; G=Gümüşler; and M=Madsan.

17

and pyroclastics altough occasionally replacements occur in silicified limestones close to the contact with the volcanics (Erler and Larson, 1992). At Çakmakdere, (İvrindi District) in particular, stibnite veinlets form a stockwork in argillically altered, locally pyritized, intermediate volcanics adjacent to a N20-30E striking fault.The stockwork zone is overlain by a silica "cap" which contains disseminated cinnabar and realgar. Localized areas of hydrothermal breccia are found at several places along the strike of the N20-30E fault. At Fatsa, in a quarry near the Dolunay hotel, 1 to 4 cm wide quartz and chalcedony veinlets containing galena, pyrite, and sphalerite form a stockwork in silicified dacites. Argillically altered volcanics crop out in the road cut across the highway from the quarry. The host rock at Akmaden is also dacite, and pyrite, stibnite, orpiment and realgar occur in N65E and N80E striking quartz-chalcedony veins ranging in width from 1/2 to 1 1/2 meters. The host rocks are silicified and argillized. At Bulancak, pyrite, chalcopyrite, sphalerite, galena, barite and hematite-bearing quartz and chalcedony veins which strike N45W and N65W and dip steeply NE, cut silicified and argillically altered dacitic volcanic tuff and agglomerate.

In summary, at all of the prospects where we have reconnaissance-level geologic information in additon to samples, mineralization is very clearly structurally controlled. Strong structural control of mineralization is characteristic of epithermal precious metal deposits as has been pointed out by Tooker (1985) and by many other authors. Wallrock alteration, only incidentally addressed in this article, is everywhere, regardless of host rock, silicification and in those prospects hosted by volcanic rocks, argillic alteration is present and occasionally is widespread. Tooker (1985) in his summary of epithermal disseminated precious metal deposit characteristics has noted that silicification is characteristic of both sediment and volcanic-hosted deposits and argillic alteration is very common in those hosted by volcanics.

4. GEOCHEMICAL SIGNATURE

All of the deposits/districts reported on in this article wrere selected for sampling on the basis (es) of known present/past production or occurence of one or more elements commonly associated with precious metal, or rock alteration (s) characteristic of epithermal mineralization elsewhere in the world. Figures 3 through 11 give minimum, maximum and median ppm geochemical values for Au, Ag, Tl, Mo, Zn, Hg, Sb and As for the 22 properties studied. Prospects are grouped and ordered by host rock type of so that on Figures 3 and 4, for example, we can compare the trace element geochemistry metamorphic rock-hosted properties such as Kurşunlu, Emirli, Madsan, Beril, Gümüşler and Celaller,while Figures 5, 6 and 7 provide the same information for melange-hosted prospects such as Evciler, Arıklar, Örencik, and the 6 prospects areas near Murat Dağı--Avdantepe, Arsaktepe, Baltalı, Çiçeklikayasıtepe, Cebrail and Karacahisar.

Inspection of Figure 3 shows that for the metamorphic rock hosted prospects Au highs
16

The melange rock affiliated group of deposits both near Dağardı and near Murat Dağı are, with some exceptions, more difficult to associate with a particular structure or specific rock type. Mineralization, however, often appears associated with highy silicified "jasperoid" breccias-- the silicification usually being so intense as to make recognation of the pre-alteration rock type difficult or impossible. Usually the breccias will be veined by late stage chalcedony and opal CT. (Yıldız and Bailey, 1978; Larson and Erler, 1992). Mapping and Örencik has shown stibnite with pyrite as disseminations, pods, and stockwork veinlets occur along and in the hanging wall of a thrust fault between serpentinites, limestones and completedly silicified jasperoidal rock of uncertain original lithology. Gold values reach up to 5 ppm, while Ag values are as much as 13 ppm. Arıklar mineralization is associaed with stibnite mineralization and jasperoid breccias at least some of which are formed along a N50-60E striking high angle fault. At Arsakkayasıtepe and Cebrail and probably at Avdantepe, the jasperoids are found at or near the contacts between silicified limestone and serpentinite. At Cebrail, jasperoids are further controlled by N12E, N20W and N30W striking faults that are apparently steeply dipping. Çiçeklikayasıtepe is somewhat different and apparently more complex with mineralization being associated with a serpentinite-silicified limestone contact, possible hot spring sinter, and an apperant explosion breccia. All of the above pospects demonstrate late stage chalcedonic to opaline silica veining, extensive intense silicifcation, breccias, and spotty stibnite and/or cinnabar plus disseminated pyrite and hematite mineralization.

Alteration and mineralization is clearly structurally controlled at the listwaenite associated Ilıcalar, Karakaya and Suluklugölköy prospects/districts. At Ilıcalar, present-day hot springs, paleosinter breccia, Sb-As mineralization and late stage barite veinlets are formed adjacent to a WNW-striking fault with serpentinite on the SW side and paleosinter overlying serpentinite on the NE side. At the Karakaya prospect along a 1.5 km long by 30 m wide E-W-striking zone between granitoids and serpentinite. Serpentinite is almost completely silicified; local areas of silicified breccia show evidence of multiple brecciation (Erler and Larson, 1992). Precious metal values reach 7 ppm Au and 7 ppm Ag. Suluklugölköy is more complex because it is a district rather than a prospect but at the largest prospect in the district, the Annocak mine, disseminated stibnite-bearing listwaenite from which samples assayed as much as 18 gm's Au/tonne crops out at the gallery portal and appears associated with silicified zones controlled by N30-60E and N40-60W trending fractures.

Prospects developed in dacitic to andesitic volcanics within the İvrindi District and near the Black Sea at Fatsa, Akmaden and Bulancak, all show strong structural control. Mineralization is in veins, stockwork veinlets and/or breccias within narrow to very broad zones of silicification and argillic alteration. In the İvrindi district most of the stibnite mineralization is hosted by argillized and locally pyritized dacitic to andezitic volcanics

15

14

Figure 2. Map showing locations and generalized primary structural control for mineralization at the 22 prospects/districts discussed in this paper.

3. PRIMARY AND SECONDARY STRUCTURAL CONTROL

Table 1 lists and Figure 2 illustrates what we belive to be the major ore controlling structures at each of the prospects/districts. In most prospects actual structural controls of mineralization are complex and often second order structures or in the intersections of structures are important to the concentration of metals.

Those deposits we list that are in metamorphic rocks of either the Menderes or Niğde massifs are, for the most part, hosted either in veins of breccias/microbreccias. Individually, however, they differ greatly. For example, extensive sampling at Emirli has shown that anomalous precious metal values are restricted in distribution to 1 or 2 meters about the flat L33 fault, and 2 or 3 smaller veins forming a small stockwork system. Precious metal values are associated with pyrite/marcasite and stibnite and seem to be at a maximum in silicified rock immediately adjacent to veins, although argillic alteration is more widespread. At Kurşunlu, precious metal values are largely within an intensely silicified microbreccia layer some 1 to 2 meters thick that forms along a 10-14 degree N-dipping fault near where it intersects the major faults that bound the Gediz graben (Larson and Erler, 1992). Associated with the gold/silver is arsenopyrite, stibnite, pyrite, possibly tetrahedrite and minute quantities of the silver selenide naumannite. However, geochemically anomalous gold and silver are also found in chalcedonic veins with realgar and stibnite and in a poorly silicified breccia which forms the distinctive black 'knob' on the hangingwall of the flat N-dipping fault and which overlooks the present-day hot spring.

About the Niğde Massif the Madsan property contains stibnite and anomaluos precious metal values in a 1 to 3+ meter wide zone at the fault contact between carbonaceous biotite-chlorite schist/gneiss and marble where the marble has been silicified. Anomalous precious metal values are also, however, found in large 'jasperoidal' breccia outcrops which are probably but not conclusively formed along E-W, N-S, N33W, N50W and N60-65E-striking fault zones. In addition to geochemically anomalous precious metal values, the jasperoids also contain disseminated barite, pyrite and, rarely, cinnabar. The Celaller mineralization is hosted by mica schist, amphibolite schist and quartzites which are cut by pegmatitic quartz veins. Gold values seem to bo associated with arsenopyrite, pyrite and iron oxides along any of the N13E, N30E, N40E, N30W or N70W-striking fracture and/or breccia zones. Rocks immediately adjacent to the fractures are very silicified and often pyritized. At Gümüşler, country rocks include marble, phyllite, quartz-mica schist and minor quartzite. Quartz veins, breccias and silicified zones along N50E, N-S, N50W, N60W and N75-80W fault contain pyrite, stibnite. cinnabar and geochemically anomalous precious metal values. Finally, at the Beril property, quartz veins and silicified breccias in quartz-mica schist and quatrzite contain pyrite, arsenopyrite, hematite, limonate and precious metal values as high as 2 ppm Au and 32 ppm Ag.

13

Province.

Volcanic hosted deposits/prospects are largely in altered andesites and dacites to rhyodacites and range from the İvrindi District southwest of Balıkesir to the prospects/mines at and about Fatsa, Akmaden, and Bulancak.

Many of the deposits/districts sampled are hosted by ophiolite associated melange terrain rocks ranging from serpentinites to graywackes and carbonates. Included in this broad group are prospects near Murat Dağı including Karacahisar and Baltalı in Uşak Province and Cebrail, Çiçeklikayasıtepe, Arsaktepe and Avdantepe--all within Kütahya Province; Ilıcalar southeast of Simav in Kütahya Province; Örencik, Evciler and Arıkler located east, north and northwest of Dağardi in Kütahya Province; and, finally, Suluklugölköy east of İnegol in Bursa Province and Karakaya, northwest of Sivrihisar in Eskisehir Province. Table 1 lists the prospects/districts we have studied and gives the abbreviation we use for that area in each of the figures used to illustrate this paper, as well as general rock environment and controlling structure (s) information.

TABLE 1
Summary Table of Prospects, Rock Environments
and Controlling Structures

Prospect Name	Abbrev	Rock Environment	Major Controlling Structural Element
Kurşunlu	K	Metamorphics	Breccia/Miçrobreccia
Emirli	E	Metamorphics	Epithermal Vein
Beril	Bl	Metamorphics	Epithermal Vein
Celaller	Cl	Metamorphics	Breccia
Gümüşler	G	Metamorphics	Epithermal Vein
Madsan	M	Metamorphics	"Jasperoid"
Evciler	Ev	Melange/Serpantinite	"Jasperoid"
Arıklar	A	Melange/Serpantinite	"Jasperoid"
Örencik	Ö	Melange/Serpantinite	"Jasperoid"
Avdantepe	Av	Melange	"Jasperoid"
Arsaktepe	As	Melange	"Jasperoid"
Baltalı	B	Melange/volcanic	"Jasperoid"
Çiçeklikayası T.	C	Melange	Siliceous Sinter
Cebrail	Ce	Melange	"Jasperoid"
Karacahisar	Kh	Melange	"Jasperoid"
Ilıcalar	Ic	Melange/Serpentinite	Siliceous Sinter
Karakaya	Ky	Melange/Serpentinite	Listwaenite
Suluklugölköy	S	Melange	Listwaenite
İvrindi	İ	Volcanics	Stockwork of Veinlets
Akmaden	Ak	Volcanics	Epithermal Vein
Fatsa	F	Volcanics	Stockwork of Veinlets
Bulancak	Bu	Volcanics	Epithermal Vein

12

Location/Host Rock Map

LEGEND

◯ VOLC. (DACITIC TO ANDESITIC)

⊕ METAMORPHIC (SCHIST/GNEISS/QTZITE)

⊕ MELANGE/SERPENTINITE
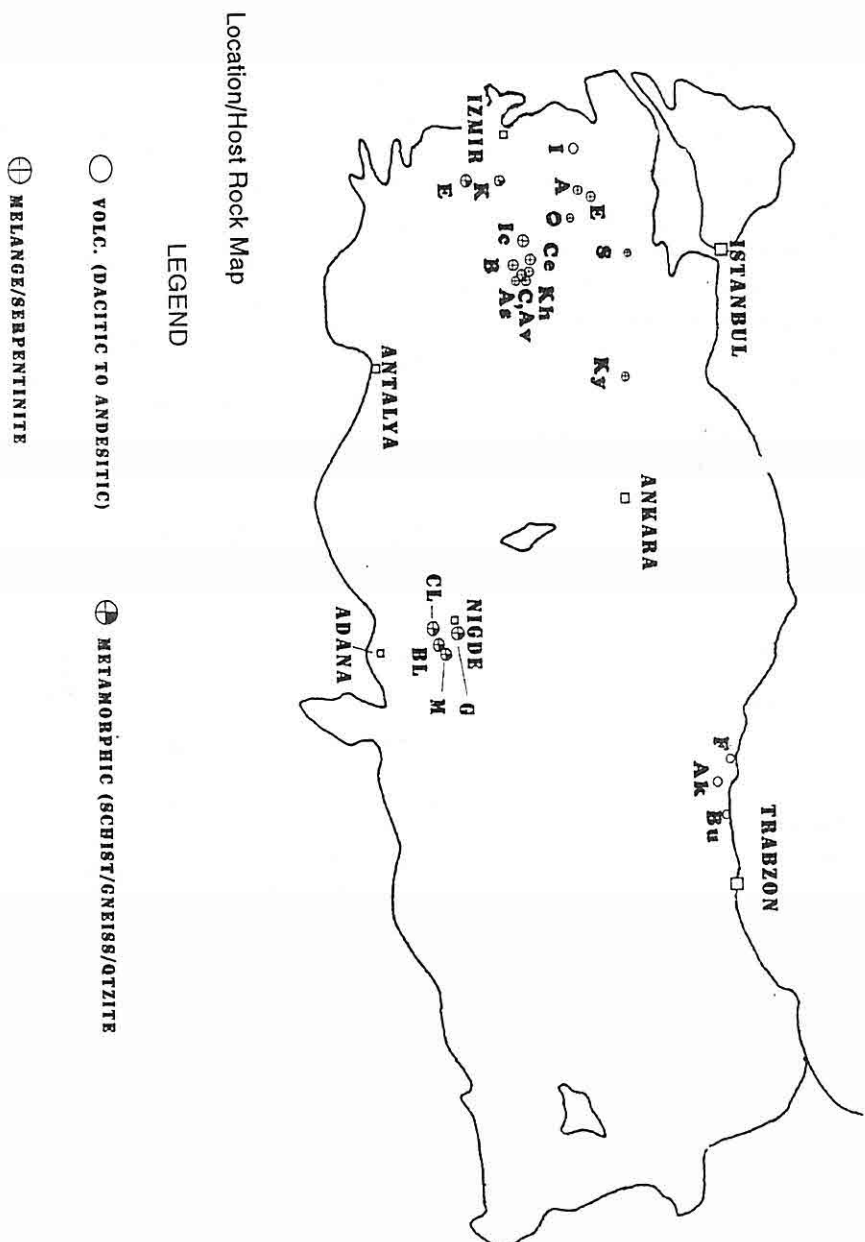
Fig. 1. Map showing locations and generalized host rocks for 22 prospects/districts discussed in this paper.

11

1. INTRODUCTION

This paper summarizes and geologically interprets the results of multi-element ICP analyses of approximately 700 rock chip samples most of which were taken from districts of known antimony (MTA, 1979) or mercury (Yıldız and Balley, 1978) mineralization throughout Turkey from near İzmir on the west to Ordu on the north and Niğde to south. A total of twenty-two (22) prospects/distdicts are considered in this paper. Samples taken in a given district vary from as few as 6 to as many as 162. Much of the sampling was done during an exploration program directed toward discovery of precious metal mineralization. An epithermal geologic model, premised upon known geological/geochemical characteristics of operating of mining properties in the western U.S. and elsewhere, was used to focus exploration (Larson, 1989).

The prospects we report on in this article may be classified on any of several bases. As in the article by Erler and Larson, 1990, we have chosen to divide them for purposes of discussion on the broad basis of generalized host rock environment/lithology (volcanics, melange, metasediments, etc.) and secondarily on what we believe to be the dominate structural control (s) of mineralization (veins, stockwork, disseminations, etc.). Most of the prospects examined appear to be distinctly epigenetic and thus to have an alteration pattern, geochemical signature and genesis more relateable to mineralizing process than to host rock environment. They are, as a group, epithermal.

All samples from all of the prospects/districts were analyzed for gold and its common epithermal indicator trace element suite of As, Ag, Hg, Sb and Tl. For many of the samples analytical data is also avaliable for Cu, Mo, Zn, Se, Te and a few other elements of less interest. As would be expected from a such a wide aggregate of deposits as is addressed in this paper, trace element concentrations vary substantially from one prospect to another. Overall, the districts/prospects show a strong epithermal geochemical signature with highly elevated values for arsenic (>1000 ppm), antimony (>1000 ppm), zinc (>250 ppm), and mercury (>10 ppm) and, less commonly high gold (0.1 to >10 ppm), silver (1 to >50 ppm) and thallium (1 to >100 ppm). A few prospects also show highly elevated values for selenium and tellurium. Interelemental correlation is positive between arsenic and gold and/or silver and locally excellent between antimony and gold/silver.

2. LOCATION AND HOST ROCK ENVIRONMENTS

Figure 1 provides a generalized location for the deposits discussed in this article and also indicates the host rock environment for each prospect. For example, the Kurşunlu prospect near Salihli in Manisa Province is hosted in metasediments (schists and gneisses) as is the Emirli District in İzmir Province. Both are, of course, in the Menderes massif. Other metasediment hosted prospects include those to the south and east of Niğde in the Niğde massif--the Gümüşler, Madsan, Beril and Celaller prospects-- all in Niğde

10

GEOLOGIC SETTINGS AND GEOCHEMICAL SIGNATURES OF TWENTY-TWO PRECIOUS METAL PROSPECTS IN TURKEY

LAWRENCE T. LARSON[1,2]   Y.AYHAN ERLER[3]

[1]*Mackay School of Mines, Univ. of Nevada, Reno, NV. (permanent address)*
[2]*Cumhuriyet University, Sivas, TÜRKİYE (present address)*
[3]*Middle East Technical University, Ankara / TÜRKİYE*

ABSTRACT: *This paper interprets the results of multi-element analyses of 700+ rock chip samples taken largely in districts of antimony/mercury mineralization throughout Turkey. A total of 22 prospects/districts were examined with exploration directed toward discovery of precious metal mineralization. Most prospects are epigenetic and exhibit alteration patterns and geochemical signatures more relateable to mineralizing process than to host rock environment. They are, as a group, epithermal.*

Dominant alteration is silicification, although locally argillic and/or acid sulfate alteration is prominent. The outcrop expression of this alteration includes silicified chalcedonic paleosinter, silicified breccias and microbreccias, pseudo-stratified silica "gel" bold jasperoid knobs, and listwaenites.

Structural control of mineralization is evident at most of the prospects, but each property seems to a degree unique in its juxtaposition of structural elements that channeled mineralizing fluids.

Trace elements concentrations overall show a strong epithermal geochemical signature with highly elevated values for arsenic (>1000ppm), antimony (>1000 ppm), zinc (>250 ppm) and mercury (>10 ppm),and less commonly high gold (1 to >10 ppm), silver (1 to >50 ppm) and thallium (1 to >100 pm) values. Arsenic appears to correlate very positively with enhanced Au and Ag.

9

Quentin, K.-E., 1957. Der Fluorgehalt Bayerischer Wasser. 1. Mitt.- Gesundh.-Ing., 78 (21/22): 329-333, München.

Şimşek, S. 1985. Geothermal Model of Denizli, Sarayköy-Buldan Area. Geothermics 14: 393-417.

so that Ca^{2+} ions adsorbed at the solid substance, in exchange adsorbed Na^+ ions go into solution.

Due to ion exchange reactions, Ca^{2+} contents decreases while Na^+ increase. Contemporaneously, fluorine contents increase, so that there is a close correlation between Na^+ und F^- contents in aqueous systems.

Finally, it can be deduced, that not one single reason is responsible for the high fluorine contents in the shallow aqueous systems of the Gölcük area, but a concurrence of several natural factors.

5. REFERENCES

Bhussry, B.R., Demole, V., Hodge, H.C., Jolly, S.S., Singh, A., and Taves, D.R., 1970. Toxic Effects of Larger Doses of Fluoride. World Health Organization Monograph Series 59 (Fluorides and Human Health): 225-271.

Oruç, N., Alpman, N., and Karamanderesi, I.H., 1976. Hydrogeology of the Spring Waters with High Fluorine Contents in Surroundings of the Tendürek Volcano. Bull. Geol. Soc. Turk. 19: 1-8, Ankara.

Özgür, N., Pekdeğer, A., Schneider, H-J., and Bilgin, A., 1990. Pliocene Volcanism of the Gölcük Area, Isparta/W-Taurides. in: Savaşçın, M.Y. and Eronat, H.H. (eds.): Proc. Internat. Earth Sci. Congr. on Aegean Regions, Izmir/Turkey, IESCA Publ. 2, Vol. II, 411-419.

Özgür, N., Pekdeğer, A., and Schneider, H-J., 1992a. High Fluorine Contents in the Pliocene Volcanic Rocks of the Gölcük Area, Isparta, SW Turkey. Bull. Geol. Soc. Greece (in print).

Özgür, N., Pekdeğer, A., and Schneider, H-J., 992b. Fluorine in Pliocene Volcanic Rocks of the Gölcük Area, SW Turkey. Proc. Ist Internat. Symp. on East Mediterranean Geology, Adana/Turkey.

Pekdeğer, A., Özgür, N., Schneider, H-J., and Bilgin, A., 1990. High Fluorine Contents in Agueous Systems of the Gölcük Area. Isparta/W-Taurides.in: Savascin, M.Y. and Eronat, H.H. (eds.): Proc. Internat. Earth Sci. Congr. on Aegean Regions, Izmir/Turkey, IESCA Publ. 2, Vol. I, 160-170.

Pekdeğer, A., Özgür, N., and Schneider, H-J.,1992a. Zur Hydrogeochemie Von Fluorid in Grundwassern und die Gesteinsgeochemie in der Provinz Isparta / Türkei. DFG-Forschungsbericht (in preep.).

Pekdeğer, A., Özgür, N., and Schneider, H-J., 1992b. Hydrogeochemistry of Fluorine in Shallow Aqueous Systems of the Gölcük Area, SW Turkey. In: Kharaka, Y.K. and Maest, A.S. (eds.): Proc. 7th Internat. Symp. on Water-Rock Interaction - WRI-7/Park City/Utah/USA, Vol. I, 821-824.

7

enhance anion exchange reactions between F⁻ and OH⁻ ions. Generally, the groundwaters are saturated with respect to calcite. However, there is only a poor vegetation cover and agricultural activity, due to unfertile soils above the volcanic rocks and dry climate in the area. Finally, the minimized microbiological activity leads to very low CO_2 contents in soil atmosphere as calculated from the carbonic acid system (Pekdeğer et al., 1992a,b).
6. Furthermore, the volcanic rocks of the Gölcük area are alkaline rocks of sodic type (Özgür et al., 1992b), so that a considerable amount of Na^+ ions are dissolved during weathering process. The Ca^{2+} ions are more readily adsorbed than Na^+ ions, so that
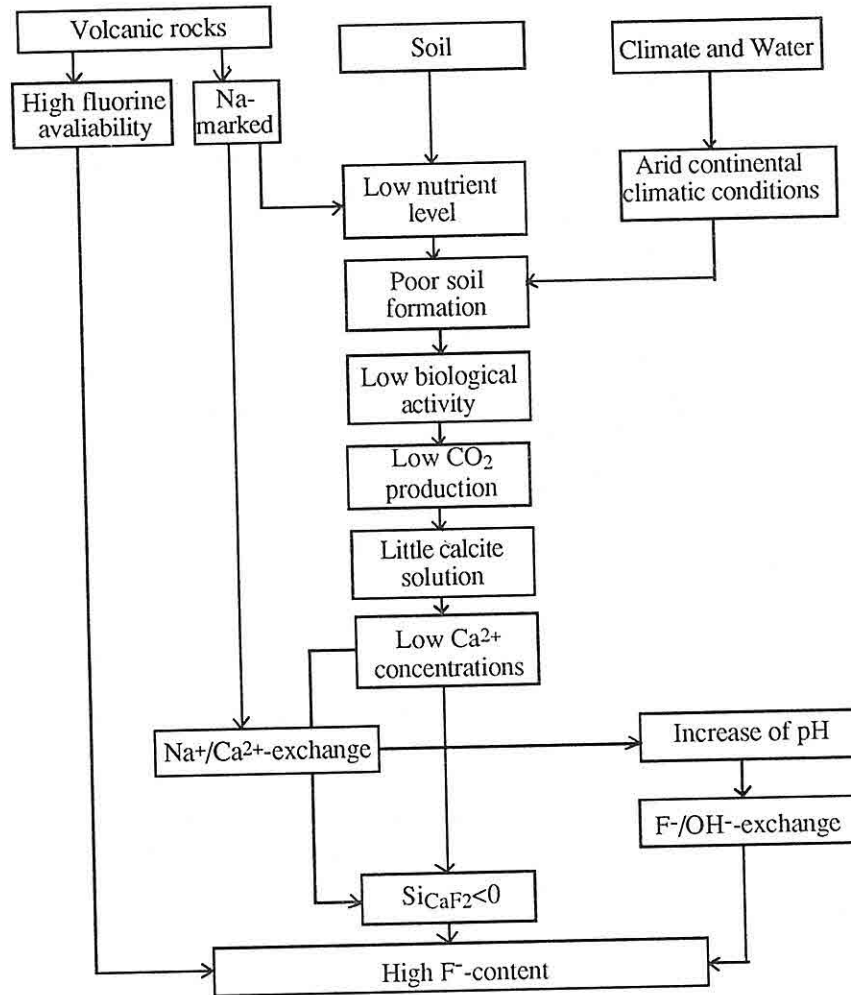
Fig. 2: Relationship between volcanic rocks, soils, and aqueous systems and schema of the increase of fluorine in the groundwater.

6

springs were studied for any indication of hydrothermal activity. All water samples show fluorine contents less than 1 mg/l. Therefore, a quantitative contribution of hydrothermal activity to the high fluorine contents in the shallow aqueous systems in the area can be ruled out.

4. DISCUSSION AND CONCLUSIONS

As the reasons for the high fluorine contents in shallow aqueous systems of the Gölcük area three aspects have to be considered:

(1) High fluorine in source rocks (Figs. 1 and 2): large amounts of fluorine are present in the volcanic rocks of the Gölcük area which can be dissolved during weathering,

(2) Hydrothermal activity: fluorine can be transported especially into the lake by ascending hydrothermal water which can be observed elsewhere in western Turkey, e.g. in Kızıldere (Şimşek 1985),

(3) Fluorite stability: fluorine contents in shallow aqueous solutions are limited by fluorite stability. Besides fluorite, fluorapatite solubility could also theoretically govern the fluorine concentration in aqueous systems.

To explain the origin of fluorine in aqueous systems the following observations are of importance (Fig.2):

1. The volcanic rocks show F-contents in a range from 32 to 3200 ppm and a background value of 1000 ppm (Özgür et al., 1990; 1992a) which can be attributed to different mineral phases, i.e. pyroxene, hornblende, biotite, fluorapatite, fluorite, and glassy groundmass. By comparison, the sedimentary rocks contain low F-contents in a range from 100 to 200 ppm.

2. F$^-$ concents in shallow aqueous systems within the volcanic rocks range from 0.7 to 5.6 mg/l with an average of 2.5 mg/l. The groundwater in the sedimentary rocks shows F$^-$contents less than 0.7 mg/l. The leachates of 40 leaching experiments carried out under controlled laboratory conditions corroborate this assumption, according to which the highest F$^-$contents were measured in the leachates of the pyroclastic series (Pekdeğer et al., 1992a).

3. In the shallow aqueous systems of the Gölcük area as well as in the Gölcük lake, the possible influence of any hydrothermal activity on the fluorine contents could not be observed.

4. High fluorine contents in the shallow aqueous systems within the volcanic rocks show a close correlation with low Ca^{2+} contents. The concentrations of the both elements are obviously limited by fluorite solubility (Pekdeğer et al., 1992a). F-apatite which forms the major F-bearing mineral phase in the volcanic rocks and may control the solution equilibria is highly supersaturated. Therefore, fluorapatite precipitation is not possible under these conditions, due to slower precipitation kinetics.

5. The low Ca^{2+} contents in the groundwater can be attributed to low pCO$_2$ during calcite dissolution. Consequently, the resulting groundwaters have high pH values which

5
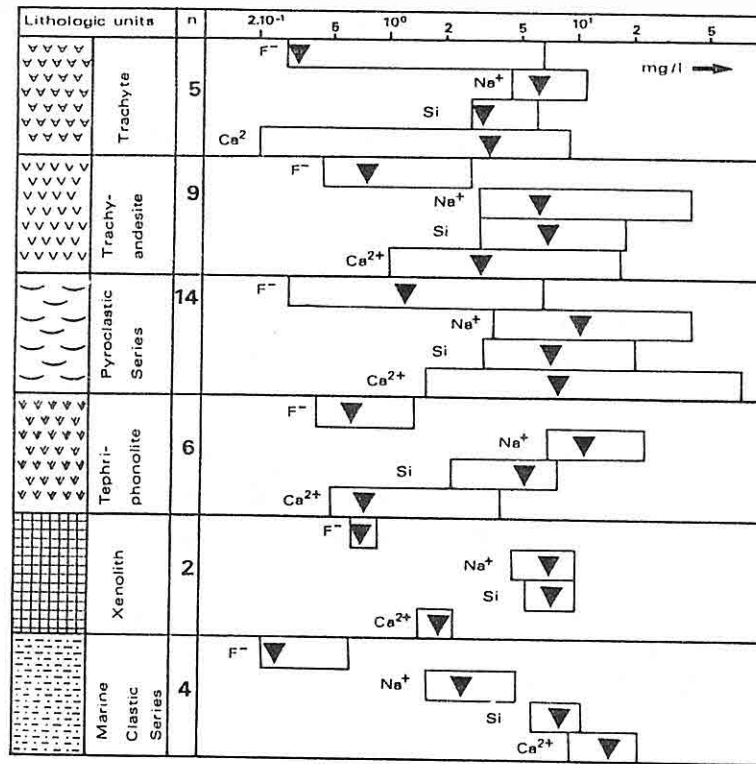
Fig. 1: F⁻ and major ion contents in shallow aqueous systems of the Gölcük area
▼: background value of the ions.

$$Ca^{2+} + 2(HCO_3^-) + Solid\text{-}2Na^+ <=> 2Na^+ + 2(HCO_3^-) + Solid\text{-}Ca^{2+} \quad (eq\ 1)..$$
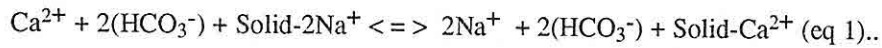
Due to ion exchange reaction, with increasing Na^+ concentrations, Ca^{2+} concentrations decrease. F^--contents increase contemporaneously, so that there is a close correlation between Na^+ and F^--contents in shallow aqueous systems of the Gölcük area (Pekdeğer et al., 1990; 1992a,b). According to the same authors, there is a negative close correlation between Ca^{2+} and F^- concentrations in the volcanic rocks. The concentration of both elements is obviously limited by fluorite solubility. By comparison, there is no correlation between Na and F contents in the volcanic rocks. With increasing SiO_2 contents in the volcanic rocks, the Ca and F contents decrease while Na increases (Özgür et al., 1990; 1992a; Pekdeğer et al., 1990; 1992a,b).

In order to investigate the possible influence of hydrothermal activity on the fluorine contents of the shallow aqueous systems in the Gölcük lake drainage area, the possible

4

surface and groundwater. The substantial amounts of groundwater are infiltrating to the lake from the subsurface. In the study area, the sedimentary rocks, i.e. limestone, marine clastic series, and conglomerate, are good aquifers, which occur mainly out of drainage area. As oldest rocks, the tephriphonolite lavas cause a pilling-up of water due to its intensely grain density and smaller jointing. Consequently, pyroclastic series with a thickness indicates a approximately horizontal layer and friable grain density and constitutes an aquifer with a high permeability.

3. HYDROGEOCHEMISTRY OF FLUORINE

Fluorine contents in shallow aqueous systems within the volcanic rocks of the Gölcük area range from 0.7 to 5.6 mg/l with an average 2.5 mg/l (Fig.1). By comparison, the groundwater in the sedimentary rock aquifers contain F^-contents less than 0.7 mg/l. By the hydrogeochemical discrimination of the elements Na^+ and Ca^{2+}, the groundwater in the Gölcük area can be divided into (1) fluorine rich and (2) fluorine poor environments. Consequently, the drainage area around the crater lake constitutes fluorine rich sphere with an exception of a few springs of the limestone. The further environment of the investigated area involving the sedimentary rocks may be regarded as fluorine poor. These determinations can be established by the leachates of 40 leaching experiments carried out under controlled laboratory conditions (Pekdeğer et al., 1992a), which yielded F^- concentrations in a range from 0.2 to 6.6 mg/l. The leachates of the pyroclastic series show highest fluorine contents. Obviously, fluorapatite and other mineral phases, i.e. biotite, pyroxene, and hornblende, are less important fluorine sources for the semi-arid hydrologic and climatological conditions, also shown by a lack of alteration when examined microscopically.

The groundwater from the drainage area and the Gölcük lake shows not only higher F^- contents but also lower Ca^{2+} contents compared with the groundwater from the sedimentary rocks. Ca^{2+} ions are derived mainly from the carbonate rocks (e.g. calcite) and partly from the volcanic rocks. Due to unfertile soils above the volcanic rocks, there is only a poor vegetation cover and little agricultural activity. Furthermore the volcanic rocks of the Gölcük area are alkaline rocks of sodic type (Özgür et al., 1990; Pekdeğer et al., 1992a), so that contemporaneously considerable amounts of Na^+ ions are dissolved. Little calcite dissolution, due to low CO_2-concentrations in soil and ion-exchange reactions with Na^+, lead to low Ca^{2+}-concentrations in groundwater. The sum of earth alkaline ions ($Ca^{2+} + Mg^{2+}$) are less then the sum of carbonate complexes ($CO_3^{2-} + HCO_3^-$), indicating an alkaline ion-exchange water of Na-HCO$_3$ type. Due to ion exchange process the Ca^{2+} ions which are more readily adsorbed than Na^+ ions, are adsorbed at the solid substance, in exchange adsorbed Na^+ ions go into solution. Calculations of ion balances show in the volcanic rocks according to (Pekdeğer et al., 1990) an ion exchange (eq 1):

3

1. INTRODUCTION

Fluorine is an essential trace element to human body, but excessive intake may cause some problems for bone and teeth. Its deficiency in drinking water leads to a caries effect of the teeth, while its surplus is a reason for the fluorosis (Bhussry et al., 1970). Therefore, the fluorine concentration in drinking water is limited by the WHO standards to 0.5-1.0 mg/l, which are depending, however, on annual average temperature. Generally, the aqueous systems contain fluorine contents in a range from 0.05 to 0.50 mg/l (Quentin, 1957) , so that supplementary F^- must be given, especially to children.

The groundwater with high F^- anomalies in the Gölcük area caused serious health problems. About 100.000 inhabitants in the province capital Isparta are supplied by this water with high F^- concentrations as high as 6 mg/l (for rock geochemistry of the investigated area see Özgür et al., this volume). The aim of this paper is to elucidate the origin of high fluorine contents in shallow aqueous systems of the study area based on the properties of geochemistry and hydrogeochemistry of the fluorine.

2. STUDY AREA

In Turkey, high fluorine contents in water have been reported in the Gölcük area in the SW part of the province capital Isparta and elsewhere as reason for dental problems (Oruç et al., 1976; Özgür et al., 1990,1992a; Pekdeğer et al., 1990, 1992a, b). The main water reserve in the investigated area constitutes the Gölcük crater lake representing fluorine contents in a range from 1.5 to 2.0 mg/l which is situated in a drainage area within the volcanic rocks.

The Gölcük area represents a post tectonic Pliocene volcanic sequence overlying a Mesozoic paleorift in the W-Taurides which consists of sedimentary and volcanic rocks. The volcanic rocks of sodic alkaline type are tephriphonolite (stage 1), pyroclastic series (stage 2), and trachyandesites and trachytes (stages 3) indicating a common magmatic origin (Özgür et al., 1992b).

The volcanic rocks show F-contents in a range from 32 to 3200 ppm and a mean value of 1000 ppm (Özgür et al., 1990; Pekdeğer et al., 1992a; Özgür et al., 1992b) which are related to different mineral phases, i.e. pyroxene, hornblende, biotite, fluorapatite, fluorite, and glassy groundmass as the main F-carriers. By comparison, the sedimentary rocks in the surrounding area contain low F-contents in a range from 100 to 200 ppm.

The drainage area of the Gölcük lake and the shallow aqueous system in the environs is situated in a semi-arid and extremely continental climate, hence a suitable environment for fluorine enrichment has been given. In the investigated area, annual average rainfall is 605 mm, while annual average temperature amounts 12 °C.

The crater lake is supplied by rainwater and perennial springs. Volcanic rock sequences with different permeabilities cause a number of aquifers and aquitards lying one above other. These aquifers are tilted towards the lake which is the main drainage area for the

2

ORIGIN OF THE HIGH FLUORINE CONTENTS IN SHALLOW AQUEOUS SYSTEMS OF THE GÖLCÜK AREA, SW TURKEY

N. ÖZGÜR, A. PEKDEĞER, and H-J. SCHNEIDER

Institut für Geologie, Geophysik und Geoinformatik der Freien Universität Berlin, Wichernstr. 16, 1000 Berlin 33, Germany

ABSTRACT : In shallow aqueous systems within the volcanic rocks of the Gölcük area, high fluorine contents up to 6 mg/l have been measured which are higher than those of sedimentary rocks. F^- ions are mainly leached from glassy groundmass, less from F^- carriers, i.e. pyroxene, hornblende, biotite, fluorapatite. Fluorine contents in groundwater of the investigated area are limited by the solubility of CaF_2, i.e. also by Ca^{2+} values. Due to low pCO_2 in the barren soils of the pyroclastic series, calcite dissolution is limited. Low Ca^{2+} concentrations are enhanced by Na^+ vs. Ca^{2+} ion exchange. Also F^- vs. OH^- ion exchange is expected at high pH-values due to calcite dissolution with low pCO_2.

1

CONTENTS

Special Issue
1st International Symposium on Eastern Mediterranean Geology

ACKNOWLEDGEMENT

PREFACE

This special issue has been prepared for the papers and abstracts which will be presented in the 1st. International Symposium on the Eastern Mediterranean Geology to be held at the University of Cukurova in Adana,Türkiye, between 13 and 16 October 1992.

The Organizing Committee of the Symposium is exceedingly honored and gratified that 170 participants and 50 accompanying persons (expected) from 12 countries, representing various universities, goverment agencies, engineering firms and industries, will be attending and contributing to the success of the Symposium.

In overwhelming response to the call for papers, 63 oral presentations originating from about 12 countries have been submitted to the 1st International Symposium on Eastern Mediterranean Geology and 24 full papers and a number of abstracts have been published here, in the Symposium Proceedings.

The Eastern Mediterranean regionally is in the very critical position where the Afro-Arabian and Anatolian plates meet each other. Therefore the main purpose of the Symposium is to provide a suitable setting for bringing together individuals from multi-disciplines of Earth Sciences to create a vehicle for the exchange of ideas and information and motivate cooperation amongst those involved in research, application and implementation. The scope of the Symposium has been planned to encompass Economic Geology, Engineering Geology, Palaemagnetism, Magmatism, Mineralogy - Petrography - Geochemistry, Paleontology, Sedimantology, Stratigraphy, Tectonics, Volcanism, and Marine Geology.

EDITORS